UCL

SCHOOL OF PHARMACY

Protein-Protein Conjugation using Interferon

A thesis submitted by

Annabelle Patricia Herrington-Symes

For the degree of:

Doctorate of Philosophy (PhD)

of

UCL School of Pharmacy,
29-39 Brunswick Square, London, WC1N 1AX, UK.

October 2014

Plagiarism statement

This thesis describes the research conducted in the UCL School of Pharmacy and PolyTherics Ltd. between 4.9.2010 and 1.9.2014, under the supervision of Professor Steve Brocchini and Dr Ji-won Choi. I, Annabelle Patricia Herrington-Symes, confirm that the work presented in this thesis is my own and that any parts of the work that have ben conducted in collaboration are clearly indicated. Where information has been derived from other sources, I confirm that this has been indicated in the thesis.

Annabelle Patricia Herrington-Symes

_____ _____

(Signed) (Dated)

Acknowledgements

I would firstly like to thank Prof. Steve Brocchini and Dr Ji-won Choi for their constant support, wisdom and patience over the last four years of my PhD. They have watched my tears, frustrations and joy and I thank them for giving me this opportunity.

I started PhD with very little experience, an absolute passion for science and an ability to work hard. My PhD journey has been tough-I have given it absolutely everything I have. I have made mistakes, but they have shaped my learning and I have grown so much over the last four years, both as a person and as a scientist.

I would like to thank PolyTherics Ltd. and the UCL School of Pharmacy for sponsoring my PhD. I am really thankful I have worked both in industry and academia; it has given me a great experience of both sides.

I would like to thank Dr Claire Ginn and Amrita Abilash, I have shared this journey with them both and they have both become life-long friends. I thank them both for the coffee breaks and catch up sessions! I am so glad to have worked with them both and for their help with the antiviral and antiproliferative assays.

I thank Farzad Khayrzad, Dr Martin Fisher and Gaidad Tekle for their reagents, chemistry knowledge and for making the 10 and 20 kDa PEG di(bis)sulfone reagents for me. I also thank Dr Emmanuelle Laurine and Dr Karolina Peciak for their help with making the His_8IFNα-2a. I thank Dr Matthew Bird and all the scientists at PolyTherics Ltd. for their advice with my conjugation reactions.

I would like to thank all my family for their support, motivational speeches, love and help over the last four years. I would also like to thank my partner, Dr Benn Jessney, for his constant love and support and always making me laugh when I was down.

I would like to dedicate this thesis to my great grandparent, Nanny and Poppy-we miss you both and I hope I have made you both proud.

Abstract

Therapeutic proteins are often potent and have rapid onsets of action. Unfortunately protein-based medicines can be immunogenic and have short half-lives. The circulation half-life of many proteins has been improved by the covalent conjugation of poly(ethylene)glycol (PEG) to the protein. For example, PEGylated interferon-α2 (PEGASYS® and PEG-INTRON®) has become a first line treatment for hepatitis C. The aim of this thesis was to examine the possibility of using a homobifunctional PEG reagent to make protein dimers.

Our group has developed PEGylation reagents that undergo conjugation by *bis*-alkylation to selectively conjugate either (i) two cysteine thiols from a native disulfide or (ii) two histidine residues in a polyhistidine tag. It was hypothesised that IFN dimers (IFN-PEG-IFN) could be prepared with higher retained activity than monoPEGylated IFN. It was also hypothesised that a heterodimer of IFN and an antibody fragment (Fab) could be made while retaining the activity of both proteins within the heterodimer.

His_8IFN-PEG-His_8IFN and IFN-PEG-IFN homodimers were prepared by site-selective conjugation to the N-terminal 8-polyhistidine tag and to one of the disulfides of IFN respectively. These homodimer conjugates were characterised in terms of purity and *in vitro* activity. The *in vitro* cell based assays were optimised to accurately elucidate the specific activities of the IFN conjugates. The His_8IFN-PEG_{20}-His_8IFN homodimer was found to retain greater activity than IFN-PEG_{20}-IFN. The increased activity was thought to be due to conjugation to the polyhistidine tag, which is distal from the IFN binding surface. It was also found that IFN-PEG_{10}-IFN homodimer retained greater activity than PEG_{10}-IFN, which could be due to the presence of the second IFN molecule in the IFN-PEG_{10}-IFN homodimer.

Two different Fabs were used to prepare the IFN-PEG-Fab heterodimers. Conjugation was conducted at one disulfide of IFN and the accessible interchain disulfide of the Fab. One Fab was derived from a polyclonal antibody to albumin (Fab_{alb}) and the rationale for this heterodimer was that a longer lasting form of IFN could be made (IFN-PEG_{20}-Fab_{alb}). The other Fab was derived from bevacizumab (Fab_{beva}) to give an IFN-PEG_{20}-Fab_{beva} heterodimer that could, in principle, display antiangiogenic properties. Both heterodimers were evaluated using antiviral and antiproliferative assays to determine the activity of IFN in the conjugate. The IFN-PEG_{20}-Fab_{alb} conjugate displayed a 10-fold reduction in activity compared to IFN-PEG_{20}-Fab_{beva}. It was thought that Fab_{alb} underwent competitive binding with components of the media. Interestingly, the IFN-PEG_{20}-Fab_{beva} heterodimer displayed greater activity than PEG_{20}-IFN and IFN-PEG_{20}-IFN in both the antiviral and antiproliferative assays. The binding

properties of Fab_{beva} were determined by SPR. It was observed that the dissociation rate of IFN-PEG_{20}-Fab_{beva} was similar to Fab_{beva} and PEG_{20}-Fab_{beva}. IFN-PEG_{20}-Fab_{alb} was found to have a similar dissociation rate to Fab_{alb}. However, PEG_{20}-Fab_{alb} was found to have a slower dissociation to both IFN-PEG_{20}-Fab_{alb} and Fab_{alb}, this result requires further investigation but was thought to be due to the sample impurity. The association rates of heterodimers were found to similar to the PEG-Fab conjugates but slower than their native Fabs. This data suggests that the novel IFN-PEG_{20}-Fab_{beva} and IFN-PEG_{20}-Fab_{alb} heterodimer conjugates have retained their binding affinities to their antigens.

Overall, it was shown that a homobifunctional *bis*-alkylating conjugation reagent (e.g. PEG di(*bis*)sulfone **4**) could be used successfully to prepare dimeric protein conjugates. This work highlighted the importance to ensure the homobifunctional conjugation reagent was pure, especially for the preparation of protein heterodimeric conjugates. To develop this work further, it would be important to investigate three broad areas: i) improving the purity of the starting homobifunctional reagents, ii) evaluate the *in vivo* efficacy of the resulting protein homo-/hetero-dimers and iii) determine the overall potential for efficient scaling of the process to make the desired protein homo-/hetero-dimers.

Table of Contents

List of Figures

List of Tables

List of Abbreviations

ABD	Albumin binding domain
AD	Anchor domain
ADC	Antibody drug conjugate
ADCC	Antibody-dependent cellular cytotoxicity
AIEC	Anion exchange chromatography
AKAP	A-Kinase anchoring proteins
BiTE	
bsmAb	Bispecific monoclonal antibody
CDC	Cell mediated cytotoxicity
CIEC	Cation exchange chromatography
DCM	Dichloromethane
DDD	Dimerization docking domain
DMAP	4-Dimethylaminopyridine
DMEM	Dulbecco's Modified Eagles Medium
DTT	Dithiothreitol
EDC	1-ethyl-3-(3-dimethylamino-propyl)carbodiimide hydrochloride
EDTA	Ethylene-diamine-tetacetic acid
EMCV	Encephalomyocarditis virus
eq.	Equivalents
Fab	Fragment antigen-binding
FBS	Foetal bovine serum
Fc	Fragment crystallisable region
FcRn	Neonatal Fc receptor
FDA	US Food and Drug Administration
FIX	Factor IX
GAS	Interferon-Gamma Activated Sequence
GM-CSF	Granulocyte Macrophage Colony-Stimulating Factor
GRS	Glutathione re-oxidising solution
GSH	Reduced glutathione solution
GSSG	Oxidised glutathione solution
HCV	Hepatitis C Virus
HER2/*neu*	Human epidermal growth factor receptor 2

HSA	Human serum albumin
IFN	Interferon α-2a
IFNAR1/IFNAR2	Interferon α receptor 1/ receptor 2
IFNGR1/IFNGR2	Interferon γ receptor 1/ receptor 2
IgG	Immunoglobulin G
IL	Interleukin
IMAC	Immobilised metal ion affinity chromatography
IPTG	Isopropyl-β-D-1-thiogalactopyranoside
ISRE	Interferon-stimulated response element
IU	International Units
JAK	Janus Kinase
LB	Lysogeny broth
MA	Malignant Ascites
mAb	Monoclonal antibody
MALDI-TOF	Matrix-Assisted Laser Desorption Ionisation Time-of-Flight
mPEG	Methoxy-Poly(ethylene glycol)
MS	Mass Spectrometry
MTT	Thiazolyl blue tetra-zolium bromide
MW	Molecular Weight
MWCO	Molecular Weight cut off
NHS	N-hydroxysuccinimide
NIBSC	National Institute for Biological Standards and Control
OD	Optical Density
PBS	Phosphate Buffered Saline
PBST	Phosphate Buffered Saline-Tween
PD	Pharmacodynamics
PEG	Poly(ethylene glycol)
PK	Pharmacokinetics
PKA	cAMP dependent protein kinase
PTM	Post-translational modification
RP-HPLC	Reverse Phase-
RPMI	Roswell Park Memorial Institute
RT	Room Temperature

scDb	Single chain diabody
scFv	Single-chain variable fragment
SDS-PAGE	Sodium dodecyl sulfate-Polyacrylamide gel electrophoresis
SEC	Size Exclusion chromatography
STAB	Sodium triacetoxyborohydride
STAT	Signal transducer and activator of transcription
TB	Terrific Broth
TCEP	Tris(2-carboxyethyl)phosphine-hydrochloride
TFA	Trifluoroacetic acid
TNF	Tumour necrosis factor
USD	United States dollar
UV	Ultra Violet
VEGF	Vascular Endothelial Growth Factor

Chapter 1 Introduction to therapeutic proteins and strategies to improve their clinical effectiveness

1.1 Therapeutic Proteins

1.1.1 Therapeutic proteins

Proteins are of critical importance as they play fundamental roles in all biological processes and their potential has now been realised as powerful therapeutic agents (Kobsa and Saltzman, 2008). Therapeutic proteins are naturally occurring macromolecules (>1000 Da), which can be used in the treatment, cure or prevention of disease. For example two prophylactic human papillomavirus (HPV) vaccines (Cervarix, GSK; Gardasil, Merck) have been recently licenced, aimed at preventing cervical cancer (Einstein et al., 2009). Currently therapeutic biologics are being used clinically to treat cancer, viral infections, diabetes, hepatitis and multiple sclerosis (Sekhon, 2010). The Food and Drugs Agency (FDA) defines biologics as any "virus, therapeutic serum, toxin, antitoxin or analogous product applicable to prevent, treat or cure of diseases or injuries to man" (Meibohm, 2006). Biologics are fundamentally different from conventional chemical drugs or small molecule drugs (e.g. aspirin, MW 180 Da), for two reasons. Firstly, therapeutic biologics are proteins (including antibodies) or nucleic acids (DNA, RNA or antisense oligonucleotides), which are much larger (e.g. interferon ~20,000 Da) than small molecules (Sekhon, 2010). Secondly, biologics are derived from living material such as human, plant, animal or microorganisms (Meibohm, 2006). Under the umbrella heading of biologics, therapeutic proteins were once a subset of medical treatments. Now they play a significant role in almost all fields of medicine (Leader et al., 2008). As of 2012, there are over 200-marketed therapeutic proteins such as recombinant blood factors, vaccines, hormones, growth factors, interferons, interleukins and antibody based products to name just a few (Mullard, 2012; Rader, 2012; Walsh, 2010).

1.1.2 Factors affecting therapeutic efficacy of proteins

From a biological and therapeutic perspective, proteins offer two unique advantages; i) having specific mechanisms of action and ii) being highly potent (Pisal et al., 2010). Crucially for therapeutic proteins to be effective, they must reach their biological target. However many biological processes hamper the ability of the therapeutic protein to meet its biological target (Kobsa and Saltzman, 2008). The reasons for this could be poor solubility of the protein or the protein being denatured by pH or enzyme degradation (Kobsa and Saltzman, 2008; Pasut and Veronese,

2012). Further, the protein could be immunogenic or cause local toxicity, such as IFN β, where neutralising antibodies against IFN β have been shown to reduce the clinical efficacy during treatment of multiple sclerosis in 20% of patients (Malucchi et al. 2004). However a more common cause for poor efficacy is that many protein therapeutics have a poor PK-PD profile. With the exception of antibodies or Fc/albumin fused proteins, the majority of protein-based medicines are below 50 kDa and tend to have a short circulating half-life. Therefore, to maintain the therapeutically effective concentration over a prolonged period of time, frequent dosing is required. This reduces patient compliance (Kontermann, 2011). Further frequent dosing can pose an increased safety risk due to potential immunogenicity and an increased incidence of side effects from non-therapeutic concentration levels between doses.

1.1.3 1st generation therapeutic proteins

The development of genetic engineering and hybridoma technology in the 1970s revolutionised the production of biopharmaceuticals. First generation therapeutic proteins were un-engineered murine monoclonal antibodies or simple replacement proteins i.e. proteins displaying an identical amino acid sequence to that of a native human protein (Sekhon, 2010; Walsh, 2004). These replacement proteins were given in order to replace or enhance the levels of that protein e.g. human insulin (Walsh, 2004). The first biologic to gain FDA approval was Humulin® (recombinant human insulin) in 1982 (Johnson, 1983).

However to improve upon these first generation biopharmaceuticals, clinical performance (dosing regimen and routes of administration), product life-cycle management, immunogenicity, toxicity and side effects needed to be improved and reduced (Martin, 2006).

Even though recombinant forms of simple replacement proteins continue to come to the market, now modern biopharmaceuticals have been engineered in some way to tailor the therapeutic proteins properties. These ‘second generation’ biopharmaceuticals aimed to improve upon the progress made with first generation biopharmaceuticals. The biopharmaceutical strategies used to modify therapeutic proteins include polymer conjugation, encapsulation, hydrogels, fusion protein, hyper-glycosylation and acylation (Table 1–1) (Veronese and Pasut, 2005). These biopharmaceutical strategies were aimed at improving the efficacy, stability,

specificity, toxicity, immunogenicity and the pharmacokinetics (PK) of therapeutic proteins, in addition to improving properties such as solubility and maintaining the desired biological activity of the therapeutic protein (Marshall et al., 2003). However it must be considered that therapeutic proteins have evolved to play fundamental roles. By modifying therapeutic proteins, for example to improve stability, the activity of the protein may be affected, thus a balanced approach should be considered when developing 'next generation biopharmaceuticals' (Figure 1-1).

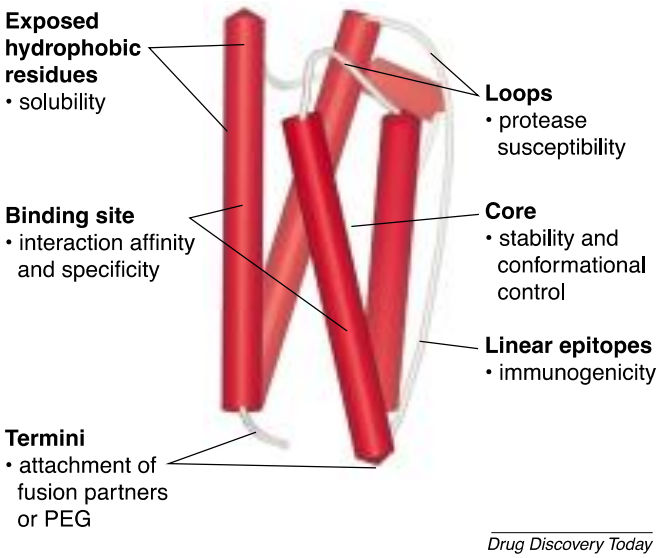

Figure 1-1. Biopharmaceutical strategies used to modify therapeutic proteins (Marshall et al., 2003). Many strategies to modify therapeutic proteins target specific areas or residues, however these changes to the protein may affect other protein properties e.g. the conjugation of PEG to the therapeutic protein may reduce the protein activity.

Table 1–1. Comparisons of biopharmaceutical strategies used to modify therapeutic proteins, adapted from (Veronese and Pasut, 2005).

Strategy	Brief Description	Advantages	Disadvantages	Marketed examples & references
Hyper-glycosylation	New glycosylation sites are engineered into the protein sequence	Glycosylation can occur away from active site, retaining protein activity	Isomers prepared with varying activity and half-lives	Aranesp® (hyperglycosylated Erythropoietin), Sigma-Tau (Elliott et al., 2003)
Protein-fusion	Protein, albumin or Fc antibody fragments fused to N or C terminus of protein	Protein obtained straight from expression system without the need for further modification	Conjugation reduces protein activity, may form new antigenic epitopes and prevent the protein from folding correctly	Etanercept® (TNF alpha receptor bound to the Fc portion of human IgG1), Amgen (Spencer-Green, 2000)
Polymer conjugation	Conjugation of polymers (PEG, PSA, PGA) to therapeutic proteins	Suitable for very immunogenic proteins, established approach with several products on the market	Reduced activity due to steric hinderance	PEGASYS® (PEG-IFN α-2a), Hoffman La Roche (Foser et al., 2003)
Hydrogels	Proteins are incorporated into a biodegrable gel, which are injected into the body	Native protein released from gel	Gel must be biodegradable which may denature the protein. Only non-immunogenic proteins can be used. Gel can form fibrotic capsules, which slows protein release.	Still in development (Tessmar and Göpferich, 2007)
Acylation	Protein or peptides modified with fatty acid to change pI and increase their affinity for albumin	Prolonged half-life by albumin binding	Mostly applicable for peptides and small proteins, may lead to large aggregates that may be immunogenic	Levemir® (Fatty acid bound to lysine residue of insulin) Novo Nordisk (Jones and Patel, 2006)
Encapsulation	Proteins are encapsulated in micro/ nanoparticles or liposomes	Protein released in native form	Not suitable for proteins, protein may be denatured in preparation	Doxil® (a Doxorubicin encapsulated in a PEGylated liposome Johnson & Johnson

1.2 Strategies to modify therapeutic proteins

Outlined are some of the most common strategies used to modify therapeutic proteins, which can be categorised into two strategies: i) increasing the MW of the therapeutic protein or ii) utilising the FcRn recycling mechanism.

1.2.1 Strategies to increase size

1.2.1.1 PEGylation

PEGylation involves the covalent chemical conjugation of poly(ethylene glycol) (PEG) to a protein, and is the most established post-translational modification (PTM) technique in the clinic for delivering and modifying the PK properties of therapeutic proteins (Jevsevar et al., 2010; Marshall et al., 2003).

Properties of PEG

PEG is made up of repeating units of ethylene glycol, which are both inert and ampiphilic in nature. Methoxy PEG (mPEG) can be made in various molecular weights (MW), structures (linear and branched, Figure 1-2) and conjugating moieties (linkers). Many PEGylation reagents have been prepared. PEG has been shown to be non-toxic, non-immunogenic, non-antigenic and is FDA approved for administration to man (Fruijtier-Pölloth, 2005; Ryan et al., 2008). Currently, there are 12 PEGylated medicines on the market (Table 1–2).

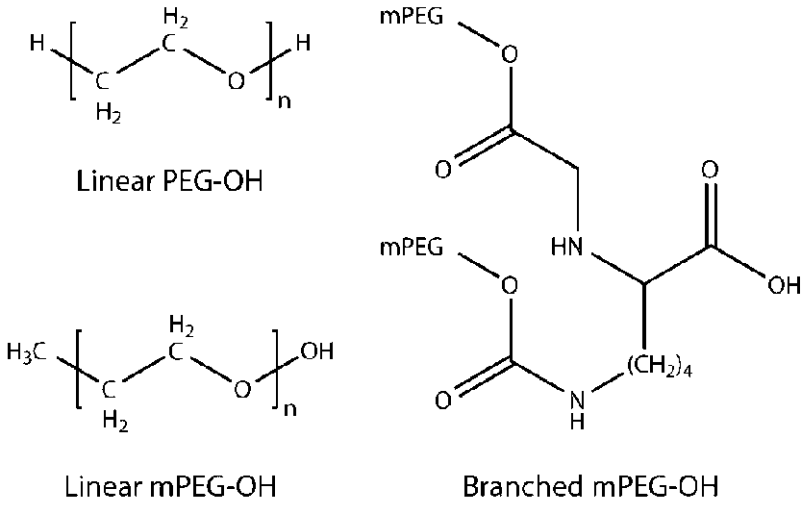

Figure 1-2. Structural formulae for linear Methoxy-PEG (mPEG), mPEG and branched mPEG (Pisal et al., 2010). mPEG can be made in various MW, structures (linear or branched) and can be conjugated to proteins with different linkers, showing the versatility of mPEG.

Table 1–2: Summary of current marketed PEGylated biologics, adapted from (Kontermann, 2011; Marshall et al., 2003).

Name	Active agent	Company	Indication	FDA approval date
Adagen® (pegademase)	Adenosine deaminase	Sigma-Tau	SCID	1990
Oncaspar® (pegaspargase)	Asparaginase	Enzon/ Schering-Plough	Cancer	1994
PEG-INTRON® (peginterferon α-2b)	IFN[1] α-2b	Schering-Plough	Hepatitis	2000
Doxil™ (Doxorubicin PEGylated	Doxorubicin	Ortho Biotech/ Schering-Plough	Cancer	2001
PEGASYS® (peginterferon α-2a)	IFN α-2a	Hoffman-La Roche	Hepatitis	2001
Somavert® (pegvisomant)	Growth hormone	Pfizer	Acromegaly	2002
Neulasta® (pegfilgrastim)	G-CSF[2]	Amgen	Leukopenia	2002
Macugen® (pegaptanib)	Anti-VEGF[3] aptamer	Eyetech pharmaceuticals/Pfizer	Age-related macular degeneration	2004
Micera® (mPEG-EPO β)	EPO[4] β	Hoffman-La Roche	Anaemia	2007
Cimzia® (Certolizumab pegol)	Anti-TNF[5] α Fab[6]	UCB Inc/Nektar	Crohn disease, Rheumatoid Arthritis	2008
Krystexxa® (pegloticase)	Uricase	Savient	Chronic Gout	2010
Omontys® (Peginesatide)	EPO	Affymax/ Takeda Pharmaceuticals	Chronic kidney disease	2012
Plegridy (Peginterferon β-1a)	IFN β-1a	Biogen-Idec	Relapsing multiple sclerosis	2014

Methods of Protein PEGylation

A variety of non-specific and specific conjugation strategies have evolved for protein PEGylation. Outlined are the most common approaches.

[1] Interferon
[2] Granulocyte-colony stimulating factor
[3] Vascular endothelial growth factor
[4] Erythropoietin
[5] Tumour necrosis factor
[6] Fragment antigen binding

- Non-specific strategies of PEGylation

Early research in PEGylation was directed at protein nucleophilic groups, typically the ε-amino group of lysine or the α-amino group of the N-terminal residue by using amine-reactive PEG reagents (Pasut and Veronese, 2012; Pisal et al., 2010). Amine-reactive PEG reagents have been developed to undergo conjugation by acylation and alkylation. PEG reagents that are functionalised as N-hydroxysuccinimide (NHS) active esters have been widely used to undergo conjugation by acylation. An amide is prepared when an amine moiety on the protein undergoes acylation. The protein amine thus loses its ability to be protonated at physiological pH, often resulting in loss of positive charge on the protein. Whereas widely used aldehyde functionalised PEG reagents undergo conjugation by alkylation. A secondary amine is prepared when the PEG-aldehyde undergoes reductive amination with the multiple amino groups within the protein. The protein amino groups therefore maintain their positive charge (Roberts et al., 2002; Veronese and Pasut, 2005).

These methods allowed non-selective conjugation of PEG to protein and resulted in heterogenous mixtures of PEG isomers. This heterogeneity is problematic for the following reasons; i) there is no control over the site(s) of conjugation, ii) there is no control over the amount of PEG conjugation and iii) this results in batch-to-batch variability, complicating purification and characterisation steps (Pasut and Veronese, 2012; Pisal et al., 2010). Further, for regulatory approval, full disclosure of the composition and evidence of process reproducibility are required, which is difficult for random conjugation strategies. Nevertheless, there are many examples of PEG-protein conjugates prepared by these non-specific acylation and alkylation routes that have achieved clinical approval, such as Adagen® and Oncaspar® (Table 1–2).

- Site-specific PEGylation

To prepare more homogenous products, site-specific techniques were developed where theoretically the final product should be easier to characterise and purify. Furthermore the activity should be more uniform with a homogenous product. Kinstler and colleagues developed one such approach using PEG aldehyde conjugation, which takes advantage of different pKa values at the N-terminal α-amino acid residues (7.6-8) or ε-amino group of lysine's (9.3-9.5) (Kinstler et al., 2002). This approach has been successful in producing monoPEGylated G-CSF conjugates in high yields (92%) (Kinstler et al., 2002). There are several challenges

with this approach, i) to find the optimum pH for conjugation and maintaining the pH throughout the process, ii) this approach may not be suitable for conjugation to all proteins due to the limited pH range required for conjugation. Nevertheless this approach has successfully prepared the FDA approved Neulasta® (Table 1–2) (Piedmonte and Treuheit, 2008).

Another well-known alternative site-specific approach is the PEGylation of thiol groups. In native proteins, 'free' cysteine's (i.e. cystine residues not involved in disulfide bonds) are rare (Doherty et al., 2005); therefore free cysteine's often have to be genetically introduced for thiol-reactive maleimide or vinyl sulfone activated PEGylation. However, engineering in an uncoupled cysteine into a protein sequence is time consuming and technically challenging as disulfide coupling or scrambling during the refolding or purification process. Further the yield of the recombinant protein could be reduced due to protein dimerisation occurring from the introduction of unpaired cysteine residues. Advantageously, the site of the genetically introduced cysteine can be selected away from the receptor-binding site in order to retain high bioactivity (Doherty et al., 2005).

This approach has demonstrated with Fab fragments as cysteine residues within the hinge region are far away from the receptor-binding region (Figure 1-3). This cysteine conjugation approach has prepared FDA approved Cimzia® (Table 1–2). A chemical-recombinant approach was taken whereby an anti-TNF Fab' was engineered to lack its interchain disulfide bond. The interchain disulfide was reduced prior to PEGylation using mild reducing agents. The final 40 kDa branched PEG-anti-TNF Fab' was devoid of a disulfide bond as the cysteine residues where conjugated to by PEG-maleimide. Humphreys and colleagues have shown Fab' devoid of a disulfide bond retained thermal stability and retained a normal PK profile (Humphreys et al., 2007). However, the main limitation with PEG-maleimide is instability whereby the reagents are labile to hydrolysis *in vivo* (Alley et al., 2008) and can undergo exchange reactions with thiol-reactive constituents in plasma (Shen et al., 2012).

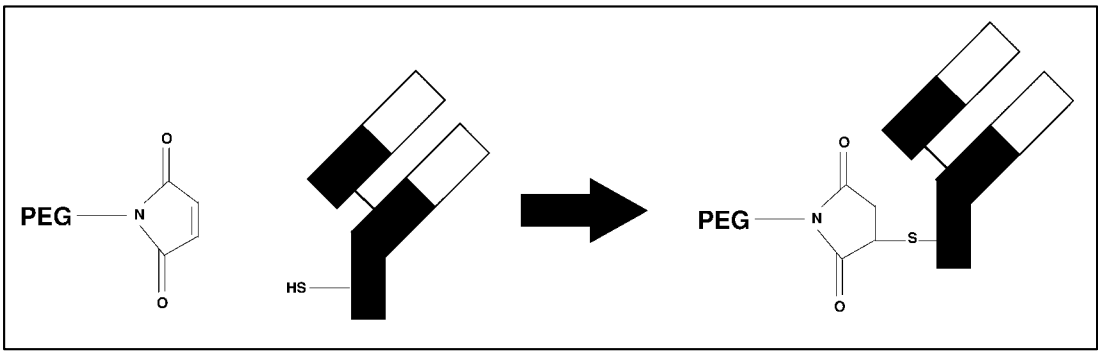

Figure 1-3. PEG maleimide conjugation to the cysteine residues of Fab'. Anti-TNF Fab' was engineered to lack the interchain disulfide and was conjugated to by a 40 kDa branched PEG-maleimide away from the receptor binding region.

How PEG modulates PK-PD

PEG is highly hydrophilic and is thought to bind to 2-3 water molecules per ethylene oxide unit. PEG is also a flexible random coiled molecule, so in water it is 5-10 times larger in solution than would be expected for a protein of the same MW. This has been confirmed by size exclusion chromatography and gel electrophoresis (Roberts et al., 2002). Therefore, when PEG is conjugated to a protein, the MW and apparent Stokes radius are increased compared to the unconjugated protein, thus extending the half-life of the protein by reducing glomerular filtration. Jorgensen and Moller have shown a direct correlation between the MW of the conjugated PEG and the half-life of the PEG-protein conjugate (Jorgensen and Moller, 1979). This has also been observed with different PEG MWs and conformations (branched vs. linear structures) with Fab fragments (Chapman et al., 1999). Interestingly, Fee found no difference in the hydrodynamic volume or viscosity radii of linear or branched PEGylated-proteins (Fee, 2007). Suggesting the longer *in vivo* half-life achieved for branched PEGylated proteins is most likely due to the PEG masking the protein surface with greater effect when compared to linear PEGs (Fee, 2007).

By increasing the overall hydrodynamic volume, protein PEGylation can reduce side effects by sustaining serum concentrations. This is well documented in the example of Hepatitis C virus (HCV) treatment where 12 kDa linear PEG-IFN α-2b (PEG-INTRON®) and 40 kDa (2× 20 kDa) branched PEG IFN α-2a (PEGASYS®) (Table 1–2) are now first line treatments when used in conjunction with ribavirin (Luxon et al., 2002a). IFN α-2b has a half-life of 7-9 h and is undetectable in the blood after 24 h (Figure 1-4) this fluctuation in effective IFN concentration may cause failure of viral suppression since HCV has a short plasma half-life and has a high turnover (Thomas et al., 1999). By conjugation to PEG,

thereby increasing the MW, PEG-INTRON® showed sustained efficacious concentration for 48-72 h, whilst PEGASYS® showed sustained concentration for up to 96 h (Table 1–3) (Glue et al., 2000; Luxon et al., 2002a). Both PEGylated IFNs were shown to be safe and well tolerated in patients, supporting once-weekly administration (Foster, 2010; Glue et al., 2000). Constant serum concentrations of the PEGylated IFNs reduced the side-effects caused by the peak and troughs caused by multiple dosing (Figure 1-4), furthermore, sustained PEG-IFN concentrations will prevent viral rebound and continued viral replication (Harris et al., 2001).

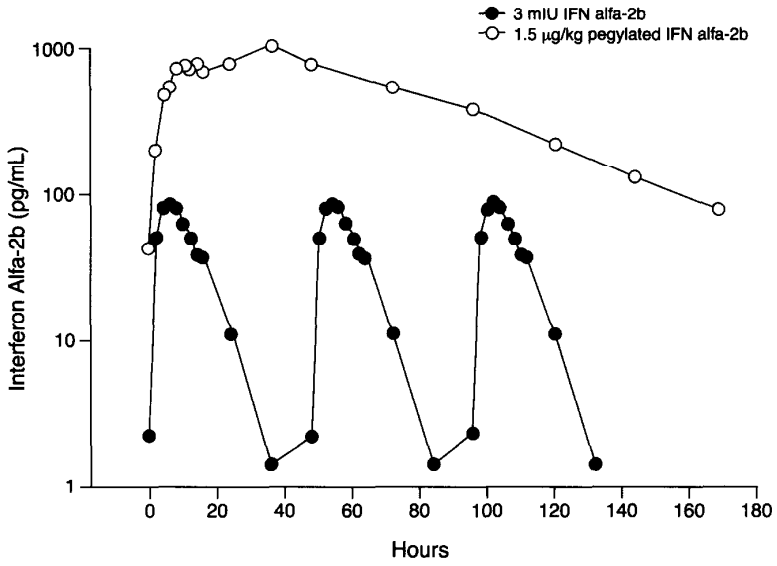

Figure 1-4. IFN α-2b (1.5 μg/ kg, SC) and PEG_{12}-IFN α-2b (3 mIU (1 IU=3.864 pg), SC) concentration-time profiles after 4 weeks of treatment. The second and third curves of IFN α-2b were superimposed on the first curve to represent sampling over 36 hours (Glue et al., 2000; Luxon et al., 2002a).

As stated previously, PEG-positional isomers arise with random PEGylation strategies such as PEGylation directed at nucleophilic groups, typically the ε-amino group of lysine or the α-amino group of the N-terminal residue. This PEGylation strategy was used by PEG-INTRON® and PEGASYS®. Both PEG-INTRON® and PEGASYS® are a mixture of PEG-positional isomers where the average antiviral activity is 28% and 7% respectively (Figure 1-4). Approximately 50% of the PEG molecules in PEG-INTRON® are attached to histidine-34, with the remaining PEG molecules attached to other amino acids, namely lysine residues (Lys^{121}, Lys^{31}, Lys^{83}, Lys^{134}, Lys^{131}) and the N-terminal cysteine residue (Cys^{1}) (Foser et al., 2003) (Table 1–3). However, even though predominant activity of PEG-INTRON is due to the PEG-H^{34} bond, the PEG-H^{34} bond is unstable in solution. The PEG-H^{34} bond

undergoes hydrolysis in aqueous solution resulting in the de-conjugation of the PEG from the protein (Pedder, 2003; Wang et al., 2000). This inherent instability of PEG-H^{34} bond contributes to the relatively short-half-life of PEG-INTRON® (Pedder, 2003).

Interestingly, the specific activity of PEGylated proteins is primarily affected by two factors; namely i) the MW of PEG and ii) the site of PEGylation. This is well demonstrated with PEG-INTRON® and PEGASYS®, where PEG-INTRON® is conjugated to a 12 kDa PEG and retains more activity than its counterpart, PEGASYS® which has an average MW of 40 kDa and only retains 7% activity (Figure 1-4). However, PEGASYS® has a longer systemic half-life, than PEG-INTRON® due to the larger PEG size. The site of PEGylation is important as conjugation near or at the binding site can drastically reduce activity, this is demonstrated with H^{34} which retained 34% activity compared to Lys^{121} which retained 9% activity of IFN (Table 1–3) (Foser et al., 2003; Grace et al., 2001). Whilst site-specific attachment of PEG to Fab fragments at the hinge region increased the *in vivo* half-life of the Fab fragments without loss of antigen binding affinity (Chapman et al., 1999). Suggesting site-specific PEGylation does not affect the activity of Fabs and is independent of PEG size, yet it can be observed with the PEG-Fab conjugates *in vivo* half-life is directly proportional to PEG size (Chapman et al., 1999). However it can be observed that the PEG sizes utilised in the study were of equivalent MWs or smaller than the Fab. It would be interesting to understand the effect of PEG on the protein activity with larger PEG MWs. For example, with PEGASYS® a 40 kDa PEG has been conjugated to a 20 kDa protein, and the resulting activity was 7%, would this be the same with site-specific conjugation.

Table 1–3. Biochemical and biological characterisation of PEG-INTRON® and PEGASYS®, adapted from (Bailon et al., 2001; Foser et al., 2003; Luxon et al., 2002a; Wang et al., 2002).

Characteristic	PEG-INTRON®	PEGASYS®
IFN isotype	IFN α-2b	IFN α-2a
PEG molecule	12 kDa linear PEG	40 kDa (2× 20 kDa) branched PEG
Positional isomers	His^{34} (> 50%); Cys^{1} (~13%); Lys^{121} (~7%), Lys^{31} (~5%); Lys^{49} (~5%); remaining 20% consists of Lys^{83}, Lys^{112}, Lys^{164}, Lys^{131}, Lys^{134}, His^{7}, Tyr^{129}, Ser^{163}	Lys^{31}, Lys121, Lys131, Lys134, reaming 6%: Lys^{164}, Lys^{70}, Lys^{83}, Lys^{49}, Lys^{112}

Antiviral activity	28% for mixture; 34% for His^{34} isomer	7% for mixture;

PEG is a common method for reducing the renal clearance of proteins but PEG can also reduce the enzymatic degradation of proteins by increased steric bulk (Veronese and Pasut, 2005). The toxicology of PEG has also been extensively reviewed (Fruijtier-Pölloth, 2005), and PEG is generally regarded as having a little toxicity (Webster et al., 2007). PEG has been shown to be eliminated from the body by either the kidneys (PEG MW < 30 kDa) or more slowly in faeces (PEG MW > 20 kDa) (Yamaoka et al., 1994). Some accumulation of PEG has been reported in the kidneys of animal models, this led to renal tubular vacuolation when PEG was given in high concentrations (Bendele et al., 1998). However the doses used in this study where far beyond that of typical therapeutic concentrations and the effects resolved after treatment finished. PEG is generally considered as weakly immunogenic. Since the 1990s, many patients have been administered with PEGylated proteins and little has been reported in literature regarding the clinical consequences of renal vacuolation. Further, the clinical doses administered to patients are much lower than those administered animal studies.

A new generation of degradable polymers are now being investigated as a possible alternatives to non-degradable polymers, such as PEG, to address possible toxicity, renal tubular vacuolation and anti-PEG antibodies (Bendele et al., 1998; Richter and Åkerblom, 1983, 1984). These new degradable biopolymers have been extensively reviewed and include HEPylation (heparosan polymer), HAPylation (homoaminoacid), PASylation (proline-alanine-serine repeats), polysialylation (polysialic acid) and HESylation (hydroxyethyl starch) (Chen et al., 2011). Alternative common polymeric delivery approaches include Polyglutamic acid (PGA), N-(2-hydroxypropyl)methacrylamide copolymer (HPMA), protein grafted copolymers PGC™ (Pasut and Veronese, 2007; Pisal et al., 2010). The majority of these new biodegradable biopolymers are within the preclinical phase. Degradable polymers are designed to be are stable when travelling to the site of action, but are degraded by intracellular degradation, by lysosomal thiol-dependent proteases or by pH dependent hydrolysis, for example PGA-paclitaxel (XYOTAX™) (Vicent and Duncan, 2006).

1.2.1.2 Glycosylation

Introduction to Glycosylation

Glycosylation represents the most widespread post-translational modification of proteins. The other main examples being; acetylation, amidation, γ-carboxylation and β-hydroxylation, disulfide bond formation, phosphorylation, proteolytic processing and sulfation (Walsh and Jefferis, 2006). Glycosylation is the addition of sugars, which can be attached by *in situ* chemical reactions or by site-directed mutagenesis. Protein glycosylation by site-directed mutagenesis is generally by N-linked or O-linked oligosaccharides. O-linked glycosylation occurs at the later stage of protein processing, where N-acetylgalactosamine (GalNAc) is linked to a hydroxyl group, notably serine or threonine residues of a polypeptide (Figure 1-5) (Bause and Lehle, 1979; Kontermann, 2011). Whereas N-linked glycosylation typically occurs in the lumen of endoplasmic reticulum and is the addition of N-acetylglucosamine (GlcNAc) to the reducing terminal of a polypeptide at the asparagine (Asn) residue (Figure 1-5) (Kontermann, 2011; Pless and Lennarz, 1977).

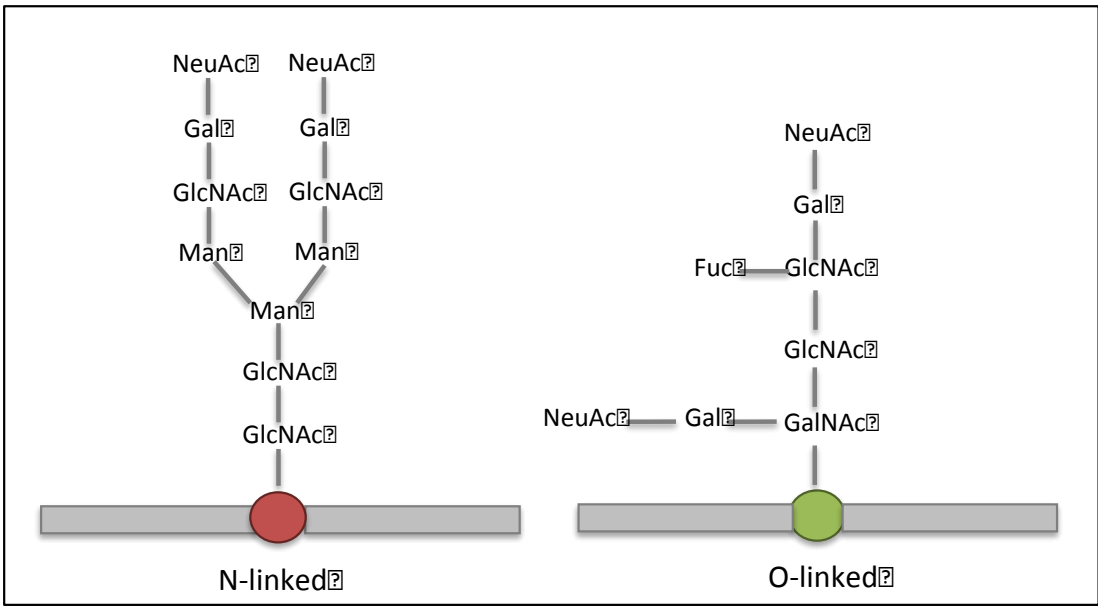

Figure 1-5. The addition of sugars to glycoproteins occurs at N-glycosidic linkages specifically N-acetylglucosamine (GlcNAc) linked to asparagine with N-linked glycosylation and N-acetylgalactosamine (GalNAc) linked to serine or threonine for O-linked glycosylation. This cellular process is dynamic and is directed by a set of glycosyltransferases, where their expression; topology and combined specificities control the glycan structures prepared. The examples outlined are usually prepared in mammalian cells.

How does glycosylation improve therapeutic proteins?

Approximately one third of biopharmaceuticals are glycosylated proteins and includes the following therapeutic protein classes; blood factors, anticoagulants,

thrombolytics, antibodies, hormones, EPO, GCSFs and IFN to name just a few (Walsh and Jefferis, 2006). These approved glycoproteins are a heterogenous mixture of glycoforms, which arise from several oligosaccharides at different N- or O-glycosylation sites. To prepare a consistent glycoform profile for therapeutic proteins still remains a challenge for the biopharmaceutical industry (Walsh and Jefferis, 2006). Additionally, producing glycoproteins within host-expression systems (e.g. CHO, NS0 or BHK) is technically challenging not only due to the intrinsically complex nature of glycan structures but also because of low glycoprotein expression yields (Solá and Griebenow, 2010).

As previously discussed with PEGylation, the attachment site of the carbohydrate is of the upmost importance. For example, if the glycosylation site is near or within the receptor binding site this could drastically reduce the activity or binding affinity of the therapeutic protein, however if the glycosylation is within an immunodominant epitope, this is advantageous as this could reduce the immunogenicity of the protein (Pisal et al., 2010). Similarly to PEGylation, glycosylation appears to modulate the *in vivo* efficacy of therapeutic proteins by altering their potency (PD) and exposure time (PK) (Solá and Griebenow, 2010). It has been reported that increased sialic acid and glycan contents within glycoproteins correlates within increased resistance times and that the naturally glycosylated proteins with sialic acid terminals have longer half-lives than partially or non-glycosylated proteins (Byrne et al., 2007) .

The first marketed glycosylated product was Aranesp® (darbepoetin α), a hyperglycosylated human erythropoietin (EPO) for the treatment of anaemia associated with chronic renal failure. Development studies of Aranesp® showed a direct relationship between carbohydrate content of the molecule, its serum half-life and *in vivo* biological activity. However there was an inverse relationship with its receptor binding (Egrie and Browne, 2002). Aranesp® was developed to have five hyperglycosylated sites, two more than human recombinant EPO (rHuEPO). Aranesp® was found to have a three-fold longer half-life than rHuEPO. In spite of Aranesp® having a four-fold lower binding affinity than rHuEPO it was found to be 13-fold more potent than rHuEPO *in vivo* when injected once weekly compared to rHuEPO which was injected thrice-weekly (Egrie et al., 2003). The greater potency of Aranesp® was found to be due to additional carbohydrate content increasing the MW of EPO, thus giving Aranesp® a longer serum half-life (Egrie and Browne,

2002). Hyperglycosylation can also improve the stability of therapeutic proteins and has been found to be essential for IgG-Fc effector functions (Walsh and Jefferis, 2006). Thus, glycosylation offers both challenges and opportunities in producing consistent reproducible glycosylated products with the optimum sites of glycosylation (Pisal et al., 2010; Walsh and Jefferis, 2006). Regardless, a glycoengineered mAb named obinutuzumab (Gazyva, Genentech) gained FDA approval in November 2013 for the treatment of chronic lymphocytic leukaemia. It selectively targets CD20 (Evans and Syed, 2014). Gazyva has an enhanced ADCC function whereby it can engage the CDC and induce caspase-independent programmed cell death. The combination of defucosylation (absence of fucosylated sugars) of this anti-CD20 mAb and the novel target has made Gazyva a successor to Rituximab (Ratner, 2014).

1.2.2 FcRn recycling

Conversely to increasing MW, there are two types of endogenous proteins that exhibit extended half-lives of weeks in humans. These are immunoglobulins (IgGs) and human serum albumin (HSA). HSA has a serum half-life of 19 days, whilst IgGs have a serum half-life of 3 to 4 weeks (Chen et al., 2011; Kontermann, 2011). The long serum half-lives of HSA and IgG are a consequence of a recycling process mediated by binding to the neonatal Fc receptor (Chaudhury et al., 2003; Rodewald, 1976). The expression, mechanism and the interaction between FcRn, the Fc portion of IgG and albumin has been extensively reviewed (Roopenian and Akilesh, 2007).

Approaches have been developed to take advantage of these long serum half-lives, these include fusion to Fc regions or albumin directly and fusion to albumin binding domains. Fusion proteins are designed to combine the properties of their component parts and are created by genetically fusing the genes encoding two or more different proteins or peptides (Carter, 2011). Often with fusion proteins, one protein overbears the function of the fusion protein partner.

1.2.2.1 Albumin fusion

HSA has been identified as an ideal ‘carrier’ protein for therapeutic proteins, not only because of its long serum half-life of 19 days but because HSA lacks both immunological and enzymatic functions (Chang et al., 2009a). Albumin is the most prevalent protein in the blood. Thus to exploit the albumin recycling mechanism,

high doses of the drug must be administered to compete for receptor sites. Albumin has been fused to peptides including, anti-HIV peptide (FB006M) (Xie et al., 2010), and proteins such as, antibody fragments (Smith et al., 2001), Factor IX (FIX), activated Factor VII, Factor VIII (Schulte, 2009, 2013). Albumin was fused to an anti-HIV peptide through Cys^{34}; the resulting FB006M conjugate is being investigated as a long-lasting, safe and effective HIV-1 fusion inhibitor. Interestingly, the FB006 was modified by 3-maleimidopropionic acid, which allows an irreversible reaction between maleimide (Figure 1-3) and the free thiol (Cys^{34}) to form a specific 1:1 peptide:albumin conjugate. Early pre-clinical studies have shown that the FB006M conjugate exhibited longer half-life and similar anti-HIV activity compared to the native anti-HIV peptide (Xie et al., 2010). However it is unclear how the anti-HIV peptide-albumin conjugate would be removed from circulation, as the peptide is irreversibly conjugated to albumin. Further, a therapeutic protein with such a long circulation half-life may cause an immune response.

Conversely, for the conjugation of albumin to Factor IX, Schulte describes the use of a cleavable peptide linker (Figure 1-6). The linker is cleaved at the same time as FIX being activated, thus the albumin-FIX fusion has a prolonged half-life. The albumin-FIX fusion was found to have ~50% potency compared to native FIX. The fusion was being developed and investigated as a possible treatment for haemophilia B (Schulte, 2009). However, it is unclear if the linker is stable for long-term storage, which may be required if the fusion protein is to be given as a treatment. Further, the cleaved albumin with the linker would be a cause of immunogenicity due to the presence of the linker.

Phase I clinical trials demonstrated the albumin-FIX fusion to have a 5-times longer half-life than FIX alone. In patients with haemophilia B, injections of 50 IU/kg were administered. The mean half-life of FIX-albumin fusion was 96 h. This was 5-times longer than the half-life of recombinant FIX. Due to these encouraging results a Phase II/III clinical trial is currently underway (Metzner et al., 2013).

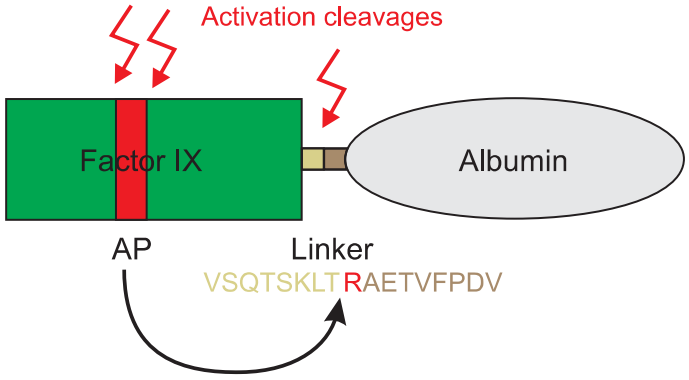

Figure 1-6. Concept of recombinant factor IX (FIX) albumin fusion protein prepared with a cleavable linker (rIX-EP). Albumin is fused to the C-terminus of FIX and the cleavable linker is inserted between FIX and albumin, thus when activated the FIX the linker is cleaved (Schulte, 2009).

The most notable albumin fusion has been Albinterferon (a HSA-Interferon α-2b fusion) which was prepared as an improved treatment for Hepatitis C. Albinterferon was composed of recombinant human albumin fused at its C-terminus to the N-terminus of IFN α (Osborn et al., 2002). Albinterferon was prepared using a genetically modified yeast strain and purified using anion, cation and semi affinity chromatography (Osborn et al., 2002; Yeh et al., 1992). It was hoped that Albinterferon would reduce dosing, thus improve patient compliance, and improve patient response to treatment. Additionally, by maintaining a constant drug concentration for a sustained period of time it was anticipated that a reduced toxicity would be observed in patients treated with Albinterferon, which had been associated with peak plasma concentrations of Interferon α and PEGylated-Interferon α (Ahad et al., 2009; Osborn et al., 2002).

In phase II clinical trials, Albinterferon was given subcutaneously and achieved a half-life of 90 h, which was 3× greater than PEG-INTRON® (30-34 h) and 18× greater than Interferon α-2b (5 h) (Osborn et al., 2002). In Phase III clinical trials, Albinterferon could be detected in blood plasma for >7 days after a single dose, supporting the administration of every 2-4 weeks (Chang et al., 2009a; Osborn et al., 2002). However, development of Albinterferon was stopped in October 2010, due to concern over dosing at 900 µg every 2 weeks. The reason for the high dose compared to PEGASYS® 180 µg per week, is that Albinterferon only possessed ~1% activity compared to native Interferon α-2b (Ahad et al., 2009; Bell et al., 2008; Osborn et al., 2002). The reduced activity of Interferon α-2b within Albinterferon could be due to either; i) the close proximity of the two proteins, as HSA (~65 kDa)

could be shielding the active site of Interferon α-2b (~20 kDa) (Figure 1-7), ii) the large size of Albinterferon (85.7 kDa) impedes the binding of Interferon α-2b to the IFNAR1/AR2 receptor (Osborn et al., 2002). Therefore, the main challenge of protein fusion is the maintenance of functional activity of the therapeutic proteins within the fusion. While linkers can be used and the orientation of the fused genes optimised to retain the biological activity, the presence of albumin can interfere with the interaction between the protein and its target(s) (Metzner et al., 2012). Secondly, minimising the risk of toxicity and immunogenicity could be an issue for new fusion partners (Subramanian et al., 2007). Thirdly, it has also been shown that predicting the *in vivo* half-lives of albumin fusion proteins may be difficult. As Andersen and colleagues have shown that there is cross-species differences in the binding of albumin fusions to the FcRn (Andersen et al., 2013). However, the application of albumin is limited to increasing the half-life and stability of proteins and does not have any secondary function, unlike Fc fusion, which does not only increase half-life but also has a cytotoxicity function (Metzner et al., 2012).

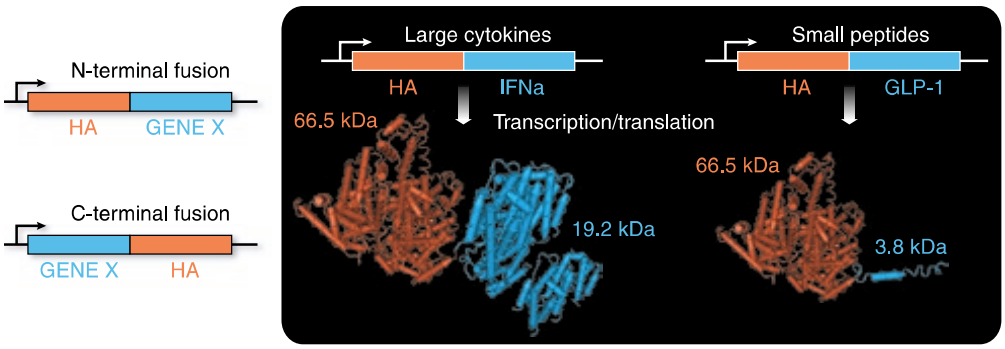

Figure 1-7. Albumin fusion to (left) cytokines and (right) to peptides by fusion of the proteins cDNA at either the N- or C-terminal of human albumin (arrows indicating transcription initiation) (Subramanian et al., 2007). (left) Human albumin is fused with IFN α-2b, 19.2 kDa and (right) human albumin is fused to glucagon-like peptide 1 (GLP-1, 3.8 kDa), demonstrating the varying sizes of biological molecules which haven been fused to albumin.

1.2.2.2 Fusion to Albumin binding domains

An alternative to albumin fusion is the preparation of therapeutic proteins or peptides that have albumin-binding domains (ABD). These ABDs bind to circulating serum albumin upon administration, thus extending the half-life of the therapeutic protein. Three high affinity ABDs are found naturally in certain streptococcus strains of protein G, of which albumin-binding domain 3 (ABD3) has been extensively studied (Akerström et al., 1987; Kraulis et al., 1996). Stork and colleagues genetically fused

ABD3 to bispecific single chain diabodies (scDb). Recombinant scDb's are composed of the variable heavy and light chain domains of two antibodies joined by three linkers as V_HA-V_LB-V_HB-V_LA (Kontermann, 2005). The scDb was developed to re-target cytotoxic T cells to CEA-expressing tumour cells (Stork et al., 2007). This scDb-ABD3 fusion protein showed a 5 to 6 fold improvement in circulation half-life, however a 3-fold reduction in activity compared to scDb. The activity was further reduced (4-fold) when ABD-scDb was bound to albumin (Stork et al., 2007).

Interestingly, it has been reported that increased ABD affinity to albumin or increasing the number of ABDs attached to scDb does not influence half-life (Hopp et al., 2010). The affinity for FcRn has been found to dictate the recycling and thus the half-life of both IgG and albumin (Hopp et al., 2010). Streptococcal ABD domains have been reported to cause immunogenicity in mice, so would be expected to pose a risk of being immunogenic in humans (Libon et al., 1999). Furthermore, increased antibody responses have been reported in ABD-fusions (Sjölander et al., 1997). Thus for ABD fusions to make successful therapeutics, the risk of immunogenicity would have to be greatly reduced. To determine accurate *in vitro* activity of ABD-fusions, accurate activity should be determined once the ABD is bound to albumin, as this will be the final product once administered. Reduced activity of the peptide or protein could be due to, i) site of ABD attachment being near or on the receptor binding site; ii) the large size of albumin and the ABD, impeding the ability of the peptide or protein to bind to its receptor.

1.2.2.3 Protein fusion to IgG or the Fc domain

The most clinically successful fusion protein therapeutics are Fc fusions with currently 10 Fc-fusions FDA approved (Table 1–4). The top selling Fc fusion is Enbrel® (50 mg/week dose) (Table 1–4), a TNF-Fc fusion for the treatment of rheumatoid arthritis (Carter, 2011; Spencer-Green, 2000). Global sales of Enbrel® in 2012 were USD $7.3 billion, exceeding the most successful therapeutic, bevacizumab (USD $6.9 billion) (Beck and Reichert, 2011). With this success, Fc-fusions represent 20% of all antibody-based medicines with FDA approval (Czajkowsky et al., 2012). Other Fc fusions include; Alprolix® (50 IU/kg/week) (coagulation factor IX-Fc fusion) which was approved in March 2014 for treatment of Haemophilia B (Shapiro et al., 2012) and Nplate® (thrombopoietin receptor

agonist-Fc fusion) (1 μg/kg/week), the first peptide-Fc fusion for the treatment of thrombocytopenia (Cines et al., 2008).

As previously discussed, the presence of the Fc-domain can increase the half-life of fused therapeutic proteins by binding to the salvage FcRn receptor (Carter, 2011; Roopenian and Akilesh, 2007) and reduces renal clearance for larger sized therapeutic proteins (Kontermann, 2011). Alprolix® (Table 1–4) for example has a half-life of 56 h, this is ~3-fold longer than the reported half-life (~18 h) of recombinant factor IX and due to this reduces the number of injections required for effective hemeostasis and controls breakthrough bleeds in patients (Shapiro et al., 2012).

An additional benefit is that the Fc domain folds independently, thus can improve the stability and solubility of a fusion protein both *in vivo* and *in vitro* (Czajkowsky et al., 2012). Whilst from a manufacturing perspective, the addition of an Fc domain allows for cost-effective purification by either protein A or G chromatography, thus leading to an easy scale-up process (Carter, 2011). Effector functions can be modified by engineering the Fc region, either to improve or reduce binding to Fc γ receptors (FcγRs) for antibody-dependent cellular cytotoxicity (ADCC) or complement receptors for cell mediated cytotoxicity (CDC) or FcRn for prolonged half-life (Kubota et al., 2009; Vincent and Zurini, 2012). Xencor uses the Fc region to improve the ADCC and CDC effector functions. The companies most advanced product is XmAb®5574 (MOR208), which targets CD19 for the treatment of B-cell lymphoblastic leukaemia and NHL (Evans and Syed, 2014). However, Fc-fusions still face the issues of insufficient efficacy and high cost of the therapeutic agent (Kubota et al., 2009).

Table 1–4: Marketed Fc-fusion protein therapeutics, adapted from (Czajkowsky et al., 2012)

Trade name (generic name)	Active fused to FC of IgG1	Indication	Company	Date of FDA approval
Alprolix™ (eftrenonacog alfa)	Factor IX	Haemophilia B	Biogen Idec	2014
Eloctate™	Factor VIII	Hemophilia A	Biogen Idec	2014
Zaltrap® (ziv-afilbercept)	VEGFR1/VEGFR2[7]	Colorectal cancer	Regeneron Pharmaceuticals	2012
Nulojix® (belatacept)	CTLA-4[8]	Organ rejection	Bristol-Myers Squibb	2011
Eylea® (aflibercept)	VEGFR1/ VEGFR2	Age related macular degeneration	Regeneron Pharmaceuticals	2011
Arcalyst® (rilonacept)	IL-1R[9]	Cryopin-associated periodic syndromes	Regeneron Pharmaceuticals	2008
Nplate® (romiplostim)	Thrombopoietin-binding peptide	Thrombocytopenia	Amgen/ Pfizer	2008
Orencia® (abatacept)	Mutated CTLA-4	Rheumatoid arthritis	Bristol-Myers Squibb	2005
Amevive® (alefacept)	LFA-3[10]	Psoriasis and transplant rejection	Astellas Pharma	2003
Enbrel® (etancept)	TNFR[11]	Rheumatoid arthritis	Amgen/ Pfizer	1998

1.3 Multifunctional proteins as 'next generation of protein therapeutics'

Next generation protein therapeutics aim to improve upon first and second generation biopharmaceuticals by having enhanced efficacy, greater safety and improved delivery (Carter, 2006; Kobsa and Saltzman, 2008). The majority of these 'next generation protein therapeutics' are multifunctional in design reflecting the complex diseases such as cancer or inflammatory disorders they are aimed at treating. Discussed in this section are the different strategies being investigated to develop multifunctional protein therapeutics.

[7] Vascular endothelial growth factor receptors-1/-2
[8] Cytotoxic T-lymphocyte-associated protein 4
[9] Interleukin-1 receptor
[10] Lymphocyte function-associated antigen 3
[11] Tumour necrosis factor receptor

1.3.1 Bispecific antibodies

Monoclonal antibodies (mAbs) have high affinity for one target however, they are only able to target a single antigen, this is a limitation when treating complex inflammatory diseases they may have several proinflammatory cytokines. Multiple targets or sites can be targeted to improve therapeutic efficacy in two ways, i) combination therapy of mAbs or other therapeutic agents or ii) creating bispecific antibodies or therapeutic agents. Success in combinational therapy has been achieved with bevacizumab and interferon α for the treatment of renal cell carcinoma (Rini et al., 2008). Where propinquity has been exploited.

Thus dual targeting within one therapeutic agent is being investigated with numerous strategies which have been extensively reviewed (Kontermann, 2012). The most clinically advanced strategy has been bispecific antibodies (bsMAb), where Removab® is FDA approved and there are many more in clinical trials (Chames and Baty, 2009). Currently there are two approaches in the production of bsMAbs; i) the fusion of two hybridoma cell lines creating a single 'quadroma' cell lines, this is a time consuming and difficult process and ii) the chemical coupling or genetic fusion of two Fab fragments. Chemical conjugation strategies are still in development, with no clinical examples yet. Bifunctional reagents such as 5,5'-dithiobis(2-nitrobenzoic acid) (Paulus, 1985) or o-phenylenedimelimide (Glennie et al., 1987) have been described to generate bsMAbs. Further, a PEG di(*bis*)sulfone **4** reagent has also been described in the conjugation of two different antigen binding fragments, to generate an anti-VEGF bispecific Fab'_2 molecule (Fab-PEG-Fab') (Khalili et al., 2013). The anti-VEGF Fab-PEG-Fab' were found to display anti-angiogenic properties comparable to or better than bevacizumab, suggesting that chemical-linkers can be used to conjugate proteins together without impeding the biological activity of the protein (Khalili et al., 2013).

Along with a long serum half-life, bispecific antibodies can bind to two adjacent targets or they can cross-link two different antigens. BsMAbs hold great promise as therapeutic agents for cancer either; i) in the recruitment of cytotoxic T cells or, ii) to effectively target tumour-associated antigens and deliver a cytotoxic payload to tumour cells (Chapman et al., 1999). Removab®, a mouse CD3-human EpCAM bispecific, was approved in 2009 for the treatment of malignant ascites (MA) due to epithelial carcinoma. One side of the antigen binding site binds to T

cells via CD3, the other side binds tumour cells via EpCAM antigen (Figure 1-8). While, the Fc region adds a third functional binding site capable of binding and activate Fcγ receptor I-, IIa or III-positive accessory cells to enhance tumour killing (Figure 1-8) (Linke et al., 2010). Removab® kills EpCAM positive tumour cells in the peritoneal cavity, which cause MAs, whilst leaving healthy cells alive, since the peritoneum lack EpCAM. Further, Removab® enhances the activation of the patients own immune system against the tumour (Linke et al., 2010). Malignant ascites as associated with ovarian cancer, gastrointestinal malignancies the prognosis of patients with MA is approximately 1-6 months (Seimetz, 2011). In phase III clinical trials, Removab® was found to improve the patients puncture free survival to 44 days compared to 15 days in the control group. Puncture-free survival was defined as the time to the next therapeutic puncture or time to death (Linke et al., 2010).

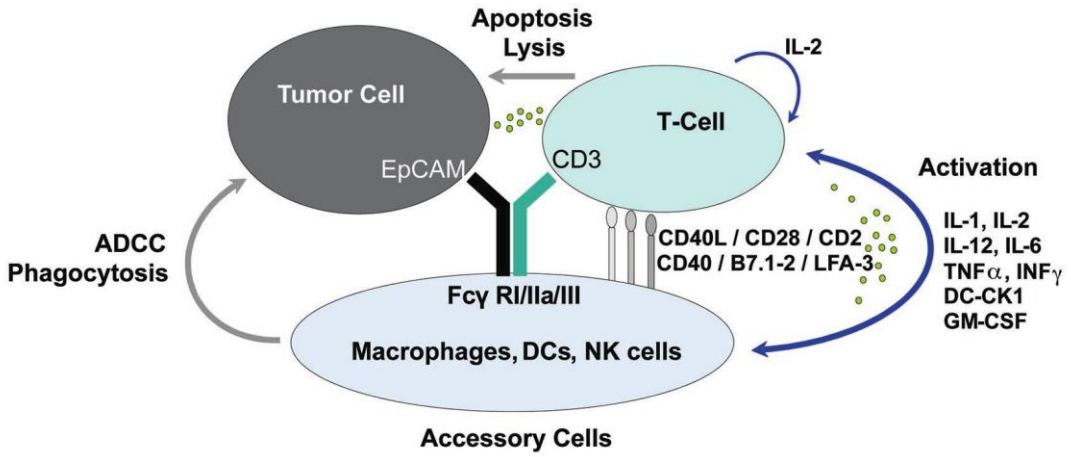

Figure 1-8. Mechanism of action of Removab®, where the intact trifunctional antibody Removab® accelerates the recognition and destruction of tumour cells by different immune cells. ADCC, antibody-dependent cellular toxicity; DC-CK1, dendritic cell cytokine 1; IL, interleukin; IFN γ, interferon gamma; TNF α, tumour necrosis factor alpha; LFA, lymphocyte function antigen; NK, natural killer; GM-CSF, granulocyte monocyte colony stimulating factor (Linke et al., 2010).

However, the major challenge with bsMAbs is to prepare them in sufficient quantity and purity to meet clinical needs (Presta, 2003). Bispecific antibodies in advanced clinical trials include Merrimack's MM-111, targeting HER2 and HER3 receptors on breast cancer cells and Trion's Lymphomun/fBTA05, which targets CD20 on lymphoma cells and CD3 on T cells to treat B cell lymphoma (Chames and Baty, 2009; McDonagh et al., 2012). In July 2014, Amgen received FDA 'breakthrough Therapy Designation' for its BiTE antibody blinatumomab which binds on T cells and CD19 which target lymphoma cells to treat acute lymphoblastic leukaemia (Davis, 2014).

1.3.2 Antibody Drug Conjugates (ADCs)

Monoclonal antibodies (mAbs) are successful therapeutics with over 20 therapeutic mAbs on the market (Wang et al., 2008). Monoclonal antibodies are successful due to their site-selectivity, where they can bind or inhibit the functions of target antigens such as trastuzumab (Herceptin®) selectively binding HER2/neu and bevacizumab (Avastin®) selectively binding VEGF (Panowksi et al., 2014). To increase the functionality of mAbs against tumour cells, there is extensive research in 'arming' mAbs with cytokines (immunocytokines), drugs (ADCs) or radionucleotides (Wu and Senter, 2005). Alone cytotoxic drugs often display substantial toxicity, as they are not site-selective. Thus ADCs, a concept that dates back to the 1970s, hold great promise as 'the magic bullets' against cancer (Panowksi et al., 2014). As ADCs combine the site-selectivity of mAbs with the cell killing ability of cytotoxic agents creating an efficient therapeutic with reduced systemic toxicity (Alley et al., 2010; Casi and Neri, 2012; Sievers and Senter, 2013).

Even though the concept of ADCs has been around since the 1970s, only now are advances being made in producing them successfully. For example, gemtuzumab ozogamicin (Mylotarg®), an anti-CD33 humanised antibody conjugated to highly potent calicheamicin derivative was granted accelerated approved by the FDA in 2000 for the treatment of acute myeloid leukaemia (Sievers and Linenberger, 2001). However, Mylotarg® was later withdrawn from the market after safety concerns and clinical benefit. The mAb-drug linker was found to be unstable where 50% of the bound drug was released in 48 h (Ravandi, 2011).

Over the last decade the understanding of factors to prepare efficacious ADCs has improved. For example, site-specific conjugation chemistry has seen recent advancements, which have been implemented resulting in homogenous ADC production and improved PK properties of ADCs. To reduce immunogenicity, now humanised or recombinant human mAbs are used, rather than chimeric or murine versions. Further, the understanding of crucial factors such as antigen selection, antibody, linker and payload has improved, enabling efficacious ADCs to be prepared (Panowksi et al., 2014). There are three key components to an ADC, which need substantial optimisation these are the mAb (and related antigen target), linker and cytotoxic drug (Figure 1-9) (Alley et al., 2010).

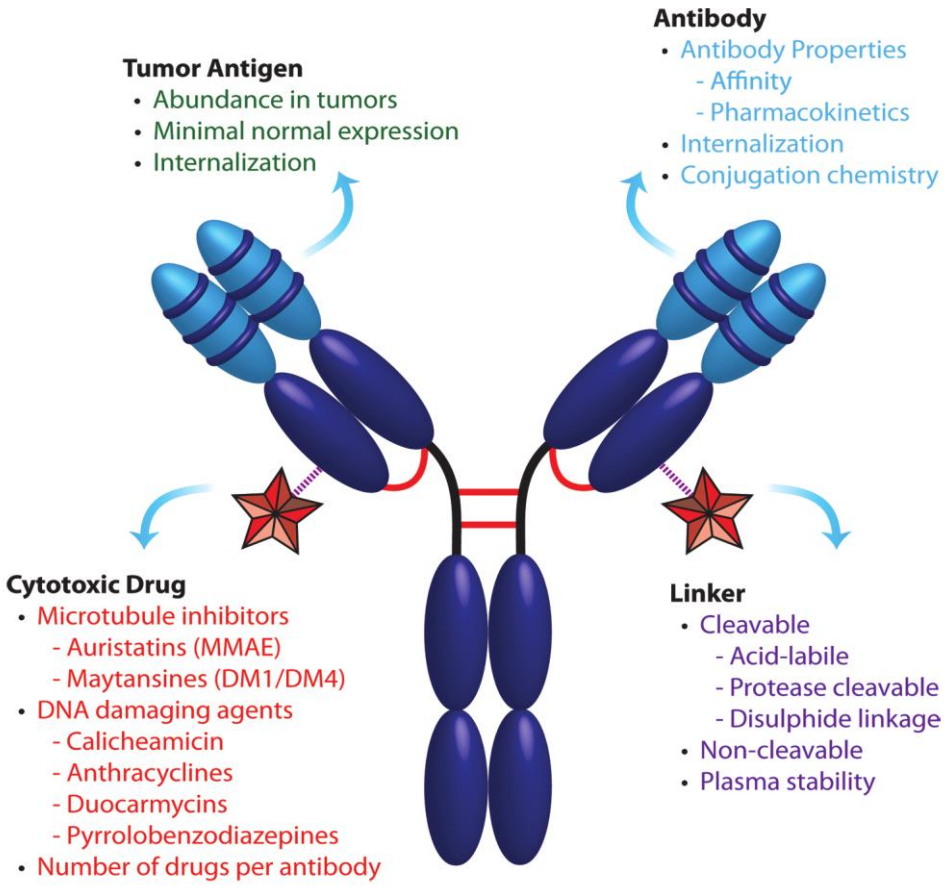

Figure 1-9. Critical parameters that influence ADC therapeutics (Panowksi et al., 2014). ADCs are made up of a mAb conjugates to a cytotoxic drug by a linker. All the components can affect the ADC performance and thus must be optimised to ensure an efficacious ADC is prepared.

Firstly, selection of the appropriate target and complementary mAb should be made. The appropriate target is the most important contributor to the antitumour activity and tolerability of an ADC (Sievers and Senter, 2013). To improve efficacy, without compromising safety, ADCs must deliver the cytotoxic payload to tumour cells specifically expressing the antigen receptor of interest without damaging healthy cells (Sievers and Senter, 2013).

Further, the linker must be considered and with this the conjugation method (Figure 1-9). The conjugation method is influenced by the mAb chosen, as developments in genetic engineering have influenced conjugation strategies away from reduced disulfide or lysine attachment where heterogenous mixtures of ADCs are prepared. Whereas, mAbs can now be engineered with cysteine residues or unnatural amino acids, resulting in homogenous ADC production and lower drug-antibody ratios (DAR), which in turn improves ADC PK properties (Panowksi et al., 2014). As it has been shown that the number of drugs per mAb and the position of

the drugs can influence ADC aggregation, antigen binding, stability, PK, potency and tolerability (Alley et al., 2010; Senter, 2009; Sievers and Senter, 2013).

Stability of the ADC is of the upmost importance. Bifunctional linkers have been designed and used to conjugate the cytotoxic payload to the mAb and allow release the cytotoxic payload at the tumour site (Casi and Neri, 2012). Linkers should deliver the cytotoxic drug in its active form to efficiently kill the tumour cells, and avoid non-specific killing and associated toxicities (Iyer and Kadambi, 2011). ADCs are internalised through receptor-mediated endocytosis. Thus most linker mechanisms of release take advantage of this where the drug is released in the lysosomal compartment, which is rich in proteolytic enzymes and is a high reducing environment (Casi and Neri, 2012; Iyer and Kadambi, 2011). The most common cytotoxic drugs (Figure 1-9) used within ADCs are maytansinoids and auristatin. These both exert their cytotoxic effects through binding to tubulin, causing cell cycle arrest at G2/M resulting in cell apoptosis (Alley et al., 2010; Casi and Neri, 2012).

Adcetris® was FDA approved in 2011 to treat large cell and Hodgkins lymphoma and Kadcyla® was approved in 2013 to treat metastatic HER2 positive breast cancer (Table 1–5). There are many more ADCs in late stage clinical trials, such as glembatumumab vedotin, which is currently undergoing accelerated clinical trials for non-metastatic melanoma (Evans and Syed, 2014). However, ADCs are costly to manufacture and often have complex PK profiles, thus ADCs can only be justified for severe diseases and must have higher therapeutic indexes than non-targeted drugs (Casi and Neri, 2012). Nevertheless, ADCs prepared a value of $501 million (Adcetris® and Kadcyla®) in 2013 and are predicted to dominate half the market in 2021.

Table 1–5: Current FDA approved antibody-drug conjugates

Trade name (generic name)	Active agent	Indication	Company	Date of FDA approval
Kadcyla® (ado-trastuzumab-emtansine)	Anti-HER2 mAb-DM1	Metastatic breast cancer (HER2 positive)	Genentech/ Roche	2013
Adcedris® (brentuximab vedotin)	CD30 mAb-MMAE	Non-Hodgkins lymphoma	Seattle Genetics	2011

1.3.3 Protein scaffolds

Even though monoclonal antibodies are very successful with >20 mAbs having gained FDA approval, they have some limitations, which reduce their clinical effectiveness. In mouse xenograph models, mAbs directed at tumour-specific antigens were found to remain in the blood and only ~20% of the dose was found to interact with the tumour (Beckman et al., 2007). ^{125}I-labelled-IgG, F(ab')$_2$, Fab' and scFv tumour penetration and PKs have been compared in human colon carcinoma xenograph models (Yokota et al., 1992). Grain density was quantified as a function of tumour penetration. The study observed scFv demonstrated maximum tumour penetration after 6 h (1953 grains), whilst the IgG did not reach the same degree of penetration until 48-96 h (~900 grains) after injection (Yokota et al., 1992). It was also observed that the IgG (2705 grains), F(ab')$_2$ (1756 grains), Fab' (3077 grains) and scFv (5921 grains) penetration correlated in a size-related manner (Yokota et al., 1992). This highlights the main limitation with mAbs, which is there large size (~150 kDa), limiting their ability to penetrate, accumulate and distribute evenly in tissues (Wurch et al., 2012). Further, Fc portion of the IgG molecule may not be required e.g. increasing the retention of the mAb in circulation or effector functions. For example, for cancer imaging and radiotherapy applications, the ideal targeting agent would have rapid tumour penetration and rapid blood clearance.

To overcome some of these shortcomings, about 50 different protein scaffolds have been documented over the past two decades (Carter, 2011; Wurch et al., 2012). 'Protein scaffold' is the term used to describe small protein domain-based frame works which can be used a therapeutic precursors. Protein scaffolds are generally understood to have distinguishing features which may include, high protein solubility and stability, single polypeptide chain format, high bacterial expression for cheap production, lack of disulfide bonds, small MW and possibly glycosylation sites (Carter, 2011; Nuttall and Walsh, 2008). Protein scaffolds can be categorised into two groups, IgG-based scaffolds and non-IgG based scaffolds (Mintz and Crea, 2013). Further, protein scaffolds represent a novel way to overcome intellectual properties rights (Gill and Damle, 2006).

The most clinically advanced non-IgG derived protein scaffolds include Kunitz domains (Dennis and Lazarus, 1994), DARPins (Tamaskovic et al., 2012), Avimers (Silverman et al., 2005), Knottins (Moore and Cochran, 2012), Affibodies

(Feldwisch et al., 2010), Adnectins (Lipovsek, 2011), Pronectins (Mintz and Crea, 2013), Fynomers (Schlatter et al., 2012), Nanofitins (Mouratou et al., 2007) and Affilins (Table 1–6) (Ebersbach et al., 2007; Mintz and Crea, 2013). These non-IgG derived protein scaffolds have naturally rigid structures, thus their existing binding sites can be genetically modified to recognise new or different target antigens (Gebauer and Skerra, 2009). Protein scaffolds are readily expressed in microbial hosts, reflecting their high stability, solubility, simple structure and small size. Plus their small size may allow for better tissue penetration vs. larger molecules such as IgG. Additionally, multivalent and/or multispecific protein biopharmaceuticals can be prepared out of the simple protein scaffold structures (Carter, 2011). Currently the only non-IgG protein scaffold to receive FDA approval is Kalbitor® (Escallantide), a Kunitz domain that inhibits kallikrein (Farkas & Varga 2011). Kalbitor® was approved in 2009 for the treatment of hereditary angioedema (Farkas and Varga, 2011; Mintz and Crea, 2013).

Table 1–6: Summary table of the most advanced types of IgG and non-IgG derived protein scaffolds (Mintz and Crea, 2013).

Name of scaffold	Characteristics
	Non IgG derived protein scaffolds
Kunitz Domains	Engineered Kunitz domains are human serine protease inhibitors can be genetically engineered for different target protease specificities
DARPins®	Engineered single domain proteins are small and can be selected to bind to any protein target
Avimers®	Prepared from multimerised low-density lipoprotein receptor class A
Knottins	Created from cysteine-rich knottin peptides
Affibodies®	Based on Z-domain of staphylococcal protein A
Adnectins® (monobodies)	Based on 10th domain of human extracellular matrix protein fibronectin type 3
Pronectins	Based on the 14th domain of human fibronectin III
Fynomers	Derived from src-homology domain 3 of tyrosine kinase fyn
Nanofitins (formerly Affitins)	Derived from Sac7d, a dsDBA-binding protein from *Sulfolobus acidocaldarius*
Affilins	Derived from human γ-B crystalin or human ubiquitin

Name of scaffold	Characteristics
	IgG derived protein scaffolds
Single domains (dAbs®)	Variable domain of heavy chain (V_H) or light chain (V_L) containing 3 CDRs[12]
Nanobody®	Derived from camels and Illamas heavy chain only antibodies
Single-chain variable fragment (scFv)	Variable chain regions (V_H and V_L) fused together with a flexible peptide linker
Antibody-binding fragment (Fab)	Composed of variable regions (one heavy, one light) with a single antigen CDR
Avibody™	VH and VL domains linked in a head-to-tail arrangement together to form multimeric antibody like proteins
Minibody	Comprised of linked V_L-V_H-C_H3 domains
Abdurins™	Variants of CH2 domains (CH2D)
Fcab	Derived from the Fc binding domain of an antibody
Bispecific T-cell engager (BiTE)	Bispecific scFv antibody fragments composed of α-CD3/mAb variable domains
Diabody	Two scFv (V_H and V_L) linked covalently or by a small peptide linker

Small antibody derived protein scaffolds include single domain (dAbs®) (Holt et al., 2003), nanobodies®, diabody, avibodies™, scFvs, Fabs, minibodies (Hu et al., 1996), Abdurins™ (Gehlsen et al., 2012), Fcabs and BiTEs (Baeuerle and Reinhardt, 2009). These IgG-based protein scaffolds are thermally stable, have retained binding and antigenic specificity (Carter, 2011; Mintz and Crea, 2013). IgG-derived protein scaffolds can be prepared either chemically or by non-mammalian expression systems, thus incurring lower manufacturing costs compared to mAbs (Mintz and Crea, 2013). Currently, the most clinically advanced product is blinatumomab, a BiTE scaffold that is in Phase III clinical trials. Blinatumomab is for the treatment of either non-Hodgkins lymphoma and/ or acute lymphoblastic leukaemia.

Protein scaffolds may potentially elicit an anti-drug response and may be potentially immunogenic in patients, however more clinical data is required to understand the factors that contribute to immunogenicity (Carter, 2011; Gebauer and Skerra, 2009). The main limiting factor of protein scaffolds is their short serum half-life due to their small size. Further, if protein scaffolds were larger they could not compete with mAbs unless they were able to recycle via the FcRn. Current options

[12] Complementary determining regions

for extending the half-lives of protein scaffolds include PEGylation, adding a second scaffold that binds to albumin, Fc fusion or attaching half-life extending peptides (Carter, 2011; Mintz and Crea, 2013).

Single domain antibodies that recognise and bind to albumin, termed 'AlbudAbs' have been developed as genetic fusions to prolong the half-life of therapeutic proteins (Holt et al., 2008). AlbudAbs have been shown in preclinical research to extend the half-life of interleukin-1 receptor antagonist and interferon α-2b (Holt et al., 2008; Walker et al., 2010). The *in vitro* potency of AlbudAb-IFN α-2b and HSA-IFN α-2b (Albuferon®) was tested using an antiviral assay (A549-EMCV, §3.3.6.1). AlbudAb-IFN α-2b and HSA-IFN α-2b achieved activities of 3.8×10^6 IU/mg and 2.4×10^6 IU/mg respectively. Compared to the IFN standard (6.6×10^7 IU/mg), AlbudAb-IFN α-2b and HSA-IFN α-2b were calculated to have fold reduction in activity of 17.4 and 265 respectively. Specifically, AlbudAb-IFN α-2b showed an 15.8-fold higher *in vitro* potency compared to the HSA-IFN α-2b (Albuferon®) and showed a half-life of 22.6 h, which was ~1.5 times longer than that observed for HSA-IFN α-2b (Walker et al., 2010). AlbudAb-IFN α-2b and HSA-IFN α-2b were also tested *in vivo* in a melanoma xenograph model, where human tumour (518A2) cells were transplanted into SCID mice. Subcutaneous injections of PBS, AlbudAb-IFN α-2b (8.75 mg/kg) and HSA-IFN α-2b (24 mg/kg) were administered 1 and 8 days post-tumour implants (Walker et al., 2010). Even when, AlbudAb-IFN α-2b was administered at a 10-fold lower dose (on a mg/kg basis) than HSA-IFN α-2b, the level of tumour growth was comparable. This is most likely due to the greater efficacy and *in vivo* half-life of the AlbudAb fused IFN α-2b compared to HSA (Walker et al., 2010). As discussed previously (§1.2.2.1), the reduced activity of Albuferon® was most likely due to HSA shielding the active site of IFN or impeding the binding of IFN to the IFNAR1/AR2 receptor. Whereas, the use of AlbudAbs are much smaller at 11-13 kDa (Walker et al., 2010), thus do not impede the activity of IFN as drastically as HSA. However, the 'AlbudAb' must be genetically fused to the protein of interest, in this case at the N-terminus of the AlbudAb, which may be complex and time consuming to do (Walker et al., 2010).

1.3.4 Protein fusion

Protein fusions can be grouped into three categories: half-life extension, targeting (or binding) and toxicity (cell killing). Half-life extension can be achieved by albumin

binding domains or AlbudAbs, fusion to HSA or Fc-fusion (§ 1.2.2). Further transferrin fusion has also been proven to extend the half-life of therapeutic agents such as in the case with transferrin-insulin fusion for diabetes treatment (Xia et al., 2000).

The cytokine family consist of interleukins, interferons, growth factors, colony stimulating factors, chemokine's and due to their > ~20 kDa MW have short serum half-lives. Many cytokines are pleiotropic, redundant (i.e. IL-4 and IL-13) and are often secreted as a result of cell signalling. Currently, >10 engineered cytokines forms are FDA approved such as PEGASYS® (PEG-IFN α) (Chang et al., 2009a; Vazquez-Lombardi et al., 2013). There has been significant clinical interest in the antitumour effects of IFNs, IL-2, IL-4, IL-12, IL-15, IL-24, GM-CSF and TNF α, where as therapeutics these cytokines can modulate tumour cells or the immune system or both (Chang et al., 2009a; Pasche and Neri, 2012). However, severe toxicities are associated with systemic infusions of cytokines (e.g. IL-12), thus dose related toxicities limit the administered dose of cytokines (Leonard et al., 1997). To utilise cytokines effectively for cancer treatment, reduced side effects would need to be achieved in conjunction with enhancing the local concentration of cytokines at the tumour site(s) (Pasche and Neri, 2012). To achieve this, different approaches have been investigated, such as fusing cytokines to HSA (Subramanian et al., 2007), Fc to improve half-life of cytokines (Bitonti et al., 2004; Jazayeri and Carroll, 2008) and transferrin fusion for specific tumours (Chang et al., 2009a). These fusions were designed to overcome the following, relative paucity of cytokine receptors on tumour, the lack of specificity of cytokines for the tumour site and their reduced half-life. Alternatively, cytokines can be injected directly into the tumour site, this requires tumours to be accessible and visualised, yet this is not always possible with micrometastatic lesions (Forni et al., 1985).

Immunocytokines provide a novel bifunctional, tumour-targeting approach, similar to ADCs, combining the anti-tumour activity of cytokines with the binding specificity of antibodies. These fused molecules are designed to enhance the concentration of cytokines at the tumour site (List and Neri, 2013; Pasche and Neri, 2012). Antibody formats being investigated to develop immunocytokines include, Fab, $F(ab')_2$, scFv, IgG, scFv-Fc and diabodies (Chang et al., 2009a; Pasche and Neri, 2012). Diabodies are well suited for immunocytokine development because they are bivalent. The combined diabody-cytokine MW is greater than renal filtration

cut-off, therefore a longer systemic half-life can be achieved (Pasche and Neri, 2012). There are currently 7 immunocytokines in clinical development (List and Neri, 2013).

The most advanced immunocytokine in clinical development is Darleukin (L19-IL-2 fusion) in Phase IIb, for the treatment of metastatic melanoma in combination with dacarbazine (Eigentler et al., 2011). Darleukin is a diabody fusion consisting of human interleukin-1 (IL-2) fused to a scFv specific to the antigenic target site EDB fibronectin (Carnemolla, 2002). To test for targeted delivery of IL-2 to the tumour site, syngeneic mice were grafted with F9 murine teratocarcinoma. Injections (12 μg in mouse of 20 g) with the fusion proteins, L19-IL-2, an irrelevant antibody (D1.3)-IL2 and saline alone occurred on days 3, 4, 5, 6, 7, 8 (Carnemolla, 2002). Histologic analysis of the F9 tumours growth found mice treated with L19-IL2 weighed 0.05 g ± 0.01. Mice treated with D1.3-IL2 and saline had tumours, which weighed 0.597 g ± 0.1 and 0.811 g ± 0.23 (Carnemolla, 2002). Immunohistochemistry analysis of the tumours treated with L19-IL-2 had a 70 times higher lymphocyte concentration compared to mice treated with D1.3-IL-2, and a 100 times higher concentration compared to mice treated with saline. These concentration in lymphocytes, may help to explain the anticancer activity of L19-IL-2 (Carnemolla, 2002). Phase I clinical trials, 83% of patients with advanced renal cell carcinoma achieved disease stabilisation after the second dose (22.5 Mio IU/patient/day three injections/week) (Johannsen et al., 2010). The study also found that the toxicities were manageable and reversible (Johannsen et al., 2010), showing the fusion of a delivery protein e.g. scFv against EDB to a cytokine e.g. IL-2 can reduce toxicity associated with cytokines to prepare a therapeutic effect. Therefore, multifunctional proteins can be used in either; i) directing therapeutic molecules to the site of need, i.e. tumour sites or ii) where proteins are in close proximity to one-another, thus they are able to work simultaneously for a therapeutic outcome such as in the case of Darleukin.

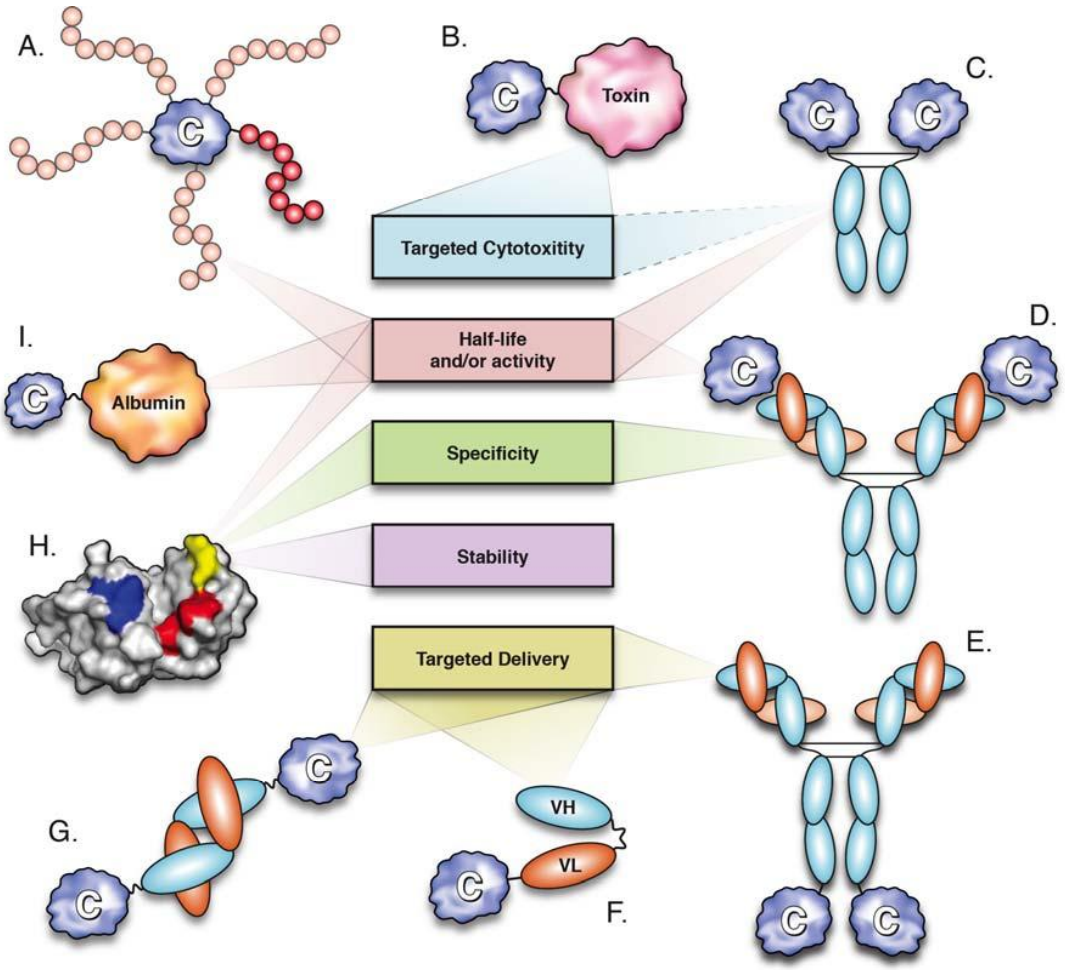

Figure 1-10. A summary of molecular engineering approaches used and their effect to improve cytokines as therapeutic agents (Vazquez-Lombardi et al., 2013). A) PEGylation (with positional isomers), B) cytokine-toxin fusion, C) cytokine-Fc fusion, D) antibody-cytokine immune complex, E-G) immunocytokines, E) cytokine-IgG, F) cytokine-scFv, cytokine-diabody, H) cytokine mutagenesis, I) cytokine-albumin fusion.

Another recombinant approach for producing novel multifunctional fusion proteins is the 'Dock-and-Lock' method. This method utilises two natural binding domains as a pair of linkers resulting in site-specific conjugation in a facile and quantitative manner (Chang et al., 2009a). The two binding domains are the dimerisation and docking domain (DDD), derived from cAMP-dependent protein kinase (PKA) and the anchor domain (AD) derived from A-kinase anchoring proteins (AKAP) (Figure 1-11). The AD and DDD peptide sequences can be fused to any protein (or other entity), once the DDD and AD are bound, they are covalently 'locked' into place by the cysteine residues which form disulfide bridges (Rossi et al., 2012) (Figure 1-11). Any AD domain can be paired with any DDD module. Further modules have included PEG, dyes, drugs, and fluorescent molecules.

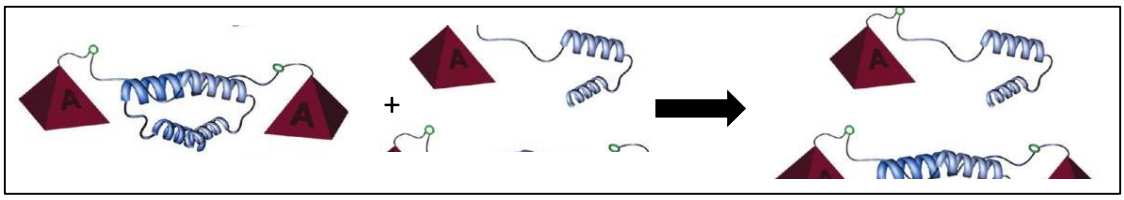

Figure 1-11. DNL method where the DDD molecule mediated protein (A) dimer e.g. Interferon, is tethered with the AD-molecule precursor (B), to prepare a DNL conjugate comprising of two copies of A and one copy of precursor B. Precursor B represents PEG, toxin or radiolabel which could be tethered to the protein dimer. Green rings indicate SH groups of the engineered cysteine residues of DDD (blue helix) and AD (yellow helix). The 'locking' disulfide bonds are depicted as interlocking green rings. Adapted from (Rossi et al., 2012).

The most reported cytokine in the DNL literature is IFN α-2b, where IFN α-2b has been included into monoPEGylated cytokine dimers (Figure 1-11) (Chang et al., 2009b), tetrameric immunocytokines (Rossi et al., 2009) and bispecific immunocytokines (Rossi et al., 2010). Chang and colleagues have prepared monoPEGylated IFN α-2b dimers with the following PEG structures and MWs, linear 20 kDa PEG, linear 30 kDa PEG and a 40 kDa branched PEG (Chang et al., 2009b) (Figure 1-11). They found that all monoPEGylated dimers retained antiviral and antiproliferative activities higher than PEGASYS® but similar or lower to PEG-INTRON®. Interestingly, the 40 kDa monoPEGylated IFN α-2b dimer is being considered for clinical evaluation as it prepared a more favourable PK, but was not as effective as PEGASYS® within the *in vivo* Daudi model, suggesting the 40 kDa monoPEGylated IFN dimer could be less toxic *in vivo* (Chang et al., 2009b).

Alternatively, IFN α-2b has been incorporated into immunocytokines using DNL, first a tetrameric immunocytokine comprised of an anti-CD20 mAb fused to four IFN α-2b as a possible B-cell lymphoma treatment (Rossi et al., 2009) and secondly, a bispecific immunocyotkine compromising of two IFN α-2b molecules, fused to anti-HLA-DR F(ab')$_2$ which is linked to veltuzumab mAb as a possible treatment for non-Hodgkin lymphoma (Rossi et al., 2010). The tetrameric IFN α-2b immunocytokine is reported to be 100 times more potent than veltuzumab or a non-targeting mAb-IFN α-2b in an IFN sensitive Daudi model. Whilst *in vitro*, the tetramer inhibited lymphoma growth at a 25-fold lower concentration of veltuzumab plus IFN α-2b. These results could be due to either the increased local tumour concentrations of IFN α-2b or that CD20 binding may inhibit the internalisation/down-regulation of IFNAR1/IFNAR2 receptors, causing prolonged and more effective IFN α-induced signalling (Rossi et al., 2009). Consequently, the

tetrameric IFN α-2b immunocytokine is now under development for CD20 targeted immunotherapy of non-Hodgkins lymphoma (Rossi et al., 2010).

However, there are two reported disadvantages with the DNL method; i) the AD and DDD peptides must be fused to the proteins of interest, this requires the establishment of two host cell lines, therefore increased production costs may be incurred; ii) the AD and DDD peptides are 'locked' together by the cysteine residues forming a disulfide bridge, however during mild redox conditions during DNL conjugation some disulfides may reduce causing some proteins to aggregate or denature along with the AD and DDD peptides (Rossi et al., 2012). However, general disadvantages encountered with producing multifunctional fusion proteins, such as with DNL include; i) in some cases fusion partners may have incompatible manufacturing properties, resulting in protein aggregation or misfolding of one of the fusion proteins, whilst the other partner may be unharmed; ii) the functionality such as activity, affinity may be severely inhibited by fusion to another protein, such as in the case of Albinterferon where IFN only retained 1% activity (Subramanian et al., 2007); iii) the dosing of each component may be complex as it difficult to control and tune the optimal amounts for efficacy and safety and iv) the high potential for immunogenicity, as novel epitopes may be prepared against the junction between fusion partners (Stefan R. Schmidt, 2013).

1.3.5 Homodimers

Within biological systems, proteins rarely act alone to prepare a biological response, rather proteins bind to other biomolecules, often self-associating to form dimers within a cascade or network to prepare a biological response (Marianayagam et al., 2004). Homodimers are two of the same protein interacting or bound to one another. It is reported in literature that eukaryotic organisms contain significantly more self-interacting proteins (homodimers) than expected which are a result of evolution (Ispolatov et al., 2005). The propensity of proteins to self-interact was found to be proportional to that of the total number of binding partners, where homodimers have twice as many binding partners than non-interacting proteins (Ispolatov et al., 2005). The ability of proteins to self-interact has several structural and functional advantages, including improved stability, specificity of active sites and greater structural complexity (Marianayagam et al., 2004). Additionally, by proteins self-associating to create homodimers or heterodimers, the genome size remains small

whilst the advantages associated with protein complex formation are maintained (Ispolatov et al., 2005; Marianayagam et al., 2004). Many functionally important proteins including receptors (G-protein-coupled receptors, tyrosine kinase receptors), enzymes, chemokine's and cytokines are homo- or heterodimers. The BRENDA enzyme database lists 452 human enzymes, of these only a third function as monomers, whilst ~70% (311) function as homo -dimeric/-multimers molecules. Important immunostimulatory and immunomodulatory cytokines such as human Interferon γ function as a dimer, formed in a head to tail conformation (Lunn et al., 1992). Interleukin-10 (IL-10), an anti-inflammatory cytokine, also activates its receptor as a dimer (Nagabhushan, TL, Reichert P, 2002).

To improve biological molecules to prepare therapeutic agents to treat disease, homo- and hetero-dimeric molecules prepared by protein fusion or biological (DNL) conjugation are under investigation. For example, immunocytokines against the HER2/*neu* antigen made up of GM-CSF in combination with Interleukin-12 (IL-12) or IL-12 in combination with interleukin-2, fused to trastuzumab are being investigated for a treatment for breast cancer (Helguera et al., 2006). Whilst the DNL method was used to prepared homodimeric PEGylated Interferon α molecules (Figure 1-12), which showed enhanced and prolonged efficacy *in vivo* (Chang, 2010; Chang et al., 2009b). The preparation of Interferon α-2b dimers is well documented in literature, where under the influence of zinc, IFN α-2b forms dimers in crystal (Nagabhushan, TL, Reichert P, 2002; Radhakrishnan et al., 1996). The IFN α-2b dimers have been found to have similar crystal structures to IL-10 and IFN γ, which interact with their receptors in the dimer form (Nagabhushan, TL, Reichert P, 2002). Nagabhushan and colleagues, modelled the structure of the IFN α-2b dimer binding its IFNAR1/IFNAR2 receptor, their findings showed that the dimer could bind to two copies of IFNAR1/IFNAR2 (Nagabhushan, TL, Reichert P, 2002). Although it is understood that IFN α-2b is active in the monomeric form, the IFN α-2b dimer has an unknown biological role. It has been suggested that the IFN α-2b dimer could serve to recruit various IFN α receptors to the signalling complex (Radhakrishnan et al., 1996).

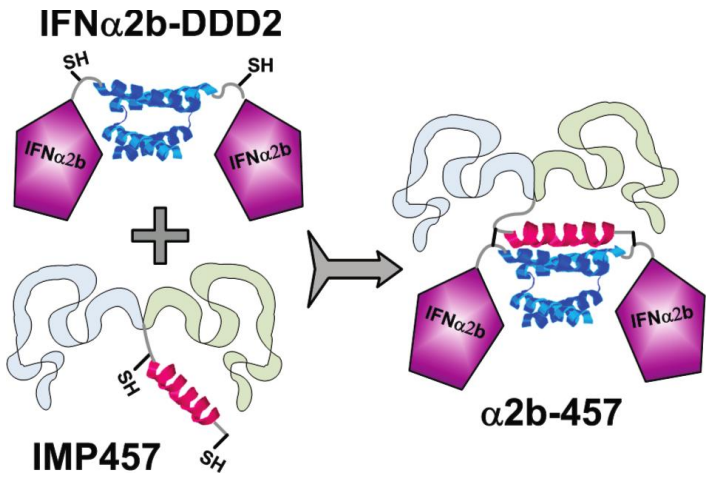

Figure 1-12. Schematic of the monoPEGylated 'dock-and-lock' Interferon α-2b dimer (Chang et al., 2009b). Green and grey ribbons indicate the 40 kDa branched PEG, red helix represents the AD2 domain whilst the blue helix indicates the DDD2 domains and the 'SH' shows the free sulfhydryl groups of engineered cysteine residues.

1.4 Recombinant-chemical approach

Bioconjugation can be defined simply as the covalent linking of a polymer molecule to a macromolecular complex (Veronese and Morpurgo, 1999). Conjugation has been around since the 1920s, however it was the pioneering work of Ringsdorf, where bioconjugation became a central role in the pharmaceutical industry. Following this, the first bioconjugated drug to be successfully marketed was SMANCs in the early 1990s (Duncan, 2003). It is thought that bioconjugation can be utilised in an attempt to address the main fusion protein shortcomings of reduced activity due to fusion site, high immunogenicity, and antibody recognition. The advantages of bioconjugation include, stabilisation of labile drugs from chemical degradation, protection from proteolytic degradation, reduction of immunogenicity, decreased antibody recognition, increased body resistance time, modification of organ disposition, drug penetration by endocytosis and new opportunities for drug targeting (Veronese and Morpurgo, 1999). Further, there is greater flexibility as to the site of conjugation and length of the linker used.

1.4.1 Site-specific conjugation

Conjugation approaches have evolved since its conceptualism, from random to site-specific conjugation approaches. For example, in the 1970s, PEGylation chemistry was limited to a single linking chemistry, succinimidyl succinate. In the 1980s succinimidyl carbonate, N-hydroxy succinimides linkages were developed (Bailon

and Won, 2009). However these linkages prepared heterogenous mixtures of conjugated product, which was problematic, resulting in batch-to-batch variability, as discussed previously (§1.2.1.1). Further linkages such as aldehyde and maleimide were then developed. However, as discussed previously (§1.2.1.1), PEG-maleimide is unstable in solution (Alley et al., 2008; Shen et al., 2012). Disulfide-bridging and histidine tag conjugation are discussed as alternative site-specific approaches for protein conjugation.

1.4.1.1 Disulfide-bridging PEGylation

As previously mentioned (§1.2.1.1), few proteins naturally contain free unpaired cysteine's that can be utilised for site-specific conjugation (Doherty et al., 2005). However many therapeutic proteins have accessible disulfides. Our first conjugation approach utilises the selective chemistry of free thiols derived from disulfide bonds. It is reported that solvent accessible disulfide bonds are thought to contribute to protein stability whilst the biological activity of a protein is dependent on their buried disulfide bonds (Thornton, 1981). Therefore, by using mild reduction conditions, solvent accessible disulfide bonds can be reduced to allow for our disulfide-bridging PEGylation, whilst having little effect on the proteins structure or biological activity.

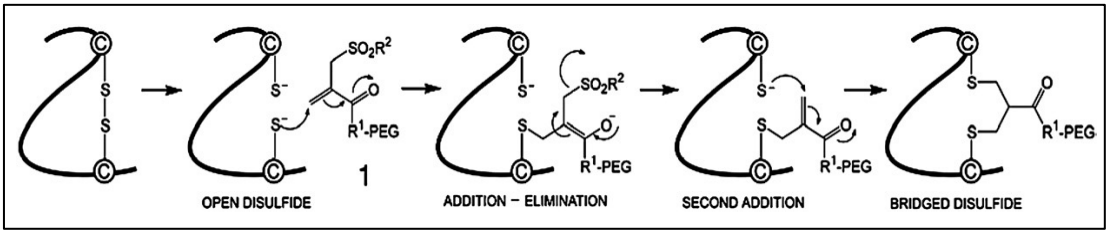

Figure 1-13. Site-specific, disulfide bridging conjugation of an accessible protein disulfide achieved by mild-disulfide reduction followed by reaction with functionalised PEG 1 (Brocchini et al., 2008). Disulfide-conjugation involves, i) first thiol addition to the PEG mono-sulfone **2**, ii) sulfinic acid elimination to generate a second double bond and iii) a second thiol addition.

The first step of disulfide-bridging PEGylation is to liberate the two free thiols for conjugation using mild reductants such as dithiothreitol (DTT) or tris (2-carboxyethyl) phosphine (TCEP-HCl). The first thiol addition to the PEG mono-sulfone **2** (l, Figure 1-13) initiates the sequential addition-elimination reactions (Figure 1-13). The addition of the first thiolate allows the elimination of a sulfinic acid derivative and allows for the addition of a second thiolate resulting in the generation of a second double bond at the α, β'-position (Brocchini et al., 2008). The addition of the second thiolate forms the three-carbon bridge (bridged-disulfide,

Figure 1-13) situated between the two-cysteine molecules, which formed the original disulfide bond. Steric hindrance from the PEG inhibits the addition of a second protein with reduced thiols and similarly prevents the attachment of a second PEG molecule conjugating.

Advantages of this approach include; a) there is no need to recombinantly engineer the therapeutically relevant protein with free cysteine's for conjugation, b) it is possible to chemically reduce the proteins to access the disulfide to its two free cysteine sulphur atoms and still maintain its tertiary structure and c) the high chemical reactivity of both sulphur atoms, which naturally occur in the disulfide and d) often disulfide bonds are in small numbers within proteins, leading to homogenous products. Conjugation is highly specific to thiols, as at neutral pH amines are protonated and thus far less reactive. Further disulfide-bridging conjugation is highly efficient as only a small stiochiometric excess of the PEG reagent is required for conjugation (typically 1 equivalent of PEG per disulfide). Further any unconjugated material can be recycled and reused. However, for proteins with more than one disulfide, the protein required careful re-folding to avoid disulfide scrambling or aggregation. The possible disadvantage with disulfide conjugation is that disulfide bonds are important for protein conformation, therefore any modification at this level could be harmful therefore the distance between the sulphur atoms must be preserved.

1.4.1.2 Polyhistidine conjugation

The second site-specific conjugation approach to be utilised is histidine conjugation. Histidine conjugation takes advantage of the histidine affinity tags (his-tags), which are used in purification of recombinant proteins during early studies of a protein, as it can increase expression yields and aid refolding. The benefits of conjugation on the his-tag are; PEGylation near or on the binding sites can be avoided, thus bioactivity of the protein is retained. Additionally, purification of the required conjugate is simpler as either ion affinity chromatography (IMAC) or ion exchange chromatography (CIEC) can be used effectively (Cong et al., 2012). Thirdly, there is control over the type of conjugate prepared whereas with random PEGylation multiple iterations are required to prepare the desired product. While there are his-tagged proteins currently being used in the clinic (Endostar) and the use of a his-tag appears to be safe, care must be taken as to the location and size of the his-tag

inserted to retain protein activity. The use of his-tags for therapeutic use has been hindered due to, a) a lack of a definitive function after purification and b) an anxiety that there may be immunogenicity against the tag. PEGylation using the his-tag may overcome the first concern and may tackle the second (Cong et al., 2012).

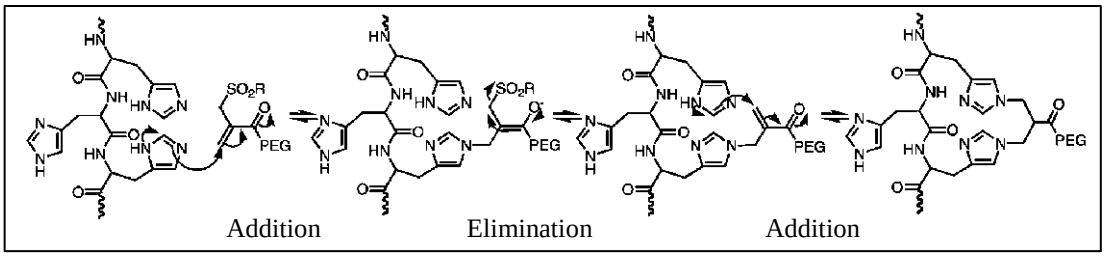

Figure 1-14. Proposed mechanism for site-specific polyhistidine conjugation with PEG mono-sulfone **2** (Cong et al., 2012). Histidine-conjugation involves, Michael addition-elimination reaction with two nitrogen's from two histidine imidazole rings, as previously observed for two thiols from a reduced disulfide.

As previously described (§1.4.1.1), PEG *bis*-sulfone **1** can be used to undergo *bis*-alkylation with two thiols derived from the two sulfurs within a disulfide bond in a protein (Brocchini et al., 2006). Similarly PEG *bis*-sulfone **1** can be used to site-specifically conjugate a polyhistidine tag on a protein by the elimination of sulfinic acid to prepare PEG mono-sulfone **2**. As with disulfide-bridging conjugation, a three-carbon bridge is prepared after the sequential addition-elimination reactions (Figure 1-14). The advantage of this conjugation approach is that few histidines are present in a row within a protein sequence; therefore a homogenous product can be prepared.

1.4.1.3 Conjugation using *bis*-alkylating PEG reagents

For both thiol and histidine specific conjugation, a *bis*-alkylating PEG reagents were used. These reagents consists of an electron-withdrawing carbonyl group, an α, β-unsaturated double bond and a β' sulfonyl group (Figure 1-15). The electron-withdrawing group is required to promote conjugation to free thiols/imidazole and lower the pKa of the α-proton so that the elimination of the β' sulfonyl leaving group takes place. This is necessary to generate the reactive mono-sulfone compound that is used for conjugation. Creation of the mono-sulfone compound can be conducted either *in situ* if the reaction is conducted in neutral or basic pH (this is dependent on protein stability and solubility) or by prior incubation (Brocchini et al., 2006). The rate of elimination of the β' sulfonyl leaving group is dependent on pH, concentration and the temperature of the solution.

Figure 1-15. Sulfinic acid **3** elimination from PEG *bis*-sulfone **1** generating PEG mono-sulfone **2** for conjugation (Brocchini et al., 2008).

For the conjugation of two proteins, PEG di(*bis*)sulfone **4** (Figure 1-16) was used. As with PEG *bis*-sulfone **1** reagent elimination of the β' sulfonyl leaving group occurs; however in the case of the PEG di(*bis*)sulfone **4** this is required at each linker terminal.

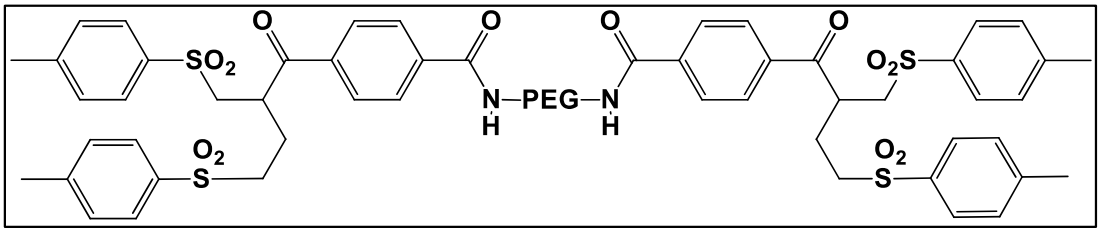

Figure 1-16. Structure of PEG di(*bis*)sulfone **4** used for homodimer or heterodimer preparation using either histidine or disulfide conjugation.

1.4.1.4 Existing research on utilising PEG as a linker

PEG di(*bis*)sulfone **4** has been used to link two Fabs using site-specific disulfide conjugation, to prepare Fab-PEG-Fab molecules. PEG di(*bis*)sulfone **4** of 6, 10 and 20 kDa was used to make corresponding Fab-PEG-Fab molecules. Bevacizumab, trastuzumab and ranibizumab were enzymatically digested to prepare the Fabs, to prepare Fab-PEG-Fab molecules. The Fab-PEG-Fab molecules were shown to display similar affinities to parent IgG, but slower dissociation rates were observed for Fab_{beva}-PEG-Fab_{beva} compared to parent bevacizumab. The apparent K_D (K_d/K_a) of the Fab_{beva}-PEG_6-Fab_{beva} (1.54 nM), Fab_{beva}-PEG_{10}-Fab_{beva} (1.27 nM), Fab_{beva}-PEG_{20}-Fab_{beva} (1.53 nM) products were found to be similar to that achieved for bevacizumab (1.33 nM). This showed that PEG size did not seem to affect the affinities of the Fab_{beva}-PEG-Fab_{beva} molecules to VEGF. Fab_{rani}-PEG-Fab_{rani} displayed *in vitro* anti-angiogenic properties comparable to or better than bevacizumab. Using a HUVEC-fibroblast angiogenesis assay, fewer angiogenesis tubules were observed in cells treated with Fab_{rani}-PEG_6-Fab_{rani} at 0.08, 0.04 and 0.013 μg/mL, 665, 294 and 73 tubule junctions were counted, respectively. While for bevacizumab at 0.12, 0.06 and 0.02 μg/mL 792, 354 and 179 tubule junctions were counted, respectively (Khalili et al., 2013). These studies suggested that the PEG

di(*bis*)sulfone **4** could be used to create Fab-PEG-Fab molecules with retained activity. Therefore it was thought that IFN dimers could be prepared using the homobifunctional reagent **4** and that these IFN-PEG-IFN dimers would retain activity.

1.4.2 IFN as a therapeutic agent

The interferons are a family of naturally secreted cytokines, which are released in response to stimulants such as viral, bacterial and tumour antigens (Ahad et al., 2009). IFNs are classified into two distinct types, Type I IFNs (α/β) and Type II IFNs (γ) (Goodbourn, 2000). Type I IFNs are either prepared by human leucocytes (IFN α) or by fibroblasts (IFN β), whereas Type II IFNs are prepared by natural killer or activated T-cells (Borden et al., 2007; Goodbourn, 2000). The biological activities of Type I and II IFNs are initiated by there binding to their specific heterodimeric cell transmembrane receptors. Type II IFNs bind specifically to IFN γ receptors 1 (IFNGR1) and 2 (IFNGR2), whilst Type I IFNs (α/β) bind specifically to IFN α receptor 1 (IFNAR1) and IFN α receptor 2 (IFNAR2) (Goodbourn, 2000).

Type I signalling occurs when IFN α/β binds to IFNAR1 and IFNAR2 resulting in the cross-phosphorylation of receptors and associated Janus kinases (Tyk2 and Jak1). This provides docking sites on the receptor complex for STAT proteins. The STAT proteins are in turn phosphorylated and form homo- and heterodimeric complexes, which dissociate from the receptor and then translocate to the nucleus and bind an ISRE or GAS elements within the promoters of interferon-regulated genes, leading to their transcription resulting in antiviral or antiproliferative activity (Figure 1-17) (Bekisz et al., 2010; de Weerd et al., 2007). IFN binding also leads to the induction of other non-canonical signalling pathways, including those pathways involving p38, MAPK, Akt and Crk. Upstream signalling from the IFNR complex leads to p38 phosphorylation, resulting in the growth inhibition of cells (Figure 1-17) (Bekisz et al., 2010). Whilst the downstream signalling of P13K, involving Akt and mTOR, or Protein Kinase C-δ confers antiviral activity regulation or regulation of apoptosis respectively (Figure 1-17) (Bekisz et al., 2010).

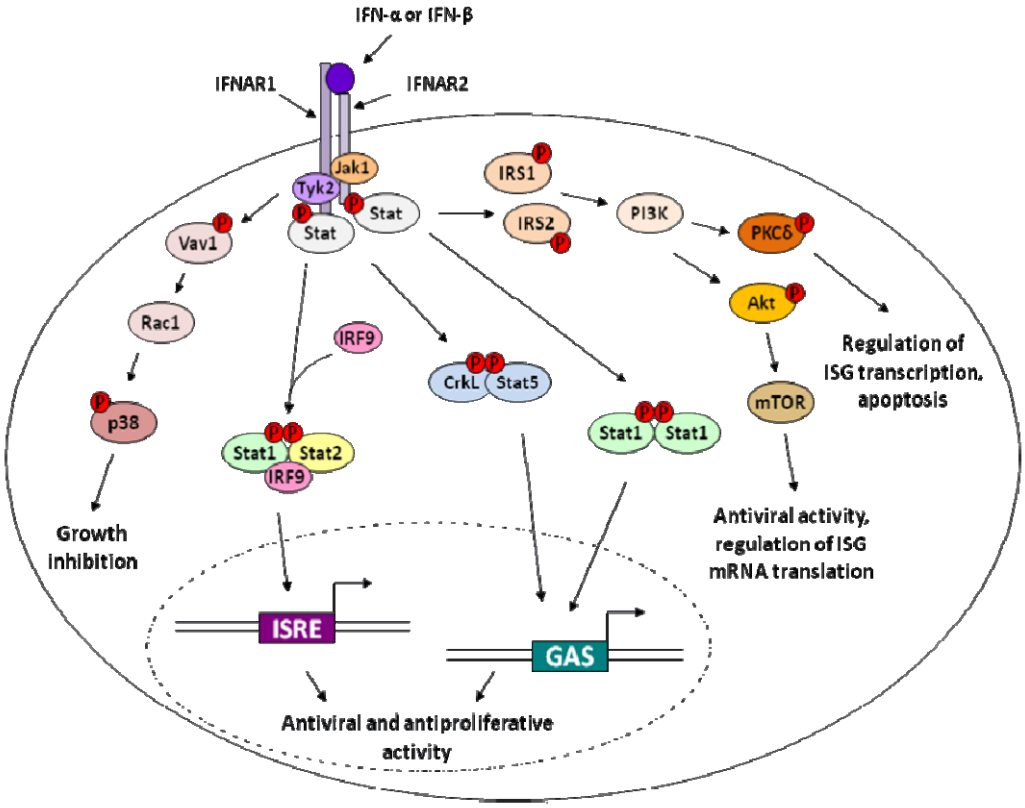

Figure 1-17. Signalling pathway for Type I IFNs (Bekisz et al., 2010). Type I IFNs bind to the transmembrane heterodimer receptor subunits of IFNAR1 and IFNAR2. This results in the activation of receptor kinases, Jak1 and Tyk2. The signal transducers and activator of transcription (Stat) proteins are recruited to the receptor docking sites, are phosphorylated and dimerise to form the active transcription factors, interferon stimulated gene factor 3 (ISGF3), IRF9 (p48/ISGF3γ) and alpha activation factor/gamma activation factor (AAF/GAF). These transcription factors induce the transcription of hundreds of interferon-stimulated genes (ISGs). Upstream signaling from IFNR complex leads to p38 phosphorylation, modulating the activity of IFN leading to growth inhibition of cells. CrkL and CrkII are phosphorylated by tyrosine (Tyk2) after IFN treatment, CrkL also can form a transcription factor complex with Stat5, leading to antiviral and antiproliferative activity downstream. IFN signal pathways downstream of P13K involve Akt and mTOR, or PKCδ mediate other biological activities of IFN, such as apoptosis.

Interferons as therapeutic medicines

Therefore, Type I IFNs are a group of heterogenous group of pleiotropic cytokines with antiviral, antiproliferative, antitumour and immunodulatory activities (Anguille et al., 2011; Goodbourn, 2000; Nanus et al., 1990). These unique biological properties have been exploited to treat a variety of clinical conditions (Table 1–7).

Table 1–7: Genetically engineered forms of IFNs approved by the FDA (Bekisz et al., 2010; Chang et al., 2009a).

Product/ Company	IFN type	Indication	FDA approval date
Actimmune® InterMune	IFN γ-1b	Chronic granulomatous disease Malignant osteopetrosis	1990 2000
Avonex® Biogen Idec	IFN β-1a	Relapsing-remitting forms of multiple sclerosis	1996
Betaseron® Berlex/Chiron	IFN β-1b	Relapsing-remitting forms of multiple sclerosis	1993
Infergen® InterMune	IFN αcon-1	Hepatitis C	1997
Intron A® Schering-Plough	IFN α-2b	Hairy cell leukemia AIDS-related Kaposi's sarcoma Hepatitis B Chronic malignant melanoma Chronic viral Hepatitis C Follicular lymphoma in chemotherapy patients Hepatitis B in pediatric patients	1986 1988 1992 1992 1997 1997 1998
PEG-INTRON® Enzon/Schering-Plough	PEGylated-IFN α-2b	Chronic Hepatitis C	2001
PEGASYS® Roche/Nektar	PEGylated-IFN α-2a	Chronic Hepatitis C	2002
Plegridy Biogen-Idec	1.4.3 PEGylated IFN β-1a	1.4.4 Relapsing multiple sclerosis	1.4.5 2014

1.4.5.1 His_8IFNα-2a used for conjugation

His_8IFNα-2a has been used previously to prepare both monoPEGylated and di-PEGylated conjugates to explore histidine PEGylation (Cong et al., 2012). An 8-polyhistidine tag was prepared recombinantly, which prepared higher yields, compared to 4 and 6-polyhistidine tags, which were expressed at lower yields. Further an 8-histidine tag was thought to allow the conjugation of two PEG molecules of moderate MW, to give a conjugate with good activity and long half-life.

To explore a recombinant-chemical approach, IFN α-2a with an 8-polyhistidine tag was prepared recombinantly to explore the preparation of IFN homodimers (IFN-PEG-IFN) and heterodimers (IFN-PEG-Fab) using PEG di(*bis*)sulfone **4**. These novel homodimers and heterodimers will be prepared using

either histidine conjugation or disulfide conjugation, as His_8IFNα-2a has both the polyhistidine tag and two disulfides (Figure 1-18), which could be conjugated to. Disulfide conjugation on His_8IFNα-2a has not been conducted before.

1.4.6 Multifunctional protein therapeutics using PEG as a linker

1.4.6.1 Approach 1: IFN-PEG-IFN as a therapeutic antiviral agent

Interferons were first described as antiviral agents in 1957 by Isaacs and Lindenmann (Isaacs and Lindenmann, 1957). They have been of particular therapeutic interest as they act on the target cell (not the virus) to inhibit replication and the lifecycle of a wide variety of viruses, thus conferring a state of resistance within the cell to viral infection (Brassard et al., 2002). There are a number of pharmaceutical forms of Type I IFNs, namely Infergen®, Intron A®, PEG-INTRON® and PEGASYS® for the treatment of viral diseases such as Hepatitis B and Hepatitis C (Bell et al., 2008).

IFN α-2a (Intron A®) is comprised of five helical barrel structures with two disulfide bonds between residues Cys1-98 and Cys29- Cys138. The ribbon structure of IFN α-2a can be seen in Figure 1-18 (Klaus et al., 1997). IFN is approximately 20 kDa, thus has a short circulation half-life of about six hours. Resulting in patients requiring an injection every other day in an attempt to keep blood concentration of IFN at an efficacious level (Glue et al., 2000; Luxon et al., 2002a). However, in reality patients are only being exposed to significant drug levels for approximately 36 hours per week (21%), as drug levels peak and trough (Ahad et al., 2009). Hence, more frequent administration of IFN α is required; however this is inconvenient and debilitating for patients. In an attempt to improve the therapeutic properties of the native protein, whilst trying to retain the biological activity of IFN α, IFN α has been conjugated to PEG in order to increase its PK properties.

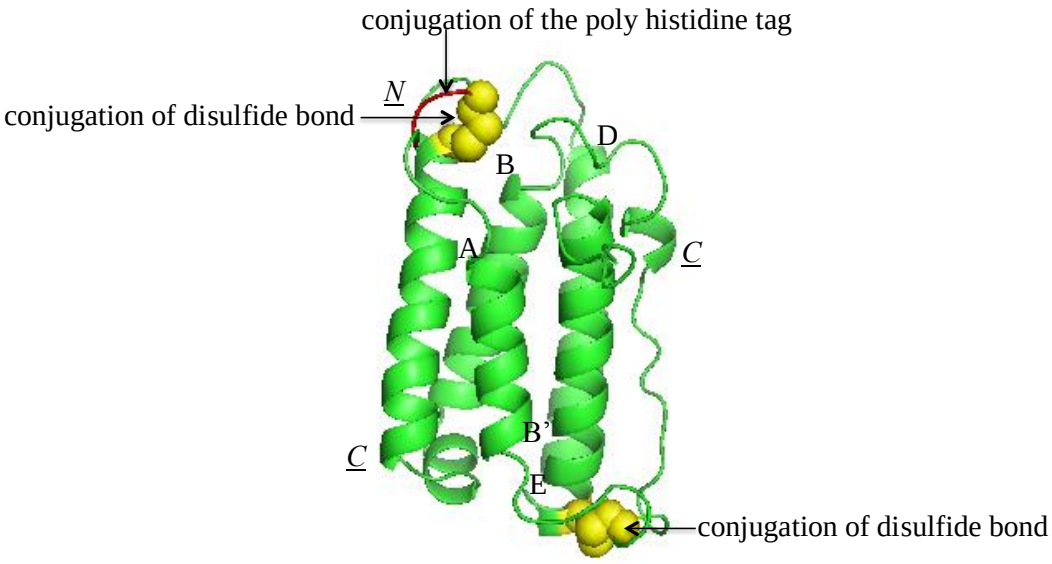

Figure 1-18. Ribbon structure of His_8IFNα-2a prepared using Pymol software. The α-helices (in green) of His_8IFN α-2a, with the two disulfide bridges shown as yellow spheres, with the 8-polyhistidine tag shown in red. The α-helicies (in green) are marked with labels A to E close to their N-terminal end. His_8IFN was used to prepare homodimeric and heterodimeric molecules using PEG di(*bis*)sulfone **4** in conjunction with site-specific conjugation approaches. The conjugation approaches used to prepare the homo- and hetero-dimeric molecules were either histidine or disulfide-bond conjugation; the sites His_8IFNα-2a conjugation are labelled.

The two most commonly used treatments for Hepatitis C are PEGASYS® and PEG-INTRON® (Figure 1-17). As discussed in §1.2.1, these current treatments have several drawbacks, namely, heterogeneity of the final products from random conjugation, reduced IFN activity due to PEG-positional isomers binding near or at the binding site and side effects from IFN treatment. Therefore, how to can we improve upon these current IFN treatments?

Fundamentally, proteins are complex and as discussed in §1.3.5 the majority of protein self-interact, very few proteins act alone to prepare a biological response. As in the case with Type I IFNs, the signalling cascade for producing an antiviral response alone is prepared by a series of at least three separate complexes of two or more proteins interacting Figure 1-17. IFN α dimers are well documented within literature, where under the influence of zinc IFN α-2b forms dimers, these have been found to have similar crystal structures to IL-10 and IFN γ, which interact with their receptors in the dimer form (Nagabhushan, TL, Reichert P, 2002; Radhakrishnan et al., 1996). The DNL method has been used to create homodimeric PEGylated Interferon α molecules, which showed enhanced and prolonged efficacy *in vivo* (Chang, 2010; Chang et al., 2009b). However, protein fusion methods such as DNL

may incur difficulties such as incompatible manufacturing properties of fusion partners, immunogenicity and reduced functionality as highlighted in §1.3.4.

Therefore, a recombinant-chemical approach will be adopted to prepare a His_8IFN-PEG-His_8IFN dimer. This approach combines the advantages of conjugation, such as reduced immunogenicity, increased body resistance time and protection from proteolytic digestion (Veronese and Morpurgo, 1999) with recombinant protein technology. IFN was expressed recombinantly with an 8-polyhistidine tag (Figure 1-18), the polyhistidine tag and the natural disulfides could both be conjugated to with the PEG di(*bis*)sulfone reagent **4**. Thus, site-specific his-tag and disulfide conjugation was conducted on the His_8IFN α-2a to create IFN homodimers. It is hypothesised that these His_8IFN α2a dimers would have greater activity than PEG-IFN conjugates, due to i) the site-specific nature of conjugation, reducing conjugation near or at the binding sites and ii) the greater number of IFNs present within the molecule which are able to bind to IFNAR complex.

1.4.6.2 Approach 2: IFN-PEG_{20}-Fab_{alb} heterodimer

Current treatments based on IFN focused on utilising PEGylated versions of IFN to improve the short serum half-life of IFN. This approach has been successful in prolonging the circulation half-life of native IFN from 7-9 h to 48-72 h or 96 h for PEG-INTRON® and PEGASYS® respectively, thus both treatments can support once-weekly administration (Table 1–3) (Glue et al., 2000; Luxon et al., 2002a). These constant serum concentrations are able to reduce the side effects caused by multiple dosing (Figure 1-4). Furthermore, sustained PEG-IFN concentrations help to prevent viral rebound and continued viral replication (Harris et al., 2001). However, the current approach is dependent on patient adherence to treatment. Therefore, there is a pharmacological rationale to prepare a longer acting IFN treatment, which provides sustained viral suppression, thus minimum side-effects, with enhanced convenience of an improved dosing regimen and may reduce viral rebounds. This was attempted in the creation of Albinterferon (Albumin-IFN α-2b fusion), which could be support a 2-4 week dosing regimen. Yet, as discussed in §1.2.2, Albinterferon only possessed ~1% activity compared to native Interferon α-2b (Ahad et al., 2009; Bell et al., 2008; Osborn et al., 2002). The reduced activity of IFN within Albinterferon highlights in crucial balance between PK and PD.

Understanding the important balance between PK and PD, whilst exploring approaches to improve the half-life of IFN beyond that of current treatments. It was thought that an anti-albumin Fab (Fab_{alb}) could be used to 'piggy-back' upon circulating albumin. Where the PEG di(*bis*)sulfone reagent **4** could be used to conjugate both IFN and anti-albumin Fab. The rationales of this approach are firstly; anti-albumin Fab has a single disulfide, which can be easily reduced using mild reductants to allow for site-specific disulfide PEGylation. As stated previously, site-specific PEGylation of Fabs with *bis*-alkylation PEG reagents has shown to retain the binding specificity (Khalili et al., 2012). Secondly, this novel approach conjugating His_8IFN α-2a and anti-albumin Fab together using the PEG_{20} (20 kDa PEG) di(*bis*)sulfone as a 'linker', the complex (~110 kDa) will be above the renal filtration threshold (~70 kDa), thus enabling the complex to stay in circulation for longer. Further, the anti-albumin Fab can also bind to circulating albumin. Thirdly, by utilising the PEG di(*bis*)sulfone **4** as a 'linker' for protein-protein conjugation in conjunction with site-specific conjugation, it is hypothesised that the functional activity of both proteins will be retained as; i) conjugation is taking place away from the binding sites and ii) it is hoped that the PEG di(*bis*)sulfone **4** will act as a 'spacer' keeping the proteins from impeding the action of one another. Forth, anti-rat albumin IgG can be digested utilising immobilised papain to prepare anti-albumin Fabs. For future investigation, anti-rat albumin Fabs were used as to assess the *in vivo* half-life of the complex within a relevant model where it can be assessed if the anti-albumin Fab can extend the half-life further.

1.4.6.3 Approach 3: IFN-PEG_{20}-Fab_{beva} a possible therapeutic for renal cell carcinoma

As discussed in §1.3.4 cytokines have three major disadvantages with cancer therapy firstly; severe toxicities are frequently associated with systemic infusions of cytokines, thus limiting the amount which can be administered to achieve an effective dose. Secondly, for a therapeutic protein to be effective it must reach its biological target, however cytokines lack tumour specificity. Thirdly, the majority of cytokines have a MW below 30 kDa, thus suffer from short serum half-lives (Vazquez-Lombardi et al., 2013). Consequently, the ultimate challenge for developing improved cytokine therapeutics for cancer is to reduce unwanted side

effects of cytokine treatment while increasing the local concentration of cytokines to the tumour microenvironment. Direct cytokine injections have been trialled with cytokines, however the major downfall of this approach is that the tumour must be accessible and visualised however this is not always possible with micrometastatic lesions (Forni et al., 1985). An intuitive approach has been to fuse cytokines to HSA, Fc regions to increase their half-life however this approach does not specifically take the cytokine to the tumour site(s) thus not reducing unwanted side effects (Bitonti et al., 2004; Jazayeri and Carroll, 2008; Subramanian et al., 2007).

Therefore, the third recombinant-chemical approach is to chemically link His_8IFN α-2a with Fab derived from bevacizumab (Fab_{beva}) using PEG di(*bis*)sulfone **4** as a linker. Bevacizumab plus interferon α has is an approved treatment for metastatic renal cell carcinoma (RCC) (Rini et al., 2008). Vascular endothelial growth factor (VEGF) is continuously expressed on many tumour cells and its the only angiogenic factor known continually expressed throughout the entire tumour life-cycle (Folkman, 2007). VEGF is a key mediator angiogenesis in cancer (Carmeliet, 2005), as the binding of VEGF to its receptor causes increased vascular permeability, induces proliferation and migration of endothelial cells (angiogenesis) and inhibits apoptosis of immature endothelial cells (Escudier et al., 2008). Therefore, bevacizumab (Avastin®) a recombinant humanised monoclonal IgG1 was developed to inhibit VEGF (Escudier et al., 2008). Interferon α has one of the longest clinical records for use in oncology, and is used to treat over 14 types of cancer including hairy cell leukaemia, RCC and Kaposi's sarcoma (Table 1–7) (Ferrantini et al., 2007). This is due to IFN α's ability to directly inhibit the proliferation of normal or tumour cells and modulate immune responses (Bekisz et al., 2010; Ferrantini et al., 2007; Wu et al., 2005). Further it is thought IFN α-2a could suppress VEGF synthesis and secretion by inhibiting P13 kinase and MAP kinase signalling pathways. This targeted dual-action treatment has become the first-line treatment for RCC as significant improvement was observed over IFN alone in progression-free survival in Phase III clinical trials (Escudier et al., 2007). However, throughout clinical trials toxicity of the combination therapy was greater than IFN α-2a alone (Rini et al., 2008). Further, the combination therapy is not a tumour specific and the combination therapy requires bevacizumab to be administered once every two weeks and IFN to be administered three times a week (Escudier et al., 2007). Adverse

effects from IFN treatment where observed, this is most likely due to either toxicity or side effects caused by multiple dosing (Figure 1-4) (Escudier et al., 2007).

By conjugating Fab_{beva} to His_8IFN α-2a, it is hoped that; i) severe toxicity associated with systemic infusion of IFN would be reduced, as the IFN-PEG_{20}-Fab_{beva} conjugate has tumour specificity from the Fab_{beva} that specifically binds to tumour expressing VEGF, thus delivering IFN to its biological target; ii) improved patient quality of life, as both Fab_{beva} and IFN alone have relatively short half-lives *in vivo*, however when conjugated together using the homobifunctional reagent the overall MW of the conjugate ~110 kDa which could improve half-life leading to fewer injections for the patient; iii) greater therapeutic efficacy by combining the tumour specificity and anti-angiogenic ability of Fab_{beva} with the antiproliferative, immunodulatory and VEGF suppression ability of IFN within one molecule; and iv) improved activity retained by the therapeutic proteins and greater homogenicity of the final product, by thiol conjugation site-specificity.

1.5 PhD hypothesis

The main hypotheses of this PhD research are:

- His_8IFN-PEG-His_8IFN homodimers can be made by selective conjugation to the N-terminal 8-polyhisitidine tag on the protein and that the homodimer will have retained *in vitro* activity.
- Disulfide-bridging conjugation can be conducted on His_8IFN with PEG di(*bis*)sulfone **4** to make IFN-PEG-IFN and this homodimer will have retained *in vitro* activity.
- The IFN-PEG-IFN dimers will have greater activity than the corresponding PEG-IFN conjugates because the IFN-PEG-IFN dimer will provide a higher concentration of IFNs at the binding site able to bind to the IFNAR complex.
- Heterodimeric protein-protein conjugates can be prepared using a homobifunctional PEG reagent **4** to make Fab-PEG-IFN conjugates. These heterodimeric conjugates will display biological properties that are associated with both of the conjugated proteins.

Chapter 2 Materials and Methods

2.1 Materials

Table 2–1: PEG reagent names, structures, previous work and purpose of the reagent used within this thesis.

PEG reagent number	PEG reagent name	PEG structure	Previous work	Purpose of reagents
1	**PEG *bis*-sulfone**	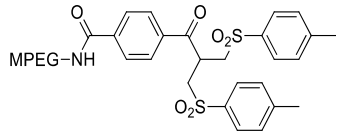	(Cong et al., 2012) (Shaunak et al., 2006) (Balan et al., 2007)	PEG-protein controls
2	**PEG mono-sulfone**	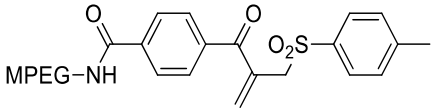	(Shaunak et al., 2006) (Balan et al., 2007) (Khalili et al., 2012)	
4	**PEG di(*bis*)-sulfone**	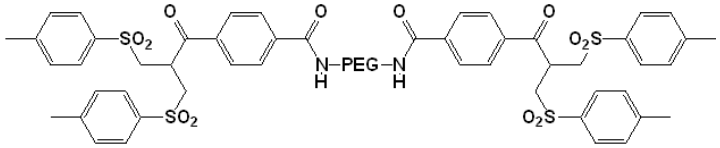	(Khalili et al., 2013)	Homo-/hetero-protein dimers
5	**PEG di(mono)sulfone**	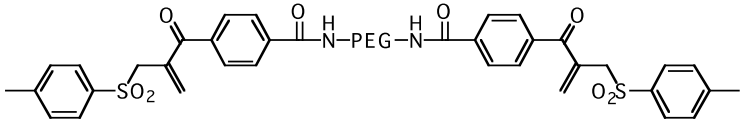	(Khalili et al., 2013)	

2.1.1 Preparation of PEG_{20} di(*bis*)sulfone **4**

For the synthesis of the homodimer (IFN-PEG-IFN) the PEG_{20} di(*bis*) sulfone **4** was made using PEG_{20} di(amine) **6** from NOF (DE-200PA) and *bis*-sulfone linker **7** was made by Martin Fisher and Farzad Khayrzad. 4-Dimethylaminopyridine (DMAP, 148270050), dry-dichloromethane (DCM, 326851000) and dry-toluene (326980010) were all supplied by Acros Organics. Oxone® (STBB229V) was brought from Sigma Aldrich. Methanol (H/4000/17) was supplied from Fisher Scientific and purified water was supplied in house at PolyTherics Ltd.

For the improved synthesis route of PEG_{20} di(*bis*) sulfone **4** which is used for the heterodimer synthesis (IFN-PEG-Fab), PEG_{20} di-amine **6** was supplied by NOF (DE-200PA) and *bis*-sulfide linker **9** was made by Gaidad Tekle. 4-Dimethylaminopyridine (DMAP, 148270050), dry-dichloromethane (DCM, 326851000) and dry-toluene (326980010) were all supplied by Acros Organics. 4-Methylbenzene thiol (1001233199) and Oxone® (STBB229V) was brought from Sigma Aldrich. Methanol (H/4000/17) was supplied from Fisher Scientific and purified water was supplied in house at Warwick Effect Polymers.

2.1.2 His_8IFN α-2a fermentation and production

For the fermentation of His_8IFN α-2a, Lysogeny Broth Miller (L3152-1KG) and isopropyl β-D-1-thiogalactopyranoside (IPTG) (I6758-5G) were both supplied from Sigma Aldrich. Ampicillin sodium salt (BPE1760-25), tryptone (BPE-1421-2), glycerol (G/0650/17/F), potassium phosphate monobasic (BP362-500) and potassium phosphate dibasic (BP363-1) were all purchased from Fisher Scientific. Yeast extract (92144) was supplied from Fluka analytical.

For the purification of His_8IFN α-2a, phosphate buffer saline (PBS) (BP399-20), imidazole (30187-0010), tris-hydrochloride (T/3710/60), sodium chloride (S/3710/60), EDTA (BP120-500F) and sodium azide (S/2360/48) were all supplied from Fisher Scientific. Protease inhibitor cocktail (P8465) was supplied from Sigma Aldrich. The following immobilised metal ion affinity chromatography (IMAC) and anion exchange chromatography (AIEC) columns were used, HisPrep™ FF 16/10 (20 mL) (28-9365-51) and HiPrep™ Q FF 16/10 (20 mL) (28-9365-43) respectively were brought from GE healthcare. For large scale lysis the QuixStand Benchtop system and pre-static pump (56-4107-78) with a hollow fibre cartridge (UFP-500-C-

4MA) were all brought from GE Healthcare. Lysozyme (L7651), protease inhibitor cocktail for His-tagged proteins, dimethyl sulfoxide solution (P8849), and deoxyribonuclease I from bovine pancreases (DN25) were supplied from Sigma Aldrich. Triton X-100 (BP151-500) was brought from Fisher Scientific.

2.1.3 Digestion and purification of Rabbit anti-rat albumin (IgG_{alb}) and Bevacizumab (IgG_{beva})

IgG_{beva} (Avastin®, 25 mg/mL, Genentech/Roche) and IgG_{alb} (Genway Biotech Inc, GWB-E3EEDA) were digested using immobilised papain from Thermo Scientific (20341). The digestion buffer was made using di-sodium hydrogen orthophosphate, dodecahydrate (S/4400/53) and sodium hydrogen orthophosphate dehydrate (S/3760/60) were supplied from Fisher Scientific, ethylene-diamine-tetraacetic acid (EDTA) was supplied from Apollo Scientific Ltd. (BIE0729) and L-cysteine was from Sigma Aldrich (168149_2.5g).

Purification of IgG_{alb} and IgG_{beva} was conducted using HiTrap™ Protein A HP column (1 mL) from GE healthcare (17-0402-01). Glycine (G/P460/53) and di-sodium hydrogen orthophosphate, dodecahydrate (S/4400/53) and sodium hydrogen orthophosphate dehydrate (S/3760/60) were supplied from Fisher Scientific.

2.1.4 Protein desalting and conjugate purification columns

For protein desalting, PD-10 and NAP-5/10 desalting columns were used from GE Healthcare (17-0851-01, 17-0853-01, 17-0854-01). For cation exchange chromatography (CIEC) HiTrap Macrocap SP HP columns (5 mL) were brought purchased from GE Healthcare (28-9508-59). Buffers A (100 mM sodium acetate, pH 4) and B (100 mM sodium acetate, 1 M sodium chloride pH 4) were made using acetic acid (A/0360/PB15), 1 M sodium hydroxide (J/7620/15), sodium chloride (BP358 212) and 1 M hydrochloric acid (J/4340/15) were brought from Fisher Scientific. For size exclusion chromatography (SEC), a HiLoad 16/60 Superdex™ 200 prep grade column from GE Healthcare (28/9893-35) column was used. The buffer used for SEC was made using di-sodium hydrogen orthophosphate, dodecahydrate (S/4400/53), sodium hydrogen orthophosphate dehydrate (S/3760/60) and sodium chloride (BP358 212) were all supplied from Fisher Scientific. Zeba™ spin desalting columns >7000 Da (2,5,10 mL) were brought from Thermo Scientific.

2.1.5 SDS-PAGE analysis

SDS-PAGE was conducted using 4-12% Bis-Tris polyacrylamide gels (NuPAGE®; NP0323BOX). Every gel was loaded with Novex® sharp pre-stained standards (Novex; P/ N 57318) and samples were loaded using an appropriately diluted 4×SDS sample buffer (NuPAGE®; NP0007). Gels were run in Xcell SureLock™ gel electrophoresis tanks (Invitrogen; EI0001) and run in MES SDS-PAGE running buffer (×20) from NuPAGE® (NP0002-02). Gels were stained using InstantBlue™ gel stain (Expedeon; ISB01L) and PEG stain (barium chloride and 0.05 M iodide were both from Fisher Scientific (B/0500/53; J/4410/15). Alternatively, silver stain (SilverXpress® Silver staining kit) was used from Invitrogen (LC6100). Densimetric analysis was conducted using ImageQuant™ LAS 4010 instrument (GE Healthcare, 28-9558-10).

2.1.6 PEGylation reagents and reactions

PEG_{20} *bis*-sulfone **1** was supplied by BioVectra Inc (6237). Acetic acid (A/0360/PB15), 1 M sodium hydroxide (J/7620/15), disodium hydrogen orthophosphate, dodecahydrate (S/4400/3), sodium dihydrogen phosphate (S/3760/60), sodium chloride (BP358 212), 1 M hydrochloric acid (J/4340/15), ammonium bicarbonate (BP2413-500) and 100 mM dithiothreitol (DTT, BP172-5) were brought from Fisher Scientific. Hydroquinone (24,012-5) and 95% sodium triacetoxyborohydride (STAB) (316393-25G) were from Sigma Aldrich. Reduced and oxidised glutathione (A0279520 and A0288123 respectively) were supplied from Acros organics. Ethylene-diamine-tetraacetic acid (EDTA) was supplied from Apollo Scientific Ltd. (BIE0729), whilst tris(2-carboxyethyl)phosphine hydrochloride solution (TCEP) was supplied from Sigma Aldrich (646547-10X1ML). Tween-20 was supplied from Fluka analytical (44112-100GF).

2.1.7 Characterisation materials

To determine His_8IFN α-2a concentration the MicroBCA™ Protein Assay Kit (Thermo Scientific, 23235) was used. Additionally for quantification of proteins in small volumes (<900 µL), the Nanodrop 2000 spectrophotometer from Thermo Scientific (SPR-700-310L) was used. BradfordUltra™ reagent from Expedeon (BFU1L) was used for the quantification of Fab concentration, where the standard

curve of bevacizumab was used to quantify unknown Fab concentrations. Sequence grade modified Trypsin was brought from Promega (100 μL; V5111).

Western blotting for assessing His-tag IFN, Fab_{beva} and Fab_{alb} was conducted using Xcell™ II blot module gel transfer apparatus (Invitrogen, EI9051). Gel contents were transferred onto nitrocellulose membrane Hybond-C that was supplied from GE Healthcare (sandwiched between 1mm thick blotting paper). Transfer buffer stock (×12.5, 1 L) consisted tris-base (Fisher Scientific), glycine (Fisher Scientific; G/460/53) in purified water (in house). The transfer buffer (1×) was made from 12.5× transfer buffer stock, methanol (laboratory grade, Fisher Scientific) and was diluted with purified water (in house). Blocking solution was made using dried skimmed milk and PBST (1× solution prepared using 10× PBS stock from Fisher Scientific (M5401) and Tween-20 from Fluka analytical).

Mouse anti-6×His monoclonal antibody (Clontech, 631212) and anti-mouse AP-conjugated antibody (Promega, S3721) were used to detect the His-tag. Samples were detected using a colorimetric detections method. Using, NBT/ BCIP (SIGMA FAST™, B5655-25TAB) alkaline phosphatase substrate tablets.

For detecting IFN, rabbit anti-IFN α polyclonal antibody (RnD Systems, 31101-1) and goat anti-rabbit HRP-conjugated antibody (AbCam, ab6721) were used.

To detect rat albumin (Sigma Aldrich, A6414-10 mg), anti-rat albumin IgG (Genway Biotech Inc, GWB-E3EEDA) and goat anti-rabbit HRP-conjugated antibody (AbCam, ab6721) were used.

For detecting bevacizumab compounds goat anti-human κ-chain (Fab'_2) (HRP-conjugated) was used (Fitzgerald, 43C-CJ0132). Pierce ECL (enhanced chemiluminescence) Western blotting substrate kit supplied from Thermo Scientific (32106) was used with the ImageQuant™ for the detection of HRP enzyme activity.

2.1.8 *In vitro* Antiviral assay

The human lung fibroblast cell line (A549) (HPACC; 86012804) was cultured in Dulbecco's Modified Eagles medium (DMEM) (Gibco/Fisher Scientific; VX21969035) and Foetal Bovine Serum (FBS) (Gibco/Fisher Scientific; VX25030024). The DMEM contained penicillin streptomycin (PAA; P11-101) and L-glutamine (Sigma; G7513-100 mL). Trypsin-EDTA (PAA; L11-004) was used for subculture. For a cell count trypan blue (Sigma Aldrich; T8154-100 mL), KOVA

glassic slide 10-grids (Hycor; FGK01) and an inverted microscope (Ceti, Jencons) were used. All cell culture work was conducted in a Bio-safety cabinet (class 2) (Biomat2), cells were kept in a CO_2 air-jacket incubator (Binder; CB15) and all reagents were warmed using a water-bath (JB series, Grant) before use. For the antiviral assay A549 cells were infected using Encephalomyocarditis Virus (EMCV) (ATCC; VR-129B). Sample controls were NIBSC IFN α-2a standard (HPACC; 95/650) and PEGASYS® (Roche). Phosphate buffered saline (PBS) pH 7.4 (BPE399-20); formaldehyde (40%) (F/145/PB17) and SDS (10%) (BPE 2436-1) were supplied from Fisher Scientific. Methyl violet 2B was from Sigma Aldrich (198099). The microplate reader was supplied from Dynex Technologies/Opsys MR and the microplate shaker was supplied from VWR/VWR (444-7094).

2.1.9 *In vitro* Antiproliferative assay

Human Negroid Burkitt lymphoma (Daudi) cell line was supplied from HPACC (85011437) and was cultured using RPMI 1960 (1×) liquid with L-glutamine from Fisher Scientific (VX21875-091). Control samples NIBSC IFN β-1b was supplied from NIBSC (00/574) and Betaferon® (250 µg/mL) was supplied from Bayer Schering Pharma (Lot No: 01062A). Dimethyl sulfoxide (DMSO) (sterile filtered) was from Sigma Aldrich, tissue culture microplate 96 well U-bottom plates were from Thermo Scientific (FB56412) and thiazolyl blue tetra-zolium bromide (MTT) was supplied by Sigma.

2.1.10 BIAcore

All BIAcore consumables were purchased from GE healthcare Ltd. (Amersham). All affinity assays were conducted using the BIAcore X-100 instrument. For essential weekly and monthly maintenance, the BIAcore Maintenance kit was used (BR-1006-66). For immobilisation the amine coupling kit (BR-1000-50) containing N-hydroxysuccinimide (NHS), 1-ethyl-3-(3-dimethylaminopropyl)-carbodiimide (EDC), ethanolamine-HCl (1.0 M, pH 8.5), glycine buffer (10 mM, pH range of 1.5 to 2.5, 22053613) and the Regeneration scouting kit (BR-1005-56) were used (including 10 mM glycine-HCl pH 2.0 and 2.5). For immobilisation, CM3 sensor chips were used (BR-1005-41). Sodium acetate pH 4.0 (BR-1003-49), 4.5 (BR-1003-50), 5.0 (BR-1003-51) and 5.5 (BR-1003-52) were used for the pH scouting experiment with 50 mM sodium hydroxide (BR-1003-58) for regeneration. For all

runs HBS-EP buffer was used (BR-1006-6) (including HEPES (0.1 M), NaCl (1.5 M), EDTA (30 mM), 0.5% V/V surfactant P20, pH 7.4). The test compounds were prepared in 1.5 mL plastic vials (BR-1002-87) and rubber caps (Type 2, BR-1004-11) were used to close the vials. The two ligands used were human vascular endothelial growth factor ($VEGF_{165}$, V7259-10 μg) were purchased from Sigma Aldrich and rat albumin (Sigma Aldrich, A6414-10 mg).

2.2 Methods

2.2.1 SDS-PAGE analysis

SDS-PAGE analysis of proteins was conducted with Novex® 4-12% Bis-Tris gels (10 or 15 wells) in an electrophoresis cell. Samples were prepared with NuPAGE® LDS sample buffer (in a 1:3 ratio) with the amount of sample loaded on the gel being approximately 1 μg. The protein molecular weight (MW) standard used was Novex® Sharp Protein Standard. NuPAGE® MES SDS running buffer (×20) was used as running buffer. The voltage applied for electrophoresis was 200 V and the run time was 35-40 min. Gels were stained by; InstantBlue™, PEG stain or SilverStain (Kurfürst, 1992).

2.2.2 Determination of protein concentration

2.2.2.1 MicroBCA assay for protein concentration

MicroBCA™ Protein Assay kit containing a solution of albumin standard (2 mg/mL) was diluted in appropriate buffer (dependent on sample buffer) to 200 μg/mL, 50 μg/mL, 25 μg/mL, 12.5 μg/mL, 6.25 μg/mL, 3.125 μg/mL and 0.0 μg/mL (blank). The samples (75-150 μL) were incubated respectively with 75-150 μL MicroBCA™ solution (prepared by mixing solutions A:B:C in the ration of 25:24:1) at 37 °C for 2 h. The absorbance was then measured at 570 nm and a standard curve was generated by plotting the absorbance values against their respective albumin concentrations. For His_8IFN α-2a samples, appropriate dilutions (~40-60 μg/mL) were made to a concentration within the linear part of the standard curve and the above steps followed. The concentration of samples was calculated based on the standard curve obtained (6.1 Appendix I).

2.2.2.2 Bradford assay for determining Fab concentration

Bevacizumab (Avastin®, 25 mg/mL, Genentech/Roche) was used as standard. Bevacizumab was first diluted in an appropriate buffer (dependent on sample buffer) to 625 μg/mL, which was then used to prepare a dilution series of 100 μg/mL, 80 μg/mL, 60 μg/mL, 50 μg/mL, 40 μg/mL, 30 μg/mL, 20 μg/mL, 9 μg/mL and 0.0 μg/mL (blank) for the standard curve. Similarly, samples were diluted to 60, 50 and 40 μg/mL in the same buffer. The standard and the samples (80 μL) were pipetted into a 96 well plate and mixed with BradfordUltra™ reagent (220 μL). The plate was then left for 10 min at RT and the absorbance read at 590 nm. The concentration of samples was then calculated based on the standard curve obtained (6.1 Appendix I).

2.2.3 Fermentation and purification of His_8IFN α-2a

2.2.3.1 Fermentation of His_8IFN α-2a

Terrific Broth (TB) was prepared using tryptone (12 g), yeast extract (24 g), glycerol (0.4% v/v), potassium phosphate dibasic (12.54 g, 0.072 M) and potassium phosphate monobasic (2.31 g, 0.017 M) per L and was supplemented with ampicillin (100 μg/mL). Lysogeny broth (LB) broth (25 g/L) was also supplemented with ampicillin (100 μg/mL). In a 0.5 L baffle flask, a pre-culture was prepared containing LB (90 mL), TB (10 mL) and glycerol stock (0.01 mL). The pre-culture was left to grow overnight at 37 °C in a shaking incubator rotating at 220 rpm. TB (500 mL) and pre-culture (50 mL) were then poured into two 2 L baffle flasks and were left to grow at 37 °C in a shaking incubator rotating at 180 rpm. The bacterial growth was monitored every hour until the absorbance reached 5.5–6.0. At this point a 1 mL aliquot from each baffled flask was taken and centrifuged for 2 min at 20,000 ×*g*. The supernatant from each aliquot was discarded and the pellet was stored at –20 °C. To each baffled flask, IPTG (1 mM) was added and further incubated at 30 °C for an additional 2.5 h shaking at 180 rpm. After this time, a 1 mL aliquot from each baffled flask was taken, centrifuged and stored as described previously. The fermentation in each baffled flask was then pipetted into 50 mL tubes and centrifuged at 3,500 ×*g*. The supernatant from all 50 mL tubes was discarded and the pellets stored at –80 °C.

2.2.3.2 Mini lysis

Cell pellets harvested before and after IPTG induction were mixed with 0.5 mL lysis buffer (lysozyme (0.4% v/v), protease inhibitor (for his-tagged proteins with no metal chelator that might inhibit binding to affinity resin (IMAC)) (0.2% v/v), DNase (0.2% v/v) in 1× PBS). The resulting mixtures were incubated at 4 °C for 30 min, then an equal volume of PBS/1% Triton X-100 was added to each mixture, vortexed until the pellet was solubilised and left to incubate for a further 30 min at 4 °C. A crude extract aliquot (100 µL) was taken from each tube to perform the mini lysis with to assess the expression and then each tube was centrifuged for 30 min, 3.5 ×*g*, 4 °C. The supernatant from each tube was then carefully transferred to pre-labelled Eppendorf tubes and the pellets were re-suspended with PBST. SDS-PAGE analysis was conducted on crude extracts, pellet and supernatant prior to and after induction with IPTG.

2.2.3.3 Large-scale lysis

Each of the pellets stored at -80 °C were weighed, and for each 1 g of pellet, 20 mL of lysis buffer was added (as in method 2.2.3.2). The pellets were vortexed until homogeneous, pooled and then sonicated for 5 min. The solution containing lysed cells was then left shaking at 4 °C for 1 h, rocking gently. Afterwards, equal volume of PBS/ 1% Triton X-100 was added and the mixture sonicated for 5 min at 100%. The mixture was then left for 1 h at 4 °C, rocking gently. His_8IFN α-2a was then purified from cell debris by cross flow filtration using the QuixStand™ System with a hollow fibre cartridge, where the flow through contained the soluble protein. SDS-PAGE analysis was conducted on crude extracts, pellet and supernatant prior to and after induction with IPTG.

2.2.3.4 Immobilised metal ion affinity (IMAC) and anion exchange chromatography (AIEC) purification of His_8IFN α-2a

Prior to IMAC purification, the supernatant from the hollow fibre purification was supplemented with 20 mM imidazole. A HisPrep™ FF 16/60 column was pre-equilibrated with buffer A (PBS pH 7.4) and the supernatant obtained from the hollow fibre purification was loaded onto the column overnight at 1 mL/min. The column was then washed with 2% buffer B (PBS, 1 M imidazole pH 7.4) at a flow rate of 5 mL/min for approximately 80 mL. A linear gradient of 2–25% buffer B was

set to flow for 25 min whilst 10 mL fractions were collected. SDS-PAGE analysis was conducted on the flow-through, loading and elution fractions.

Prior to AIEC purification, fractions containing His_8IFN α-2a were pooled and diluted 4-fold using buffer C (20 mM Tris-HCl, pH 8.0). The HiPrep™ Q FF 16/60 column was pre-equilibrated with buffer C; following this the protein was loaded onto the column at 1 mL/min. The column was then washed with ~80 mL of 2% buffer D (20 mM tris-HCl, 1 M sodium chloride, pH 8.0) at 5 mL/min. A linear gradient of 2-30% buffer D was set to flow for 30 min whilst collecting 10 mL fractions. SDS-PAGE analysis was conducted on the flow-through, loading and elution fractions.

Following SDS-PAGE analysis, the fractions containing pure His_8IFN α-2a were pooled and the concentration measured by UV absorbance at 280 nm (ε=0.914, 0.9 mg/mL, 70 mL). The concentration was made to 0.5 mg/mL and the solution supplemented with 100 mM sodium chloride, 10% glycerol, protease inhibitor (dilution 1/5000), 1 mM EDTA and 1 mM sodium azide. His_8IFN α-2a was then aliquoted into 5 mL cryovials and snap-frozen in liquid nitrogen and stored at -80 °C. The production of His_8IFN α-2a was conducted three times with the yields achieved being between 60-70 mg.

2.2.4 Digestion and purification of IgG_{alb} and IgG_{beva}

2.2.4.1 Protein A purification of IgG_{alb}

Purification of IgG_{alb} was performed using Protein A to separate IgG_{alb} from albumin impurities. The IgG_{alb} mixture was loaded onto a 1 mL HiTrap Protein A HP column using an ÄKTA prime plus which had been pre-equilibrated with buffer A (20 mM sodium phosphate pH 6.5). The IgG_{alb} was eluted with 100% buffer B:0.1 M glycine pH 2.0. The IgG_{alb} mixture was manually loaded onto the column (*ca.*=10 mL), and the system was washed for 30 mL with buffer A and then 100% B was used to elute the IgG_{alb}. Throughout the manual run, 2 mL fractions were collected and for the IgG_{alb} eluted with buffer B, 200 µL of neutralising buffer (1 M Tris, 1 mM EDTA, pH 8.0) was added. SDS-PAGE was used to characterise the peak fractions and the resulting gel was stained by InstantBlue™ stain. The purest IgG_{alb} fractions were combined and buffer exchanged using a pre-equilibrated 10 mL Zeba™ spin column (1000 ×*g*, 2 min, 4 °C). The IgG_{alb} concentration was estimated by UV absorbance at

280 nm, the concentration and yield were calculated using the extinction coefficient of IgG_{alb} (ε=1.4, 0.95 mg/mL, 4.75 mg, final yield=47.5%).

2.2.4.2 Optimisation of IgG_{alb} digestion using papain

Immobilised papain was mixed by inversion to obtain an even suspension, then 1 mL of the immobilised papain was pipetted into a 15 mL tube. The Immobilised papain was resuspended into 20 mM cysteine, 2 mM EDTA, sodium phosphate pH 7.0 (digestion buffer) and centrifuged for 2 min at 4000 ×*g*. The supernatant was discarded and the step was repeated. After this, the Immobilised papain was re-suspended into 0.9 mL of the digestion buffer. Three enzyme:IgG ratios were investigated, 1:10, 1:20 and 1:50. The enzyme was pipetted into the three Eppendorf tubes containing 0.2 mg/mL of anti-rat albumin IgG. The mixtures were left to shake at speed 200 at 37 °C. Aliquots were taken at 0,1,2,3,4,5,6,8 h and 16 h. SDS-PAGE analysis was conducted on these aliquots with the resulting gels stained by InstantBlue™ and silver stain. Further, SEC analysis was conducted at 0,2,4,6 and 8 h following the method outlined by Zhao et al. 2009.

2.2.4.3 Digestion of IgG_{alb}

Immobilised papain was mixed by inversion-shaking to obtain an even suspension, then 2 mL of 50% immobilized papain was transferred into a 15 mL falcon. The gel slurry was equilibrated with digestion buffer (8 mL) (20 mM sodium phosphate, 2 mM EDTA, 20 mM cysteine, pH 7.0) and centrifuged (4 min, 400 ×*g* at RT), where the supernatant was discarded. This wash procedure was repeated, after this the gel slurry was re-suspended in 2.0 mL of digestion buffer. The digestion was conducted for 4 h at 37 °C (210 speed of shaking) in a shaker incubator and a ratio of 1:20 (w/w) of papain:purified IgG_{alb} (237.5 µg papain:4750 µg IgG_{alb}). After 4 h, the immobilised papain was removed by filtering the digestion mixture through a polypropylene barrel with polyethylene frit (left after removing medium from PD-10 column). The visible amount of papain captured by the frit was washed four times with 2 mL with buffer A (20 mM sodium phosphate pH 6.5). SDS-PAGE was carried on the digestion IgG_{alb} mixture; the resulting gel was stained using InstantBlue™.

2.2.4.4 Purification of digested IgG_{alb}

A protein A column was used to purify the Fab_{alb} from undigested IgG_{alb} and Fc_{alb}. The HiTrap Protein A HP 1 mL column was pre-equilibrated with buffer A (20 mM sodium phosphate pH 6.5); following this the digested mixture was loaded onto the column at 1 mL/min. The column was then washed with ~30 mL of buffer A and then IgG_{alb}/Fc_{alb} was eluted from the column with 100% buffer B (0.1 M glycine pH 2.0). Throughout the manual run, 2 mL fractions were collected and for the Fc_{alb} eluted with buffer B, 200 µL of neutralising buffer (1 M Tris, 1 mM EDTA, pH 8.0) was added. SDS-PAGE analysis was conducted on the flow-through, loading and elution fractions, with the resulting gel analysed by InstantBlue™. The Fab_{alb} fractions were combined and concentrated in a pre-equilibrated Vivaspin 10,000 MWCO (3000 ×*g*, 30 min, 4 °C). Once the Fab_{alb} is concentrated to *ca.*=2 mL, the Fab_{alb} was diluted to 20 mL with reaction buffer (50 mM sodium phosphate, 20 mM EDTA, 150 mM sodium chloride, 0.01% Tween-20, pH 8.2). This was repeated thrice, until the Fab_{alb} (2 mL) was buffer exchanged into the reaction buffer. The Fab_{alb} concentration was estimated by UV absorbance at 280 nm, the concentration and yield were calculated using the extinction coefficient of Fab_{alb} (ε=1.4, 0.67 mg/mL, 1.99 mg, final yield=41.9%). SDS-PAGE was conducted on the Fab_{alb} and the resulting gel was stained with InstantBlue™.

2.2.4.5 Digestion of IgG_{beva}

Immobilised papain was mixed by inversion-shaking to obtain an even suspension, then 1 mL of 50% immobilized papain was transferred into a 15 mL falcon. The gel slurry was equilibrated with digestion buffer (9 mL) (20 mM sodium phosphate, 2 mM EDTA, 20 mM cysteine, pH 7.0) and centrifuged (4 min, 400 ×*g* at RT), where the supernatant was discarded. This wash procedure was repeated, after this the gel slurry was re-suspended in 1.0 mL of digestion buffer. The digestion was conducted for 5.5 h at 37 °C (210 speed of shaking) in a shaker incubator and a ratio of 1:100 (w/w) of papain: IgG_{beva} (250 µg papain:25,000 µg IgG_{beva}). After 5.5 h, the immobilised papain was removed by filtering the digestion mixture through a polypropylene barrel with polyethylene frit (left after removing medium from PD-10 column). The visible amount of papain captured by the frit was washed four times with 2 mL with buffer A (100 mM Tris, 1 mM EDTA, pH 8.0). SDS-PAGE was

carried on the digestion mixture of IgG_{beva} (1 μg) and the gel was then stained using InstantBlue™.

2.2.4.6 Purification of digested IgG_{beva}

The digested IgG_{beva} was loaded onto two 1 mL HiTrap Protein A HP column using an ÄKTA prime plus fitted with two 5 mL loops which had been pre-equilibrated with buffer A (100 mM Tris, 1 mM EDTA, pH 8.0). The IgG_{beva} was eluted with 100% buffer B: 100 mM glycine pH 2.8. The digested IgG_{beva} was manually loaded onto the column (~10 mL), and the system was washed for 30 mL with buffer A and then 100% buffer B was used to elute the Fc_{beva}. Throughout the manual run, 2 mL fractions were collected and for the Fc_{beva} eluted with buffer B, 200 μL of neutralising buffer (1 M Tris, 1 mM EDTA, pH 8.0) was added. SDS-PAGE was used to characterise the peak fractions and the resulting gel was stained by InstantBlue™ stain. The Fab_{beva} fractions were combined and concentrated in a pre-equilibrated Vivaspin 10,000 MWCO (3000 ×*g*, 30 min, 4 °C). Once the Fab_{beva} is concentrated to ~2 mL, the Fab_{beva} was diluted to 20 mL with reaction buffer (50 mM sodium phosphate, 20 mM EDTA, 150 mM sodium chloride, 0.05% Tween-20, pH 8.2). This was repeated thrice, until the Fab_{beva} (2 mL) was buffer exchanged into the reaction buffer. The Fab_{beva} concentration was estimated by UV absorbance at 280 nm, the concentration and yield were calculated using the extinction coefficient of Fab_{beva} (ε=1.4, 4.89 mg/mL, 9.77 mg, final yield=39%). SDS-PAGE was conducted on the Fab_{beva} and the resulting gel was stained with InstantBlue™.

2.2.5 Synthesis and activation of PEG reagents

2.2.5.1 Activation of PEG_{20} *bis*-sulfone **1** for his-tag conjugation

To obtain an improved yield of PEG_{20}-His_8IFN and $(PEG_{20})_2$-His_8IFN conjugates**,** the PEG *bis*-sulfone reagent **1** (Table 2–1) was pre-incubated for 8 h at 37 °C in 50 mM sodium phosphate buffer pH 7.4 containing 150 mM sodium chloride. These conditions allow for the elimination of one of the β-sulfonyl groups generating a reactive PEG_{20} mono-sulfone **2** (Figure 2-1). In a similar manner, PEG_{20} di(*bis*)-sulfone **4** can be activated to PEG_{20} di(mono)sulfone **4**. The activation of PEG mono-sulfone **2** does not go to completion, thus leaving a mixture of both un-activated *bis*-sulfone and activated mono-sulfone PEG reagents.

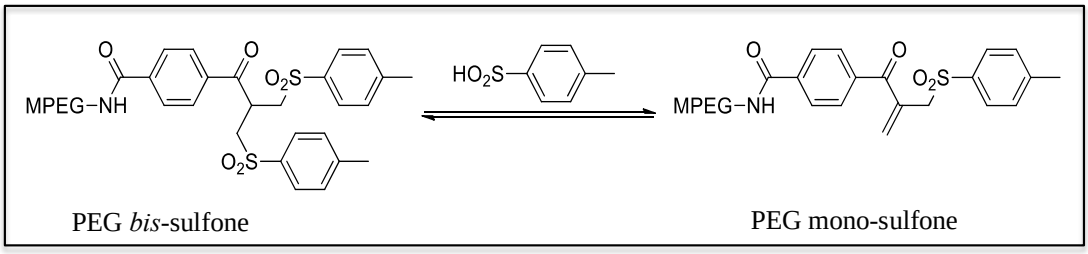

Figure 2-1. Activation of PEG *bis*-sulfone **1** reagent by the elimination of one β-sulfonyl group **3** to PEG mono-sulfone **2**.

2.2.5.2 Synthesis of PEG_{20} di(*bis*) sulfone **4** for homodimer production

PEG_{20} di(amine) **6** (20 mg, 0.001 mmol) was added to a single-neck Schlenk flask (50 mL) along with toluene (2.5 mL). The PEG was dried by azeotropic distillation by use of toluene at RT. In another single neck Schlenk flask, *bis*-sulfone linker **7** (7 mg, 5 mg/mL) was weighed and dissolved in dichloromethane. The *bis*-sulfone linker **7** was then added to the dried PEG_{20} di(amine) **6** and a magnetic stirring bar added to the mixture. The mixture was then purged with argon and the reaction mixture was left stirring for 48 h at RT. After this time, volatiles were removed by rotary evaporation at RT and the crude mixture was placed under vacuum for 15 min. The crude product was re-dissolved in acetone (5-10 mL) and filtered through a cotton-wool filled pipette into a pre-weighed centrifuge tube. The dissolved PEG was placed in dry ice for precipitation to occur and centrifuged for 30 min, at -9 °C, 4000 rpm. The supernatant was discarded and the white precipitant was re-dissolved in fresh acetone, allowed to precipitate and centrifuged as before. This procedure was repeated three times, discarding the supernatant each time. After the last round, the white precipitate was allowed to dry in vacuum at ambient temperature to afford a white solid product. The product (~7 mg) was weighed and analysed by ^{1}H-NMR (400/300 MHz).

2.2.5.3 Synthesis of PEG_{20} di(*bis*) sulfone **4** for heterodimer production

PEG_{20} di(amine) **6** (20 kDa, 1.09 mg, 54.5 μmol, 1 eq.) was dissolved in warm dry toluene (100 mL) in a round bottom flask. Residual water trapped in the PEG was removed through azeotropic distillation, and the solid was then dissolved in dry-DCM (114 mL). *Bis*-sulfide linker **9** (349 mg, 654 μmol, 12 eq.) was then added to the solution and the mixture was left stirring at RT, overnight. The mixture was then passed through a glass wool plug to filter off particulates before removing the solvent under pressure for 1 h to yield a white solid. This was then dissolved in warm

acetone (109 mL) and cooled down on dry-ice to form a white precipitate. After cooling, the sample was then centrifuged at -78 °C, 7800 rpm for 15 min and the supernatant was then decanted off. This acetone precipitation procedure was repeated twice using fresh acetone each time. Once completed, the solid was re-suspended in DCM in a round bottom flask and the solution was then dried under reduced pressure and subsequently on high vacuum, 1.1 mg of clean product (PEG_{20} di(*bis*) sulfide **8**) was recovered (96.2 % yield).

PEG_{20} di(*bis*) sulfide **8** (1.480 g, 70.5 μmol, 1 eq.) was dissolved in dry-DCM (20.5 mL) with 4-methylbenzene thiol (87.5 mg, 705 μmol, 200 eq.) in a sealed-round bottom flask and the solution as left stirring at RT, overnight. After this, the solvent was removed under reduced pressure and the resulting solid was dissolved in warm acetone (150 mL). The solution was then cooled using dry ice and precipitated by centrifugation at 7800 rpm at -78 °C for 15 min. Following this the supernatant was removed. This acetone precipitation was repeated thrice, each time using fresh acetone. The solid was then dissolved in DCM in a round bottom flask. Subsequently the solvent was removed under reduced pressure before being exposed to high vacuum for 3 h, 1.4 g of the final deactivated PEG_{20} di(*bis*) sulfide **8** product was recovered (94.6 % yield).

Following the deactivation of PEG_{20} di(*bis*) sulfide **8**, is the oxidation to di(*bis*)-sulfone PEG **4**. PEG_{20} di(*bis*) sulfide **8** (1.4 mg, 66 μmol, 1 eq.) was dissolved in a 50/50 mixture of water/methanol (50 mL) in a round bottom flask. To this solution, 246 mg of Oxone® (800 μmol, 1 eq.) was added and the reaction was allowed to proceed overnight. Methanol was removed under reduced pressure and the remaining solution was frozen after the addition of 15 mL of water. The frozen solution was then freeze dried overnight. The dried solid was then dissolved in DCM and filtered using 3 μm and 0.22 μm hydrophobic membranes successively to remove Oxone® and afford a clear solution. The DCM was the removed under high pressure and the resulting solid dried under high vacuum to give 1.38 g of PEG_{20} di(*bis*)sulfone **4** (98% yield).

2.2.5.4 Purity assessment of PEG_{20} di(*bis*)sulfone **4** by RP-HPLC

Buffer A (94% filtered water, 5% HPLC grade acetonitrile and 1% TFA) and buffer B (99% HPLC grade acetonitrile, 1% TFA) were freshly prepared. RP-HPLC was conducted using a PLRP-S (1000 Å, C3) RP column, which had been pre-

equilibrated with buffer B then buffer A. The PEG_{20} di(*bis*)sulfone **4** was injected (50 µL) onto the column and a gradient of 0% to 100% buffer B was conducted assessing the chromatogram at both 214 nm and 280 nm.

2.2.5.5 Purity assessment of PEG_{20} di(*bis*)sulfone **4** by SDS-PAGE

MES (1×; 1 L) running buffer was freshly prepared with 75 µL of antioxidant. PEG_{20} di(*bis*)sulfone **4** from synthesis routes 1 and 2 was weighed and made into a 1 mg/mL solution with purified water. A Bis-Tris (4-12 %) was then loaded with 1 and 5 µg of PEG_{20} di(*bis*)sulfone **4** from synthesis routes 1 and 2. The gel was then run for 35 min at 200 V, 500 mA. The resulting gel was stained for 1 h with InstantBlue™ and then washed for 1 h with purified water. The gel was stained with PEG stain (25 mL barium chloride, 5 mL iodine) for 5 min and rinsed for 10 min with purified water and the resulting gel was then scanned.

2.2.6 Protein reduction and re-oxidation

2.2.6.1 His_8IFN α-2a reduction using Dithiothreitol (DTT)

Dithiothreitol (0.15425 g, 1 M) was diluted in purified water (1 mL). For the complete reduction of His_8IFN α-2a, 25 mM DTT for 30 min at RT was found to be optimum. Desalting columns were used to remove the DTT from His_8IFN α-2a, and reduction was confirmed using SDS-PAGE analysis.

2.2.6.2 Glutathione re-oxidising of His_8IFN α-2a

A glutathione reoxiding solution (GSH) of 50 mM oxidized glutathione (GSSG, 30.6 mg): 50 mM reduced glutathione (GSH, 15.4 mg) was made in purified water (1 mL) and stored at -80 °C as 150 µL aliquots. Reduced His_8IFN α-2a once reacted with PEG, the un-reacted disulfide bond of His_8IFN α-2a was re-oxidised using 0.5 mM oxidised glutathione: 0.5 mM reduced glutathione for 16 h at RT. Re-oxidation of His_8IFN α-2a was confirmed using SDS-PAGE analysis.

2.2.6.3 Reduction of Fab_{beva} with Tris(2-carboxyethyl)phosphine (TCEP)

The optimum conditions established for the full reduction of Fab_{beva} were 1.4 equivalents (eq.) TCEP (0.5 M, 1 mL) for 2 h at 37 °C. After 1.5 h, SDS-PAGE analysis was conducted on the TCEP-Fab_{beva} mixture to confirm reduction.

2.2.6.4 Reduction of Fab_{alb} with DTT

DTT (0.15425 g, 1 M) was diluted in purified water (1 mL). For the complete reduction of Fab_{alb} 5 mM DTT for 30 min at RT was found be optimum. After reduction, DTT was removed using a pre-equilibrated PD-10 desalting column. SDS-PAGE analysis was used to confirm the reduction of Fab_{alb}.

2.2.7 Preparation of his-tag PEGylated His_8IFN α-2a conjugates

2.2.7.1 PEGylation of His_8IFN α-2a using PEG_{20} reagent **2** to prepare PEG_{20}-His_8IFN and $(PEG_{20})_2$-His_8IFN

The activated PEG_{20} reagent **2** (0.502 mL, 2.5 eq.) was added to the His_8IFN α-2a solution (2.837 mL at 1.41 mg/mL) and incubated at 20 °C for 16 h. The reaction mixture was then analysed by SDS-PAGE, the gel was stained with InstantBlue™ followed by PEG stain. The conjugated His_8IFN α-2a conjugate was stabilised by the addition of 50 mM sodium triacetoxyborohydride (STAB) dissolved in DMSO at 4 °C for 1.5 h (Figure 2-2). The crude mixture (2× 2.5 mL) was then buffer exchanged into 100 mM sodium acetate pH 4.0 using a pre-equilibrated PD-10 desalting column.

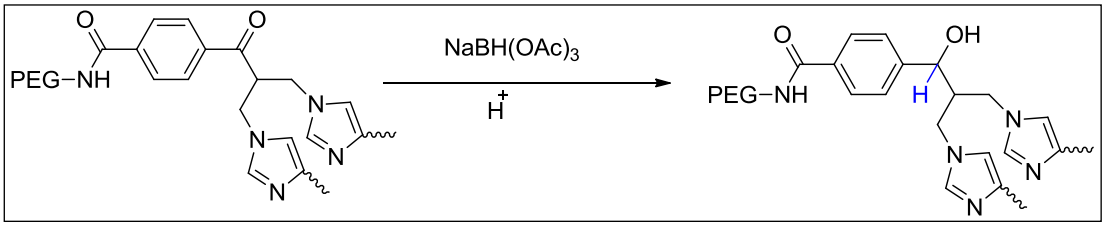

Figure 2-2. Reduction of PEG linker ketone group by STAB

2.2.7.2 Purification of the PEG_{20} mono-sulfone **2**-His_8IFN α-2a reaction mixture

Purification of the reaction mixture was performed using CIEC to separate $(PEG_{20})_2$-His_8IFN, unreacted PEG_{20} reagent **2**, PEG_{20}-His_8IFN and unconjugated His_8IFN α-2a. The reaction mixture was loaded into a 5 mL HiTrap Macrocap SP cation exchange column using an ÄKTA prime plus fitted with a 5 mL loop which had been pre-equilibrated with buffer A (100 mM sodium acetate pH 4.0). The His_8IFN α-2a species were eluted using a step gradient of buffer B (1.0 M sodium chloride in 100 mM sodium acetate pH 4.0) with the following steps 27, 36, 55 and 100%, with each step eluting over six column volumes. Fractions (2 mL) collected over the step gradient were then analysed by SDS-PAGE and stained using InstantBlue™ and PEG

stain. Fractions containing the desired conjugates were combined and centrifugally concentrated using a VivaSpin column with 10,000 MWCO at 3000 ×*g*, 4 °C until >1.5 mL. Once concentrated the PEG_{20}-His_8IFN and $(PEG_{20})_2$-His_8IFN conjugates were buffer exchanged into buffer A, to decrease the salt concentration and enable the conjugates to bind to the column during the further purification. Protein concentration and yield was estimated by measuring UV absorbance at 280 nm for both PEG_{20}-His_8IFN and $(PEG_{20})_2$-His_8IFN conjugates (1.054 mg, 26% and 0.483 mg, 12% respectively).

2.2.7.3 Further CIEC purification of PEG_{20}-His_8IFN and $(PEG_{20})_2$-His_8IFN

PEG_{20}-His_8IFN and $(PEG_{20})_2$-His_8IFN conjugates were further purified using a buffering CIEC step using the same column and buffers as in method 2.2.7.2. For PEG_{20}-His_8IFN the step gradient of buffer B was 40, 55 and 100%, with each step eluting over six column volumes, whilst for $(PEG_{20})_2$-His_8IFN the step gradient was 27, 36, 55 and 100% buffer B with each step also eluting over six column volumes. Analysis of the collected fractions was performed by SDS-PAGE, with the gels being stained with InstantBlue™, PEG stain and silver stain. Once analysed, the purest and most concentrated fractions were combined and centrifugally concentrated in a VivaSpin (10,000 MWCO) at 3000 ×*g*, 4 °C until ~1.5 mL. The concentrated PEG-His_8IFN and PEG_2-His_8IFN products (1× 2.5 mL) were then buffer exchanged into 50 mM sodium phosphate pH 7.4 containing 150 mM sodium chloride using pre-equilibrated PD-10 desalting columns. SDS-PAGE analysis was conducted on both PEG-His_8IFN and PEG_2-His_8IFN products and InstantBlue™, PEG stain and silver stain were conducted on the gels. UV absorbance at 280 nm and MicroBCA™ assay were conducted to quantify protein concentration and final yields of PEG_{20}-His_8IFN and $(PEG_{20})_2$-His_8IFN conjugates (0.7 mg, 17.6% and 0.29 mg, 7.13% respectively).

2.2.7.4 Conjugation of His_8IFN α-2a with PEG_{20} di(mono)sulfone **5** to prepare His_8IFN-PEG_{20}-His_8IFN

Pre-activated PEG_{20} di(*bis*)sulfone **5** (0.515 mL,1 eq.) was added to His_8 IFN α-2a solution (0.5 mL at 3 mg/mL) and incubated overnight (16 h) at 20 °C. Analysis of the reaction mixture was performed by SDS-PAGE, with the resulting gels initially stained by InstantBlue™ followed by PEG stain. To prevent de-PEGylation the conjugated His_8IFN α-2a conjugates were stabilised by the addition of 100 mM

STAB dissolved in DMSO at 4 °C for 1.5 h. The crude mixture was then buffer exchanged into 100 mM sodium acetate pH 4.0 using a pre-equilibrated PD-10 desalting column.

2.2.7.5 Purification of His_8IFN-PEG_{20}-His_8IFN using CIEC

Purification of PEG_{20} di(mono)sulfone-His_8IFN α-2a reaction mixture was performed using CIEC to separate PEG_{20}-His_8IFN, His_8IFN-PEG_{20}-His_8IIFN, unreacted PEG di(mono)sulfone **5** and unconjugated His_8IFN α-2a. The reaction mixture was loaded into a 5 mL HiTrap Macrocap SP CIEC column using an ÄKTA prime plus fitted with a 5 mL loop which had been pre-equilibrated with buffer A (100 mM sodium acetate pH 4.0). A buffer B (1 M sodium chloride, 100 mM sodium acetate pH 4.0) step gradient of 27, 36, 55, 80 and 100 % was used to elute the different His_8IFN α-2a species. Fractions collected were then analysed by SDS-PAGE and stained using silver stain. Fractions containing PEG_{20}-His_8IFN and His_8IFN-PEG_{20}-His_8IFN were combined and centrifugally concentrated using a VivaSpin column with 10,000 MWCO at 3000 ×*g*, 4 °C until ~1.5 mL. Once concentrated PEG_{20}-His_8IFN and His_8IFN-PEG_{20}-His_8IFN conjugates were buffer exchanged into 50 mM sodium phosphate containing 150 mM sodium chloride pH 7.4 for size exclusion chromatography (SEC). The protein concentration and yield was estimated by measuring UV (abs= 280 nm) for the PEG_{20}-His_8IFN and His_8IFN-PEG_{20}-His_8IFN (0.092 mg/mL, 3% yield and 0.407 mg/mL, 13.5% yield respectively).

2.2.7.6 Further purification of His_8IFN-PEG_{20}-His_8IFN using SEC

SEC was used to separate His_8IFN-PEG_{20}-His_8IFN from native His_8IFN α-2a. The mixture was loaded into a 120 mL Superdex™ 200 prep grade column 16/60 using an ÄKTA prime plus fitted with a 2 mL loop which had been pre-equilibrated with 50 mM sodium phosphate containing 150 mM sodium chloride pH 7.4. The protein conjugates were eluted according size over one column volume (120 mL), and the fractions collected (2 mL) analysed using SDS-PAGE. The resulting gel was stained using silver stain and the purest fractions of His_8IFN-PEG_{20}-His_8IFN were combined and centrifugally concentrated using pre-equilibrated VivaSpin column with 10,000 MWCO at 3000 ×*g*, 4 °C until ~1.5 mL. The His_8IFN-PEG_{20}-His_8IFN concentration

and yield (0.030 mg/mL, ~1.5%) was estimated by UV absorbance (280 nm) and MicroBCA™ assay.

2.2.8 Preparation of disulfide conjugated IFN conjugates

2.2.8.1 Optimisation of PEG_{20} *bis*-sulfone **1** molar equivalents for PEG_{20}-IFN and $(PEG_{20})_2$-IFN preparation

His_8IFNα-2a (0.438 mg/mL, 0.1 mL) was reduced using 20 mM DTT for 30 min at RT. After reduction DTT was removed by PD-10 buffer exchange using a pre-equilibrated PD-10 column. Scouting experiments were conducted with increasing molar equivalents (eq.) of PEG_{20} *bis*-sulfone **1** ranging from 0.8 to 2.5 eq. (Table 2–2). The reactions were allowed to proceed for 4 h at 4 °C, then 1 mM GRS solution (2 µL) was added and the reaction mixture as allowed to react for a further 16 h at 4 °C. After the incubation period the reaction mixture was assessed using SDS-PAGE analysis.

Table 2–2: Molar equivalents of PEG_{20} *bis*-sulfone **1** tested to prepare disulfide conjugated PEG_{20}-IFN and $(PEG_{20})_2$-IFN

Reagent	Molar equivalent	Volume (µL)
PEG_{20} *bis*-sulfone **1** (20 mg/mL)	0.8	0.85
	1.0	1.0
	1.5	1.6
	2.0	2.0
	2.5	2.7

2.2.8.2 Disulfide conjugation of IFN with PEG_{20} *bis*-sulfone **1**

His_8IFN α-2a (5 mg; 4.875 mL) was reduced using DTT (1 M, 15.4 mg, 125 µL) for 30 min at RT. Once reduced, DTT was removed from the His_8IFN α-2a solution by buffer exchange using two pre-equilibrated PD-10 columns. The concentration was quantified using UV at absorbance 280 nm (0.797 mg/mL, 6.5 mL) and was diluted to 0.5 mg/mL (10 mL). PEG_{20} *bis*-sulfone **1** was weighed (5.9 mg) and added to the reduced His_8IFN α-2a (250 µL) in a 1:1 ratio (PEG_{20} *bis*-sulfone **1**:IFN). The PEG_{20}-IFN reaction mixture was left to react for 3 h at RT, then 1 mM GRS (50 µL of 50 mM GSH:50 mM GSSG in 50 mM sodium acetate pH 4.0) was added, and the reaction allowed to proceed for a further 16 h at 20 °C. SDS-PAGE analysis was conducted the reaction mixture prior to CIEC purification.

2.2.8.3 CIEC purification of PEG_{20} *bis*-sulfone **1**- IFN reactions mixture

CIEC purification of the reaction mixture was performed to separate $(PEG_{20})_2$-IFN, unreacted PEG_{20} reagent **1**, PEG_{20}-IFN and unconjugated His_8IFN α-2a. The reaction mixture was loaded onto a 5 mL HiTrap Macrocap SP column using an ÄKTA prime which had been pre-equilibrated with buffer A (100 mM sodium acetate pH 4.0). The protein conjugates were eluted with a step gradient of buffer B (1.0 M sodium chloride in 100 mM sodium acetate pH 4.0) where the reaction mixture was loaded manually onto the column (*ca*.=10 mL), and the system was washed for 30 mL, then the method in Table 2–3 was conducted.

Table 2–3. CIEC purification method for PEG_{20} *bis*-sulfone **1**-IFN reaction mixture

Volume (mL)	% Buffer B	Flow Rate (mL/ min)	Fraction Size (mL)	Position	Auto zero
0.0	0	2.0	0	Load	No
2.0	0	2.0	0.0	Load	Yes
20.0	0	2.0	1.5	Load	No
20.1	40	2.0	1.5	Load	No
60.1	40	2.0	1.5	Load	No
60.2	45	2.0	1.5	Load	No
100.2	45	2.0	1.5	Load	No
100.3	55	2.0	1.5	Load	No
140.3	55	2.0	1.5	Load	No
140.4	100	2.0	1.5	Load	No
180.4	100	2.0	1.5	Load	No
180.5	0	2.0	0.0	Load	No
220.5	0	2.0	0.0	Load	No

Fractions collected were then analysed by SDS-PAGE and stained using InstantBlue™ and PEG stain. Fractions containing the desired conjugates were combined and centrifugally concentrated using a VivaSpin column with 10,000 MWCO at 3000 ×*g*, 4 °C until ~1.5 mL. Once concentrated the PEG_{20}-IFN and $(PEG_{20})_2$-IFN conjugates were buffer exchanged into 50 mM sodium phosphate containing 20 mM EDTA pH 7.8. Protein concentration was estimated by measuring UV absorbance at 280 nm and was confirmed by MicroBCA assay for both PEG_{20}-IFN and $(PEG_{20})_2$-IFN conjugates (330 μg/mL, 147.5 μg/mL respectively). Then approximate yield was calculated for both PEG_{20}-IFN and $(PEG_{20})_2$-IFN conjugates (28.8% and 12% respectively).

2.2.8.4 Disulfide conjugation of IFN with PEG_{10} *bis*-sulfone **1**

His_8IFN α-2a (3 mg; 4.875 mL) was reduced using DTT (1 M, 15.4 mg, 125 µL) for 30 min at RT. Once reduced, DTT was removed from the His_8IFN α-2a solution by buffer exchange using two pre-equilibrated PD-10 columns. The concentration was quantified using UV at absorbance 280 nm (0.480 mg/mL, 7 mL) and was diluted to 0.5 mg/mL (10 mL). PEG_{10} *bis*-sulfone **1** was weighed (2.2 mg) and added to the reduced His_8IFN α-2a (220 µL) in a 1:1 ratio (PEG_{10} *bis*-sulfone **1**:IFN). The PEG_{10} *bis*-sulfone **1**-IFN reaction mixture was left to react for 3 h at RT, then 1 mM GRS (204.1 µL of 50 mM GSH:50 mM GSSG in 50 mM sodium acetate pH 4.0) was added, and the reaction was allowed to proceed for a further 16 h at 20 °C. SDS-PAGE analysis was conducted the reaction mixture prior to CIEC purification.

2.2.8.5 CIEC purification of PEG_{10} *bis*-sulfone **1**-IFN reaction mixture

Purification of the PEG_{10} *bis*-sulfone **1**-IFN reaction mixture was performed in the same procedure outlined in method 2.2.8.3, however the ÄKTA prime method used was optimised to the following percentages of buffer B: 0, 50, 55, 60 and 100. The protein concentration was estimated by measuring UV absorbance at 280 nm for both PEG_{20}-IFN and $(PEG_{20})_2$-IFN conjugates (1 mg/mL = 0.130 and 0.261 Abs=280 nm respectively) and then approximate yield was calculated (14% and 16% respectively).

2.2.8.6 Disulfide conjugation of His_8IFN α-2a with PEG_5 *bis*-sulfone **1**

His_8IFN α-2a (4.18 mg/mL; 4 mL) was reduced using DTT (1 M, 15.4 mg, 80 µL) for 30 min at RT. Once reduced, DTT was removed from the His_8IFN α-2a solution by buffer exchange using two pre-equilibrated PD-10 columns. The concentration was quantified using UV at absorbance 280 nm (0.523 mg/mL, 7 mL). PEG 5 kDa *bis*-sulfone **1** was weighed (2.1 mg) and added to the reduced His_8IFN α-2a (430 µL) in a 1:1 ratio (PEG_5 *bis*-sulfone **1**:IFN). The PEG_5 *bis*-sulfone **1**-His_8IFN α-2a reaction mixture was left to react for 3 h at RT, then 1 mM GRS (142.9 µL of 50 mM GSH:50 mM GSSG in 50 mM sodium acetate pH 4.0) was added, and the reaction was allowed to proceed for a further 16 h at 20 °C. SDS-PAGE analysis was conducted the reaction mixture prior to CIEC purification.

2.2.8.7 CIEC purification of PEG_5 *bis*-sulfone **1**-IFN reaction mixture

Purification of the PEG_5 *bis*-sulfone **1**- His_8IFN α-2a reaction mixture was performed in the same procedure outlined in method 2.2.8.3, however the ÄKTA prime method used was optimised to the following percentages of buffer B: 0, 48, 55, 60 and 100. The protein concentration was estimated by measuring UV absorbance at 280 nm for both PEG_5-IFN and $(PEG_5)_2$-IFN conjugates (0.304 mg/mL and 0.36 mg/mL respectively) and the approximate yield was calculated (29% and 34.5% respectively).

2.2.8.8 Disulfide conjugation of IFN with PEG_{20} di(*bis*)sulfone **4** to prepare IFN-PEG_{20}-IFN

His_8IFN α-2a (2 mg/mL, 5 mL) was buffer exchanged into 50 mM sodium phosphate 20 mM EDTA pH 7.8 using two pre-equilibrated PD-10 columns. His_8IFN α-2a was reduced using 25 mM DTT (1 M, 15.8 mg, 180 µL) for 30 min. The reduced His_8IFN α-2a was buffer exchanged into 50 mM sodium phosphate 20 mM EDTA pH 7.8 using three pre-equilibrated PD-10 columns. The concentration was quantified using UV at absorbance 280 nm (0.752 mg/mL, 11 mL) and was diluted to 0.5 mg/mL (15 mL), where half (7.5 mL, 4.1 mg) of this reduced His_8IFN α-2a was used for the synthesis of IFN-PEG_{10}-IFN. PEG_{20} di(*bis*)sulfone **4** was weighed (2.5 mg) and added to the reduced His_8IFN α-2a (106 µL) in a 2:1 ratio (PEG_{20} di(*bis*)sulfone **4**:IFN). The PEG_{20} di(*bis*)sulfone-His_8-IFN α-2a reaction mixture was left to react for 5 h at 20 °C, then 1 mM GRS (153.1 µL of 50 mM GSH:50 mM GSSG in 50 mM sodium acetate pH 4.0) was added, and the reaction was allowed to proceed for a further 16 h at 20 °C. SDS-PAGE analysis was conducted the reaction mixture prior to and after GRS addition. The IFN-PEG_{20}-IFN conjugate was then stabilized by the addition of 100 mM STAB dissolved in DMSO at 4 °C for 1.5 h. The reaction mixture (7.5 mL) was then buffer exchanged into 100 mM sodium acetate pH 4.0 using three pre-equilibrated PD-10 desalting columns.

2.2.8.9 Disulfide conjugation of IFN with PEG_{10} di(*bis*)sulfone **4** to prepare IFN-PEG_{10}-IFN

Reduced His_8IFN α-2a (7.5 mL, 4.1 mg) from method 2.2.8.8 was used for this reaction. PEG_{10} di(*bis*)sulfone **4** was weighed (2.9 mg) and added to the reduced His_8IFN α-2a (110 µL) in a 2:1 ratio (PEG_{20} di(*bis*)sulfone **4**:IFN). The PEG_{10}

di(*bis*)sulfone **4**-IFN mixture was left to react for 5 h at 20 °C, then 1 mM GRS (153.1 µL of 50 mM GSH:50 mM GSSG in 50 mM sodium acetate pH 4.0) was added, and the reaction was allowed to proceed for a further 16 h at 20 °C. SDS-PAGE analysis was conducted the reaction mixture prior to and after GRS addition. The IFN-PEG_{10}-IFN conjugate was then stabilized by the addition of 100 mM STAB dissolved in DMSO at 4 °C for 1.5 h. The reaction mixture (7.5 mL) was then buffer exchanged into 100 mM sodium acetate pH 4.0 using three pre-equilibrated PD-10 desalting columns.

2.2.8.10 CIEC purification of IFN-PEG_{20}-IFN and IFN-PEG_{10}-IFN reaction mixtures

CIEC purification of the reaction mixtures was performed to separate unreacted PEG reagent **4**, PEG-IFN from IFN-PEG-IFN and unconjugated His_8IFN α-2a, which would be separated using SEC (method 2.2.8.11). The reaction mixture was loaded onto a 5 mL Macrocap SP ion exchange column using an ÄKTA prime plus fitted with two 5 mL loops which had been pre-equilibrated with buffer A (100 mM sodium acetate pH 4.0). The protein conjugates were eluted with a step gradient of buffer B: 1.0 M sodium chloride in 100 mM sodium acetate pH 4.0 of 45,55 and 100%. Fractions collected were then analysed by SDS-PAGE and stained using InstantBlue™ and silver stain. Fractions (57-63 and 60-62) containing IFN-PEG_{20}-IFN+His_8IFN α-2a, IFN-PEG_{10}-IFN+His_8IFN α-2a mixtures respectively were combined and centrifugally concentrated using a VivaSpin column with 10,000 MWCO at 3000 ×*g*, 4 °C until >1.5 mL. The mixtures were buffer exchanged using pre-equilibrated NAP-10 columns into 50 mM sodium phosphate containing 150 mM sodium chloride pH 7.8. Protein concentration and yield was calculated by measuring UV absorbance at 280 nm for both IFN-PEG_{20}-IFN+His_8IFN α-2a, IFN-PEG_{10}-IFN+His_8IFN α-2a mixtures (0.682 mg/mL, 27.3% and 1.12 mg/mL, 27.3% respectively).

2.2.8.11 SEC purification of IFN-PEG_{20}-IFN and IFN-PEG_{10}-IFN mixtures

SEC purification of IFN-PEG_{20}-IFN + His_8IFN α-2a and IFN-PEG_{10}-IFN + His_8IFN α-2a mixtures was performed to separate His_8IFN α-2a from IFN-PEG_{20}-IFN and IFN-PEG_{10}-IFN. The mixtures were loaded separately onto the Superdex 200 Prep Grade Column 16/60 120 mL column, which had been pre-equilibrated with 50 mM sodium phosphate containing 20 mM EDTA pH 7.8 using an ÄKTA prime, plus

fitted with a 2 mL loop. The protein conjugates were eluted over 120 mL and the fractions collected were then analysed by SDS-PAGE and stained using silver stain. Fractions (26-29 and 22-28) containing IFN-PEG_{20}-IFN or IFN-PEG_{10}-IFN were combined and centrifugally concentrated using a VivaSpin column with 10,000 MWCO at 3000 ×*g*, 4 °C until >1.5 mL. Protein concentration for both IFN-PEG_{20}-IFN and IFN-PEG_{10}-IFN were estimated by measuring UV absorbance at 280 nm and confirmed by MicroBCA assay (0.035 and 0.046 mg/mL respectively). Final yields for IFN-PEG_{20}-IFN and IFN-PEG_{10}-IFN conjugates were 1.4% and 1.12% respectively. SDS-PAGE analysis was carried on the final conjugates.

2.2.9 Preparation of disulfide PEGylated IFN-PEG-Fab heterodimer conjugates and PEG-Fab controls

2.2.9.1 Optimisation of TCEP equivalents for Fab_{beva} reduction

Fab_{beva} (0.38 mg/mL, 0.19 mg) in reaction buffer (50 mM sodium phosphate, 150 mM sodium chloride, 40 mM EDTA, 0.05% Tween-20 pH 8.2) was pipetted into five 0.1 mL aliquots. TCEP (0.5 mM) was then diluted using purified water. The ratios of TCEP were then added to the Fab_{beva} aliquots following Table 2–4 volumes. All TCEP eq. volumes were made up to 2.74 µL by the addition of extra reaction buffer, to keep the concentration of Fab_{beva} the same throughout. The aliquots were then left for 2 h at 37 °C. After 1.5 h, SDS-PAGE analysis was conducted on the TCEP-Fab_{beva} mixtures to determine the optimum eq. for full reduction of Fab_{beva}. It was determined that 1.4 eq. of TCEP enough to reduce Fab_{beva} after 2 h incubation at 37 °C.

Table 2–4. Fab_{beva} reduction optimisation with TCEP: molar equivalents and volumes

Reagent	Molar equivalent	Volume (µL)
TCEP (2.1 mM)	1	1.52
	1.2	1.82
	1.4	2.12
	1.8	2.74

2.2.9.2 Optimisation of PEG_{20} *bis*-sulfone **1** equivalents for PEG_{20}-Fab_{beva}

A 100 µL aliquot of Fab_{beva} at 3.02 mg/mL was defrosted at RT. From a stock of 0.5 M TCEP a 2.1 mM TCEP stock was prepared using purified water. Fab_{beva} (150 µg) was reduced using 2 µL of 2.1 mM TCEP stock, resulting in the final molar equivalents of TCEP being 1.4. The mixture was then incubated at 37 °C for 2 h.

After 1.5 h SDS-PAGE analysis was conducted on the TCEP-Fab_{beva} mixture to confirm reduction.

Following completion of reduction of Fab_{beva} with TCEP, different molar equivalents (1,1.2, 1.5,1.7, 2 eq.) of PEG_{20} *bis*-sulfone **1** were trialled to optimise yield of PEG_{20}-Fab_{beva}.Fab_{beva} (20 μg, 6.9 μL) was pipetted into five 0.5 tubes and Table 2–5 was followed for the addition of PEG_{20} *bis*-sulfone **1**. All PEG_{20} *bis*-sulfone **1** eq. volumes were made up to 3.2 μL by the addition of extra reaction buffer, to keep the concentration of Fab_{beva} the same throughout. The reactions were allowed to proceed for 16 h at 25 °C.

Table 2–5. Conjugation of Fab_{beva} to PEG_{20} *bis*-sulfone **1** optimisation: amounts and volumes used of reagent.

Reagent	Molar equivalent	Volume (μL)
PEG_{20} *bis*-sulfone **1** (5 mg/mL)	1	1.59
	1.2	1.92
	1.5	2.4
	1.7	2.72
	2	3.2

After 16 h, SDS-PAGE analysis was conducted on all reactions and densimetric analysis was conducted on the InstantBlue™ stained gel using ImageQuant™. It was found that 2 eq. of PEG_{20} *bis*-sulfone **1** was optimum for PEG_{20}-Fab_{beva} production.

2.2.9.3 Disulfide conjugation of Fab_{beva} with PEG_{20} *bis*-sulfone **1** to prepare PEG_{20}-Fab_{beva}

Three 100 μL aliquots of Fab_{beva} at 3.02 mg/mL was defrosted at RT and pooled. From a stock of 0.5 M TCEP a 14 mM TCEP stock was prepared using purified water. Fab_{beva} (1 mg, *ca.*=331 μL) was reduced using 2 μL of 14 mM TCEP stock, resulting in the final molar equivalents of TCEP being 1.4. The mixture was then incubated at 37 °C for 2 h. After 1.5 h SDS-PAGE analysis was conducted on the TCEP-Fab_{beva} mixture to confirm reduction.

Following completion of reduction of Fab_{beva} with TCEP, 2.0 eq PEG_{20} *bis*-sulfone **1** (40 mg/mL, 20 μL) was added and the reaction allowed to proceed for 16 h at 25 °C. After 16 h, SDS-PAGE analysis was conducted on the reaction mixture.

2.2.9.4 Optimisation of CIEC purification of PEG_{20}-Fab_{beva} reaction mixture

The reaction mixture from method 2.2.9.3 (*ca.* 353 µL) was diluted 8.3× in buffer A (100 mM sodium acetate pH 4.0, 0.01% Tween-20 (*ca.*=2.9 mL). The reaction mixture was purified by CIEC using a HiTrap Macrocap SP column connected to an AKTA prime plus purifier, which had been pre-equilibrated with buffer A. To determine the percentage of buffer B (100 mM sodium acetate, 1 M sodium chloride, 0.01% Tween-20 pH 4.0) at which the conjugates elute a linear gradient was performed from 0-100 % buffer B over 30 mL. The peak fractions (27-45) collected were then analysed by SDS-PAGE and stained using InstantBlue™ and PEG stain.

Fractions 29 to 45 were pooled and diluted 10× with buffer A (*ca.*=340 mL). The diluted protein was then re-loaded onto the pre-equilibrated HiTrap Macrocap SP column at 5 mL/min. The CIEC step gradient shown in Table 2–6 was then used to purity PEG_{20} *bis*-sulfone **1**-Fab_{beva} reaction mixture. The peak fractions (5-32) were then analysed by SDS-PAGE.

Table 2–6. Details of first CIEC step gradient used to purity PEG_{20} *bis*-sulfone 1-Fab_{beva}

Volume (mL)	% Buffer B	Flow Rate (mL/ min)	Fraction Size (mL)	Position	Auto zero
0.0	0	5.0	0	Load	No
2.0	0	5.0	0.0	Load	Yes
10.0	0	5.0	2.0	Load	No
10.1	14	5.0	2.0	Load	No
30.1	14	5.0	2.0	Load	No
30.2	20	5.0	2.0	Load	No
60.2	20	5.0	2.0	Load	No
60.3	100	5.0	2.0	Load	No
65.3	100	5.0	2.0	Load	No
65.4	0	5.0	0.0	Load	No
95.4	0	5.0	0.0	Load	No

2.2.9.5 CIEC purification of PEG_{20} *bis*-sulfone **1**-Fab_{beva}

From the first CIEC in method 2.2.9.5, no separation was between PEG_{20}-Fab_{beva} and Fab_{beva} was observed in the SDS-PAGE analysis. Therefore, fractions 6-31 were pooled and diluted 10× with buffer A (*ca.*=468 mL). The diluted mixture was re-loaded onto the pre-equilibrated HiTrap Macrocap SP column at 5 mL/min. The second step gradient method shown in Table 2–7 was followed.

Table 2–7. Second CIEC step gradient method for purifying PEG_{20} *bis*-sulfone **1**-Fab_{beva}

Volume (mL)	% Buffer B	Flow Rate (mL/ min)	Fraction Size (mL)	Position	Auto zero
0.0	0	5.0	0	Load	No
2.0	0	5.0	0.0	Load	Yes
10.0	0	5.0	2.0	Load	No
10.1	17	5.0	2.0	Load	No
30.1	17	5.0	2.0	Load	No
30.2	30	5.0	2.0	Load	No
60.2	30	5.0	2.0	Load	No
60.3	100	5.0	2.0	Load	No
90.3	100	5.0	2.0	Load	No
90.4	0	5.0	0.0	Load	No
120.4	0	5.0	0.0	Load	No

The peak fractions (5-14, 15-25, 29-35) were then analysed by SDS-PAGE and the resulting gel was stained by InstantBlue™ and PEG stain. Fractions 5-13 were pooled (*ca.*=18 mL) and centrifugally concentrated in a pre-equilibrated Vivaspin MWCO 10,000 at 4 °C, 3000 ×*g*. The concentrated PEG_{20}-Fab_{beva} (*ca.*=1 mL) was then buffer exchanged into 1×PBS using a pre-equilibrated NAP-10 column; 1 mL of conjugate was loaded onto the column and eluted. PSB (1×, 1.5 mL) was loaded onto the column and the conjugate eluted and collected in a 2 mL tube. Protein concentration for both PEG_{20}-Fab_{beva} was estimated by measuring UV absorbance at 280 nm (0.440 mg/mL). The final yield for PEG_{20}-Fab_{beva} was 44% and then SDS-PAGE analysis was conducted on the final conjugate were the resulting gel was stained by InstantBlue™ and PEG stain.

2.2.9.6 Disulfide conjugation of Fab_{beva} with PEG_{20} di(*bis*)sulfone **4** to prepare Fab_{beva}-PEG_{20}-X

Fab_{beva} was reduced following method 2.2.6.3, the reduced Fab_{beva} (4 mg, 2 mL) in 50 mM sodium phosphate, 150 mM sodium chloride, 20 mM EDTA, 0.005% Tween-20 pH 8.2 was allowed to react with 2 eq. PEG_{20} di(*bis*)sulfone **4**. PEG_{20} di(*bis*)-sulfone **4** was solubilised in 50 mM sodium phosphate, 150 mM sodium chloride, and 20 mM EDTA pH 7.4. The reaction was allowed to proceed for 2 h at 25℃. After this time, SDS-PAGE analysis of the reaction mixture was conducted and the subsequent gel was stained by InstantBlue™ and PEG stain (BaI_2).

2.2.9.7 CIEC purification of PEG_{20} di(*bis*)sulfone **4**-Fab_{beva} (Fab_{beva}-PEG_{20}-X)

The PEG_{20} di(*bis*)sulfone **4**-Fab_{beva} reaction mixture (*ca.*=5 mL) was diluted 10× (*ca.*=50 mL) in buffer A (100 mM sodium acetate pH 4.0) and was manually loaded onto a 5 mL Macrocap SP ion exchange column using an ÄKTA prime plus which had been pre-equilibrated with buffer A. The protein conjugates were eluted with a linear gradient over 30 mL with a target of 100% buffer B:100 mM sodium acetate, 1 M sodium chloride pH 4.0. Fractions collected were then analysed by SDS-PAGE and stained using InstantBlue™ and PEG stain (BaI_2). Fractions (3-27) containing X-PEG_{20}-Fab_{beva} were combined, centrifugally concentrated and buffer exchanged into 50 mM sodium phosphate, 150 mM sodium chloride, 20 mM EDTA pH 7.8 using a pre-equilibrated VivaSpin column with 10,000 MWCO at 3000 ×g, 4 °C until >1.5 mL. The protein concentration of Fab_{beva}-PEG_{20}-X was estimated using UV absorbance 280 nm (4.35 mg/mL, ε=1.4).

2.2.9.8 Conjugation of IFN with Fab_{beva}-PEG-X to prepare IFN-PEG_{20}-Fab_{beva}

IFN was reduced according to method 2.2.6.1, the reduced IFN (2 eq, 3.55 mg) was then added to Fab_{beva}-PEG_{20}-X (1 eq.) and the reaction allowed to proceed for 5 h at 25 °C. After this time, glutathione re-oxidising solution was added the reaction mixture and the re-oxidising of IFN was allowed to proceed for 16 h at 25 °C. The IFN-PEG_{20}-Fab_{beva} reaction mixture was then stabilised by the addition of 100 mM STAB dissolved in DMSO at 4 °C for 1.5 h (Figure 2-2). The crude mixture (*ca.*= 6 mL) was then diluted 10-fold in 100 mM sodium acetate pH 4.0 for CIEC.

2.2.9.9 CIEC purification of the IFN-PEG_{20}-Fab_{beva} reaction mixture

The IFN-PEG_{20}-Fab_{beva} reaction mixture (*ca.*=60 mL) was manually loaded onto a 5 mL Macrocap SP cation exchange column using an ÄKTA prime plus which had been pre-equilibrated with buffer A (100 mM sodium acetate pH 4.0). The protein conjugates were eluted with a step gradient of buffer B:1.0 M sodium chloride in 100 mM sodium acetate pH 4.0 of 30,60, 80 and 100%. Fractions collected were then analysed by SDS-PAGE and stained using InstantBlue™ and PEG stain. Fractions (27-31) containing IFN-PEG_{20}-Fab_{beva} were combined, centrifugally concentrated and buffer exchanged into 50 mM sodium phosphate containing 150 mM sodium chloride pH 7.8 using a pre-equilibrated VivaSpin column with 10,000 MWCO at 3000 ×*g*, 4 until ~2 mL. Protein concentration was estimated by measuring UV

absorbance at 280 nm for IFN-PEG_{20}-Fab_{beva} (Fab: ε=1.4 0.489 mg/mL, yield=12%; IFN: ε=0.914, 0.749 mg/mL, yield=21%).

2.2.9.10 Optimisation of Fab_{alb} reduction using DTT

Fab_{alb} (0.736 mg/mL; 10 μL aliquots) was reduced using 2.5, 5, 10 mM DTT for 1 h at RT. The reduced Fab_{alb} mixtures were then analysed using SDS-PAGE. The resulting SDS-PAGE gel was stained using InstantBlue™. It was observed that 5 mM was required to fully reduce Fab_{alb}.

2.2.9.11 Control Fab_{alb}-PEG_{20} *bis*-sulfone reaction

To confirm site-specific disulfide conjugation of Fab_{alb}, a control reaction was conducted. Fab_{alb} (10 μg; 0.15 mL) (in 50 mM sodium phosphate, 20 mM EDTA, 50 mM sodium chloride) was not reduced and incubated for 5 h at RT with PEG_{20} *bis*-sulfone **1** in a ratio of 1:1 PEG:Fab. The mixture was analysed by SDS-PAGE, with the resulting gel stained with InstantBlue™ and PEG stain. PEG *bis*-sulfone **1** was also run on the gel for comparison.

2.2.9.12 Optimisation of reaction buffer pH to prepare PEG_{20}.Fab_{alb}

Fab_{alb} (0.736 mg/mL, 1.0 mL) was reduced with 5 mM DTT for 1 h at RT. Confirmation of reduction was conducted by SDS-PAGE. To remove the DTT the reduced Fab_{alb} was buffer exchanged into 50 mM sodium phosphate, 40 mM EDTA, 150 mM sodium chloride (reaction buffer) pH 6.5, pH 7.0 and pH 7.4 by pre-equilibrated PD-10 columns. Fab_{alb} (1 eq., 1 mL) was reacted with PEG_{20} *bis*-sulfone **1** (1 eq., 20 mg/mL) for 1,3,16 h at 25 °C at each pH (Table 2–8). SDS-PAGE analysis was conducted at each time point to monitor the reactions. The optimum reaction conditions to prepare PEG_{20}-Fab_{alb} were found to be pH 6.5 for 3 h.

Table 2–8: Conjugation of Fabalb to PEG_{20} *bis*-sulfone 1 optimum pH determination, conditions and volumes used for reactions

Reaction buffer pH	Fab_{alb} concentration (mg)	Volume (μL) of PEG_{20} *bis*-sulfone 1
6.5	0.171	3.41
7.0	0.197	3.94
7.4	0.196	3.90

2.2.9.13 Disulfide conjugation of Fab_{alb} with PEG_{20} *bis*-sulfone **1**-Fab_{alb} to prepare PEG_{20}-Fab_{alb}

Fab_{alb} (0.3 mg/mL, 1.0 mL) was defrosted at RT, and then reduced using 20 mM DTT for 1 h at RT. Confirmation of reduction was conducted by SDS-PAGE. To remove the DTT, the reduced Fab_{alb} was buffer exchanged into 50 mM sodium phosphate, 20 mM EDTA, 150 mM sodium chloride and 0.01% Tween-20 pH 6.5 (reaction buffer) by pre-equilibrated PD-10 column. The reduced Fab_{alb} concentration was assessed by UV absorbance (280 nm, 0.285 mg/mL, 2 mL). PEG_{20} *bis*-sulfone **1** was weighed out (3.4 mg) and solubilised in reaction buffer (20 mg/mL, 170 μL). The PEG_{20} *bis*-sulfone **1** (0.163 mg, 8.15 μL) was then added in a 1:1 eq. ratio to the reduced Fab_{alb} and the reaction allowed to proceed for 4 h at 25 °C. After overnight incubation, SDS-PAGE was conducted on the reaction mixture and the resulting gel was stained by InstantBlue™ and PEG stain.

2.2.9.14 SEC purification of PEG_{20} *bis*-sulfone **1**-Fab_{alb} reaction mixture

The PEG_{20} *bis*-sulfone **1**-Fab_{alb} reaction mixture from method 2.2.9.12 was purified by SEC purification in an effort to separate PEG_{20}-Fab_{alb} from Fab_{alb} and high MW impurities ((PEG_n)-Fab_{alb}). The mixture was loaded onto the Superdex 200 Prep Grade Column 16/60 120 mL column, which had been pre-equilibrated with 50 mM sodium phosphate containing 20 mM EDTA pH 7.8 using an ÄKTA prime, plus fitted with a 2 mL loop. The protein conjugates were eluted over 120 mL and the fractions collected were then analysed by SDS-PAGE and stained using silver stain. Fractions (23-28) containing PEG_{20}-Fab_{alb} were combined and centrifugally concentrated using a VivaSpin column with 10,000 MWCO at 3000 ×*g*, 4 °C until >2 mL. Protein concentration for PEG_{20}-Fab_{alb} was estimated by measuring UV absorbance at 280 nm (41 μg/mL, 2 mL). The final yield of PEG_{20}-Fab_{alb} was calculated to be 28.8%. SDS-PAGE analysis of the final product was conducted and the resulting gel stained with InstantBlue™ and PEG stain.

2.2.9.15 Disulfide conjugation of Fab_{alb} with PEG_{20} di(*bis*)sulfone **4** to prepare Fab_{alb}-PEG_{20}-X

Fab_{alb} (0.37 mg, 1 mL) was reduced according to method 2.2.6.4 in 50 mM sodium phosphate, 150 mM sodium chloride, 20 mM EDTA, and 0.005% Tween-20 pH 7.0 and was subsequently reacted with 5 eq PEG_{20} di(*bis*) sulfone **4** (0.732 mg, 36.6 μL).

The PEG_{20} di(*bis*)sulfone **4** was solubilised in 50 mM sodium phosphate, 150 mM sodium chloride, and 20 mM EDTA pH 7.4. The reaction was allowed to proceed for 3 h at 25℃. After this time, SDS-PAGE analysis of the reaction mixture was conducted and the subsequent gel was stained by InstantBlue™ and PEG stain.

2.2.9.16 CIEC purification of PEG_{20} di(*bis*)sulfone **4**-Fab_{alb} (Fab_{alb}-PEG_{20}-X)

To remove excess PEG_{20} di(*bis*)sulfone **4**, a linear CIEC was performed. The PEG_{20} di(*bis*)-sulfone-Fab_{alb} reaction mixture (*ca.*=1 mL) was diluted 10-fold in buffer A (100 mM sodium acetate pH 4.0). The diluted mixture was then manually loaded onto the 5 mL Macrocap SP column using an ÄKTA prime plus which had been pre-equilibrated with buffer A. The protein conjugates were eluted with a linear gradient over 30 mL with a target of 100% buffer B (100 mM sodium acetate, 1 M sodium chloride pH 4.0). Fractions collected were then analysed by SDS-PAGE and stained using InstantBlue™ stain. Fractions (29-39) containing PEG_{20}-Fab_{alb} were combined, centrifugally concentrated and buffer exchanged into 50 mM sodium phosphate, 150 mM sodium chloride, 20 mM EDTA pH 7.4 using a pre-equilibrated VivaSpin column with 10,000 MWCO at 3000 ×*g*, 4 °C until *ca.*=6 mL. The concentration of X-PEG_{20}-Fab_{alb} was estimated to be 0.17 mg using UV absorbance 280 nm (Fab_{alb} ε=1.4) with a resulting yield of 46.7%.

2.2.9.17 Disulfide conjugation of IFN with PEG_{20} di(*bis*)sulfone **4**-Fab_{alb} (Fab_{alb}-PEG_{20}-X)

IFN was reduced following method 2.2.6.1. Reduced IFN (2 eq, 0.25 mg) was then added to X-PEG_{20}-Fab_{alb} (1 eq, 0.17 mg) and the reaction allowed to proceed for 4 h at 25 °C. After this time, glutathione re-oxidising solution (40 μL) was added the reaction mixture and re-oxidising of IFN was allowed to proceed for 16 h a 25 °C. The IFN-PEG_{20}-Fab_{alb} conjugate was then stabilised by two additions (80 μL) of 100 mM STAB dissolved in DMSO at 4 °C for 1.5 h (Figure 2-2). The crude mixture (*ca.*=2 mL) was then diluted 10-fold in 100 mM sodium acetate pH 4.0 for CIEC to reduce the salt concentration and allow the proteins to bind to the column.

2.2.9.18 CIEC purification of the IFN-PEG_{20}-Fab_{alb} reaction mixture

The IFN-PEG-Fab_{alb} reaction mixture (*ca.*=2 mL) was manually loaded at a flow rate of 2 mL/min onto a pre-equilibrated (buffer A:100 mM sodium acetate pH 4.0) 5 mL

Macrocap SP cation exchange column using an ÄKTA prime plus. The protein conjugates were eluted with a step gradient of buffer B:1.0 M sodium chloride in 100 mM sodium acetate pH 4.0 of 30,60,80 and 100 %. Fractions collected (2 mL) were then analysed by SDS-PAGE and stained using InstantBlue™ and silver stain. Fractions (4-24) containing IFN-PEG_{20}-Fab_{alb} were combined, centrifugally concentrated and buffer exchanged into 50 mM sodium phosphate containing 150 mM sodium chloride pH 7.8 using a pre-equilibrated VivaSpin column with 10,000 MWCO at 3000 ×*g*, 4 °C until ~1.5 mL. Protein concentration was estimated by measuring UV absorbance (280 nm) for IFN-PEG_{20}-Fab_{alb} (IFN ε=0.914, 0.11 mg/mL, yield=44%; Fab_{alb} ε=1.4, 0.0725 mg/mL, yield=20.5%).

2.2.10 Characterisation of protein species

2.2.10.1 Western blot for protein species characterisation

Protein species were loaded (1 μg protein) and run on SDS-PAGE gels (35 min, 200 V, 500 mA). The transfer buffer stock (12.5×) was made in advance; it consisted of tris-base (37.8 g), glycine (181.7 g) and was made up to 1 L with purified water. Transfer buffer (1×) was prepared by diluting 100 mL of transfer stock (12.5×) with methanol (250 mL) and 900 mL of purified water. The gels and transfer equipment were soaked for 10 min in transfer buffer (1×) and the protein samples in the SDS-PAGE gel were transferred to a nitrocellulose membrane for 1 h, 30 V. After the transfer, the membrane was blocked with 20 mL PBST (1×PBS, 0.01% Tween-20) containing 5% skimmed milk for 1 h at RT.

For His_8IFN α-2a detection, the membrane was washed briefly with PBST and then left overnight at 4 °C with a ratio of 1:5000 antibody:PBST. The primary antibody used was anti-IFN α-2 rabbit polyclonal antibody, followed by anti-rabbit AP-conjugated (H&L) antibody in a ratio of 1:10000 in PBST for 1 h at RT. The membrane was washed trice with PBST. The samples were detected by a colorimetric detection method. Therefore, one Sigma Fast™ NBT/BCIP alkaline phosphatase substrate tablet was dissolved in 10 mL deionized water and poured over the membrane. Incubation was conducted in the dark for 20 min and stopped by washing the membrane with water.

For detecting the his-tag only PEGylation, mouse anti-6×His monoclonal antibody was used and was conjugated to by anti-mouse AP-conjugated antibody at

1:5000 in PBST for 1 h at RT. The membrane was washed trice with PBST and was detected by a colorimetric detection method. Therefore, one Sigma Fast™ NBT/BCIP alkaline phosphatase substrate tablet was dissolved in 10 mL deionized water and poured over the membrane. Incubation was conducted in the dark for 20 min and stopped by washing the membrane with water.

For detecting the rabbit anti-rat albumin species a polyclonal anti-rabbit IgG (H&L) AP-conjugated IgG was used. The membrane was used thrice with PBST and was developed by a colorimetric method. One Sigma Fast™ NBT/BCIP alkaline phosphatase substrate tablet was dissolved in 10 mL deionized water and poured over the membrane. Incubation was conducted in the dark for 20 min and stopped by washing the membrane with water.

For detecting bevacizumab species goat anti-human κ-chain HRP-conjugated Fab'$_2$ was used in a 1:10,000 ratio of antibody:PBST. The membrane was briefly washed with PBST and left overnight at 4 °C with the antibody. Following this, the membrane was washed 6 times with PBST. The samples were detected using Enhanced Chemiluminescence (ECL) and visualised by a digital imaging system (ImageQuant™ LAS 4000). Detecting substrates A and B were mixed in a 40:1 ratio (2 mL), poured on the membrane and left to incubate for 1 min in the dark. After this, the ECL solution was poured off the membrane and with the ImageQuant™ set to chemiluminescence, pictures of the developed membrane were taken at 5,10,30 sec, 1 and 3 min.

2.2.10.2 NMR analysis of PEG_{20} di(mono)sulfone **5**

To investigate how the PEG_{20} di(mono)sulfone **5** and buffer interact, PEG_{20} di(mono)sulfone **5** was left for 16 h at 20 °C in 50 mM sodium phosphate pH 6.5. This sample was then buffer exchanged using a PD-10 column into purified water and then freeze dried for 24 h. The freeze-dried PEG_{20} di(mono)sulfone **5** was re-suspended in 200 μL deuterated water. The sample was then pipetted into an NMR tube and analysed by NMR.

2.2.10.3 Matrix-Assisted Laser Desorption Ionisation Time of Flight (MALDI-TOF) Mass Spectrometry of analysis of IFN conjugates

Mass spectra were acquired using an Applied Biosystems Voyager DE-PRO Biospectrometry workstation MALDI-TOF mass spectrometer using a nitrogen laser

(345-347 nm). Two matrix solution were used, firstly 25-dihydroxbenzoic acid (DHB) and secondly, sinapinic acid (SA) (3-(4-hydroxy-3-5-dimethoxyphenyl) pro2-enoic). The matrix was a solution of either DHB or SA in a 50:50 mixture of acetonitrile and water containing 0.01% trifluoroacetic acid. The sample and matrix were mixed in a 1:1 ratio and 1 µL was spotted onto a 100-well stainless steel plate. All spectra were acquired in positive mode over a range of 2-100 kDa under linear conditions (25 kV accelerating voltage, 750 ns extraction time delay).

2.2.10.4 7 day stability study of conjugated protein species

To assess the stability of all PEGylated proteins prepared a 7-day stability study was conducted. Samples were incubated at 4 °C for 7 days and SDS-PAGE analysis was conducted on the incubated samples, with the resulting gels stained by InstantBlue™ and PEG stain. For conjugated proteins with a low concentration, silver stain was used to detect the conjugate and determine if there was any free protein.

2.2.10.5 Accelerated stability assessment of PEGylated products

PD-10 desalting columns were used to buffer exchange PEGylated protein samples into 10 mM ammonium bicarbonate pH 8.0 and the protein concentration quantified by UV absorbance at 280 nm. The protein concentrations were then diluted to 50 µg/mL, and for each protein concentration, 27 µL was transferred into 4×0.5mL sample vials. For each of the protein products two of the sample vials were made up to 30 µL with the addition of 3 µL of 10 mM ammonium bicarbonate pH 8.0 while the two remaining sample vials are made up to 30 µL with 100 mM DTT solution. For each protein product, two sample vials (one with DTT and one without) were heated on a metal heating block to 90 °C for 10 min. The two remaining sample vials (one with DTT and one without) were then heated in the metal heating block for 1 h at 50 °C. Once all sample vials for each protein product were cooled to RT, 22 µL was taken from each sample vial and transferred into new labelled sample vials containing 11 µL loading dye. The sample/loading dye mixtures were subsequently analysed by SDS-PAGE and stained with InstantBlue™ and PEG stain, to identify if the protein conjugates are stable by the absence of unreacted His_8IFN α-2a.

2.2.10.6 Assessment of EMCV titre (50 % Tissue Culture Infective dose ($TCID_{50}$) assay) in A549 cells

For the $TCID_{50}$ assay, A549 cells (9×10^5 cells/mL) were added at 0.1 mL/well in 96 well microtitre plates (assay plates) and incubated for 24 h at 37 °C, 5% CO_2 to allow the cells to adhere. Serial dilutions (10-fold, 10^{-1} to 10^{-9}) of EMCV stock were prepared in 2 mL tubes using DMEM/2% FBS, serial dilutions (10^{-2} to 10^{-9}, 150 µL/well) were transferred into V-bottom microtitre assay plates (sample plates) in rows A to H and columns 2 to 11 (Figure 2-3). Columns 1 and 12 were the negative control wells where 150 µL DMEM/2% FBS was added (Figure 2-3). Media in the assay plates was aspirated and replaced with 0.1 mL of the EMCV dilutions. Sample transfer was rapidly performed using a multichannel pipette. Assay plates were then incubated for 72 h in 37 °C, 5% CO_2. From 72 h to 120 h the numbers of wells showing a cytopathic effect (CPE) was monitored using an inverted microscope and pictures were taken of the positive and negative control wells. After 120 h, 50 µL of MTT (5 mg/mL) was added to all wells in the assay plates and incubated for 3 h at 37 °C, 5 % CO_2. MTT is metabolised by live cells to insoluble purple formazan crystals. The plates were then centrifuged for 5 min at 1500 ×*g* to sediment formazan crystals and the medium carefully aspirated. The crystals were then solubilised using 0.1 mL/well of dimethyl sulfoxide (DMSO) for 20 min at RT and the absorbance at 570 nm determined using a microplate reader. The plaque forming units (PFU) were determined from the $TCID_{50}$/mL (6.3 Appendix III). Plaque forming units are the measure of the number of viruses capable of causing cell lysis from viral replication and forming a plaque.

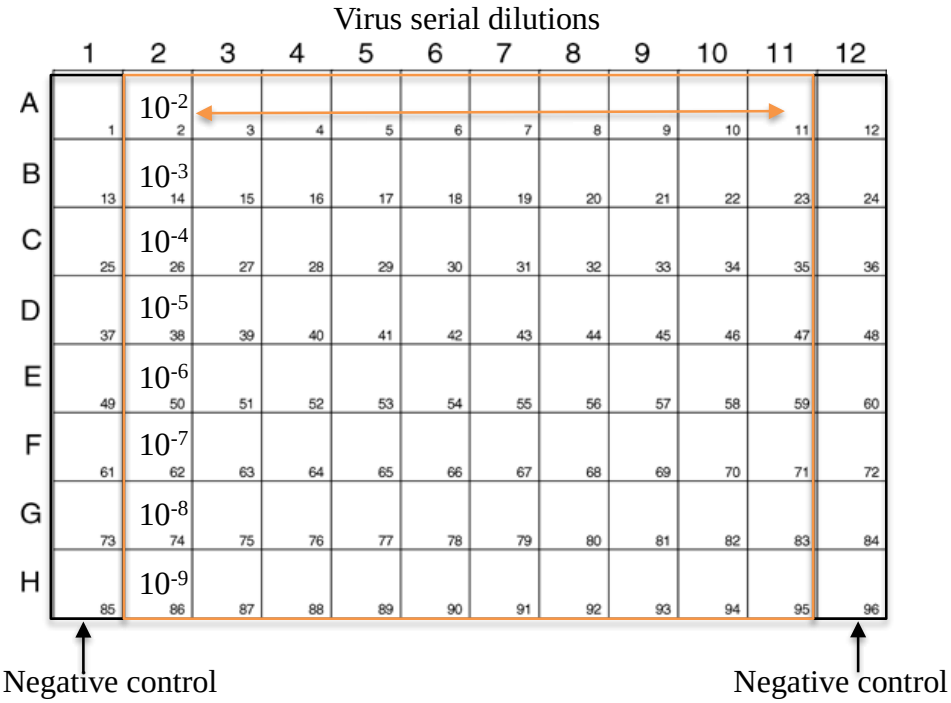

Figure 2-3. Plate layout for the EMCV titre $TCID_{50}$ assay. Negative controls (media and A549 cells) are in columns 1 and 12 seen in the black boxes. EMCV serial dilutions (10^{-2} to 10^{-9}) were conducted in columns 2-11 seen in the orange box.

2.2.10.7 *In vitro* antiviral assay for potency testing of IFN species

The human lung fibroblast cell line A549 was maintained in DMEM media supplemented with 10% foetal bovine serum (FBS), 50 units/mL penicillin, 2 mM L-glutamine and 50 µg/mL streptomycin. For the antiviral assay, A549 cells were plated (1.7×10^5 cells/mL at 50 µL/well) in 96 well flat-bottomed tissue culture plates, then incubated at 37 °C, 5% CO_2 overnight until the cells were 80% confluent. Serial dilutions (2-fold) of the His_8IFN α-2a samples were prepared in DMEM/10% FBS in 96 well V-bottom plates. Fifty µL of the diluted samples was transferred to flat-bottom plates and incubated for 24 h at 37 °C, 5% CO_2. Protein samples were tested in triplicate (Figure 2-4). Control wells contained only cells (negative control) or cells with virus (positive control) (Figure 2-4). After incubation, the sample and media were discarded. Following this, 50 µL/well of EMCV, pre-titrated to achieve complete killing in 24 h in control wells, was added to all wells except for the negative control wells where, 50 µL/well of DMEM/2% FCS was added. The plate was then incubated for 21 h at 37 °C after which ~80% cell death occurred in the control wells. Media was then discarded and the wells were washed with 300 µL/well of PBS added. Plates were then incubated for 30 min at RT with 50 µL/well of 4% formaldehyde/0.5% methyl violet. After incubation the plates were washed

twice with PBS (200 µL/well) and tap-dried. Dye was solubilised by 20 min agitation in 50 µL/well of 2% SDS and the absorbance measured at 570 nm.

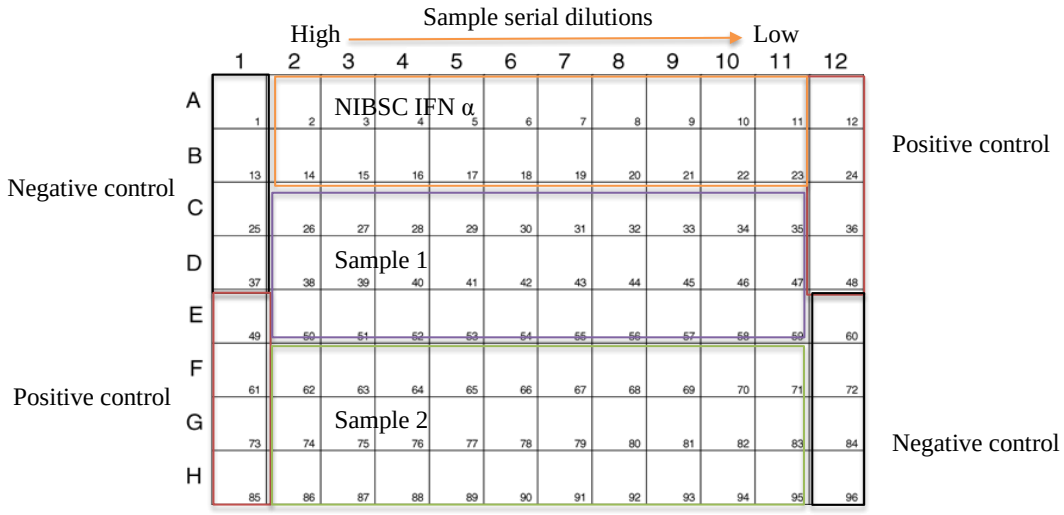

Figure 2-4. Antiviral assay plate layout. Negative control (A549 cells and media) can be seen in the black boxes (columns 1 and 12), whilst the positive controls (A549 cells plus virus) can be seen in the red boxes (columns 1 and 12). The serial dilutions were conducted in columns 2-11 from high to low sample concentration. NIBSC IFN α was conducted on every plate as an internal control in duplicate (orange box). Samples 1 and 2 were conducted in triplicate (purple and green box).

2.2.11 Resuscitation and growth profile assay for the A549 cell line

A549 cells previously stored in liquid nitrogen were thawed at 37 °C in a water bath, then immediately re-suspended in 10 mL of DMEM/20% FBS. Thawed cells were centrifuged for 5 min at 1500 ×*g* and the supernatant was carefully removed. The cells were then re-suspended in 20 mL of DMEM/20% FBS and transferred to a T75 tissue culture flask and incubated at 37 °C, 5% CO_2. A549 cell growth was monitored daily by visual inspection every 4 days and photography of the cells under an inverted microscope.

2.2.11.1 Effect of different EMCV concentrations on NIBSC IFN α-2a

A549 cells were re-suspended in DMEM/10% FBS at 1.7×10^5 cells/mL and seeded at 8,500 cells/well (50 µL/well) in four 96 well microtitre plates (assay plates) for 24 h. A serial dilution (2-fold) of NIBSC IFN α-2a was prepared in DMEM/10% FBS in 96 V-bottom microtitre plates (sample plates, 300 µL). Fifty µL was then transferred to the four assay plates using a multichannel pipette and the assay plates incubated for a further 24 h. Four EMCV titres were prepared (1×10^5, 2×10^5, 3×10^5 and 4×10^5 PFU/mL) in DMEM/2% FBS. The IFN-containing media was aspirated from the assay plates and was replaced with media containing EMCV titres (50 µL/well) in

duplicate. Viral inoculation was allowed to occur for 19 h. The plates were then washed once with PBS (200 µL/well), 0.1% methyl violet in 4% formaldehyde-PBS added (50 µL/well) and incubated for 20 min at RT. The staining solution was aspirated and the plates washed thrice with PBS (200 µL/well). The dye was then solubilised in 2% SDS (50 µL/well) for 20 min on a plate shaker at RT and the absorbance measured at 570 nm using a microplate reader.

2.2.11.2 Effect on EMCV incubation time on A549 cell death

A549 cells were re-suspended in DMEM/10% FBS and diluted to 1.7×10^5 cells/mL then 50 µL of the cell suspension seeded into the wells of a 96 well flat-bottom plate. Cells were then allowed to adhere to the plate surface overnight at 37 °C until they reach ~80 % confluency. After 24 h, 50 µL of DMEM/10% FBS was added to all wells and the plates incubated for a further 24 h. EMCV stock was diluted to 1×10^5 PFU/mL in DMEM/2% FBS, and 50 µL added to all wells except the control columns (columns 1 and 12) where only medium was added. The plates (2 per incubation time) were then incubated with the virus for different lengths of time (4, 8, 16, 20, 24 and 28 hour). Pictures of the A549 cells controls with and without virus were taken prior to harvesting, to observe how cell death is affected by EMCV incubation time. Plates were then washed once with PBS (150 µL) and the viable adherent cells detected by staining with 50 µL of 4.0 % formaldehyde/0.5 % methyl violet for 20 min at RT. Plates were then washed twice with 200 µL of PBS and remaining dye solubilised by the addition of 50 µL of 2 % SDS. Plates were agitated on a plate shaker for 20 min before the absorbance was read at 570 nm using a spectrometer.

2.2.11.3 Data analysis of Antiviral assay results

In line with the British pharmacopoeia, the interferon concentration (the log reciprocal of the interferon dilution) was plotted against the absorbance achieved. The reduction in cell viability fits a sigmoidal dose-response curve, thus the distance between the linear portions of the curves is used to compare the response and relative potencies of the standards and samples tested. Data was only considered valid under two criterion, i) the variation between the straight part of the sigmoidal curve and the data points was small enough to be accurately represented by a straight line (absolute sum of squares (r value)) and ii) the ED_{50} for the internal control, NIBSC IFN α, is

within the expected range. If the data achieved was not in line with this criterion, the data was not used. Accepted potency data was then turned into international units (IU) to allow for direct comparisons to be made to literature data. GraphPad Prism 5 was used for all data analysis.

2.2.11.4 *In vitro* antiproliferative assay for the potency testing of IFN species

The human Negroid Burkitt's lymphoma (Daudi) cell line was maintained in RPMI 1640 media supplemented with 10 % foetal bovine serum (FBS), 50 units/mL penicillin and 50 µg/mL streptomycin. For the antiproliferative assay Daudi cells were plated (1.7×10^5 cells/mL at 100 µL/well) in a 96 well round-bottomed tissue culture plates and these were incubated at 37 °C, 5% CO_2 whilst the sample serial dilutions were being conducted. Serial dilutions (three-fold) of IFN α controls (NIBSC IFN α-2a and Pegasys®) were conducted in 1.5 mL centrifuge tubes using RPMI 1640/10% FBS. IFN α controls were pipetted into the plate (100 µL/well) from low to high dilutions in duplicates, with each well having a final volume of 200 µL/well. Control wells contained only media without cells (negative control) or cells with media (as positive control). The plate layout was the same as with the antiviral assay (Figure 2-4). The plates were then incubated for 72 h at 37 °C, 5% CO_2. Methyl thiazolyl tetrazolium (MTT), a soluble metabolic substrate which is converted into formazan salt, was used to determine the Daudi cell viability (Wang et al., 1996). MTT solution (5 mg/mL) was dissolved in PBS and was prepared 10 min before addition to the wells. MTT solution was filtered through a 0.2 µm syringe filter. Twenty µL/well MTT was added to each well and the plates incubated for 3 h at 37 °C, 5% CO_2. Plates were then centrifuged at 1500 ×*g* for 10 min, allowing formazan crystals to sediment. Using a multichannel pipette, the supernatant was carefully removed and 100 µL/well non-sterile DMSO was added to solubilise the crystals by agitation. Absorbance was then measured at 570 nm.

2.2.11.5 Growth characteristics of Daudi cells

A marked antiproliferative effect typically requires an incubation period of several days, thus a growth curve for Daudi cells was conducted to determine the stage of growth the Daudi cells are in typically when carrying out the antiproliferative assay. Daudi cells were seeded (250,000 cells/flask) in four T25 flasks, these were then incubated at 37 °C, 5% CO_2, whilst recording the time. At the same time 24 h later, a

manual cell count was conducted on one of the T25 flasks, and the cell number recorded. This procedure was conducted for 7 days.

2.2.11.6 Daudi cell density optimisation by MTT colorimetric response

Daudi cells were diluted in RPMI/10% FBS to 200,000 cells/well, 100,000 cells/well, 50,000 cells/well, 25,000 cells/well and 12,500 cells/well. Five U-bottom microtitre assay plates were seeded with each cell density (100 µL/well) in duplicate with the 96 well plates, 100 µL/well of media was then added to replace sample volume. Control wells were included in each experiment to serve as positive control (media without cells). The plates were incubated at 37 °C, 5% CO_2 and harvested after 0,1,2,3 and 4 days. A 5 mg/mL solution of MTT in PBS was prepared and filter-sterilised. MTT was added at 20 µL/ well and the plates incubated for 3 h at 37 °C, 5% CO_2. Plates were then centrifuged at 1500 ×*g* for 10 min, allowing formazan crystals to sediment. Using a multichannel pipette, supernatant was carefully removed and 100 µL/well of non-sterile DMSO was added to solubilise the crystals by agitation. Absorbance was then measured at 570 nm.

2.2.11.7 Effect of cell seeding density on IFN response

A variation on method 2.2.11.4 was conducted whereby standards were prepared in a two-fold serial dilution in assay media instead of a three-fold dilution. Incubation periods of 72 h and 96 h were also conducted.

2.2.11.8 Effect of sample incubation time on cell viability

Following method 2.2.11.4, plates were incubated for 72 h, 96 or 120 h at 37 °C in a humidified atmosphere of 5% CO_2.

2.2.11.9 Data analysis for the antiproliferative assay

GraphPad Prism 5 was used for all data analysis. For optimisation work, cell viability (%) was plotted against control wells using site-specific binding with Hill slope on a semi-log graph. For sample potency testing, as with the antiviral assay, the interferon concentration (the log reciprocal of the interferon dilution) was plotted against the absorbance achieved. The reduction in cell viability fits a sigmoidal dose-response curve, thus the distance between the linear portions of the curves is used to compare the response and relative potencies of the standards and samples tested. Data was only accepted if the variation between the straight part of the sigmoidal curve and the

data points was small enough to be accurately represented by a straight line (absolute sum of squares (r value)).

2.2.11.10 BIAcore kinetic and affinity assay of Fab species

Binding affinity assays were conducted for a) anti-albumin and b) bevacizumab compounds. For the anti-rat albumin species, rat albumin (~65 kDa) was immobilised on a CM3 chip as the ligand whilst for bevacizumab compounds VEGF (~38 kDa) was immobilised as on another CM3 chip. Three steps were optimised for the two chips preparations; 1) pH scouting, 2) immobilisation and 3) regeneration prior to kinetic and affinity analysis of the compounds.

2.2.11.11 pH scouting assay

To find the best electrostatic interaction between the rat albumin with the dextran chip, a pH scouting assay was performed. Rat albumin (1 μg/mL) was dissolved in 10 mM sodium acetate buffer at pH (4, 4.5, 5 and 5.5) and run through flow channel 2 (Fc=2). A contact time of 200 sec was applied. To regenerate the CM3 chip surface, 50 mM sodium hydroxide was used to remove any bound rat albumin. It was found that Rat albumin (1 μg/mL) in 10 mM sodium acetate pH 5.0 was the optimum pH for the binding of the rat albumin to the dextran matrix on the chip.

2.2.11.12 Immobilisation optimisation assay

Rat albumin and VEGF were immobilised by carbodiimide mediated coupling onto separate CM3 chips. $VEGF_{165}$ (38 kDa, 0.2 μg/mL) was immobilised to a level of 110 RU and rat albumin (65 kDa, 0.2 μg/mL) was immobilised to a level of 72 RU. Ligand immobilisation was conducted by firstly docking the new CM3 chip inside the BIAcore. A manual run was conducted as because it was possible to better control contact time and ligand immobilisation level. The flow rate was set to 5 μL/min through Fc=2 and the chip was washed for 60 sec with 50 mM sodium hydroxide. The chip dextrin carboxyl groups were activated by an injection of NHS:EDC (1:1 ratio) solution for 200 sec to give reactive succinimides esters. After this, the HBS-ES buffer was allowed to wash over the chip surface for ~200 sec. The ligand, rat albumin or VEGF, was then injected for 180 or 150 sec respectively. Lastly, 1.0 M ethanolamine-HCL solution was injected for 180 sec to inactivate any remaining succinimides esters on the chip surface and remove non-covalent bound ligand.

2.2.12 Regeneration optimisation assay

A regeneration scouting experiment was performed to find the potential conditions for the regeneration of the rat albumin immobilised chip, where the ligand level of the chip stays the same and only bound analyte was removed. Scouting was performed by testing repeated cycles (5 cycles) of rat albumin binding and regeneration with differing 10 mM glycine-HCL conditions (pH 2.25, pH 2.5) and examining the response levels within each condition. To avoid complicating the interpretation, a new CM3 bound with rat albumin was made and the high pH was tested first. It was found that using 10 mM glycine-HCL pH 2.25 achieved the baseline. Only a slight increase in analyte/baseline response was observed a pH 2.25, which is due to the dextran matrix taking longer to equilibrate at lower pHs.

2.2.12.1 Kinetics and affinity assay analysis

All analyte samples were freshly prepared in the standard HBS-EP running buffer (10 mM HEPES pH 7.4, 150 mM sodium chloride, 3 mM EDTA and 0.005% P20) before the run. All kinetic measurements were conducted at 25 °C at a flow rate of 30 μL/min with an association time of 180 sec and a dissociation time of 1200 sec for bevacizumab compounds and 1600 sec for anti-albumin compounds. Double-referencing (buffer blanks) was conducted in every analyte kinetic run as a control to account for bulk effects caused by changes in buffer composition or non-specific binding (Myszka, 2000; Rich and Myszka, 2000). Further it improves the quality and reproducibility of data achieved at low RUs, by subtracting the average response of the blank injections from the entire data set (Myszka, 2000; Rich and Myszka, 2000).

2.2.12.2 Data analysis

All kinetic data was analysed with the BIAevaluation software (version 2.1) and the best fit (lowest Chi^2) was obtained using a 1:1 binding model. Kinetics and affinity analysis was performed by fitting the 1:1 binding model, globally over five sensogram association and dissociation curves of varying analyte concentrations. Equilibrium dissociation constants (K_D) were calculated from the rate constants ($K_D=k_{off}/k_{on}$). k_{off} is also known as k_d or the dissociation rate constant, whilst k_{on} is also known as k_a or the association constant.

Chapter 3 Preparation and functional activity studies of IFN-PEG-IFN homodimers

3.1 Introduction

As discussed, proteins rarely act alone to prepare a biological response. Instead, proteins bind to other biomolecules, often self-associating to form dimers within a network to prepare a biological response (Marianayagam et al., 2004). For example, the active form of interleukin-12 (IL-12) is a heterodimer comprised of p35 and p40. IL-12 is responsible for triggering the production of interferon γ (IFN γ) during acute inflammation (Marianayagam et al., 2004). However, the activity of IL-12 is regulated by the production of p40 homodimers, where p40 homodimers can bind to the IL-12 receptor and inhibit the production of IFN γ (Heinzel et al., 1997). This example shows that within a biological network, both homodimers and heterodimers can be involved and that the same protein can associate to different proteins depending on the function required. The ability to self-associate to prepare homo- or hetero-dimers allows the genome size to stay small whilst maintaining the advantages associated with protein complex formation (Ispolatov et al., 2005; Marianayagam et al., 2004).

There are many approaches being investigated to prepare multifunctional proteins (§ 1.3). The PEG di(*bis*)sulfone **4** reagent has been used to prepare dimers of Fabs, Fab-PEG-Fab homo- and hetro-dimers (Khalili et al., 2013) and peptides, specifically Octreotide. The aim of the work described in this chapter was to explore methods to make IFN dimers (IFN-PEG-IFN) utilising site-specific *bis*-alkylation conjugation using PEG as a linker to dimerise IFN. A recombinant-chemical approach was investigated to prepare IFN dimers. Where, IFN was expressed recombinantly with an 8-polyhistidine tag (Figure 1-18). Both the polyhistidine tag and the natural disulfides can both be conjugated to with the PEG di(*bis*)sulfone reagent **4**. Firstly, site-specific his-tag conjugation was conducted to take advantage of the 8-polyhistidine tag to create novel His_8IFN-PEG_{20}-His_8IFN dimers using PEG_{20} di(mono)sulfone **5**. His-tag conjugation has been investigated previously with His_8IFN to prepare the monomeric variants of His_8IFN (PEG-His_8IFN) (Cong et al., 2012). It was hypothesised that the novel IFN dimers would retain their biological activity, due to the site-specific conjugation used.

His_8IFN-PEG_{20}-His_8IFN dimers were prepared by his-tag conjugation by reacting His_8IFN α-2a with PEG_{20} di(*bis*)sulfone **4** **(**Figure 3-1**)**. While for disulfide conjugation, His_8IFN α-2a was reduced with DTT prior to conjugation with PEG_{20}

di(*bis*)sulfone **4** **(**Figure 3-1**)**. The IFN dimers were then isolated in a two-step purification process. The IFN dimers were isolated from X-PEG_{20}-IFN (X being the unconjugated linker end) by CIEC. The IFN dimers were then isolated from unconjugated His_8IFN α-2a and higher MW impurities by SEC purification. The IFN dimers were then characterised in terms of purity, identity, stability and activity. Anti-IFN Western blot was used to determine the purity and identity of the conjugates. The activity of the IFN dimers was assessed by two cell-based assays: antiviral and antiproliferative assays. These assays examined two aspects of the pleiotropic nature of IFN.

As previously discussed, Type I IFNs are a group of heterogenous group of pleiotropic cytokines with antiviral, antiproliferative, antitumour and immunodulatory activities (Anguille et al., 2011; Goodbourn, 2000; Nanus et al., 1990). The antiviral activity of IFN is currently being used to treat Hepatitis B and C with treatments such as PEGASYS® and PEG-INTRON®. However, these PEGylated forms of IFN have several drawbacks, namely, heterogeneity of the final products from random conjugation, reduced IFN activity due to PEG-positional isomers binding near or at the binding site and side effects from IFN treatment. In an attempt to improve upon these treatments for Hepatitis B and C, a recombinant-chemical approach was used to prepare IFN dimers. His_8IFN α-2a was used to prepare the IFN dimers. His_8IFN α-2a has been previously used to prepare monoPEGylated and diPEGylated conjugates to explore histidine PEGylation, while disulfide conjugation has not been conducted on His_8IFN α-2a before. Advantageously, His_8IFN α-2a has both a polyhistidine-tag and two disulfide bonds, therefore both histidine and disulfide conjugation can therefore be conducted to prepare the IFN homodimers. It was found that PEG di(*bis*)sulfone **4** can be used as a linker and prepare IFN dimers. These IFN-PEG-IFN dimers were prepared utilising both histidine and thiol conjugation strategies. It was found that His_8IFN-PEG_{20}-His_8IFN retained greater activity than IFN-PEG_{20}-IFN within the antiviral assay, where both conjugates demonstrated higher activity than PEGASYS® (Table 3–6). This shows that the PEG di(*bis*)sulfone **4** reagent in conjunction with site-specific conjugation could be used to prepared multifunctional proteins, such as IFN dimers. However the PEG di(*bis*)sulfone **4** reagent needs further investigation regarding purity, conjugation process and final yield to make the approach scalable.

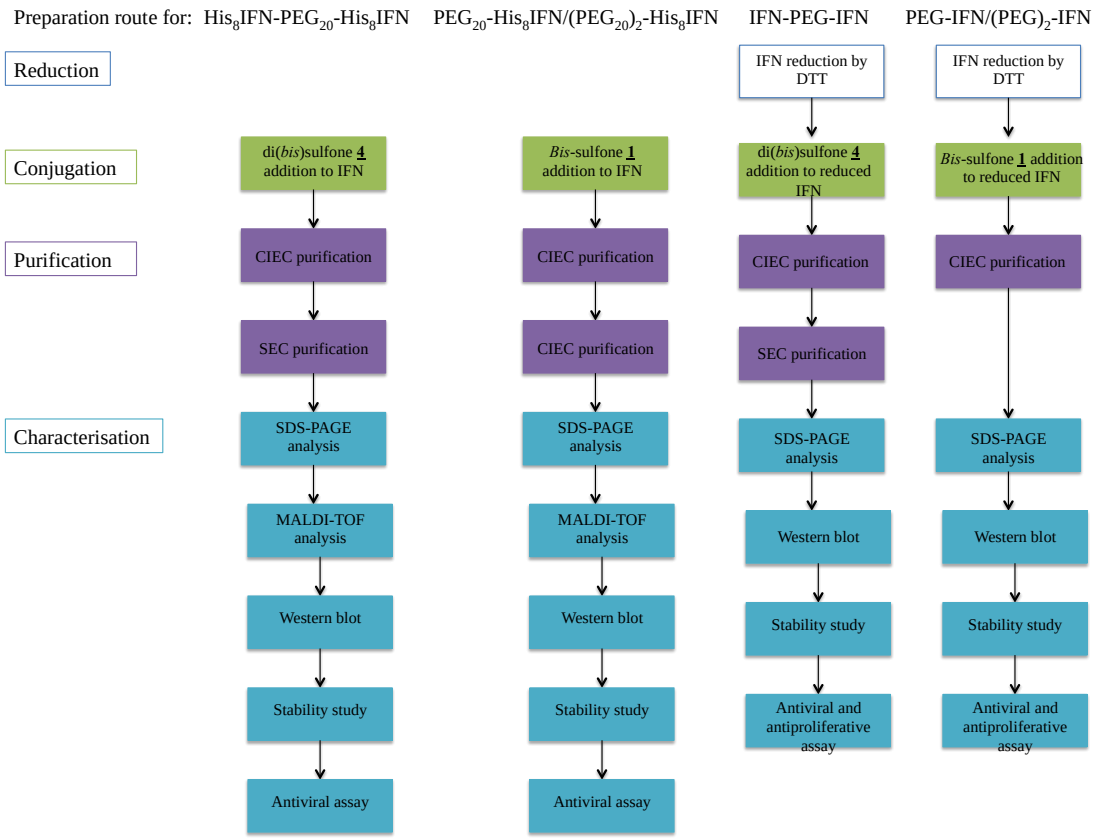

Figure 3-1: Experimental plan of the IFN homodimers and controls prepared in this chapter. The $His_8IFN\text{-}PEG_{20}\text{-}His_8IFN$ dimer was prepared by his-tag conjugation by reacting His_8IFN with PEG_{20} di(*bis*)sulfone **4**. The $PEG_{20}\text{-}His_8IFN$, $(PEG_{20})_2\text{-}His_8IFN$ controls were prepared by reacting His_8IFN with PEG_{20} *bis*-sulfone **1**. For preparing the IFN-PEG-IFN dimers by disulfide conjugation, His_8IFN was first reduced before being allowed to react with PEG di(*bis*)sulfone **4**. Whilst for preparing PEG-IFN and $(PEG)_2$-IFN controls by disulfide conjugation, His_8IFN was reduced with DTT and then allowed to react with PEG *bis*-sulfone **1**. A two-step chromatography process of CIEC and SEC was used to purify the IFN dimers whereas the mono- and di-PEGylated IFN controls were purified by CIEC only. All conjugates prepared where characterised in terms of their purity, identity, stability and biological activity by SDS-PAGE, anti-IFN Western blot, stability studies and antiviral and antiproliferative assays respectively.

3.2 Results and Discussion

3.2.1 Synthesis of 10 kDa and 20 kDa PEG di(*bis*)sulfone 4

The 10 and 20 kDa PEG di(*bis*)sulfone **4** reagents were prepared by F Khayrzad (Figure 3-2) and donated by PolyTherics for use in this PhD project. The PEG di(*bis*)sulfones **4** were prepared following method 2.2.5.2.

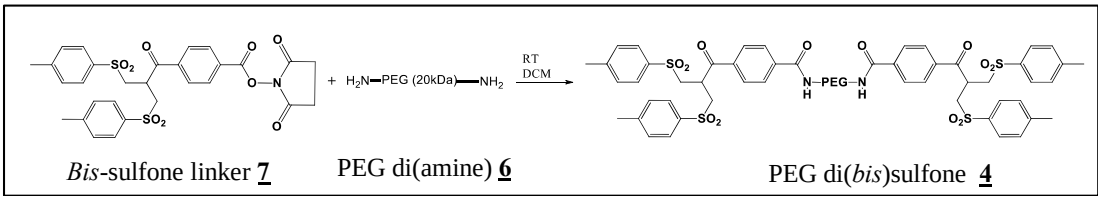

Bis-sulfone linker **7** PEG di(amine) **6** PEG di(*bis*)sulfone **4**

Figure 3-2. Synthesis route for PEG di(*bis*)sulfone **4** used in the IFN-PEG-IFN homodimer production. PEG di(amine) **6** was reacted with the *bis*-sulfone linker **7** at RT with DCM to prepare PEG di(*bis*)sulfone **4**. Acetone precipitation purification was used to purify the PEG di(*bis*)sulfone **4**, the purified homobifunctional reagent **4** was analysed by ^{1}H-NMR.

Prior to conjugation to prepare the IFN-PEG-IFN dimer, ^{1}H-NMR (400/300 MHz) was used to analyse the final 10 and 20 kDa PEG di(*bis*)sulfone **4** reagents in deuterated chloroform (Figure 3-3). The PEG_{20} can be seen between 3.25-4.5 ppm. Theoretically the integration value should be ~1900 relative to 12 protons for the 4 aryl methyl groups (2.49 ppm) indicate there was excess PEG species within the sample. There did not appear to be any elimination of the tolyl sulfinic acid groups. It is possible that unreacted PEG *bis*-amine was carried through the purification, which was addition of the crude reaction mixture to cold acetone to precipitate the PEG di(*bis*)sulfone **4** reagents. Protons labelled number 4 the PEG di(*bis*)sulfone **4** have a similar chemical shift as the methylene proteins in PEG, so cannot be seen in the ^{1}H-NMR spectrum. The aromatic compounds (labelled 2, 3, 6, 7) can be seen at ~7 ppm.

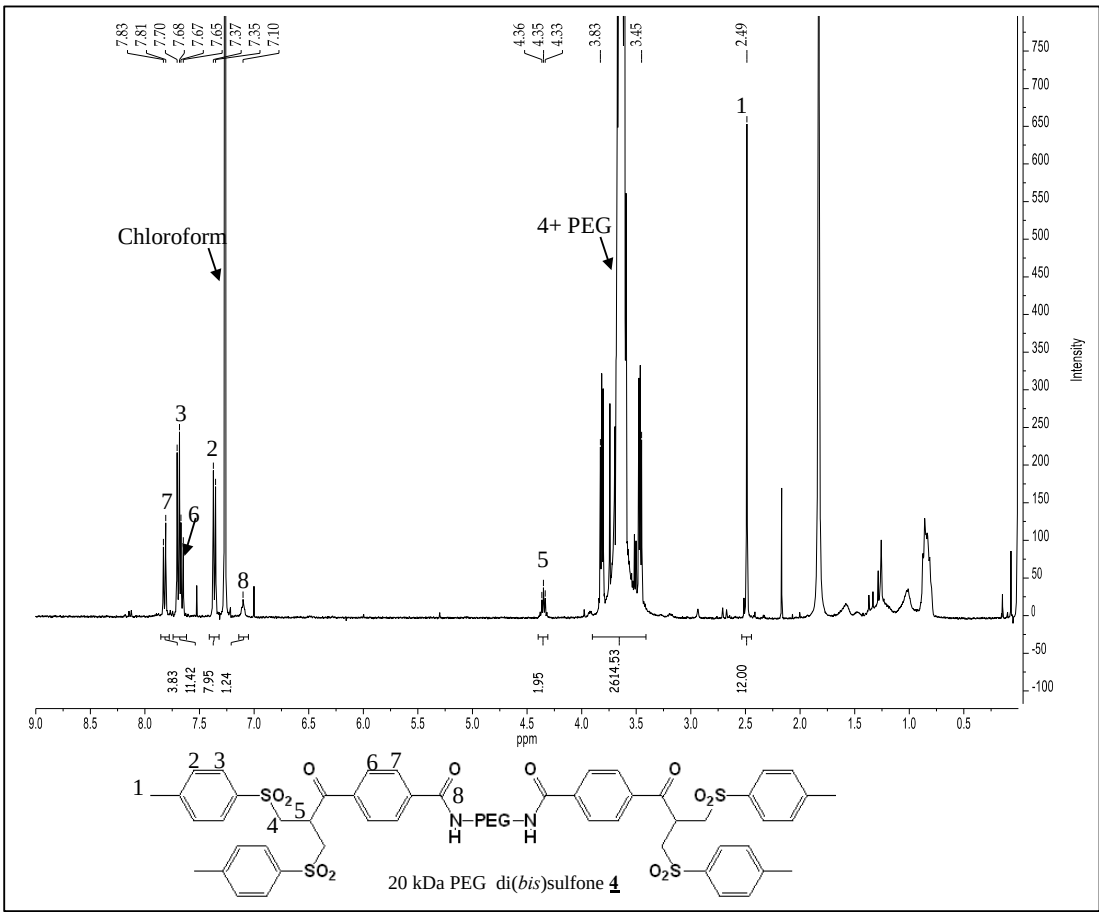

Figure 3-3. ^{1}H-NMR of PEG_{20} di(*bis*)sulfone **4** in deuterated chloroform. Analysis by ^{1}H-NMR has revealed that PEG_{20} di(*bis*)sulfone **4** was successfully made, however it contains excess PEG revealed from the integration, possibly unreacted PEG *bis*-amine **6**. Conjugation with His_8IFN α-2a was then conducted to prepare the IFN homodimer using the homobifunctional reagent **4**.

For his-tag conjugation to proceed, the PEG di(mono)sulfone **5** was expected to be a better reagent to use (Figure 3-4). This is due to the his-tag conjugation taking place at slightly acidic conditions, meaning the generation of PEG di(mono)sulfone **5** which would normally happen *in situ* at neutral or slightly basic conditions is unable to occur (Brocchini et al., 2006). Therefore, PEG di(mono)sulfone **5** was prepared following method 2.2.5.1.

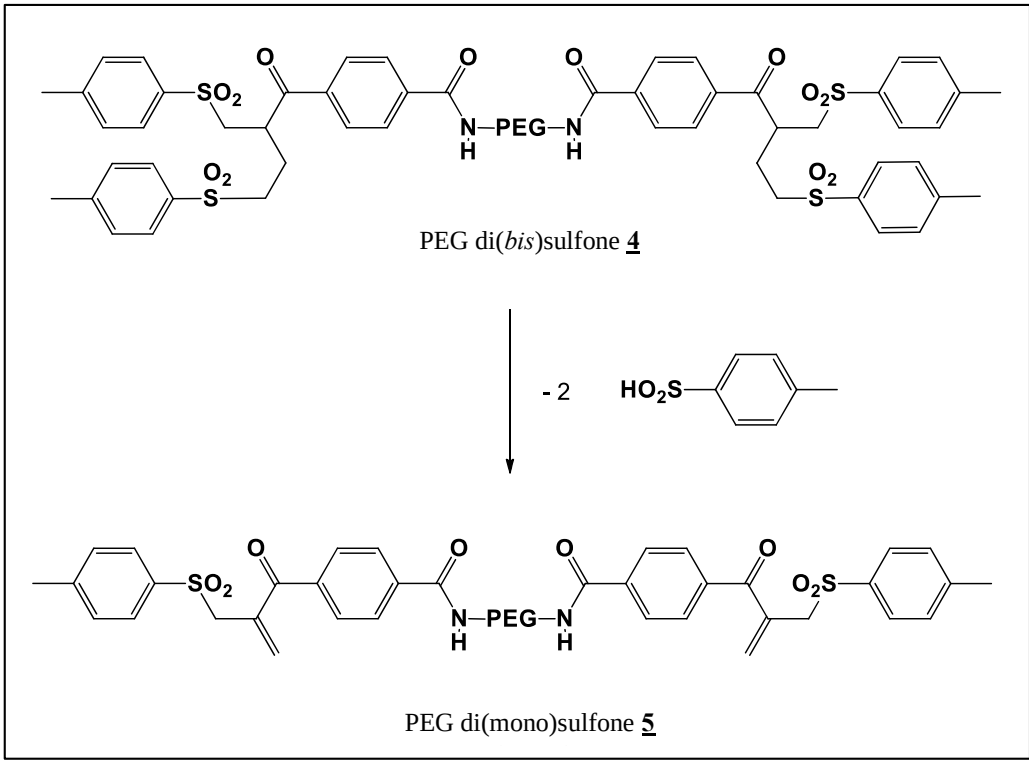

Figure 3-4. Activation of PEG_{20} di(*bis*)sulfone **4** reagent by the elimination of two β-sulfonyl groups **3** to prepare PEG_{20} di(mono)sulfone **5**. PEG_{20} di(mono)sulfone **5** was used to prepare the His_8IFN-PEG_{20}-His_8IFN dimers, due to his-tag conjugation taking place at lower pHs. Thus, the generation of PEG_{20} di(mono)sulfone **5** is unable to occur *in situ*.

It was observed during the preparation of the His_8IFN-PEG_{20}-His_8IFN dimer that there was low conversion to the His_8IFN-PEG_{20}-His_8IFN dimer, when compared to the preparation of the monomeric PEG_{20}-His_8IFN with PEG_{20} *bis*-sulfone **1**. One reason for low conversion to His_8IFN-PEG_{20}-His_8IFN may have been due to competitive addition of water to the PEG_{20} di(mono)sulfone **5** reagent. Addition of water would lead to the formation of allylic alcohol adducts (Figure 3-5) that would undergo subsequent elimination of hydroxide to allow addition to occur at the β-carbon.

The ^{1}H-NMR analysis of PEG_{20} di(mono)sulfone **5** after eight months storage at -20ºC under argon (Figure 3-6 B) was the same as the ^{1}H-NMR obtained when the reagent was prepared (Figure 3-6 A). However, when the PEG_{20} di(mono)sulfone reagent **5** was incubated for 16 h in 50 mM sodium phosphate containing 150 mM sodium chloride pH 6.5 (Figure 3-6 C) the ^{1}H-NMR spectrum changed with the presence of new peaks (black circle).

Peak integration (Figure 3-6 C) indicated that approximately a third of the PEG_{20} di(mono)sulfone **5** had changed, presumably having undergone addition of water or hydrolysis. This hydrolysis can occur at one of the 4 reactive β-carbons,

where conjugation is designed to occur on the PEG_{20} di(mono)sulfone **5** (Figure 3-5). Because of the slow addition of the imidazole amine in the his-tag and the fact that a reactive form of the reagent is present in high concentration throughout the conjugation period, it is not surprising that hydrolysis was observed.

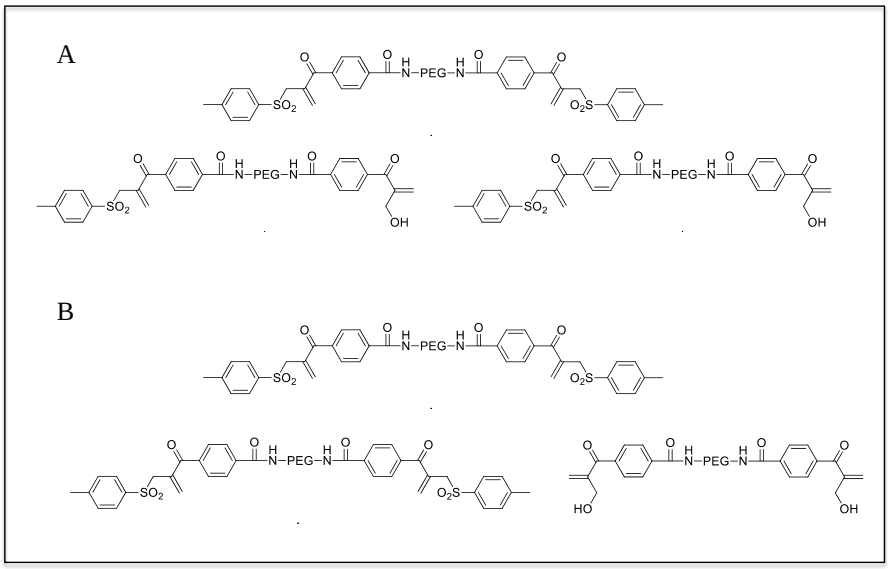

Figure 3-5. Possible mixtures of hydrolysed PEG_{20} di(mono)sulfone **5**. A) one third of the bi-functional PEG reagent **4** is hydrolysed at one linker end, B) one third of the bi-functional PEG reagent **4** mixture is hydrolysed at both ends of the linker. As ^{1}H-NMR analysis revealed one third of the PEG_{20} di(mono)sulfone **5** mixture had hydrolysed.

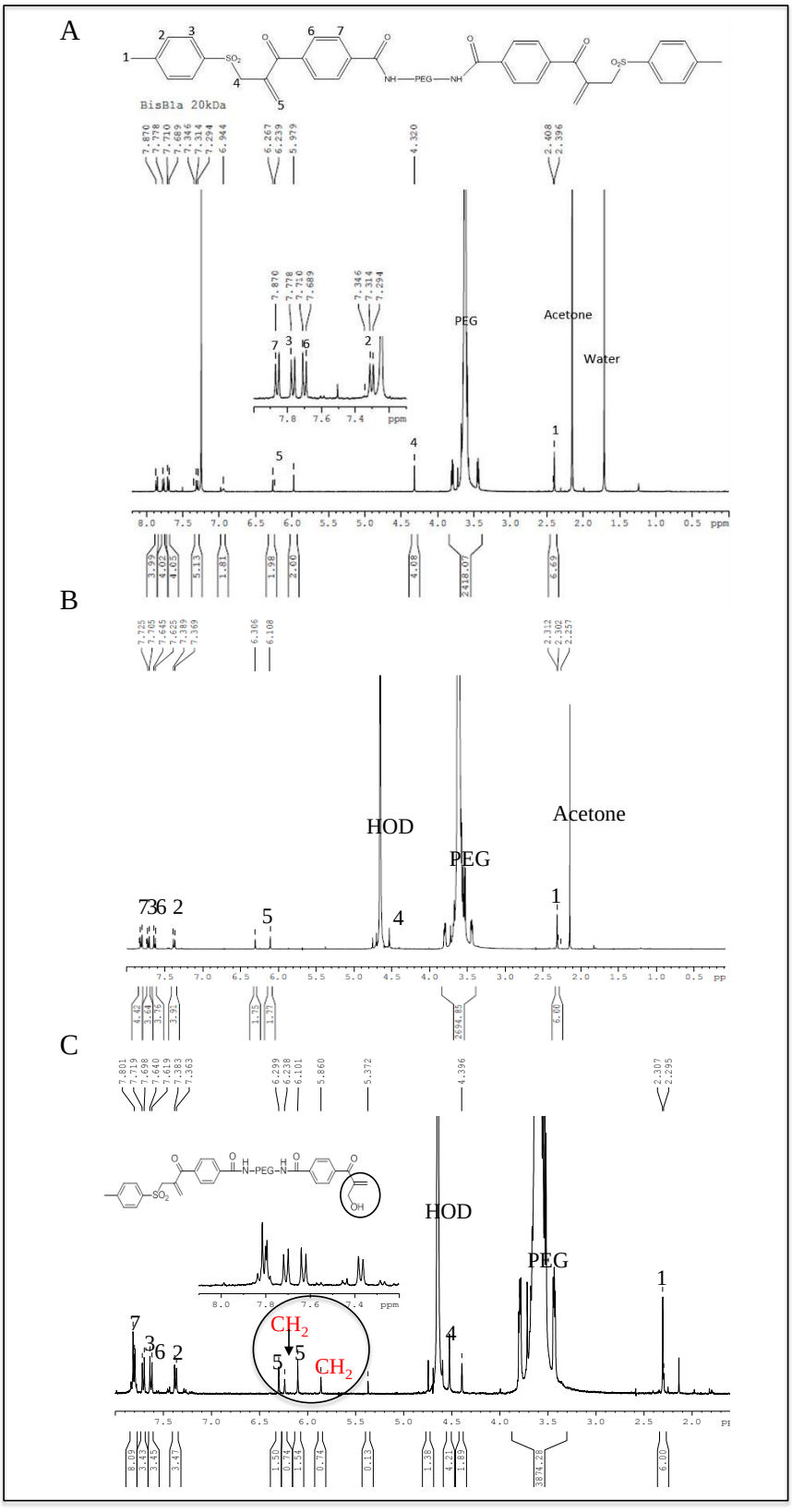

Figure 3-6. NMR analysis of PEG_{20} di(mono)sulfone **5** A) immediately after preparation, B) after eight months at -20 °C under argon and C) after 16 h at 20 °C in 50 mM sodium phosphate containing 150 mM sodium chloride pH 6.5. ^{1}H-NMR analysis reveals some changes have occurred (black circle) to PEG_{20} di(mono)sulfone **5** presumably from water addition or hydrolysis. Peak integration suggests one third of the PEG_{20} di(mono)sulfone **5** mixture has changed.

Alternatively, PEG_{20} di(*bis*)sulfone **4** purity or purity of the starting reagents could also be a reasons for the low conversion of the $His_8IFN\text{-}PEG_{20}\text{-}His_8IFN$ dimer. Therefore, to investigate the purity of the PEG_{20} di(*bis*)sulfone **4**, SDS-PAGE of the PEG_{20} di(*bis*)sulfone **4** was conducted. SDS-PAGE of the PEG_{20} di(*bis*)sulfone **4** reveals 2 impurities at 80-110 kDa and 110-160 kDa, which could affect the conversion of IFN dimers.

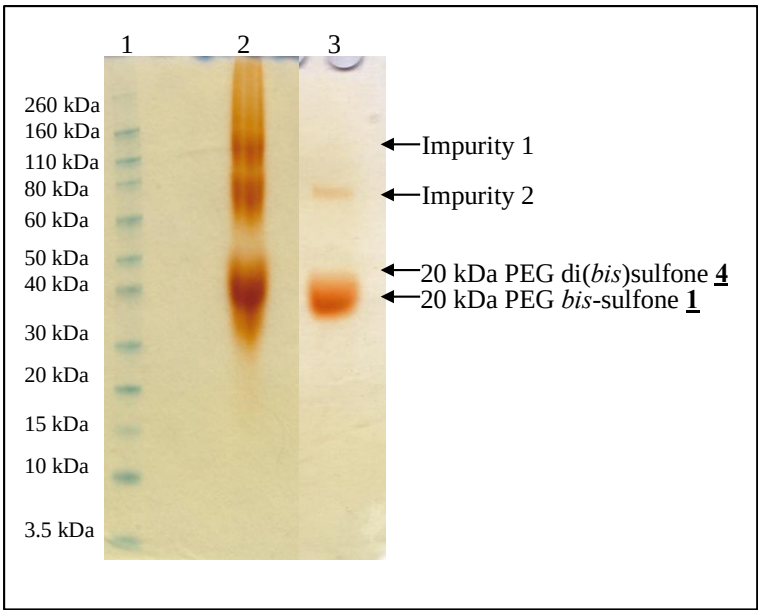

Figure 3-7. SDS-PAGE analysis of PEG_{20} di(*bis*)sulfone **4**. Lane 1: Novex pre-stained markers, Lane 2: PEG_{20} di(*bis*)sulfone **4**, Lane 3: PEG_{20} *bis*-sulfone **1**. Two impurities can be seen in at 160 and 110 kDa (Impurity 1 and 2), which could affect the conversion and yield of homodimer production.

The SDS-PAGE (Lane 2, Figure 3-7) shows that PEG_{20} di(*bis*)sulfone **4** is a mixture, as three bands at 40-50 kDa, 80-110 kDa and 110-160 kDa. The main band at between 40-50 kDa is the PEG_{20} di(*bis*)sulfone **4**. However the two bands above are impurities (impurities 1 and 2), which could be multi-PEG derivatives, whereby the PEG_{20} di(*bis*)sulfone has undergone a reaction with the starting PEG *bis*-amine. Furthermore, it can be observed that the purity of PEG_{20} *bis*-sulfone **1** (Lane 3, Figure 3-7) is greater than that of PEG_{20} di(*bis*)sulfone **4**, as there are fewer impurity bands observed for PEG_{20} *bis*-sulfone **1**. These differences could be the cause of the low yields observed for the IFN dimer and also explain the differences in conversion observed between the $PEG_{20}\text{-}His_8IFN$, $(PEG_{20})_2\text{-}His_8IFN$ and that of the $His_8IFN\text{-}PEG_{20}\text{-}His_8IFN$ dimer.

Moreover, the behaviour of the PEG_{20} di(*bis*)sulfone **4** in solution could affect the conversion of the $His_8IFN\text{-}PEG_{20}\text{-}His_8IFN$. As it has been reported that by

dynamic light scattering, the solution size of PEG_{20}-Fab was 21.2 ± 1.8 nm, whilst for solution size for Fab-PEG_{20}-Fab was 11.6 ± 0.2 nm, which is half the PEG_{20}-Fab molecule size (Khalili et al., 2013). This data suggests that in solution the PEG_{20} di(*bis*)sulfone **4** could be more compact in nature than that of the PEG_{20} *bis*-sulfone **1**. This behaviour could impede the conjugation of the PEG_{20} di(*bis*)sulfone with His_8IFN, thus explaining the low conversions.

It was hoped that by improving the purity of the PEG_{20} di(*bis*)sulfone **4**, a higher conversion of His_8IFN-PEG_{20}-His_8IFN would be achieved. First, F Khayrzad conducted RP-HPLC purification of the PEG_{20} di(*bis*)sulfone **4** mixture (10 mg) using a gradient of 0-100% acetonitrile (§2.2.5.4).

As can be seen in Figure 3-8 there are three peaks at min 20.69, 21.87 and 22.2. The most intense peak, 1000 absorbance (mAu) being that of PEG_{20} di(*bis*)sulfone **4** at 22.2 minutes. The three peaks observed by RP-HPLC were also observed in the SDS-PAGE analysis (Figure 3-7). As the small-scale separation was successful, the scale was then increased to 90 mg. This scale was conducted in the hope that enough PEG_{20} di(*bis*)sulfone **4** could be successfully purified and used for further conjugation studies. This conjugation could determine if the purified PEG_{20} di(*bis*)sulfone **4** would improve the conversions and yields of the homodimer.

The 90 mg RP-HPLC chromatogram at both 214 and 280 nm showed no separation of the three peaks. This is due to the absorbance being above the maximum intensity levels detectable by the HPLC. Therefore, an alternative synthesis route for the PEG_{20} di(*bis*)sulfone **4** was examined in an effort to improve the purity of the reagent. It is important that each terminus on the PEG is appropriately functionalised to ensure that protein conjugation can occur.

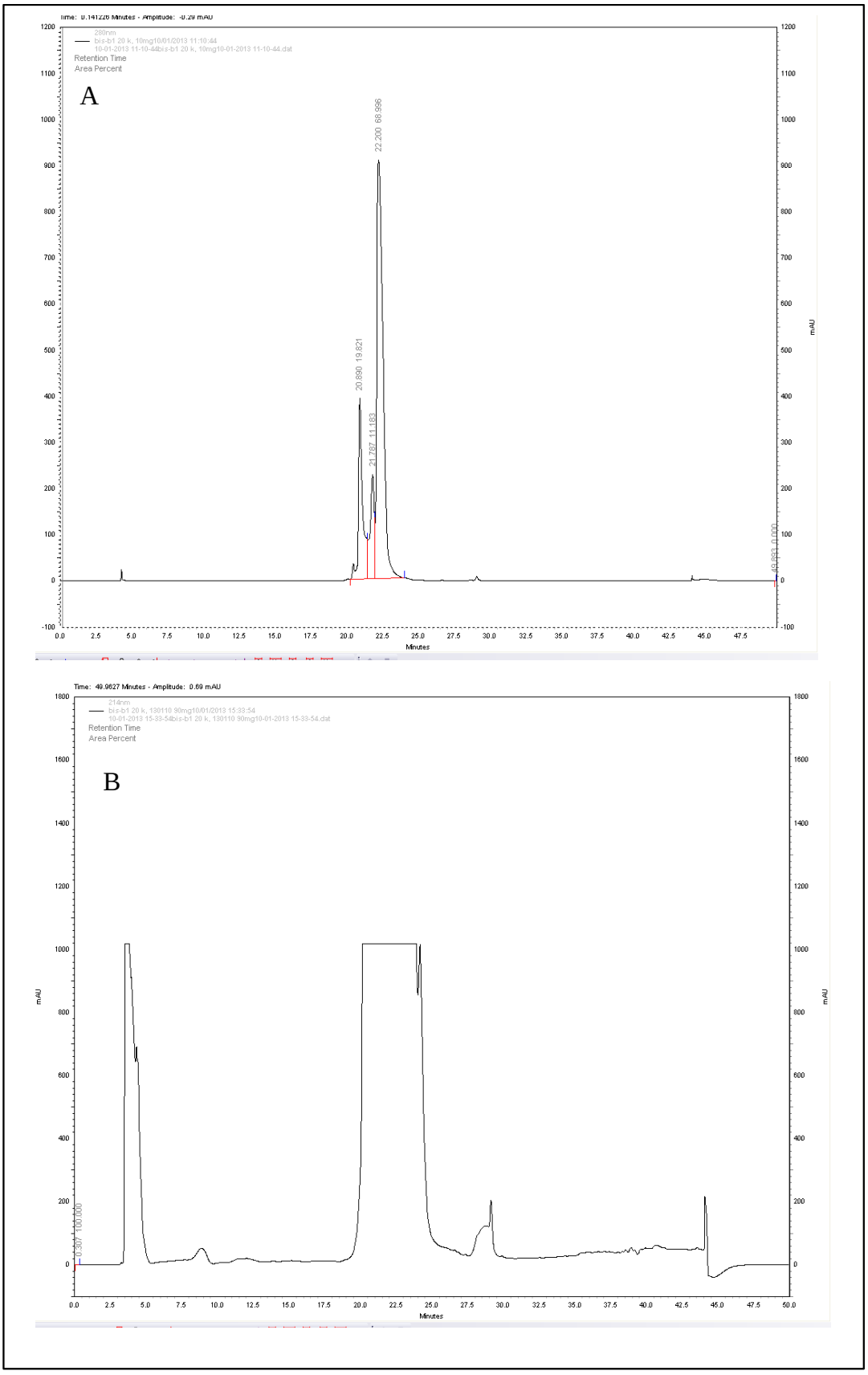

Figure 3-8. Reverse phase-HPLC analysis of PEG_{20} di(*bis*)sulfone **4** at A280 nm A) 10 mg scale and B) 90 mg scale. PEG_{20} di(*bis*)sulfone **4** was purified at the 10 mg scale, but no separation occurred at the 90 mg scale.

An alternative synthesis route for the PEG_{20} di(*bis*)sulfone **4** was used to improve the purity of the reagent. The PEG_{20} di(*bis*)sulfone **4** was prepared by G. Tekle (Figure 3-9) and donated by PolyTherics for use in this PhD project following method 2.2.5.3. The final PEG_{20} di(*bis*)sulfone **4** prepared by synthesis route 2 was characterised by ^{1}H-NMR, SDS-PAGE and RP-HPLC.

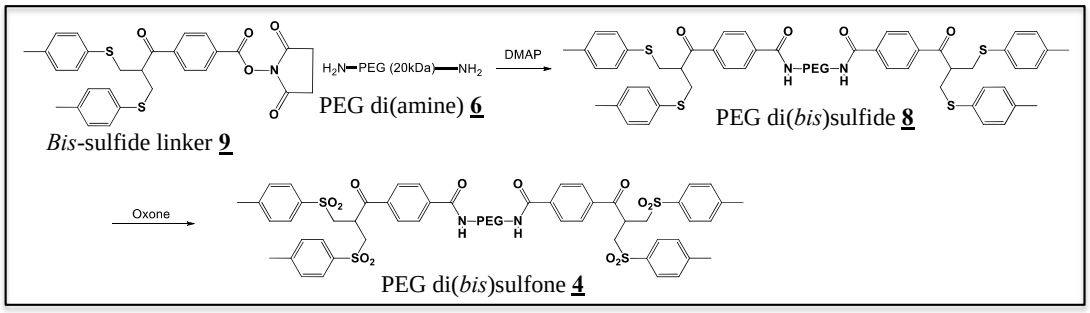

Figure 3-9. PEG_{20} di(*bis*) sulfone **4** synthesis route 2 for heterodimer preparation. PEG_{20} di(amine) **6** was reacted with the *bis*-sulfide linker **9** with DMAP to prepare PEG_{20} di(*bis*)sulfide **8**. PEG_{20} di(*bis*)sulfide **8** was reacted with Oxone® to prepare PEG_{20} di(*bis*)sulfone **4**. Acetone precipitation purification was used to purify the PEG_{20} di(*bis*)sulfone **4**, the purified homobifunctional reagent **4** was analysed by ^{1}H-NMR.

The ^{1}H-NMR (Figure 3-10) was obtained for PEG_{20} di(*bis*)sulfone **4** synthesised by route 2. The integration of the 4 methyl peaks (~2.5 ppm) was set to 12 protons (Figure 3-10). The PEG protons appear between ~3.4-4.5 ppm with an integration of 2400.12. The theoretical integration value for PEG_{20} is ~1900, therefore there was excess PEG within the mixture, which cannot be removed by acetone precipitation explaining the higher integration value. However, it can be observed that the PEG_{20} integration is lower in Figure 3-10 than in Figure 3-3, showing improved quality of the PEG_{20} di(*bis*)sulfone **4**.

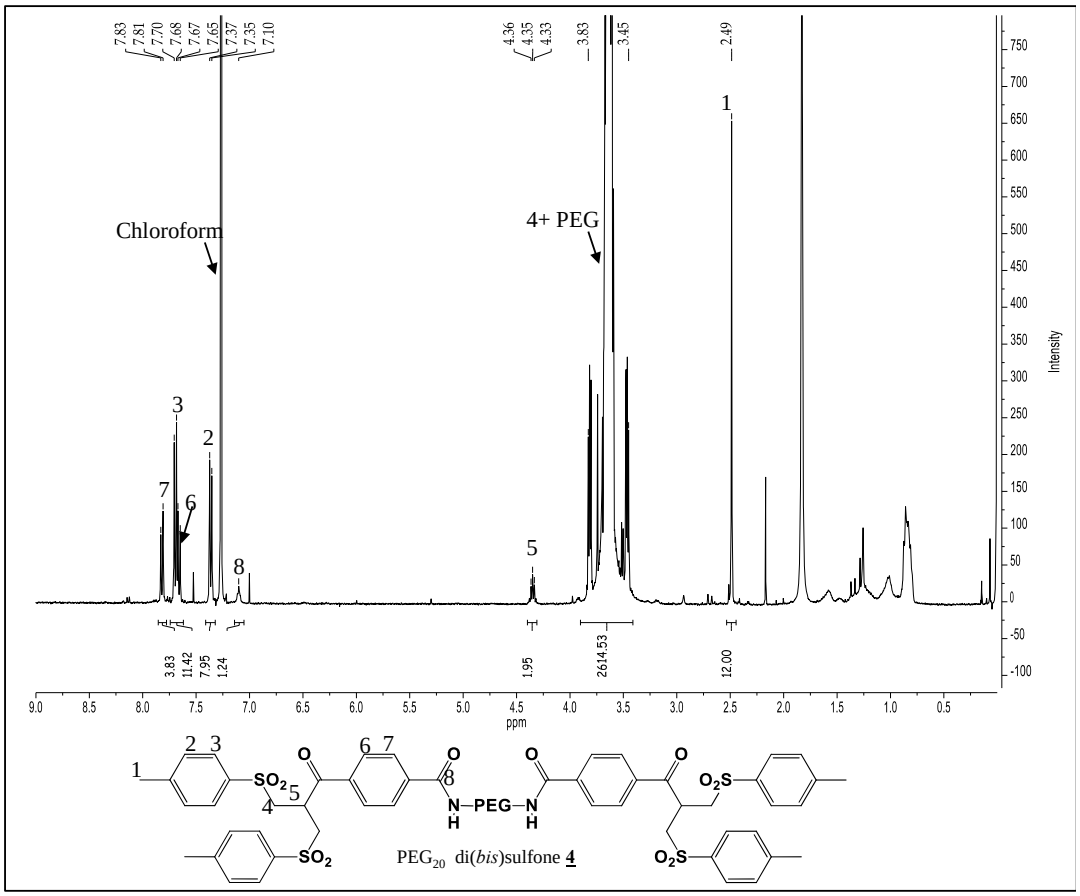

Figure 3-10. ^{1}H-NMR analysis of the PEG_{20} di(*bis*)sulfone **4** prepared using synthesis route 2 (**Figure 3-9**). Analysis by ^{1}H-NMR has revealed that PEG_{20} di(*bis*)sulfone **4** was successfully made. Integration revealed excess PEG (3.4-4 ppm), possibly from the starting material. Disulfide conjugation with His_8IFN α-2a was then conducted to prepare the IFN-PEG_{20}-Fab heterodimers using PEG_{20} di(*bis*)sulfone **4**.

RP-HPLC (method 2.2.5.4) was conducted on the PEG_{20} di(*bis*)sulfone **4** prepared using synthesis route 2. RP-HPLC allows for the separation of components within the PEG_{20} di(*bis*)sulfone **4** mixture and to identify and quantify each separated component/peak. The RP-HPLC chromatograms (Figure 3-11) at 214 nm and 280 nm showed two peaks. The first peak eluted at 28.68 min (15% relative area) and the second peak eluted at 29.89 min (84.9% relative area). The smaller peak could be an impurity from the synthesis route or starting PEG material. The larger peak was deduced to be PEG_{20} di(*bis*)sulfone **4** as this has a longer retention time compared to the impurity. The amount of peaks observed in the RP-HPLC chromatogram (Figure 3-11) also correlates with the amount of bands observed in the SDS-PAGE analysis for PEG_{20} di(*bis*)sulfone **4** synthesised by route 2 (Figure 3-12). When the RP-HPLC chromatograms of the two synthesised PEG_{20} di(*bis*)sulfone **4** were compared, the

second synthesis route has a higher purity (84% relative area, Figure 3-11) of the PEG_{20} di(*bis*)sulfone **4** than synthesis route 1 where there are two impurity peaks.

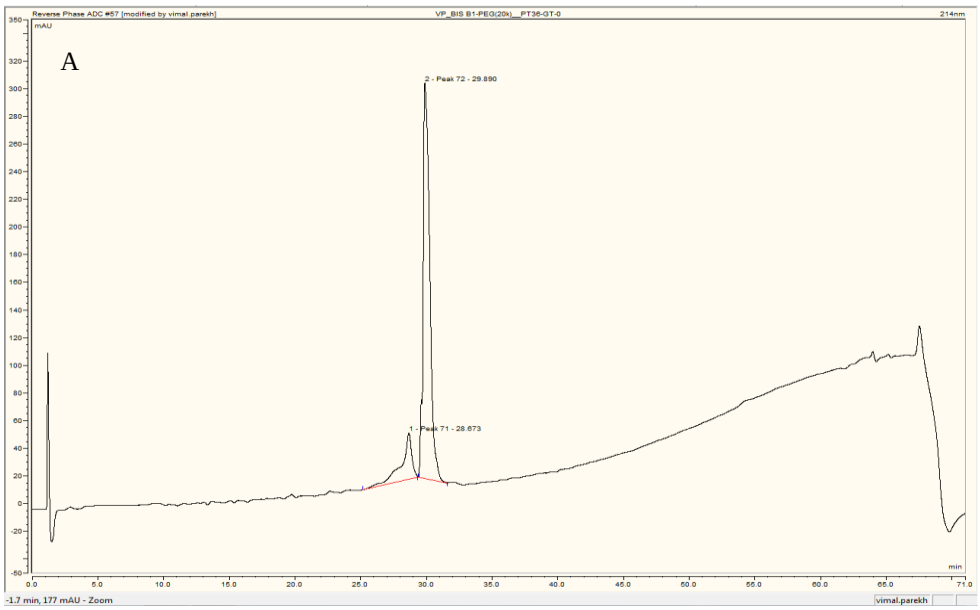

Peak No.	Retention Time (min)	Area (mAU* min)	Height (mAU)	Relative Area (%)	Resolution
1	28.673	29.965	33.321	15.16	1.41
2	29.89	167.6779	285.725	84.84	n.a.
Total:		197.6429	319.046	100	

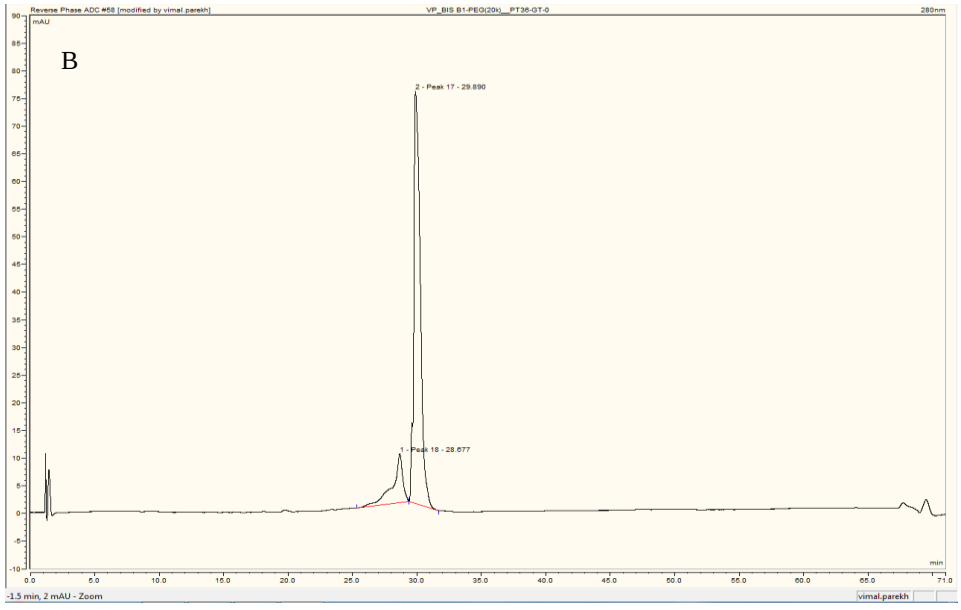

Peak No.	Retention Time (min)	Area (mAU* min)	Height (mAU)	Relative Area (%)	Resolution
1	28.677	7.9104	8.776	15.4	1.4
2	29.89	43.4482	74.467	84.6	n.a.
Total:		51.3586	83.243	100	

Figure 3-11. RP-HPLC purity analysis of PEG_{20} di(*bis*)sulfone **4** prepared by synthesis route 2 at A) 214 nm and B) 280 nm. Peak 1 is an impurity possibly from the PEG starting material or synthesis and Peak 2 is the PEG_{20} di(*bis*)sulfone **4**. Purity is assessed to be 84% by RP-HPLC.

SDS-PAGE analysis (Figure 3-12) showed that PEG_{20} di(*bis*)sulfone **4** prepared from route 2 (Lane 3) was more pure than when prepared by route 1 (Lanes 2). The PEG_{20} di(*bis*)sulfone **4** was observed between 40-50 kDa on the Bis-Tris gel (Figure 3-12) , this is due to PEG_{20} running on the SDS-PAGE gel at double its MW, as the PEG binds 2-3 water molecules (Roberts et al., 2002). In Lane 2 (Figure 3-12) there was a laddering effect of the PEG_{20} di(*bis*)sulfone **4** and two impurity bands could be seen at 80 and 100 kDa; where the band at 80 kDa could be seen in Lane 3.

The SDS-PAGE results agree with the RP-HPLC analysis results on the PEG_{20} di(*bis*)sulfone **4** prepared from routes 1 and 2. For synthesis route 1 three peaks were seen on the chromatogram (Figure 3-8) whilst two peaks could be seen on the chromatogram (Figure 3-11) for synthesis route 2. It can be observed Figure 3-8 and Figure 3-11 the HPLC retention times vary. This can be due to variations in the SEC column used, small changes in mobile phase composition, flow rate and temperature (Brocchini et al., 2006).

For the preparation of His_8IFN-PEG_{20}-His_8IFN and IFN-PEG-IFN, PEG_{20} di(*bis*)sulfone **4** synthesised using synthesis route 1 was used. As knowledge of the homobifunctional reagent **4** and preparation of the IFN dimers grew through the project, it was decided to use PEG_{20} di(*bis*)sulfone **4** prepared by synthesis route 2 for the preparation of the IFN-PEG_{20}-Fab heterodimers. As this was the purest reagent prepared, thus it was hoped that a greater yield of the final IFN-PEG_{20}-Fab heterodimers would be prepared.

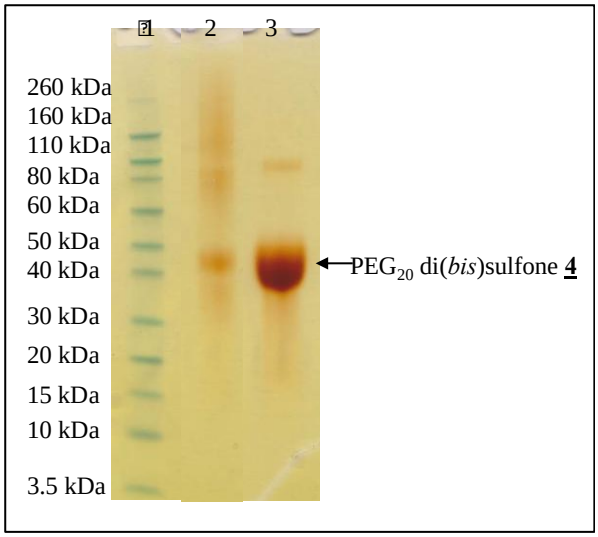

Figure 3-12. SDS-PAGE (PEG stain) analysis (InstantBlue™ and PEG stain) of PEG_{20} di(*bis*)sulfone **4** prepared by synthesis route 1 (Lanes 2) and synthesis route 2 (Lanes 3). Lane 1: Novex pre-stained makers, Lane 2: synthesis route 1 PEG_{20} di(*bis*)sulfone **4** (5 µg), Lane 3: synthesis route 1 PEG_{20} di(*bis*)sulfone **4** (5 µg).

3.2.2 Production of His_8IFN α-2a

The aim here was to prepare a good yield of active recombinant IFN α-2a in fusion with an eight-histidine tag (His_8) in *Escherichia coli* (*E.coli*) for conjugation to PEG di(*bis*)sulfone **4** to prepare novel IFN dimers (His_8IFN-PEG-His_8IFN). The eight-histidine tag was attached between the cysteine and methionine at the N-terminus end of IFN α-2a (Cong et al., 2012). The His_8IFN α-2a gene was cloned into an expression vector utilising a T7 promotor inducible by isopropyl-β-D-1-thiogalactopyranoside (IPTG) on an ampicillin resistance backbone. PolyTherics kindly donated the clone for expression in E. coli.

The SHuffle™ T7 Express strain of *E.coli* was selected as the expression host for His_8IFN α-2a. The SHuffle™ T7 Express system prepares correctly disulfide bonded active proteins in high yields within the cytoplasm of *E.coli* (Lobstein et al., 2012). Additionally, the SHuffle™ *E.coli* have also been engineered to express DsbC, which promotes the correction of mis-oxidised proteins into their correctly folded form (Lobstein et al., 2012). A preculture (method 2.2.3.1) was set up overnight with a chunk of glycerol stock and then the next day the culture was added to the optimised fermentation buffer and the growth of the *E.coli* followed by optical density (OD) readings taken once an hour (Figure 3-13). Once an OD of 5 was reached, IPTG was added to allow the transcription of the lac operon which was stopped at an OD of *ca.*=9 by the centrifuging of the solution to obtain the bacterial pellets.

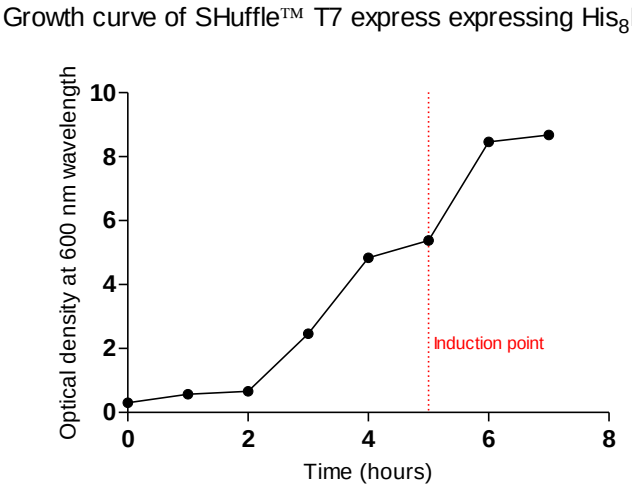

Figure 3-13. Representative growth curve of SHuffle™ Express expressing His_8IFN when grown at 30 °C and induced with 1 mM IPTG after an OD of *ca.*=9 (red line). His_8IFN α-2a successfully expressed in SHuffle™ express system, the His_8IFN α-2a was purified by IMAC. His_8IFN was expressed twice (n=2) within the SHuffle™ Express system.

Prior to and after IPTG induction an aliquot of the SHuffle™ T7 expression strain *E.coli* growth was taken and frozen at -80 °C. The non-induced and induced samples were lysed (method 2.2.3.2). The crude extract, supernatant and pellet from each sample (non-induced/induced) were evaluated by SDS-PAGE to compare the expression of soluble His_8IFN.

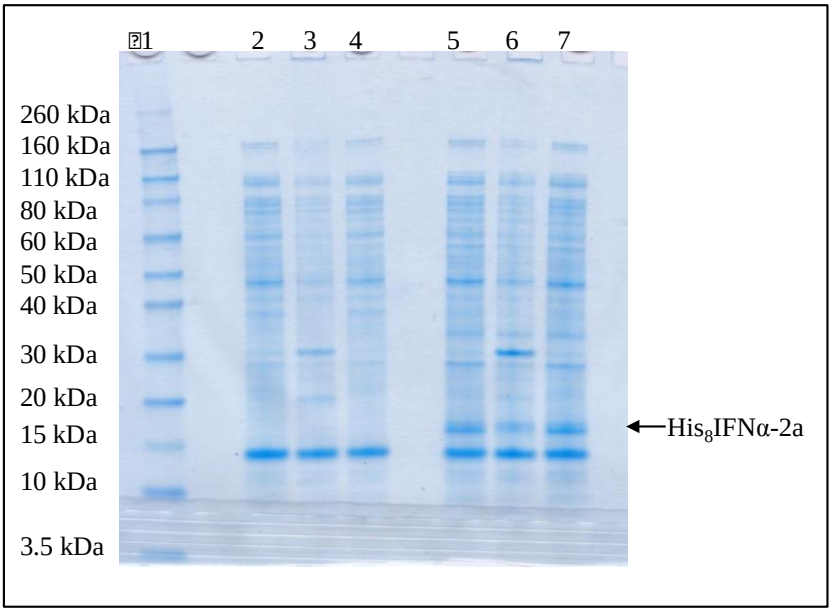

Figure 3-14. Example SDS-PAGE analysis (InstantBlue™ stain) of prior to and after induction effect on His_8IFN expression in SHuffle™ T7 Express system (n=2). Lane 1: Novex pre-stained markers, Lane 2: non-induced crude extract, Lane 3: non-induced pellet, Lane 4: non-induced supernatant, Lane 5: IPTG induced crude extract, Lane 6: IPTG induced pellet and Lane 7: IPTG induced supernatant. High yield of soluble recombinant His_8IFN expressed after IPTG induction.

It can be observed (Figure 3-14) that a high yield of soluble recombinant His_8IFN was expressed after IPTG induction in the SHuffle™ T7 express *E.coli.* The His_8IFN can be seen at between 15-20 kDa in the crude extract and supernatant when IPTG induced. A small amount can also be seen in the pellet fraction, but this could be due to some protein that had remained after pipetting off the supernatant. The band below His_8IFN (between 10-15 kDa) could be lysozyme as it can be seen in both the crude extract and pellet.

After confirmation of recombinant His_8IFN expression with the small-scale lysis, a larger scale lysis was conducted firstly by sonication and then cross flow-filtration to remove the soluble His_8IFN from the cell debris. The soluble protein was then collected for purification.

His_8IFN was purified by an optimised two-step purification method 2.2.3.4. First, IMAC purification was conducted to take advantage of the poly-histidine tag of

His_8IFN. As His_8IFN was expressed as a soluble protein, an optimised purification method working at physiological pH was chosen to maintain the stability/activity of the protein. Firstly, the HisPrep™ FF 16/60 column was pre-equilibrated with buffer A (PBS, 20 mM imidazole), then the supernatant was loaded onto the column and the column was then washed with 2% buffer A; this was to elute non-specific interactions and improve the purity of His_8IFN. His_8IFN was then eluted with a linear gradient of 2-25% buffer B (PBS, 1 M imidazole) (Figure 3-15). The fractions from purification were then analysed using SDS-PAGE (Figure 3-15) and the fractions containing His_8IFN were then diluted 4-fold in 20 mM Tris pH 8.0 to allow the proteins to bind to the anion column for further purification.

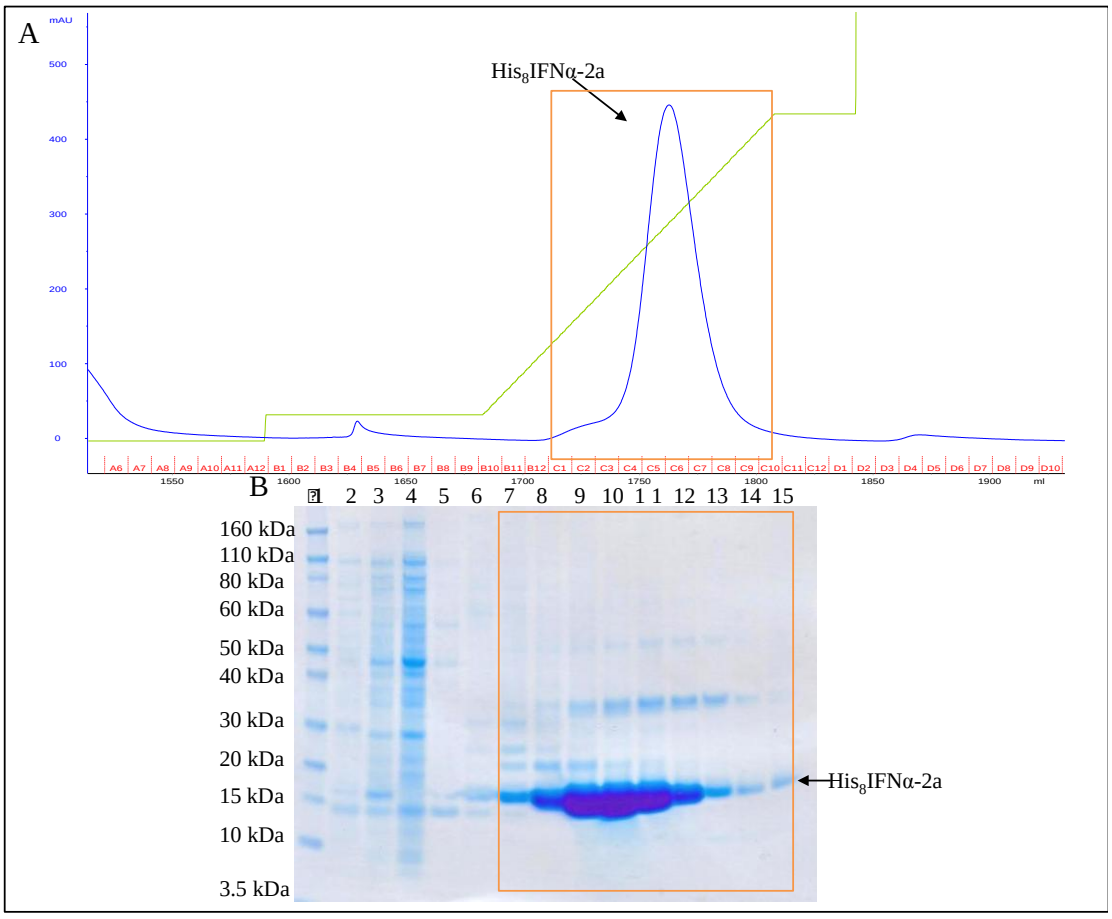

Figure 3-15. Example IMAC purification of His_8IFN bacterial lysis mixture. A) IMAC purification chromatogram, B) SDS-PAGE analysis (InstantBlue™ stain) of IMAC purification fractions, Lane 1: Novex pre-stained markers, Lane 2: pellet (17.5× diluted), Lane 3: supernatant after filtration, Lane 4: flow through, Lane 5: fraction B4, Lane 6-14: fractions C1-12 and Lane 15: fraction D4. His_8IFN was successfully purified by IMAC from bacterial lysis mixture (n=2); a polishing AIEC purification step was next used on the IMAC purified His_8IFN.

In the second purification step, His_8IFN was passed through an AIEC column (Figure 3-16). The HiTrap Q HP column was first equilibrated in 20 mM Tris pH 8.0

and the diluted protein was loaded onto the column and as before the column was washed with buffer C (20 mM Tris, pH 8.0) to elute molecules with non-specific interactions. His_8IFN was then eluted by a 2-20% gradient over 30 min of buffer D (20 mM Tris, 1 M sodium chloride pH 8.0). Fractions from purification were collected and analysed by SDS-PAGE (Figure 3-16 B).

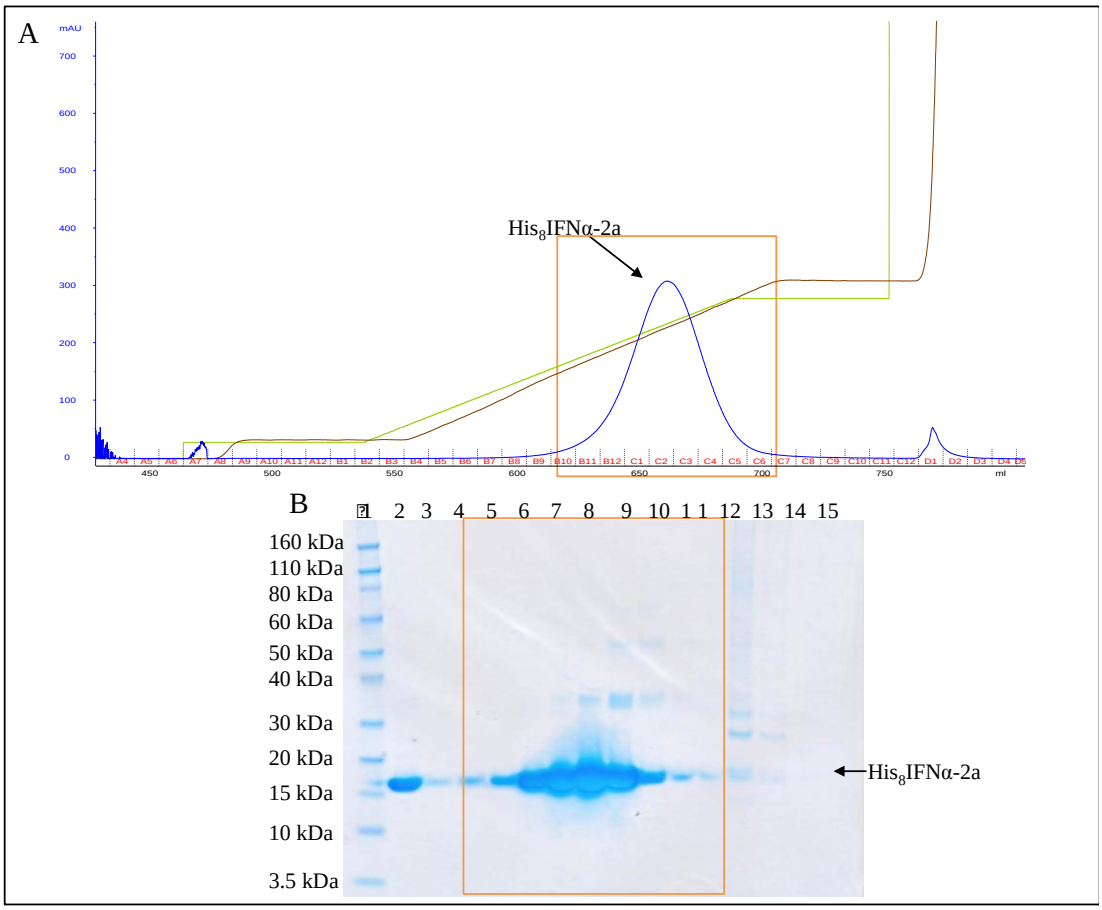

Figure 3-16. Representative AIEC purification of IMAC purified His_8IFN, A) AIEC purification chromatogram, B) SDS-PAGE analysis of AIEC purification fractions, Lane 1: Novex pre-stained markers, Lane 2: IMAC purified His_8IFN, Lane 3-6: fractions B8-12, Lane 7-8: fractions C1-2, Lane 9: C4, Lane 10: C6, Lane 11: C8, Lane 12: C9, Lane 13: D1, Lane 14: D2 and Lane 15: flow through. Pure His_8IFN was prepared from a polishing AIEC step was successfully conducted twice, the His_8IFN was then characterised.

Fractions B8-C9 (Figure 3-16) containing pure His_8IFN were pooled and quantified by UV (abs=280 nm) and MicroBCA™ assay to be 62.8 mg. His_8IFN was prepared two times, each as a 500 mL culture with a yield of between 60-70 mg of His_8IFN being prepared each time. This shows that the production of His_8IFN was quite reproducible as loss of material could be due to i) variations in expression levels, ii) loss during purification process. His_8IFN was stored at a concentration of 0.5 mg/mL, which was suitable for conjugation reactions. The purified His_8IFN buffer was then supplemented with 1 mM EDTA, protease inhibitor cocktail, 1 mM

sodium azide and 10% glycerol for long-term storage at -80 °C. The final His_8IFN product was then characterised in terms of its identity, purity (SDS-PAGE, MALDI-TOF, Western blot) and biological activity (antiviral assay).

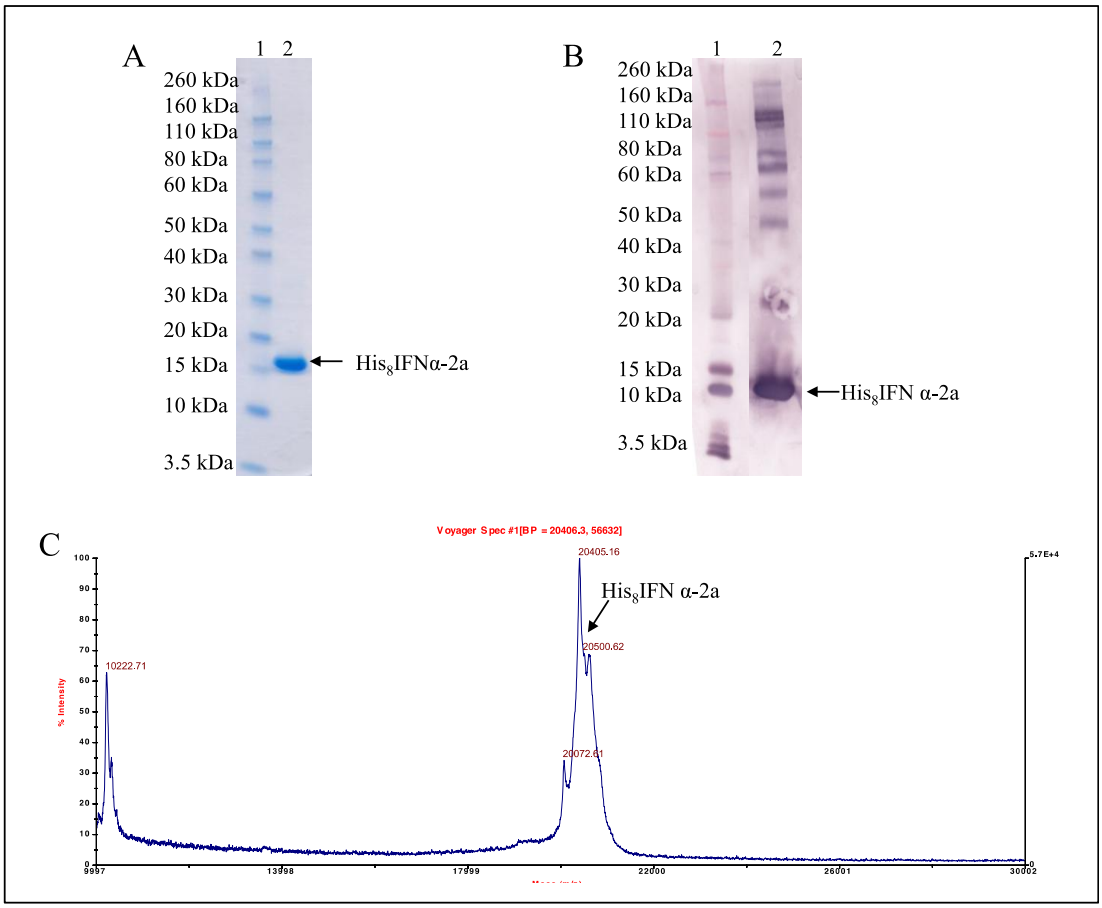

Figure 3-17. Characterisation of final His_8IFN product by A) SDS-PAGE (n=2), B) anti-IFN western blot (n=1) and C) MALDI-TOF spectrum (n=1), Lane 1: Novex pre-stained markers, Lane 2: His_8IFN. Purity characterisation identifies the His_8IFN α-2a prepared is pure and ~20 kDa.

SDS-PAGE analysis was conducted to assess the purity of His_8IFN. For this 1 µg of the final His_8IFN product was loaded into a 4-12% Bis-Tris gel and stained using InstantBlue™. His_8IFN migrates at ~16 kDa (Cong et al., 2012) and has no visible impurities (Figure 3-17 A). His_8IFN was expression was conducted twice and for each expression, SDS-PAGE was conducted. His_8IFN was found to consistently migrate at ~16 kDa on the Bis-Tris gel.

To further corroborate the identity and purity of His_8IFN an anti-IFN α-2a Western blot was conducted. The purified final His_8IFN (1 µg) product was loaded into a SDS-PAGE 4-12% Bis-Tris gel and the gel was transferred onto nitrocellulose membrane which was subject to rabbit anti-IFN α antibody followed by anti-rabbit-AP conjugated antibody (method 2.2.10.1). First to load 1 µg of His_8IFN required the

concentration of His_8IFN to be quantified and then dilutions (i.e. 10×) were made for the final loading of 1 µg onto the SDS-PAGE. His_8IFN was successfully identified by the anti-IFN α antibody, as a band can be observed at approximately ~15 kDa (Figure 3-17 B). Other bands were observed in Figure 3-17 B, could be due to i) over-sensitivity of the primary or secondary antibody or ii) over-development of the membrane with the alkaline phosphatase tablet and/or iii) insufficient time in the blocking step that leads to high background signals. To improve the Western blot, increasing the washing time could help to reduce the background signal. Further too high of an exposure can lead to increased background; therefore reducing/optimising the development time can help to reduce the background signal. Additionally, a lower concentration of IFN could be used to help reduce the high background signal. Some of the bands in Figure 3-17 B, can be seen to be blurry, this is caused by air bubbles present during transfer, this can be avoided by rolling a tube across the gel and nitrocellulose membrane to remove air bubbles (Mahmood and Yang, 2012).

MALDI-TOF analysis was conducted to determine the molecular weight (MW) and further characterise the identity of the expressed His_8IFN α-2a. His_8IFN was buffer exchanged into water using a PD-10 column (method 2.2.10.2). Prior to MALDI-TOF analysis, His_8IFN was freeze-dried and subsequently re-suspended into ammonium bicarbonate pH 8.0. The MALDI-TOF spectrum for His_8IFN showed a peak molecular weight of ≈20405.2 Da (Figure 3-17 C), this is comparable to that stated in literature of 20 kDa (Ahad et al., 2009; Vanden Broecke and Pfeffer, 1988). However, the MW may be slightly higher taking into account the eight-histidine tag (1.2 kDa) (Cong et al., 2012).

The biological potency of His_8IFN was assessed *in vitro* by the prevention of infection of human lung carcinoma (A549) cells by encephalomyocarditis virus (EMCV) (Grace et al., 2005). The His_8IFN displayed a specific activity of 231 ± 10.95 MIU/mg (Table 3–3), whilst the positive control of NIBSC (non-his-tagged) IFN α-2a displayed an activity of 254 MIU/mg. In literature His_8IFN has been reported to display an ED_{50} of 7 pg/mL (Cong et al., 2012). The activity of non-his-tagged interferon α is reported to be 1.4×10^8 IU/mg (British pharmacopoeia 7.0).

3.2.3 Preparation of His_8IFN-PEG_{20}-His_8IFN using his-tag conjugation

3.2.3.1 Preparation of His_8IFN-PEG_{20}-His_8IFN

Novel His_8IFN-PEG_{20}-His_8IFN dimers were prepared using PEG_{20} di(mono)sulfone **5** (1 eq. in 200 mM sodium phosphate containing 150 mM sodium chloride) and three molar equivalents of His_8IFN in 50 mM sodium acetate pH 5.3 containing 35 µM hydroquinone. Hydroquinone was added to all of the his-tag conjugation reaction buffers. Due to PEG_{20} di(*bis*)sulfone **4** undergoing conjugation by addition reactions to a double bond, it is possible that radical induced side-reactions can occur. Previous investigations in house have shown that the addition of hydroquinone to conjugation buffers prevents the polymerisation of *bis*-alkylating PEG reagents. As fewer side reactions occur, resulting in better conversion of the his-tag conjugated protein.

The pH of the reaction mixture was ≈ pH 6.5. The high IFN concentration (3.3 mg/mL, 0.5 mL) and stoichiometry were used to promote the formation of His_8IFN-PEG_{20}-His_8IFN. The reaction mixture was for 16 h at 20 °C, which is similar to what is used to prepare PEG_{20}-His_8IFN (§ 2.2.7.4). The reaction mixture was analysed by SDS-PAGE (Figure 3-18**)** where a band (Lane 4) at 50-60 kDa consistent for the formation of His_8IFN-PEG_{20}-His_8IFN was evident. However conversion was low as there was a significant amount of un-conjugated IFN still present.

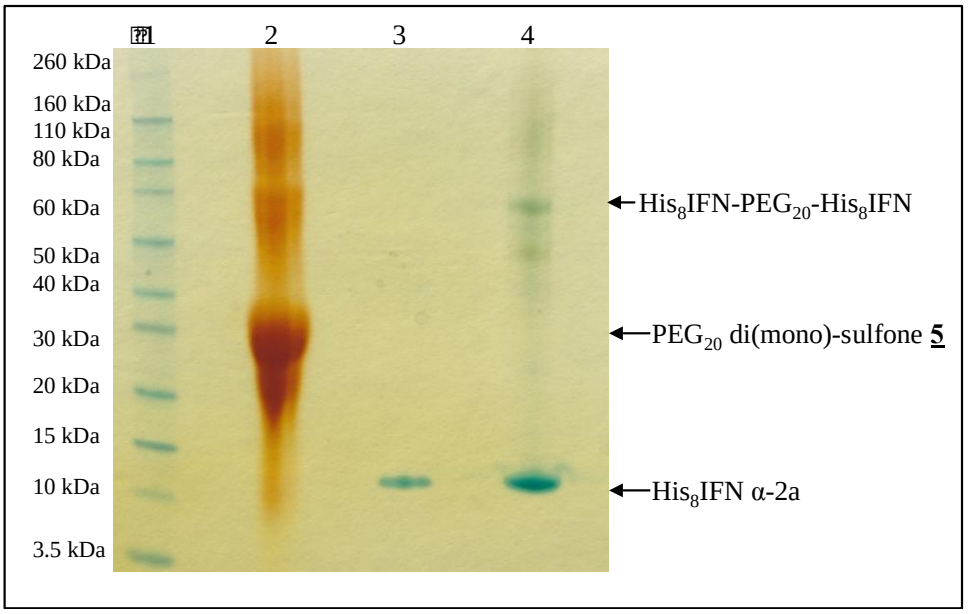

Figure 3-18. Example SDS-PAGE analysis (InstantBlue™ and PEG (BaI_2 stain) of His_8IFN reaction with PEG_{20} di(mono)sulfone **5** (n=2), Lane 1: Novex pre-stained markers, Lane 2: PEG_{20} di(mono)sulfone **5**, Lane 3: His_8IFN, Lane 4: PEG_{20} di(mono)sulfone **5**-His_8IFN reaction mixture. SDS-PAGE analysis shows the formation of His_8IFN-PEG_{20}-His_8IFN.

After SDS-PAGE analysis the reaction mixture was stabilised using an excess of 100 mM sodium triacetoxyborohydride (STAB). STAB, a mild reducing agent, reduces the electron withdrawing ketone group located on the PEG reagent to an alcohol group to stabilise His_8IFN-PEG_{20}-His_8IFN by preventing de-PEGylation (Figure 2-2). The reaction mixture was then buffer exchanged into 100 mM sodium acetate pH 4.0 for CIEC purification.

Initially a single His_8IFN CIEC purification step was used to separate the His_8IFN-PEG_{20}-His_8IFN from un-conjugated PEG_{20} di(mono)sulfone **5** species, unreacted His_8IFN and low and high MW impurities (§ 2.2.7.5). However, as seen in Figure 3-19 (Lane 3), a single CIEC step was unable to separate the His_8IFN-PEG_{20}-His_8IFN from high and low MW impurities. A polishing second CIEC step was conducted, but the impurities remained (Figure 3-19, Lane 4).

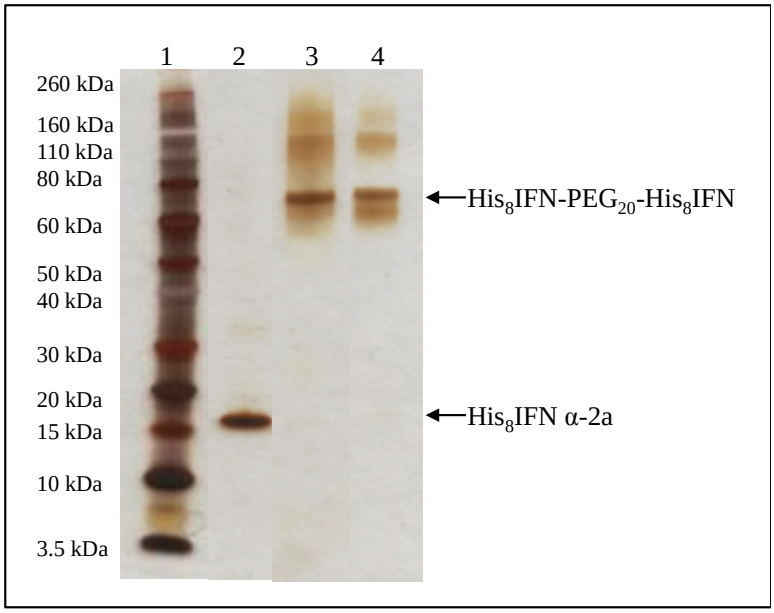

Figure 3-19. SDS-PAGE (silver stain) of CIEC purified His_8IFN-PEG_{20}-His_8IFN. Lane 1: Novex pre-stained markers, Lane 2: His_8IFN α-2a, Lane 3: one-step CIEC purified His_8IFN-PEG_{20}-His_8IFN, Lane 4: two-step CIEC purified His_8IFN-PEG_{20}-His_8IFN. One and two step CIEC unable to purity His_8IFN-PEG_{20}-His_8IFN from high and lower MW impurities.

Seeley J.E and colleagues have reported different methods to purity PEG dimers (one PEG conjugated to two proteins) made using PEG_{20} *bis*-vinyl sulfone (Seely and Richey, 2001). Cation exchange purification was successful for purify the PEG dimer from PEG monomer (one protein with one PEG conjugated) and unconjugated protein. Size exclusion chromatography (SEC) characterises proteins according to size (Tayyab et al., 1991). SEC was successful in separating the unPEGylated from the PEGylated proteins, but could not purify the PEG dimer from

the PEG monomer (James E Seely et al., 2005). Therefore, the reaction was repeated and CIEC used to remove unconjugated PEG_{20} di(*bis*)sulfone **4** and PEG_{20}-His_8IFN from His_8IFN-PEG_{20}-His_8IFN. SEC purification was then used in an attempt to separate His_8IFN-PEG_{20}-His_8IFN dimer from low and high MW impurities (method 2.2.7.6). The SEC chromatogram (Figure 3-20 A), shows that low and high MW impurities were separated with the first peak (Figure 3-20 C) being the high MW impurities (22% of the purified reaction mixture, SEC analysis), then the His_8IFN-PEG_{20}-His_8IFN (38% of the purified reaction mixture, SEC analysis) and then the unreacted His_8IFN α-2a (40% of the purified reaction mixture, SEC) (Figure 3-20 B).

To determine the best purification method, the final His_8IFN-PEG_{20}-His_8IFN from the different purification methods was compared by SDS-PAGE analysis (Figure 3-20 D). Each His_8IFN-PEG_{20}-His_8IFN sample was stored at 4 °C in 50 mM sodium phosphate containing 150 mM sodium chloride pH 7.8 for approximately 2 months. Silver stain was used, as it is a highly sensitive and quick method of detecting low concentrations (very low nanogram detection level) of protein (Chevallet et al., 2006). The best method to obtain a pure His_8IFN-PEG_{20}-His_8IFN conjugate was after one cycle of CIEC and SEC, as seen in Figure 3-20 D (Lane 4). Low and high MW can be seen in Lanes 2 and 3 (Figure 3-20 D) after one or two cycles of CIEC, thus the His_8IFN-PEG_{20}-His_8IFN dimer could not be obtained in high enough purity without using SEC. The high MW impurities observed (Lane 3-7, Figure 3-20 C) could be $(PEG)_n$-His_8IFN, where the polyhistidine tag has two or more PEG di(*bis*)sulfone **4** conjugated to it, producing $(PEG)_n$-His_8IFN. No free His_8IFN α-2a can be seen in any homodimer samples, indicating that the His_8IFN-PEG_{20}-His_8IFN dimer is stable for 2 months at 4 °C.

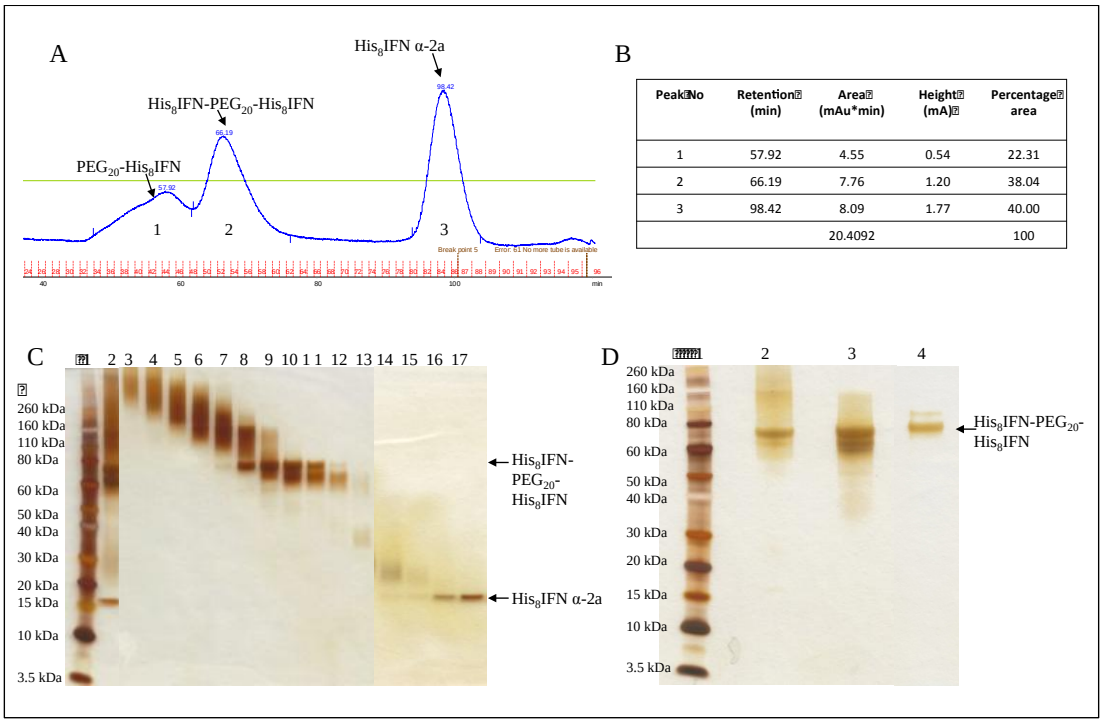

Peak No	Retention (min)	Area (mAu*min)	Height (mA)	Percentage area
1	57.92	4.55	0.54	22.31
2	66.19	7.76	1.20	38.04
3	98.42	8.09	1.77	40.00
		20.4092		100

Figure 3-20. SEC purification of $His_8IFN\text{-}PEG_{20}\text{-}His_8IFN$ fractions. A) SEC purification chromatogram and B) peak information table, C) SDS-PAGE (Silver stain) of fractions from SEC purification, Lane 1: Novex markers, Lane 2: CIEC purified mixture, Lane 3-7: high MW species, Lane 8-12: $His_8IFN\text{-}PEG_{20}\text{-}His_8IFN$, Lane 13-15: low MW impurities, Lane 16-17: unreacted His_8IFN α-2a. D) SDS-PAGE analysis of different purification methods, Lane 1: Novex pre-stained markers, Lane 2: $His_8IFN\text{-}PEG_{20}\text{-}His_8IFN$ after two CIEC steps, Lane 3: $His_8IFN\text{-}PEG_{20}\text{-}His_8IFN$ after one CIEC step, Lane 4: $His_8IFN\text{-}PEG_{20}\text{-}His_8IFN$ after one CIEC and one SEC step. The best method to obtain a pure $His_8IFN\text{-}PEG_{20}\text{-}His_8IFN$ conjugate was one cycle of CIEC and SEC.

The yield of $His_8IFN\text{-}PEG_{20}\text{-}His_8IFN$ dimer (0.030 mg/mL, from 3 mg/mL) after one cycle of CIEC followed by one cycle of SEC purification was found to be ≈1.5 % after UV and MicroBCA™ assay to ascertain the His_8IFN α-2a concentration. This is a very low yield compared to that obtained for $PEG_{20}\text{-}His_8IFN$ and $(PEG_{20})_2\text{-}His_8IFN$, 0.7 mg, 17.6% yield and 0.29 mg, 7.1 % yield respectively (§ 3.2.4). The preparation of $His_8IFN\text{-}PEG_{20}\text{-}His_8IFN$ dimer was conducted twice where the low conversion was consistently observed.

The low yield for the $His_8IFN\text{-}PEG_{20}\text{-}His_8IFN$ dimer results from a low conversion, which could be due to the impure PEG_{20} di(mono)sulfone **5** as can observed in Lane 2 (Figure 3-18) and/or long reaction time (16 h), which may be causing hydrolysis of the PEG reagent **5**. Histidine is less reactive as a nucleophile than a free thiol, so there was concern about the $His_8IFN\text{-}PEG_{20}\text{-}His_8IFN$ dimer could be improved with purer reagents and possibly with reagent that had different leaving groups (Cong et al., 2012). However, the aim was to prepare the His_8IFN-

PEG_{20}-His_8IFN dimer and to characterise the dimer in terms of activity, purity and identity. Thus, the His_8IFN dimer was prepared in enough quantity to characterise it in terms of purity, identity and activity along with the PEG_{20}-His_8IFN and $(PEG_{20})_2$-His_8IFN controls.

3.2.4 Preparation of PEG_{20}-His_8IFN and $(PEG_{20})_2$-His_8IFN using his-tag conjugation

His-tag conjugation of His_8IFN was conducted with PEG_{20} mono-sulfone **2**. The PEG_{20}-His_8IFN and $(PEG_{20})_2$-His_8IFN were prepared to evaluate the different properties of the His_8IFN-PEG_{20}-His_8IFN dimer to that of both mono- and di-PEGylated His_8IFN. In an effort to increase the yield of PEG_{20}-His_8IFN and $(PEG_{20})_2$-His_8IFN, the PEG_{20} *bis*-sulfone reagent **1** was activated by the elimination of one of the β-sulfonyl groups generating a reactive PEG mono-sulfone **2** (§ 2.2.5.1). As a slightly acid pH is required for conjugation to one of the amines in the imidazole ring of histidine, preparation of PEG *bis*-sulfone **1** to PEG mono-sulfone **2** was conducted prior to the reaction, as the elimination reaction of β-sulfonyl groups would be very slow (Brocchini et al., 2008).

His-tag conjugation was conducted using 2.5 eq. of PEG_{20} mono-sulfone **2** to 1 eq. of His_8IFN, the reaction was left for 16 h at 20 °C. The slight excess of PEG reagent and the longer incubation time are required to maximise the conjugation yields, as histidine is less reactive as a nucleophile than a free thiol (Brocchini et al., 2006; Cong et al., 2012). Factors also affecting the conjugation include, protein concentration and pH (Brocchini et al., 2008). SDS-PAGE analysis was then conducted on the reaction mixture (Figure 3-21). The conditions for PEG_{20} *bis*-sulfone **1** reaction with IFN were taken from Cong et al. (Cong et al., 2012), which was based on extensive optimisation. Due to the his-tag having eight-histidine's, two molecules of PEG can conjugate to the his-tag, producing a $(PEG_{20})_2$-His_8IFN species. The conjugation of His_8IFN was successful with $(PEG_{20})_2$-His_8IFN migrating to between ~80-110 kDa. PEG_{20}-His_8IFN α-2a migrated on the gel between ~50-60 kDa and native His_8IFN is seen at ~16 kDa (Figure 3-21).

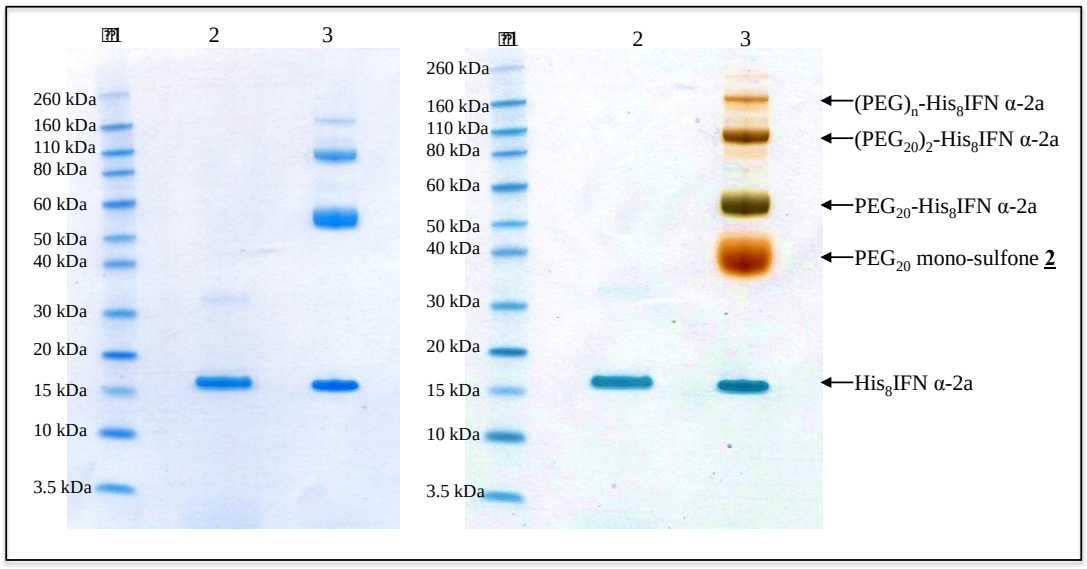

Figure 3-21. Representative SDS-PAGE (left: InstantBlue™ stain, right: InstantBlue™ and PEG (BaI_2) stain) analysis of PEG_{20} mono-sulfone **2** reaction with His_8IFN (n=4), Lane 1: Novex markers, Lane 2: His_8IFN and Lane 3: His_8IFN incubated with 2.5 eq. of PEG_{20} mono-sulfone **2**. SDS-PAGE shows successful his-tag conjugation of His_8IFN, to prepare PEG_{20}-His_8IFN and $(PEG_{20})_2$-His_8IFN.

After the reaction incubation period, the solution containing the reaction mixture (in pH 7.4 buffer) was buffer exchanged into 50 mM sodium acetate buffer, pH 4.0. This was done due to the pI of IFN being ~6.0, meaning the His_8IFN would be positively charged at pH 4.0 to bind efficiently to the CIEC column. The recommended buffer for CIEC at pH 4.0 was sodium acetate with the HiTrap™ sulphopropyl (SP) MacroCap™ column (GE Healthcare HiTrap™ SP MacroCap™ product literature). The reaction mixture was purified by the different positively charged His_8IFN species having different affinities to the column, which were eluted with a step gradient (method 2.2.7.2). Collected fractions, were analysed for each peak by gel electrophoresis (Figure 3-22).

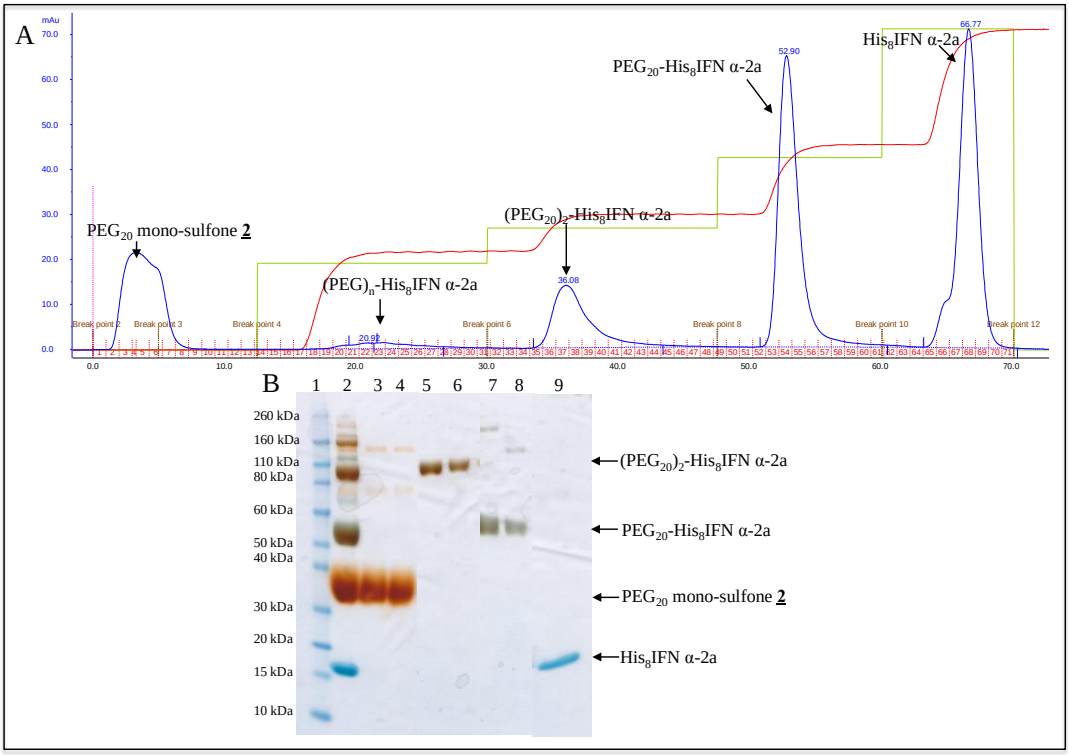

Figure 3-22. Example analysis of CIEC purification of PEG_{20} mono-sulfone **2**-His_8IFN reaction mixture (n=4). A) CIEC chromatogram and B) SDS-PAGE (InstantBlue™ and PEG stain) analysis of CIEC fractions, Lane 1: Novex markers, Lane 3: reaction mixture prior to CIEC, Lane 3-4: PEG_{20} mono-sulfone **2**, Lane 5-6: $(PEG_{20})_2$-His_8IFN, Lane 7-8: PEG_{20}-His_8IFN and Lane 9: His_8IFN. CIEC successfully purified $(PEG_{20})_2$-His_8IFN and PEG_{20}-His_8IFN from His_8IFN.

Analysis of the chromatogram showed the major peak maxima were at 20.92, 22.21, 36.08, 52.90 and 66.77 min (Figure 3-22 A). The first peak corresponds to unconjugated PEG_{20} reagent **2**, which does not bind to the CIEC column, this can be seen in lanes 3-4 (Figure 3-22 B) at ~40 kDa. The second peak corresponds to multimers or $(PEG)_n$-His_8IFN, which bind loosely to the column due to steric hinderance from the conjugated PEGs. $(PEG_{20})_2$-His_8IFN and PEG_{20}-His_8IFN elute prior to unconjugated His_8IFN, which bound strongest to the column and therefore required the highest concentration of buffer B to elute from the column (Figure 3-22). Purification was found to be very reproducible, where the elution pattern was consistent for each of the four separate occasions it was conducted.

PEG_{20}-His_8IFN and $(PEG_{20})_2$-His_8IFN fractions (52-60 and 35-44 respectively) were subsequently centrifugally concentrated using VivaSpin column 10,000 MWCO, combined and purified further by CIEC separately (§ 2.2.7.3). The CIEC chromatogram peaks and SDS-PAGE analysis of the CIEC peak fractions for PEG_{20}-His_8IFN and $(PEG_{20})_2$-His_8IFN respectively are shown in Figure 3-23. PEG_{20}-

His_8IFN was observed as single peak (Figure 3-23 A) and can be seen between 50-60 kDa by SDS-PAGE analysis (Figure 3-23 B). The chromatogram of $(PEG_{20})_2$-His_8IFN CIEC purification showed two peaks (Figure 3-23 C), the larger peak between 30-40 min was confirmed to be $(PEG_{20})_2$-His_8IFN by SDS-PAGE (~110 kDa, Figure 3-23 D), whilst the smaller peak at 50 min was confirmed to be PEG_{20}-His_8IFN (50-60 kDa) (Lanes 7-9, Figure 3-23 D).

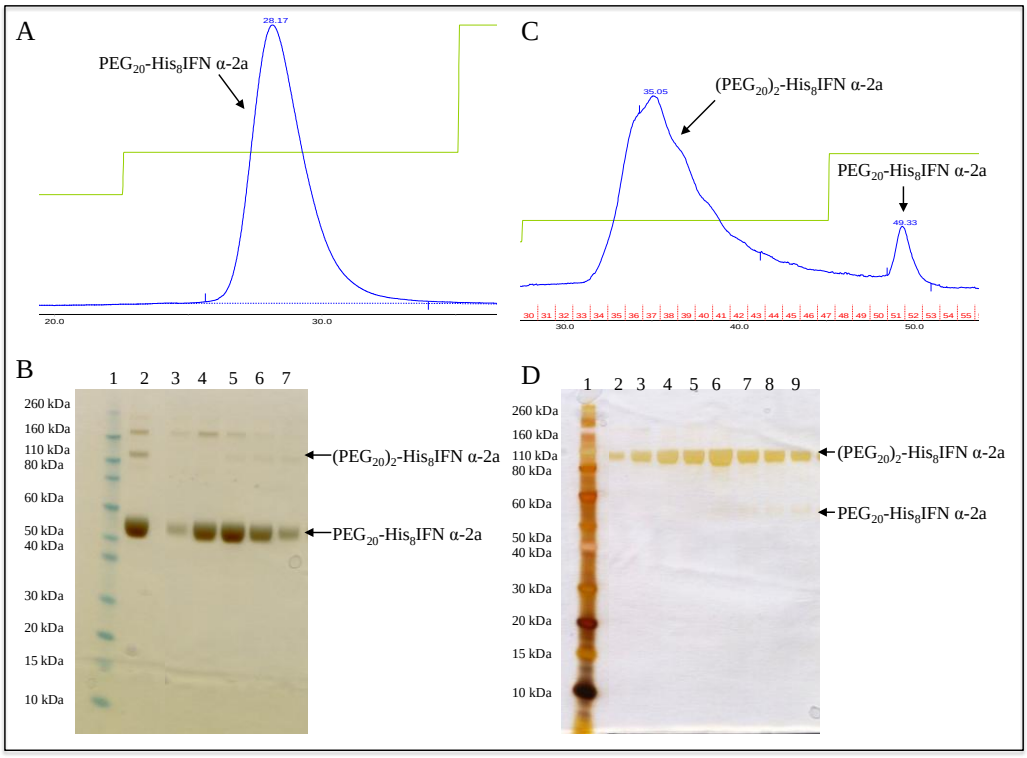

Figure 3-23. Example of further CIEC purification analysis of A) PEG_{20}-His_8IFN, C) $(PEG_{20})_2$-His_8IFN and SDS-PAGE (silver stain) analysis of peak fractions of B) PEG_{20}-His_8IFN and D) $(PEG_{20})_2$-His_8IFN. Further purification of PEG_{20}-His_8IFN and $(PEG_{20})_2$-His_8IFN was consistently successful at isolating the final PEG_{20}-His_8IFN and $(PEG_{20})_2$-His_8IFN conjugates (n=4).

Fractions containing pure PEG_{20}-His_8IFN and $(PEG_{20})_2$-His_8IFN were then combined and centrifugally concentrated until approximately 2.5 mL remained so the conjugates could be buffer exchanged into storage buffer (§ 2.2.7.3). The storage buffer was 50 mM sodium phosphate containing 150 mM sodium chloride pH 7.4 and was chosen as this buffer is often used for the storage of proteins (Cong et al., 2012). A final SDS-PAGE analysis was conducted on the final conjugates to confirm their purity, as seen in Figure 3-24. Quantification of protein concentration was conducted by MicroBCA™ assay and UV absorbance at 280nm (§ 2.2.2.1). The final yields for PEG_{20}-His_8IFN and $(PEG_{20})_2$-His_8IFN were calculated by MicroBCA™ quantification of protein concentration were 0.7 mg, 17.6% yield for PEG_{20}-His_8IFN

and 0.29 mg, 7.1 % yield for $(PEG_{20})_2$-His_8IFN. The preparation of PEG_{20}-His_8IFN and $(PEG_{20})_2$-His_8IFN was conducted four times, with yields were found to be reproducible at ~17% and 7-9% for PEG_{20}-His_8IFN and $(PEG_{20})_2$-His_8IFN respectively. Samples were then aliquoted into cryovials, and flash frozen using liquid nitrogen, and stored at -80 ºC ready for identity, purity, stability and activity characterisation tests to be conducted with the His_8IFN-PEG_{20}-His_8IFN dimer.

The His_8IFN-PEG_{20}-His_8IFN (~1.5%) was prepared along with controls PEG_{20}-His_8IFN (17.6%) and $(PEG_{20})_2$-His_8IFN (7.1%). The yields were lower than those reported for thiol-conjugation of non-his-tagged IFN, where a 65% yield of PEG_{10}-IFN was reported (Balan et al., 2007). This could be due to histidine being a less reactive nucleophile than thiol. Further, investigations (§3.2.1) into the PEG di(*bis*)sulfone **4** revealed that the reagent purity was low, which could have impeded on the yield/conversion of the His_8IFN-PEG_{20}-His_8IFN.

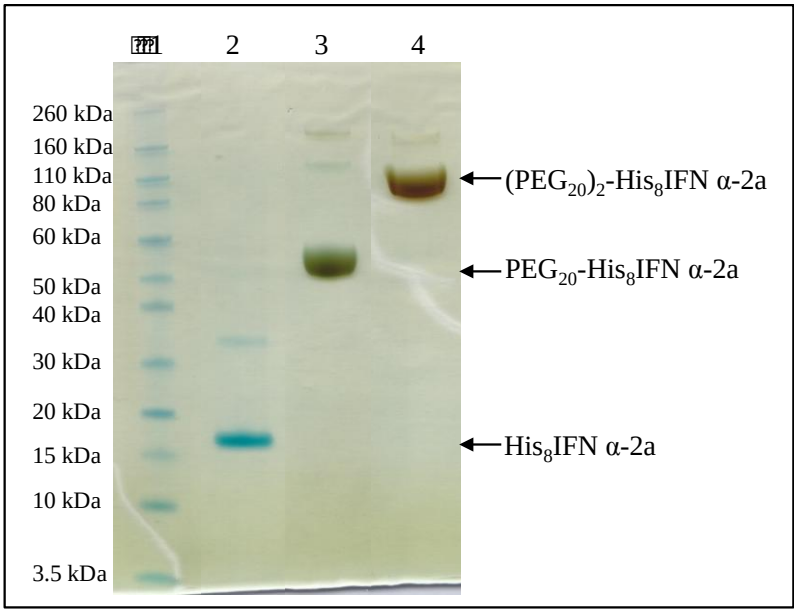

Figure 3-24. SDS-PAGE (InstantBlue™ stain) analysis of final PEG_{20}-His_8IFN and $(PEG_{20})_2$-His_8IFN, Lane 1: Novex pre-stained markers, Lane 2: His_8IFN, Lane 3: PEG_{20}-His_8IFN, Lane 4: $(PEG_{20})_2$-His_8IFN. PEG_{20}-His_8IFN and $(PEG_{20})_2$-His_8IFN successfully prepared for identity, purity and activity characterisation for comparison to the His_8IFN-PEG_{20}-His_8IFN.

3.2.5 Characterisation of His_8IFN-PEG_{20}-His_8IFN dimer

3.2.5.1 Accelerated stability study of His_8IFN-PEG_{20}-His_8IFN dimer

An accelerated stability study was conducted on the His_8IFN-PEG_{20}-His_8IFN dimer in comparison to the PEG_{20}-His_8IFN and $(PEG_{20})_2$-His_8IFN conjugates in order to assess the STAB treatment on the conjugates using DTT and high temperatures (50

°C and 90 ºC). DTT was used to act as a nucleophile. De-conjugation of the conjugate may occur by DTT reacting with the linker, but STAB would prevent this as the amide/ester bonds within the linker are already reduced.

The His_8IFN-PEG_{20}-His_8IFN dimer, PEG_{20}-His_8IFN and $(PEG_{20})_2$-His_8IFN conjugates were shown to be stable (Figure 3-25) as no free His_8IFN α-2a from de-conjugation was observed in those samples subject to DTT reduction. In addition, this accelerated stability study showed that the His_8IFN-PEG_{20}-His_8IFN dimer, PEG_{20}-His_8IFN and $(PEG_{20})_2$-His_8IFN remain conjugated to PEG up to 90 ºC, as no free or aggregated His_8IFN was observed.

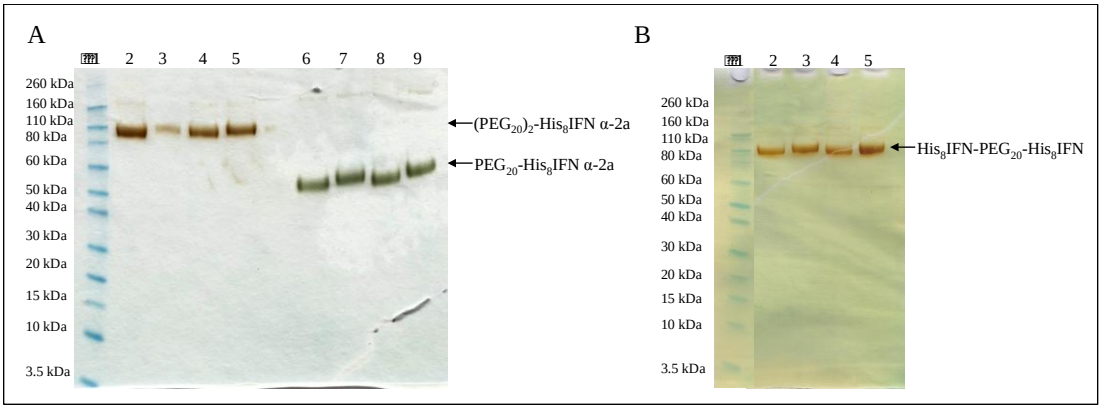

Figure 3-25. A) SDS-PAGE (InstantBlue™ and PEG stain) analysis of PEG_{20}-His_8IFN (Lanes 6-9) and $(PEG_{20})_2$-His_8IFN (Lanes 2-5) stressed with ± DTT at 50 and 90 °C. Lane 1: Novex pre-stained markers, Lane 2: -DTT 50 °C, Lane 3: +DTT 50 °C, Lane 4: -DTT 90 °C, Lane 5: +DTT 90 °C, Lane 6: -DTT 50 °C, Lane 7: +DTT 50 °C, Lane 8: -DTT 90 °C, Lane 9: +DTT 90 °C. B) SDS-PAGE (InstantBlue™ and PEG stain) analysis of His_8IFN-PEG_{20}-His_8IFN dimer stressed with ± DTT at 50 and 90 °C, Lane 1: Novex pre-stained markers, Lane 2: -DTT 50 °C, Lane 3: +DTT 50 °C, Lane 4: -DTT 90 °C, Lane 5: +DTT 90 °C. His_8IFN-PEG_{20}-His_8IFN, PEG_{20}-His_8IFN and $(PEG_{20})_2$-His_8IFN found stable when reduced ± DTT at 50 °C and 90 °C, as no free His_8IFN was observed by SDS-PAGE.

3.2.5.2 Anti-IFN α-2a Western blot of his-tag conjugated His_8IFN α-2a conjugates

To confirm the identity of His_8IFN-PEG_{20}-His_8IFN dimer, PEG_{20}-His_8IFN and $(PEG_{20})_2$-His_8IFN, an anti-IFN α-2a Western blot was conducted to confirm the presence of IFN. Samples were loaded (1 µg) into a SDS-PAGE 4-12% Bis-Tris gel. The resulting gel was transferred onto nitrocellulose membrane, which was subject to rabbit anti-IFN α-2a antibody followed by anti-rabbit-AP conjugated antibody (method 2.2.10.1).

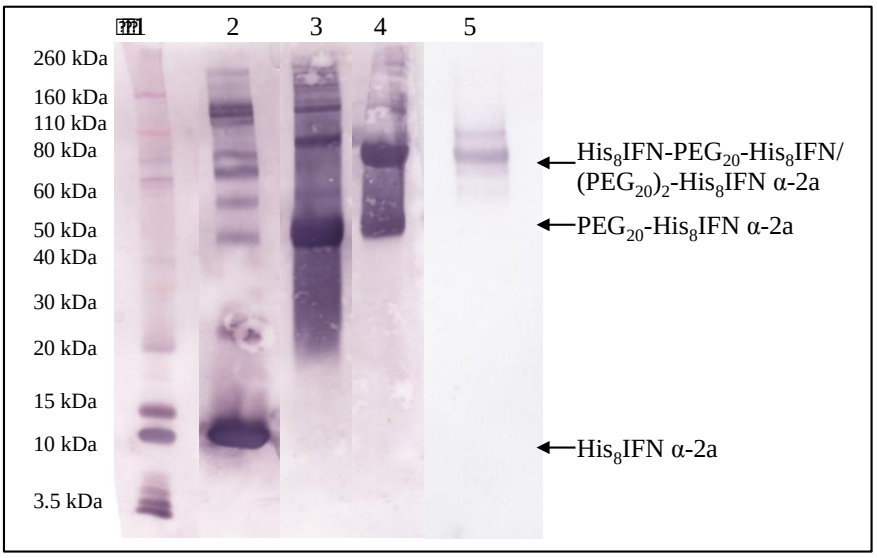

Figure 3-26. Anti-IFN α-2a Western blot of $His_8IFN\text{-}PEG_{20}\text{-}His_8IFN$ dimer**,** $PEG_{20}\text{-}His_8IFN$ and $(PEG_{20})_2\text{-}His_8IFN$. Lane 1: Novex markers, Lane 2: His_8IFN α-2a, Lane 3: $PEG_{20}\text{-}His_8IFN$, Lane 4: $(PEG_{20})_2\text{-}His_8IFN$, Lane 5: $His_8IFN\text{-}PEG_{20}\text{-}His_8IFN$. Anti-IFN α-2a antibody identifies all His_8IFN α-2a species confirming their identities.

The anti-IFN α-2a identifies $His_8IFN\text{-}PEG_{20}\text{-}His_8IFN$ dimer, which can be clearly observed at ~80 kDa (Lane 5, Figure 3-26). This is 20 kDa larger than that observed for $PEG_{20}\text{-}His_8IFN$, which can be seen at ~60 kDa (Lane 3, Figure 3-26). This 20 kDa difference could be explained by the conjugation of one more His_8IFN molecule within $His_8IFN\text{-}PEG_{20}\text{-}His_8IFN$ dimer compared to that of $PEG_{20}\text{-}His_8IFN$. Interestingly, the MW of the $His_8IFN\text{-}PEG_{20}\text{-}His_8IFN$ dimer is similar to that of $(PEG_{20})_2\text{-}His_8IFN$, where $(PEG_{20})_2\text{-}His_8IFN$ can be seen at ~80 kDa in lane 4 (Figure 3-26). Unconjugated His_8IFN was analysed as a control, which is seen at ~15 kDa in Lane 1 (Figure 3-26). This anti-IFN Western blot therefore confirms the identity of $His_8IFN\text{-}PEG_{20}\text{-}His_8IFN$ dimer, $PEG_{20}\text{-}His_8IFN$ and $(PEG_{20})_2\text{-}His_8IFN$ as they were successfully detected.

The Western blot (Figure 3-26) has a high background signal, with some smearing of His_8IFN α-2a (Lane 2), $PEG_{20}\text{-}His_8IFN$ (Lane 3), $(PEG_{20})_2\text{-}His_8IFN$ (Lane 4). Optimising the development time of the membrane could reduce the background signal. Additionally, longer washing steps would also help to reduce the background signal, however, too long a washing steps can also reduce the signal. An optimised lower concentration of IFN species could be used to help reduce the high background signal. The patchiness of the Western blot could be prevented by rolling a tube across the gel and nitrocellulose membrane to remove air bubbles (Mahmood and Yang, 2012).

3.2.5.3 MALDI-TOF analysis of his-tag PEGylated His_8IFN α-2a conjugates

To confirm the MW and thus identity of His_8IFN-PEG_{20}-His_8IFN dimer in comparison to controls (His_8IFN, PEG_{20}-His_8IFN and $(PEG_{20})_2$-His_8IFN) MALDI-TOF analysis was conducted. MALDI-TOF mass spectrometry (MS) is widely used technique for the precise mass determination of proteins, peptides or glycan's and has also been used for the analysis of post-translational modifications (Fenselau, 1997). MALDI-TOF can ionise molecules with molecular masses of 100-1,000,000 Da for analysis and can be a highly sensitive technique. As MALDI-TOF was conducted n=1 for His_8IFN-PEG_{20}-His_8IFN, His_8IFN, PEG_{20}-His_8IFN and $(PEG_{20})_2$-His_8IFN, the achieved MS data was analysed to one significant figure since the accuracy of MS is often between 0.1-0.01% (Fenselau, 1997). One significant figure was used as no repeats were conducted to determine the reproducibility of the MALDI-TOF data.

Typically, for MALDI-TOF analysis, the amount of salts in the samples should be as low as possible. Thus, the samples (His_8IFN-PEG_{20}-His_8IFN, His_8IFN, PEG_{20}-His_8IFN and $(PEG_{20})_2$-His_8IFN) were concentrated by freeze-drying. Prior to freeze-drying the samples were desalted using a PD-10 column to buffer exchange the samples into deionised water. These freeze-dried samples were then re-suspended in ammonium bicarbonate pH 8.0. PEG_{20} di(mono)sulfone **2** was re-suspended into ammonium bicarbonate pH 8.0; then all the samples were then analysed by MALDI-TOF MS (method 2.2.10.2).

As discussed previously (§ 3.2.2), the MALDI-TOF spectrum for His_8IFN α-2a showed a peak MW of ≈20405.2 Da (Figure 3-27 A), this was found to be comparable to that stated in literature (Ahad et al., 2009; Vanden Broecke and Pfeffer, 1988), but the MW was slightly larger taking into account the eight-histidine tag (1.2 kDa) (Cong et al., 2012). The PEG_{20} di(mono)sulfone **2** MALDI-TOF spectrum showed a peak at ≈22940.6 Da (E). The MALDI-TOF spectrum of His_8IFN-PEG_{20}-His_8IFN dimer showed a peak MW of ≈63106.7 (Figure 3-27 D), suggesting the conjugate obtained was His_8IFN-PEG_{20}-His_8IFN (2× His_8IFN α-2a's ≈20405.2 Da each + PEG_{20} ≈22940.6 Da). SDS-PAGE analysis of His_8IFN-PEG_{20}-His_8IFN dimer was observed on the gel at ≈70 kDa such as observed for the anti-IFN Western blot (Figure 3-26).

The His_8IFN-PEG_{20}-His_8IFN dimer was found to be difficult to prepare pure and in good yield (n=2). Optimisation reactions investigating PEG_{20} di(*bis*)sulfone **4** vs. PEG_{20} di(mono)sulfone **5**, incorporating DMSO, PEG:IFN equivalents and reaction times were all investigated. The purity of the His_8IFN-PEG_{20}-His_8IFN was improved with optimisation of the purification procedure, whereby CIEC followed by SEC was used.

Whereas, the PEG_{20}-His_8IFN MALDI-TOF spectrum showed a peak of ≈40686.0 Da (Figure 3-27 B), confirming the conjugate's identity as PEG_{20}-His_8IFN (His_8IFN α-2a≈20405.2 Da + PEG≈20 kDa). Comparing the MW of the PEG_{20}-His_8IFN (≈40686.0 Da) to His_8IFN-PEG_{20}-His_8IFN (≈63106.7 Da) there is a 20 kDa difference in MW between the two molecules. As the His_8IFN-PEG_{20}-His_8IFN is conjugated to one more His_8IFN molecule compared to that of the dimer, thus confirming the identity of both the PEG_{20}-His_8IFN and His_8IFN-PEG_{20}-His_8IFN. Whilst for $(PEG_{20})_2$-His_8IFN, the MALDI-TOF spectrum (Figure 3-27 C) of ≈60688.3 Da, this confirms the identity of $(PEG_{20})_2$-His_8IFN (His_8IFN α-2a≈20405.2 Da + PEG≈40 kDa). Compared to PEG_{20}-His_8IFN, the MW of $(PEG_{20})_2$-His_8IFN is 20 kDa larger, taking into account the conjugation of the second PEG *bis*-sulfone **1**. Whilst compared to the His_8IFN-PEG_{20}-His_8IFN the MW is similar, however the slightly larger for the His_8IFN-PEG_{20}-Hi_8IFN dimer, taking into account the polyhistidine tags attached to IFN.

To conclude, the aim was to prepare His_8IFN-PEG_{20}-His_8IFN utilising a recombinant-chemical approach, taking advantage of the 8-polyhistidine-tag on the recombinantly prepared IFN. However, it was found that pure His_8IFN-PEG_{20}-His_8IFN, were more difficult to prepare than thought in a good yield, even after numerous optimisation experiments and attempts. Enough was prepared to test the activity of the His_8IFN-PEG_{20}-His_8IFN within the *in vitro* assays. However, to investigate whether pure IFN-PEG-IFN could be prepared and possibly in higher yields, disulfide conjugation was used due to free thiols being a better nucleophile than free histidines (Cong et al., 2012). Therefore, it was hoped that the free thiols would be more reactive with the PEG di(*bis*)sulfone **4** and prepare IFN-PEG-IFN dimers. Disulfide conjugation on His_8IFN was conducted with PEG di(*bis*)sulfone **4** to make IFN-PEG-IFN dimers to evaluate the different properties of the IFN-PEG-IFN dimers.

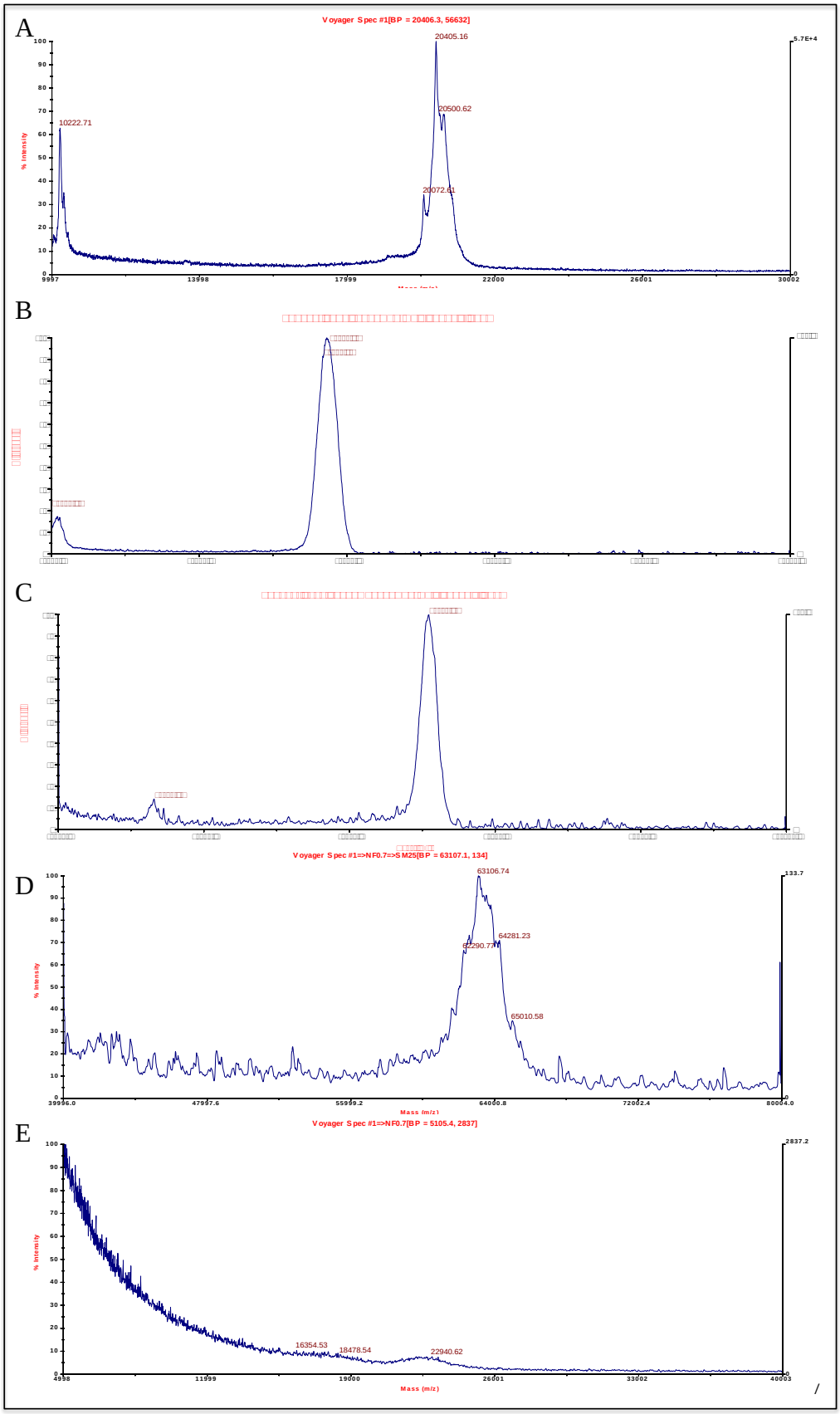

Figure 3-27. MALDI-TOF spectrum for His_8IFN α-2a species and PEG_{20} di(mono)sulfone **5**. A) His_8IFN α-2a B) PEG_{20}-His_8IFN, C) $(PEG_{20})_2$-His_8IFN, D) His_8IFN-PEG_{20}-His_8IFN, E) PEG_{20} di(mono)sulfone **5**. MALDI-TOF confirmed the MW of the his-tag conjugates.

3.3 Disulfide-bridging conjugation to prepare IFN-PEG-IFN

3.3.1 Optimisation of reduction conditions for His_8IFN α-2a using DTT

The most commonly used thiol reductant is dithiothreitol (DTT) (Hansen and Winther, 2009). Disulfide reduction with requires only one molecule of DTT for each disulfide to be reduced. DTT is converted into a stable cyclic disulfide which drives the reduction of the accessible protein disulfides (Getz et al., 1999; Hansen and Winther, 2009). Scouting experiments were conducted with increasing concentrations of DTT to evaluate the conditions to reduce the disulfides in His_8IFN α-2a. His_8IFN α-2a (0.1 mg/mL; 0.1 mL) was reduced using DTT concentrations ranging from 10-100 mM for 30 min and 1 h at RT (Figure 3-28). The reduction was conducted at pH 7.8 (method 2.2.6.1) as DTT has been shown to be most effective at pH values above pH 7.0 (protonated sulfurs have lowered nucleophilicities) (Cleland, 1964; Hermanson, 2008).

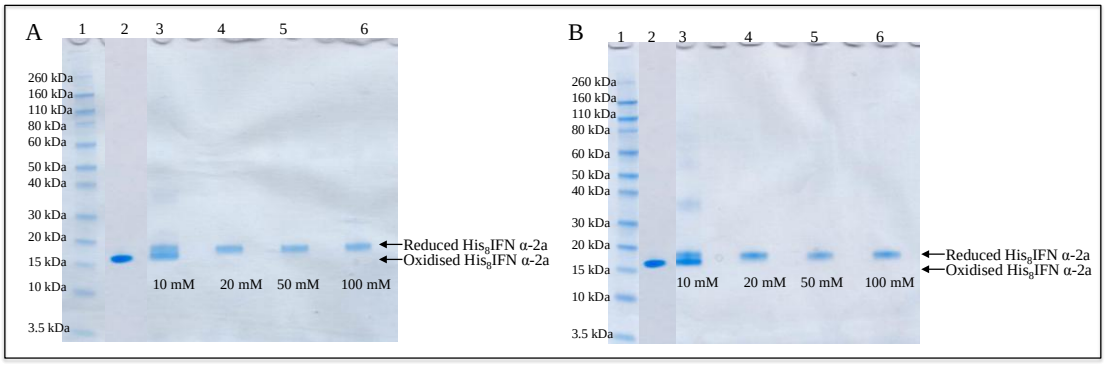

Figure 3-28. DTT (10-100 mM) reduction study of His_8IFNα-2a (0.1 mg/mL) for A) 30 min and B) 1 h. Lane 1: Novex pre-stained markers, Lane 2: 10 mM DTT, Lane 3: 20 mM DTT, Lane 4: 50 mM DTT and Lane 5: 100 mM DTT. His_8IFN α-2a was completely reduced by 20 mM DTT after 30 min. The reduced disulfides in His_8IFN α-2a are then able to undergo *bis*-alkylation reactions with PEG di(*bis*)sulfone **4** to prepare IFN-PEG-IFN homodimers.

SDS-PAGE analysis (Figure 3-28) indicated that His_8IFN is completely reduced at DTT concentrations above 20 mM from 30 min (Lanes 3-5,Figure 3-28). Fully reduced protein (Lanes 2-5, Figure 3-28) migrated more slowly compared to native His_8IFN α-2a with its two disulfides oxidised. This is due to the disulfide reduced IFN being able to be completely unfolded in the presence of SDS to have a larger solution structure than the oxidised IFN. His_8IFN α-2a was not fully reduced using 10 mM DTT (Lane 2, Figure 3-28) even after 1 h, therefore 20 mM DTT for 30 min was considered best for reducing His_8IFN α-2a.

Another common method to reduce disulfide bonds in proteins is to use tris (2-carboxyethyl) phosphine (TCEP). TCEP has been shown to be significantly more stable over a wider pH range (1.5-8.5) than DTT (Getz et al. 1999). However, there are two main disadvantages of using TCEP. Firstly, TCEP does not have a long shelf life (Getz et al., 1999); hence its reducing efficiency declines over time as it degrades. Secondly, DTT is more stable in buffers containing a metal chelator whereas the stability of TCEP can be affected for example by the presence of phosphates (Getz et al., 1999). Therefore, DTT was used for reduction.

Removal of the reductant (TCEP or DTT) from the reduced protein, elution over a PD-10 column is necessary. As, the reductant (TCEP or DTT) could react with the *bis*-sulfone linker, reducing the yield of the desired PEGylated conjugate. However, as the protein is within the reduced state, it is more amenable to precipitation or dimerisation. No precipitation was observed when eluting reduced IFN from the PD-10 column during preparation of the IFN-PEG-IFN dimers.

3.3.2 Glutathione re-oxidation of His_8IFN α-2a

IFN has two disulfide bonds that are amenable to reduction by DTT. To prepare the mono-PEG IFN conjugate, only one disulfide bond was conjugated by PEG *bis*-sulfone **1**. Upon conjugation it is necessary to ensure the unconjugated disulfide is reoxidised.

Glutathione is one of the most abundant thiol compounds found in cells, and plays a major role in the formation of disulfide bonds in proteins in the endoplasmic reticulum (Okumura et al., 2011). Glutathione is widely used to assist protein reoxidation *in vitro* with proteins containing disulfide bond(s) (Okumura et al., 2011).

The formation of a disulfide bond in a protein in the presence of glutathione occurs via 'oxido-shuffling' (thiol/disulfide exchange reaction) process. Initially, a mixed disulfide of the reduced protein and glutathione forms (Figure 3-29). However, this mixed disulfide is often less stable than the protein disulfide which then forms. Fahey et al (2000) have shown the effect of GSH:GSSG on the reoxidation of the reduced disulfides and recovery of activity of serine protease domain of urokinase plasminogen activator (Fahey et al., 2000). They found that the optimum ratio of GSH:GSSG for efficient reoxidation to be 0.5:0.5 mM (Fahey et al., 2000). Further, glutathione has been described to reoxidise IFN α-2b after

conjugation with PEG *bis*-sulfone **1**. This work demonstrated glutathione could be utilised in the reoxidation of IFN after disulfide conjugation (Balan et al., 2007). As disulfide-conjugation was to be conducted on His_8IFN, the optimum reoxidation conditions for His_8IFN were investigated.

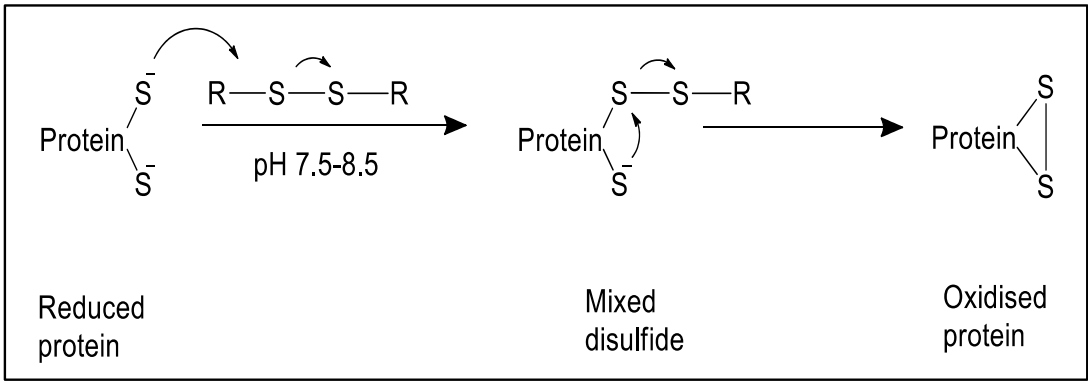

Figure 3-29. The process of protein disulfide bond formation via thiol/disulfide exchange process initiated by small MW disulfide compounds (R) such as glutathione. His_8IFN has two disulfide bonds, which can be conjugated to. Conjugation to one reduced disulfide was required, therefore, once conjugated to, the other disulfide bond needs to be reoxidised, for this glutathione was used.

To determine the optimum incubation time and temperature for the complete reoxidation of the reduced cysteine-thiols of His_8IFN, an investigation was undertaken using glutathione at RT and 4 °C over time points (0, 1, 3, 5, 8 and 16 h). This is due to the reduced disulfide to take time to reoxidise, as the disulfide-exchange reactions are the rate-determining step (Okumura et al., 2011). His_8IFN (0.5 mg/mL, 2 mL) was reduced with DTT (20 mM), the DTT was removed and the reduced His_8IFN α-2a was aliquoted into two 1 mL fractions. Glutathione (50 mM GSH:50 mM GSSG) was added to each aliquot, where one was placed at RT and the other at 4 °C, and SDS-PAGE analysis run at the determined time points (method 2.2.6.2). Densimetric analysis of the InstantBlue™ stained gels was conducted, as InstantBlue™ is a quantitative stain.

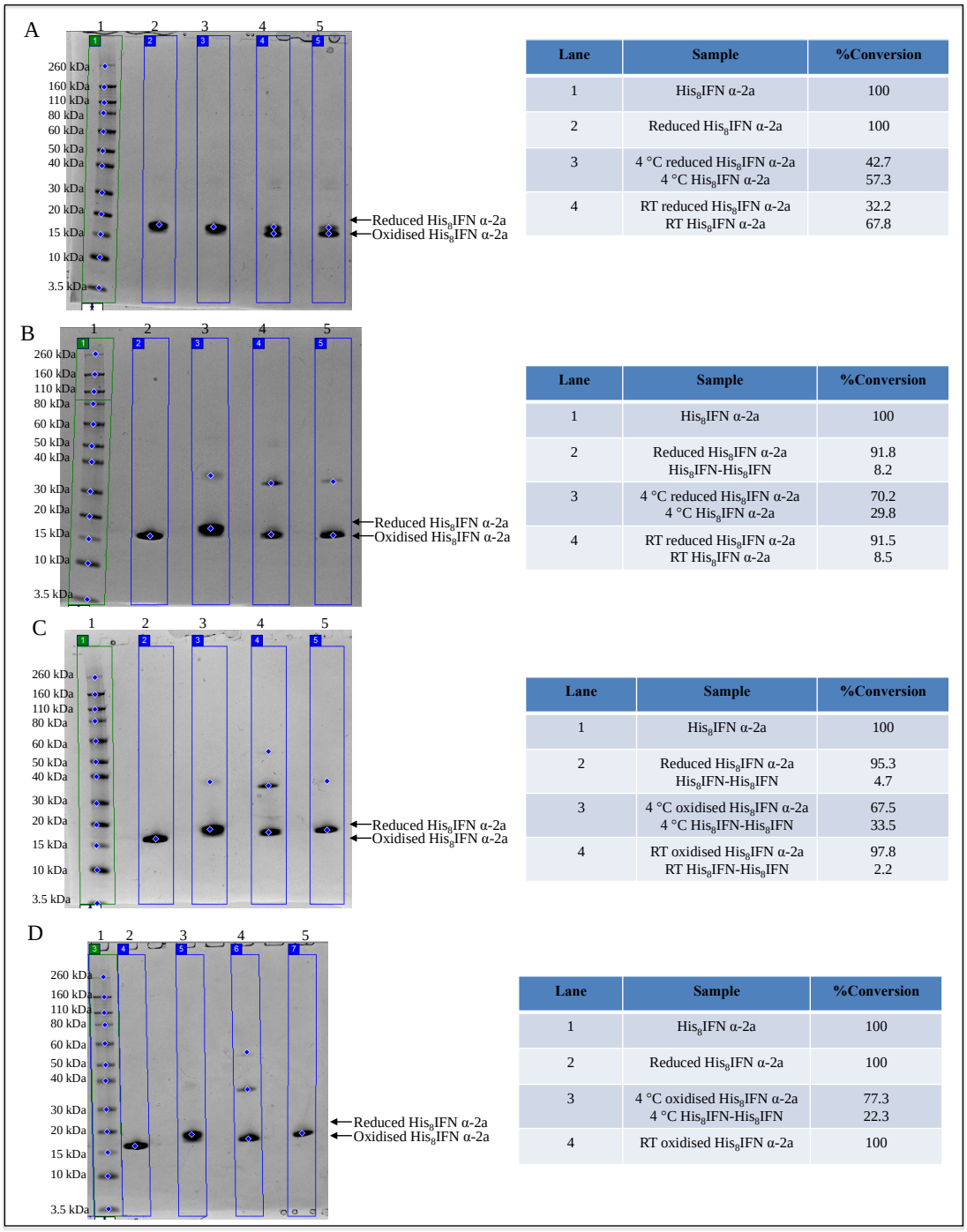

Lane	Sample	%Conversion
1	His_8IFN α-2a	100
2	Reduced His_8IFN α-2a	100
3	4 °C reduced His_8IFN α-2a 4 °C His_8IFN α-2a	42.7 57.3
4	RT reduced His_8IFN α-2a RT His_8IFN α-2a	32.2 67.8

Lane	Sample	%Conversion
1	His_8IFN α-2a	100
2	Reduced His_8IFN α-2a His_8IFN-His_8IFN	91.8 8.2
3	4 °C reduced His_8IFN α-2a 4 °C His_8IFN α-2a	70.2 29.8
4	RT reduced His_8IFN α-2a RT His_8IFN α-2a	91.5 8.5

Lane	Sample	%Conversion
1	His_8IFN α-2a	100
2	Reduced His_8IFN α-2a His_8IFN-His_8IFN	95.3 4.7
3	4 °C oxidised His_8IFN α-2a 4 °C His_8IFN-His_8IFN	67.5 33.5
4	RT oxidised His_8IFN α-2a RT His_8IFN-His_8IFN	97.8 2.2

Lane	Sample	%Conversion
1	His_8IFN α-2a	100
2	Reduced His_8IFN α-2a	100
3	4 °C oxidised His_8IFN α-2a 4 °C His_8IFN-His_8IFN	77.3 22.3
4	RT oxidised His_8IFN α-2a	100

Figure 3-30. Glutathione reoxidisation of DTT reduced His_8IFN α-2a time point (0,1,3,5,8,16 h) studies, A) 0 h, B) 3 h, C) 8 h, D) 16 h. Lane 1: Novex pre-stained markers, Lane 2: His_8IFN α-2a, Lane 3: reduced His_8IFN α-2a, Lane 4: 4 °C glutathione-His_8IFN α-2a mixture, Lane 5: RT glutathione-His_8IFN α-2a mixture. Complete reoxidation of reduced His_8IFN α-2a was observed when His_8IFN α-2a was incubated with glutathione at RT for 16 h.

From the results (Figure 3-30) it was deduced that the most favourable conditions for glutathione reoxidisation of the reduced His_8IFN was to allow incubation to proceed for 16 h at RT, which led to complete reoxidation of His_8IFN. In contrast, the reactions at 4 °C did not go to full conversion to prepare oxidised His_8IFN, as ~23%

of the mixture was His_8IFN-His_8IFN. Similarly, at 8 h at RT had a 94% yield of oxidised His_8IFN as some of the mixture had formed His_8IFN-His_8IFN. To conclude, it was chosen to combine the conjugation reaction time and after this add the GRS (50 mM GSH:50 mM GSSG) and allow the reoxidising of the reduced His_8IFN to be conducted for 16 h at RT. Balan and colleagues reported using a 1 mM solution of glutathione (50 mM oxidised glutathione: 50 mM reduced glutathione) for 24 h at 4 °C (Balan et al., 2007).

3.3.3 Preparation of IFN-PEG_{20}-IFN and IFN-PEG_{10}-IFN

To investigate whether pure IFN-PEG-IFN could be made and possibly in higher yields, disulfide conjugation was used. Disulfide conjugation had not previously been conducted on His_8IFN. Disulfide conjugation was conducted on His_8IFN with PEG di(*bis*)sulfone **4** to make IFN-PEG-IFN dimers to evaluate the different properties of the IFN-PEG-IFN dimers. IFN-PEG_{10}-IFN was prepared to determine i) how varying the PEG di(*bis*)sulfone **4** size (20 kDa vs. 10 kDa) affects the reaction conversion/yield and ii) how varying the PEG di(*bis*)sulfone **4** sizes affect the bioactivity of IFN in comparison to their mono- or di-PEGylated counterparts. Further, PEG di(*bis*)sulfone **4** had been previously used to prepare Fab-PEG-Fab dimers using disulfide-conjugation (Khalili et al., 2013). When tested *in vitro,* the Fab-PEG-Fab dimers binding activity mimicked that of mAbs (§1.4.1.4) (Khalili et al., 2013), therefore it was thought that the PEG di(*bis*)sulfone **4** with disulfide conjugation could be used sucessfully to prepare IFN-PEG-IFN dimers.

For conjugation with the 10 and 20 kDa PEG di(*bis*)sulfone **4**, His_8IFN α-2a (4.1 mg) was first reduced using 20 mM DTT (Figure 3-31). Reduced His_8IFN was buffer exchanged into 50 mM sodium phosphate 20 mM EDTA pH 7.8 for conjugation, as thiols are nucleophilic at neutral pH, therefore thiol-specific conjugation can take place (Brocchini et al., 2008).

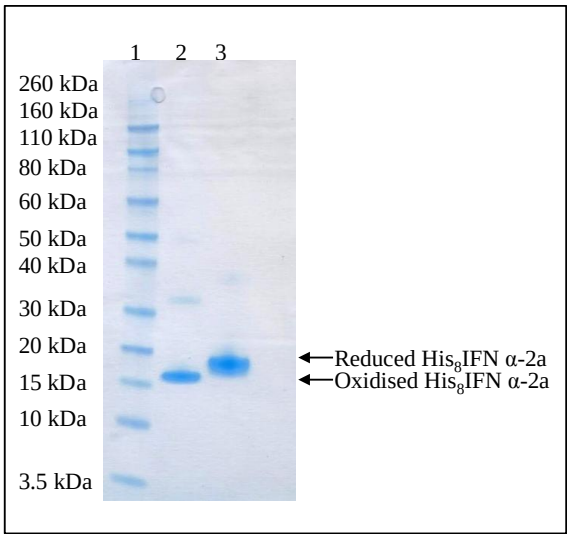

Figure 3-31. SDS-PAGE of His_8IFN α-2a reduced using DTT for 10 and 20 kDa PEG di(*bis*)sulfone **4** conjugation. Lane 1: Novex pre-stained markers, Lane 2: His_8IFN α-2a and Lane 3: reduced His_8IFN α-2a. Successful reduction of His_8IFN α-2a with 20 mM DTT for 10 and 20 kDa PEG di(*bis*)sulfone **4** conjugation.

The reduced His_8IFN was conjugated to using PEG_{20} di(*bis*)sulfone **4** in a 2:1 ratio. This stoichiometry was selected to promote the formation of IFN-PEG_{20}-IFN, as there was excess of His_8IFNα-2a to PEG to minimise the formation of X-PEG_{20}-IFN (§ 2.2.8.8). The same ratio was used of PEG_{10} di(*bis*)sulfone **4** to promote the formation of IFN-PEG_{10}-IFN (§ 2.2.8.9). To reduce the risk of hydrolysis, the PEG reagent was activated *in situ* by the elimination of two β sulfonyl groups generating reactive PEG di(mono)sulfone **4** (Figure 2-1). Reduced His_8IFN α-2a (0.5 mg/mL, 7.5 mL) was allowed to incubate for 5 h at 20 °C separately with the 10 kDa and 20 kDa PEG di(*bis*)sulfone **3**. To re-oxidise the unconjugated thiol of the remaining disulfide, GRS was added (50 mM, 153.1 μL) and left to reaction for a further 16 h at 20 °C. Confirmation of re-oxidisation was conducted by SDS-PAGE analysis (Figure 3-32).

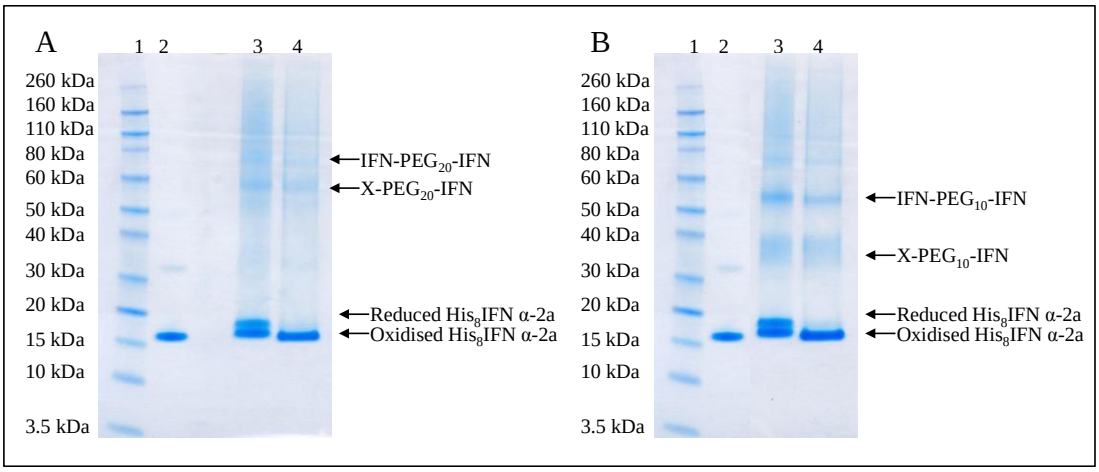

Figure 3-32. Example Glutathione reoxidation of His_8IFN α-2a unconjugated thiols in A) PEG_{20} di(*bis*)sulfone **4**-His_8IFN α-2a reaction mixture, Lane 1: Novex pre-stained markers, Lane 2: His_8IFNα-2a, Lane 3: PEG_{20} di(*bis*)sulfone **4**-His_8IFNα-2a reaction mixture, Lane 4: PEG_{20} di(*bis*)sulfone **4**-His_8IFNα-2a reaction mixture with GRS solution. B) PEG_{10} di(*bis*)sulfone **4**-His_8IFN α-2a reaction mixture. Lane 1: Novex pre-stained markers, Lane 2: His_8IFNα-2a, Lane 3: PEG_{10} di(*bis*)sulfone **4**-His_8IFNα-2a reaction mixture, Lane 4: PEG_{10} di(*bis*)sulfone **4**-His_8IFNα-2a reaction mixture with GRS solution. Complete re-oxidation of reduced His_8IFNα-2a by glutathione after 16 h. Low conversion of IFN-PEG-IFN dimers observed when using both 10 and 20 kDa PEG di(*bis*)sulfone **4** and was observed for each of the three repeats conducted.

Prior to purification, two additions (0.15 mL) of STAB were added to 'lock' the IFNs in place (Figure 2-2) by preventing de-conjugation. Cation exchange chromatography (CIEC) was used to purify X-PEG-IFN from His_8IFNα-2a and IFN-PEG-IFN. CIEC was unable to purify His_8IFN from IFN-PEG-IFN; due to the later having the same affinity to the column as native His_8IFN. CIEC was successful in purifying X-PEG-IFN from both His_8IFN and IFN-PEG-IFN, which could be separated by SEC (§ 2.2.8.10 and 2.2.8.11). One step of SEC was tried but it was unable to separate X-PEG-IFN from His_8IFN and IFN-PEG-IFN.

The reactions to prepare IFN-PEG_{20}-IFN and IFN-PEG_{10}-IFN were repeated three times, with low conversions observed each time to the homodimers. These low conversions suggest that the reactivity or purity of the PEG di(*bis*)sulfone **4** maybe impeding the conversion to the homodimer product rather than the conjugation chemistry, as conversion to the homodimer was low for both disulfide and his-tag conjugation.

A CIEC step gradient of 0, 45, 55, 100% was used to purify the PEG_{20} di(*bis*)sulfone **4**-His_8IFN reaction mixture, with aim of purifying X-PEG_{20}-IFN from His_8IFN and IFN-PEG_{20}-IFN (Figure 3-33 A). Fractions were collected and analysed using SDS-PAGE (Figure 3-33 B) following method 2.2.8.10.

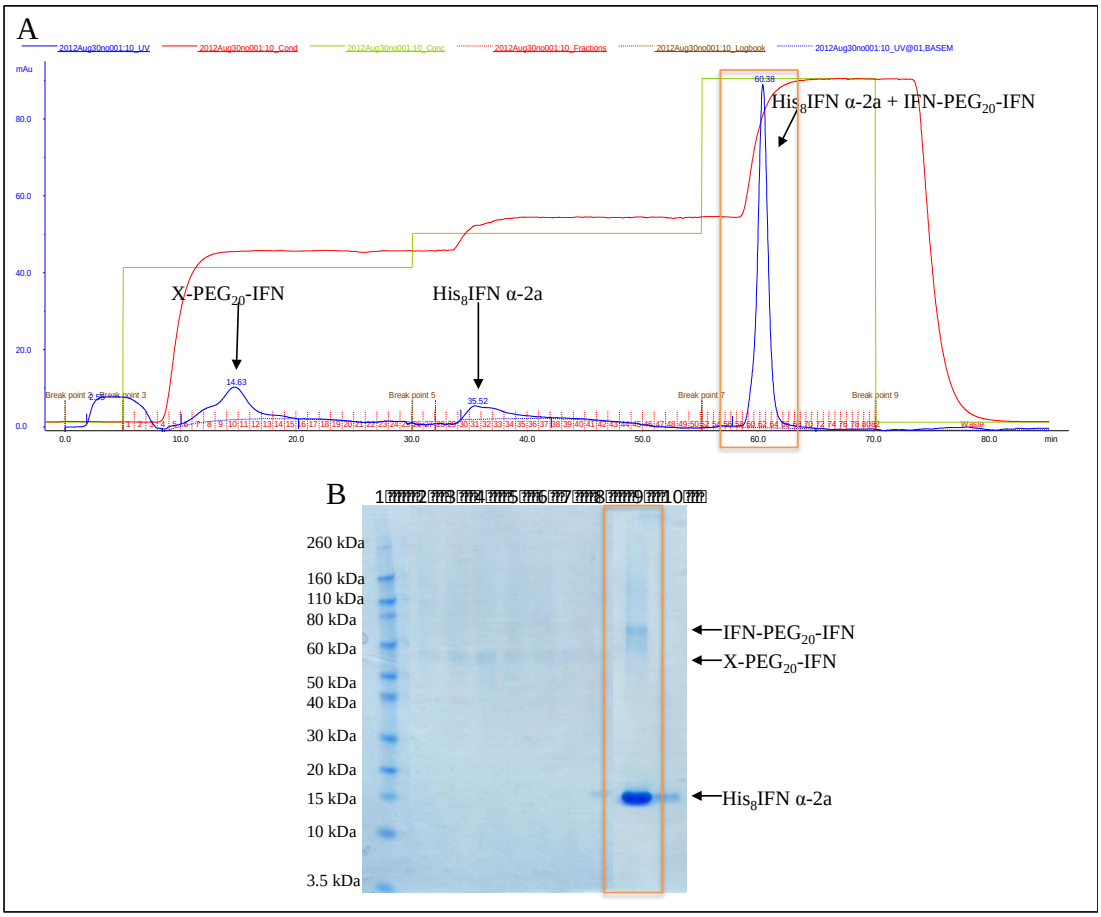

Figure 3-33. A) CIEC chromatogram and B) SDS-PAGE analysis (InstantBlue™) of CIEC purification of PEG_{20} di(*bis*)sulfone **4**-His_8IFNα-2a reaction mixture. Lane 1: Novex pre-stained markers, Lane 2-7: X-PEG_{20}-IFN fractions 7-19, Lane 9-10: His_8IFN α-2a and IFN-PEG_{20}-IFN fractions 57-63. His_8IFN α-2a and IFN-PEG_{20}-IFN were successfully purified from X-PEG_{20}-IFN by CIEC.

Analysis of the chromatogram shows the major peaks at 2.58, 14.63, 35.52 and 60.38 min (Figure 3-33 A). The first peak corresponds to PEG_{20} di(*bis*)sulfone **4**, which is flowing straight through the column as it does not bind. The next peak at 14.63 min (Figure 3-33 A) corresponds to X-PEG_{20}-IFN which can be seen between 50-60 kDa in Lanes 2-8 in Figure 3-33 B. The peak at 60.38 min corresponds to His_8IFN α-2a (15-20 kDa) and IFN-PEG_{20}-IFN (between 60-80 kDa) which bind tightly to the column eluting at ~80% buffer B, the mixture can be seen in Lane 9 (Figure 3-33 B).

To purify X-PEG_{10}-IFN from IFN-PEG_{10}-IFN and some His_8IFN, an optimised CIEC step gradient of 0, 45, 55, 100% was used. This was developed by carrying out a linear gradient from 0-100% buffer B, the fractions where collected and analysed by SDS-PAGE. Using the chromatogram and SDS-PAGE results, the

percentage of buffer B where each conjugate elutes is calculated, to develop the draft step gradient-this is then further adjusted for optimum separation.

Analysis of the chromatogram (Figure 3-34 A) shows the major peaks at 4.33, 16.98, 39.10 and 62.91 min. The first two peaks correspond to PEG_{10} di(*bis*)sulfone **4**, which has flowed straight through the CIEC column as it does not bind. The next peak at 39.10 min (Figure 3-34 A) corresponds to X-PEG_{10}-IFN, which can be seen between 30-40 kDa in Lanes 8-11 in Figure 3-34 B and His_8IFN α-2a between 15-20 kDa that co-eluted with X-PEG_{10}-IFN. The peak at 62.91 min corresponds to His_8IFN α-2a (15-20 kDa) and IFN-PEG_{10}-IFN (~50 kDa) which bind tightly to the column eluting at ~80% buffer B, the mixture can be seen in Lane 12 (Figure 3-34 B).

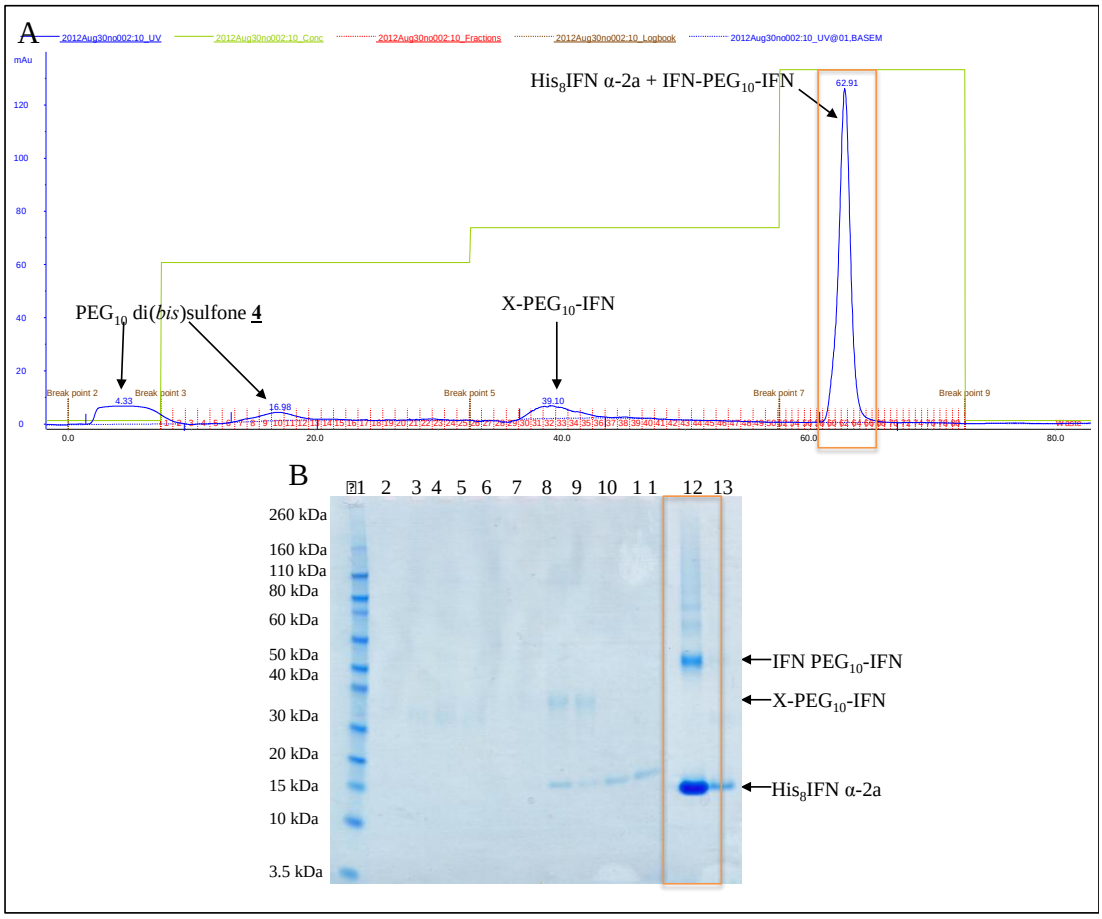

Figure 3-34. A) CIEC chromatogram and B) SDS-PAGE analysis of PEG_{10} di(*bis*)sulfone **4**-His_8IFN α-2a reaction mixture purification. Lane 1: Novex pre-stained markers, Lane 2-7: PEG_{10} di(*bis*)sulfone **4**, Lane 8-11: X-PEG_{10}-IFN+ His_8IFN α-2a, Lane 12-13: IFN-PEG_{10}-IFN and His_8IFN α-2a. His_8IFN α-2a and IFN-PEG_{10}-IFN successfully purified from X-PEG_{10}-IFN.

For SEC purification, CIEC fractions 57-63 were pooled of His_8IFN α-2a and IFN-PEG_{20}-IFN and CIEC fractions 61-64 were pooled of His_8IFN and IFN-PEG_{10}-

IFN. The pooled fractions were diluted into 50 mM sodium phosphate pH 7.8 for SEC purification (method 2.2.8.11).

SEC successfully purified IFN-PEG$_{20}$-IFN from His$_8$IFN α-2a (Figure 3-35), therefore fractions 26-30 were centrifugally concentrated until <~1 mL. No buffer exchanged was necessary due to the SEC running buffer being 50 mM sodium phosphate pH 7.8.

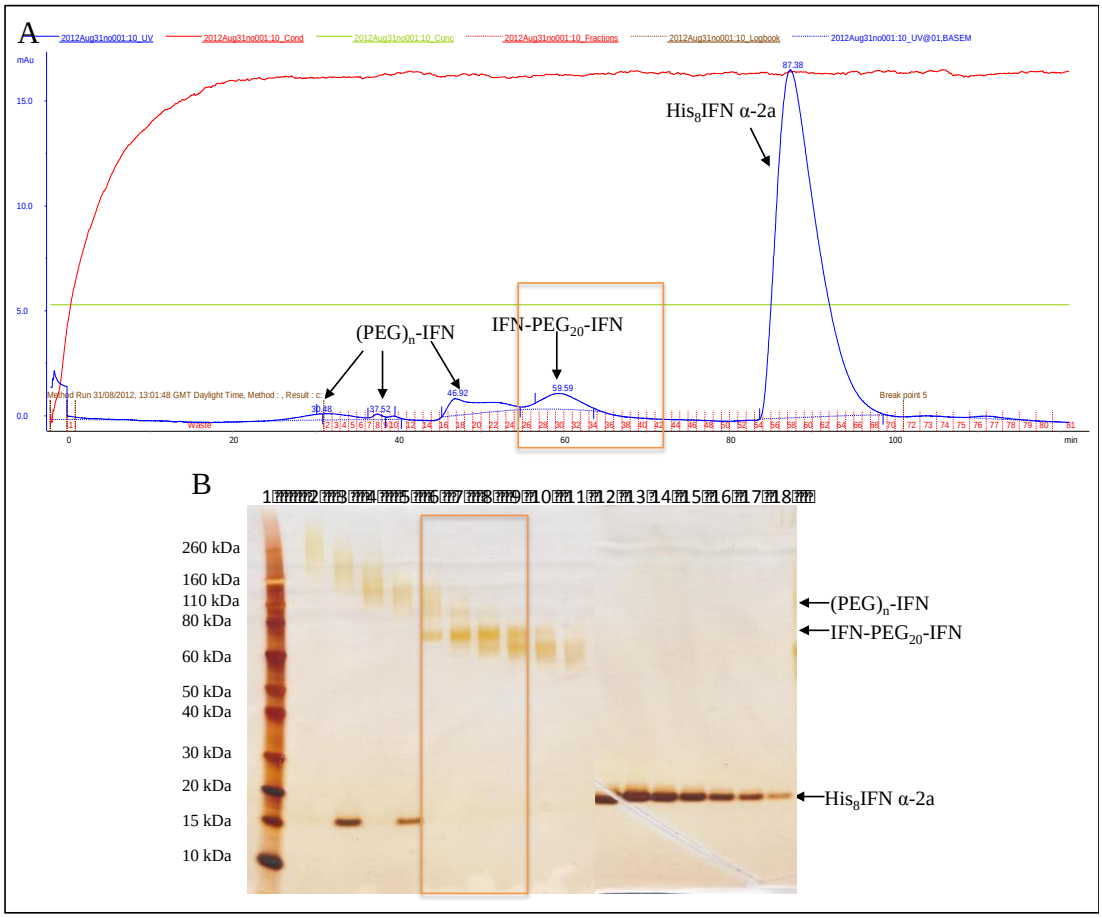

Figure 3-35. SEC purification A) chromatogram and B) SDS-PAGE analysis (silver stain) of peak fractions of PEG$_{20}$ di(*bis*)sulfone **4**-His$_8$IFNα-2a CIEC purified mixture. Lane 1: Novex pre-stained markers, Lane 2-5: (PEG)$_n$-IFN fractions 18-24, Lane 6-9: IFN-PEG$_{20}$-IFN fractions 26-30, Lane 10-11: low MW impurities fractions 32-36, Lane 12-18: His$_8$IFN α-2a. SEC purification successfully purified IFN-PEG$_{20}$-IFN from His$_8$IFN α-2a, for further characterisation in terms of activity, identity and purity.

Analysis of the SEC chromatogram obtained (Figure 3-36 A) shows three major peaks at 47.58, 67.73 and 86.23 min. The first peak could possibly be (PEG)$_n$-IFN where two or more PEGs have linked to one IFN and/or where more than two IFNs have conjugated to one PEG in which mis-bridging has allowed more than one IFN to bind at either linker end. The second peak at 67.73 min is IFN-PEG$_{10}$-IFN, this can be seen on the gel between 50-60 kDa, lanes 7-10 (Figure 3-36 B). His$_8$IFN is the smallest and therefore last to elute from the SEC column at 86.23 min (Figure

3-36 A) and can be observed on the gel in lanes 11-17 (Figure 3-36 B). Further, the two chromatograms Figure 3-35, Figure 3-36, show the same trend in elution, showing how reproducible the purification process is for PEG di(*bis*)sulfone **4**-His_8IFN.

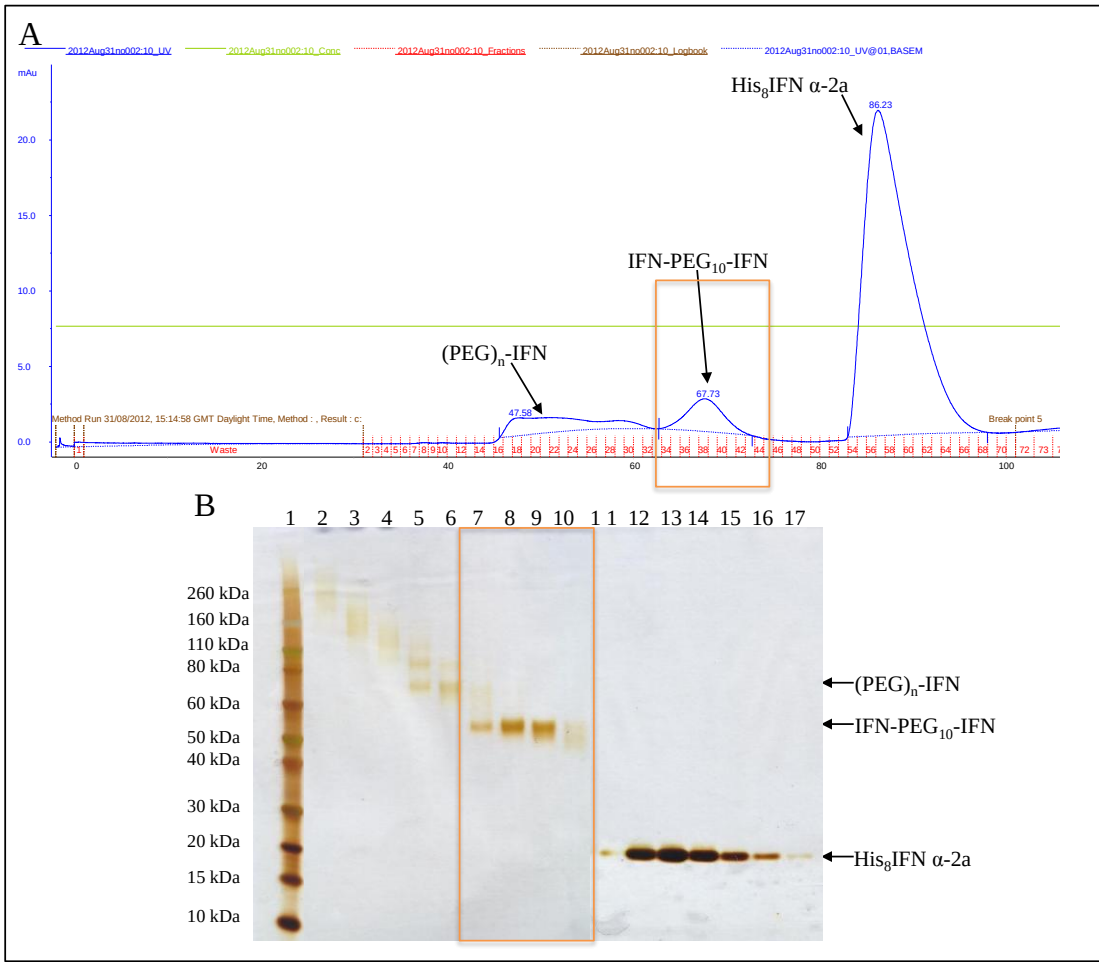

Figure 3-36. SEC purification A) chromatogram and B) SDS-PAGE analysis (silver stain) of peak fractions of PEG_{10} di(*bis*)sulfone **4**-His_8IFN α-2a CIEC purified reaction mixture. Lane 1: Novex pre-stained markers, Lane 2-6: $(PEG)_n$-IFN fractions 19-34, Lane 7-10: IFN-PEG_{10}-IFN fractions 31-43, Lane 11-17: His_8IFN α-2a fractions 49-70. SEC purification successfully purified IFN-PEG_{10}-IFN from His_8IFN α-2a for further characterisation studies.

From the SDS-PAGE analysis it can be observed that SEC (Figure 3-36 B) successfully purified IFN-PEG_{10}-IFN from His_8IFN α-2a, therefore fractions 31-43 were centrifugally concentrated until ~1 mL remained. For IFN-PEG_{20}-IFN fractions 26-30 were pooled and also concentrated until ~1 mL. No buffer exchanged was necessary because SEC running buffer (50 mM sodium phosphate pH 7.8) was compatible with the biological assay media which is used to test potency.

UV and BCA quantification was conducted and the yields obtained for IFN-PEG_{20}-IFN and IFN-PEG_{10}-IFN were 0.85% (35 μg/mL) and 1.1% (46 μg/mL)

respectively. The yields of the IFN-PEG-IFN dimers were very low, this was also found for the His_8IFN-PEG_{20}-His_8IFN dimer (§ 3.2.3.1), where the yield achieved was ~1.5%. These low yields could be due to i) a two-step purification which involves SEC which causes reduced yields and ii) the PEG di(*bis*)sulfone **4** reagent which causes low conversion. The IFN-PEG-IFN were prepared n=2, however the low yield was reproducible. It was found upon investigation into the PEG di(*bis*)sulfone **4** that the reagent was impure, this was thought to be the cause of the low yields. Thus, a different synthesis route (2) was developed to prepare a pure PEG di(*bis*)sulfone **4** for heterodimer preparation. The PEG di(*bis*)sulfone **4** has been used to prepare Fab-PEG-Fab dimers (§1.4.1.4). However, the aim was to prepare IFN-PEG-IFN dimers, which were pure to investigate their properties.

SDS-PAGE of the final IFN-PEG_{10}-IFN and IFN-PEG_{20}-IFN conjugates can be seen in Figure 3-37 where it can be seen that the conjugates was made to high purity. Purity assessment of the IFN-PEG-IFN dimers was confirmed by Western blotting.

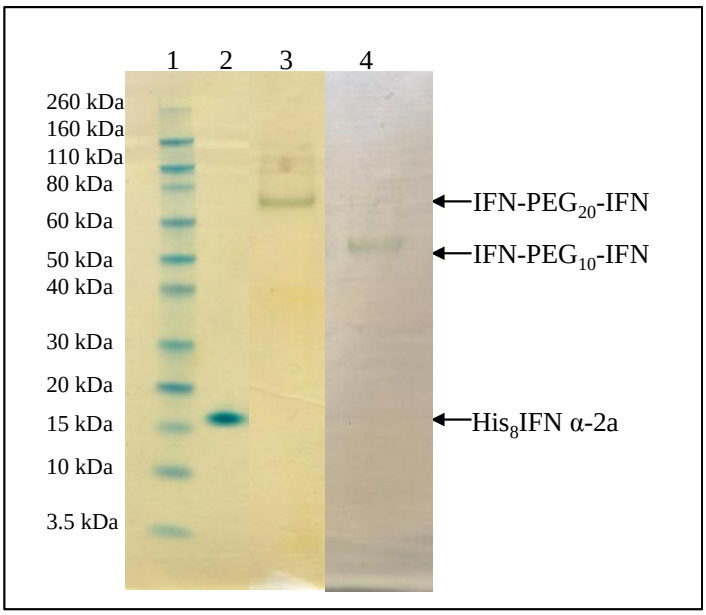

Figure 3-37. SDS-PAGE (InstantBlue™ and PEG stain) analysis of final IFN-PEG_{10}-IFN and IFN-PEG_{20}-IFN conjugates. Lane 1: pre-stained Novex markers, Lane 2: His_8IFN α-2a, Lane 3: IFN-PEG_{20}-IFN, Lane 4: IFN-PEG_{10}-IFN. IFN-PEG_{10}-IFN and IFN-PEG_{20}-IFN conjugates successfully prepared using disulfide-bridging conjugation of His_8IFN and purified.

3.3.4 Preparation of 5, 10 and 20 kDa PEG-IFN α-2a and $(PEG)_2$-IFN α-2a

Disulfide conjugation was conducted on His_8IFN α-2a, this had not been explored previously. As His_8IFN has two disulfide bonds (Figure 1-18), a PEG molecule can

conjugate to each of the disulfide bonds, producing the $(PEG_{20})_2$-IFN species. To evaluate the IFN-PEG-IFN dimers to see if they have different properties of PEG-IFN and $(PEG)_2$-IFN, PEG-IFN and $(PEG)_2$-IFN were prepared. For preparing the PEG-IFN and $(PEG)_2$-IFN, PEG *bis*-sulfone **1** was used, with PEG MW of 5, 10 and 20 kDa. These PEG MW were used to evaluate how the PEG MW affects the activity of His_8IFN and how this compares to that of the IFN-PEG-IFN dimers.

3.3.4.1 Optimisation of PEGylation conditions for the synthesis of PEG_{20}-IFN α-2a and $(PEG_{20})_2$-IFN α-2a

After it was determined that 20 mM DTT was sufficient to reduce completely the two disulfides in His_8IFN α-2a, PEG_{20} *bis*-sulfone **1** was used to optimise the molar equivalents required to prepare PEG_{20}-IFN and $(PEG_{20})_2$-IFN. Scouting experiments were conducted with increasing molar equivalents (eq.) of PEG_{20} *bis*-sulfone **1** ranging from 0.8 to 2.5 eq., the reactions were incubated for 4 h at 4 °C (method 2.2.8.1). The glutathione solution (1 mM) was added and the reaction was allowed to proceed for a further 16 h at 4 °C. The GRS was added to reoxidise the reduced disulfide bond, which had not been PEGylated. After reoxidation the reaction mixture was assessed using SDS-PAGE analysis.

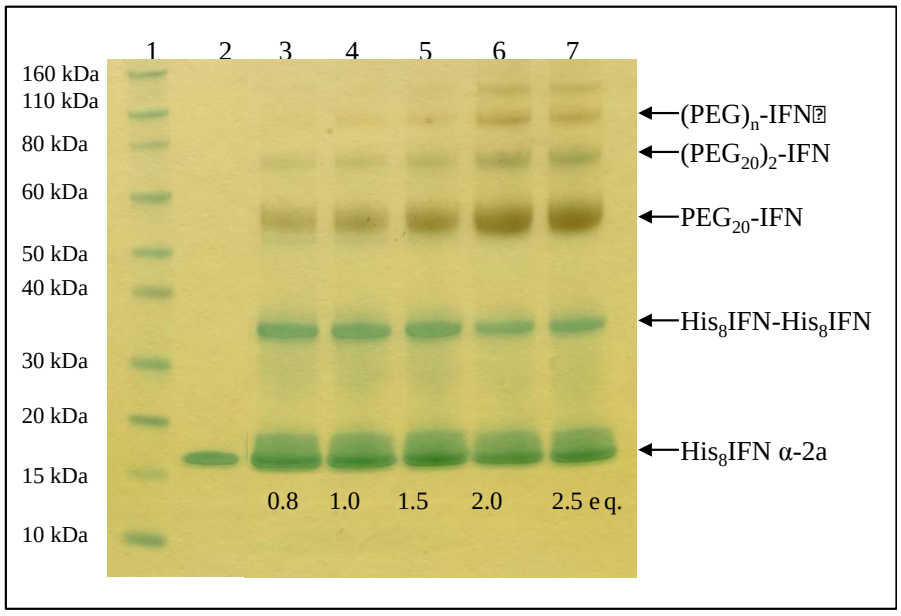

Figure 3-38. Optimisation of PEG:IFN ratios for disulfide-conjugation of His_8IFN with PEG_{20} *bis*-sulfone **1**. Lane 1) Novex pre-stained markers, Lane 2) His_8IFN α-2a, Lanes 3-7) 0.8-2.5 eq PEG-His_8IFN α-2a reaction mixture. Optimum ratio for preparing PEG_{20}-IFN and $(PEG_{20})_2$-IFN, was found to be 1:1 PEG: His_8IFN α-2a for thiol PEGylation.

It was observed (Figure 3-38) that with increasing PEG eq. more PEG molecules conjugate to one IFN molecule creating $(PEG)_n$-IFN species. Therefore, a balance is

required between PEG stoichiometry and the conversion of PEG_{20}-IFN and $(PEG_{20})_2$-IFN and limiting the conversion of $(PEG)_n$-IFN. To achieve the highest conversion of PEG_{20}-IFN and $(PEG_{20})_2$-IFN, 1 eq. (Lane 4, Figure 3-38) of PEG_{20} *bis*-sulfone **1** was chosen. One eq. was observed to prepare both PEG_{20}-IFN and $(PEG_{20})_2$-IFN, but only trace amounts of $(PEG)_n$-IFN species, thus maximising conversion of PEG_{20}-IFN and $(PEG_{20})_2$-IFN. In comparison, 2.5 eq. PEG yielded more high MW impurities of $(PEG)_n$-IFN as seen in lane 7 (Figure 3-38). The use of 1 eq. PEG for disulfide-bridging conjugation of non-his-tagged IFN α-2 has also been described for the preparation of PEG-IFN (Brocchini et al., 2008). Interestingly, the non-his-tagged IFN is not reported to dimerise during disulfide-conjugation (Balan et al., 2007). Suggesting the presence of the his-tag within His_8IFN increases the propensity of His_8IFN to dimerise, as seen at 35 kDa in Figure 3-38.

3.3.4.2 Preparation of 5, 10 and 20 kDa PEG-IFN and $(PEG)_2$-IFN

Prior to the disulfide-bridging conjugation of the his-tag IFN, 20 mM DTT (1.0 M, 0.15 g) was used to reduce the two disulfides in His_8IFN α-2a (1.0 mg/mL, 3.13 mL) (Figure 3-39). Disulfide-bridging conjugation was conducted (method 2.2.8.1) using 1 eq. of PEG *bis*-sulfone **1** to 1 eq. of reduced His_8IFN α-2a, the reaction was conducted for 20 h at 20 °C.

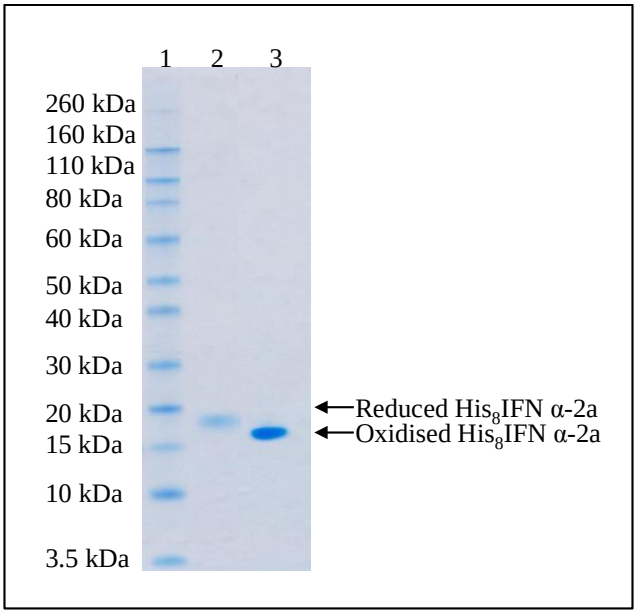

Figure 3-39. Example SDS-PAGE (InstantBlue™ stain) analysis of reduced His_8IFN -2a with 20 mM DTT for 30 min, Lane 1: Novex pre-stained markers, Lane 2: reduced His_8IFN α-2a for conjugation to PEG *bis*-sulfone **1**, Lane 4: oxidised His_8IFN α-2a. His_8IFN α-2a was fully reduced to react with PEG *bis*-sulfone **1**. Reduction was conducted six times (2 times per PEG size used) as conjugation was conducted twice (n=2) for each PEG size (20, 10 and 5 kDa).

As the free thiol is more reactive as a nucleophile than the histidine residue, less equivalents of PEG can be used than in his-tag conjugation. As discussed previously, due to His_8IFN α-2a having two disulfide bonds, it is possible to prepare both PEG-IFN and $(PEG)_2$-IFN in one reaction (Figure 3-40). The reaction mixture for 20, 10 and 5 kDa PEG *bis*-sulfone **1**-His_8IFN α-2a were analysed using SDS-PAGE (Figure 3-40).

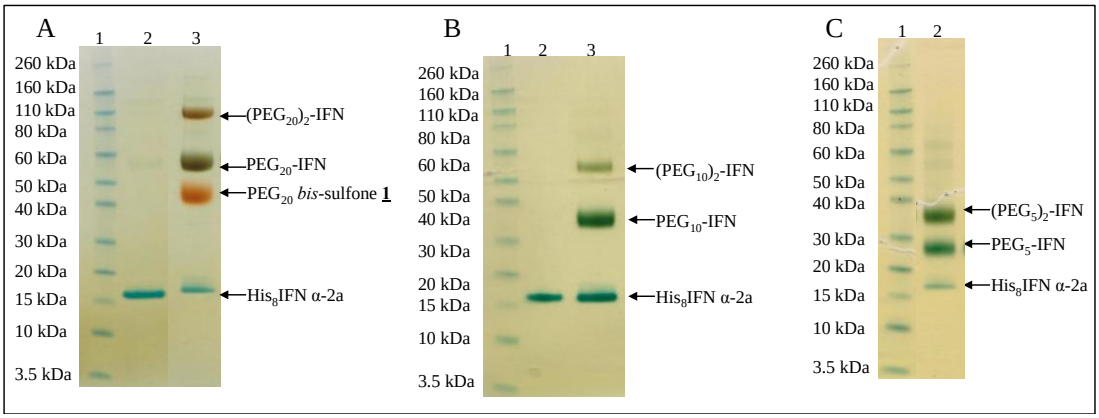

Figure 3-40. Representative SDS-PAGE (InstantBlue™ and PEG stain) of the A) 20, B)10 and C) 5 kDa PEG *bis*-sulfone **1**-IFN reaction mixtures. A) Lane 1: Novex pre-stained markers, Lane 2: His_8IFN α-2a and Lane 3: PEG_{20} *bis*-sulfone **1**-IFN reaction mixture. B) A) Lane 1: Novex pre-stained markers, Lane 2: His_8IFN α-2a and Lane 3: PEG_{10} *bis*-sulfone **1**-IFN reaction mixture. C) A) Lane 1: Novex pre-stained markers, Lane 2:PEG_5 *bis*-sulfone **1**-IFN reaction mixture. Successfully disulfide-bridging conjugation of His_8IFN α-2a with 20, 10 and 5 kDa *bis*-sulfone PEG **1** to prepare PEG-IFN and $(PEG)_2$-IFN. Conjugation was conducted twice for each PEG size; the SDS-PAGE shown is an example for each PEG size reaction.

After the incubation period, the solution was diluted 3- to 4- fold with 50 mM sodium acetate pH 4.0. The pI of IFN is ~6.0, thus to bind to the cation exchange column resin, His_8IFN would be positively charged at ~ pH 4.0. The recommended buffer for CIEC at pH 4.0 was sodium acetate with the HiTrap™ sulphopropyl (SP) MacroCap™ column (GE Healthcare HiTrap™ SP MacroCap™ product literature). The PEG_{20} *bis*-sulfone **1**-IFN reaction mixture was purified by the different positively charged His_8IFN species having different affinities to the column, which were eluted with a step gradient of 0, 40, 45, 55 and 100% sodium chloride (§ 2.2.8.3). For each peak the fractions were collected and analysed by SDS-PAGE (Figure 3-41 B**)**.

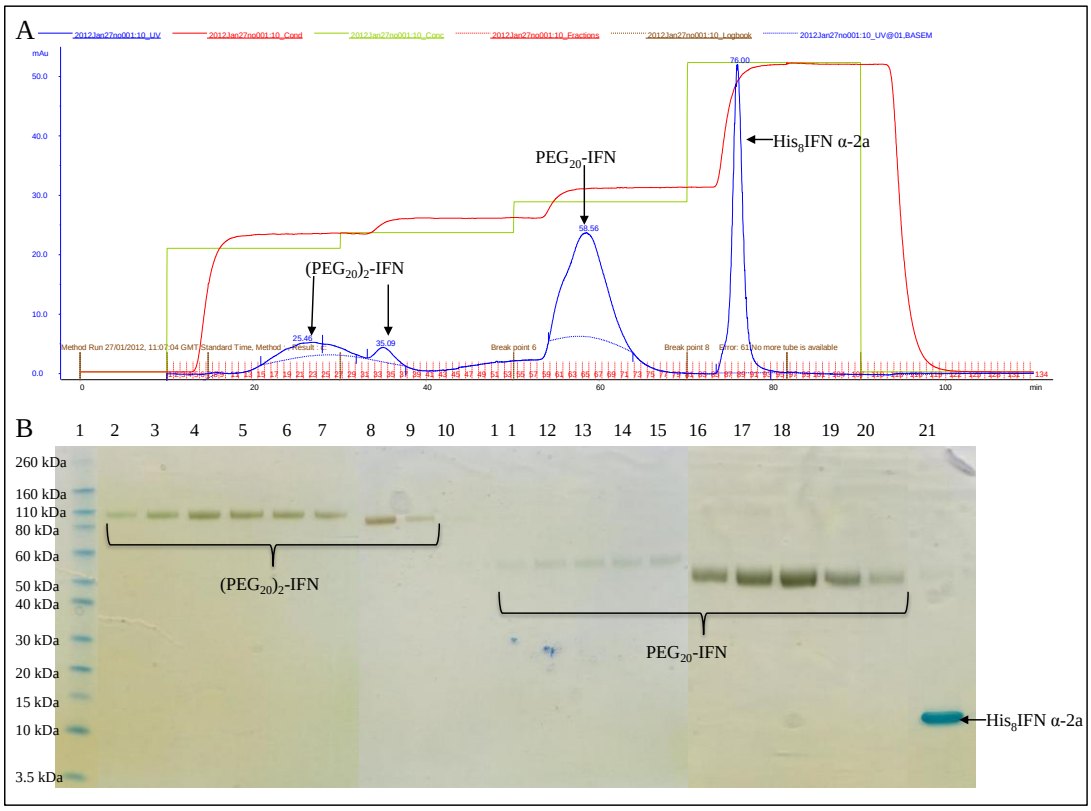

Figure 3-41. Representative CIEC chromatogram of A) PEG_{20} *bis*-sulfone **1**-His_8IFNα -2a reaction mixture (n=2) and B) SDS-PAGE analysis (InstantBlue™ and PEG stain) of CIEC peak fractions, Lane 1: Novex pre-stained markers, Lane 2-9: fractions 16-37 of $(PEG_{20})_2$-IFN, Lane 11-20: fractions 46-75 of PEG_{20}-IFN, Lane 21: His_8IFN α-2a. PEG_{20}-IFN and $(PEG_{20})_2$-IFN were successfully purified by CIEC using a sodium chloride step gradient of 0, 40, 45, 55 and 100%.

For PEG_{10} *bis*-sulfone **1**-IFN, reaction mixture was purified using a step gradient of 0, 50, 55, 60 and 100% sodium chloride (method 2.2.8.5). While the PEG_5 *bis*-sulfone **1**-IFN reaction mixture was purified using a step gradient of 0, 48, 55, 60 and 100% sodium chloride (method 2.2.8.7).

Analysis of the chromatogram obtained shows the major peaks at 25.46, 35.09, 58.56 and 76.00 min (Figure 3-41 A). The first two peaks correspond to $(PEG_{20})_2$-IFN, which binds least strongly due to steric hindrance from the two PEGs conjugated to the two disulfide bonds of His_8IFN. The next peak (58.56 min, Figure 3-41 A) corresponds to PEG_{20}-IFN, which can be seen in Lanes 11-20 (Figure 3-41 B). His_8IFN α-2a binds strongest to the column and elutes at approximately 80% buffer B, this can be seen in Lane 21 (Figure 3-41 B).

The CIEC chromatograms for both 10 kDa (Figure 3-42 A) and 5 kDa PEG (Figure 3-43 A) *bis*-sulfone **1**-His_8IFN α-2a reaction mixtures showed the same elution trend as observed with PEG_{20} *bis*-sulfone **1**-His_8IFN α-2a reaction mixture, where $(PEG)_2$-IFN eluted first followed by PEG-IFN and then His_8IFN α-2a eluted

last. However, the percentage of sodium chloride required to elute the different conjugated species differed with PEG MW and required optimisation to elute pure conjugates. For example, 40% sodium chloride was required to elute PEG_{20}-IFN, while ~50% sodium chloride was required to elute PEG_{10}-IFN and PEG_5-IFN. This is due to the smaller PEG MW having less of a steric shielding effect over His_8IFN α-2a. Interestingly, PEG-positional isomers have been described with PEG-INTRON® and PEGASYS® where by the PEG conjugates to different lysine residues and it has been described that each PEG-positional isomers retained different levels of activity (§1.2.1.1). Therefore, different potencies may be found for each of the disulfide PEG-positional isomers in Figure 3-42. However, this has not been described before using disulfide conjugation of non-his-tagged IFN. Possibly this could be due to the sensitivity of the AKTA, where the purification is monitored by UV, compared to the use of a pre-static pump for purification as described by Balan and co-workers (Balan et al., 2007).

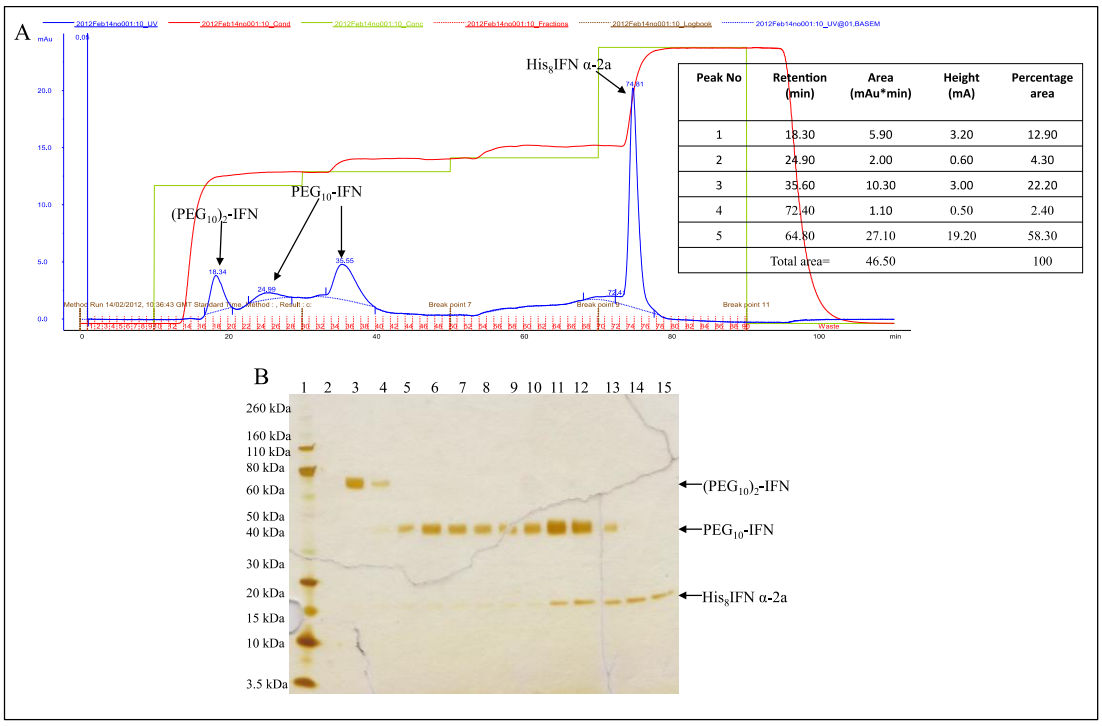

Figure 3-42. A) Representative CIEC chromatogram and peak information table of PEG_{10} *bis*-sulfone **1**-His_8IFNα -2a reaction mixture and B) SDS-PAGE analysis (InstantBlue™ and PEG stain) of CIEC peak fractions (n=2), Lane 1: Novex pre-stained markers, Lane 3-4: fractions 18-20 of $(PEG_{10})_2$-IFN, Lane 5-13: fractions 22-32 of PEG_{10}-IFN, Lanes 11-15: His_8IFN α-2a. PEG_{10}-IFN and $(PEG_{10})_2$-IFN were successfully purified by CIEC using a sodium chloride step gradient of 0, 50, 55, 60 and 100%.

PEG_{20}-IFN and $(PEG_{20})_2$-IFN fractions (16-37 and 46-75 respectively) were pooled, concentrated using a VivaSpin column and buffer exchanged into 50 mM sodium

phosphate pH 7.8 (method 2.2.8.3). While for PEG_{10}-IFN and $(PEG_{10})_2$-IFN and PEG_5-IFN and $(PEG_5)_2$-IFN fractions 17-21, 22-39 and 11-18, 23-43 respectively were each pooled and buffer exchanged (methods 2.2.8.5 and 2.2.8.7 respectively). Final SDS-PAGE analysis (Figure 3-44) was conducted on the final disulfide conjugated IFN samples. Interestingly, it was observed that the yields for 10 kDa PEG *bis*-sulfone **1** samples were lower than when using the 20 and 5 kDa *bis*-sulfone **1** (Table 3–1). However, the yields obtained for PEG-IFN and $(PEG)_2$-IFN samples where greater than those achieved for IFN-PEG-IFN dimers. These yields highlight there are obvious differences between the PEG *bis*-sulfone **1** and PEG di(*bis*)sulfone **4**.

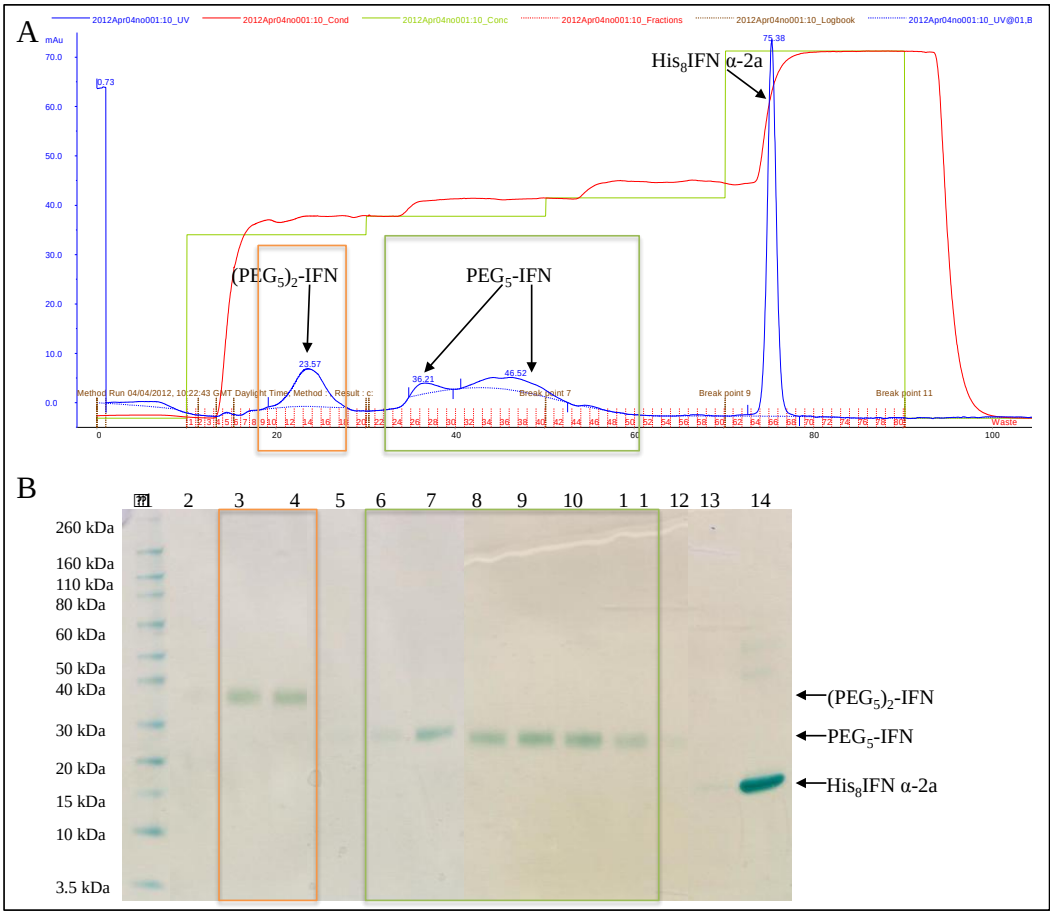

Figure 3-43. A) Representative CIEC chromatogram of PEG_5 *bis*-sulfone **1**-His_8IFNα -2a reaction mixture and B) SDS-PAGE analysis (InstantBlue™ and PEG stain) of CIEC peak fractions (n=2), Lane 1: Novex pre-stained markers, Lane 3-4: fractions 10-19 of $(PEG_5)_2$-IFN, Lane 5-13: fractions 22-44 of PEG_5-IFN, Lanes 11-15: His_8IFN α-2a. PEG_5-IFN and $(PEG_5)_2$-IFN were successfully purified by CIEC using a sodium chloride step gradient of 0, 48, 55, 60 and 100%.

The differences in yields between the PEG *bis*-sulfone **1** and PEG di(*bis*)sulfone **4**, is the same even when using different conjugation strategies (his-tag vs. disulfide conjugation). As the IFN dimer has a reduced yield when using both

conjugation strategies, as for IFN-PEG_{10}-IFN a 1.1% yield was achieved. While for IFN-PEG_{10}-IFN a 0.85% yield was achieved compared to the 1.5% yield of His_8IFN-PEG_{20}-His_8IFN. The low yields were thought to be due to the PEG di(*bis*)sulfone **4** being an impure mixture compared to the pure PEG *bis*-sulfone **1** (Figure 3-12), thus a purer homobifunctional reagent **4** was prepared using synthesis route 2 in an attempt to improve the conversion and yields products prepared (§3.2.1).

Interestingly, higher yields were achieved for the disulfide-conjugated $(PEG_{20})_2$-IFN (12%) compared to that of his-tag conjugated (PEG_{20})-His_8IFN (7.1% yield). This could possibly due to the greater reactivity of the thiols than the amines or could it be due to steric shielding of one PEG conjugated to the his-tag reducing the conjugation of a second PEG molecule to the histidine tag. Overall, the yields achieved for PEG-IFN (Table 3–1) where quite similar to that achieved for PEG_{20}-His_8IFN (17.1%). The yields achieved of the disulfide-conjugated his-tag IFN were lower than that reported for non-his-tagged IFN (56% PEG-IFN) (Balan et al., 2007). This could be due to variations in conjugation procedure such as using PEG mono-sulfone **2** for conjugation, rather than PEG *bis*-sulfone **1** and using different purification columns (Balan et al., 2007).

As is stated in Table 3–1, the reactions for each PEG size (i.e. 20, 10 and 5 kDa) were repeated twice. The yields achieved for each of the thiol-conjugates His_8IFN being found consistent for each replicate, showing the reproducibility of the conjugate and purification processes developed.

Table 3–1. Summary of thiol-conjugates His_8IFN α-2a samples and the achieved yields

Thiol conjugated His_8IFN	**Average Yield (%)**	***n***
PEG_{20}-IFN	29	2
$(PEG_{20})_2$-IFN	12	2
PEG_{10}-IFN	14	2
$(PEG_{10})_2$-IFN	16	2
PEG_5-IFN	29	2
$(PEG_5)_2$-IFN	35	2

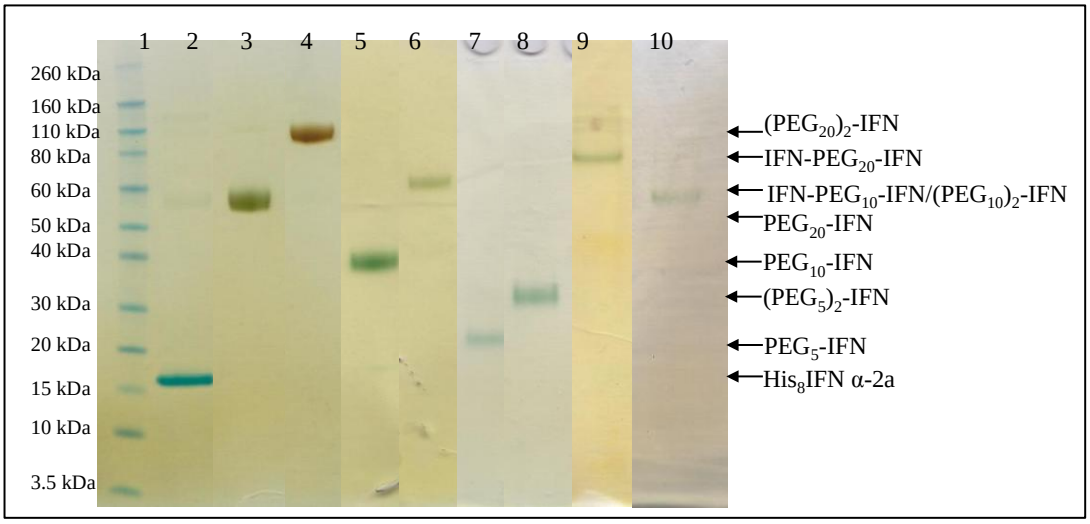

Figure 3-44. Final SDS-PAGE analysis (InstantBlue™ and PEG stain) of disulfide-conjugated His_8IFN α-2a species. Lane 1: Novex pre-stained markers, Lane 2: His_8IFN α-2a, Lane 3: PEG_{20}-IFN, Lane 4: $(PEG_{20})_2$-IFN, Lane 5: PEG_{10}-IFN, Lane 6: $(PEG_{10})_2$-IFN, Lane 7: PEG_5-IFN, Lane 8: $(PEG_5)_2$-IFN. Novel disulfide-conjugated his-tagged IFN species successfully prepared.

3.3.5 Characterisation of thiol conjugated IFN-PEG-IFN dimers

3.3.5.1 Stability study of thiol PEGylated IFN α-2a conjugates

Stability studies were performed for all *bis*-thiol selective PEG conjugated IFN α-2a species. First the purity of the thiol conjugated IFN α-2a species was first determined to confirm the absence of free IFN α-2a before starting the stability studies (Figure 3-45). For that reason, the products were analysed by SDS-PAGE and the resulting gels were stained with InstantBlue™ and PEG stain followed by Western blotting using anti-IFN α-2a antibody (1 μg of protein/well, Figure 3-45, method 2.2.10.1). The results revealed no free IFN α-2a was present in any of the thiol conjugated IFN α-2a species prepared.

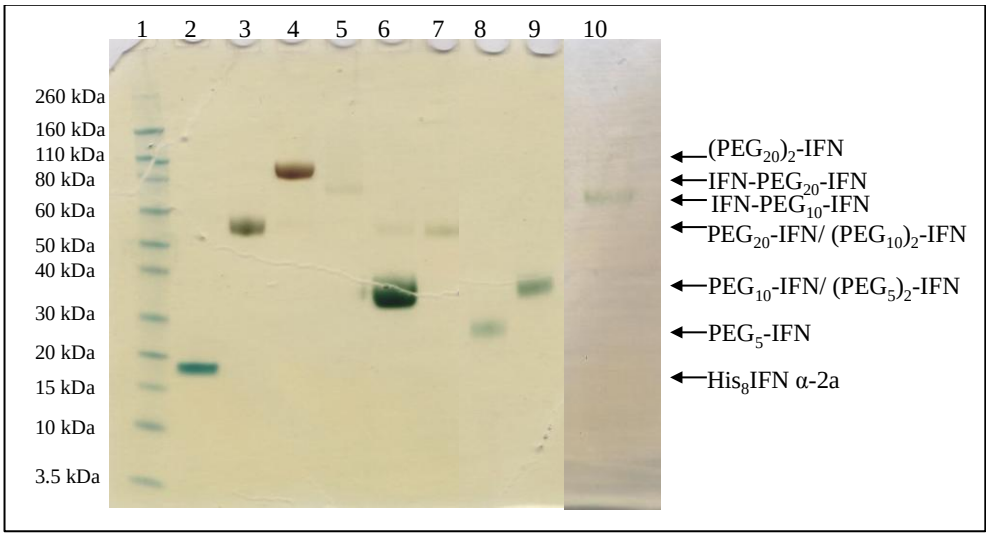

Figure 3-45. SDS-PAGE (InstantBlue™ and PEG stain) analysis of thiol PEGylated IFN α-2a species. Lane 1: Novex pre-stained markers, Lane 2: His_8IFN α-2a, Lane 3: PEG_{20}-IFN, Lane 4: $(PEG_{20})_2$-IFN, Lane 5: IFN-PEG_{20}-IFN, Lane 6: PEG_{10}-IFN, Lane 7: $(PEG_{10})_2$-IFN, Lane 8: PEG_5-IFN, Lane 9: $(PEG_5)_2$-IFN, Lane 10: IFN-PEG_{10}-IFN. No un-conjugated His_8IFN α-2a is observed from any of the thiol PEGylated IFN α-2a species.

In addition, longer term stability studies were conducted by incubating the compounds in 50 mM sodium phosphate buffer, 150 mM NaCl pH 7.8 for 7 days at 4 °C. The results showed no evidence of aggregation or free protein being released when analysed by SDS-PAGE (Figure 3-46).

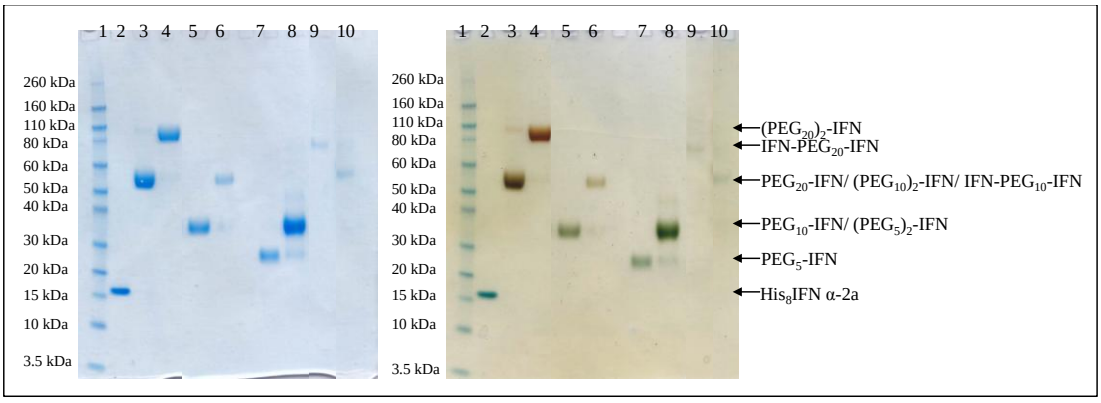

Figure 3-46. Thiol conjugated IFNα-2a conjugates incubated at 4 °C for 7 days. Lane 1: Novex pre-stained markers, Lane 2: His_8IFN α-2a, Lane 3: PEG_{20}-IFN, Lane 4: $(PEG_{20})_2$-IFN, Lane 5: PEG_{10}-IFN, Lane 6: $(PEG_{10})_2$-IFN, Lane 7: PEG_5-IFN, Lane 8: $(PEG_5)_2$-IFN, Lane 9: IFN-PEG_{20}-IFN, Lane 10: IFN-PEG_{10}-IFN. No evidence of free or aggregated protein was observed by SDS-PAGE analysis using InstantBlue™ and PEG stain.

Accelerated stability studies were also performed by incubating the thiol PEGylated IFN α-2a compounds (~40 µg/mL) at 90 ºC (10 min) with or without 20 mM DTT (method 2.2.10.5). Sample analysis was conducted by SDS-PAGE with the resulting gel stained using silver stain (Figure 3-37).

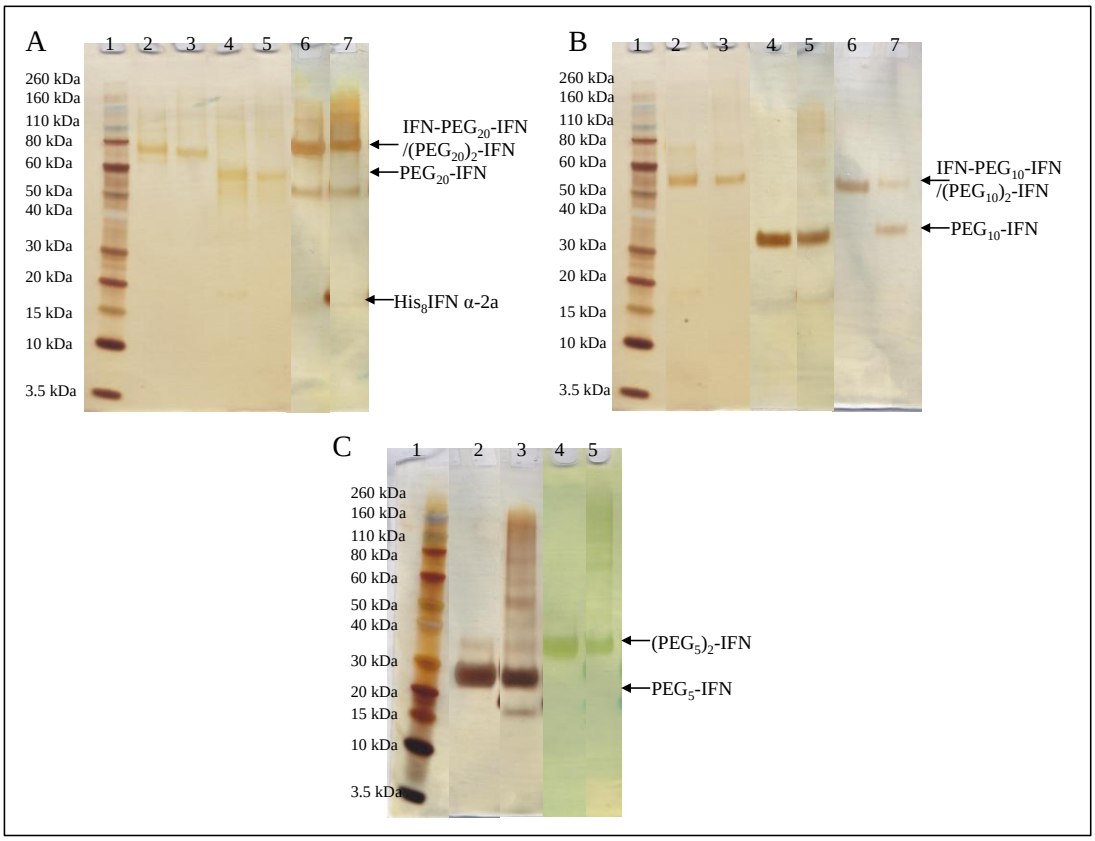

Figure 3-47. SDS-PAGE (silver stain) analysis of disulfide-conjugated IFN conjugates stressed with ± DTT for 10 min at 90 °C. A) Lane 1: Novex pre-stained markers, Lane 2: IFN-PEG_{20}-IFN +DTT, Lane 3: IFN-PEG_{20}-IFN -DTT, Lane 4: PEG_{20}-IFN +DTT, Lane 5: PEG_{20}-IFN -DTT, Lane 6: $(PEG_{20})_2$-IFN +DTT, Lane 7: $(PEG_{20})_2$-IFN -DTT. B) Lane 1: Novex pre-stained markers, Lane 2: IFN-PEG_{10}-IFN +DTT, Lane 3: IFN-PEG_{10}-IFN -DTT, Lane 4: PEG_{10}-IFN +DTT, Lane 5: PEG_{10}-IFN –DTT , Lane 6: $(PEG_{10})_2$-IFN +DTT, Lane 7: $(PEG_{10})_2$-IFN -DTT. C) Lane 1: Novex pre-stained markers, Lane 2: PEG_5-IFN +DTT, Lane 3: PEG_5-IFN -DTT, Lane 4: $(PEG_5)_2$-IFN +DTT (InstantBlue™ and PEG stain), Lane 5: $(PEG_5)_2$-IFN –DTT (InstantBlue™ and PEG stain). The conjugates were shown to be stable when stressed with DTT for 10 min at 90 °C.

The results indicated that when the thiol conjugated IFN α-2a were visualised on the gel by silver stain, no free protein was observed for the IFN-PEG_{20}-IFN, PEG_{20}-IFN, IFN-PEG_{10}-IFN and $(PEG_5)_2$-IFN in the presence or absence of DTT, showing the conjugates to be stable even when stressed under reducing conditions and high temperatures (90 °C). A trace amount of free protein was observed for the PEG_{10}-IFN, $(PEG_{10})_2$-IFN and PEG_5-IFN conjugates when incubated for 10 min with DTT. Considering the acutely high sensitivity of the silver stain technique and the artificial design of the condition tested, this observation is unlikely to represent their stability under physiological conditions. Overall, these results suggest that the conjugates are stable. This shows that the 3-carbon bridge is highly thermodynamically stable, as the disulfide-conjugated IFN samples were not treated with STAB.

3.3.5.2 Anti IFN α Western blot of thiol PEGylated IFN conjugates

To assess the purity and to prove the identity of the conjugates in terms of IFN α-2a content, an anti-IFN α Western blot was conducted. One µg of His_8IFN α-2a and thiol conjugated IFN α-2a species were loaded onto a SDS-PAGE 4-12 % Bis-Tris gel. The resulting gel was transferred onto nitrocellulose membrane, which was subject to rabbit anti-IFN α antibody followed by anti-rabbit-AP conjugated antibody (method 2.2.10.1).

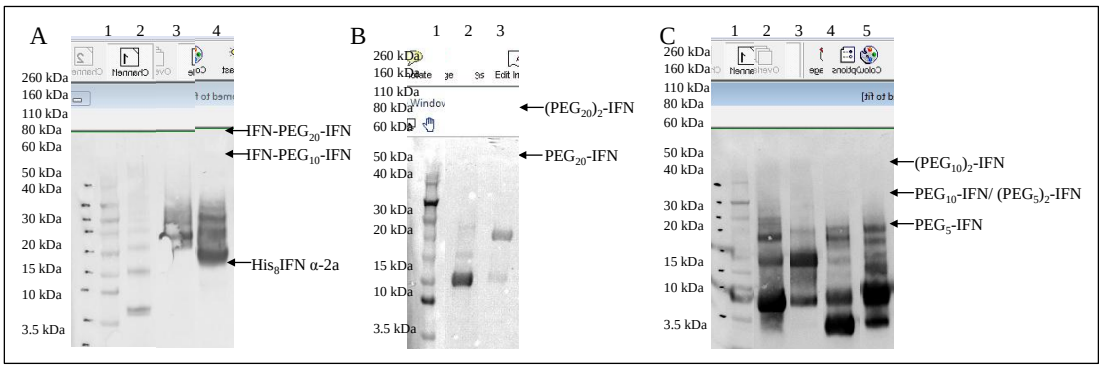

Figure 3-48. Anti IFN α western blot of A) His_8IFN, IFN-PEG_{20}-IFN and IFN-PEG_{10}-IFN, B) PEG_{20}-IFN and $(PEG_{20})_2$-IFN, C) PEG_{10}-IFN, $(PEG_{10})_2$-IFN, PEG_5-IFN and $(PEG_5)_2$-IFN. A) Lane 1: Novex pre-stained markers, Lane 2: His_8IFN α-2a, Lane 3: IFN-PEG_{20}-IFN, Lane 4: IFN-PEG_{10}-IFN, B) Lane 1: Novex pre-stained markers, Lane 2: PEG_{20}-IFN, Lane 3: $(PEG_{20})_2$-IFN, C) Lane 1: Novex pre-stained markers, Lane 2: PEG_{10}-IFN, Lane 3: $(PEG_{10})_2$-IFN, Lane 4: PEG_5-IFN, Lane 5: $(PEG_5)_2$-IFN. Anti-IFNα Western blot identified all the thiol conjugated species.

All thiol-conjugates IFN α-2a species were observed by anti-IFN α Western blot. First, His_8IFN was seen in Lane 2 (Figure 3-48 A) between 15-20 kDa. IFN-PEG_{20}-IFN (Lane 3) and IFN-PEG_{10}-IFN (Lane 4, Figure 3-48 A) were observed at 80 kDa and 60 kDa respectively. PEG_{20}-IFN conjugate was identified and was observed at ~60 kDa (Lane 2, Figure 3-48 B), where as $(PEG_{20})_2$-IFN was observed at ~100 kDa. This is 40 kDa larger than PEG_{20}-IFN, and 20 kDa larger than IFN-PEG_{20}-IFN, this is due to the $(PEG_{20})_2$-IFN having two PEG molecules conjugated, which are 40 kDa, each in solution. IFN-PEG_{10}-IFN is 20 kDa larger than PEG_{10}-IFN (~40 kDa) (Lane 2, Figure 3-48 C), due to the addition of an extra IFN molecule. While $(PEG_{10})_2$-IFN was seen at ~60 kDa in Lane 3 (Figure 3-48 C). $(PEG_5)_2$-IFN (Lane 4, Figure 3-48 C) can be seen at 40 kDa, the same MW as PEG_{10}-IFN. While PEG_5-IFN was observed at 30 kDa in Lane 5, Figure 3-48 C.

Trace amounts of $(PEG)_n$-IFN can be seen in many of the conjugated species in Figure 3-48. Interesting, no un-conjugated His_8IFN was observed in any of the thiol-conjugated samples. The blurry bands observed in the anti-IFN Western blot

could be caused by high voltage or air bubbles present during the transfer process. These could be avoided by ensuring that the gel is run using a lower voltage and that the transfer is rollered to remove air bubbles prior to transfer. Considering the acutely high sensitively of the detection antibodies and Western blot technique, these observations are unlikely to represent the actual purity of the samples. Overall, the results confirm the identity of the thiol-conjugated conjugates.

3.3.6 *In vitro* biological potency of IFN-PEG-IFN dimers

3.3.6.1 Antiviral activity testing of his-tag conjugated His_8IFN-PEG_{20}-His_8IFN dimer

IFN α-2a has numerous distinct biological properties; one of these is antiviral activity. This can be assessed *in vitro*, by the prevention of infection of human lung carcinoma (A549) cells by encephalomyocarditis virus (EMCV) (Grace et al., 2005) (Figure 3-49). The relative activity of the PEGylated His_8IFN α-2a conjugates was determined by comparing the dose (concentration) of the sample, which displays 50 % prevention of infection in cells or (50 % effective dose- ED_{50}) *in vitro* to the dose of the National Institute for Biological Standards and Control (NIBSC) reference standard IFN α-2a. The ED_{50} was then used to calculate the specific activity of each of the His_8IFN α-2a compounds (6.1 Appendix I).

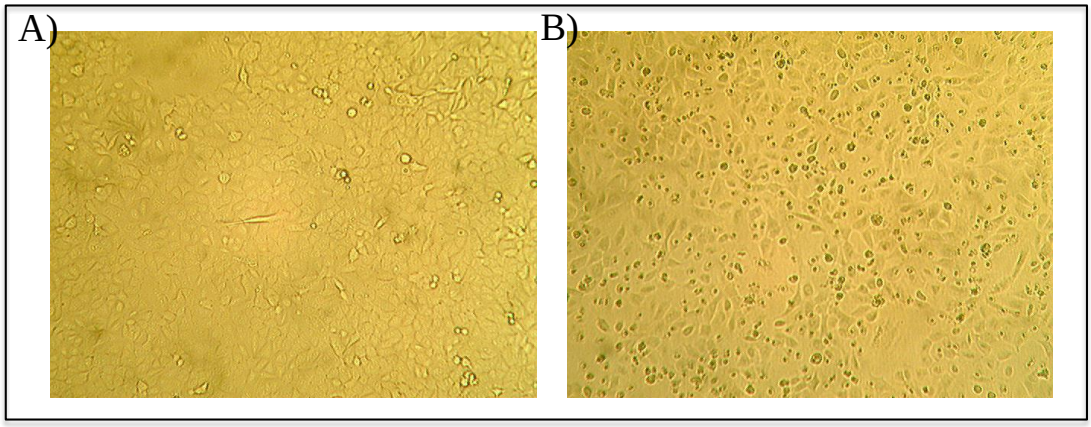

Figure 3-49. Microscope pictures of antiviral assay positive and negative controls, A) A549 cells incubated without virus (negative), B) A549 cells incubated with EMCV virus (positive).

Cell-based assays are inherently variable (Meager, 2006). The use of international standards can significantly reduce inter-assay and even inter-laboratory variability. However, even optimised assays can lead to different specific activities being achieved by different laboratories (Giard and Fleischaker, 1984). The activity

of an IFN product is usually compared against the WHO international standard (IS) matching subtype, which is assigned an agreed specific activity per milligram (Meager, 2006). The WHO IS for IFNs are a homogenous standard of individual subtypes with separate unitage (Meager et al., 2001). The use of IS allows for comparisons to be made between different IFN preparations in a variety of biological assays including antiviral assays (Meager, 2002; Meager et al., 2001; Mire-Sluis et al., 1996).

Within this antiviral assay, two controls were used to ensure the data achieved was 'real' and not an artefact of the cell-based assay. First, on each plate an International standard was used, NIBSC IFN α-2a, which allows IFN potency to be reported in universally accepted International Units (IU) (Meager, 2006). Thus, direct comparisons can be made between IFN samples from different laboratories. Secondly, PEGASYS® was also used concomitantly as a PEGylated IFN α control. As discussed (§ 1.2.1.1), PEGASYS®, a 40 kDa branched PEG-IFN α-2a, is a marketed product for the treatment of HCV. To further ensure the data achieved was accurate the assay was optimised as outlined in 6.3 Appendix III.

First, His_8IFN α-2a, PEG_{20}-His_8IFN, $(PEG_{20})_2$-His_8IFN and His_8IFN-PEG_{20}-His_8IFN were subject to antiviral assay testing (§ 2.2.10.7). The raw data was plotted as shown for His_8IFN-PEG_{20}-His_8IFN (Figure 3-50). The effective dose at 50% (ED_{50}) was calculated into specific activity (MIU/mg) using the calculations in 6.1 Appendix I.

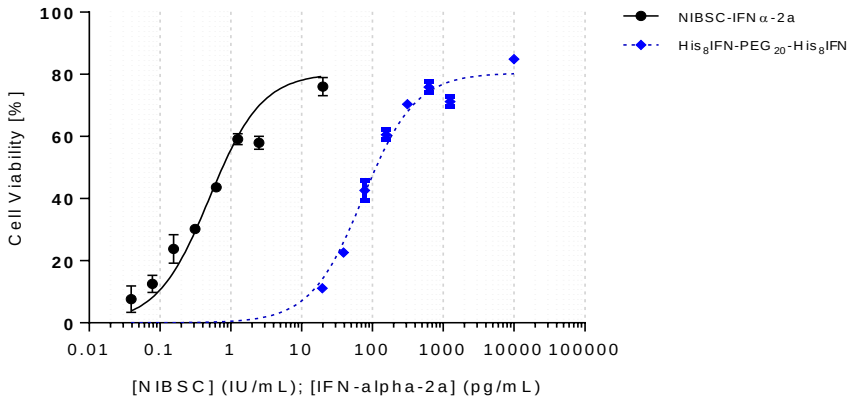

	NIBSC-IFNα-2a	His8IFN-PEG20-His8IFN	Global (shared)
One site -- Specific binding with Hill slope			
Best-fit values			
Bmax	80.43	80.43	80.43
h	1.174	1.174	1.174
Kd	0.4995	73.31	
Goodness of Fit			
Robust Sum of Squares	7.682	9.154	16.84
RSDR			5.994
Constraints			
Bmax	Bmax is shared	Bmax is shared	
h	h is shared	h is shared	
Number of points			

Figure 3-50. Representative graph of $His_8IFN\text{-}PEG_{20}\text{-}His_8IFN$ with the ED_{50} for calculating the specific activity (MIU/mg). The Kd value in the table is the EC_{50} on the graph. The $His_8IFN\text{-}PEG_{20}\text{-}His_8IFN$ was tested twice within the antiviral assay.

The specific activity for NIBSC IFN is 63,000 IU/mL. Given that the vial contains *ca.* 250 ng of IFN, the specific activity would be *ca.* 254 MIU/mg. As stated cell based assays are inherently variable, therefore the inclusion of the NIBSC standard allows for any drifts in the values achieved for specific activity but may also indicate any negative changes within the assay or its components. Therefore a range for NIBSC IFNα-2a was set to 200-300 MIU/mg allowing for 20% variation or %CV. This 20% CV of specific activity for compounds would be taking this drift of NIBSC standard into account.

The mean specific activity achieved for PEGASYS® (n=6) was 2.75 ± 0.37 MIU/mg (Table 3–2). For His_8IFN α-2a, the specific activity achieved was 195.5 ± 66.8 MIU/mg (n=3) (Table 3–3). The specific activity achieved for $PEG_{20}\text{-}His_8IFN$ was 9.84 ± 2.08 MIU/mg (5% retained activity, n=3) (Table 3–2). The novel $His_8IFN\text{-}PEG_{20}\text{-}His_8IFN$ dimer achieved a specific activity of 5.78 ± 1.62 MIU/ mg (2.95% retained activity, n=2, Table 3–2), whereas, $(PEG_{20})_2\text{-}His_8IFN$ achieved a specific activity of 0.38 ± 0.16 MIU/mg (0.19% retained activity, n=3, Table 3–2).

Despite having a reduced antiviral activity all of the his-tag conjugates achieved complete inhibition of cell death from EMCV infection at saturating doses.

Table 3–2. Summary of *in vitro* specific activity values achieved and n numbers for his-tag conjugated His_8IFN-PEG_{20}-His_8IFN and controls. His_8IFN-PEG_{20}-His_8IFN retained greater activity than PEGASYS and all his-tag conjugates achieved complete inhibition of cell death, thus retaining biological activity.

Value	His_8IFN α-2a	PEGASYS®	PEG_{20}-His_8IFN	$(PEG_{20})_2$-His_8IFN	His_8IFN-PEG_{20}-His_8IFN
Mean specific activity (MIU/mg)	195.50	2.75	9.84	0.38	5.78
ST.DEV of specific activity (MIU/mg)	66.83	0.37	2.08	0.16	1.62
retained activity (%)	100	-	5	0.19	2.95
n	3	6	3	3	2

Specific activities achieved for the novel His_8IFN-PEG_{20}-His_8IFN and the controls were plotted onto a bar graph and a one-way analysis of variance (ANOVA) was conducted. The one-way ANOVA was used to test that the null hypothesis that the sets of bioactivity data have the same mean (Dytham, 2011). One-way ANOVA was used in conjunction with a *post hoc* test, the Tukey's test. The Tukey's test is a multiple comparison test, which compares all possible pairs of means to find which are statistically different from one another and is based on studentised range of distribution (q). The assumption of the Tukey's test are that i) the observations being tested are independent and ii) there is equal variation across the sets of data (Dytham, 2011).

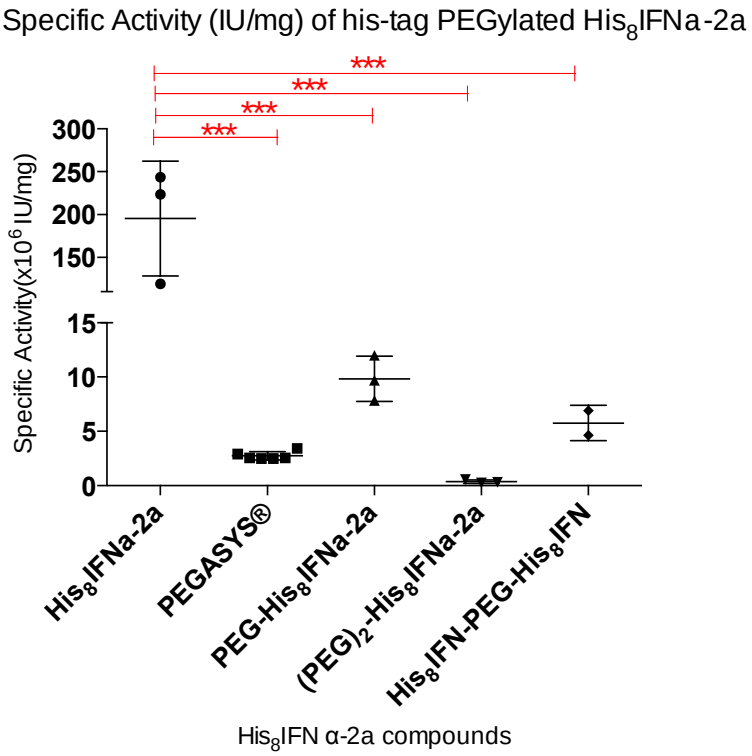

Tukey's multiple comparisons test	Mean Diff.	95% CI of diff.	Significant?	Summary
His_8IFNa-2a vs. PEGASYS®	192.7	131.2 to 254.3	Yes	****
His_8IFNa-2a vs. PEG-His_8IFNa-2a	185.7	114.6 to 256.7	Yes	****
His_8IFNa-2a vs. $(PEG)_2$-His_8IFNa-2a	195.1	124.1 to 266.2	Yes	****
His_8IFNa-2a vs. His_8IFN-PEG-His_8IFN	189.7	110.3 to 269.2	Yes	****
PEGASYS® vs. PEG-His_8IFNa-2a	-7.088	-68.62 to 54.45	No	ns
PEGASYS® vs. $(PEG)_2$-His_8IFNa-2a	2.375	-59.16 to 63.91	No	ns
PEGASYS® vs. His_8IFN-PEG-His_8IFN	-3.023	-74.08 to 68.03	No	ns
PEG-His_8IFNa-2a vs. $(PEG)_2$-His_8IFNa-2a	9.463	-61.59 to 80.52	No	ns
PEG-His_8IFNa-2a vs. His_8IFN-PEG-His_8IFN	4.065	-75.38 to 83.51	No	ns
$(PEG)_2$-His_8IFNa-2a vs. His_8IFN-PEG-His_8IFN	-5.398	-84.84 to 74.04	No	ns

Figure 3-51. One-way ANOVA analysis of the specific activity (MIU/mg) data achieved for the novel His_8IFN-PEG_{20}-His_8IFN and controls. Statistically different ($P < 0.05$) conjugates are marked (*).

The one-way ANOVA in conjunction with the Tukey test showed that all the conjugated His_8IFN species were significantly different ($P < 0.05$) when compared to un-conjugated His_8IFN α-2a (Figure 3-51). Interestingly, there is not a significant difference ($P < 0.05$) between any of the conjugated His_8IFN α-2a conjugates made. This was an unexpected result for the His_8IFN-PEG_{20}-His_8IFN, as the make up of the conjugate is quite different compared to that of PEG_{20}-His_8IFN and $(PEG_{20})_2$-His_8IFN. Perhaps this difference in activity and statistical difference could be due to the presence of the PEG attached to the homobifunctional linkers as the difference is between native His_8IFN and not vs. the controls (PEG_{20}-His_8IFN and $(PEG_{20})_2$-

His_8IFN). It is well documented in literature that the conjugation of PEGs to proteins reduces the activity of the protein (Bailon et al., 2001; Monkarsh et al., 1997; Wang et al., 2002). However, as discussed (§ 1.2.1.1) conjugation is used to improve the PK of the proteins, so reduction in activity is not always detrimental if the proteins effect *in vivo* is prolonged. Further the reduction in activity can be overcome by increasing the dose. Therefore, the reduction in activity of the His_8IFN-PEG_{20}-His_8IFN is not detrimental if there is prolonged half-life, which could be assumed due to the MW of the conjugate (~80 kDa).

To better compare the specific activity achieved between the novel His_8IFN-PEG_{20}-His_8IFN and the controls. The achieved specific activities of all his-tag conjugated His_8IFN species were plotted onto a scatter graph (Figure 3-51). It is observed that the order of activity is His_8IFN with 100% retained activity, followed by PEG_{20}-His_8IFN (5%), His_8IFN-PEG_{20}-His_8IFN (2.95%), $(PEG_{20})_2$-His_8IFN (0.19%). It was unexpected that the His_8IFN-PEG_{20}-His_8IFN dimer activity was less than that of PEG_{20}-His_8IFN (Figure 3-51). The data achieved suggests that may be the second His_8IFN molecule within the His_8IFN-PEG_{20}-His_8IFN is impeding the activity of the other His_8IFN molecule. His_8IFN-PEG_{20}-His_8IFN was shown to have ~2-fold greater activity than PEGASYS®. The reduction in IFN dimer activity has also been reported with DNL IFN α-2b dimers (§1.3.5). It was reported that a DNL monoPEGylated (20 kDa PEG) IFN α-2b dimer (10×10^{12} IU/mmol) had greater *in vitro* activity compared to PEGASYS® when tested within the antiviral assay (Chang et al., 2009b). They accounted that site-specific PEGylation may preserve biological better, when using larger PEG MW (Chang et al., 2009b). The specific activity data achieved is in agreement with this, as the his-tag conjugates, PEG_{20}-His_8IFN and His_8IFN-PEG_{20}-His_8IFN, achieved greater retained activity than that PEGASYS®, which is prepared using random conjugation. However, $(PEG_{20})_2$-His_8IFN retained less activity than PEGASYS®, this is most likely due to the conjugation of two PEG molecules masking the binding site or impeding the IFN binding to the IFNAR1/AR2 (Bailon and Won, 2009).

It is well documented in literature that conjugating proteins to PEG results in a reduction in protein activity, there is a directly proportional trend of reduced protein activity with increasing PEG MW (Grace et al., 2005). This trend can be seen when comparing the activity of the activity of PEG_{20}-IFN to $(PEG_{20})_2$-IFN or PEG_{20}-IFN to PEGASYS®. In both cases, the PEG_{20}-IFN has a greater activity of 25- and 4-

fold respectively. When compared to His_8IFN-PEG_{20}-His_8IFN, PEG_{20}-IFN has a 1.7-fold better activity.

3.3.6.2 Antiviral activity assessment of thiol conjugated IFN conjugates

Antiviral assay was also performed on the disulfide-conjugated IFN-PEG_{20}-IFN dimers and control conjugates, to compare the effect of the PEG MW on the IFN-PEG-IFN *in vitro* activity and how the activity of the IFN-PEG-IFN dimers compares to the conjugated controls.

As with the his-tag conjugated samples, ED_{50} values were used to calculate specific activity (MIU/mg) according to the method described in 6.1 Appendix I. The specific activity achieved for His_8IFN was 231.31 ± 10.95 (n=3, Table 3–2), while for PEGASYS® was 2.43 ± 0.06 MIU/mg (n=3, Table 3–2). PEG_5-IFN and $(PEG_5)_2$-IFN achieved specific activities of 51.89 ± 10.45 MIU/mg (n=2, 22.4% retained activity, Table 3–2) and 0.84 ± 0.03 MIU/mg (n=3, 0.36% retained activity, Table 3–2) respectively. Specific activities of 4.86 ± 1.77 MIU/mg (2.1% specific activity, n=5, Table 3–2) and 0.12 ± 0.04 MIU/mg (0.05% retained activity, n=3, Table 3–2) for PEG_{10}-IFN and $(PEG_{10})_2$-IFN respectively. IFN-PEG_{10}-IFN achieved a specific activity of 5.99 MIU/mg (2.59% retained activity, n=3, Table 3–2). The specific activities of PEG_{20}-IFN and $(PEG_{20})_2$-IFN were 3.95 ± 1.69 MIU/mg (1.7% retained activity, n=5, Table 3–2) and 0.55 ± 0.04 MIU/mg (0.24% retained activity, n=3, Table 3–2), respectively. A specific activity of 2.12 ± 0.64 MIU/mg (0.95% retained activity, n=4, Table 3–2) was achieved for IFN-PEG_{20}-IFN.

To better compare the specific activities of the IFN-PEG-IFN dimers with the controls, the specific activities of all the thiol-conjugated IFN species were plotted on a graph (Figure 3-52). The graph shows that both the IFN-PEG-IFN dimers have retained activity. The IFN-PEG_{10}-IFN dimer (2.59% retained activity, Figure 3-52) has greater activity than both PEG_{10}-IFN (2.1%, Table 3–3) and $(PEG_{10})_2$-IFN (0.05%, Table 3–3). This could possibly be the smaller homobifunctional PEG **4** allowing both the IFN molecules to bind to the IFNAR1/AR2 on the cell surface. Interestingly, IFN-PEG_{20}-IFN achieved a specific lower activity (2.12 ± 0.64 MIU/mg, Table 3–3) compared to IFN-PEG_{10}-IFN (5.99 ± 2.08 MIU/mg, Figure 3-52). This could be due to the increasing PEG size affecting the IFN binding to IFNA receptors. Even so, both the IFN-PEG_{20}-IFN and IFN-PEG_{10}-IFN dimers were found to be more active that PEGASYS® (Figure 3-52). IFN-PEG_{20}-IFN (2.12 ± 0.64

MIU/mg, Figure 3-52) had a greater specific activity than $(PEG_{20})_2$-IFN (0.55 ± 0.04 MIU/mg) but a slightly lower activity than PEG_{20}-IFN (3.95 ± 1.69 MIU/mg, Table 3–3). Suggesting the addition a second PEG molecule has greater detriment to retained activity than a second protein. The only thiol-conjugate to have a greater specific activity than IFN-PEG_{10}-IFN (5.99 ± 2.08 MIU/mg) was PEG_5-IFN (51.89 ± 10.45 MIU/mg, Figure 3-52). This observation highlights the correlation that with increasing PEG MW a decrease in specific activity is observed with the IFN-PEG-IFN dimers and controls (Figure 3-52). The trend of decreasing activity of PEGylated proteins with increasing PEG MW trend is well documented in literature (Grace et al., 2005). It was also observed that all $(PEG)_2$-IFN molecules had a much lower activity than IFN-PEG-IFN dimers and mono-PEGylated-IFNs, suggesting the conjugation of two PEG molecules must reduce the ability of IFN to bind to the IFNA receptors, thus reducing the activity of IFN (Figure 3-52).

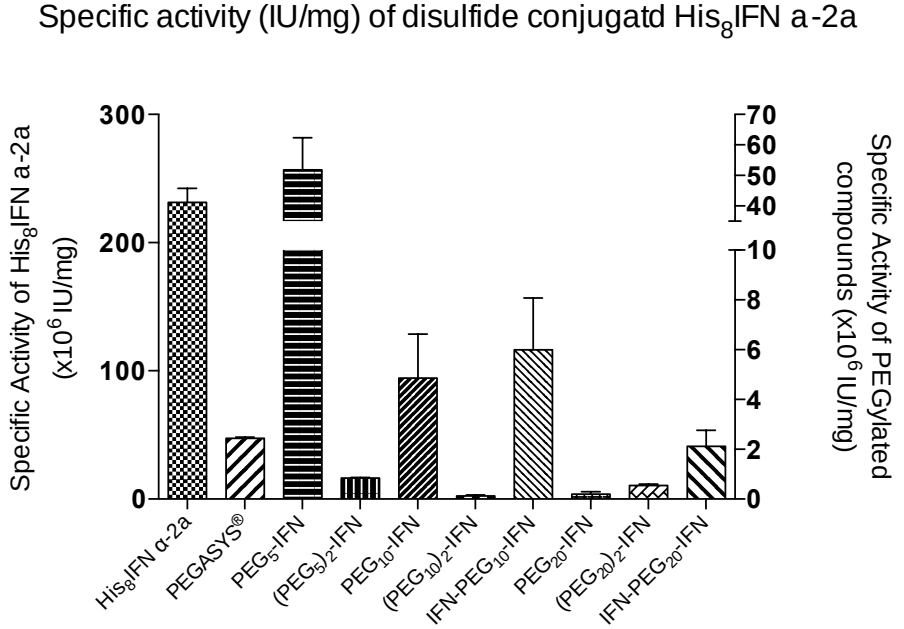

Figure 3-52. Specific Activities achieved for IFN-PEG-IFN dimers and control prepared using thiol-conjugation.

Table 3–3. Antiviral specific activity achieved for disulfide conjugated IFN-PEG-IFN dimers and controls (PEG-IFN and $(PEG)_2$-IFN). All disulfide conjugates have retained biological potency.

Value	His_8IFN α-2a	PEGASYS®	PEG_5-IFN	$(PEG_5)_2$-IFN	PEG_{10}-IFN	$(PEG_{10})_2$-IFN	IFN-PEG_{10}-IFN	PEG_{20}-IFN	$(PEG_{20})_2$-IFN	IFN-PEG_{20}-IFN
Mean specific activity (MIU/mg)	231.31	2.43	51.89	0.84	4.86	0.12	5.99	3.95	0.55	2.12
ST.DEV of specific activity (MIU/mg)	10.95	0.06	10.45	0.03	1.77	0.04	2.08	1.69	0.04	0.64
Percentage (%) retained activity	100	-	22.4	0.36	2.1	0.05	2.59	1.7	0.24	0.92
n	3	3	2	3	5	3	3	5	3	4

3.3.6.3 Comparison between the specific activities of thiol and his-tag IFN-PEG-IFN dimers and controls

As IFN-PEG-IFN dimers prepared using both his-tag and thiol conjugation of His_8IFN. To observe if there were any differences within the specific activities achieved between the IFN dimer samples and their controls, their specific activity data and percentage retained activity data was summarised in Table 3–4. Interestingly, His_8IFN-PEG_{20}-His_8IFN had a greater specific activity compared to both IFN-PEG_{10}-IFN and IFN-PEG_{20}-IFN (Table 3–4). Further PEG_{20}-His_8IFN retained greater specific activity than PEG_{20}-IFN. This data suggests the conjugation at the his-tag has a higher retained activity compared to thiol conjugation of His_8IFN. The IFN α-2a domains thought to interact with the IFNA receptors are A (Met16-Ser28), AB (Cys29-Phe36), C (Glu78-Asp95) and DE (Tyr122-Ala139) (Figure 3-53) (Fish, 1992; Mitsui et al., 1993; Uzé et al., 1994; Waine et al., 1992). Figure 3-53 of the binding domains shows that one disulfide bond is between binding domains A and B, therefore conjugation at this disulfide bond (Cys29-Cys138) would drastically reduce the specific activity of His_8IFN. It is understood that the disulfide conjugation reaction mixture of IFN is a mixture of two 'PEG position isomers' where the PEG conjugated at Cys1-CC[PEG]-C-Cys98 and Cys29-CC[PEG]C-Cys138 (Balan et al., 2007). CIEC purification of PEG-IFN reaction mixtures showed two peaks of PEG-IFN, these are thought to be the two disulfide PEG positional isomers (§ 3.3.4.2). While, the higher specific activity of His_8IFN-PEG_{20}-His_8IFN and controls could be due to location of the polyhistidine-tag away from the binding domains, thus there is less steric hinderance from the conjugated PEG. Interestingly, $(PEG_{20})_2$-His_8IFN (0.38 ± 0.16 MIU/mg, Table 3–4) retained similar activity to $(PEG_{20})_2$-IFN (0.55 ± 0.04 MIU/mg, Table 3–4) suggesting steric hinderance of two conjugated PEGs effect the binding of IFN in a similar way.

Table 3–4. Summary of specific activities and percentage retained activity achieved for IFN-PEG-IFN dimers and the controls prepared. Grey colour indicates His-tag conjugated species, while white shows thiol-conjugated species. All site-specifically conjugated IFN conjugates retained biological activity, with His_8IFN-PEG_{20}-His_8IFN retaining the highest biological activity of the IFN dimers prepared.

Sample	Specific Activity (MIU/mg)	Percentage (%) retained activity
His_8IFN-PEG-$_{20}$-His_8IFN	5.78 ± 1.62	2.95
PEG_{20}-His_8IFN	9.84 ± 2.08	5
$(PEG_{20})_2$-His_8IFN	0.38 ± 0.16	0.19
IFN-PEG_{20}-IFN	2.12 ± 0.64	0.92
PEG_{20}-IFN	3.95 ± 1.69	1.7
$(PEG_{20})_2$-IFN	0.55 ± 0.04	0.24
IFN-PEG_{10}-IFN	5.99 ± 2.08	2.59
PEG_{10}-IFN	4.86 ± 1.77	2.1
$(PEG_{10})_2$-IFN	0.12 ± 0.04	0.05

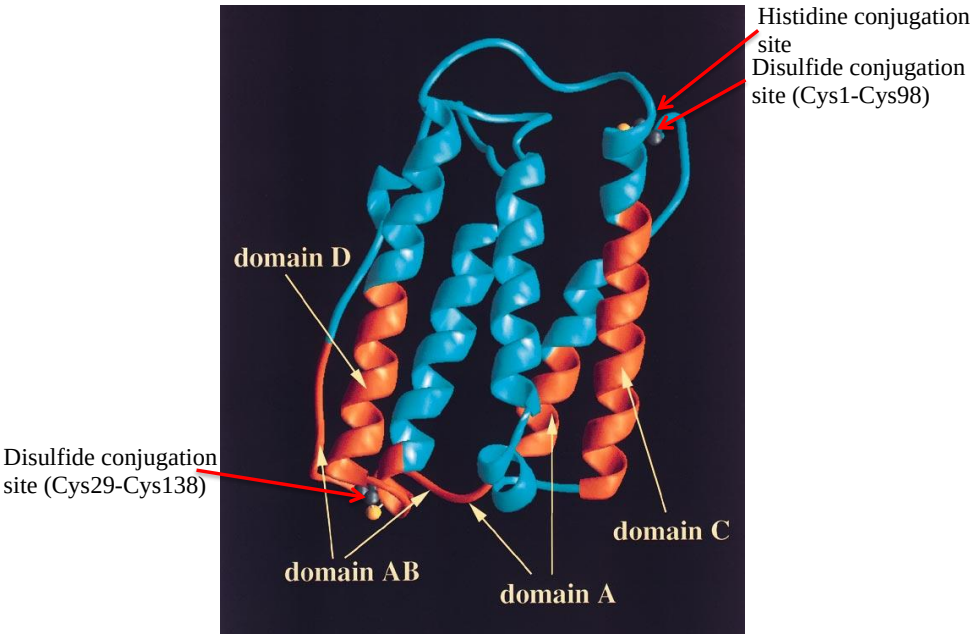

Figure 3-53. A) Receptor binding sites located on IFN α-2a, with binding domains A, AB, C and D labelled, sulphur atoms are coloured yellow and carbon atoms in grey (adapted from Klaus et al. 1997) to show the conjugation sites used for preparing the homo- and hetero-dimeric molecules of IFN. The disulfide and histidine conjugation sites are labelled, taking into account where the location of the histidine tag would be located within His_8IFN α-2a. Conjugation between Cys29-Cys138 would result in reduced IFN activity due to conjugation being located within the binding domains, whereas conjugation at Cys1-98 or on the histidine tag would result in higher retained activity of IFN due to the conjugation being away from the binding domains.

3.3.6.4 Antiproliferative assay to assess the biological potency of thiol PEGylated IFN conjugates

IFN is a pleiotropic protein, therefore to better judge the specific activity of the IFN-PEG-IFN dimers and controls, the disulfide-conjugates were subject to an antiproliferative assay. The antiproliferative activity of IFNs was first described by Paucker in 1962 and colleagues who demonstrated that a 24 h exposure of L-cells to either UV-irradiated Newcastle disease virus or to IFN led to a temporary decline in cell growth. Interferons exert antiproliferative effects though cell cycle arrest particularly of the G0 and G1 phases (Sangfelt et al., 1997; Tiefenbrun et al., 1996).

The antiproliferative assay used to Daudi (human Burkitts Lymphoma) cells, the most widely utilised cell line, to assess the antiproliferative activity of the IFN-PEG-IFN conjugates and mono-PEGylated controls. Due to the large quantity of sample required to run the assay, di-PEGylated samples as well as PEG_5-IFN could not be assayed. The antiproliferative assay was optimised as outlined in 6.2 Appendix II to ensure the data achieved was accurate and reproducible. As in the antiviral assay, NIBSC IFN α-2a was run on every plate as a control.

Raw data was plotted as shown for IFN-PEG_{10}-IFN. The effective dose at 50% (ED_{50}) was calculated from the normalised graph (Figure 3-54) into specific activity (MIU/mg) using the calculations in 6.1 Appendix I.

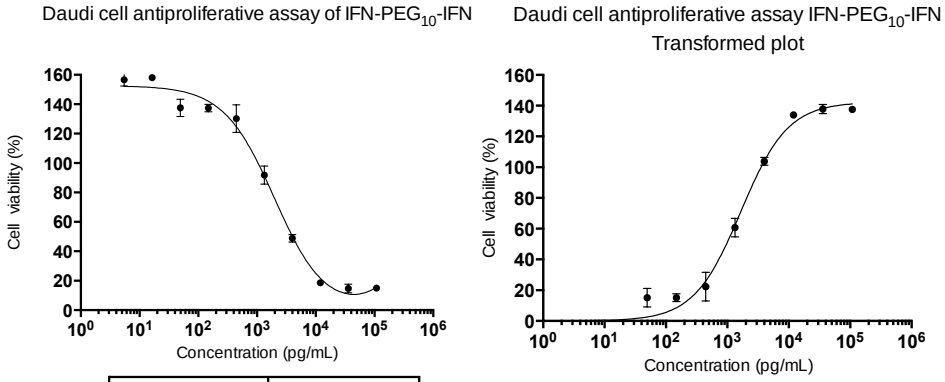

	IFN-PEG_{10}-IFN
One site -- Total	
Best-fit values	
Bmax	-155.0
Kd	2018
NS	0.0001430
Background	152.6

	IFN-PEG_{10}-IFN
One site -- Specific binding with Hill slope	
Best-fit values	
Bmax	142.3
h	1.136
Kd	1661

Figure 3-54. Representative Left) plotted data for IFN-PEG_{10}-IFN and right) transformed data plot for IFN-PEG_{10}-IFN with analysis tables (n=3). In the analysis table, the Kd is the EC_{50}.

The specific activity achieved for His_8IFN was 329.36 ± 97.98 MIU/mg (n=5, Table 3–5). PEG_{10}-IFN achieved a specific activity of 2.95 ± 0.21 MIU/mg (0.90% retained activity, n=2, Table 3–5). IFN-PEG_{10}-IFN achieved a specific activity of 1.52 ± 0.47 MIU/mg (0.46% retained activity, n=3, Table 3–5). The specific activity of PEG_{20}-IFN was 5.13 ± 1.44 MIU/mg (1.56% retained activity, n=4, Table 3–5). Specific activity of 0.81 ± 0.09 MIU/mg (0.25% retained activity, n=3, Table 3–5) was achieved for IFN-PEG_{20}-IFN.

Table 3–5. Summary of antiproliferative activity (MIU/mg) achieved for IFN-PEG-IFN dimers and controls (PEG-IFN and $(PEG)_2$-IFN). All tested samples retained biological activity.

Sample	Specific Activity (MIU/mg)	Percentage (%) retained activity	n number
His_8IFN α-2a	329.36 ± 87.98	100	5
IFN-PEG_{20}-IFN	0.81 ± 0.09	0.25	3
PEG_{20}-IFN	5.13 ± 1.44	1.56	4
IFN-PEG_{10}-IFN	1.52 ± 0.47	0.46	3
PEG_{10}-IFN	2.95 ± 0.21	0.90	2

The specific activity and the percentage retained activity achieved for IFN-PEG_{10}-IFN in the antiproliferative assay was higher than that for IFN-PEG_{20}-IFN. This shows that the PEG size affects the activity of the conjugated IFN molecule, where the larger PEG_{20} has reduced activity compared to the smaller PEG_{10} version of the dimer. However, the contrary is true for the mono-PEGylated controls. The PEG_{10}-IFN has a lower activity than the PEG_{20}-IFN control. This is not the same trend observed within literature or previous antiviral assay results as it is well documented that the larger PEG MW correlates with a reduction in protein activity (Grace et al., 2005). Thus, it is thought that further experiments should be conducted to increase the number of replicates on both PEG_{20}-IFN and PEG_{10}-IFN to better assess the true antiproliferative activity of these conjugates.

IFN-PEG_{10}-IFN in both the antiviral and antiproliferative assays was shown to be more active than IFN-PEG_{20}-IFN (Table 3–6). This could be due to the smaller PEG MW having less steric hinderance on the functional binding of IFN to its IFNAR receptors. This trend has also been reported in literature with IFN, where larger PEG sizes correlates with reduced activity (Grace et al., 2005). This trend was

also seen for the PEG-IFN controls within the antiviral assay, where PEG_{10}-IFN had greater activity compared to PEG_{20}-IFN (Table 3–6). However, for the antiproliferative data, PEG_{10}-IFN achieved a lower specific activity than PEG_{20}-IFN (Table 3–6). This is against the trend observed seen in the antiviral assay and in the literature, thus the data is questionable. Thus, it is difficult to ascertain whether the IFN-PEG_{10}-IFN is more active than the PEG_{10}-IFN as seen in the antiviral assay. However, both assays showed that the IFN-PEG-IFN dimers had retained activity.

Table 3–6. Summary table of antiviral and antiproliferative specific activity data achieved for IFN-PEG-IFN dimers and monoPEGylated controls

Sample	Antiviral specific activity (MIU/mg)	Antiproliferative specific activity (MIU/mg)
His_8IFN α-2a	231.31 ± 10.95	329.36 ± 87.98
IFN-PEG_{20}-IFN	2.17 ± 0.77	0.81 ± 0.09
PEG_{20}-IFN	3.95 ± 1.69	5.13 ± 1.44
IFN-PEG_{10}-IFN	5.99 ± 2.08	1.52 ± 0.47
PEG_{10}-IFN	4.86 ± 1.76	2.95 ± 0.21

3.4 Conclusion

This work has shown that PEG di(*bis*)sulfone **4** can be used as a linker to make IFN-PEG-IFN dimers. These IFN-PEG-IFN dimers were prepared utilising both histidine and thiol conjugation strategies. It was found that His_8IFN-PEG_{20}-His_8IFN retained greater activity than IFN-PEG_{20}-IFN (Table 3–6). This is thought to be due to the conjugation site. The polyhistidine tag is thought to be further away from the protein-binding site than the thiols from the disulfides.

Interestingly, it was found that the IFN-PEG_{10}-IFN dimer was found to be more active than PEG_{10}-IFN in the anti-viral assay (Table 3–6). This could be due to the presence of the second IFN molecule and the lower MW PEG used. However, this observation was reversed for IFN-PEG_{20}-IFN, where PEG_{20}-IFN displayed a higher specific activity in both the antiviral and antiproliferative assays. These results indicate that each conjugate should each be evaluated.

The trend where smaller PEG MW have greater retained activity was observed for the novel IFN-PEG-IFN dimers, PEG-IFN and $(PEG)_2$-IFN, where increasing PEG size correlates with greater reductions in protein activity. This was

shown where IFN-PEG_{10}-IFN had greater retained activity compared to IFN-PEG_{20}-IFN (Table 3–6). To further develop the IFN-PEG_{10}-IFN homodimer into a possible treatment for hepatitis C, two areas need to be further investigated: i) experimental process and i) pharmacokinetics (PK). First, the experimental process to make the IFN-PEG_{10}-IFN dimers would need to be improved to give higher conversions and yields of IFN-PEG_{10}-IFN dimer to make the process scalable. Regarding purification, a SEC purification step that is readily scalable would need to be replaced by a CIEC step. Additionally, investigations into improving the purity of the PEG_{10} di(*bis*)sulfone **4** would need to be conducted in an effort to improve the conversion of IFN-PEG_{10}-IFN. As for *in vivo* studies, larger quantities of the IFN-PEG_{10}-IFN heterodimer made from a single batch would be required. Second, investigations into the dosing and pharmacokinetic properties of the homodimer would be necessary. For the IFN-PEG_{10}-IFN dimer to become a possible treatment for hepatitis C, it would need to have more favourable PK properties than current treatments PEGASYS® and PEG-INTRON® resulting in less frequent injections and greater patient compliance.

It was observed that the conversion and yield of the IFN-PEG-IFN dimers were much lower than those observed when preparing the PEG-IFN conjugates (Table 3–6), using either the polyhistidine or thiol conjugation strategies. One reason for this difference is the PEG di(*bis*)sulfone **4** used for conjugation was found to be less pure (§ 3.2.1) than the mono PEGylation reagents used to prepare the PEG-IFN conjugates. Utilising an alternative synthesis route (synthesis route 2, § 3.2.1), PEG di(*bis*)sulfone **4** was used to investigate producing multifunctional proteins (IFN-PEG-Fab) using PEG di(*bis*)sulfone **4** as a linker.

Table 3–7. Summary of all the prepared conjugates, demonstrating reaction conditions, yields and biological activities. ND=not determined

PEGylated conjugate	PEG eq. in reaction	Purification method	Conversion (%)	Yield (%)	AV mean Specific activity (MIU/mg)	Percentage retained activity (%)	AP mean Specific activity (MIU/mg)	Percentage retained activity (%)
His-tag conjugated conjugates								
PEG_{20}-His_8IFN	2.5	2x CIEC	17.6	17.6	9.84 ± 2.08	5	ND	ND
$(PEG_{20})_2$-His_8IFN	2.5	2x CIEC	7.1	7.1	0.38 ± 0.16	0.19	ND	ND
His_8IFN-PEG_{20}-His_8IFN	1	CIEC, SEC	1.5	~1.5	5.78 ± 1.62	2.95	ND	ND
Disulfide conjugated conjugates								
PEG_{20}-IFN	1	CIEC	28.8	29	3.95 ± 1.69	1.7	5.13 ± 1.44	
$(PEG_{20})_2$-IFN	1	CIEC	12.0	12	0.55 ± 0.04	0.24	ND	ND
IFN-PEG_{20}-IFN	1	CIEC, SEC	0.8	0.85	2.12 ± 0.64	0.92	0.81 ± 0.09	0.25
PEG_{10}-IFN	1	CIEC	14.0	14	4.86 ± 1.76	2.1	2.95 ± 0.21	0.25
$(PEG_{10})_2$-IFN	1	CIEC	16.0	12	0.12 ± 0.04	0.052	ND	ND
IFN-PEG_{10}-IFN	1	CIEC, SEC	1.1	1.1	5.99 ± 2.08	2.59	1.52 ± 0.47	0.46
PEG_5-IFN	1	CIEC	29.0	29	32.31 ± 23.66	14.0	ND	ND
$(PEG_5)_2$-IFN	1	CIEC	34.5	34.5	0.84 ± 0.03	0.36	ND	ND

Chapter 4 Preparation and *in vitro* functional activity studies of IFN-PEG-Fab heterodimers

4.1 Introduction to IFN-PEG-Fab heterodimers

There are many approaches being investigated to prepare multifunctional proteins (§ 1.3). The PEG di(*bis*)sulfone **4** reagent has been used to prepare dimers of IFN (Chapter 3), Fabs (Khalili et al., 2013) and peptides, specifically Octreotide. The aim of this chapter was to explore a recombinant-chemical method to make heterodimers. IFN-PEG_{20}-Fab heterodimers were hoped to be prepared, utilising the 20 kDa PEG di(*bis*)sulfone **4** as a linker to conjugate the two proteins together by site-specific disulfide conjugation.

The aim to prepare and characterise IFN-PEG_{20}-Fab_{beva} and IFN-PEG_{20}-Fab_{alb} heterodimers required utilising the 20 kDa PEG di(*bis*)sulfone **4** as a linker to conjugate both IFN and Fab_{beva} or Fab_{alb} by disulfide PEGylation (§1.4.1.1). A 20 kDa PEG derived reagent was chosen because i) 20 kDa PEG-protein conjugates are easier to purify by CIEC, due to the greater size of the PEG ii) by using a 20 kDa PEG, the MW of the desired conjugate would be approximately ~90 kDa which is above the renal filtration cut-off of 50-60 kDa which could be useful to help achieve a prolonged half-life *in vivo*.

As discussed in §1.4.6.3 cytokines have three major disadvantages with cancer therapy firstly; severe toxicities are frequently associated with systemic infusions of cytokines, thus limiting the amount, which can be administered to achieve an effective dose. Secondly, for a therapeutic protein to be effective, it must reach its biological target, however cytokines lack tumour specificity. Thirdly, the majority of cytokines have a MW below 30 kDa, thus suffer from short serum half-lives (Vazquez-Lombardi et al., 2013). Consequently, the ultimate challenge for developing improved cytokine therapeutics for cancer is to reduce unwanted side effects of cytokine treatment while increasing the local concentration of cytokines to the tumour microenvironment. Bevacizumab (Avastin) plus interferon α is an approved first-line dual-action treatment for metastatic renal cell carcinoma (RCC) (Escudier et al., 2007; Rini et al., 2008). In an attempt to overcome the shortcomings associated with cytokine treatment, a novel therapeutic IFN-PEG_{20}-Fab_{beva} heterodimer using disulfide conjugation was made. The heterodimer was made by firstly conjugating Fab_{beva} to PEG_{20} di(*bis*)sulfone **4** to prepare Fab_{beva}-PEG-X (Figure 4-1). Fab_{beva}-PEG_{20}-X was purified by a linear CIEC step to remove unreacted PEG_{20} di(*bis*)sulfone **4** and then was allowed to react with reduced IFN.

An optimised CIEC step gradient was used to isolate the IFN-PEG_{20}-Fab_{beva} heterodimer (Figure 4-1). The IFN-PEG_{20}-Fab_{beva} was then characterised in terms of purity (SDS-PAGE), identity (anti-IFN, anti-human Western blots) and stability prior to functionality testing.

Second, it was hoped a novel IFN-PEG_{20}-Fab_{alb} heterodimer could be prepared. It was thought that an anti-albumin Fab (Fab_{alb}) could be used to 'piggy-back' upon circulating albumin. This approach was explored in an attempt to improve the half-life of IFN beyond that of current treatments of hepatitis C. This approach used the PEG_{20} di(*bis*)sulfone **4** as a linker to conjugate IFN to Fab_{alb}. A similar experimental process was used as for preparing the IFN-PEG_{20}-Fab_{beva} heterodimer. Whereby, first the Fab_{alb} was reduced using DTT, the reduced Fab_{alb} was then allowed to react with PEG_{20} di(*bis*)sulfone **4** (Figure 4-1). The X-PEG_{20}-Fab_{alb} conjugate was isolated from the unreacted PEG_{20} di(*bis*)sulfone **4** by CIEC. The purified X-PEG_{20}-Fab_{alb} conjugate was then allowed to react with reduced IFN to prepare IFN-PEG_{20}-Fab_{alb}. An optimised CIEC step gradient was used to isolate the IFN-PEG_{20}-Fab_{alb} heterodimer (Figure 4-1). The IFN-PEG_{20}-Fab_{alb} was then characterised in terms of purity (SDS-PAGE), identity (anti-IFN, anti-rat Western blots) and stability prior to functionality testing.

The purified IFN-PEG_{20}-Fab_{beva} and IFN-PEG_{20}-Fab_{alb} heterodimers were characterised in terms of functional activity. It was hoped that both IFN and Fab_{beva}/Fab_{alb} would both retain activity within the heterodimer complex, as i) site-specific disulfide conjugation was used and ii) the PEG_{20} di(*bis*)sulfone **4** was used a 'spacer' as well as a 'linker' to conjugate the two proteins together.

Antiviral and antiproliferative assays were conducted to determine if IFN had retained activity within the heterodimers. Functionality testing determined that IFN within the IFN-PEG_{20}-Fab_{beva} heterodimer had retained activity. It was found that the IFN-PEG_{20}-Fab_{alb} heterodimer bound to the FBS within the cell media, therefore it was difficult to determine the activity of the heterodimer, however the results obtained suggest that the IFN-PEG_{20}-Fab_{alb} heterodimer has retained some activity. BIAcore using a VEGF coated chip was used to determine if Fab_{beva} within the heterodimer had retained activity. While, BIAcore using a rat albumin coated chip was used to determine if Fab_{alb} within the heterodimer had retained activity. Functionality testing determined that both Fab_{beva} and Fab_{alb} within the heterodimers, IFN-PEG_{20}-Fab_{beva} and IFN-PEG_{20}-Fab_{alb} respectively, had retained activity.

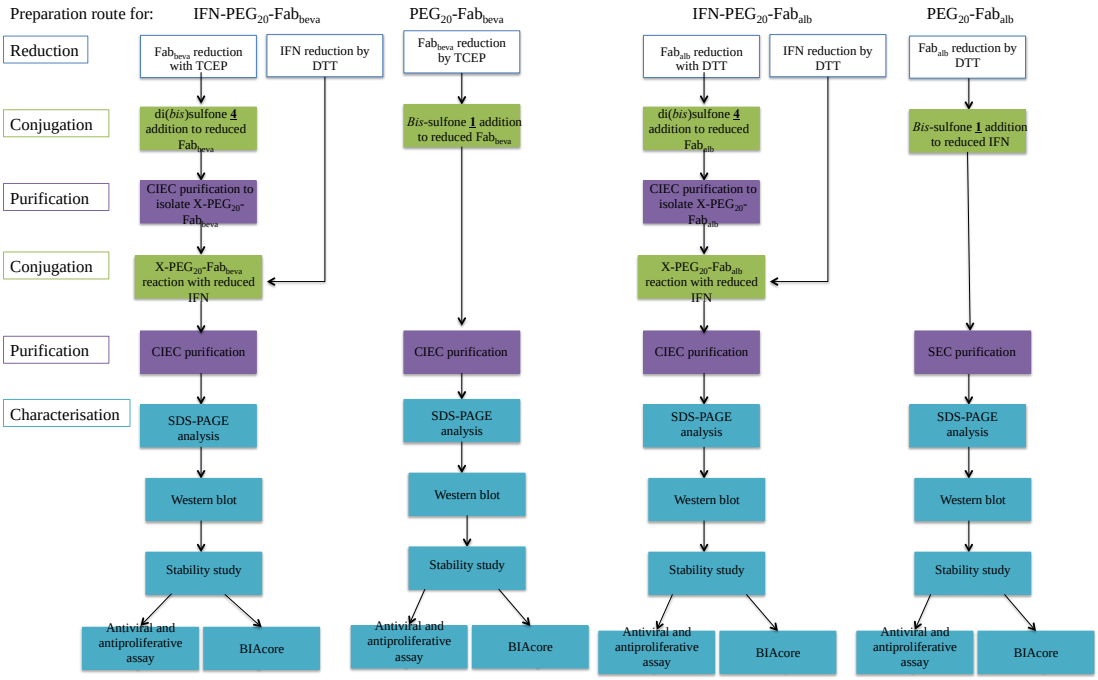

Figure 4-1: Experimental plan for preparing the IFN-PEG_{20}-Fab_{beva} and IFN-PEG_{20}-Fab_{alb} heterodimers. The IFN-PEG_{20}-Fab_{beva} heterodimer was prepared by a two-step disulfide conjugation process, first by reacting reduced Fab_{beva} with PEG_{20} di(*bis*)sulfone **4**. The X-PEG_{20}-Fab_{beva} conjugate was purified from the unconjugated PEG_{20} di(*bis*)sulfone **4** by a linear CIEC purification step. The X-PEG_{20}-Fab_{beva} was then allowed to react with reduced His_8IFN, following this IFN-PEG_{20}-Fab_{beva} was isolated by CIEC purification. For preparing IFN-PEG_{20}-Fab_{alb}, the same process was conducted by first reacting Fab_{alb} with PEG_{20} di(*bis*)sulfone 4, the X-PEG_{20}-Fab_{alb} conjugate was then isolated by CIEC. The X-PEG_{20}-Fab_{alb} conjugate was then allowed to react with reduced IFN. A step gradient was then used to isolate the IFN-PEG_{20}-Fab_{alb} heterodimer. The controls, PEG_{20}-Fab_{beva} and PEG_{20}-Fab_{alb}, were prepared by allowing reduced Fab_{beva} or Fab_{alb} to react with PEG_{20} *bis*-sulfone **1** respectively. PEG_{20}-Fab_{beva} was purified using a single CIEC step, while PEG_{20}-Fab_{alb} was purified by SEC. All conjugates prepared where characterised in terms of their purity, identity, stability and biological activity by SDS-PAGE, Western blot, stability studies and antiviral/antiproliferative assays and BIAcore respectively.

4.2 Results and discussion

4.2.1 Digestion and purification of bevacizumab

4.2.1.1 Digestion and purification of bevacizumab to prepare Fab_{beva}

Bevacizumab was proteolytically digested with immobilised papain to obtain Fab_{beva} (method 2.2.4.5). Papain is a thiol protease, which has a sulfhydryl group in the active site, which must be reduced for enzymatic activity (Goding, 1996). Papain reduction by disulfide exchange is possible by the addition of free thiol to the digestion mixture. Cysteine is generally used. Papain digestion of an IgG generally prepares two Fab fragments and one Fc fragment by cleaving peptides in the hinge region (Figure 4-2). Unlike pepsin, papain can prepare Fab fragments from all IgG

subclasses from all species (Andrew and Titus, 2001; Mage, 1980), but it can be inactivated by heavy metals. Therefore, to ensure maximal activity of the enzyme, EDTA was incorporated into the digestion buffer as a metal chelator (Goding, 1996). Immobilised papain (i.e. papain agarose resin) was chosen over crystalline papain or mercuripapain, as it does not require an oxidant to end digestion. Additionally, immobilised papain is easy to remove by passing the digestion mixture over a PD-10 frit, so there is no need to optimise an ion exchange method for papain removal (Mage, 1980).

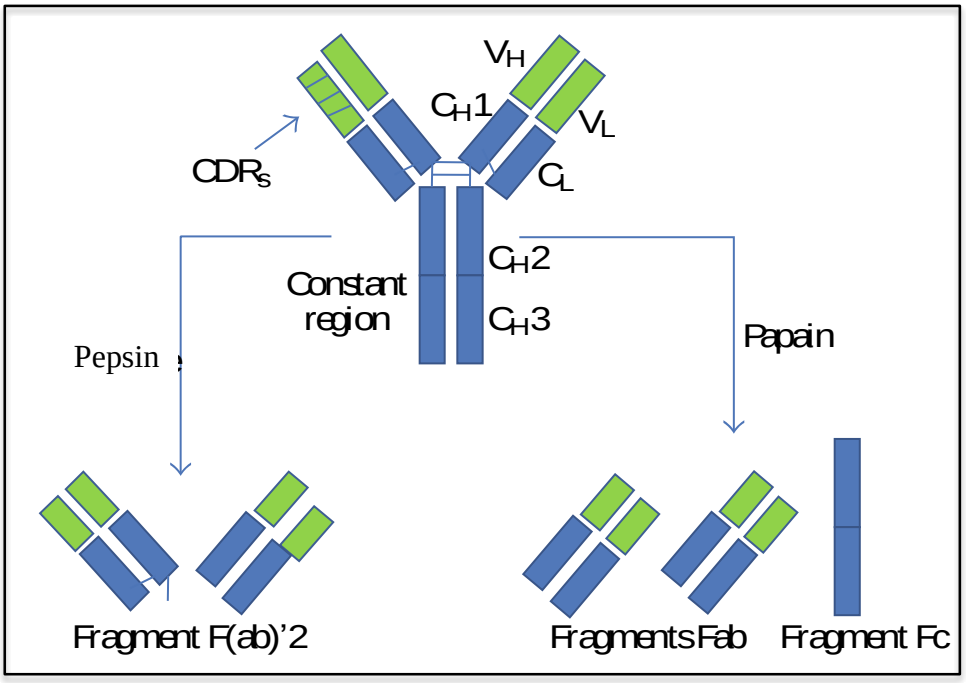

Figure 4-2: IgG antibody structure and the resulting products after enzyme (pepsin or papain) digestion (Arruebo et al., 2009). The antibody is made up a heavy chain (H) and a light chain (L). The heavy chain consists of four constant domains (CH1, CH2, CH3, CH4) and a variable region (VH), whilst the light chain is made up of two domains; variable and constant, VL and CL respectively. The complementary determining region (CDR) responsible for antigen binding is found on the VH and VL domains.

Antibody to enzyme ratio, digestion time and purification of bevacizumab digestion was optimised. The optimised conditions (method 2.2.4.5) were a 5 h digestion period using a 1:100 papain:antibody ratio, which allows for the near complete digestion of bevacizumab (150 kDa) to Fab (~45 kDa) and Fc (~50 kDa) (25 mg scale, n=2) (Figure 4-3). Interestingly, it appeared by SDS-PAGE (Figure 4-3) there were also bands of heavy chain of bevacizumab (~110 kDa), half a chain of bevacizumab (~80 kDa), reduced Fc_{beva} (~30 kDa) and reduced Fab_{beva} (~20 kDa). These could be the result of proteolytic cleavage and/or partial reduction by cysteine. Thiol exchange reducing agents such as cysteine have been reported for their ability

to cleave the interchain disulfide bonds of immunoglobulins (Andrew and Titus, 2001; Goding, 1996).

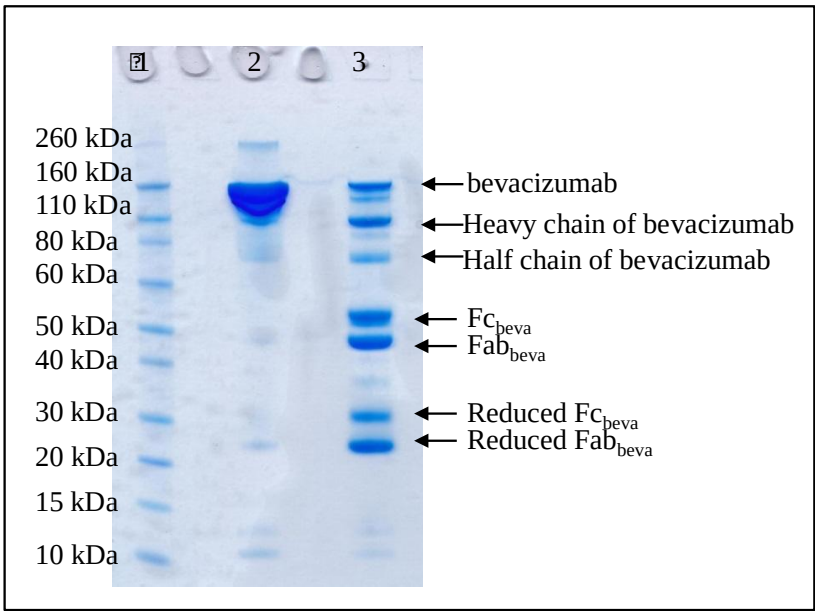

Figure 4-3. Representative SDS-PAGE analysis (InstantBlue™) of bevacizumab digestion with immobilised papain (n=2). Lane 1: Novex pre-stained markers, Lane 2: bevacizumab, Lane 3: bevacizumab digestion mixture. Successful immobilised papain digestion of bevacizumab to prepare Fab_{beva} and Fc_{beva}.

Protein purification was used to isolate of the Fab_{beva} from the papain digested bevacizumab mixture, (method 2.2.4.6). Staphylococcal protein A is a single polypeptide chain of ~45 kDa (Goding, 1996; Verwey, 1940). The protein A molecule has four high affinity ($K_a=10^8$/ M) binding sites within the Fc region capable of binding several species (Hjelm et al., 1975), which makes it ideal for the purification of Fab from Fc within digestion mixtures. Protein A was used successfully to isolate the Fab_{beva} from the undigested bevacizumab and Fc_{beva} (Figure 4-4) with a yield of 39% based on total starting IgG protein. Digestion of bevacizumab was conducted twice with the yields achieved being 39% and 33%. This could be due to incomplete digestion as previously discussed as well as some material loss during buffer exchange and papain removal steps.

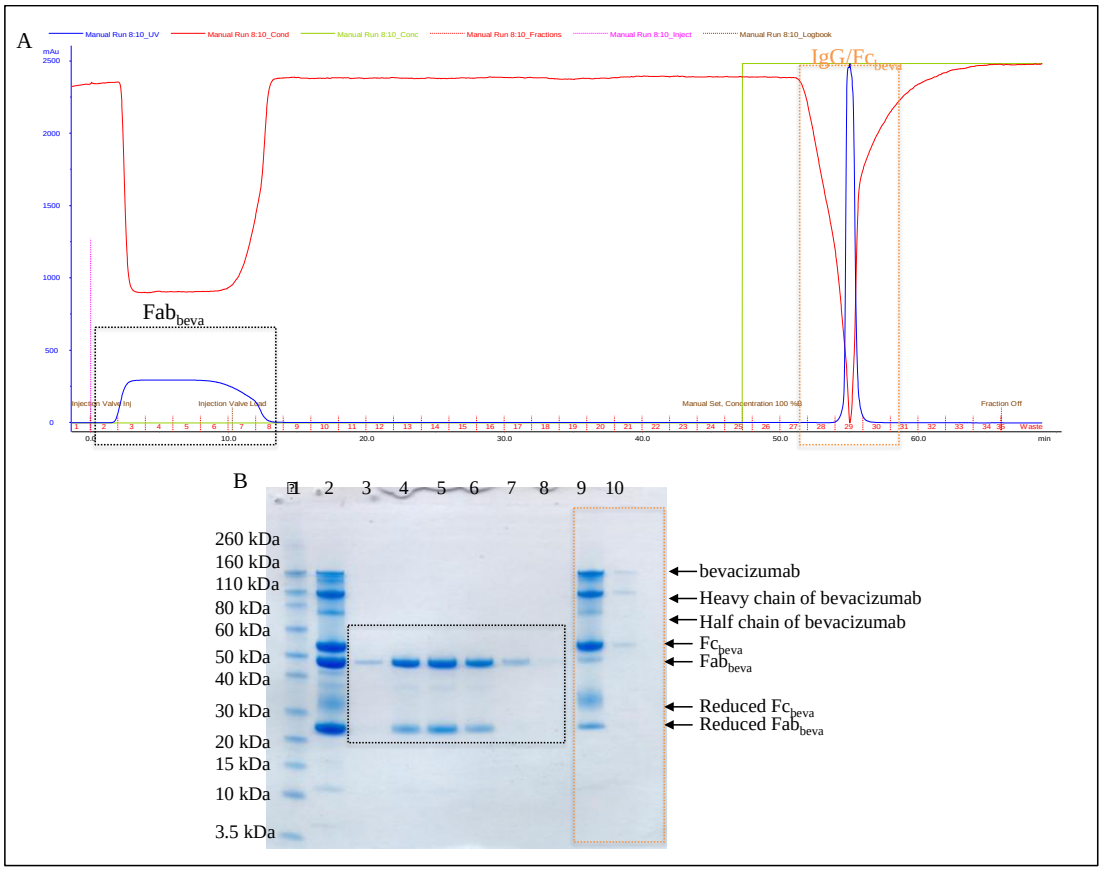

Figure 4-4. Representative A) Chromatogram and B) SDS-PAGE analysis of Protein A purification of papain digested bevacizumab mixture (n=2). Lane 1: Novex pre-stained markers, Lane 2: papain digested bevacizumab mixture, Lanes 3-8: Fab_{beva}, Lanes 9-10: bevacizumab/Fc_{beva}. Protein A purification successfully isolates Fab_{beva} from the digestion mixture.

4.2.1.2 Characterisation of Fab_{beva}

Prior to conjugation, the Fab_{beva} prepared from bevacizumab digestion was characterised in terms of its identity (Western blot), purity (SDS-PAGE) and size (MALDI-TOF). SDS-PAGE (Figure 4-5) analysis showed one band at ~50 kDa, which is the Fab_{beva}. No other bands were observed. Since InstantBlue™ stain has a detection level of 5 ng, we deduce that the Fab_{beva} was essentially pure and certainly pure enough for conjugation (Expedeon product information).

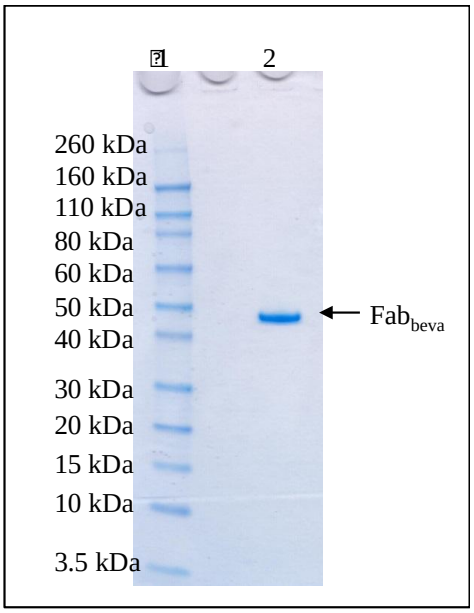

Figure 4-5. Representative SDS-PAGE analysis (InstantBlue™) of Fab$_{beva}$ prepared from bevacizumab digestion (n=2). Lane 1: Novex pre-stained markers, Lane 2: Fab$_{beva}$ (1 µg). Fab$_{beva}$ prepared by digestion of bevacizumab shows good purity.

To confirm the identity of Fab$_{beva}$, an anti-human IgG Western blot was conducted (method 2.2.10.1). A goat anti-human κ-chain HRP-conjugated Fab´$_2$ was used to detect the κ-light chains on bevacizumab and Fab$_{beva}$. As the anti-human IgG detection antibody is specific to the κ-light chain, it would not be able to detect the Fc$_{beva}$ that is made up of heavy chains. The anti-human IgG detection antibody was HRP-conjugated hence enhanced chemiluminescence (ECL) was applied directly. The HRP enzyme catalyses the conversion of luminol to 3-aminophthalate via intermediates in the presence of chemicals to enhance the emitted light. The emitted light was detected by ImageQuant™ where both bevacizumab and Fab$_{beva}$ were successfully visualised confirming the identities of the bevacizumab and Fab$_{beva}$ (Figure 4-6).

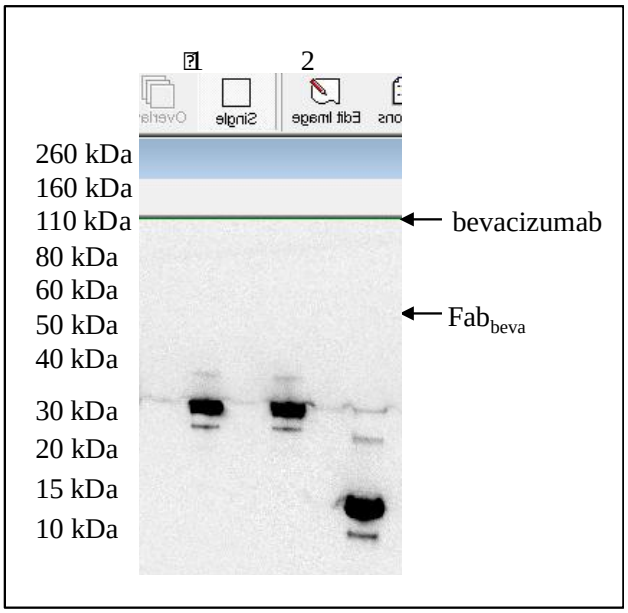

Figure 4-6. Anti-human Western blot of bevacizumab and Fab$_{beva}$ visualised by ECL. Lane 1 and 2: bevacizumab, Lane 3: Fab$_{beva}$. The detection of bevacizumab and Fab$_{beva}$ was successful using anti-human k-chain HRP-conjugated F(ab')$_2$.

For accurate calculations of molar equivalents for conjugation, MALDI-TOF (method 2.2.10.3) was used to quantify the size of Fab$_{beva}$ once (n=1). The MW achieved for Fab$_{beva}$ was 48204.1 Da (Figure 4-7), which is in agreement with the theoretical MW for digested Fabs (Andrew and Titus, 2001). The spectra (Figure 4-7) shows three other peaks at 23419.8, 23601.2 and 24141.6 Da, which are doubly (+2) charged species of Fab$_{beva}$. Therefore, the MW based on singly (+1) charged Fab$_{beva}$ was 48.2 kDa, the MW is expressed to one significant figure due reported sensitivity of MS (Fenselau, 1997).

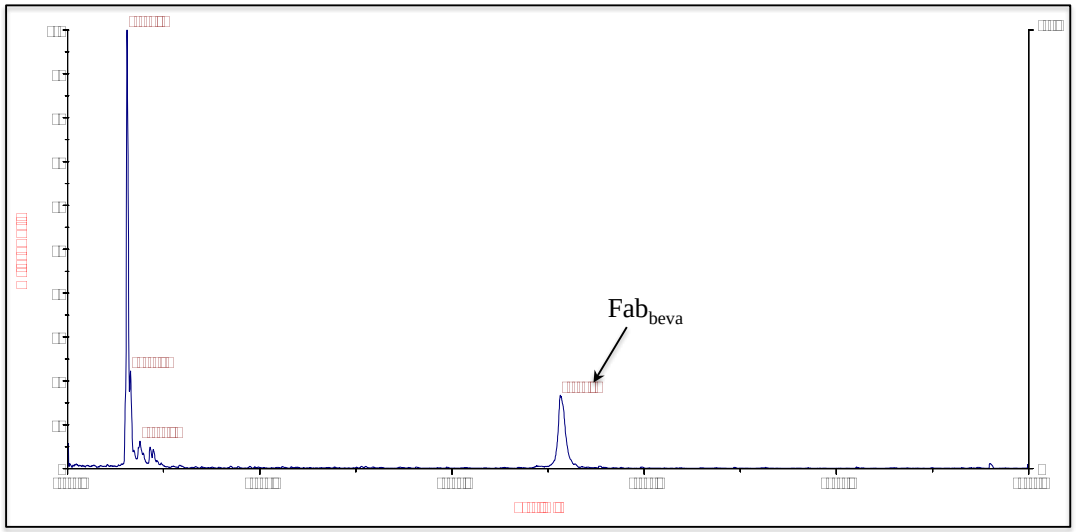

Figure 4-7. MALDI-TOF spectra achieved for Fab$_{beva}$. MALDI-TOF shows the MW of Fab$_{beva}$ to be 48.2 kDa (n=1).

4.2.2 Preparation of IFN-PEG_{20}-Fab_{beva} heterodimer

The IFN-PEG_{20}-Fab_{beva} synthesis is summarised in Figure 4-8. Firstly, the interchain disulfide of Fab_{beva} is reduced and then the TCEP is removed. The reduced Fab_{beva} is then allowed to react with PEG_{20} di(*bis*)sulfone **4** to prepare Fab_{beva}-PEG_{20}-X (X being the unconjugated linker end). After the incubation of PEG_{20} di(*bis*)sulfone **4** with Fab_{beva} this reaction mixture is purified by CIEC purification to remove unreacted PEG_{20}. The second conjugation reaction is then conducted by allowing reduced IFN to react with Fab_{beva}-PEG_{20}-X to prepare IFN-PEG_{20}-Fab_{beva}. The reaction mixture is then purified by CIEC to isolate the IFN-PEG_{20}-Fab_{beva} conjugate.

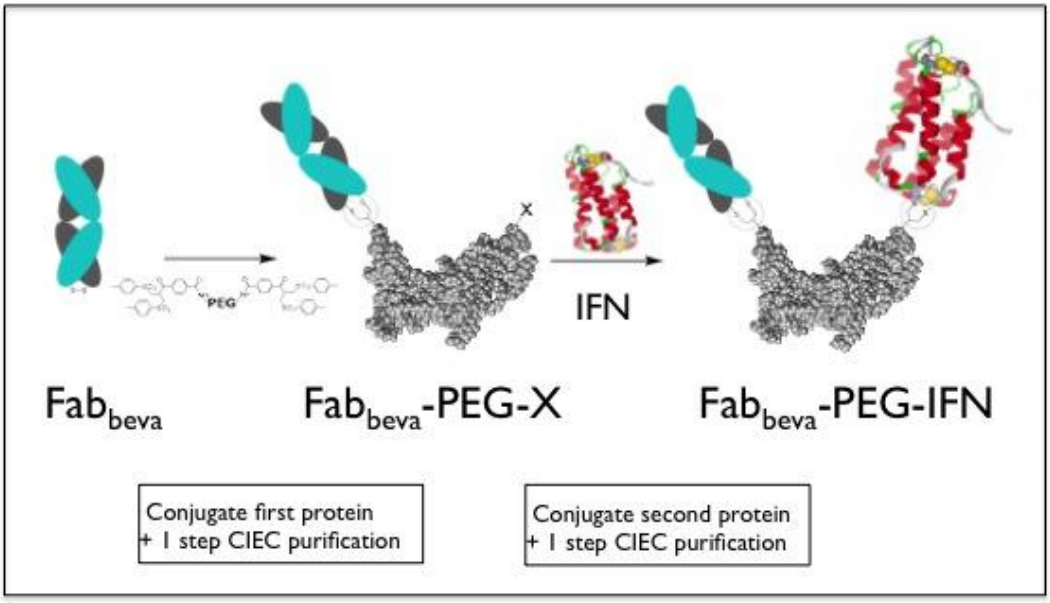

Figure 4-8. Summary of IFN-PEG_{20}-Fab_{beva} preparation**.** First, Fab_{beva} is reduced using mild reductants, then the Fab_{beva} is reacted with PEG_{20} di(*bis*)sulfone **4**. The purified Fab_{beva}-PEG_{20}-X conjugate is then reacted with reduced IFN to prepare the IFN-PEG_{20}-Fab_{beva} heterodimer.

4.2.2.1 Fab_{beva} reduction using tris(2-carboxyethyl)phosphine (TCEP)

For conjugation, mild reduction of the accessible native disulfide bond within Fab_{beva} is necessary to liberate the cysteine thiols for the conjugation of PEG di(*bis*)sulfone **4** (Balan et al., 2007). Optimisation of reduction of Fab_{beva} with TCEP was conducted (method 2.2.9.1). TCEP was introduced in 1992 as an alternative to DTT. TCEP was chosen for the mild reduction of Fab_{beva} because it is more stable over a wider pH range (1.5-8.5) than DTT (Getz et al., 1999; Hansen and Winther, 2009). TCEP can be used quite accurately in stoichiometric amount to avoid eluting the reduction mixture over a PD-10 column. However care must be taken because TCEP can

undergo reaction with the *bis*-alkylating PEG reagents, reducing the yield of the desired PEGylated conjugate.

As shown in Figure 4-9, increasing molar equivalents of TCEP resulted in more of the Fab_{beva} to have been reduced. The reduced Fab_{beva} can be seen on the gel at ~25 kDa due to the dissociation of the two heavy and light chain polypeptides in the presence of SDS. As unreacted TCEP can impede conjugation by reacting with the PEG *bis*-sulfone **1**, a slightly longer reduction period with a lower TCEP stoichiometry would ensure all the TCEP has undergone reaction. Therefore, reduction of Fab_{beva} was conducted with 1.4 eq TCEP for 2 h. This ensured complete reduction of Fab_{beva}, with only a trace amount of unreduced Fab_{beva} present after 1.5 h (Lane 5, Figure 4-9).

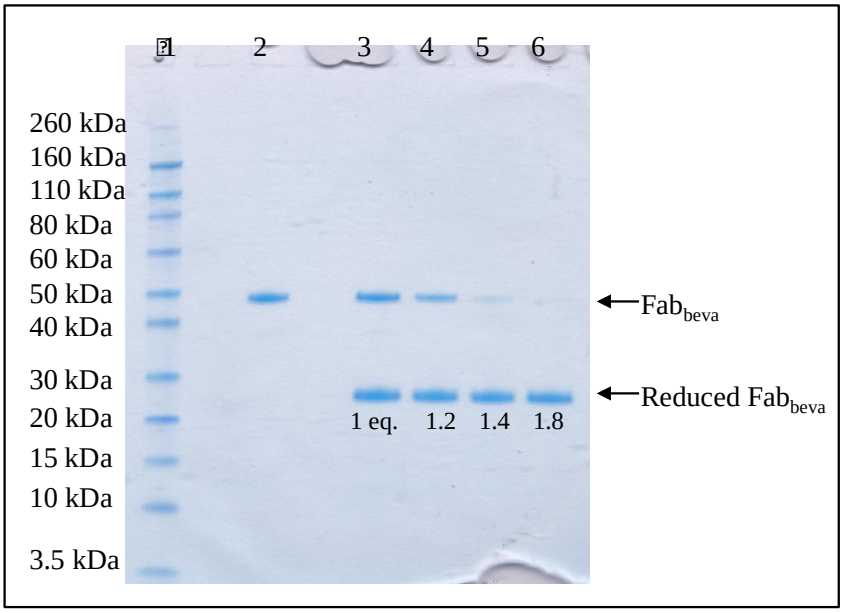

Figure 4-9. SDS-PAGE analysis (InstantBlue™) of the optimisation of TCEP molar equivalents (eq.) for the complete reduction of Fab_{beva} after 1.5 h. Lane 1: Novex pre-stained markers, Lane 2: Fab_{beva}, Lane 3: Fab_{beva} + 1 eq TCEP, Lane 4: Fab_{beva} + 1.2 eq TCEP, Lane 5: Fab_{beva} + 1.4 eq TCEP, Lane 6: Fab_{beva} + 1.8 eq TCEP. Optimum reduction conditions for Fab_{beva} are 1.4 eq. TCEP for 2 h.

4.2.2.2 Preparation of Fab_{beva}-PEG_{20}-X

First the Fab_{beva} (1 eq.) was reduced with TCEP (as optimised in §4.2.2.1) and then reacted with PEG_{20} di(*bis*)sulfone **4** (2 eq.) for 2 h at 25 °C. These conditions were optimised to promote the formation of Fab_{beva}-PEG_{20}-X, as by using excess PEG than Fab_{beva} the reaction is more driven to prepare Fab_{beva}-PEG_{20}-X rather than Fab_{beva}-PEG_{20}-Fab_{beva}. No TCEP was removed prior to conjugation.

In a 16 h hydrolysis study of the PEG_{20} di(mono)sulfone **5**, ^{1}H-NMR results indicated that approximately a third of the PEG_{20} di(mono)sulfone **5** had changed (§ 3.2.1), presumably having undergone addition of water to the double bond in the linker moiety. In an effort to maximise yield and conversion of Fab_{beva}-PEG_{20}-IFN, short reaction times were conducted. Further conjugation and purification was conducted quickly (less than 12 h) to reduce the risk of hydrolysis to the PEG_{20} di(*bis*)sulfone **4**.

On SDS-PAGE analysis, for a given molecular weight of PEG, it will run at double the molecular weight of the marker protein due to the hydrophilic and flexible nature of PEG. This can be seen in Lane 4 (Figure 4-10) where PEG_{20} di(*bis*)sulfone **4** is stained orange from barium iodide and has migrated to ~40 kDa. Fab_{beva}-PEG_{20}-X can be seen on the gel in Lane 3 (Figure 4-10) at ~90 kDa (50 kDa=Fab_{beva} + 40 kDa=PEG_{20}). Fab_{beva}-PEG_{20}-X is stained a green colour from a mixture of protein being stained blue from the InstantBlue™ stain and the orange colour from the PEG stained with barium iodide. A faint band of oxidised Fab_{beva} (50 kDa) can be seen. The oxidation of Fab_{beva} could be prevented by argon purging buffers and the use EDTA. PEG reagent and protein stoichiometry is important and although only a ratio of 2:1 was used, some high MW impurities of Fab_{beva}-PEG_{20}-Fab_{beva} or $(Fab_{beva})_n$-$(PEG)_n$ appeared to be present. Future optimisation could be conducted to optimise PEG:protein stoichiometry and time of conjugation, as fewer protein eq. and a shorter time of conjugation may improve the conversion to Fab_{beva}-PEG_{20}-X.

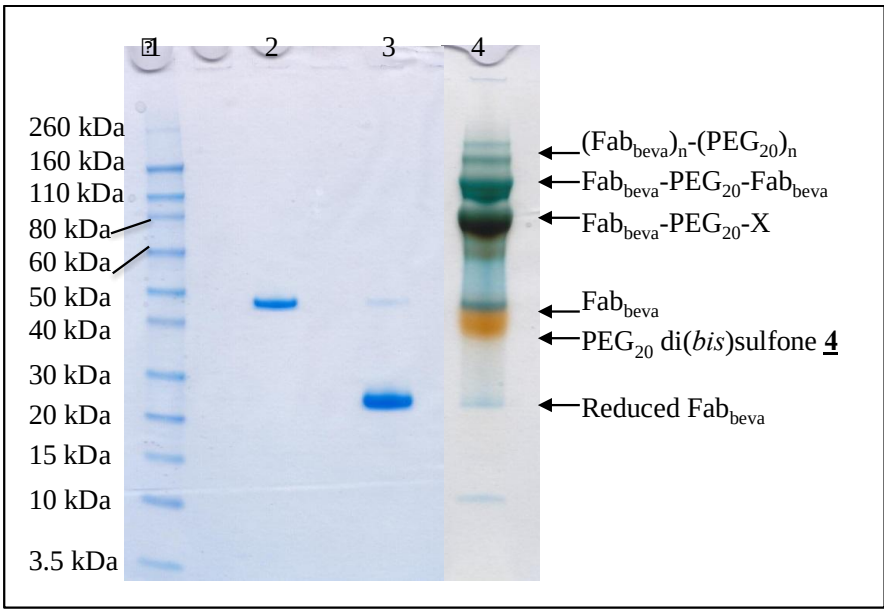

Figure 4-10. Representative SDS-PAGE analysis of reduced Fab_{beva} (InstantBlue™) and 20 kDa PEG di(*bis*)sulfone **4**-Fab_{beva} reaction mixture (IntantBlue™ + PEG stain, n=2). Lane 1:

Novex pre-stained markers, Lane 2: Fab_{beva}, Lane 3: TCEP reduced Fab_{beva}, Lane 4: PEG_{20} di(*bis*)sulfone **4**-Fab_{beva} reaction mixture. Successful conjugation of Fab_{beva} with PEG_{20} di(*bis*)sulfone **4** to prepare Fab_{beva}-PEG_{20}-X.

4.2.2.3 CIEC purification of the Fab_{beva}-PEG_{20}-X reaction mixture

CIEC purification (§ 2.2.9.7) was used to purify Fab_{beva}-PEG_{20}-X from the unconjugated PEG_{20} di(*bis*)sulfone **4**. This was a necessary step to prepare the heterodimer, as the presence of excess PEG_{20} di(*bis*)sulfone **4** would compete with Fab_{beva}-PEG_{20}-X for conjugating the reduced IFN. Therefore CIEC was used to purify the PEG_{20} di(*bis*)sulfone **4**. PEG is a neutral water soluble organic polymer, so will not bind to the column (Molineux, 2002), whilst the Fab_{beva}-PEG_{20}-X conjugates will bind to the column. The chromatogram (Figure 4-11 A) shows a single peak which is a mixture of Fab_{beva}-PEG_{20}-X (~90 kDa), Fab_{beva}-PEG-Fab_{beva} (160 kDa) and $(Fab_{beva})_n$-$(PEG_{20})_n$ (>160 kDa) (Figure 4-11 B).

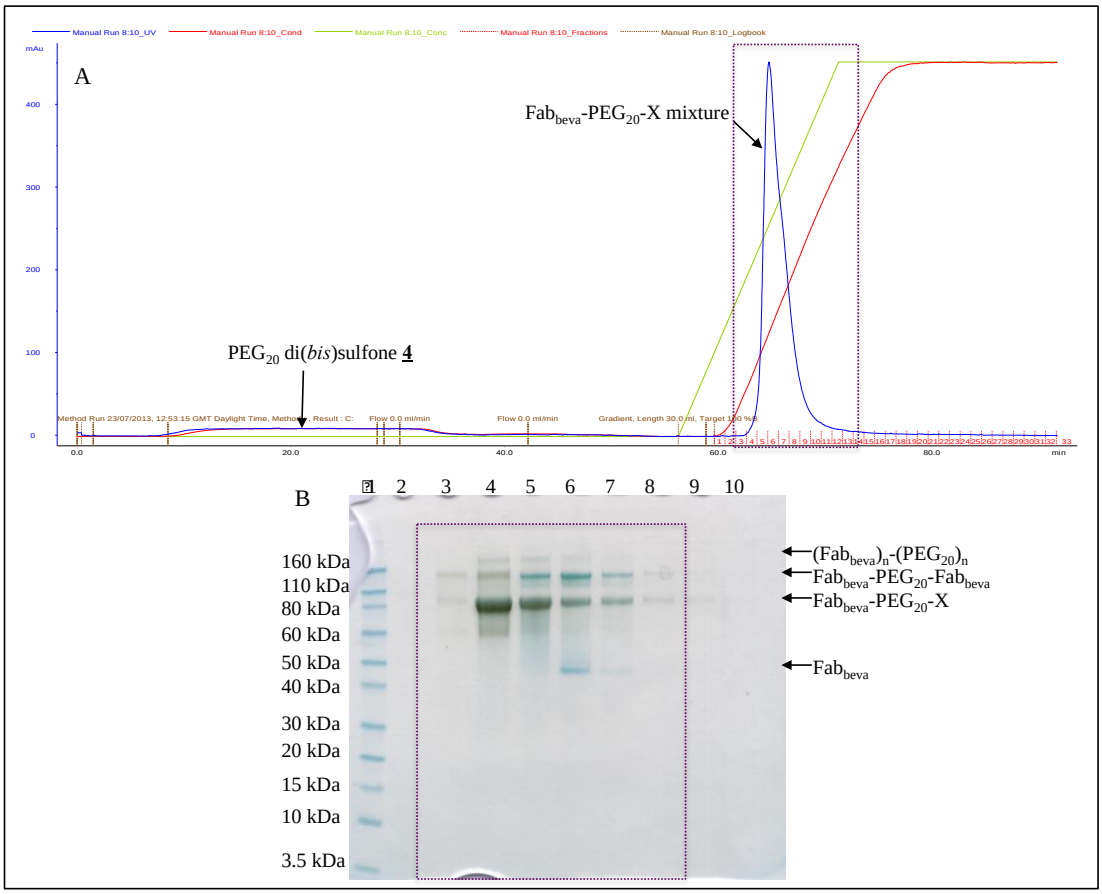

Figure 4-11. Representative A) Chromatogram and B) SDS-PAGE analysis of Fab_{beva}-PEG_{20}-X CIEC purification (n=2). Lane 1: Novex pre-stained markers, Lane 2-9: fractions 3-13. Successful isolation of Fab_{beva}-PEG_{20}-X by CIEC purification from unconjugated PEG_{20} di(*bis*)sulfone **4**.

There is an absence of an orange band at 40 kDa on the SDS-PAGE (Figure 4-11 B) of the PEG_{20} di(*bis*)sulfone **4** showing that it has been successfully removed by CIEC

purification. The HiTrap Macrocap SP column used is designed for the CIEC purification of large PEGylated proteins as it is a strong cation exchanger and is made of a highly porous base matrix, which allow for the binding of large proteins. Bevacizumab has a pI of 7.6, so pH 4.0 was used where Fab_{beva} would have a net positive charge to bind tightly to the CIEC column.

4.2.2.4 Conjugation of IFN with Fab_{beva}-PEG_{20}-X

Following the successful isolation of the Fab_{beva}-PEG_{20}-X conjugate from unreacted 20 kDa PEG di(*bis*)sulfone **4** by CIEC; the fractions containing Fab_{beva}-PEG-X were pooled and quantified by UV ready for conjugation to IFN (§ 2.2.9.7). The two disulfides in IFN were first reduced using DTT (25 mM) and then IFN (2 eq.) was allowed to undergo reaction with Fab_{beva}-PEG_{20}-X (1 eq.) to form IFN-PEG_{20}-Fab_{beva} (§ 2.2.9.8). Conjugation of the reduced IFN to the remaining linker group (X) within Fab_{beva}-PEG_{20}-X may be difficult due to the hydrophilic nature of the PEG. The end groups on PEG comprise the Fab and the remaining linker. While the PEG is hydrophilic, it is not miscible with proteins. So it is possible the end groups of the intermediate conjugate Fab_{beva}-PEG_{20}-X can self associate and become less accessible to solvent. This could result in a slower second conjugation step, with hydrolysis becoming more competitive. The net result being the second conjugation step becomes much less efficient than the first conjugation step. Therefore, a high concentration of IFN was used to promote the reaction with the remaining linker.

As IFN as two disulfide bonds (Figure 1-18), once reduced by DTT, both reduced disulfides are accessible for conjugation as shown in §3.3.4. However, within the Fab_{beva}-PEG_{20}-X conjugate only one linker group (X) is available for conjugating to IFN. Once formed the IFN within the IFN-PEG_{20}-Fab_{beva} conjugate has one reduced unconjugated disulfide. For IFN to retain its activity this disulfide bond must be oxidised and this was done using glutathione (§2.2.9.8). As discussed in §3.3.2, reduced and oxidised glutathione has been shown to re-oxidise and maintain the activity of proteins (Fahey et al., 2000). No reduced unconjugated IFN can be seen in Lane 3 at between 10-15 kDa (Figure 4-12) after glutathione treatment; oxidised unconjugated IFN can be seen between 15-20 kDa. IFN-PEG_{20}-Fab_{beva} conjugate can be seen in Lane 3 (Figure 4-12) at 110 kDa. This was inferred because i) the MW corresponds to what is expected (50 kDa=Fab_{beva} + PEG_{20}=40 kDa + oxidised IFN=~20 kDa) and ii) this band is not observed in the reaction

mixture prior to IFN conjugation i.e. Fab_{beva}-PEG_{20}-X reaction mixture which can be seen in Lane 2 (Figure 4-12). Interestingly, there is still a band of Fab_{beva}-PEG_{20}-X, meaning the reaction has not gone to completion even though excess reduced IFN was within the reaction mixture. This could be due to i) some of the di(*bis*)sulfone linker may have hydrolysed due to the long synthesis route or ii) a longer incubation time is required with the IFN, as a 4 h incubation time may not have been sufficient time for all the IFN to react with the Fab_{beva}-PEG_{20}-X. The purity of the starting PEG_{20} di(*bis*)sulfone **4** is also important to ensure there are no dead chain ends in Fab_{beva}-PEG_{20}-X.

Following glutathione re-oxidisation of the IFN in the IFN-PEG_{20}-Fab_{beva} conjugate, the reaction mixture was then subjected to STAB treatment (§ 2.2.9.8). This was conducted to 'lock' the linker into place by reducing the linker ends.

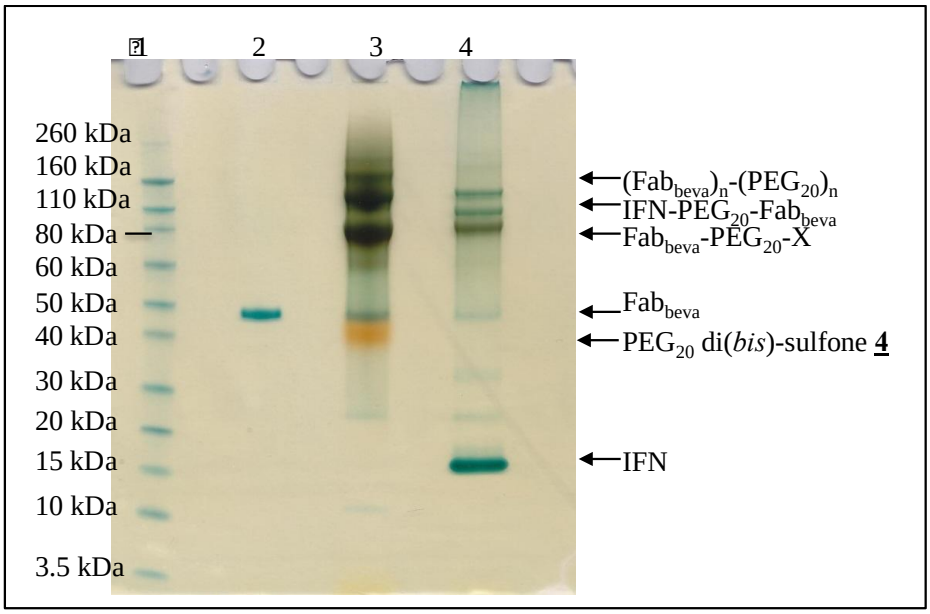

Figure 4-12. Example SDS-PAGE (InstantBlue™ and PEG stain) of the IFN-PEG_{20}-Fab_{beva} reaction mixture. Lane 1: Novex pre-stain markers, Lane 2: Fab_{beva}-PEG_{20}-X reaction mixture prior to CIEC purification, Lane 3: IFN-PEG_{20}-Fab_{beva} reaction mixture prior to CIEC purification. Successful conjugation of reduced IFN to Fab_{beva}-PEG_{20}-X to prepare IFN-PEG_{20}-Fab_{beva}, this was conducted twice to ensure conjugation was reproducible.

4.2.2.5 CIEC purification of the IFN-PEG_{20}-Fab_{beva} reaction mixture

A step CIEC gradient was used to purify the IFN-PEG_{20}-Fab_{beva} conjugate from the unreacted IFN and Fab_{beva}-PEG_{20}-X, and higher MW impurities of $(Fab_{beva})_n$-$(PEG_{20})_n$ (Figure 4-13 A). This step gradient of 30, 60, 80 and 100% buffer B (§ 2.2.9.9) was optimised to isolate the IFN-PEG_{20}-Fab_{beva} conjugate by CIEC purification in an effort to maximise yield. SDS-PAGE analysis (Figure 4-13 B)

shows that the step gradient CIEC was successful to isolate the IFN-PEG_{20}-Fab_{beva} (Lane 6), conjugate from the unreacted IFN (Lanes 7-10) and Fab_{beva}-PEG_{20}-X (Lane 3), and higher MW impurities of $(Fab_{beva})_n$-$(PEG_{20})_n$ (Lane 3). It can be seen that the mAu (absorbance at 280 nm) of the Fab_{beva}-PEG_{20}-X peak (Figure 4-13 A) is greater than that of the IFN-PEG_{20}-Fab_{beva} peak, this is due to Fab_{beva}-PEG_{20}-X, and higher MW impurities of $(Fab_{beva})_n$-$(PEG_{20})_n$ co-eluting as can be seen on the SDS-PAGE analysis.

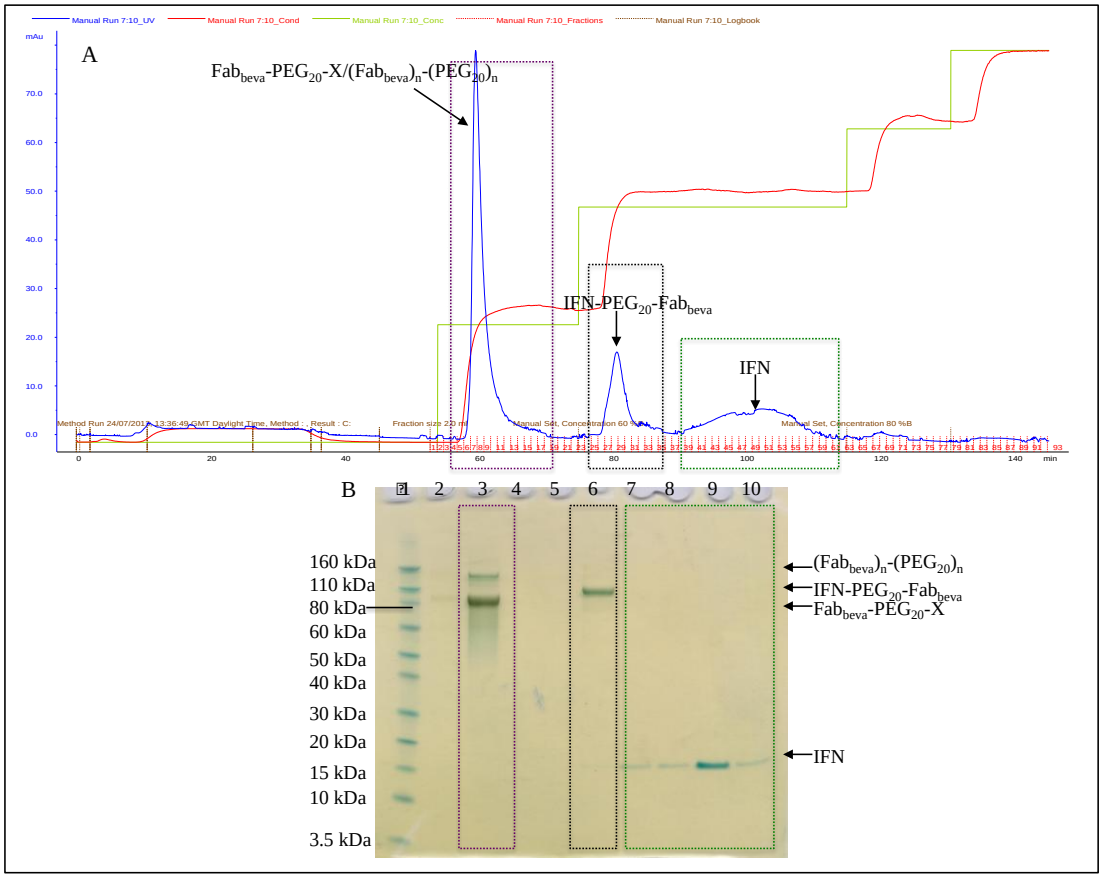

Figure 4-13. Example A) Chromatogram and B) SDS-PAGE of IFN-PEG_{20}-Fab_{beva} reaction mixture CIEC purification. Lane 1: Novex pre-stained markers, Lane 3: Fab_{beva}-PEG_{20}-X/$Fab_{beva})_n$-$(PEG_{20})_n$, Lane 6: IFN-PEG_{20}-Fab_{beva}, Lanes 7-10: IFN. Successful step CIEC purification to purify out the IFN-PEG_{20}-Fab_{beva} conjugate. Purification was found to be reproducible with each repeat (n=2).

The fractions for IFN-PEG_{20}-Fab_{beva} were pooled and the concentration of Fab_{beva} and IFN quantified by UV (Fab_{beva}: ε=1.4 0.489 mg/mL, yield=12%; IFN: ε=0.914, 0.749 mg/mL, yield=21%). The yields of the repeat were found be very reproducible, with the repeat yields being Fab_{beva}=19.4% and IFN=23.4%. The yields achieved for IFN-PEG_{20}-Fab_{beva} were found to be comparable to that achieved for the PEG *bis*-sulfone **1**. This shows that synthesis route 2 (Figure 3-9) for PEG_{20} di(*bis*)sulfone **4** has a greater reactivity compared to the previously used PEG_{20}

di(*bis*)sulfone **4** synthesised by route 1 (Figure 3-2). This could be due to i) the improved purity of the PEG_{20} di(*bis*)sulfone **4** which was quantified by RP-HPLC (§ 2.2.5.4) and SDS-PAGE (§ 2.2.5.5); ii) the better understanding of hydrolysis and its effect on the PEG di(*bis*)sulfones, whereby the synthetic approach was conducted in under 12 hours, reducing the risk of hydrolysis to the di(*bis*)sulfone linkers.

SDS-PAGE analysis was conducted with the final IFN-PEG_{20}-Fab_{beva} conjugate to assess its purity. It can be seen in Lane 5 (Figure 4-14) that the IFN-PEG_{20}-Fab_{beva} conjugate at 110 kDa was prepared and purified in good purity as no other bands can be seen by InstantBlue™ or PEG stain.

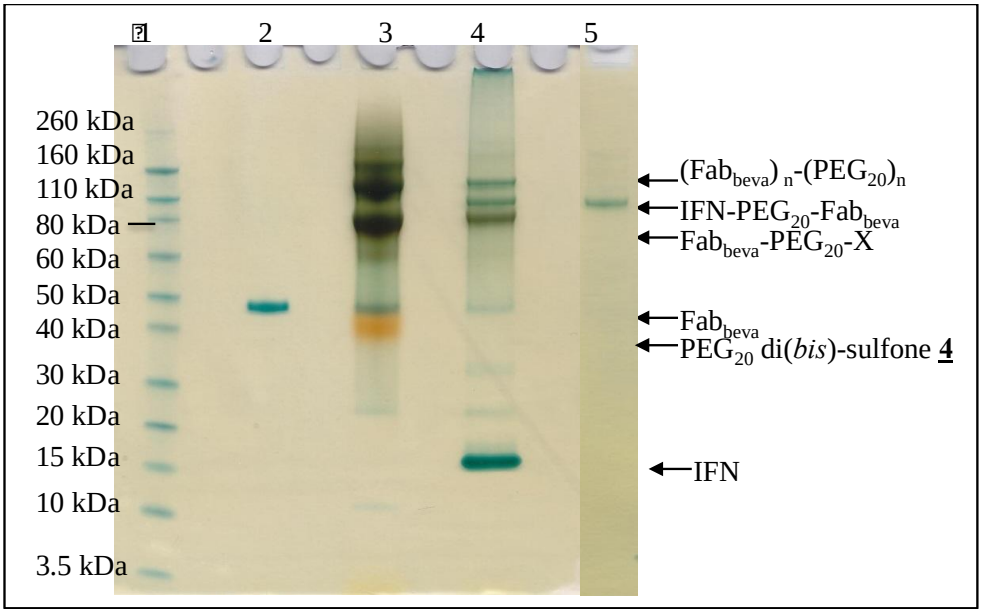

Figure 4-14. SDS-PAGE analysis of final IFN-PEG_{20}-Fab_{beva} conjugate prepared. Lane 1: Novex pre-stained markers, Lane 2: Fab_{beva}, Lane 3: Fab_{beva}-PEG_{20}-X reaction mixture, Lane 4: IFN-PEG_{20}-Fab_{beva} reaction mixture, Lane 5: final IFN-PEG_{20}-Fab_{beva} conjugate. Final IFN-PEG_{20}-Fab_{beva} conjugate successfully prepared and purified.

4.2.3 Preparation of PEG_{20}-Fab_{beva}

4.2.3.1 Optimisation of PEG_{20} *bis*-sulfone **1** conjugation to Fab_{beva}

It was necessary to prepare PEG_{20}-Fab_{beva} as a control to compare the binding kinetics to that of IFN-PEG_{20}-Fab_{beva}. To ensure the highest yield of PEG_{20} *bis*-sulfone **1**-Fab_{beva} was achieved, the stoichiometry for PEG_{20} *bis*-sulfone **1** was optimised (method 2.2.9.2). It has been shown that 1.4 eq. TCEP (§ 4.2.2) can successfully liberate the Fab cysteine thiols for the conjugation of PEG_{20} *bis*-sulfone to the Fab_{beva}. For the conjugation, 50 mM sodium phosphate buffer pH 7.8 was used as pH 7.8 allows the PEG *bis*-sulfone **1** to undergo elimination *in situ* to prepare PEG

mono-sulfone **2** (Figure 2-1) (Brocchini et al., 2006). It can be seen (Figure 4-15) that with increasing PEG eq. there is a directly proportional increase in the conversion of PEG_{20}-Fab_{beva} being prepared. Within SDS-PAGE analysis PEG_{20} *bis*-sulfone can be observed on the SDS-PAGE gel at ~40 kDa (Figure 4-15 A). PEG_{20}-Fab_{beva} can be seen at ~90 kDa by SDS-PAGE analysis (50 kDa=Fab_{beva} + 40 kDa =PEG_{20}, Figure 4-15). The highest percentage conversion (66%) to PEG_{20}-Fab_{beva} was observed at 2 eq (Figure 4-15 B). Therefore, a 2:1 molar ratio of PEG_{20} *bis*-sulfone **1**:Fab_{beva} was used to scale up the preparation of PEG_{20}-Fab_{beva}.

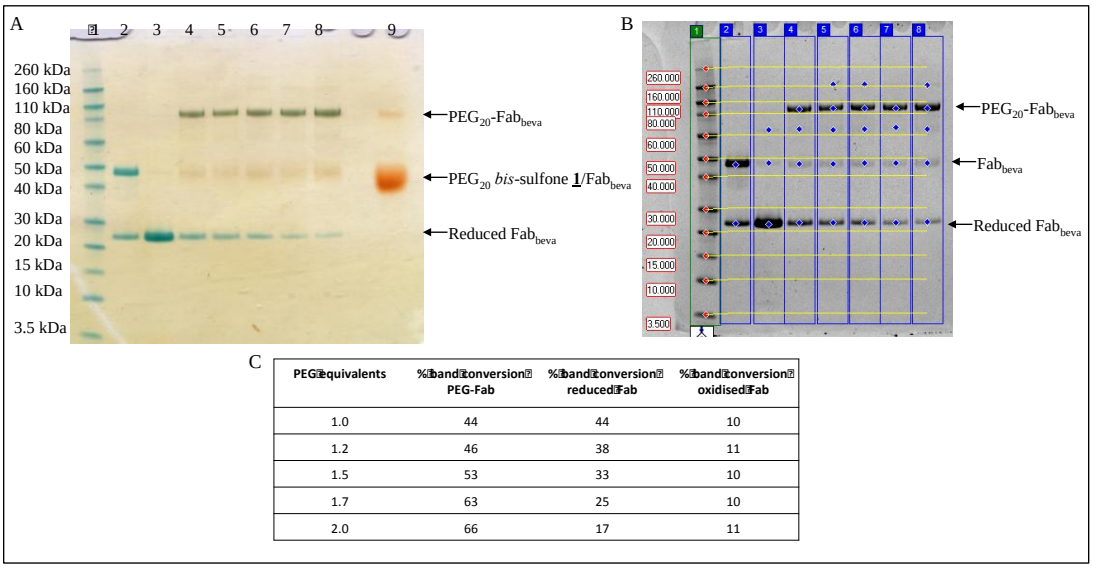

PEG equivalents	% band conversion PEG-Fab	% band conversion reduced Fab	% band conversion oxidised Fab
1.0	44	44	10
1.2	46	38	11
1.5	53	33	10
1.7	63	25	10
2.0	66	17	11

Figure 4-15. A) SDS-PAGE and B) ImageQuant™ analysis and C) Densimetric information table of Fab_{beva} conjugation with varying PEG_{20} *bis*-sulfone **1** equivalents (1, 1,2, 1,5, 1,7, and 2). Lane 1: Novex pre-stained markers, Lane 2: Fab_{beva}, Lane 3: TCEP reduced Fab_{beva}, Lane 4: Fab_{beva} + 1 eq PEG, Lane 5: Fab_{beva} + 1.2 eq. PEG, Lane 6: Fab_{beva} + 1.5 eq., Lane 7: Fab_{beva} + 1.7 eq., Lane 8: Fab_{beva} + 2.0 eq. PEG, Lane 9: PEG_{20} *bis*-sulfone **1**. PEG_{20} *bis*-sulfone **1** to PEG ratio found to be 2:1 eq. for 16 h at 25 °C.

4.2.3.2 Optimisation of PEG_{20} *bis*-sulfone **1**-Fab_{beva} purification

To isolate the PEG_{20}-Fab_{beva} from the unreacted PEG reagent species and Fab_{beva}, CIEC was used. Elution of the different molecules from the CIEC column occurs with different percentages of buffer. For use in the CIEC purification optimisation, a 1 mg reaction of Fab_{beva} with PEG_{20} *bis*-sulfone **1**-Fab_{beva} was conducted (§ 2.2.9.3). The reaction mixture of the PEG_{20} *bis*-sulfone **1**-Fab_{beva} can be seen in Lane 10, Figure 4-16 A where PEG_{20}-Fab_{beva} can be seen at ~90 kDa. To determine the different elution percentages for the PEG_{20}-Fab_{beva} and Fab_{beva} a linear gradient from 0 to 100% of salt was conducted (§ 2.2.9.4).

The percentage at which the PEG_{20}-Fab_{beva} and Fab_{beva} eluted from the column was calculated by determining the delay in millilitres from when the linear

gradient started. The volume of the middle of the two peak columns was subtracted from the delayed linear gradient volume. This gave the accurate volume at which buffer B was eluting the PEG_{20}-Fab_{beva} and Fab_{beva}, taking into account the volume delay. The percentage of buffer B at the calculated volume was then determined from the chromatogram. It was calculated that ~17% and ~30% buffer B were eluting PEG_{20}-Fab_{beva} and Fab_{beva} respectively. A step gradient method was designed using 17% and 30% buffer B to in an effort to elute PEG_{20}-Fab_{beva} and Fab_{beva} in separate peaks and thus prepare pure PEG_{20}-Fab_{beva}.

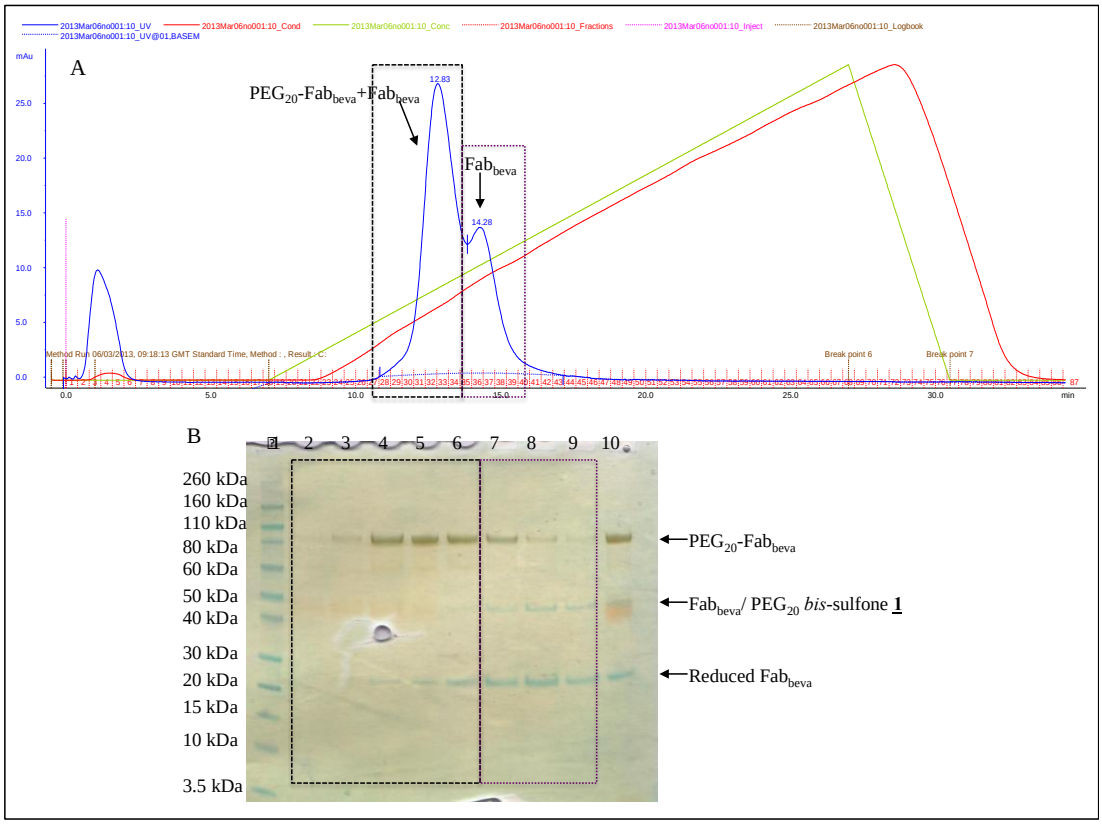

Figure 4-16. Linear CIEC A) chromatogram and B) SDS-PAGE analysis of PEG_{20} *bis*-sulfone **1**-Fab_{beva} reaction mixture. Lane 1: Novex pre-stained markers, Lanes 2-6: PEG_{20}-Fab_{beva} + Fab_{beva}, Lanes 7-9: Fab_{beva} + PEG-Fab_{beva}, Lane 10: PEG_{20} *bis*-sulfone **1**-Fab_{beva} reaction mixture prior to CIEC.

4.2.3.3 Scaled up preparation of PEG_{20}-Fab_{beva}

Using the optimised conditions, PEG_{20}-Fab_{beva} was prepared for kinetic and affinity binding studies. Reduced Fab_{beva} (1 mg) was allowed to react with PEG *bis*-sulfone **1** as stated in §2.2.9.3. The reaction was then purified by a step gradient of 17, 30 and 100% PBS with 1 M sodium chloride (buffer B) (§ 2.2.9.5). It can be observed (Figure 4-17 A) that at 17% buffer B, the salt dissociates the PEG_{20}-Fab_{beva} conjugate from the column where as a higher salt concentration (30%) is required to dissociate

the Fab_{beva} from the column, as the PEG reduces the ability of the Fab_{beva} to bind to the cation exchange column. It can be observed that the step gradient has successfully purified out the PEG_{20}-Fab_{beva} (Lanes 2-5) from the Fab_{beva} (Lanes 6-9, Figure 4-17 B).

The final PEG_{20}-Fab_{beva} conjugate was then assessed regarding concentration (UV at A280 nm) and purity (SDS-PAGE). The final yield for the PEG_{20}-Fab_{beva} conjugate was 44% (0.440 mg/mL, § 2.2.9.5), which can be seen in lane 3 at ~90 kDa (Figure 4-17 C). No other bands were observed in lane 3 (Figure 4-17 C).

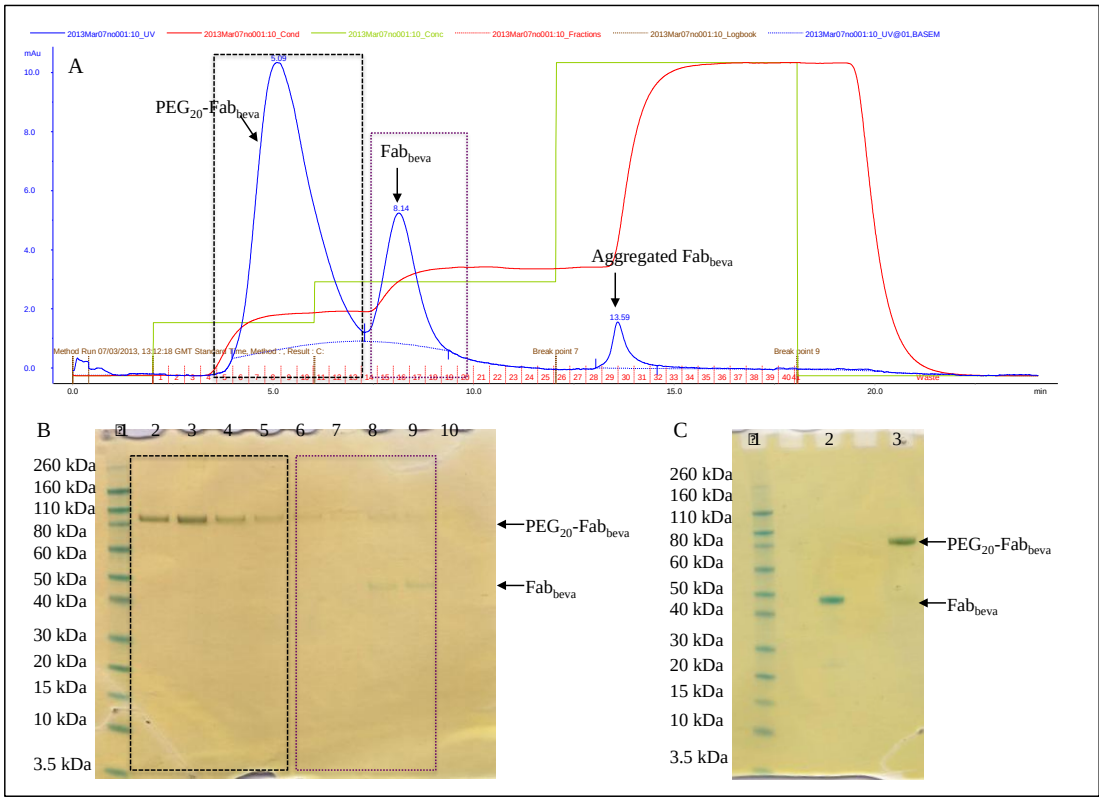

Figure 4-17. Step CIEC gradient A) chromatogram, B) SDS-PAGE analysis (InstantBlue™ + PEG stain) of PEG_{20} *bis*-sulfone **1**-Fab_{beva} purification fractions and C) Final purified PEG_{20}-Fab_{beva}. B) Lanes 1-5: PEG_{20}-Fab_{beva}, Lanes 6-9: Fab_{beva}, Lane 10: aggregated Fab_{beva}, C) Lane 1: Novex pre-stained markers, Lane 2: Fab_{beva}, Lane 3: PEG_{20}-Fab_{beva}. Step CIEC successfully purified PEG_{20}-Fab_{beva} from Fab_{beva}.

4.2.4 Characterisation and purification of anti-albumin IgG

The aim of this section is to prepare an IFN-PEG_{20}-Fab_{alb} heterodimer, using Fab enzymatically generated from polyclonal rabbit anti-rat albumin IgG. The IFN-PEG_{20}-Fab_{alb} heterodimer was prepared as a longer acting therapeutic for Hepatitis C virus. The heterodimer prepared was utilising disulfide conjugation of both Fab_{alb} and His_8IFN. The PEG_{20} di(*bis*)sulfone **4** was used which had been prepared using

synthesis route 2 (Figure 3-9). The synthesis route for preparing the IFN-PEG_{20}-Fab_{alb} is outlined in Figure 4-8.

4.2.4.1 Characterisation of anti-albumin IgG by SDS-PAGE and Western blotting

Polyclonal anti-rat albumin IgG was purchased from GenWay Biotech. To ensure the anti-rat albumin IgG was pure for digestion and specific to rat albumin, the following studies were conducted. First, SDS-PAGE was conducted (§ 2.2.1) to determine if the anti rat albumin IgG was pure for papain digestion as impurities within the IgG may impede digestion or purification. InstantBlue™ and silver staining were both performed on the gel (Figure 4-18). Silver stain is more sensitive than InstantBlue™ (Chevallet et al., 2006).

Two main bands could be identified in the SDS-PAGE analysis (Figure 4-18). One band between 110 kDa and 160 kDa is the polyclonal rabbit anti-rat albumin IgG of 150 kDa in size (Andrew and Titus, 2001). The band second was between 50 kDa and 60 kDa, which could be a stabiliser such as bovine serum albumin (BSA) and gelatin, which is used in purified antibody stock solutions for long term storage. The presence of such stabilisers usually does not interfere with immunodetection methods, however its presence could interfere with antibody digestion. This problem is well understood so 'antibody clean-up' kits are available with Protein A or Protein G spin-columns. Thus, it was necessary to purify the anti-albumin IgG from the stabiliser for enzymatic digestion.

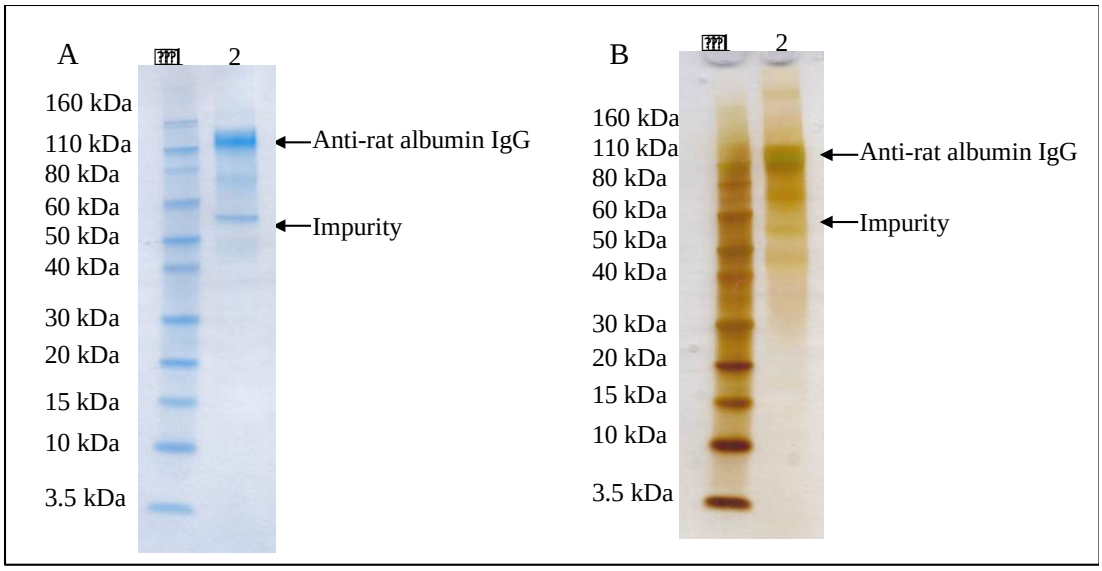

Figure 4-18. SDS-PAGE of anti-rat albumin IgG stained with A) InstantBlue™ and B) silver stain. Lane 1: Novex pre-stained markers, Lane 2: anti-rat albumin IgG. SDS-PAGE analysis reveals anti-rat albumin has been stored with stabiliser protein.

Prior to further studies, it was important to determine if the commercially available anti-rat albumin IgG (from a rabbit host) would bind to the rat serum albumin. To determine this, the anti-rat albumin IgG was used as a primary antibody to detect rat serum albumin that had run on a SDS-PAGE gel. A secondary AP-conjugated antibody against the rabbit anti-rat albumin IgG was used to visualise binding (§ 2.2.10.1).

SDS-PAGE analysis (§ 2.2.1) was performed initially to assess the purity of the rat albumin and for comparison by western blot. Two bands can be seen in the SDS-PAGE analysis (Figure 4-19 A), the main band can be seen at ~60 kDa and the other band at ~120 kDa (Figure 4-19 A). According to the product information from Sigma-Aldrich, the main band is likely to be rat albumin, which is 65 kDa in size. The other high MW bands could be the dimer of rat albumin (130 kDa), as the second band is between 110 kDa and 160 kDa.

The two bands of albumin (~60 kDa) and possible albumin dimer (~120 kDa) identified in the SDS-PAGE analysis (Figure 4-19 A) could also be observed by Western blot (Figure 4-19 B). As the rat albumin was visualised by Western blot, this suggests the anti-rat albumin IgG has bound to the rat albumin. Additionally, it also suggests that the high MW impurity is an albumin dimer for it to be detected by the anti-rat albumin IgG.

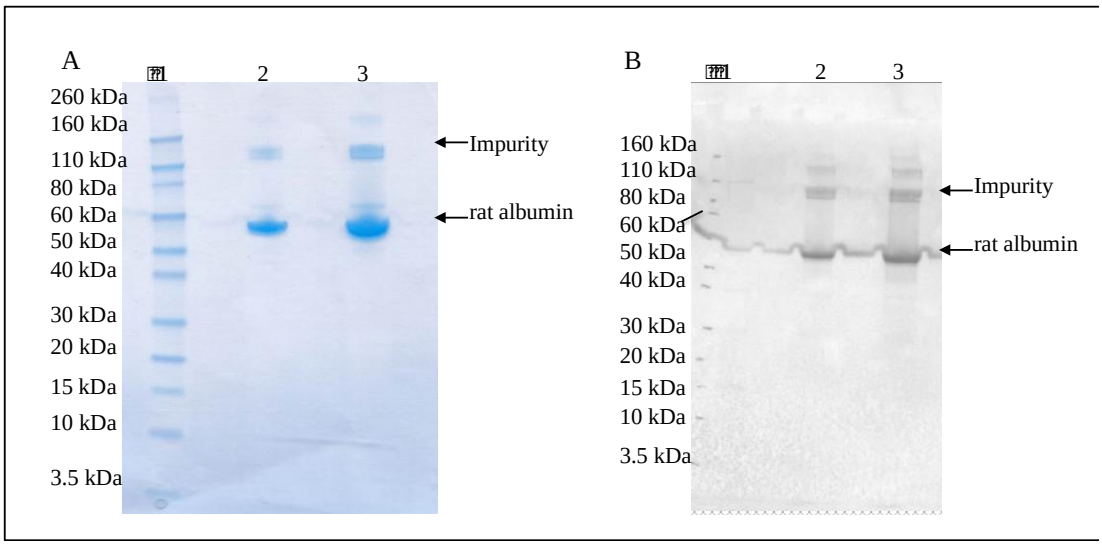

Figure 4-19. A) SDS-PAGE and B) Western blot of rat albumin. Lane 1: Novex pre-stained markers, Lane 2: rat serum albumin (1 μg), Lane 3: rat serum albumin (5 μg). Detection of rat albumin by Western blot confirmed the anti-rat albumin IgG has bound to rat serum albumin.

In the Western blot of rat albumin (Figure 4-19 B) there is a band in all wells at ~50 kDa. This could be rat albumin that when the SDS-PAGE was loaded has

spilled into other wells and due to the sensitivity of the Western blot, has been detected by the primary and secondary antibodies. This shows that when loading the SDS-PAGE care must be taken to ensure all the sample is loaded carefully into the wells. Overspill can be avoided by reducing the volume loaded into the SDS-PAGE wells ensuring the sample stays within one well.

4.2.4.2 Purification of anti-rat albumin IgG for digestion

From the SDS-PAGE analysis of the rabbit anti-rat albumin IgG it was found that a protein stabiliser, most probably HSA, was in the IgG stock solution (§ 4.2.4.1). To remove BSA, we elected to use HiTrap Protein A columns. Protein A has been used to purity monoclonal or polyclonal IgG ascites, serum and tissue culture and bioreactor supernatants. However, variation in the strength of binding between species of animal and species of IgG subclasses has been reported. The polyclonal anti-rat albumin IgG was prepared in rabbits and the strength of binding of rabbit IgG or IgG fragments to Protein A is stronger than Protein G (Antibody purification handbook from GE-healthcare). Therefore, a HiTrap Protein A column was used to isolate the anti-rat albumin IgG from BSA and other potential impurities (§ 2.2.4.1).

Following Protein purification, two peaks were observed (Figure 4-20 A). The first, small and wide peak (< 500 mAu, Figure 4-20 A) is the loading peak and any molecules not bound to the Protein A resin are eluted. The second, large and sharp peak (>2000 mAu, Figure 4-20 A) represents the elution peak where the pH is changed to pH 2.0 which caused the bound molecules to dissociate from the Protein A resin to then elude from the column. SDS-PAGE analysis, Lanes 2-6 (Figure 4-20 B) of the peak fractions revealed that the first peak was a mixture of BSA (between 50 kDa and 60 kDa) and anti-rat albumin IgG (between 110 kDa and 160 kDa). The anti-rat albumin IgG may have eluted during loading as the concentration of the IgG may have exceeded the capacity of the Protein A column.

In the second peak (Lanes 7-8,Figure 4-20 B) the main band was the anti-rat albumin IgG. Importantly, the band associated with BSA was not present. The bands above and below the ~150 kDa IgG band are most likely from the high concentration of IgG, as these were not observed in the SDS-PAGE analysis prior to Protein A purification (Figure 4-18).

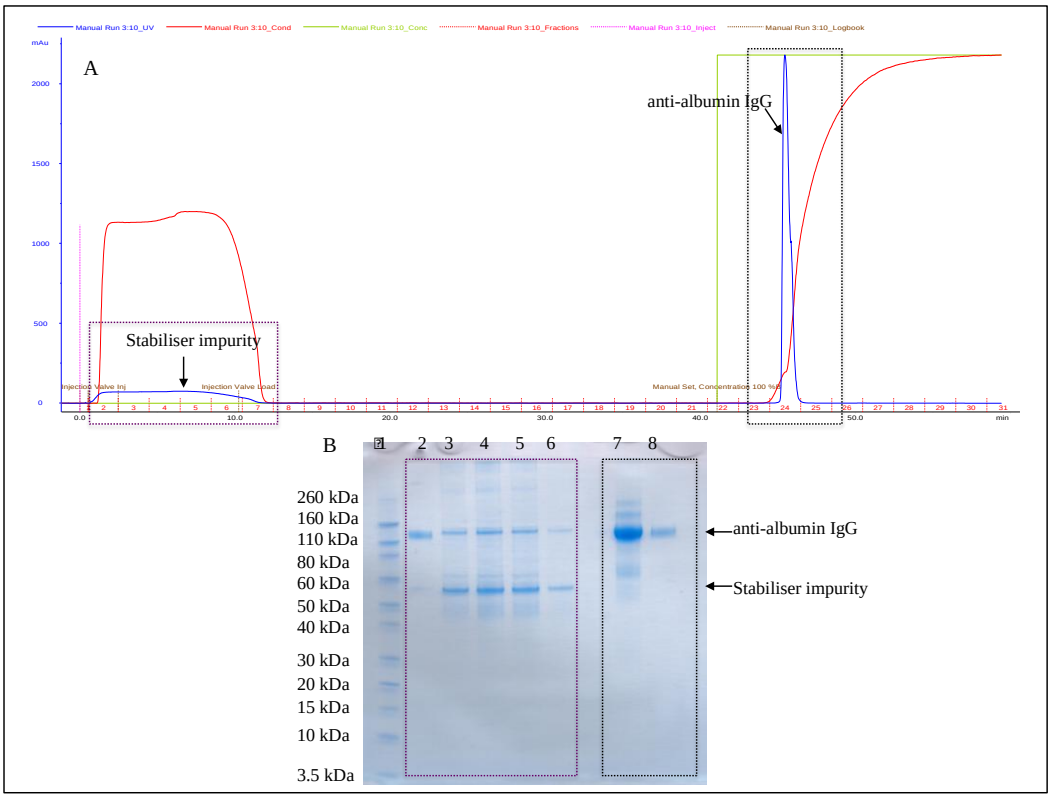

Figure 4-20. Example A) Chromatogram and B) SDS-PAGE analysis of fractions collected from Protein A purification of anti-rat albumin IgG. Lane 1: Novex pre-stained markers, Lanes 2-6: stabilising protein + anti-rat albumin IgG, Lanes 7-8: anti-rat albumin IgG. Successful removal of stabilising protein from anti-rat albumin IgG by Protein purification. Purification of anti-rat albumin IgG from the stabiliser protein was found to be consistent in all four repeats conducted.

The yield of the purified anti-rat albumin IgG was found to be consistent in in all three purifications conducted, with the yields achieved of anti-albumin IgG being 54.6%, 47.5% and 50.7%. These yields demonstrate the reproducibility of the Protein A purification process to isolate the anti-albumin IgG from the stabiliser protein, with the average recovery of IgG_{alb} being 51%.

4.2.5 Digestion and purification of anti-rat albumin IgG to prepare Fab_{alb}

4.2.5.1 Optimisation of enzymatic digestion of anti-rat albumin and purification to prepare Fab_{alb}

The aim was to optimise the digestion conditions of polyclonal anti-rat albumin IgG to obtain Fab_{alb}. It was necessary to optimise the digestion conditions as i) individual IgG classes and species vary in their susceptibility to digestion and ii) the rate of digestion is influenced by papain concentration (Andrew and Titus, 2001; Goding, 1996). The two variables that were examined for optimisation were the papain:IgG

ratio and the length of time to allow for papain digestion. Papain :IgG ratio for the rabbit anti-rat albumin IgG was conducted (§ 2.2.4.2) and the digestion mixture was analysed by SDS-PAGE. The cleavage of IgG by papain was then monitored by SE-HPLC over an 8 h period (§ 2.2.4.2) to determine the optimum digestion time.

The following papain:IgG concentrations were investigated: 1:10, 1:20 and 1:50. Coulter reported a concentration of 1:10 for the digestion of rabbit IgG, whilst typical concentrations reported for mouse, rat, human are 1:20-1:100 (Andrew and Titus, 2001; Coulter and Harris, 1983; Mage, 1980; Zhao et al., 2009). Therefore experiments were conducted to find the optimum concentration for the polyclonal rabbit anti-rat albumin IgG. A concentration of 20 mM cysteine was used as previously reported (Goding, 1996; Zhao et al., 2009).

SDS-PAGE analysis was performed on the anti-rat albumin IgG as a control (Figure 4-21 A) to compare the digestion mixture to over the time points (1-6 h). The SDS-PAGE analysis revealed two bands for anti-rat albumin IgG (~150 kDa) and BSA (~60 kDa) as previously observed. SDS-PAGE analysis revealed that with all concentrations of papain and digestion lengths (1-6 h) tested that the IgG was fully digested with no IgG visible at 150 kDa (Figure 4-21 B-E). Fab_{alb} was observed at ~40-50 kDa with a band that was interpreted to be the Fc at ~50 kDa (Figure 4-21 B-E), which are in agreement with reported literature (Zhao et al., 2009).

Due to the presence of the cysteine, some reduced Fab_{alb} and Fc could be seen at 30 kDa and 25 kDa, respectively (Figure 4-21 B-E). As the incubation period increases, greater amounts of the Fab_{alb} and Fc were seen. However, with higher ratios (1:10) more reduced species were observed at ~30 kDa and below with longer incubation time. On the contrary, at a lower papain concentration (1:50) some higher MW bands representing un-digested anti-rat albumin IgG were detected (Figure 4-21 B-E), suggesting a longer incubation necessary. Therefore, the 1:20 papain:IgG appeared to be the best condition because there was little anti-rat albumin IgG observed in the incubation times and less reduced impurities below ~30 kDa (Figure 4-21 B-E).

To then define the optimum digestion period and in an effort to improve the yield of Fab_{alb}, analytical SEC was conducted. SEC has been previously reported for a similar purpose and was employed to analyse the extent of papain digestion with time at the 1:20 papain to IgG ratio (Zhao et al., 2009).

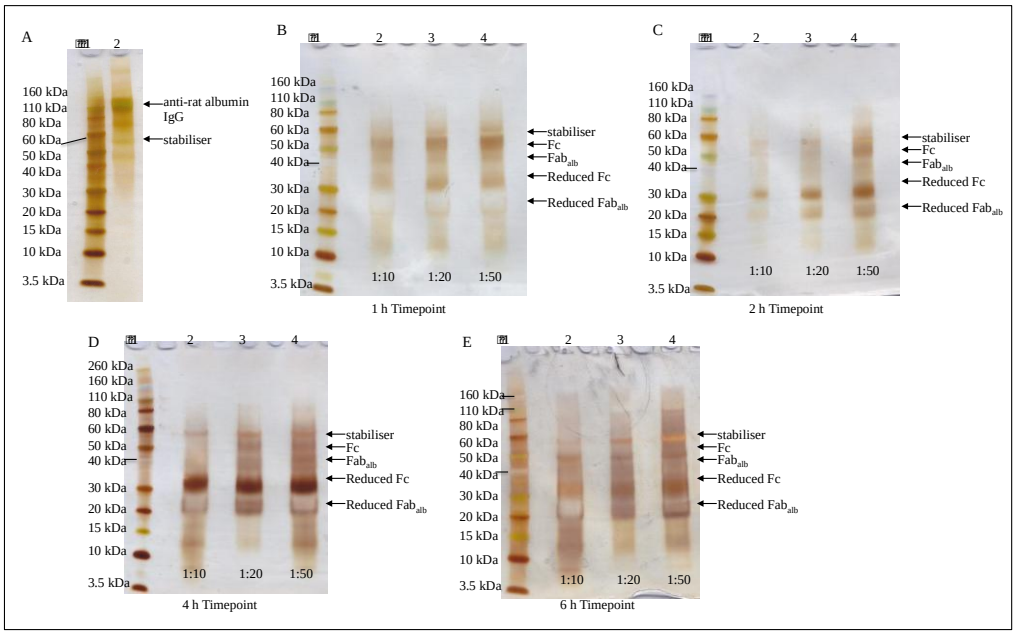

Figure 4-21. SDS-PAGE analysis (silver stain) of A) anti-rat albumin IgG, B) 1 h, C) 2 h, D) 4 h, E) 6 h incubation of anti-rat albumin IgG with varying papain concentrations (1:10,1:20,1:50). A) Lane 1: Novex pre-stained markers, Lane 2: anti-rat albumin IgG. B-E) Lane 1: Novex pre-stained markers, Lane 2: papain: IgG 1:10 ratio, Lane 3: papain: IgG 1: 20 ratio, Lane 4: papain: IgG 1: 50 ratio. Optimum papain: anti-albumin IgG concentration was found to be 1:20.

Zhao and colleagues demonstrated by using SEC, that papain digestion of IgG over time can be analysed by integrating the area under the curve of chromatograms at different incubation times, which can then compared (Zhao et al., 2009). The optimum incubation time was defined as the time in which the IgG peak area under the curve reaches or is close to zero absorbance (A280 nm). SE-HPLC analysis (Figure 4-22,Table 4–1) of the peaks was performed as detailed in § 2.2.4.2.

The first two peaks seen in the chromatograms (Figure 4-22) at 8 and 9 min are the largest MW species as these have eluted first. These impurities were not visualised by SDS-PAGE analysis (Figure 4-22) by silver stain or InstantBlue™ thus the impurities must be in very low concentration, which the small peak area also confirms this. The impurity could be aggregates of IgG due to the MW being >150 kDa. The peak at ~10.5 min corresponds to the undigested anti-rat albumin IgG molecule, and as the digestion time proceeds, the area under the curve (Table 4–1) can be seen to decrease in size (Figure 4-22). The Fab_{alb} and Fc fragments are of similar size ~50 and 55 kDa respectively, there elution is seen as one peak at ~13 min. This peak increases in size as the digestion time proceeds and can be seen to plateau at 4 h of digestion (Figure 4-22).

As previously discussed, the presence of cysteine is for papain activation, however cysteine can cleave the interchain disulfide of IgG (Andrew and Titus, 2001; Goding, 1996). This was seen in SDS-PAGE analysis with bevacizumab where approximately half IgG molecules were observed (Figure 4-3) and has been observed in SE-HPLC analysis by Zhao and colleagues (Zhao et al., 2009). This would explain the peak observed at ~11 min on the SE-HPLC chromatograms (Figure 4-22) as the peak is after the elution of IgG (~150 kDa) but before the elution of Fab_{alb}/Fc (~50 kDa).

As for bevacizumab, a band for approximately half IgG was seen at ~80 kDa (Figure 4-3). This strongly suggests the peak at ~11 min is the IgG heavy chain prepared by cysteine reduction. The peaks observed after 13 min are buffer components absorbed at 280 nm. The SE-HPLC results suggest that a digestion period 4 h using 1:20 papain to anti-rat albumin IgG ratio digestion is sufficient to prepare Fab_{alb}. The SEC results achieved for the papain digestion of polyclonal anti-albumin IgG are comparable to those achieved for the digestion of monoclonal antibodies reported by Zhao and colleagues (Zhao et al., 2009) confirming the reliability of the results achieved.

Table 4–1. Area under the peak integrated from the SEC chromatograms in **Figure 4-22**. ND=could not be determined due to software failure.

Time (h)	**Area under peak (% total area)**		
	10.5 min	11.3 min	13 min
0	ND	ND	ND
1	202.67 (22.13)	144.40 (157.77)	148.68 (16.24)
2	108.45 (11.39)	144.73 (15.2)	248.46 (26.10)
4	ND	ND	ND
6	ND	ND	ND

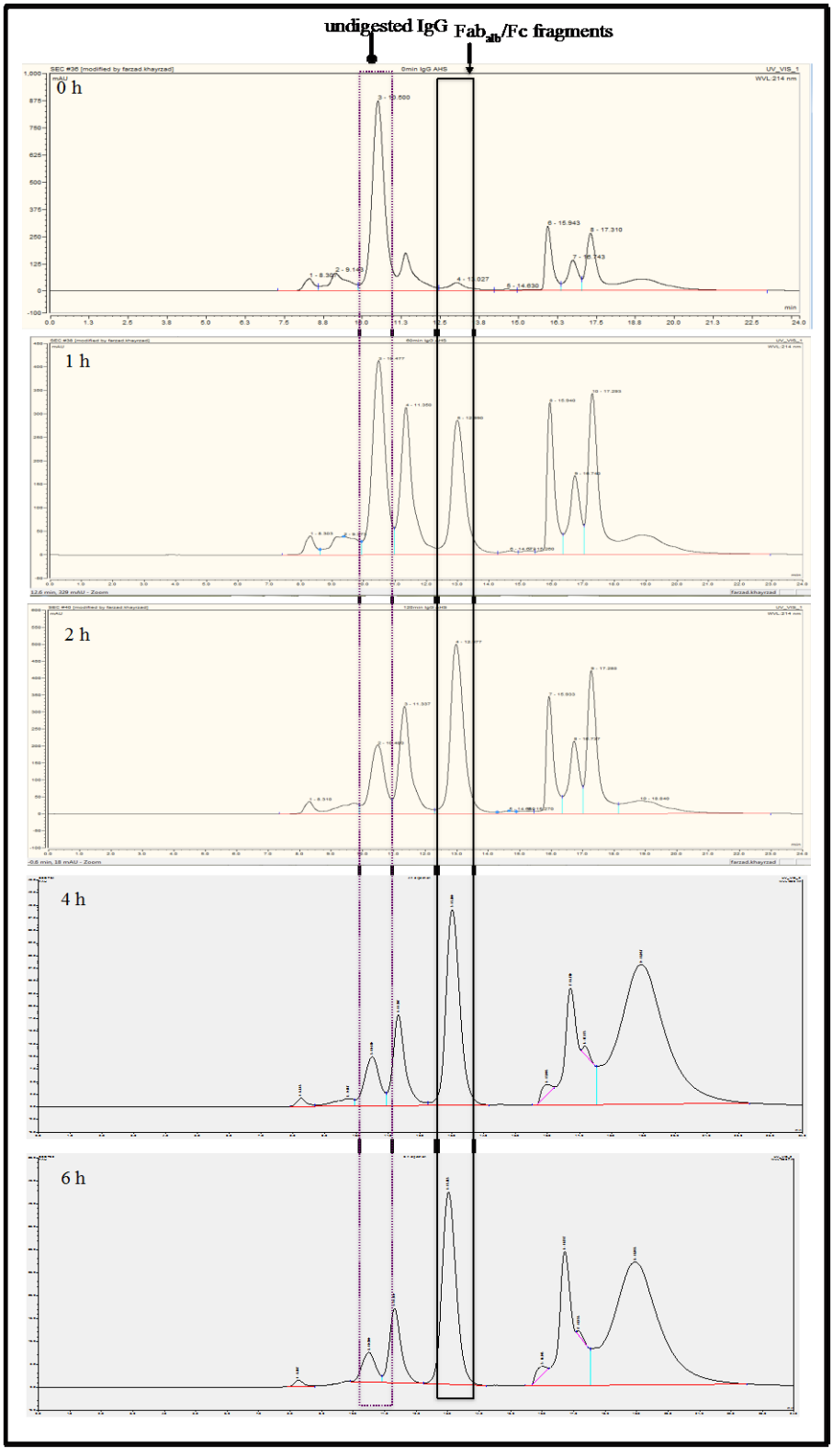

Figure 4-22. Papain digestion of polyclonal anti-rat albumin IgG analysed by analytical SEC. The peak at ~10.5 min corresponds to the undigested anti-rat albumin IgG molecule. As the size of Fab_{alb}/Fc are similar, these make up the peaks at ~13 min. The peak at ~11 min is from the partial reduction of the IgG (i.e. light chain falling off under cysteine reduction). Peaks before 10 min could be high MW impurities and the peaks after 13 min are due to buffer components absorbed at 280 nm.

4.2.5.2 Digestion and purification of anti-rat albumin IgG to isolate Fab_{alb}

Utilising the optimised papain concentration of 1:20 papain to anti-albumin IgG ratio and the optimum incubation time of 4 h (§ 2.2.4.2) Fab_{alb} was prepared for conjugation studies. Digestion of anti-albumin IgG (4.75 mg) was complete as no whole IgG was observed at ~150 kDa. The fragments of Fab_{alb} (~45 kDa) and Fc (~50 kDa) can be seen as well as there reduced forms at ~25 kDa and ~30 kDa, respectively (Figure 4-23 B). The reduced Fab_{alb} and Fc migrate faster by SDS PAGE than their oxidised forms; this could be due to the structure being open and spread out in the reduced form.

Prior to Protein purification, the digestion mixture was pipetted through a PD-10 frit to remove the immobilised papain. This method is quicker and more accurate than using iodoacetamide to stop digestion or centrifugation (Goding, 1996; Zhao et al., 2009). This is due to the frit being washed five times with binding buffer or until no protein is detected by UV (A280 nm).

Protein A purification was chosen over conventional methods of ion exchange, DEAE cellulose or Protein G because, i) the protein A molecule has a high binding affinity specifically for the Fc region (Hjelm et al., 1975), which makes it ideal for the purification of Fab from Fc within digestion mixtures, ii) the anti-rat albumin IgG is of rabbit origin, rabbit IgG binds strongly to Protein A, where it has week binding to Protein G, iii) Protein A columns were used for the purification of the anti-rat albumin IgG and could be easily used for digestion mixture purification (§4.2.4.2). Additionally, Protein A has been shown to be more efficient at purifying rabbit Fab fragments over conventional ion exchange procedures (Coulter and Harris, 1983).

The chromatogram (Figure 4-23 A) shows a small peak from 20-80 min at ~100 mAu, this is the loading peak, where any molecules not bound to the Protein A resin, namely Fab_{alb}, elute. The eluting Fab_{alb} can be seen in the SDS-PAGE analysis (Lanes 2-6, Figure 4-23 C) at ~40 kDa, reduced Fab_{alb} can be also be observed between 20-30 kDa. The second large and sharp peak (>2000 mAu) is the elution peak where the pH was dropped to pH 2.0, causing bound Fc molecules to dissociate from the Protein A resin. As pH 2.0 was used to dissociate the anti-rat albumin IgG/Fc from the Protein A, a neutralising solution (1 M Tris) was pipetted into the collected fractions as they were eluted to increase the pH to ~pH 7 which is a more appropriate physiological pH (§ 2.2.4.4).

SDS-PAGE analysis (Lane 9, Figure 4-23 C) of the eluted peak fractions showed three bands. The first band is at ~110 kDa, this could be heavy chain of the anti-rat albumin molecule. The heavy chain molecule is most likely a product of cysteine reduction from digestion (Andrew and Titus, 2001). The ~50 kDa band (Lane 9, Figure 4-23 C) is the Fc fragment and the reduced Fc can be seen at ~30 kDa. The digestion has gone to completion, as no whole anti-rat albumin IgG can be seen in Lane 9 at 150 kDa, indicating that the selected digestion conditions were successful. This method was utilised three times within the study to isolate Fab_{alb} for conjugation, the average yield achieved was ~39% (yields achieved: 35%, 42% and 39%). Some Fab_{alb} may have been lost through the digestion and purification process or within other fragments such as heavy chain. The yields achieved of Fab_{alb} are very similar to those achieved for Fab_{beva} (39% and 33%, §4.2.1.1), showing the consistency of the papain digestion and protein A purification process.

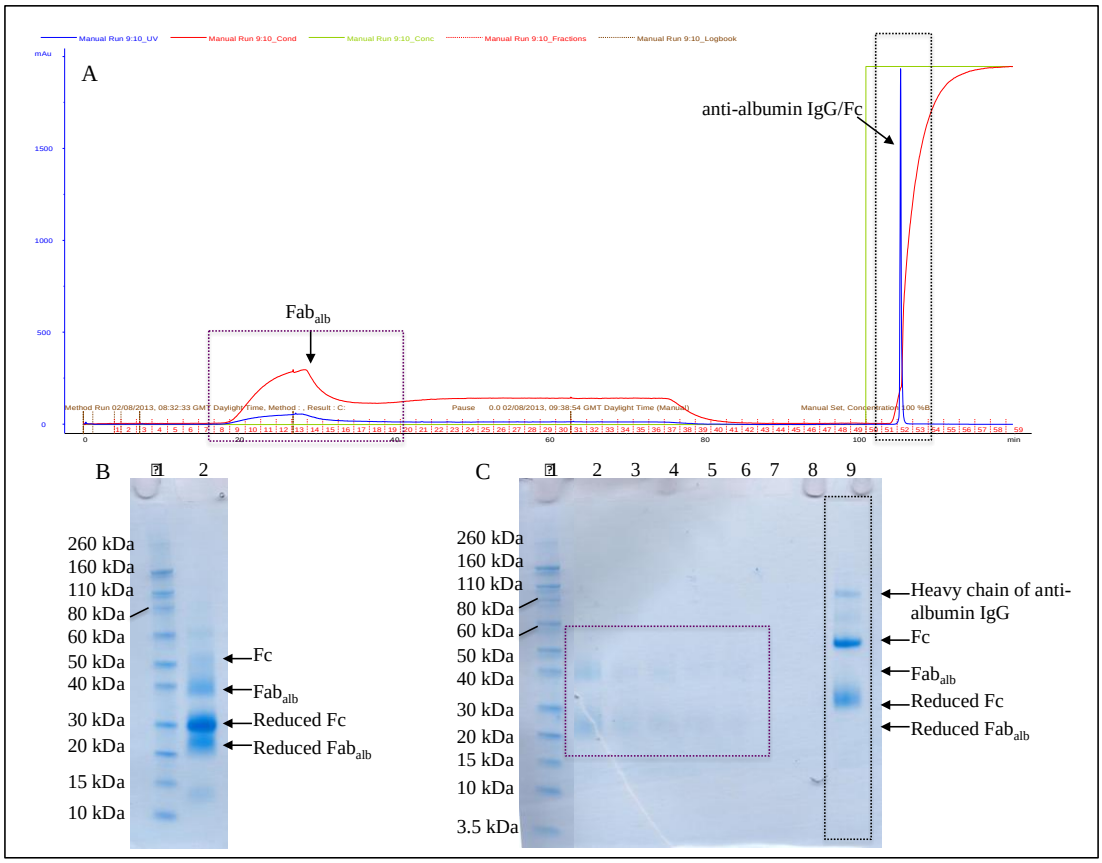

Figure 4-23. Representative B) Papain digestion mixture of anti-rat albumin IgG, A) Protein A purification chromatogram of anti-rat albumin IgG digestion mixture and C) SDS-PAGE analysis of Protein A purification fractions. B) Lane 1: Novex pre-stained markers, Lane 2: anti-rat albumin IgG digestion mixture; C) Lane 1: Novex pre-stained markers, Lane 2-6: Fab_{alb}, Lane 9: Fc. Successful papain digestion of anti-rat albumin IgG and isolation of Fab_{alb} by Protein A purification. The purification process was found to be reproducible in all three repeats conducted.

4.2.5.3 Characterisation of Fab_{alb}

Prior to conjugation, the Fab_{alb} was characterised. SDS-PAGE analysis (Figure 4-24) showed one band at ~45 kDa, which is the Fab_{alb}. No other bands were observed.

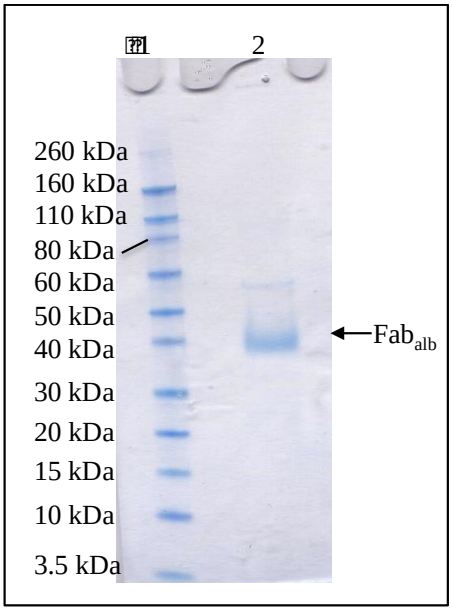

Figure 4-24. Example SDS-PAGE analysis (InstantBlue™ stain) of Fab_{alb} prepared from anti-rat albumin IgG (n=3). Lane 1: Novex pre-stained markers, Lane 2: Fab_{alb}. Fab_{alb} prepared from anti-rat albumin IgG is pure to the 5 ng level.

To confirm the identity of the Fab_{alb} isolated from papain digestion of anti-rat albumin IgG an anti-rabbit Western blot was performed (§ 2.2.10.1). A polyclonal anti-rabbit IgG (H&L) AP-conjugated IgG was used and a colorimetric method of detection was used. The anti-rabbit IgG has positively identified the Fab_{alb} prepared from anti-rat albumin IgG digestion, as a ~45 kDa band is visible by colorimetric detection (Figure 4-25). This MW is the same as that observed by other SDS-PAGE analysis, such as that seen in Figure 4-23 C, thus confirming the identity of Fab_{alb}. A faint band is visible between 20-30 kDa; this is the reduced Fab_{alb}, which is also observed on SDS-PAGE as in Figure 4-23 C.

MALDI-TOF (§ 2.2.10.3) indicated the MW for Fab_{alb} was 45883.8 Da (Figure 4-26). This is in agreement with the theoretical MW for digested rabbit Fab_{alb} (Coulter and Harris, 1983). The MALDI-TOF spectra (Figure 4-26) show's two other peaks at 22805.4 and 91914.7 Da. The peak at 22805.4 Da is a result of double charged species of Fab_{alb}, whilst the other peak at 91914.7 Da is a result of Fab_{alb} dimers^{1+}. Therefore, the MW based on singly charged Fab_{alb} was 45.9 kDa from n=1, this is expressed to one significant figure due to the reported accuracy of MS being 0.1-0.01% (Fenselau, 1997).

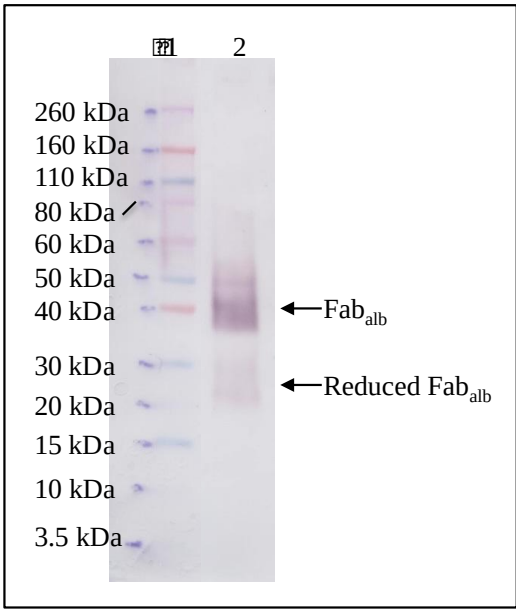

Figure 4-25. Anti-rabbit Western blot of Fab$_{alb}$. Lane 1: Novex pre-stained markers, Lane 2: Fab$_{alb}$. Successful identification of Fab$_{alb}$ by anti-rabbit IgG by Western blotting.

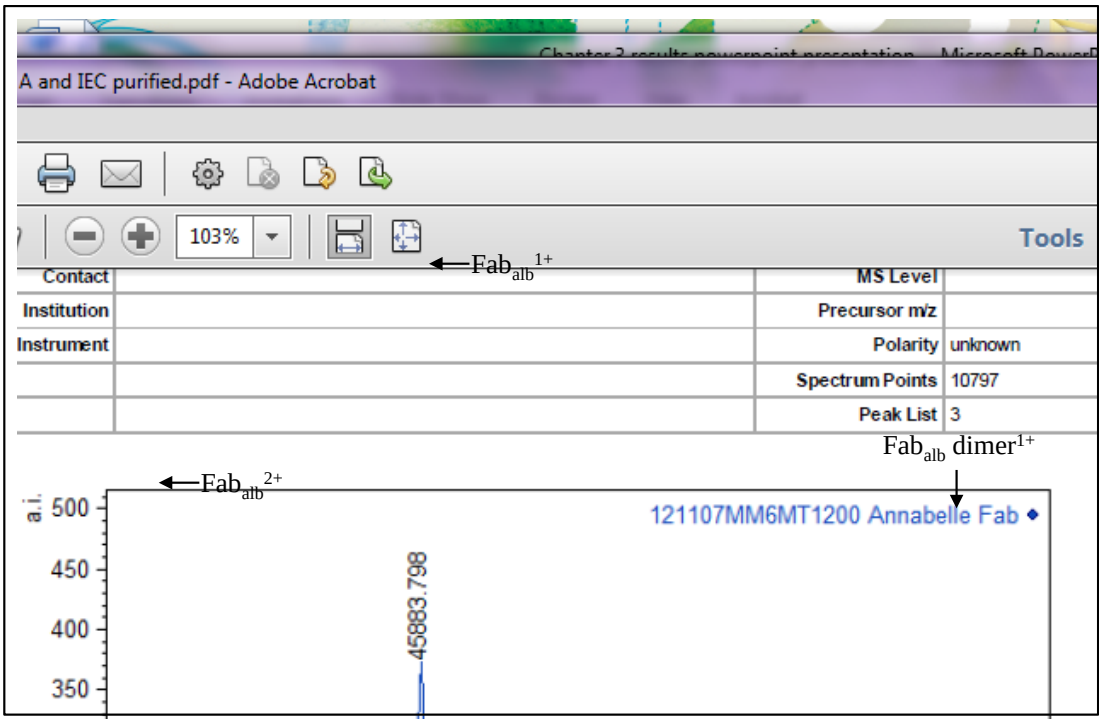

Figure 4-26. MALDI-TOF spectrum of Fab$_{alb}$ conducted once. Singley charged Fab$_{alb}$ can be seen at 45883.8 Da, whilst a double charged Fab$_{alb}$ was observed at 22805.4 Da. A singly charged Fab$_{alb}$ dimer can be seen at 91914.7 Da.

4.2.6 Preparation of IFN-PEG$_{20}$-Fab$_{alb}$ heterodimer

The aim was to prepare an IFN-PEG$_{20}$-Fab$_{alb}$ heterodimer utilising the PEG$_{20}$ di(*bis*)sulfone **4** as a linker to conjugate both IFN and Fab$_{alb}$ by disulfide PEGylation following the same strategy used to prepare IFN-PEG$_{20}$-Fab$_{beva}$ (Figure 4-8). The aim

was to prepare a therapeutic IFN-PEG_{20}-Fab_{alb} heterodimer in an effort to elongate the half-life of IFN, where the Fab_{alb} would 'piggy back' on circulating albumin, thus elongating the half-life of IFN beyond that of monoPEGylated IFN.

4.2.6.1 Optimisation of Fab_{alb} reduction using DTT

The aim was to optimise the mild reduction of Fab_{alb} to liberate the accessible sulfur atoms, which in turn can be conjugated to by the *bis*-thiol alkylating reagent (Brocchini et al., 2006). For the mild reduction of Fab_{alb}, TCEP was tested, however a large excess of TCEP (>4 eq.) was required to reduce the single disulfide bond. Further, when using 4 eq. of TCEP, Fab_{alb} was not fully reduced. Thus, DTT was used to reduce the disulfide of Fab_{alb}. Scouting experiments were conducted with increasing concentrations of DTT (2.5 mM-25 mM) to evaluate the optimum conditions for Fab_{alb} reduction (§ 2.2.9.10). The reduction was conducted at pH 7.8 (§ 2.2.9.10) as DTT has been shown to be most effective at pH values above pH 7.0 (protonated sulfurs have lowered nucleophilicities) (Cleland, 1964; Hermanson, 2008).

A trend was observed where as the concentration of DTT increases, the amount of oxidised Fab_{alb} was seen to decrease (Figure 4-27). Fab_{alb} was observed to be completely reduced with 5 mM DTT, as no oxidised Fab_{alb} was present at ~40 kDa (Lane 4, Figure 4-27). With 2.5 mM DTT, Fab_{alb}, and both reduced and oxidised Fab_{alb} were observed (Lane 3, Figure 4-27). When preparing the heterodimer (IFN-PEG_{20}-Fab_{alb}) it was necessary to try to reduce the risk of hydrolysis to the PEG di(*bis*)sulfone **4**. Therefore, by using a higher DTT concentration and a shorter incubation time, reduction is preferred. Thus, the minimum amount of DTT for reduction of Fab_{alb} is 5 mM for 1 h at RT.

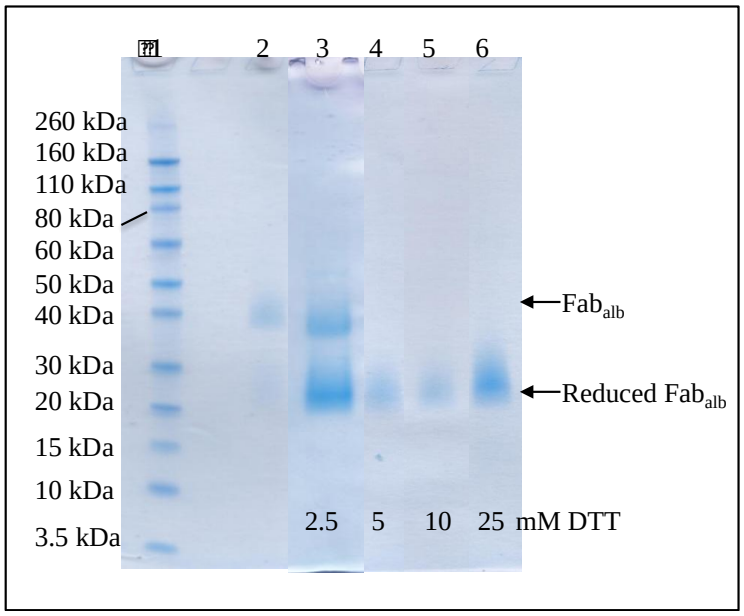

Figure 4-27. SDS-PAGE analysis of Fab_{alb} reduction by varying DTT concentrations. Lane 1: Novex pre-stained markers, Lane 2: Fab_{alb}, Lane 3: 2.5 mM DTT+ Fab_{alb}, Lane 4: 5 mM DTT + Fab_{alb}, Lane 5: 10 mM DTT+ Fab_{alb}, Lane 6: 25 mM DTT + Fab_{alb}. Optimum DTT concentration for Fab_{alb} reduction was found to be 5 mM.

4.2.6.2 Conjugation of Fab_{alb} with PEG_{20} di(*bis*)sulfone **4** to prepare Fab_{alb}-PEG_{20}-X

Analogous to the sequence of steps to prepare Fab_{beva}-PEG_{20}-IFN, the initial step to prepare the IFN-PEG_{20}-Fab_{alb} heterodimer was first to reduce the accessible disulfide of Fab_{alb} for conjugation to PEG_{20} di(*bis*)sulfone **4** to give Fab_{alb}-PEG_{20}-X. Fab_{alb} (1 eq., 0.37 mg Fab_{alb}) was reduced with DTT and then allowed to react with PEG_{20} di(*bis*)sulfone **4** (5 eq.) for 3 h at 25 °C (§2.2.9.15). As before (§ 4.2.2.2) excess PEG di(*bis*)sulfone **4** was used to cause the formation and efficient purification of Fab_{alb}-PEG_{20}-X, while minimising the formation of Fab_{alb}-PEG_{20}-Fab_{alb}.

In an effort to maximise yield and conversion of the conjugation reactions to make Fab_{alb}-PEG_{20}-IFN, while avoiding the potential hydrolysis reactions to the reagent, short reaction times were conducted. Further conjugation and purification was conducted in one day to reduce the risk of changes to the PEG di(*bis*)sulfone **4**, from the PEG di(*bis*)sulfone **4** being present in solution for long periods of time. Further, the purity of the reagent is also an important factor in producing good yields of Fab_{alb}-PEG_{20}-IFN heterodimers, as discussed in §3.2.1.

Fab_{alb}-PEG_{20}-X was observed at ~80 kDa (~45 kDa=Fab_{alb}+ 40 kDa=PEG_{20}, Figure 4-28). Fab_{alb}-PEG_{20}-X is a green band, where the InstantBlue™ stains proteins blue, whilst PEG is stained orange. A clear blue band of un-conjugated

Fab_{alb} can be seen between 20-30 kDa in Figure 4-28. The band at ~110 kDa could be Fab_{alb}-PEG-Fab_{alb}, as (2× Fab_{alb}= ~60 kDa+ 40 kDa=PEG_{20}).

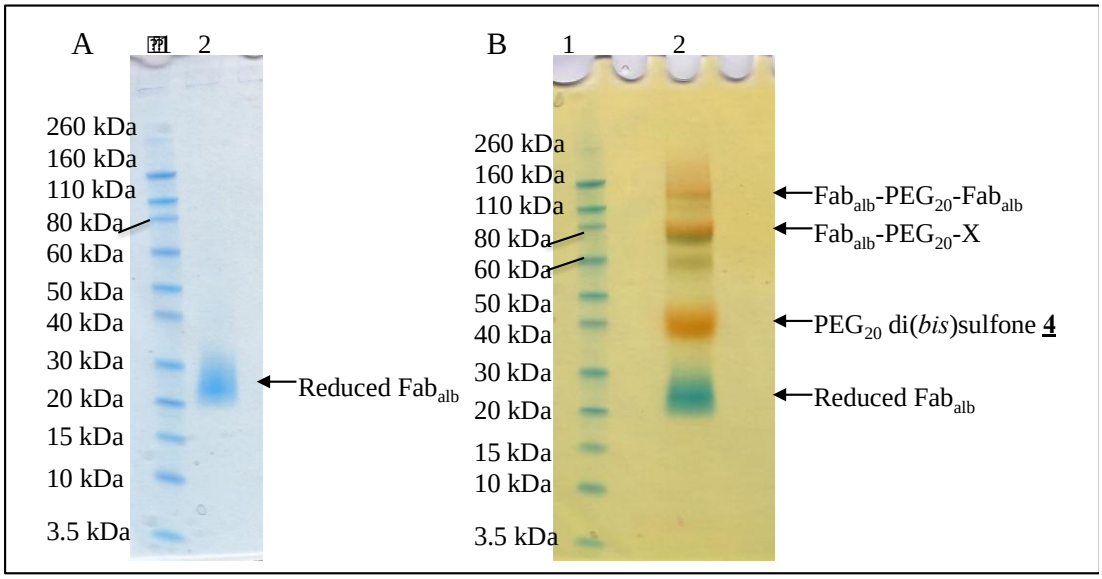

Figure 4-28. Example SDS-PAGE analysis of (InstantBlue™) A) reduced Fab_{alb} and (PEG stain) B) PEG_{20} di(*bis*)sulfone **4**-Fab_{alb} reaction mixture. A) Lane 1: Novex pre-stained markers, Lane 2: reduced Fab_{alb}. B) Lane 1: Novex pre-stain markers, Lane 2: PEG_{20} di(*bis*)sulfone **4**-Fab_{alb} reaction mixture. Successful conjugation of Fab_{alb} with di(*bis*)sulfone **4** to prepare Fab_{alb}-PEG_{20}-X, this was conducted n=2.

4.2.6.3 CIEC purification of the Fab_{alb}-PEG_{20}-X reaction mixture

CIEC purification (§2.2.9.16) was used to purify the Fab_{alb}-PEG_{20}-X from the unreacted PEG_{20} di(*bis*)sulfone **4**. This again was a necessary step for creating the heterodimer, as unreacted PEG_{20} di(*bis*)sulfone **4** would compete against the Fab_{alb}-PEG_{20}-X for conjugating the reduced IFN.

The CIEC chromatogram (Figure 4-29 A) shows two peaks at 20 min and 70 min respectively. The first peak at 20 min is PEG_{20} di(*bis*)sulfone **4** which can be seen in Lane 2 (Figure 4-29 B), where the PEG stained orange from the barium chloride. The second peak at 70 min (~45 mAu) is the Fab_{alb} species eluting from the column due to the salt gradient causing the Fab_{alb} species to dissociate from the cation exchange resin. The SDS-PAGE analysis of the peak fractions shows both un-conjugated Fab_{alb} between 20-30 kDa and 20 kDa Fab_{alb}-PEG_{20}-X (~80 kDa) have co-eluted. However, this is of no consequence as the aim was to remove the un-reacted PEG_{20} di(*bis*)sulfone **4**, which would otherwise compete against the Fab_{beva}-PEG_{20}-X for conjugating the reduced IFN.

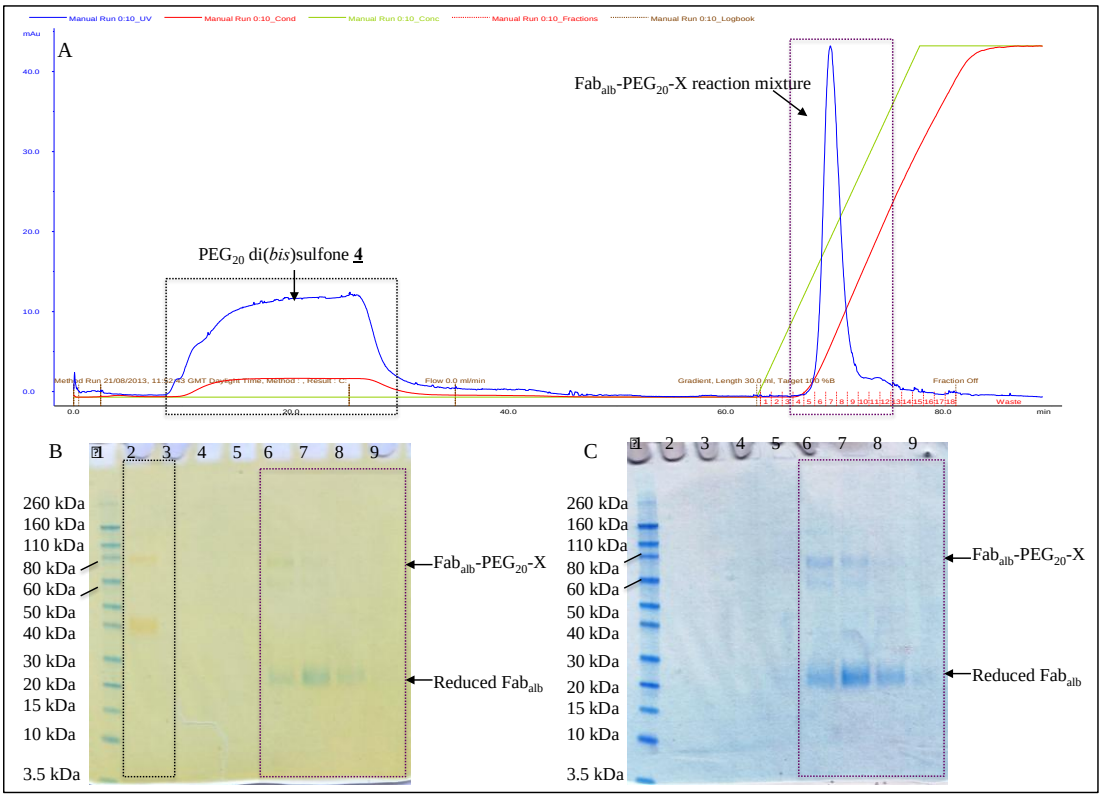

Figure 4-29. Representative A) Chromatogram and SDS-PAGE analysis (B) PEG stain, C) InstantBlue™ stain) of the linear CIEC purification of PEG$_{20}$ di(*bis*)sulfone **4**-Fab$_{alb}$ reaction mixture. Lane 1: Novex pre-stained markers, Lane 2: PEG$_{20}$ di(*bis*)sulfone **4**, Lane 6-9: Fab$_{alb}$-PEG$_{20}$-X mixture. Successful removal of un-reacted PEG$_{20}$ di(*bis*)sulfone 4 from Fab$_{alb}$-PEG$_{20}$-X mixture, this was repeated n=2.

4.2.6.4 Disulfide conjugation of IFN with Fab$_{alb}$-PEG$_{20}$-X

In an effort to maximise the yield of Fab$_{alb}$-PEG$_{20}$-IFN, Fab$_{alb}$-PEG$_{20}$-X was in solution for as short as time as possible. Fab$_{alb}$ was reacted with PEG$_{20}$ di(*bis*)sulfone **4** for 3 h and purified at once. Once quantified the Fab$_{alb}$-PEG$_{20}$-X was reacted straight away with reduced IFN. Following the isolation of the Fab$_{alb}$-PEG$_{20}$-X conjugate from unreacted PEG$_{20}$ di (*bis*)sulfone **4** by CIEC; the fractions containing Fab$_{alb}$-PEG$_{20}$-X were pooled and quantified by UV (0.17 mg, yield=46.7%) ready for conjugation to IFN (§ 2.2.9.16). The disulfide reduced IFN (2 eq., 0.25 mg) was then allowed to undergo conjugation with Fab$_{alb}$-PEG$_{20}$-X (1 eq.) in an effort to form IFN-PEG$_{20}$-Fab$_{alb}$ (§ 2.2.9.17). To promote the conjugation of IFN to Fab$_{alb}$-PEG$_{20}$-X an excess of reduced IFN were used.

As before (§ 4.2.2.4), once the IFN-PEG$_{20}$-Fab$_{alb}$ conjugate had been formed the unconjugated disulfide in IFN was oxidised using glutathione. Prior to glutathione treatment, SDS-PAGE analysis was conducted on the IFN-PEG$_{20}$-Fab$_{alb}$ reaction mixture. The IFN-PEG$_{20}$-Fab$_{alb}$ conjugate can be seen in Lane 2 (Figure

4-30) at a new band ~110 kDa, which is the expected MW (~50 kDa=Fab_{alb} + PEG_{20}=40 kDa + IFN=~20 kDa) (Figure 4-30). A faint band of Fab_{alb}-PEG_{20}-X can be observed in Lane 2 at ~80 kDa (Figure 4-30), meaning the reaction has not gone to completion or that some of the Fab-PEG-X had a dead chain end due to hydrolysis or because the reagent was not pure at the start of the conjugation sequence.

Following glutathione re-oxidisation of IFN within the IFN-PEG_{20}-Fab_{alb} conjugate, the reaction mixture was then subject to STAB treatment (§ 2.2.9.17) to reduce the electron withdrawing carbonyl to stop de-conjugation.

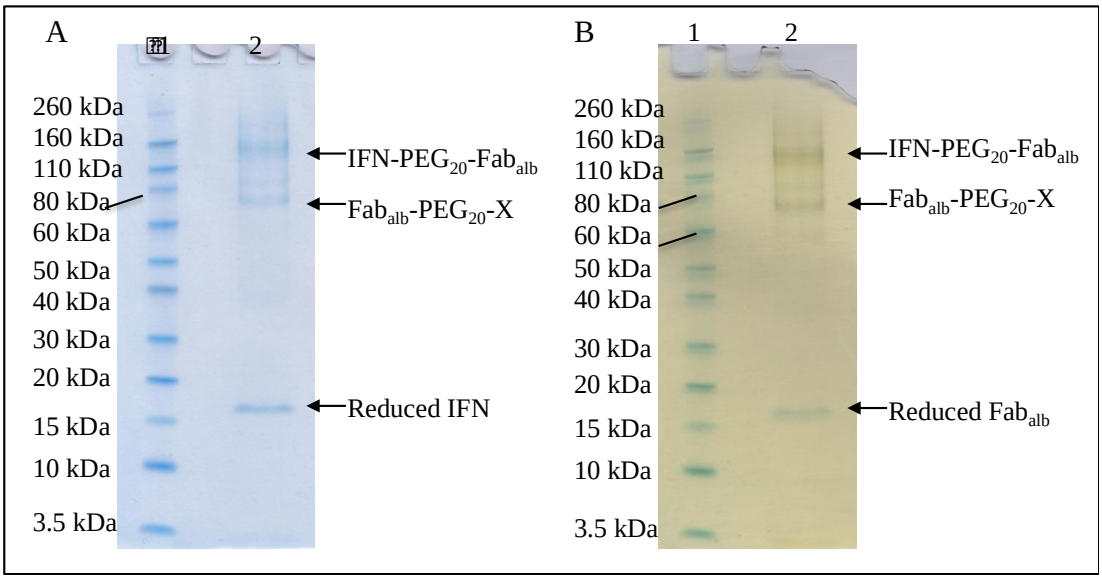

Figure 4-30. Example SDS-PAGE analysis A) InstantBlue™ B) PEG stain of the IFN-PEG_{20}-Fab_{alb} reaction mixture. Lane 1: Novex pre-stained markers, Lane 2: IFN-PEG_{20}-Fab_{alb} reaction mixture. Successful conjugation of reduced IFN to Fab_{alb}-PEG_{20}-X to prepare IFN-PEG_{20}-Fab_{alb}. This was repeated twice independently.

4.2.6.5 CIEC purification of the IFN-PEG_{20}-Fab_{alb} reaction mixture

A step CIEC gradient was used to purify the IFN-PEG_{20}-Fab_{alb} conjugate from the unreacted IFN and Fab_{alb}-PEG_{20}-X, and higher MW impurities of Fab_{alb}-PEG_{20}-Fab_{alb} (Figure 4-31 A). This step gradient of 30, 60, 80 and 100% buffer B (§ 2.2.9.18) was optimised to isolate the IFN-PEG_{20}-Fab_{alb} conjugate in a single step CIEC purification in an effort to maximise yield. SDS-PAGE analysis (Figure 4-31 B) shows that the step gradient CIEC was successful at isolating the IFN-PEG_{20}-Fab_{alb} heterodimer (Lane 7) from the unreacted IFN (Lanes 8-9), Fab_{alb}-PEG_{20}-X and Fab_{alb} (Lanes 3-5), plus higher MW impurities of Fab_{alb}-PEG_{20}-Fab_{alb} (Lanes 3-5). As the Fab_{alb}-PEG_{20}-X (~80 kDa), Fab_{alb} (~45 kDa), Fab_{alb}-PEG_{20}-Fab_{alb} (~140 kDa) (Lanes 3-5) co-eluted this suggests that their binding affinity for the column is similar as they all required 30% salt to elute from the column.

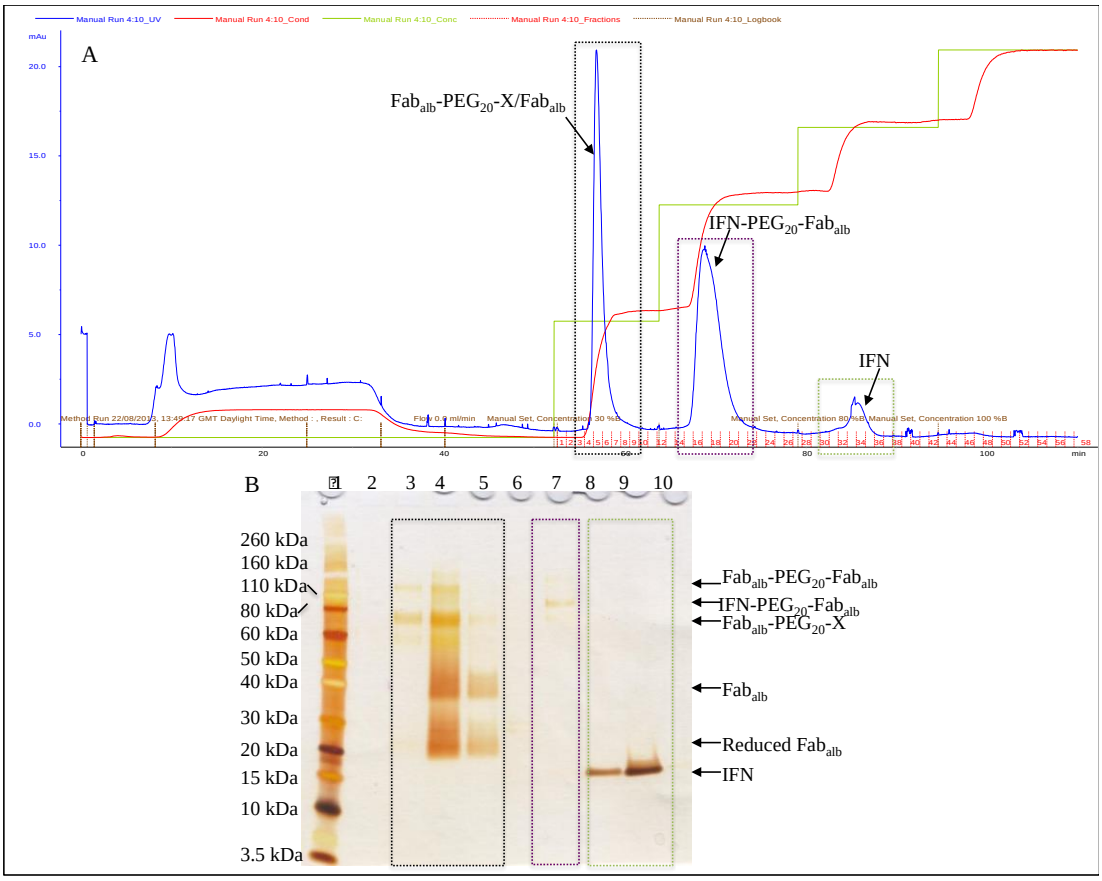

Figure 4-31. Representative A) Chromatogram and B) SDS-PAGE analysis of IFN-PEG$_{20}$-Fab$_{alb}$ CIEC purification to isolate IFN-PEG-Fab$_{alb}$. Lane 1: Novex pre-stained markers. Lanes 3-5: Fab$_{alb}$-PEG$_{20}$-X/Fab$_{alb}$/Fab$_{alb}$-PEG$_{20}$-Fab$_{alb}$ mixture, Lanes 7: IFN-PEG$_{20}$-Fab$_{alb}$, Lane 8-9: IFN. Successful CIEC purification was conducted to isolate IFN-PEG$_{20}$-Fab$_{alb}$. Purification was found to be reproducible, as IFN-PEG$_{20}$-Fab$_{alb}$ was successfully isolated twice.

Whilst 60% salt was required to elute the IFN-PEG$_{20}$-Fab$_{alb}$ (~110 kDa, Lane 7, Figure 4-31) from the resin, as the binding affinity of the conjugate is an average of both proteins, thus it is in the middle of the Fab$_{alb}$ (~20 mAu) and IFN (5 mAu) peaks within the chromatogram. Interestingly, the Fab$_{alb}$ mixture peak (~20 mAu) is the largest of the three peaks; this peak is a mixture of Fab$_{alb}$-PEG$_{20}$-X (~ 80 kDa), Fab$_{alb}$ (~45 kDa) and Fab$_{alb}$-PEG$_{20}$-Fab$_{alb}$ (~140 kDa) explaining the higher absorbance.

The fractions for IFN-PEG$_{20}$-Fab$_{alb}$ were pooled and the concentration of Fab$_{alb}$ and IFN quantified by UV (IFN ε=0.914, 0.11 mg/ mL, yield=44%; Fab$_{alb}$ ε=1.4, 0.0725 mg/ mL, yield=20.5%). The yields achieved for Fab$_{alb}$ and IFN are comparable to that achieved for the PEG$_{20}$ *bis*-sulfone **1** and that achieved for the IFN-PEG$_{20}$-Fab$_{beva}$ heterodimer (§ 4.2.2.5). As discussed these results show that synthesis route 2 for PEG$_{20}$ di(*bis*)sulfone **4** has a greater reactivity compared to the

PEG_{20} di(*bis*)sulfone **4** synthesised by route 1. This could be due to i) the improved purity of the PEG_{20} di(*bis*)sulfone **4** which was quantified by RP-HPLC (§ 2.2.5.4) and SDS-PAGE (§ 2.2.5.5); ii) the better understanding of hydrolysis and its effect on the di(*bis*)sulfones, whereby the synthesis approach was conducted in under 12 hours, reducing the risk of hydrolysis to the di(*bis*)sulfone linkers.

SDS-PAGE analysis was conducted on the final IFN-PEG_{20}-Fab_{alb} conjugate to assess its purity. It can be seen in Lane 2 (Figure 4-32) that the IFN-PEG_{20}-Fab_{alb} conjugate at ~110 kDa was prepared and purified in good purity as no other bands can be seen by InstantBlue™ stain.

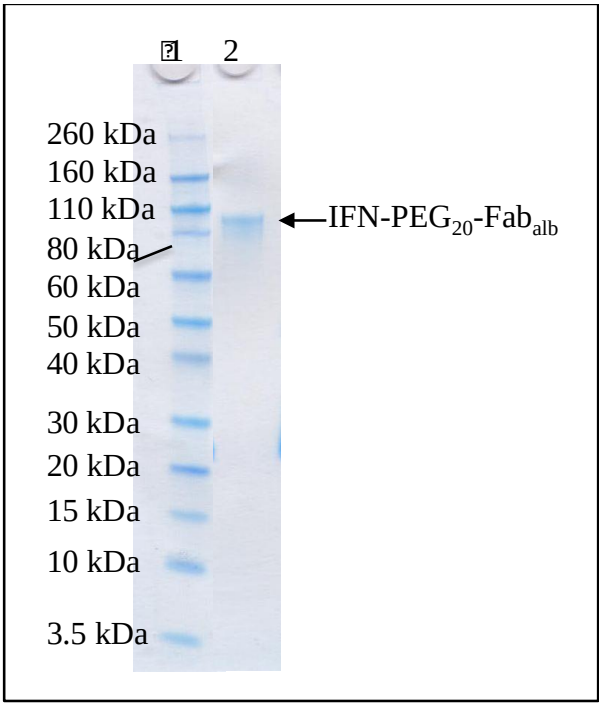

Figure 4-32: Example SDS-PAGE analysis (InstantBlue™ stain) of final IFN-PEG_{20}-Fab_{alb} conjugate (n=2). Lane 1: Novex pre-stained markers, Lane 2: IFN-PEG_{20}-$Fab_{alb.}$ IFN-PEG_{20}-Fab_{alb} was successful prepared and in good purity.

4.2.7 Preparation of PEG_{20}-Fab_{alb}

PEG_{20}-Fab_{alb} was prepared as a control for the binding studies, to compare the binding affinities of IFN-PEG_{20}-Fab_{alb}, PEG_{20}-Fab_{alb} and Fab_{alb} to rat albumin, and how the conjugation of IFN and PEG_{20} affect the binding of Fab_{alb} to rat albumin.

4.2.7.1 Reaction optimisation of PEG_{20} *bis*-sulfone **1**-Fab_{alb} production

As Fab_{alb} had not been conjugated to PEG before, little was known about the optimised reaction conditions (pH and reaction time) to prepare PEG_{20}-Fab_{alb}. Therefore, to confirm the site-specific PEGylation of Fab_{alb}, a control reaction was

conducted (§ 2.2.9.11) by allowing non-reduced Fab_{alb} to incubate with PEG_{20} *bis*-sulfone **1** in 1:1 molar ratio. This ratio was used as Fab_{alb} only has one disulfide to which the PEG_{20} *bis*-sulfone **1** could generate the 3-carbon linkage and conjugate. The reaction was conducted at pH 7.8 for 5 h hours at RT. This allows for the PEG *bis*-sulfone **1** to generate PEG mono-sulfone **2** by an *in situ* elimination reaction as shown in Figure 2-1 (§2.2.9.11, Brocchini et al. 2006).

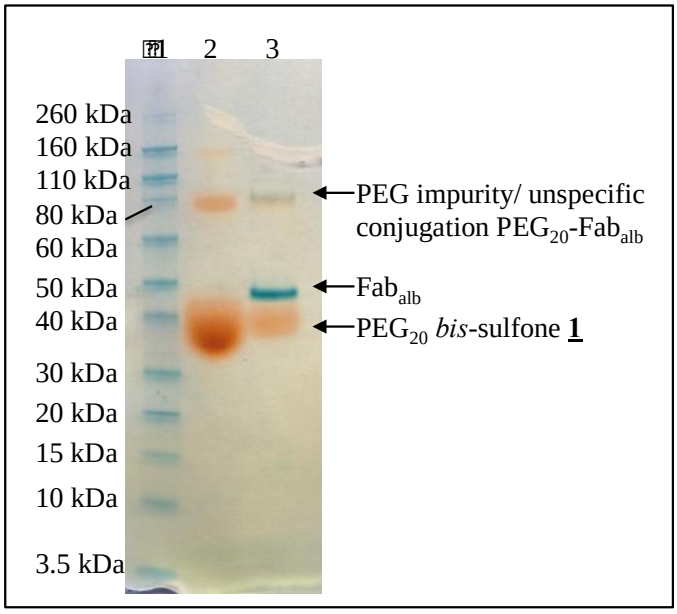

Figure 4-33. SDS-PAGE analysis (InstantBlue™/PEG stain) of PEG_{20} *bis*-sulfone **1**-Fab_{alb} control reaction. Lane 1: Novex pre-stained markers, Lane 2: PEG_{20} *bis*-sulfone **1**, Lane 3: PEG_{20} *bis*-sulfone **1**-Fab_{alb} control reaction. Unspecific conjugation of PEG_{20} *bis*-sulfone **1** to Fab_{alb} was observed (~85 kDa).

SDS-PAGE analysis was conducted on the PEG_{20} *bis*-sulfone **1**-Fab_{alb} mixture (Figure 4-33). Two PEG bands can be observed on the gel at ~40 kDa and ~80 kDa; the band at ~ 40 kDa is PEG *bis*-sulfone **1** (Lane 2, Figure 4-33). The band observed at ~80 kDa is most likely to be a PEG impurity. Oxidised Fab_{alb} can be seen as a clear blue band at ~45 kDa (Lane 3, Figure 4-33). A PEG-protein band can be seen at ~85 kDa (Lane 3, Figure 4-33). Additionally, due to the MW, it is most likely a Fab_{alb} (45 kDa)-PEG_{20} (~40 kDa) conjugate prepared from unspecific binding of PEG_{20} *bis*-sulfone **1** to the Fab_{alb}. This indicates that tailored reaction conditions, specifically pH, need to be found to reduce the likelihood of this taking place.

As unspecific conjugation had occurred to a small extent at pH 7.8, lower pH values were evaluated in an effort to minimise unspecific conjugation to Fab_{alb}. Reducing the pH was expected to protonate any nucleophilic residues available for conjugation. *Bis*-thiol alkylation occurs efficiently at slightly acidic pH (Brocchini et

al., 2006), therefore activation *in situ* to PEG mono-sulfone **2** would not be effected by reducing the pH (Figure 2-1).

First, Fab_{alb} was reduced using DTT; the reduced Fab_{alb} can be seen in Lane 2 at between 20 kDa-30 kDa (Figure 4-34 A). Varying pH's (pH 6.5, 6.0, 7.8) were tested to prepare PEG_{20}-Fab_{alb} at 25 °C. After 1 h little conjugation of the reduced Fab_{alb} was observed at of the pH values tested (Figure 4-34 A), this could be due to the *in situ* activation of the PEG_{20} *bis*-sulfone **1** occurring at this time. However, at 3 h of reaction time, conjugation of Fab_{alb} appeared to occur at all pH values tested as seen in Figure 4-34 B. The band of interest is PEG_{20}-Fab_{alb}, which can be seen at ~80 kDa (~45 kDa=Fab_{alb} + PEG_{20}=40 kDa).

Interestingly, it can be seen in Figure 4-34 B and C, that the higher the pH the more bands for conjugated Fab_{alb} can be seen. The band observed at ~110 kDa could be $(PEG_{20})_2$-Fab_{alb}. This is unusual as Fab_{alb} is thought to have only one accessible disulfide that could be reduce and to which the PEG reagent can conjugate. The starting antibody was polyclonal and it is possible that there are many Fab variants in the solution. However, non-specific binding or mis-bridging of PEG_{20} *bis*-sulfone **1** cannot be ruled out.

It was interesting that at pH 6.5 at 3 h (Lane 2, Figure 4-34 B), no $(PEG_{20})_2$-Fab_{alb} is observed; only PEG_{20}-Fab_{alb}, suggesting this pH and reaction time is favourable for preparing PEG_{20}-Fab_{alb}. Also it can be seen that after 16 h, there was no remaining Fab_{alb} at pH 7.0 and pH 7.4. There was excess PEG *bis*-sulfone **1**, so this could explain why more $(PEG_{20})_2$-Fab_{alb} was prepared. However, at pH 6.5, $(PEG_{20})_2$-Fab_{alb} was also prepared yet there was still some reduced Fab_{alb} remaining. This suggested conjugation of two PEG *bis*-sulfone **1** molecules is due to unspecific conjugation.

The band at ~60 kDa is thought to be the heavy or light chains from Fab_{alb}, from reduction of Fab_{alb}, which has been conjugated by PEG_{20} *bis*-sulfone **1**. It was observed as incubation time increased from 3 h to 16 h, the band of PEG_{20}-heavy or light chain of Fab_{alb} band was seen to reduce at pH 7.0 and pH 7.4 (Lanes 3-4, Figure 4-34 B/C). The bands of $(PEG_{20})_2$-Fab_{alb} and PEG_{20}-Fab_{alb} were seen to be deeper in colour, suggesting more of these conjugates had been made. Possibly, conjugation of the heavy or light chain of Fab_{alb} prepared PEG_{20}-Fab_{alb} or $(PEG_{20})_2$-Fab_{alb} explaining the increased prominence of these bands on the gel. However, the aim was to prepare PEG_{20}-Fab_{alb}, therefore the best conditions found where 3 h at pH 6.5,

as no higher MW impurities ($(PEG_{20})_2$-Fab_{alb}) were prepared (Lane 2, Figure 4-34 C).

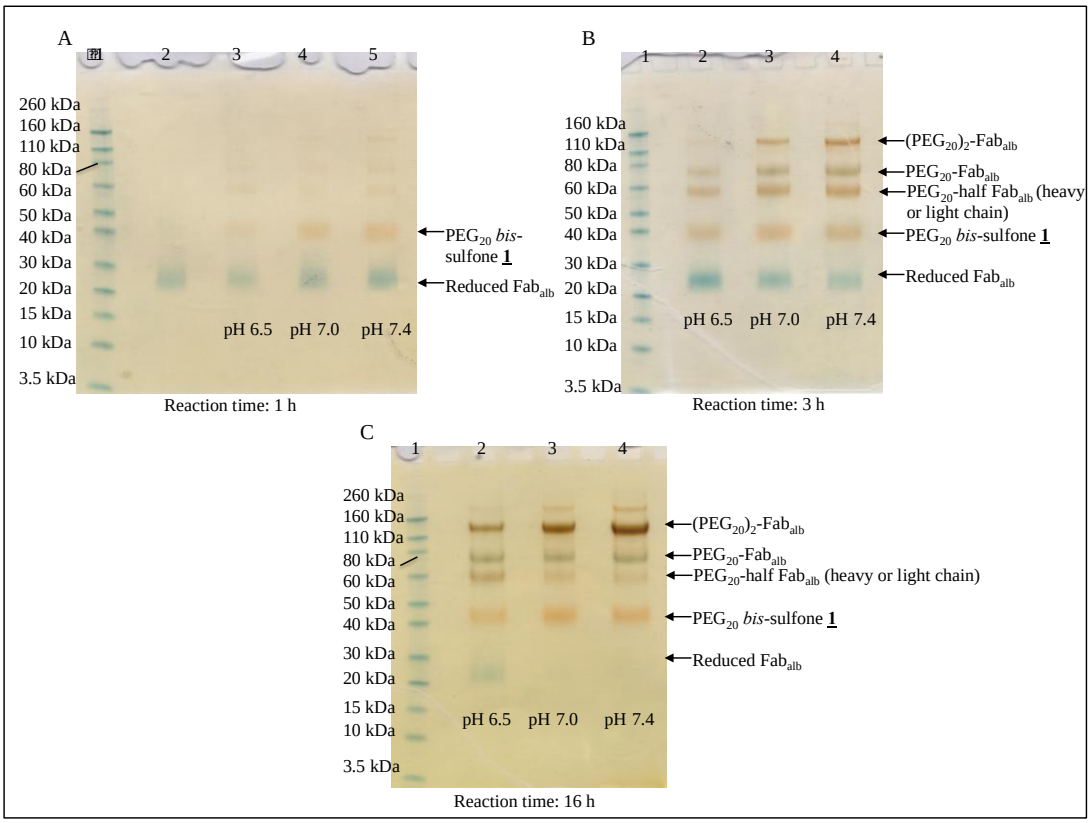

Figure 4-34. SDS-PAGE of the PEG_{20} *bis*-sulfone **1**-Fab_{alb} reactions with pH (pH 6.5,7, 7.4) and reaction time, A) 1 h, B) 3 h, C) 16 h optimisation. A) Lane 1: Novex pre-stained markers, Lane 2: reduced Fab_{alb}, Lane 3: pH 6.5, Lane 3: pH 7.0, Lane 4: pH 7.4. B/ C) Lane 1: Novex pre-stained markers, Lane 2: pH 6.5, Lane 3: pH 7.0, Lane 4: pH 7.4. For the preparation of PEG_{20} *bis*-sulfone **1**-Fab_{alb} 1:1 ratio of 3 h conjugation pH 6.5 found to optimum at 25 °C.

4.2.7.2 Conjugation of Fab_{alb} with PEG *bis*-sulfone **1**

The optimum conditions to prepare PEG_{20}-Fab_{alb} and to avoid high MW impurities were pH 6.5 for 3 h. However it was observed that there was some unreacted reduced Fab_{alb} (1:1 eq. PEG:Fab_{alb}) so in an effort to increase the yield of PEG_{20}-Fab_{alb} the reaction time was increased to 4 h instead of 3 h (Figure 4-34).

First, Fab_{alb} (Lane 2, Figure 4-35) was reduced with DTT (§2.2.9.12). The reduced Fab_{alb} was then allowed to react with PEG_{20} *bis*-sulfone **1** (~80 kDa, Lane 4-5, Figure 4-35). Unreacted reduced Fab_{alb} can be seen in Lanes 4 and 5 between 20-30 kDa, however as discussed there was a balance between PEG_{20}-Fab_{alb} yield, pH and conjugation specificity. Therefore, as no high MW impurities of $(PEG_{20})_2$-Fab_{alb} were observed in the reaction mixture (Lane 4-5, Figure 4-35), conjugation was viewed as successful, as only the conjugate of interest was prepared.

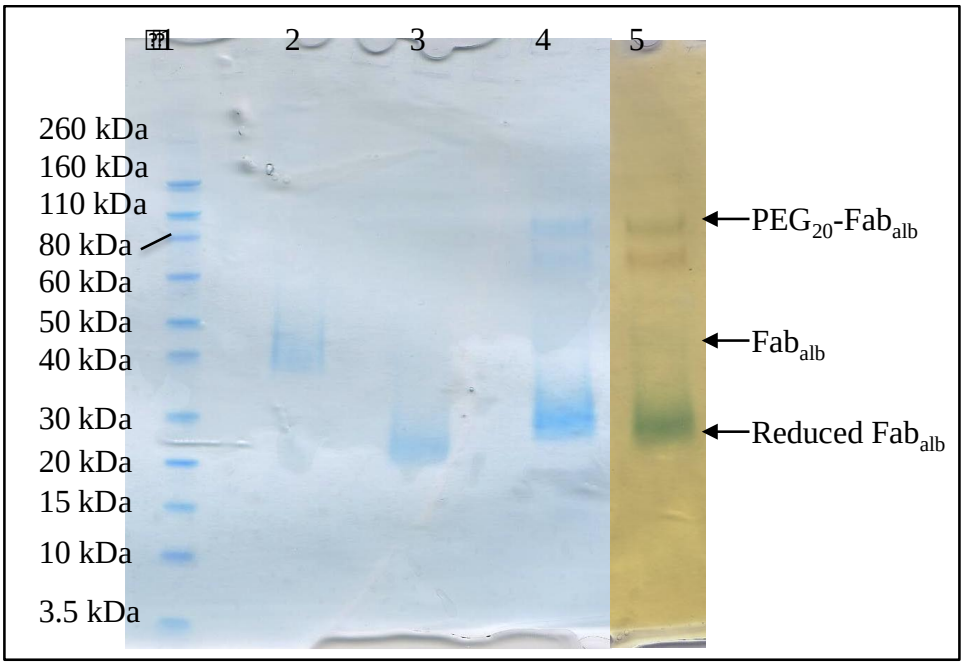

Figure 4-35. SDS-PAGE analysis (InstantBlue™ stain) on PEG_{20} *bis*-sulfone **1** –Fab_{alb} reaction mixture. Lane 1: Novex pre-stained markers, Lane 2: Fab_{alb}, Lane 3: DTT reduced, Lane 4: PEG_{20} *bis*-sulfone **1**-Fab_{alb} reaction mixture, (PEG stain) Lane 5: PEG_{20} *bis*-sulfone **1**-Fab_{alb} reaction mixture. Successful conjugation of reduced Fab_{alb} to prepare PEG_{20}-Fab_{alb}.

4.2.7.3 SEC purification of the PEG_{20} *bis*-sulfone **1** –Fab_{alb} reaction mixture

To purify PEG_{20}-Fab_{alb} from the reaction mixture, SEC purification was used (§2.2.9.14). CIEC was first tried twice however, but no separation of the PEG_{20}-Fab_{alb} from the reaction mixture could be achieved. As CIEC is the purification is the separation of proteins by differences in binding affinity for the resin, this suggests the conjugation of PEG_{20} *bis*-sulfone **1** to Fab_{alb} has not drastically changed the binding affinity of Fab_{alb} due to CIEC not being able to purify PEG_{20}-Fab_{alb} from Fab_{alb}. This was unexpected since PEGylation typically results in a conjugate that is less able to bind to the column than the unmodified protein.

SDS-PAGE analysis (Figure 4-36 B) of the fractions collected from SEC purification (Figure 4-36 A) shows PEG_{20}-Fab_{alb} was purified from Fab_{alb}. However, PEG_{20}-Fab_{alb} (Lane 3-4, Figure 4-36) could not be purified from PEG_{20}-half Fab_{alb}. The final yield of PEG_{20}-Fab_{alb} successfully purified from Fab_{alb} was 28.8% (n=1). Although this was lower than that achieved for PEG_{20}-Fab_{beva} (44%, 41μg/mL, 2 mL, §4.2.3.3), the yield was sufficient for the binding studies. Yields of ~65% have been stated in literature for disulfide-conjugated Fabs (Khalili et al., 2012), however, this was the first time polyclonal anti-rat albumin Fab had been conjugated to, thus more

optimisation regarding pH, reaction time, purification and equivalents could be conducted to improve the yield.

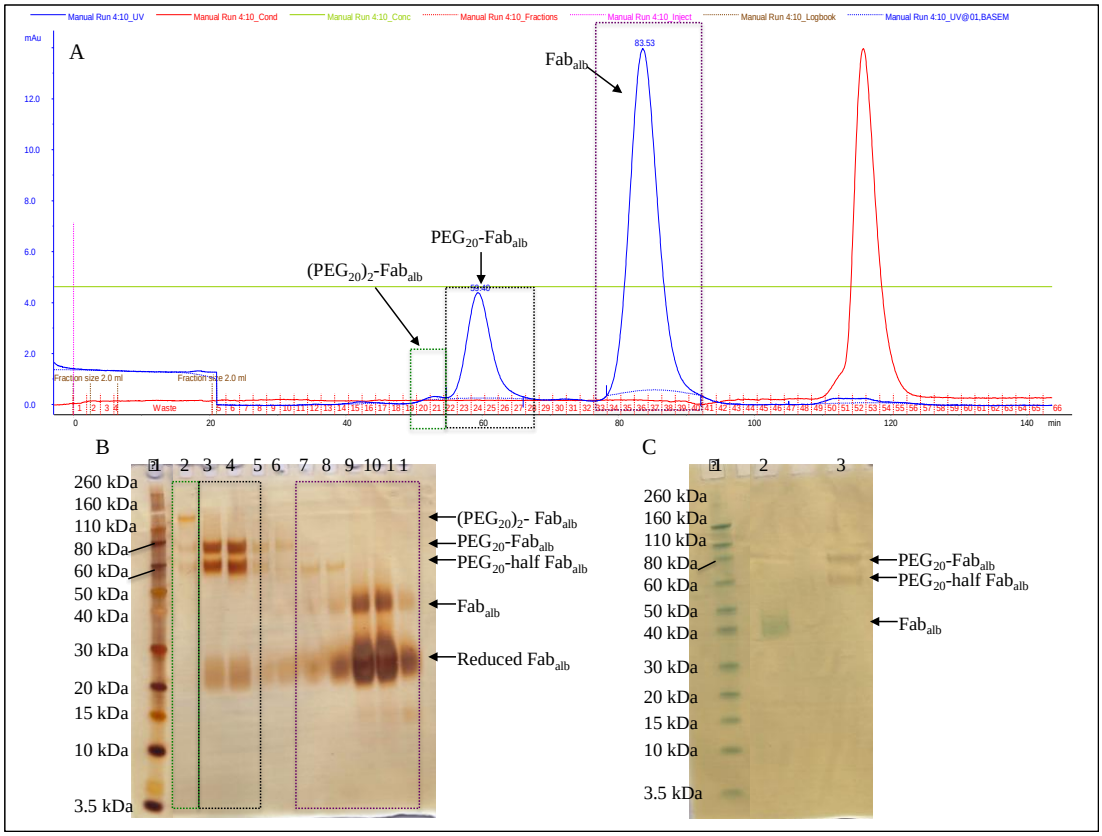

Figure 4-36. A) Chromatogram and B) SDS-PAGE (silver stain) of fractions from SEC purification of PEG_{20} *bis*-sulfone 1-Fab_{alb} reaction mixture, C) SDS-PAGE (InstantBlue™ and PEG stain) of final PEG_{20}-Fab_{alb} conjugate. B) Lane 1: Novex pre-stained markers, Lane 2: $(PEG_{20})_2$-Fab_{alb}, Lanes 3-4: PEG_{20}-Fab_{alb}/PEG_{20}-half Fab_{alb}, Lanes 7-11: Fab_{alb} and reduced Fab_{alb}. C) Lane 1: Novex pre-stained markers, Lane 2: Fab_{alb}, Lane 3: final PEG_{20}-Fab_{alb}. SEC purified PEG_{20}-Fab_{alb} was used as a control in IFN-PEG_{20}-Fab_{alb} functionality testing.

4.2.8 Characterisation of Fab_{beva}-PEG_{20}-IFN and Fab_{alb}-PEG_{20}-IFN

Characterisation in terms of purity (SDS-PAGE) and identity (Western blot) was conducted on the IFN-PEG_{20}-Fab heterodimers and PEG_{20}-Fab controls prior to functionality testing (binding affinity and *in vitro* activity assays).

4.2.8.1 Characterisation of IFN-PEG_{20}-Fab and PEG_{20}-Fab conjugates

SDS-PAGE analysis of the final bevacizumab compounds was performed, where after InstantBlue™ stain, densitometric analysis was conducted on the gel (§2.2.1). Bevacizumab and Fab_{beva} were also run for comparison (Figure 4-37 B), PEG_{20}-Fab_{beva} was present as a band at ~90 kDa (50 kDa for Fab_{beva} + 40 kDa for PEG_{20}) (Lane 4, Figure 3-37). In Lane 5 (Figure 4-37 B), IFN-PEG-Fab_{beva} conjugate was

visible as being 110 kDa in size (20 kDa for IFN + 50 kDa for Fab_{beva} + 40 kDa for PEG_{20}). It was also noted that on the SDS-PAGE gel (Figure 4-37 B) the bands for PEG_{20}-Fab_{beva} and IFN-PEG_{20}-Fab_{beva} had a green colour compared to those for bevacizumab and Fab_{beva}. This is due to the overlapping colours for the protein (stained blue) and the PEG moiety (stained orange). In addition, the band for IFN-PEG_{20}-Fab_{beva} was less green in colour in comparison to the PEG_{20}-Fab_{beva} band due to the additional IFN conjugated to the PEG di(*bis*)sulfone **1**.

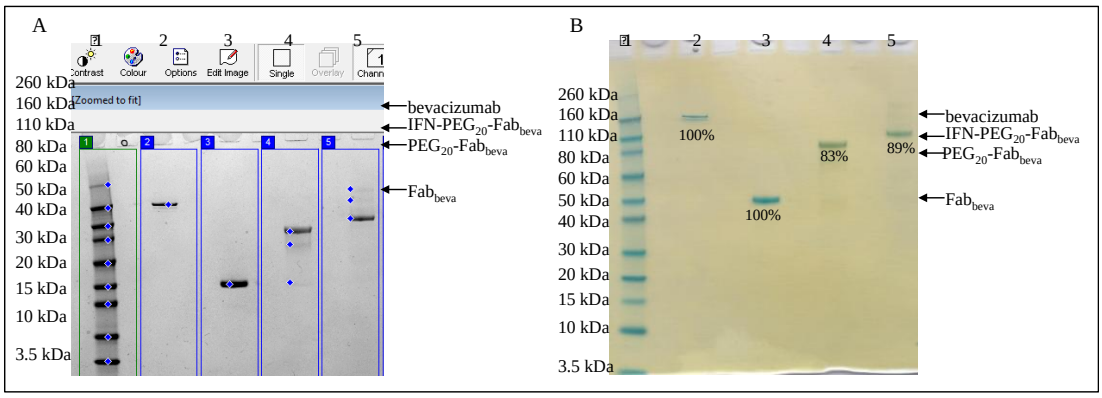

Figure 4-37. A) ImageQuant™ densimetric image and B) SDS-PAGE analysis (InstantBlue™ + PEG stain) of bevacizumab compounds. Lane 1: Novex pre-stained markers, Lane 2: bevacizumab, Lane 3: Fab_{beva}, Lane 4: PEG_{20}-Fab_{beva} and Lane 5: IFN-PEG_{20}-Fab_{beva}. Densimetric analysis showed that the bevacizumab conjugates were prepared in good purity (>80%).

ImageQuant™ LAS 4000 digital imaging system was used with the transillumination setting for densitometric analysis (Figure 4-37 A). The results showed that Fab_{beva} prepared from digested bevacizumab was 100% pure while PEG_{20}-Fab_{beva} and IFN-PEG_{20}-Fab_{beva} were 83% and 89% pure respectively. In Lane 4 (Figure 4-37 A), several bands below ~90 kDa were observed which could be Fab_{beva} at 50 kDa and PEGylated single chain at ~80 kDa. In Lane 5 (Figure 3-37 A), two impurity bands above 110 kDa could be Fab_{beva}-PEG-Fab_{beva} (~140 kDa) or $(PEG_{20})_n$-$(Fab_{beva})_n$ (~170 kDa). However, as these bands were in trace amounts as they could not be visible with InstantBlue™ stain whose limit of detection is 5 ng. These impurities were considered to be due to the purification conditions used rather than product instability, thus stability studies were conducted to confirm this.

SDS-PAGE analysis of IFN-PEG_{20}-Fab_{alb} showed the samples to be pure by silver stain analysis, as no other bands were visible (Figure 4-38, Lane 4). SDS-PAGE PEG_{20}-Fab_{alb} showed some faint bands above and below the PEG_{20}-Fab_{alb} at ~80 kDa. However, these are in very low concentration due to being only slightly

visible by silver stain (Lane 3, Figure 4-38). Fab_{alb} was shown to be ~50 kDa and pure by InstantBlue™ stain (Lane 2, Figure 4-38).

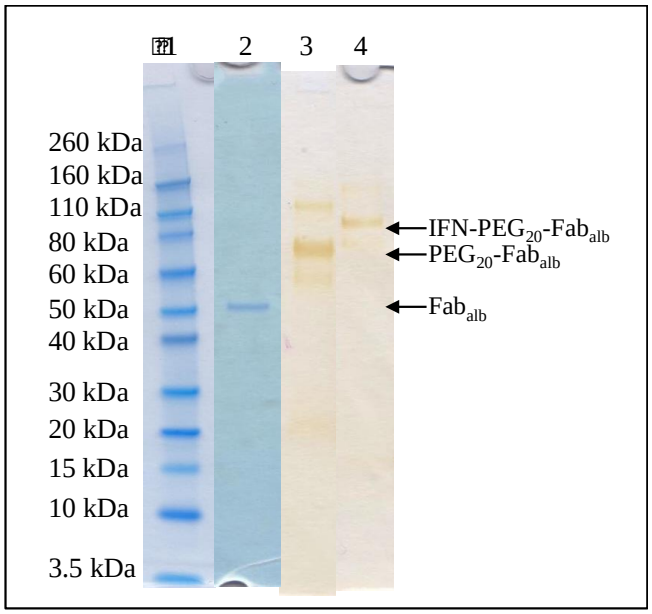

Figure 4-38. SDS-PAGE analysis of IFN-PEG_{20}-Fab_{alb}, PEG_{20}-Fab_{alb} (silver stain) and Fab_{alb} (InstantBlue™ stain). Lane 1: Novex pre-stained markers, Lane 2: Fab_{alb}, Lane 3: PEG_{20}-Fab_{alb} and Lane 4: IFN-PEG_{20}-Fab_{alb}. SDS-PAGE analysis shows the samples to be pure, with light impurity bands visible for PEG_{20}-Fab_{alb}.

4.2.8.2 Identity confirmation by Western blot of IFN-PEG_{20}-Fab heterodimers and controls

Western blot of anti-IFN α-2 and anti-human were used to identify the bevacizumab and IFN samples (§ 2.2.10.1.). Goat anti-human κ-chain HRP-conjugated Fab'_2 was used to detect the κ-light chains on bevacizumab and Fab_{beva} samples. The anti-human detection antibody is HRP-conjugated which can be detected by enhanced chemiluminescence (ECL). All the bevacizumab samples were visualised and thus the identities of bevacizumab, Fab_{beva}, PEG_{20}-Fab_{beva} and IFN-PEG_{20}-Fab_{beva} were confirmed by their detection and migration patterns (Figure 4-39 A).

The anti-human IgG Western blot successfully detected the κ-light chain of Fab_{beva} within the IFN-PEG_{20}-Fab_{beva} conjugate, but to confirm the identity of the IFN-PEG_{20}-Fab_{beva} conjugate, IFN must also be identified. For this an anti-IFN α-2 Western blot was conducted (§ 2.2.10.1.). Here, a colorimetric method of detection was used using a substrate for alkaline phosphatase, so the Novex pre-stained markers could also be observed. IFN was included as a positive control (Lane 2) and detected near the 15 kDa ladder (Figure 4-39 B). Similarly, IFN-PEG_{20}-Fab_{beva} conjugate was also detected near the 110 kDa ladder and confirmed the presence of

IFN within the IFN-PEG_{20}-Fab_{beva} conjugate. Impurities, also discussed previously (Figure 4-39 B), were more prominent in this study due to the greater sensitivity of the Western blot method.

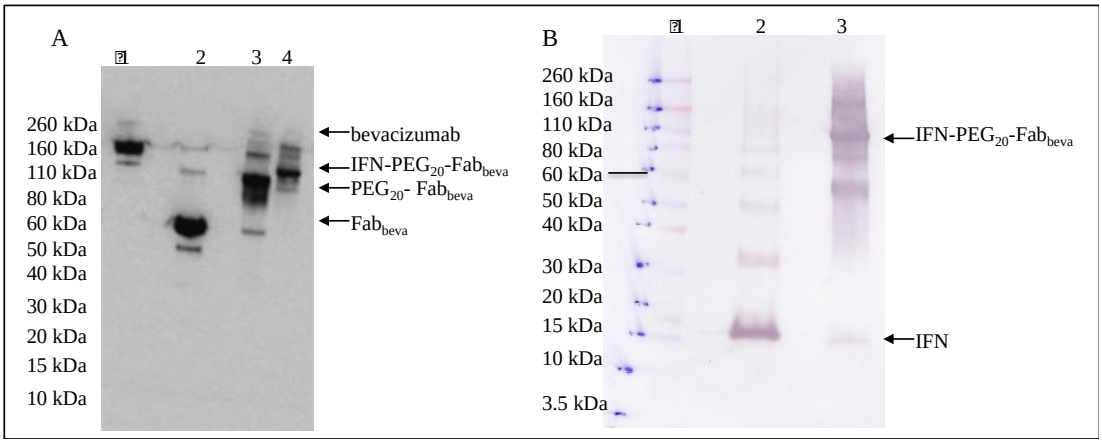

Figure 4-39. A) anti-human and B) anti-IFN α-2 Western blot of bevacizumab samples. A) Lane 1: bevacizumab, Lane 2: Fab_{beva}, Lane 3: PEG_{20}-Fab_{beva}, Lane 4: IFN-PEG_{20}-Fab_{beva}. B) Lane 1: Novex pre-stained markers, Lane 2: IFN, Lane 3: IFN-PEG_{20}-Fab_{beva}. Anti-human and anti-IFN α-2 Western blots successfully identify all bevacizumab samples.

To confirm the identity of the anti-rat albumin conjugates prepared, anti-IFN α-2 and anti-rabbit Western blots were conducted (§ 2.2.10.1). For the detection of the rabbit anti-rat albumin species a polyclonal anti-rabbit IgG (H&L) AP-conjugated IgG was used. A colorimetric method of detection was used, so the Novex pre-stained markers could also be observed. In the resulting Western blot (Figure 4-40 A) Fab_{alb}, PEG_{20}-Fab_{alb} and IFN-PEG_{20}-Fab_{alb} were successfully identified, positively identifying the presence of the rabbit Fab_{alb} within in the conjugates. Furthermore, as the ladder is present, the MW of the conjugates could be assessed. In Lane 2 (Figure 4-40 A) Fab_{alb} was visualised at ~45 kDa, this MW confirmed the identity of Fab_{alb}, as this was the MW achieved in previous SDS-PAGE analysis (Figure 4-24). In Lane 3 (Figure 4-40 A) PEG_{20}-Fab_{alb} can be seen at ~70 kDa, whilst in Lane 4, IFN-PEG_{20}-Fab_{alb} was identified at ~90 kDa. The MW's achieved in the Western blot for these conjugates, match those achieved in previous SDS-PAGE analysis (Figure 4-38).

However, to successfully identify the IFN-PEG-Fab_{alb} conjugate, IFN must be identified, to confirm its presence within the conjugate. For this an anti-IFN α-2 Western blot was performed (§ 2.2.10.1.). In Lane 2 (Figure 4-40 B) IFN was observed between 15-20 kDa, this MW is the same as that achieved in previous analysis (Figure 4-38). Whilst in Lane 3, the IFN-PEG_{20}-Fab_{alb} can be seen at ~110

kDa (Figure 4-40 B). This confirms the presence of IFN within the IFN-PEG_{20}-Fab_{alb} conjugate and its identity. Therefore, from the anti-rabbit and anti-IFN α-2 Western blots conducted, the identity of Fab_{alb}, PEG_{20}-Fab_{alb} and IFN-PEG_{20}-Fab_{alb} were confirmed.

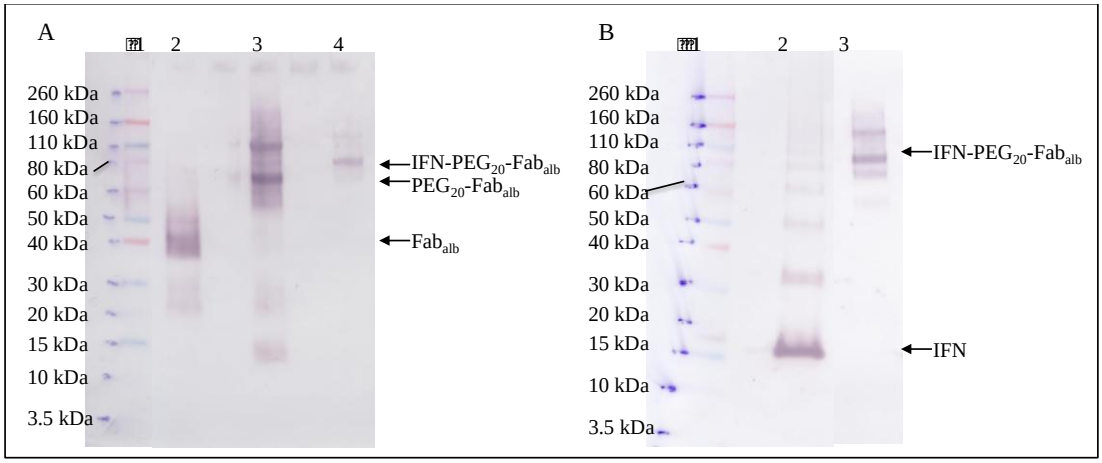

Figure 4-40. A) anti-rabbit and B) anti-IFN α-2 Western blots of anti-rat albumin compounds. A) Lane 1: Novex pre-stained markers, Lane 2: Fab_{alb}, Lane 3: PEG_{20}-Fab_{alb}, Lane 4: IFN-PEG_{20}-Fab_{alb}. B) Lane 1: Novex pre-stained markers, Lane 2: IFN, Lane 3: IFN-PEG_{20}-Fab_{alb}. The anti-rabbit and anti-IFN α-2 Western blots conducted positively identified Fab_{alb}, PEG_{20}-Fab_{alb} and IFN-PEG_{20}-Fab_{alb}.

It can be observed in Figure 4-39 and Figure 4-40 that there are two areas where the Western blots could be improved. First, there is a smearing of the protein bands; which is caused by high voltage or air bubbles present during transfer (Mahmood and Yang, 2012). This can be overcome by ensuring that a lower voltage and thus longer transfer is conducted. Further prior to transfer, the gel and nitrocellulose membrane are rollered to ensure no air bubbles are between them. Second, there is high background observed in some sample columns (e.g. Figure 4-40 A, Lane 3), this could be avoided by using a lower sample concentration.

4.2.8.3 Stability assessment of IFN-PEG_{20}-Fab

Stability studies were conducted with Fab_{beva}, PEG_{20}-Fab_{beva} and IFN-PEG_{20}-Fab_{beva} to determine if they underwent de-conjugation or non-reversible aggregation in simulated storage and *in vitro* assay conditions. As shown in §4.2.2.5, all samples were considered stable at the time they were made and at the start of the stability studies, with no changes observed by SDS PAGE.

Firstly, one-week stability studies were conducted by incubating the compounds in 50 mM sodium phosphate buffer, 150 mM NaCl pH 7.8 for 7 days at 4 °C. The results showed no evidence of free protein (IFN or Fab_{beva}) or de-PEGylation

when analysed by SDS-PAGE (Figure 4-41 A). This study indicates that Fab_{beva}, PEG_{20}-Fab_{beva} and IFN-PEG_{20}-Fab_{beva} were stable for at least 7 days at 4 °C.

Accelerated stability studies were also performed by incubating IFN-PEG-Fab_{beva} conjugate (40 µg/mL) at 50 ºC (1 h) with or without 20 mM DTT (§ 2.2.10.5). DTT was added to induce de-PEGylation. Sample analysis was conducted by SDS-PAGE with the resulting gel stained using InstantBlue™ and PEG stain. The results showed no de-PEGylation from incubation with DTT, this demonstrates that STAB treatment has fully reduced the ketone group within the di(*bis*)sulfone linker (Figure 2-2) as the DTT could not react with the ketone group to induce de-conjugation.

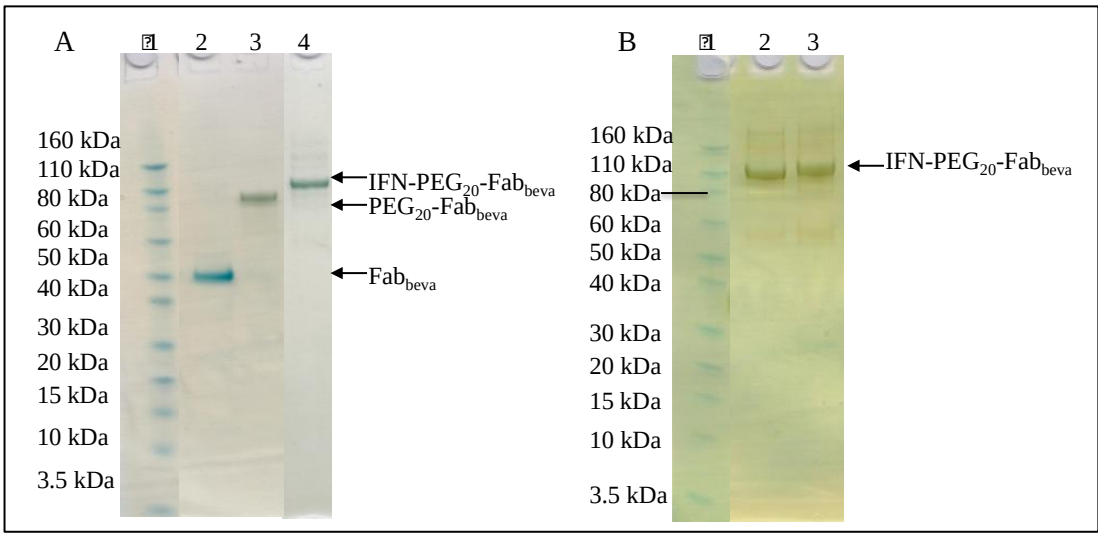

Figure 4-41. SDS-PAGE analysis of Fab_{beva} samples stability studies at A) 4 °C for 7 days and B) 50 °C for 1 h. A) Lane 1: Novex pre-stained markers, Lane 2: Fab_{beva}, Lane 3: PEG_{20}-Fab_{beva}, Lane 4: IFN-PEG_{20}-Fab_{beva}, B) Lane 1: Novex pre-stained markers, Lane 2: IFN-PEG_{20}-Fab_{beva} –DTT and Lane 3: IFN-PEG_{20}-Fab_{beva} +DTT. All Fab_{beva} compounds were shown to be stable at 4 °C for 7 days and IFN-PEG_{20}-Fab_{beva} shown to be stable for 1 h at 50 °C ±DTT.

A one-week stability study was then conducted with PEG_{20}-Fab_{alb} and IFN-PEG_{20}-Fab_{alb}. As shown in §4.2.6.5, the Fab_{alb} samples were stable at day 0, where no free IFN or Fab_{alb} was observed in the conjugated compounds. The compounds were again stored in 50 mM sodium phosphate buffer, 150 mM NaCl pH 7.8 for 7 days at 4 °C. Analysis by SDS-PAGE (Figure 4-42) indicated there was no free IFN (~20 kDa) or Fab_{alb} (45 kDa) in either sample. In Lane 3 (Figure 4-42), PEG-Fab_{alb} can be observed at ~80 kDa (Fab_{alb}= ~45 kDa + PEG_{20}=40 kDa), while in Lane 2 (Figure 4-42), IFN-PEG_{20}-Fab_{alb} can be seen at ~110 kDa (IFN=20 kDa+ PEG_{20}=40

kDa+ Fab_{alb}=~45 kDa). These observations indicate that PEG_{20}-Fab_{alb} and IFN-PEG_{20}-Fab_{alb} are stable for 7 days at 4 °C.

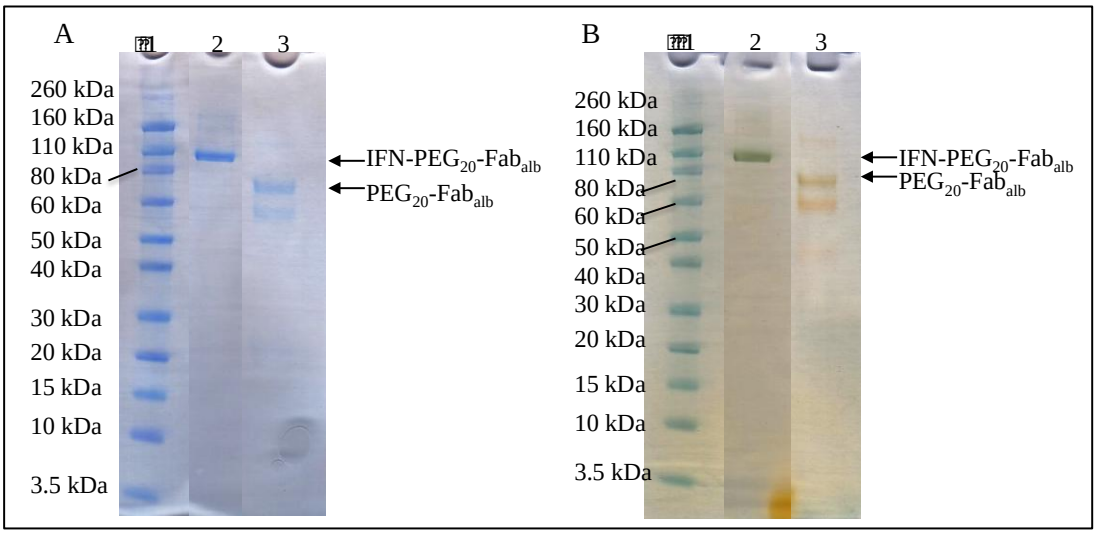

Figure 4-42. 7 day at 4 °C stability study of PEG_{20}-Fab_{alb} and IFN-PEG_{20}-Fab_{alb} analysed by SDS-PAGE A) InstantBlue™, B) PEG stain. Lane 1: Novex pre-stained markers, Lane 2: IFN-PEG_{20}-Fab_{alb}, Lane 3: PEG_{20}-Fab_{alb}. No free protein (IFN or Fab_{alb}) can be observed by SDS-PAGE analysis, therefore PEG_{20}-Fab_{alb} and IFN-PEG_{20}-Fab_{alb} are stable for 7 days at 4 °C.

4.2.9 Functional activity assessment of IFN-PEG_{20}-Fab heterodimers

Both IFN-PEG_{20}-Fab_{beva} and IFN-PEG_{20}-Fab_{alb} were then evaluated by *in vitro* assays to determine if there was any retained Fab binding and IFN activity. The results were compared against controls, IgG, Fab and PEG_{20}-Fab for anti-rat albumin and bevacizumab. As IFN is a pleiotropic protein, both antiviral and antiproliferative assays were used to better assess the conjugates retained *in vitro* activity. SPR was used to assess the Fab_{beva}/Fab_{alb} retained binding kinetics.

4.2.9.1 Binding properties of IFN-PEG_{20}-Fab heterodimers

The affinity and avidity of a mAb with its antigen is crucial for biological activity (Rudnick and Adams, 2009). Affinity and avidity, although often confused, are related to describe the binding properties of mAbs (Rudnick and Adams, 2009). Avidity is often referred to as functional affinity and is the accumulated strength of multiple affinities from multiple, often cooperative, binding interactions (Rudnick and Adams, 2009). Affinity is a thermodynamic term to describe the strength of interaction between the single antigen and a single binding region of the mAb (Rudnick and Adams, 2009). Affinity is calculated from the formation a complex (AB) between interacting proteins, for example mAb (A) and its antigen (B)

(Myszka, 1997). However, affinity is often expressed as its reciprocal, which is known as the equilibrium dissociation constant ($K_D=k_d/k_a$).

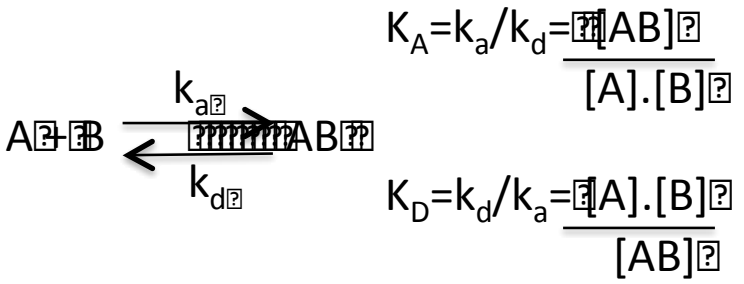

Figure 4-43. Affinity can be expressed as K_D or K_A but is often expressed as K_D (Myszka, 1997)

The binding of IgG is bivalent, whereas the binding of Fab is monovalent. IFN-PEG-Fab heterodimers were prepared to assess if PEG_{20} di(*bis*)sulfone **4** can be used to conjugate two therapeutic proteins site-specifically and that the proteins will retain their functional activity. The end groups in polymers are thought to be close spatially in solution and move more frequently compared to the rest of the polymer structure (Shewmake et al., 2008). It has been shown that the conjugates prepared with PEG di(*bis*)sulfone **4** have smaller dynamic volumes than those prepared using PEG *bis*-sulfone **1** with the same PEG MW (Khalili et al., 2013). Site-specific conjugation of PEG molecules to antibody fragments (Fab) have shown no significant conformational changes to the Fabs itself (Lu et al., 2008). To determine if the Fab retained activity within the IFN-PEG_{20}-Fab heterodimers, it was necessary to determine their binding affinities and compare them to Fab and PEG_{20}-Fab. Surface plasmon resonance (SPR) was used for these studies.

SPR biosensors have become an established method to measure protein-protein interactions, such as antibody-antigen interactions in real time, without labelling requirements (Markey, 1999; Myszka, 1997). In SPR, one protein or ligand is immobilised onto the chip surface (termed 'ligand') and monitoring its interaction with a second component flowing over the chip in solution (termed 'analyte') (Myszka, 1997). The SPR instrument measures the change in refractive index of the solvent near the surface chip of the immobilised ligand that occurs during complex formation and dissociation (Figure 4-44) (Cooper, 2002; Markey, 1999). For the binding affinity measurements of the heterodimers and controls, a commercially available SPR instrument, BIAcore X100 (Biomolecular Interaction Analysis) was used.

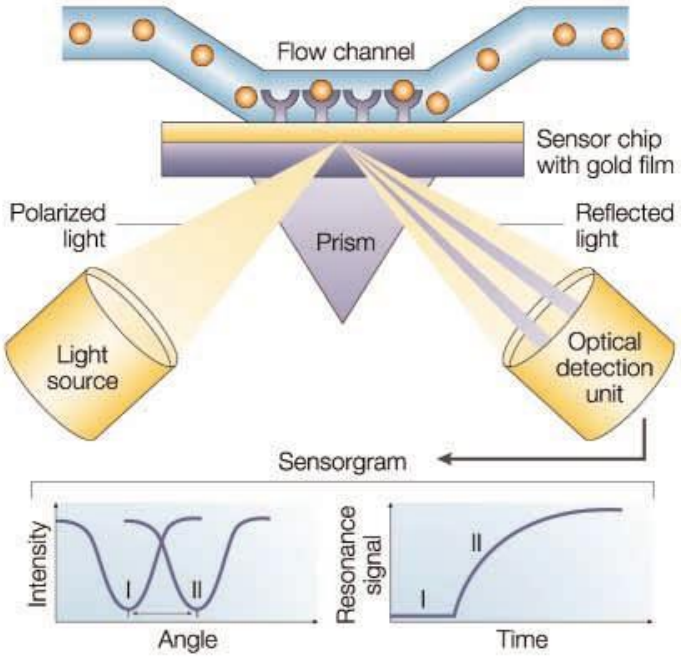

Figure 4-44. Typical SPR biosensor set up (Cooper, 2002)

The sensor chips used for immobilisation are coated in a gold layer (50 nm thick). These provide the conditions for the SPR phenomenon (Figure 4-44) (Cooper, 2002). Carboxymethylated dextran of varying lengths is covalently attached to the gold surface. These chips are called CM chips (e.g. CM3 and CM5). CM3 chips were used due to their shorter dextran strands, which reduce surface interactions and rebinding effects. To study the binding of bevacizumab conjugates, vascular endothelial growth factor (VEGF, ~38 kDa) was immobilised on a CM3 chip. Rat albumin (~65 kDa) was immobilised on another CM3 chip to study the Fab anti-rat albumin conjugates.

The binding response is related to mass changes on the chip surface and results in changes in the measured intensity of the refractive index. The signal generated is given in resonance units (RU), which are approximately proportional to a change in mass (few pg per millimetre squared) (Myszka, 1997). The resulting plot is known as a sensogram and involves three steps: association, dissociation and regeneration (Figure 4-45). The association step is the analyte in running buffer flowing over the immobilised ligand. Association relates the analyte binding to the immobilised ligand. The dissociation phase occurs when the analyte is replaced by buffer to allow the analyte-ligand complex to dissociate. The regeneration step involves flowing a buffer solution to remove remaining bound analyte from the immobilised receptor without causing any damage to the immobilised ligand. The regeneration step

prepares the chip surface for the next kinetic analysis cycle (Figure 4-45) (Cooper, 2002).

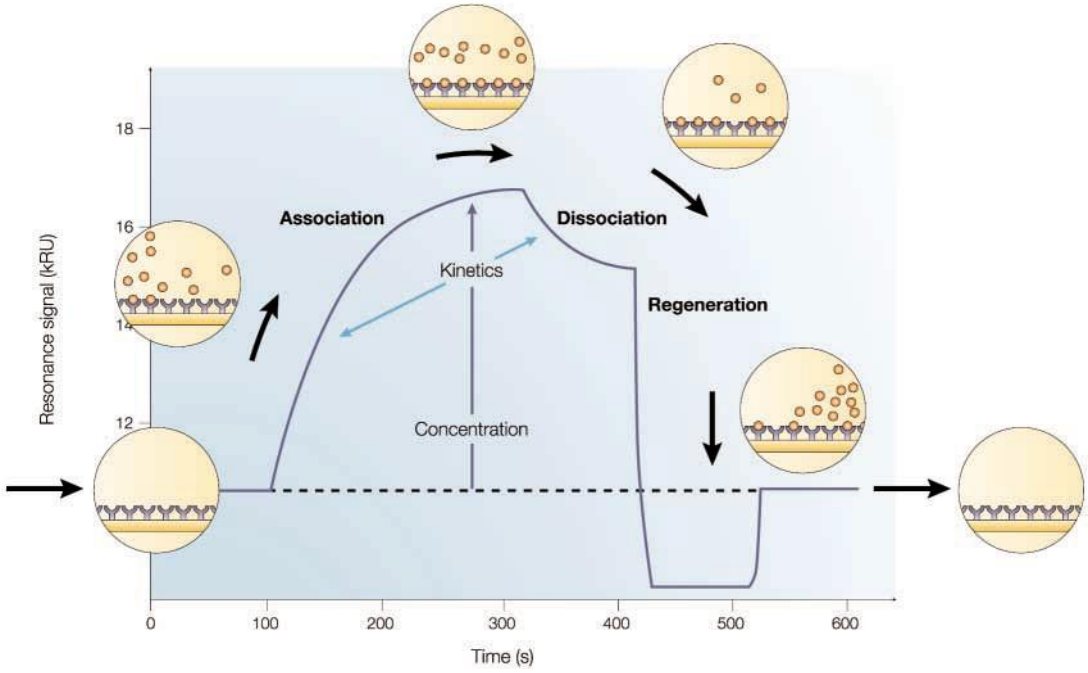

Figure 4-45. Typical sensogram binding curve observed on SPR (Cooper, 2002)

Since Fab_{beva} and Fab_{alb} were obtained by proteolytically digesting bevacizumab and polyclonal anti-rat albumin IgG, it was necessary to determine the binding affinity of these Fabs. It was also necessary to evaluate the corresponding PEG-Fab conjugates as controls. These controls were prepared to understand how the PEG *bis*-sulfone **1** affects the binding affinity of the parent Fabs and how this compared to the heterodimer binding affinities. Heterodimers, IFN-PEG_{20}-Fab_{beva} and IFN-PEG_{20}-Fab_{alb} were prepared to assess if the PEG_{20} di(*bis*)sulfone **4** can be used to conjugate two proteins and while retaining their activities. A summary of all the constructs that were prepared and tested regarding their binding affinity is seen in Table 4–2.

Table 4–2. Summary table of prepared constructs tested by SPR

Antibody	Fab	PEG-Fab	Heterodimer
Bevacizumab	Fab_{beva}	PEG_{20}-Fab_{beva}	IFN-PEG_{20}-Fab_{beva}
Anti-rat albumin IgG	Fab_{alb}	PEG_{20}-Fab_{alb}	IFN-PEG_{20}-Fab_{alb}

Binding capacity of the chip surface is dependent on the level and activity of the immobilised ligand. The SPR response correlates with mass concentration of material on the chip surface. This depends on the relative MW of the analyte and

ligand, and on the stoichiometry of interaction between analyte and ligand. The maximum binding capacity (R_{max}) of the sensor surface ligand with analyte in RU can be calculated as follows:

$$R_{max}=\text{MW analyte/ MW ligand} \times S_m \times R_L$$

R_{max} is the maximum capacity of binding analyte, where R_L is the actual level or amount of ligand on the chip surface; S_m is the binding stoichiometry between analyte and ligand. Not all of the immobilised ligand will be available for binding to the analyte, as some of the ligand may be damaged during immobilisation and regeneration, thus the theoretical R_{max} is often higher than the experimental R_{max}. The R_{max} of immobilised ligand is optimally between 50 to 150 RU for conducting kinetic studies. The use of a low ligand density will help to minimise mass transfer and rebinding limitations.

Three steps are performed to immobilise a ligand on a CM3 chip:

1. Ligand pre-concentration
2. Immobilisation step
3. Regeneration step.

Pre-concentration assay

Electrostatic attraction provides an efficient means for associating positively charged ligands onto the negatively charged carboxymethylated dextran on the sensor surface. To do this, the pH of the ligand solution should between pH 3.5 and the isoelectric point of the ligand, so that the sensor surface and the ligand carry opposite charges. The pI of rat albumin is 5.7 (Sigma product information). Human $VEGF_{165}$ has a pI value of 8.6. Many proteins have a tendency to aggregate or denature at low pH, so it is necessary to determine an optimum pH, which is a compromise between efficient pre-concentration and not denaturing/precipitating the ligand. To determine the optimum pH for interactions between the ligand and the sensor chip, a pH scouting experiment was performed for rat albumin with sodium acetate at pH 4,4.5,5, 5.5 (§ 2.2.11.11).

Interestingly, at pH 5.5 (pink line, Figure 4-46), low association of the rat albumin to the sensor chip was observed. However, at pH 5.0 (blue line, Figure 4-46) the highest binding of rat albumin to the sensor chip was observed, so this pH was used for immobilisation of rat albumin to the CM3 chip. Lower interaction was observed at pH 4.0 and 4.5 (green and orange lines respectively, Figure 4-46). Since

the response correlated with pH, until pH 5.5, this shows the interactions are driven primarily by electrostatic interactions. However at pH 5.5, there is sharp drop in associated compared to pH 5.0, this is due to the pH being close the pI of rat albumin (pI=5.7). Sodium hydroxide (50 mM) was used to regenerate the CM3 chip for immobilisation.

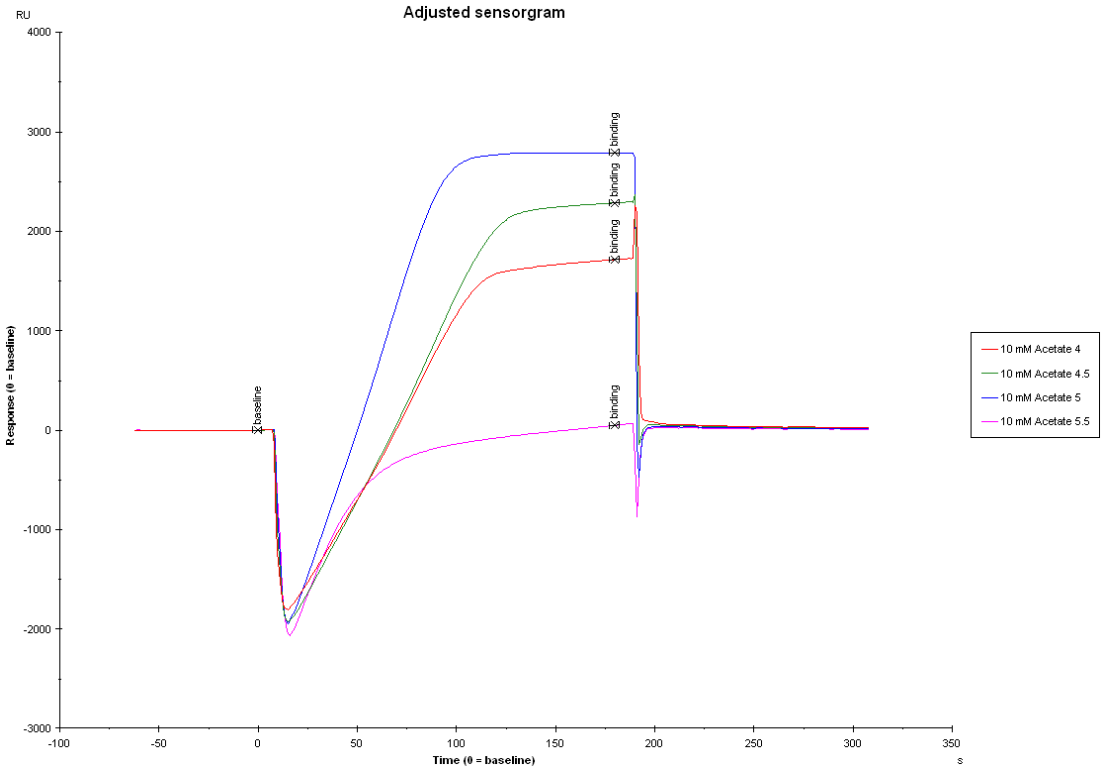

Figure 4-46. pH scouting assay using rat albumin (1 µg/mL) in sodium acetate buffer. It was found that 10 mM sodium acetate pH 5.0 was the optimum pH for the immobilisation of rat albumin to the CM chips.

Ligand Immobilisation

Immobilisation of the CM3 chip by amine coupling is conducted in three steps:

1. *Activation:* For coupling to take place, the carboxylic acids on the sensor chip surface are modified into activated esters using a 1:1 ratio of 1-theyl-3-(3-dimethylaminopropyl)-carbodiimide (EDC) and N-hydroxysuccinimide (NHS). (Figure 4-47).

2. *Coupling*: The ligand was injected over the NHS-activated carboxymethyl dextran surface. Amines in the ligand undergo reaction to covalently bond to the activated carboxylic acids on the dextran matrix (Figure 4-47). The ligand binds in a non-specific way to the chip surface. As most proteins contain several amine groups, efficient attachment to the sensor surface can be achieved while maintaining ligand-

binding surfaces that can then be utilised to evaluate the analyte. Amine coupling is the most widely used coupling technique; other techniques include thiol and ligand coupling.

3. *Deactivation*: Since not all the activated dextran carboxylic acids will have undergone a reaction with the ligand to be immobilised, a blocking amine solution such as ethanolamine is injected to quench remaining active succinimide ester moieties. This avoids covalent binding of the analyte to the sensor chip surface.

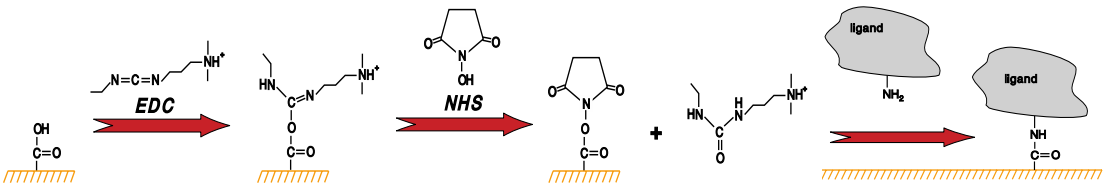

Figure 4-47. Activation by EDC/NHS of carboxymethyl dextran sensor surface and amine-coupling mechanism (adapted from BIAcore Sensor Surface Handbook).

Manual control on the BIAcore was used to immobilise separate CM3 chips with both VEGF and rat albumin. The optimum conditions for VEGF immobilisation was found to be 0.2 µg/mL in sodium acetate pH 5.5 for 150 sec to immobilise with the R_{max} of ~100 RU (Figure 4-48). For rat albumin immobilisation, the optimum conditions were 0.2 µg/mL in sodium acetate pH 5.5 for 180 sec, to immobilise CM3 with the R_{max} of ~70 RU (Figure 4-49). The theoretical R_{max} for VEGF (100 RU=38,000/50,000 ×1 ×R_L) and rat albumin (100 RU=65,000/50,000 ×1 ×R_L) were 76 RU and 130 RU respectively. Prior to achieving the optimum conditions for rat albumin immobilisation, different concentrations of rat albumin (0.1 to 1 µg/mL) were tried in conjunction with different contact times (120 sec-180 sec), to achieve a low RU. A low RU was necessary to avoid bulk transport effects and achieve accurate affinity data.

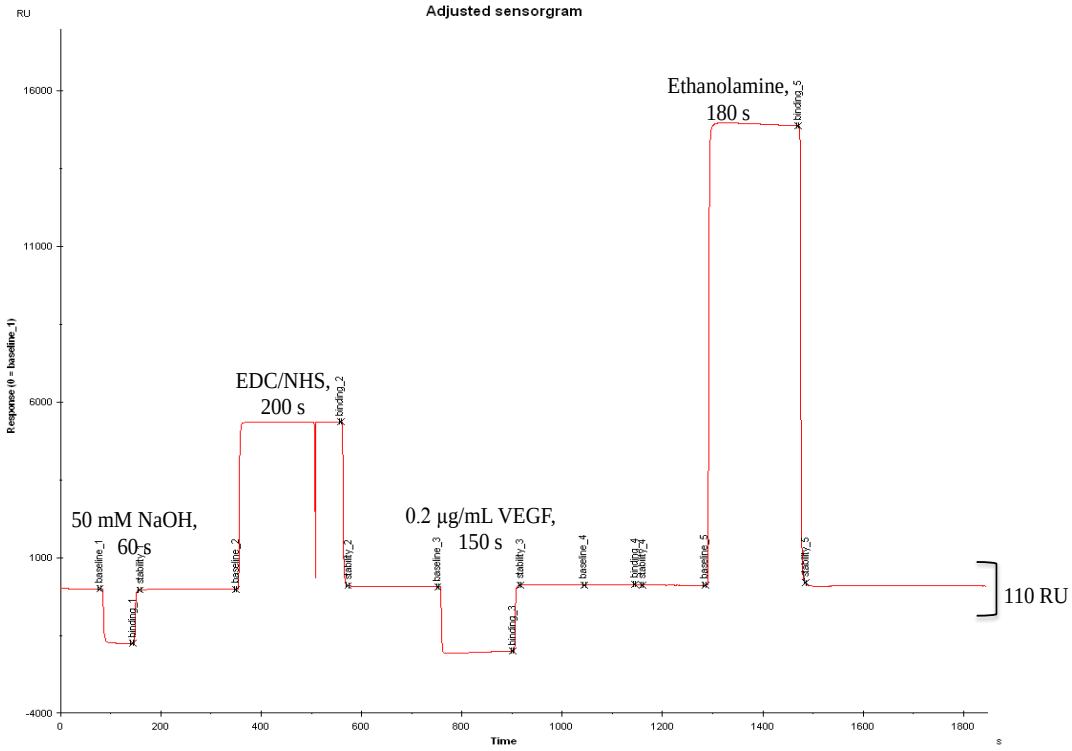

Figure 4-48. Manual immobilisation of VEGF (0.2 µg/mL) onto a CM3 chip using amine coupling to achieve 110 RU.

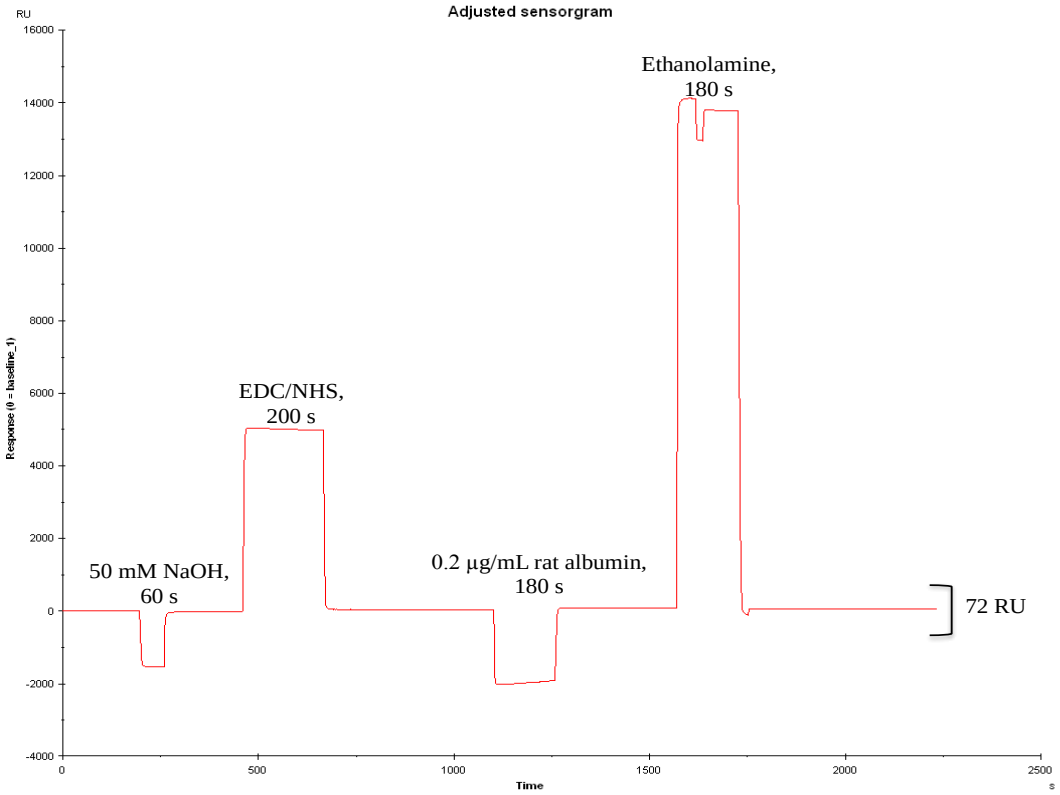

Figure 4-49. Manual immobilisation of rat albumin (0.2 µg/mL) onto a CM3 chip using amine coupling to achieve 72 RU.

The VEGF and rat albumin immobilised chips were then used for kinetic assays involving the novel heterodimeric constructs.

Regeneration

Regeneration is the process to remove bound analyte from the immobilised ligand while causing minimal change or damage to the immobilised ligand. Regeneration is required to prepare the chip for he next analysis. To determine the optimum regeneration conditions for rat albumin, scouting experiments were conducted. Scouting experiments were performed by repeated cycles of analyte binding and chip regeneration and examining the response level after each cycle. Recommended regeneration buffers include, sodium hydroxide, sodium chloride, magnesium chloride and SDS. The most widely used regeneration solution is 10 mM glycine-HCl at pH 1.5-3. Regeneration conditions were examined at pH 2.25 and pH 2.75 (§ 2.2.12).

It was found that glycine-HCl pH 2.25 was the optimal regeneration condition for rat albumin. This was determined, as literature recommends no more than 10% increase in baseline after repeated cycles of binding and regeneration. A decrease in the baseline can be observed for pH 2.75, showing the removal of rat albumin after regeneration. Regeneration using glycine-HCl pH 2.25 showed a steady baseline, after 4 binding and regeneration cycles, thus pH 2.25 was used for the regeneration of the rat albumin chip after kinetic analysis of the rat albumin derivatives. For VEGF immobilisation the optimum regeneration condition was pH 2.0 (Khalili et al., 2012, 2013).

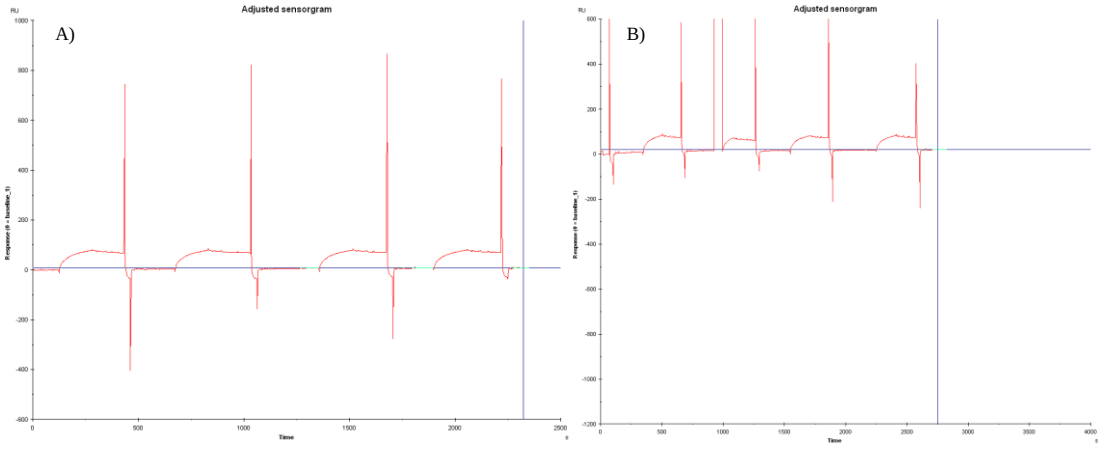

Figure 4-50. Regeneration optimisation of rat albumin immobilised chip using glycine-HCl A) pH 2.25 and B) pH 2.75. Results showed the glycine-HCl pH 2.25 was optimum for regeneration of the immobilised rat albumin chip.

A control-binding assay was conducted using the VEGF immobilised chip to determine whether IFN binds to VEGF. No increase in RU was observed after IFN

injection (Figure 4-51), showing IFN does not bind to VEGF, thus binding data achieved for IFN-PEG-Fab_{beva}, is from the Fab_{beva} binding to VEGF not IFN.

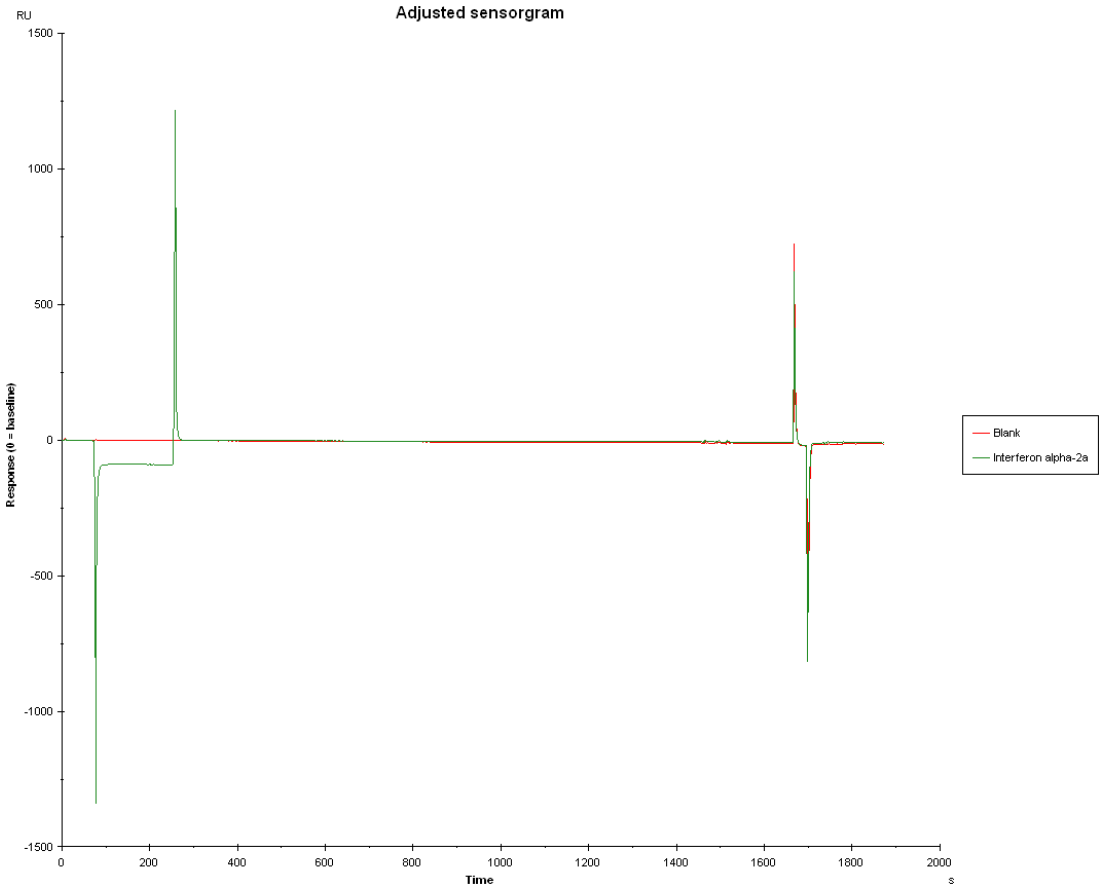

Figure 4-51. Binding assay of His_8IFN (green line; 100 µg/mL) and blank (red line; HBS+ EP running buffer) using VEGF immobilised CM3 chip. No binding observed for His_8IFN to VEGF.

4.2.9.2 Kinetic assay for IgG, Fab and PEG_{20}-Fabs

As discussed in §1.2.1.1, protein activity is dependent on conjugation chemistry, site of conjugation, size of conjugating moiety and the number of conjugating moieties. For example, protein activity can be reduced by PEG conjugation near or at the receptor-binding site. Fee has shown as five-fold decrease in antibody binding affinity by conjugating at cysteine residues compared to non-conjugated antibodies (Fee, 2007). This reduction in activity is thought to be due to steric hinderance from the conjugated moiety (Luxon et al., 2002b; Subramanian et al., 2007).

For the kinetic and affinity analysis, different concentrations of IgG, Fab and PEG_{20}-Fab were allowed to flow over the chip with the corresponding immobilised ligand. For bevacizumab the concentration range was from 0.5 µM to 0.015625 µM and for Fab_{beva} the range was from 1.0 µM to 0.0625 µM (Figure 4-51 A and B). While for anti-rat albumin IgG the concentration range used for kinetics analysis was

from 0.167 μM to 0.0209 μM and for Fab_{alb} was from 0.5 μM to 0.03125 μM (Figure 4-52 A and B). PEG_{20}-Fab_{beva} (range of 0.5 μM to 0.03125 μM, VEGF, 110 RU, Figure 4-51 C) and PEG_{20}-Fab_{alb} (0.5 μM to 0.03125 μM, rat albumin, 72 RU, Figure 4-52 C) were also examined to calculate their kinetic constants. The concentration of the bevacizumab derivatives and anti-rat albumin derivatives were calculated from Bradford assay and UV (A280 nm) respectively, with respect to protein molecular weight. The kinetic fitting curves and residual plots of bevacizumab derivatives and anti-rat albumin derivatives were calculated using a 1:1 binding model. The fitting parameters were determined to ensure the kinetic rate constants and binding data achieved were significant and within the acceptable ranges.

The residual plots (Figure 4-51 A-C) of the bevacizumab derivatives suggested that there was no difference between the experimental curve (coloured curves) and the fitted cube (black curve) when applying the 1:1 binding model as it scattered around zero. The Chi^2 values were <1 suggesting a good fit (Table 4–3). The SE value of K_a and K_d for bevacizumab, Fab_{beva} and PEG_{20}-Fab_{beva} were less than two orders of magnitude for the K_a and K_d values (Table 4–3). The experimental R_{max} achieved for the bevacizumab samples was lower than the immobilisation level for VEGF (110 RU) and the theoretical R_{max} (76 RU). If a greater experimental R_{max} had been achieved for the bevacizumab samples, it would suggest that the 1:1 binding model was not fitting or that there were impurities within the analyte samples. The tc values were greater than 10^9 indicating that no mass transfer was observed within the bevacizumab samples kinetic analysis (Table 4–3). As the kinetic analysis parameters (Chi^2, SE, R_{max} and tc) achieved for the bevacizumab samples were within the acceptable ranges, therefore the kinetic analysis data achieved could be taken as valid (Table 4–3). The kinetic and affinity analysis was conducted twice for bevacizumab and three times for Fab_{beva} and PEG_{20}-Fab_{beva}, the average K_a, K_d and K_D achieved can be seen in Table 4–4.

Table 4–3. Kinetic constants and parameters of bevacizumab and its derivatives using the VEGF immobilised chip (110 RU)

Sample	k_a ($\times 10^4$ M^{-1} s^{-1})	SE (k_a)	k_d (s^{-1})	SE (k_d)	K_D $\times 10^{-9}$ (M)	R_{max}	SE (R_{max})	Chi^2	tc
Bevacizumab	6.77	2.50×10^{2}	2.25×10^{-4}	2.40×10^{-6}	3.40	21.9	0.047	0.569	6.63×10^{15}
Fab_{beva}	2.81	54	1.54×10^{-4}	1.40×10^{-6}	5.47	23.02	0.024	0.308	2.83×10^{14}
PEG_{20}-Fab_{beva}	2.23	52	1.73×10^{-4}	1.70×10^{-6}	7.78	20.57	0.026	0.5	1.33×10^{15}

The k_d represents the strength in the interactions between the antibody and antigen, where a slower dissociation rate (smaller k_d value) results in a stronger binding interaction between analyte and ligand. While, a smaller k_a value is related to a slower association rate, thus there is less binding between analyte and ligand. Therefore k_a and k_d allow a great insight into the behaviour of the antibody fragment and how conjugation affects it.

Fab_{beva} and PEG_{20}-Fab_{beva} were observed to have a slower k_a compared to bevacizumab. This could be due to the monovalent nature of Fab_{beva} and PEG_{20}-Fab_{beva} when compared to bevacizumab. However, Fab_{beva} and PEG_{20}-Fab_{beva} both displayed faster dissociation rates compared to bevacizumab, 6.23×10^{-4} s^{-1} and 6.04×10^{-4} s^{-1} respectively. These results show how the PEG_{20} *bis*-sulfone **1** conjugation to the disulfide interchain did not affect the binding of the Fab_{beva} to VEGF.

Table 4–4. Average kinetic constants and parameters of bevacizumab and its derivatives using the VEGF immobilised chip (110 RU).

Sample	ka ($\times10^4$ M^{-1} s^{-1})	k_d ($\times10^{-4}$ s^{-1})	K_D ($\times10^{-9}$ M)	*n*
Bevacizumab	6.70 ± 0.10	2.24 ± 0.02	3.34 ± 0.08	2
Fab_{beva}	2.51± 0.32	1.55 ± 0.10	6.23 ± 0.67	3
PEG_{20}-Fab_{beva}	2.38 ± 0.30	1.53 ± 0.20	6.04 ± 1.49	3

A) IgG_{beva}

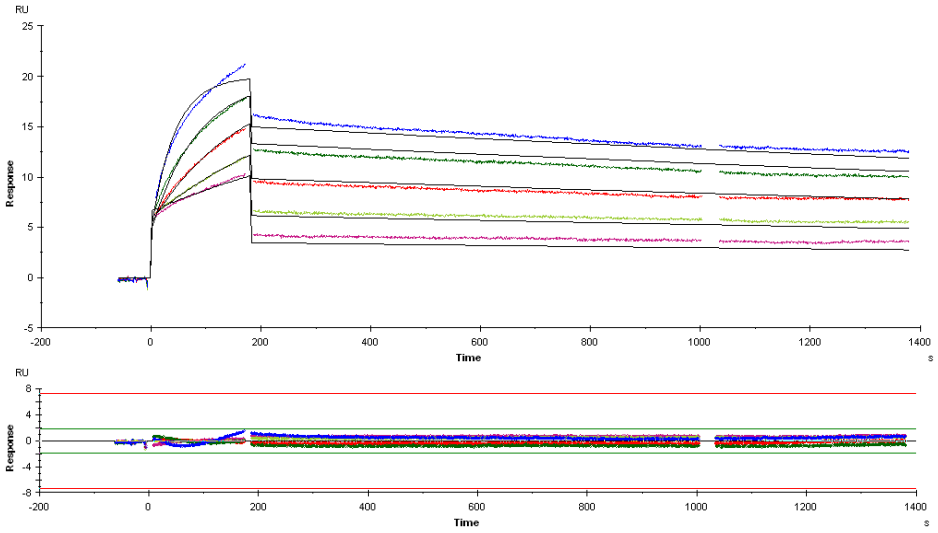

B) Fab_{beva}

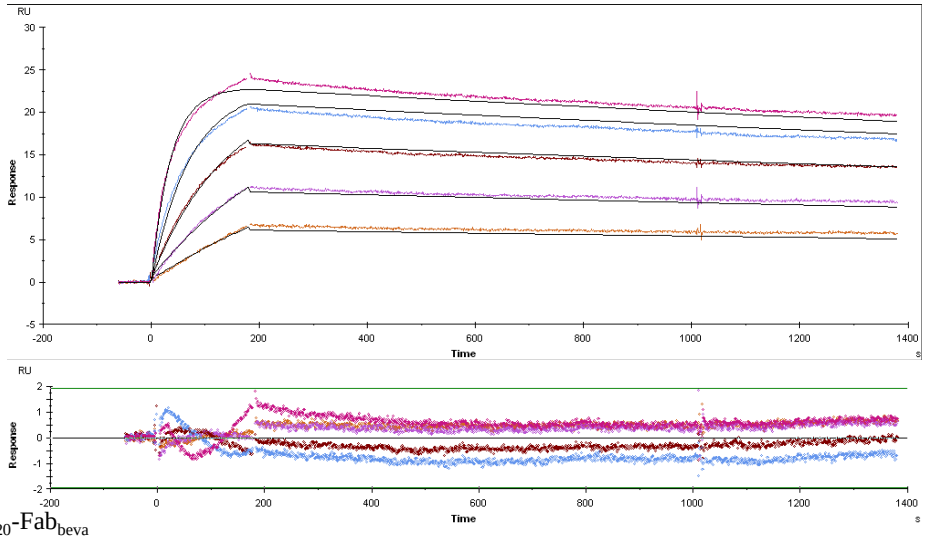

C) PEG_{20}-Fab_{beva}

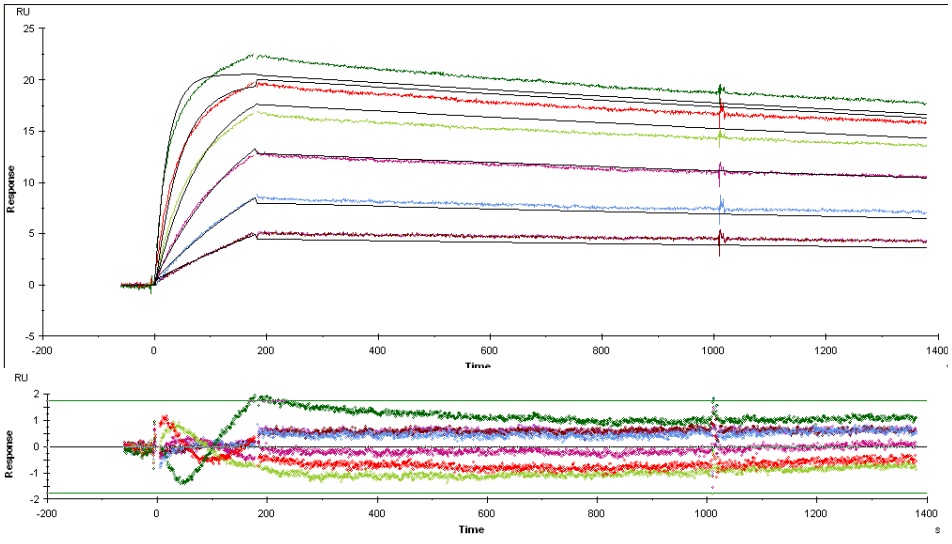

Figure 4-52. The fitting curve and residual plot applying the 1:1 fitting model of A) bevacizumab, B) Fab_{beva}, C) PEG_{20}-Fab_{beva}.

IgG_{alb}

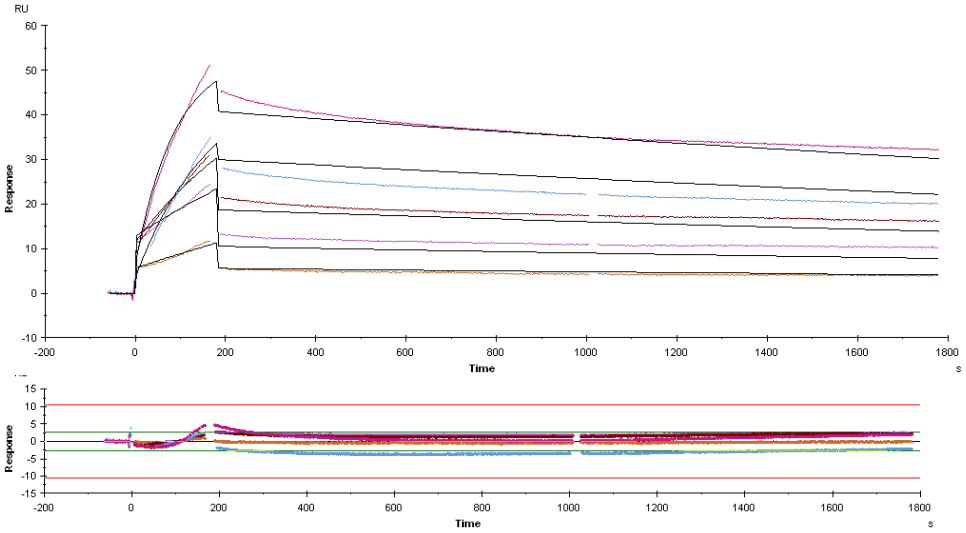

Fab_{alb}

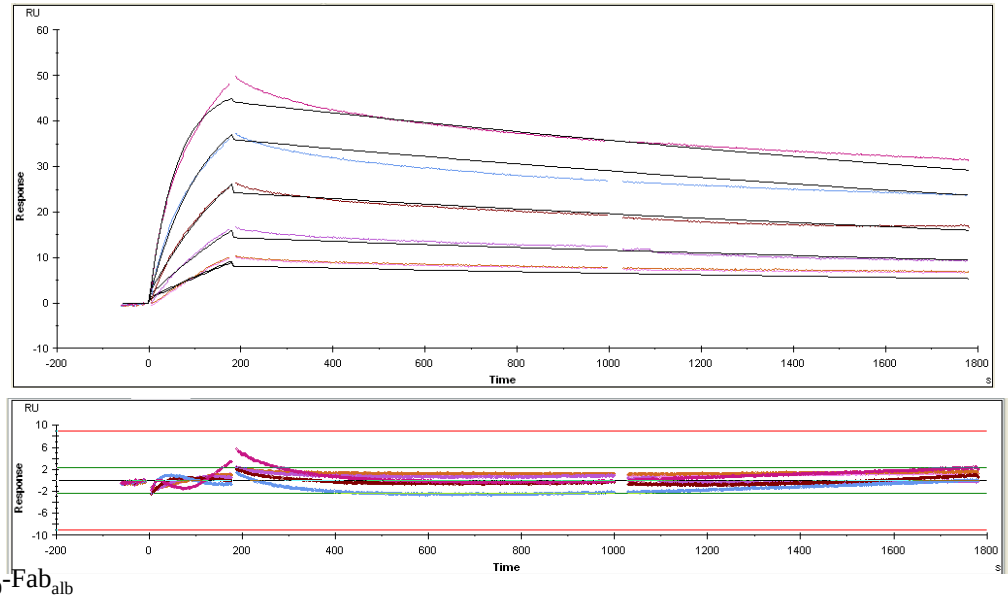

PEG_{20}-Fab_{alb}

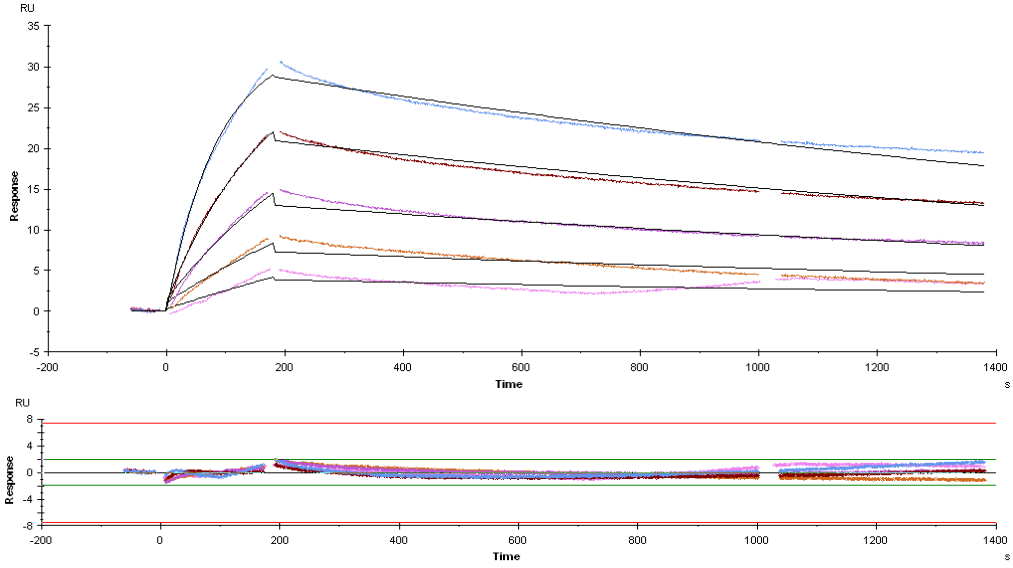

Figure 4-53. The fitting curve and residual plot using the 1:1 fitting model of A) anti-rat albumin IgG, B) Fab_{alb} and C) PEG_{20}-Fab_{alb}.

The residual plots (Figure 4-52 A-C) of the anti-rat albumin derivatives suggested that there was no difference between the experimental curve (coloured curves) and the fitted cube (black curve) when applying a 1:1 binding model as it scattered around zero. The Chi^2 values achieved for anti-rat albumin IgG, Fab_{alb} and PEG_{20}-Fab_{alb} were below 1, showing the 1:1 binding model is a good fit to the data obtained (Table 4–5). The experimental R_{max} achieved for the anti-rat albumin IgG samples were lower than the immobilisation level for rat albumin (72 RU) and the theoretical R_{max} (130 RU), showing that the samples fit to the 1:1 binding model (Table 4–5). The tc values were greater than 10^9 indicating that no mass transfer was observed within the anti-rat albumin samples kinetic analysis (Table 4–5). As the kinetic analysis parameters (Chi^2, SE, R_{max} and tc) achieved for the anti-rat albumin samples were within the acceptable ranges, therefore the kinetic analysis data achieved could be taken as valid (Table 4–5). The average kinetic and affinity analysis for anti-rat albumin IgG (n=1), Fab_{alb} (n=4) and PEG_{20}-Fab_{beva} (n=3) can be seen in Table 4–6.

Table 4–5. Kinetic constants and parameters of anti-rat albumin IgG and its derivatives using the rat albumin immobilised chip (72 RU). ND=not determine as data lost.

Sample	k_a ($\times 10^4$ M^{-1} s^{-1})	SE (k_a)	k_d (s^{-1})	SE (k_d $\times 10^{-6}$)	K_D (M)	R_{max}	SE (R_{max})	Chi^2	tc
anti-rat albumin IgG	3.56	ND	4.33×10^{-5}	ND	1.22×10^{-9}	2.426	ND	0.029	1.79×10^{18}
Fab_{alb}	3.02	65	2.61×10^{-4}	1.00	8.66×10^{-9}	48.8	0.059	0.96	1.50×10^{23}
PEG_{20}-Fab_{alb}	1.92	49	2.91×10^{-4}	1.30	15.1×10^{-8}	26.9	0.043	0.14	2.16×10^{15}

For the polyclonal anti-rat albumin IgG (Table 4–6), a slower association and dissociation was observed compared to monoclonal bevacizumab (Table 4–4). The association rate for Fab_{alb} was found to be similar to anti-rat albumin IgG, but Fab_{alb} was found to have a slower dissociation rate compared to anti-rat albumin (Table 4–6). This slower dissociation rate for Fab_{alb} was thought to be due to the monovalent binding to rat albumin compared to anti-rat albumin IgG. PEG_{20}-Fab_{alb} was found to have a much slower association compared to both Fab_{alb} and anti-rat albumin IgG. However, PEG_{20}-Fab_{alb} was found to have a slower dissociation rate than anti-rat albumin IgG but a comparable dissociation rate than Fab_{alb} (Table 4–6). The association rate for PEG_{20}-Fab_{alb} (1.92×10^4 M^{-1} s^{-1}) is slower compared to both Fab_{alb}

(3.02×10^4 M^{-1} s^{-1}) and anti-rat albumin IgG (3.56×10^4 M^{-1} s^{-1}, Table 4–6). This result implies that the strength of binding to rat albumin was affected by the interchain disulfide conjugation. This is quite different to the findings for PEG_{20}-Fab_{beva}, where the k_a and k_d were not changed drastically by disulfide conjugation (Table 4–4). This is most likely due to the polyclonal nature of Fab_{alb}, therefore it can be determined that the binding affinity has been retained. However, the exact binding affinity is difficult to determine due to the polyclonal nature of the antibody, where there are many different binding and rebinding effects. With PEG-Fab_{alb} there may be effects from PEG shielding, and the lack of bivalency compare to IgG.

Table 4–6. Average kinetic constants and parameters of anti-rat albumin IgG and its derivatives using the rat albumin immobilised chip (72 RU)

Sample	k_a ($\times 10^4$ M^{-1} s^{-1})	k_d ($\times 10^{-4}$ s^{-1})	K_D (M)	*n*
anti-rat albumin IgG	3.56	4.33×10^{-5}	1.22×10^{-9}	1
Fab_{alb}	3.13 ± 0.13	2.41 ± 0.22	$7.72 \pm 0.70 \times 10^{-9}$	4
PEG_{20}-Fab_{alb}	1.66 ± 0.47	3.34 ± 0.56	$22.2 \pm 1.15 \times 10^{-8}$	3

4.2.9.3 Kinetic and affinity analysis of novel IFN-PEG-Fab heterodimers

The binding properties for the Fabs in the heterodimers, IFN-PEG_{20}-Fab_{beva} and IFN-PEG_{20}-Fab_{alb} were then evaluated by SPR. The concentration ranges tested for IFN-PEG_{20}-Fab_{beva} and IFN-PEG_{20}-Fab_{alb} were 1.0 μM to 0.0625 μM and 0.125 μM to 0.0078125 μM respectively. The residual plots (Figure 4-54) achieved for IFN-PEG_{20}-Fab_{beva} and IFN-PEG_{20}-Fab_{alb} suggested that the experimental curves (coloured curves) fitted in the 1:1 binding model curves (black curves) well, as the residual plots were scattered around zero, except for the highest IFN-PEG_{20}-Fab_{alb} concentration tested (Figure 4-54 B). The Chi^2 value achieved for IFN-PEG_{20}-Fab_{beva} was less than 1 suggesting a good fit to the 1:1 binding model (Table 4–7). However, the Chi^2 value for IFN-PEG_{20}-Fab_{alb} was greater than one, suggesting it does not fit the 1:1 binding model well, this is most likely due to the polyclonal nature of Fab_{alb} within the heterodimer. Where Fab_{alb} is binding to different epitopes on rat albumin. However, the experimental R_{max} (43.17 RU, Table 4–7) achieved for IFN-PEG_{20}-

Fab_{alb} was less than the R_{max} achieved, suggesting the IFN-PEG_{20}-Fab_{alb} analysis fits with the 1:1 binding model.

A) IFN-PEG_{20}-Fab_{beva}

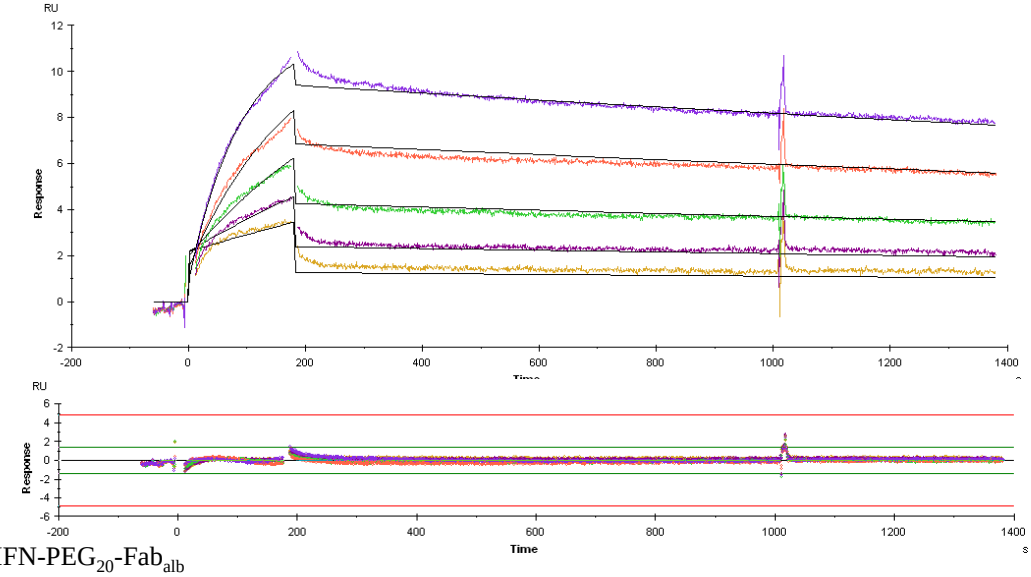

B) IFN-PEG_{20}-Fab_{alb}

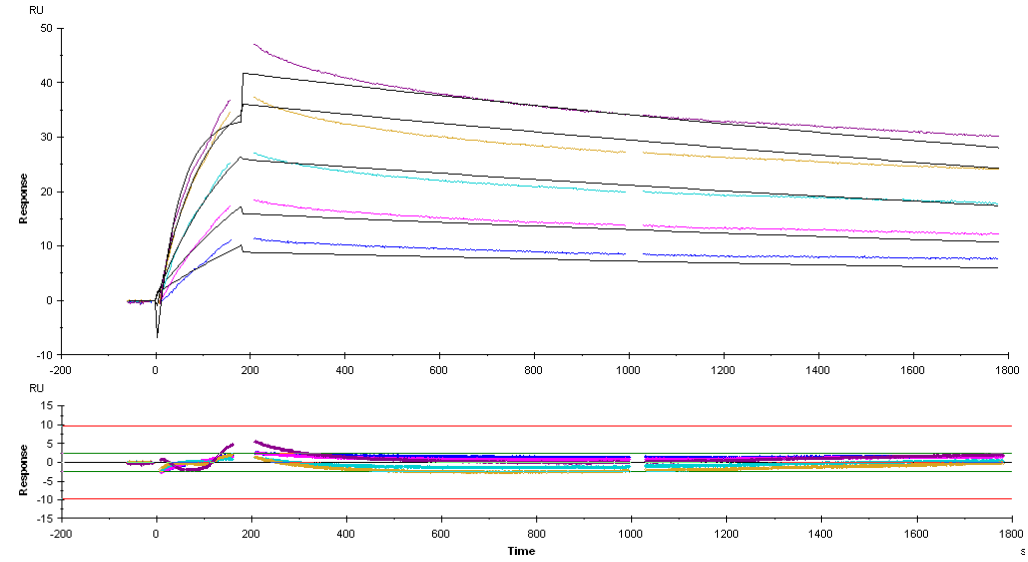

Figure 4-54. The fitting curve and residual plot using the 1:1 fitting model of A) IFN-PEG_{20}-Fab_{beva} and B) IFN-PEG_{20}-Fab_{alb}.

The tc values were greater than 10^9 for both heterodimeric molecules indicating that no mass transfer was observed within the samples kinetic analysis (Table 4–7). As the kinetic analysis parameters (Chi^2, SE, R_{max} and tc) achieved for IFN-PEG_{20}-Fab_{beva} were within the acceptable ranges, the kinetic analysis data achieved could be taken as valid (Table 4–7). As the SE, R_{max} and tc parameters were within the acceptable ranges for IFN-PEG_{20}-Fab_{alb}, the data achieved was viewed as preliminary. The kinetic and affinity analysis was conducted three times for IFN-

PEG_{20}-Fab_{beva} and two times for IFN-PEG_{20}-Fab_{alb}, the average K_a, K_d and K_D achieved can be seen in Table 4–7.

Table 4–7. Kinetic constants and parameters achieved by IFN-PEG_{20}-Fab_{beva} and IFN-PEG_{20}-Fab_{alb}. The affinity is achieved by Fab_{alb} and Fab_{beva} within the heterodimers.

Sample	k_a (M^{-1} s^{-1})	SE (k_a)	k_d (s^{-1})	SE (k_d)	K_D (M)	R_{max}	SE (R_{max})	Chi^2	tc
IFN-PEG_{20}-Fab_{beva}	1.05×10^4	39	1.55×10^{-4}	1.90×10^{-6}	14.7×10^{-8}	12.01	0.059	0.0835	1.04×10^{15}
IFN-PEG_{20}-Fab_{alb}	1.68×10^5	4.7×10^2	2.48×10^{-4}	1.50×10^{-6}	1.47×10^{-8}	43.17	0.067	1.88	3.12×10^{17}

The results show that both IFN-PEG_{20}-Fab_{beva} and IFN-PEG_{20}-Fab_{alb} retained binding to their respective antigens. It was observed that the dissociation rate of IFN-PEG_{20}-Fab_{beva} was similar to Fab_{beva} and PEG_{20}-Fab_{beva}, suggesting conjugating the interchain disulfide of Fab_{beva} does not change the dissociation rate or binding of Fab_{beva} to VEGF. This is in agreement with the finding by Khalili and co-workers (Khalili et al., 2012, 2013). This observation was also found for IFN-PEG_{20}-Fab_{alb} where the dissociation rate was similar to Fab_{alb} binding to rat albumin. However, it was noted that the dissociation rate for PEG_{20}-Fab_{alb} was not similar to those observed for Fab_{alb} and IFN-PEG-Fab_{alb}, suggesting this result needed further investigation. This result could be due to the sample purity, as it was difficult to prepare PEG_{20}-Fab_{alb} in good purity (§ 4.2.7).

Nonetheless, the trend observed that conjugation to the interchain disulfide does not affect the strength of binding to the antigen (k_d) (Khalili et al., 2012; Yang et al., 2014). Interestingly, it has also been found that the dissociation rate of Fab_{beva} did not vary with different sizes of PEG *bis*-sulfone **1** (Khalili et al., 2012). This could possibly be due to the site-specific nature of disulfide conjugation meaning the PEG molecule is away from the binding region. Further, Fab_{beva}-PEG-Fab_{beva} constructs were found to have a decreased dissociation rate, showing a tighter interaction between antibody and antigen (Khalili et al., 2013). This finding was thought to be a reflection of the bivalent nature of the construct and the flexibility of the PEG di(*bis*)sulfone **4** linker allowing for better binding to the antigen, compared to bevacizumab IgG. Interestingly, when calculating the retained k_a for IFN-PEG_{20}-Fab_{beva} and IFN-PEG_{20}-Fab_{alb} in comparison to Fab_{beva} and Fab_{alb} respectively, both

heterodimers retained ~54% association (Table 4–8). While, the dissociation constant for IFN-PEG_{20}-Fab_{beva} (1.79 ± 0.30 $\times 10^{-4}$ s^{-1}) and IFN-PEG_{20}-Fab_{alb} (2.51 ± 0.04 $\times 10^{-4}$ s^{-1}) were found to increase slightly compared to Fab_{beva} and Fab_{alb} (Table 4–8). The fast dissociation rates observed for Fab vs. IgG is thought to be due to i) monovalent binding of Fab and ii) the mass difference between the two molecules, where the Fab can diffuse from the bulk to the sensor surface more quickly than IgG. Where IgG is bivalent and allows rebinding to the ligand. Thus, the faster dissociation rates observed for the IFN-PEG_{20}-Fab heterodimers are thought to be due to the monovalent binding of the Fab to the antigen, but also possibly the conjugation to the PEG may aid the diffusion from the bulk to the sensor surface. Nonetheless, this data suggests that the novel IFN-PEG_{20}-Fab_{beva} and IFN-PEG_{20}-Fab_{alb} heterodimer conjugates have retained their binding affinities to their antigens.

Table 4–8. Average kinetic constants and parameters achieved for IFN-PEG_{20}-Fab_{beva} and IFN-PEG_{20}-Fab_{alb} and controls (Fab and PEG_{20}-Fab). Association (k_a) was found to be similar between Fab, PEG-Fab and IFN-PEG-Fab heterodimers suggesting retained association. However, dissociation rates were found to be faster, possibly due to the monovalent nature of Fabs vs. IgG.

Sample	k_a (M^{-1} s^{-1})	k_d ($\times 10^{-4}$ s^{-1})	K_D (M)
Fab_{beva}	2.51± 0.32 $\times 10^4$	1.55 ± 0.10	6.23 ± 0.67$\times 10^{-9}$
PEG_{20}-Fab_{beva}	2.38 ± 0.30 $\times 10^4$	1.53 ± 0.20	6.04 ± 1.49$\times 10^{-9}$
IFN-PEG_{20}-Fab_{beva}	1.37 ± 0.50 $\times 10^4$ (54%)	1.79 ± 0.30	1.36 ± 0.24$\times 10^{-8}$
Fab_{alb}	3.13 ± 0.13 $\times 10^4$	2.41 ± 0.22	7.72 ± 0.70$\times 10^{-9}$
PEG_{20}-Fab_{alb}	1.66 ± 0.47 $\times 10^4$	3.34 ± 0.56	2.22 ± 1.15$\times 10^{-8}$
IFN-PEG_{20}-Fab_{alb}	1.68 $\times 10^5$ (53.7%)	2.51 ± 0.04	1.49 ± 0.03$\times 10^{-9}$

To assess if the binding affinities of the IFN-PEG_{20}-Fab_{beva} and IFN-PEG_{20}-Fab_{alb} conjugates were statistically different from their respective controls, a one-way ANOVA was conducted on the K_D data achieved for the conjugates. As previously, the one-way ANOVA was used in conjunction with a *post hoc* test, the Tukey's test. The assumptions of the Tukey's test are that i) the observations being tested are independent and ii) there is equal variation across the sets of data (Dytham, 2011).

It was found that the equilibrium dissociation constant (K_D) IFN-PEG_{20}-Fab_{beva} was statistically different from both Fab_{beva} and PEG_{20}-Fab_{beva} (Figure 4-55). This statistical difference between the heterodimers and controls could be due to the addition of the IFN molecule on the PEG_{20} di(*bis*)sulfone **4**. As, IFN-PEG_{20}-Fab_{alb}

was also shown to be statistically different from both Fab_{alb} and PEG_{20}-Fab_{alb} (Figure 4-56). The KD is calculated as K_d/K_a. Therefore, the K_D is statistically different to PEG-Fab and IFN-PEG-Fab most likely due to the association rates slowing, therefore differing KD are achieved for both Fab_{alb} and Fab_{beva} conjugates.

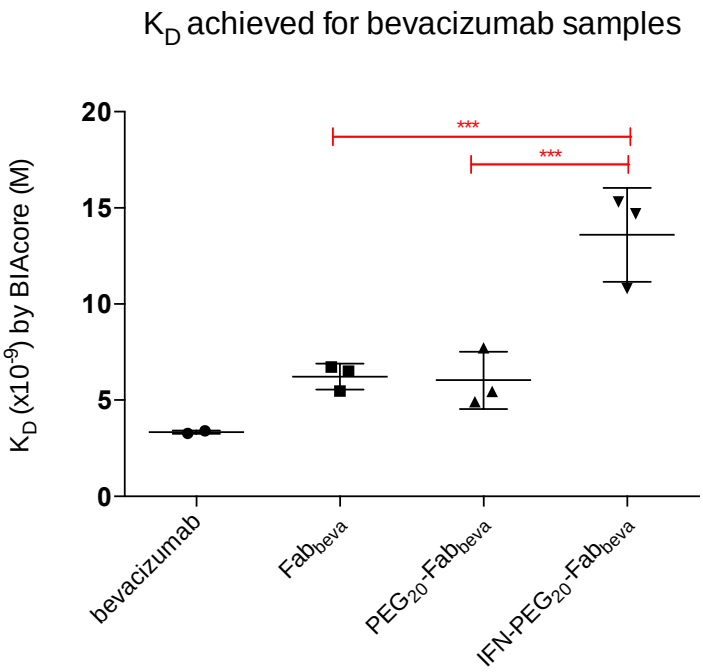

Figure 4-55. One-way ANOVA conducted on K_D data achieved for bevacizumab samples, statistical different samples are marked with red stars (*). IFN-PEG_{20}-Fab_{beva} is shown to be statistically different from Fab_{beva} and PEG_{20}-Fab_{beva}.

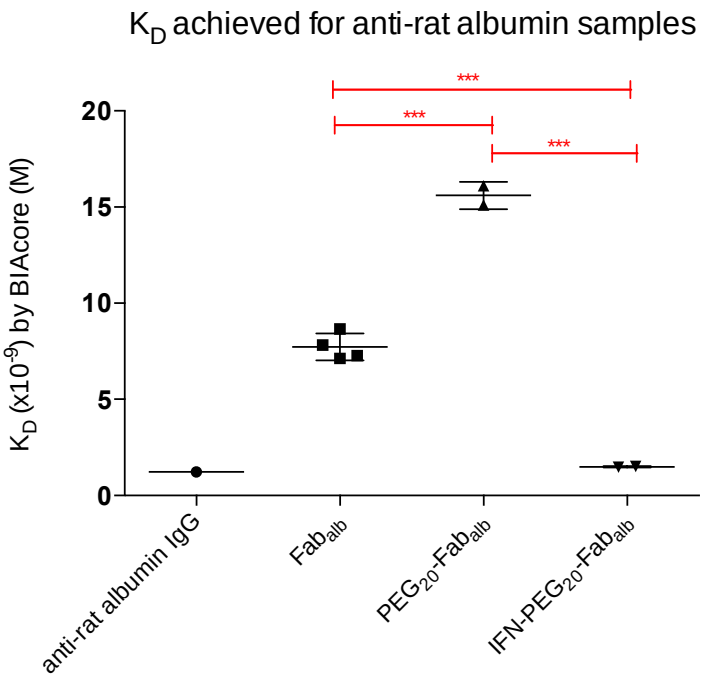

Figure 4-56. One-way ANOVA conducted on K_D data achieved for anti-rat albumin samples, statistical different samples are marked with red stars (*). IFN-PEG_{20}-Fab_{alb} is shown to be statistically different from Fab_{alb} and PEG_{20}-Fab_{alb}.

4.2.9.4 *In vitro* cell based evaluation of IFN-PEG_{20}-Fab heterodimers

To assess the retained biological activity of the interferon component of the IFN-PEG_{20}-Fab_{beva} and IFN-PEG_{20}-Fab_{alb} heterodimers, two *in vitro* assays were used. An antiviral and an antiproliferative assay were used. Since cell based assays are inherently variable (Meager, 2006) efforts for their optimisation are described in 6.2-6.3 Appendices I and II. NIBSC IFNα-2a was used as control in these assays. As described (§3.3.6.1), NIBSC IFNα-2a allows for uniform reporting of IFN potency in universally accepted International Units (IU) (Meager, 2006). Therefore, direct bioactivity comparisons can be made between IFN conjugates prepared and tested from different laboratories.

First, IFN-PEG_{20}-Fab_{beva} and IFN-PEG_{20}-Fab_{alb} were subjected to testing in the antiviral assay. The raw data are plotted as shown for both IFN-PEG_{20}-Fab_{beva} and IFN-PEG_{20}-Fab_{alb} (Figure 4-57). The effective dose at 50% (ED_{50}) was calculated into specific activity (MIU/mg) using the calculations in 6.1 Appendix I. As discussed previously (§3.3.6.1), the accepted range for the experiments conducted with NIBSC IFNα-2a was 200-300 MIU/mg allowing for 20% variation or %CV in the experiments conducted.

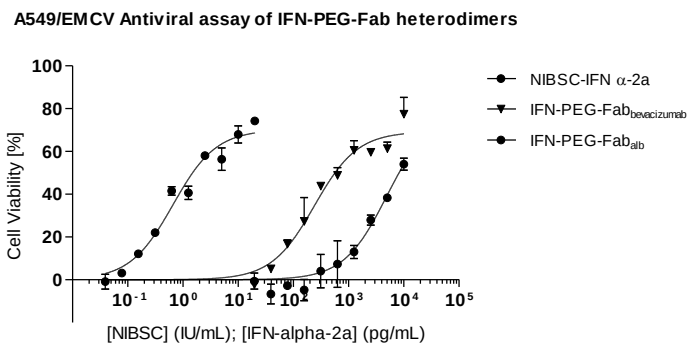

	NIBSC-IFN α-2a	IFN-PEG-Fab avastin	IFN-PEG-Fabalb	Global (shared)
One site -- Specific binding with Hill slope				
Best-fit values				
Bmax	70.15	69.30	78.33	
h	1.112	1.112	1.112	1.112
Kd	0.6585	240.0	4899	
Std. Error				
Bmax	2.588	2.348	12.76	
h	0.09388	0.09388	0.09388	0.09388
Kd	0.08778	30.95	1586	
95% Confidence Intervals				
Bmax	65.00 to 75.31	64.62 to 73.98	52.90 to 103.8	
h	0.9251 to 1.299	0.9251 to 1.299	0.9251 to 1.299	0.9251 to 1.299
Kd	0.4837 to 0.8334	178.3 to 301.6	1740 to 8058	

Figure 4-57. Representative graph of NIBSC IFN α-2a, IFN-PEG_{20}-Fab_{beva} and IFN-PEG_{20}-Fab_{alb} with the ED_{50} (Kd) for calculating the specific activity (MIU/mg).

Full sigmoid curves were achieved for NIBSC IFN α-2a and IFN-PEG-Fab_{beva}, however for IFN-PEG_{20}-Fab_{alb} a full sigmoid curve was not achieved. Further, a 10-fold lower Kd was observed for IFN-PEG_{20}-Fab_{alb} than IFN-PEG-Fab_{beva}. It was thought this stunted curve observed for IFN-PEG_{20}-Fab_{alb} was due to the Fab_{alb} binding to albumin within the media composition. The antiviral assay was conducted three times for both IFN-PEG_{20}-Fab_{alb} and IFN-PEG-Fab_{beva}, in all cases the stunted curve for IFN-PEG_{20}-Fab_{alb} was observed (Figure 4-57).

In an attempt to prepare a full curve for IFN-PEG_{20}-Fab_{alb}, different media compositions were investigated (DMEM+FCS, DMEM-FCS, DMEM+RPMI, RPMI-FCS) to conduct the antiviral assay with which did not contain albumin. As a positive control DMEM+FCS was also tested. The antiviral assay was conducted using NIBSC IFN α-2a in order to assess how the different media compositions affected the antiviral assay results, and if an alternative media composition could be used to test the bioactivity of IFN-PEG_{20}-Fab_{alb}.

As discussed previously, specific activity range for NIBSC IFNα-2a is 254 MIU/mg. Therefore, the accepted range for the experiments conducted with NIBSC IFNα-2a was 200-300 MIU/mg ± 20% CV. Thus, NIBSC IFN α-2a achieves a Kd (ED_{50}) between 0.5-1. Using DMEM+FCS, NIBSC IFNα-2a achieved an ED_{50} of

0.53 (Figure 4-58), which is within the expected range. When NIBSC IFNα-2a was in the presence of different media compositions, an increase in the Kd was observed. The shift observed was from 0.5 (positive control) to ~2.0 (different media compositions) (Figure 4-58). The higher Kd's observed were for all media compositions with no FCS, suggesting no media with no FCS would be suitable for conducting the antiviral assay to test IFN-PEG_{20}-Fab_{alb}. For assessing the activity of IFN-PEG_{20}-Fab_{alb}, possibly different cell lines e.g. 2D9 cells could be investigated or the antiviral assay could be optimised with an alternative media e.g. serum free media for testing the biological activity of IFN-PEG_{20}-Fab_{alb} (Meager, 2006).

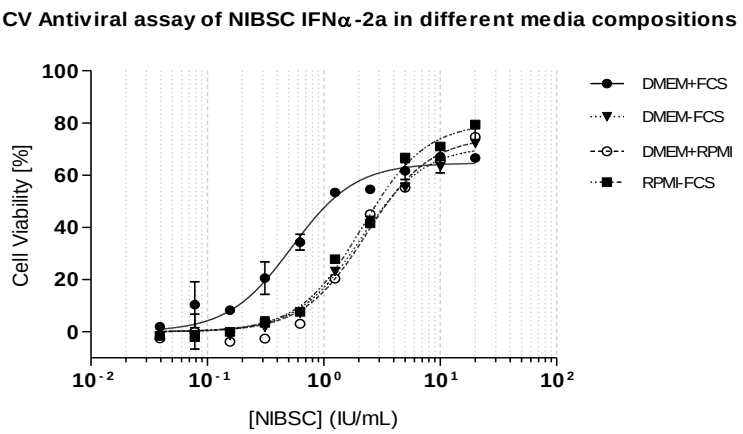

	DMEM+FCS	DMEM-FCS	DMEM+RPMI	RPMI-FCS
One site -- Specific binding with Hill slope				
Best-fit values				
Bmax	64.69	71.25	74.78	80.21
h	1.595	1.595	1.595	1.595
Kd	0.5305	2.081	2.320	2.140
Std. Error				
Bmax	1.581	2.436	2.579	2.521
h	0.09420	0.09420	0.09420	0.09420
Kd	0.04446	0.1858	0.2026	0.1726
95% Confidence Intervals				
Bmax	61.53 to 67.84	66.39 to 76.11	69.63 to 79.93	75.18 to 85.24
h	1.407 to 1.783	1.407 to 1.783	1.407 to 1.783	1.407 to 1.783
Kd	0.4417 to 0.6193	1.710 to 2.452	1.916 to 2.725	1.796 to 2.485

Figure 4-58. Graph and table of NIBSC IFN α-2a antiviral activity in different media types (DMEM+FCS, DMEM-FCS, DMEM+RPMI, RPMI-FCS). A shift in Kd for NIBSC IFN α-2a was observed when conducting the antiviral assay with different media compositions.

The mean specific activity achieved for the novel IFN-PEG_{20}-Fab_{beva} was 7.60 ± 2.56 MIU/mg (3.3% retained activity; n=3) (Table 4–9). For His_8IFN α-2a, the mean specific activity achieved was 231.31 ± 10.95 MIU/mg (n=3) (Table 4–9). The mean specific activity achieved for PEG_{20}-IFN was 3.95 ± 1.69 MIU/mg (1.7% retained activity, n=3) (Table 4–9). IFN-PEG_{20}-IFN dimer achieved a mean specific activity of 2.12 ± 0.64 MIU/mg (0.94% retained activity, n=4) (Table 4–9). Despite

having a reduced antiviral activity all of the disulfide conjugates achieved complete inhibition of cell death from EMCV infection at saturating doses.

Table 4–9. Summary of *in vitro* specific activity values achieved and n numbers for disulfide conjugated IFN-PEG_{20}-Fab_{beva}, IFN-PEG_{20}-IFN conjugates and controls. The IFN-PEG_{20}-Fab_{beva} heterodimer has retained the greatest specific activity, followed by disulfide conjugated PEG_{20}-IFN, IFN-PEG_{20}-IFN when compared to native His_8IFN α-2a.

Value	His_8IFN α-2a	PEG_{20}-IFN	IFN-PEG_{20}-IFN	IFN-PEG_{20}-Fab_{beva}
Mean specific activity (MIU/mg)	231.31	3.95	2.12	7.60
ST.DEV of specific activity (MIU/mg)	10.95	1.69	0.64	2.56
Retained activity (%)	100	1.7	0.94	3.3
n number	3	3	4	3

To better compare the specific activity achieved between the novel IFN-PEG_{20}-Fab_{beva} heterodimer and controls, the achieved specific activities of all the disulfide conjugated IFN species were plotted onto a bar graph (Figure 4-59). It can be seen that the order of activity is IFN with 100% retained activity, followed by IFN-PEG_{20}-Fab_{beva} (3.3%), PEG_{20}-IFN (1.7%) and IFN-PEG_{20}-IFN (0.94%) (Figure 4-59). Interestingly the IFN-PEG_{20}-Fab_{beva} had greater retained activity than the IFN-PEG_{20}-IFN homodimer. This could be possibly due to the 1:1 binding required between IFN and IFNAR receptor, therefore by conjugating two IFNs together the second IFN is unable to bind to its own receptor or both IFNs are trying to bind to one receptor and impeding one-another. However, the data shows that the novel IFN-PEG_{20}-Fab_{beva} has retained activity. Overall, the IFN disulfide conjugates have reduced activity compared to native IFN. It is well documented in literature that conjugating proteins to PEG results in a reduction in activity (Grace et al., 2005).

Analogous to conjugating PEG to a protein, conjugating (or fusing) two proteins together will invariably reduce the binding properties, and hence the activity, of each protein. For example, the IFN within Albuferon™ (recombinantly expressed Albumin-IFN fusion) retained 2% activity (Subramanian et al., 2007). The length, flexibility and non-covalent properties of the linker is thought to be an important consideration to help ensure the two protein moieties can maintain their

binding characteristics (Arai et al., 2001; Shewmake et al., 2008). It is also reported that longer flexible linkers could lead to greater retained binding affinity (Reeves et al., 2011; Shewmake et al., 2008). From the results achieved, it is thought that with site-specific conjugation and the linker length and the flexibility of the PEG in the PEG_{20} di(*bis*)sulfone **4**, that allowed for retained activity of IFN.

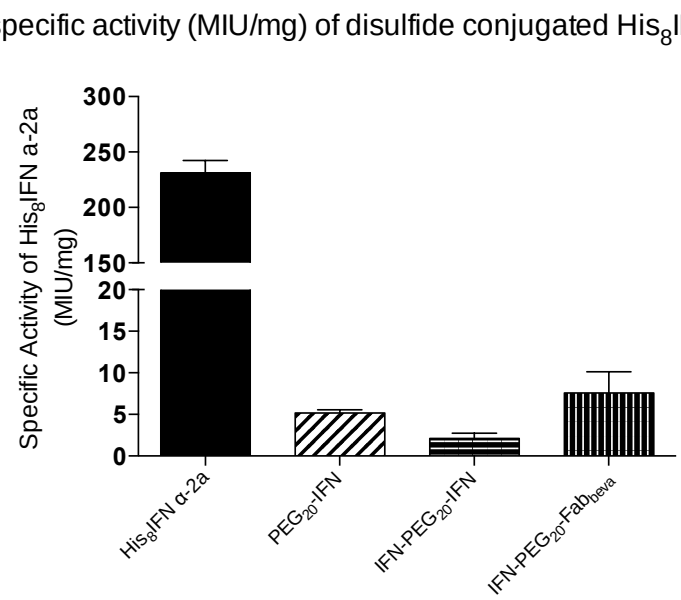

Figure 4-59. Specific activity (MIU/mg) of IFN, PEG_{20}-IFN, IFN-PEG_{20}-IFN, IFN-PEG_{20}-Fab_{beva} tested within the antiviral (A549/EMCV) assay. IFN-PEG_{20}-Fab_{beva} retained activity when assayed in the antiviral assay.

IFN is a pleiotropic protein; therefore to better judge the specific activity of the IFN-PEG_{20}-Fab_{beva} heterodimer and controls, the disulfide-conjugates were subjected to an *in vitro* antiproliferative assay. As outlined in §3.3.6.4, Daudi cells were used to assess the antiproliferative activity of IFN-PEG_{20}-Fab_{beva}. The antiproliferative assay was optimised as outlined in 6.1 Appendix II, in order to ensure the data achieved was accurate and reproducible. As in the antiviral assay, NIBSC IFN α-2a was run on every plate as a control.

Raw data was plotted as shown for IFN-PEG_{20}-Fab_{beva} (Figure 4-60 B). The effective dose at 50% (ED_{50}) was calculated from the normalised graph (Figure 4-60 B) into specific activity (MIU/mg) using the calculations in 6.1 Appendix I.

A

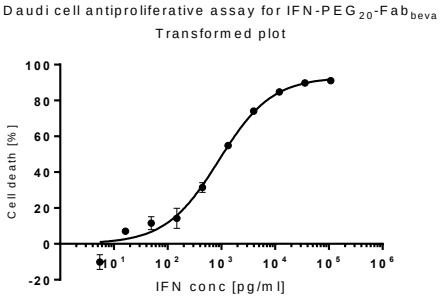

	IFN-PEG20-Fabbeva
One site -- Specific binding with Hill slope	
Best-fit values	
Bmax	93.09
h	0.8808
Kd	895.5

B

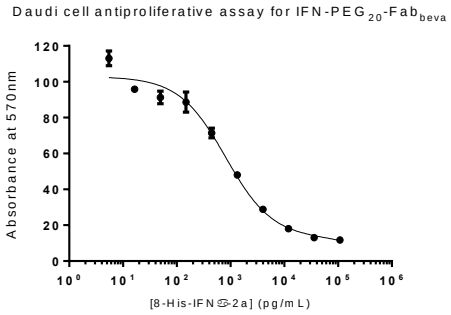

	IFN-PEG20-Fabbeva
One site -- Total	
Best-fit values	
Bmax	-89.89
Kd	810.2
NS	-2.065e-005
Background	102.9

C

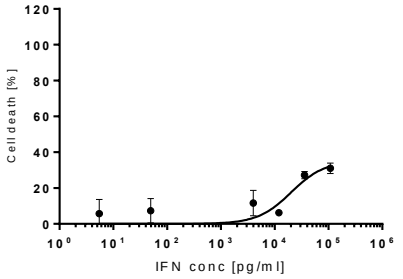

	IFN-PEG20-Fabalb
One site -- Specific binding with Hill slope	
Best-fit values	
Bmax	35.27
h	1.394
Kd	20275

D

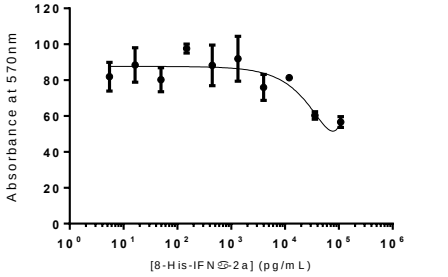

	IFN-PEG20-Fabalb
One site -- Total	Ambiguous
Best-fit values	
Bmax	~ -4830
Kd	~ 818120
NS	~ 0.004927
Background	87.66

Figure 4-60. Representative graphs of A) Transformed plot of IFN-PEG_{20}-Fab_{beva}, B) normal plot of IFN-PEG_{20}-Fab_{beva}, C) transformed plot of IFN-PEG_{20}-Fab_{alb} and D) normal plot of IFN-PEG_{20}-Fab_{alb} achieved within the antiproliferative assay. IFN-PEG_{20}-Fab_{alb} can be seen to have achieved a stunted curve compared to IFN-PEG_{20}-Fab_{beva}, this is thought to be due to the Fab_{alb} binding to components within the media and thus not achieving a full sigmoid curve.

IFN-PEG_{20}-Fab_{alb} can be seen to have achieved a stunted sigmoid curve compared to IFN-PEG_{20}-Fab_{beva} (Figure 4-60), this is thought to be due to the Fab_{alb} binding to components within the media and thus not achieving a full sigmoid curve. This was also found within the antiviral assay. Therefore, no accurate specific activity data could be achieved for IFN-PEG_{20}-Fab_{alb}, however, it can be determined that the IFN within the heterodimer has retained some activity being as a small curve was achieved.

The IFN-PEG_{20}-Fab_{beva} heterodimer achieved a specific activity of 34.72 ± 6.30 MIU/mg (n=2) and retained 10.5% activity (Table 4–10). The mean specific

activity achieved for IFN was 329.36 ± 97.98 MIU/mg (n=5, Table 3–5). The mean specific activity of PEG_{20}-IFN was 5.13 ± 1.44 MIU/mg (1.56% retained activity, n=4) (Table 4–10). A specific activity of 0.81 ± 0.09 MIU/mg (0.25% retained activity, n=3) (Table 4–10) was achieved for IFN-PEG_{20}-IFN. This shows that the IFN-PEG_{20}-Fab_{beva} retained antiproliferative activity.

Table 4–10. Summary of antiproliferative activity (MIU/mg) achieved for IFN-PEG_{20}-Fab_{beva} heterodimer and controls (IFN, PEG_{20}-IFN and (IFN-PEG_{20}-IFN)

Sample	Specific Activity (MIU/mg)	Percentage (%) retained activity	n number
His_8IFN α-2a	329.36 ± 87.98	100	5
IFN-PEG_{20}-IFN	0.81 ± 0.09	0.25	3
PEG_{20}-IFN	5.13 ± 1.44	1.56	4
IFN-PEG_{20}-Fab_{beva}	34.72 ± 6.30	10.5	2

To better compare the antiproliferative activity of the heterodimer to IFN-PEG_{20}-IFN and controls, all of the disulfide conjugates were plotted on a bar graph (Figure 4-61). It can be seen that the order of highest activity precedes as follows IFN (100%), IFN-PEG_{20}-Fab_{beva} (10.5%), PEG_{20}-IFN (1.56%) and IFN-PEG_{20}-IFN (0.25%). Interestingly, IFN-PEG_{20}-Fab_{beva} has greater activity than PEG_{20}-IFN. The greater retained antiproliferative activity of IFN-PEG_{20}-Fab_{beva} could be due to the flexibility of the linker allowing IFN to bind more effectively to the IFNAR and start the JAK/STAT pathways resulting in antiproliferative activity (Bekisz et al., 2010).

Therapeutically, IFN-PEG_{20}-Fab_{beva} could be used as a treatment for renal cell carcinoma, where IFN is currently used as an antiproliferative agent, thus these results show that IFN within the IFN-PEG_{20}-Fab_{beva} conjugate has retained activity.

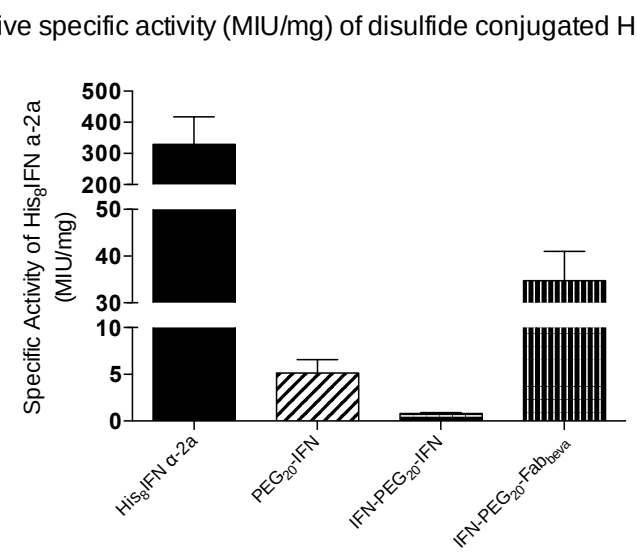

Figure 4-61. Specific activity (MIU/mg) of IFN, PEG_{20}-IFN, IFN-PEG_{20}-IFN, IFN-PEG_{20}-Fab_{beva} within the antiproliferative (Daudi cell) assay. IFN-PEG_{20}-Fab_{beva} retained activity when assayed in the antiviral assay.

To best determine the activity of the novel IFN-PEG_{20}-Fab_{beva} in comparison to IFN-PEG_{20}-IFN and controls (IFN and PEG_{20}-IFN) both the antiviral and antiproliferative data achieved were compared. Conducting both assays to assess the activity of IFN biologics is well documented in literature (Chang et al., 2009b; Subramanian et al., 2007). The antiviral and antiproliferative results suggest the order of activity achieved for the PEG and bevacizumab derived conjugates to be IFN, IFN-PEG_{20}-Fab_{beva}, PEG_{20}-IFN and IFN-PEG_{20}-IFN (Table 4–11). Interestingly, the IFN-PEG_{20}-Fab_{beva} conjugate was found to be more active in both the antiviral and antiproliferative assays than the PEG_{20}-IFN conjugate. This is possibly due to the linker length and flexibility of the linker, allowing IFN to better bind to the IFNAR. As it is well documented in literature that linker length and flexibility are important factors in affecting protein activity (Arai et al., 2001; Shewmake et al., 2008). Reduced activity of PEG conjugated proteins is well reported in literature. The reduction in protein activity is associated with the steric hinderance from the PEG. The results obtained suggest that the PEG_{20} di(*bis*)sulfone **4** can be used to efficiently link two proteins together, where the retained activity of IFN is greater than that of PEG_{20}-IFN. The greater retained activity observed in both the antiviral and antiproliferative assays could possibly be the result of the smaller solution structure of the PEG_{20} di(*bis*)sulfone **4** compared to PEG_{20} *bis*-sulfone **1**, which has been reported (Khalili et al., 2013).

Table 4–11. Summary table of antiviral and antiproliferative specific activity data achieved for IFN-PEG_{20}-Fab_{beva}, IFN-PEG_{20}-IFN and monoPEGylated controls

Sample	Antiviral specific activity (MIU/mg)	Antiproliferative specific activity (MIU/mg)
His_8IFN α-2a	231.31 ± 10.95	329.36 ± 87.98
IFN-PEG_{20}-IFN	2.17 ± 0.77	0.81 ± 0.09
PEG_{20}-IFN	3.95 ± 1.69	5.13 ± 1.44
IFN-PEG_{20}-Fab_{beva}	7.60 ± 2.56	34.72 ± 6.30

4.3 Conclusion

The aim of this chapter was to investigate the use of PEG_{20} di(*bis*)sulfone **4** prepared by synthesis route 2 (§3.2.1) to make IFN-PEG_{20}-Fab heterodimers. It was hoped that both IFN and Fab_{alb}/Fab_{beva} would retain functionality once conjugated to PEG_{20} di(*bis*)sulfone **4** and that the final heterodimers would be prepared in good yield and purity.

The data achieved for this chapter suggests that PEG_{20} di(*bis*)sulfone **4** can be used successfully as a linker/spacer to prepare heterodimers in good yield. The IFN-PEG_{20}-Fab_{alb} heterodimer was prepared as a possible treatment for hepatitis C, which could possibly 'piggy' back on albumin to last longer in circulation than current PEGylated treatments. To investigate the IFN-PEG_{20}-Fab_{alb} heterodimer further the activity of the IFN-PEG_{20}-Fab_{alb} would need to be determined. Possibly using serum free media within cell based assays or using BIAcore where the binding of IFN to IFNAR could be quantified without the need for the use of media. As anti-rat albumin Fab was used, the PK properties of the IFN-PEG_{20}-Fab_{alb} could be compared to PEG_{20}-IFN and IFN-PEG_{20}-Fab_{beva} in rats to determine if the PK properties of the heterodimer are prolonged due to the Fab_{alb} 'piggy' backing onto circulating albumin or if the half-life is due to the size of the heterodimer.

For determining the binding affinity properties, IFN-PEG_{20}-Fab_{alb} was compared to PEG_{20}-Fab_{alb}, to understand how the addition of IFN affected the binding properties of Fab_{alb} to rat albumin. PEG_{20}-Fab_{alb} was found to be very difficult to produce and purify. SE chromatography was used to purify PEG_{20}-Fab_{alb} from what was thought to be PEG_{20}-half Fab_{alb}. This could possibly be due to the polyclonal nature of the anti-rat albumin Fab. Therefore, if IFN-PEG_{20}-Fab_{alb} was to

be further investigated, possibly expressing the anti-rat albumin IgG could be investigated as a monoclonal antibody to produce homogenous products.

To investigate the IFN-PEG_{20}-Fab_{beva} heterodimer as a possible treatment for RCC, two areas would need to be further investigated, i) a relevant model for RCC, ii) PK properties. The relevant model for RCC where the IFN-PEG_{20}-Fab_{beva} heterodimer could be tested next to bevacizumab and IFN given separately. This would be interesting to see to determine if: i) the activity of the IFN-PEG_{20}-Fab_{beva} heterodimer is sustained over a longer period than that of bevacizumab, ii) the IFN-PEG_{20}-Fab_{beva} heterodimer is a more direct therapy for RCC and if this results in reduced cytokine related cytotoxicity. A possible model for determining if IFN-PEG_{20}-Fab_{beva} heterodimer can effectively reduce tumours of RCC is using a patient derived model, where a piece of tumour from a RCC patient is inserted into immunocompetent humanised mice. A study could then be conducted to determine if different doses of IFN-PEG_{20}-Fab_{beva} and controls (IFN + Fab_{beva}, IFN-PEG_{20}-Fab_{alb}) where successful in reducing or eradicating the tumour. Alternatively, a 3D tumour model could be used to assess the activity of the IFN-PEG_{20}-Fab_{beva} conjugate prior to *in vivo* studies and aid the doses used. 3D *in vitro* models are advantageous as they are more realistic as to the cell environment found in the body, compared to 1D *in vitro* cell cultures.

To further develop the use of PEG_{20} di(*bis*)sulfone **4** to heterodimeric molecules, the scalability of the approach would need to be improved. For example if Fabs were to be conjugated at one end of the linker, a more scalable approach could be to express the Fab's in mammalian cells (NS0, Sp20, CH0 cells) rather than the digestion of whole IgGs, this could afford greater yields.

Further, the PEG_{20} di(*bis*)sulfone **4** when made using synthesis route 2 produced higher yields of IFN-PEG-Fab heterodimers. Therefore, if further investigations into the reagent purity, purity of the starting materials and synthesis route was conducted, possibly the conversions and final yields of homodimers and heterodimers could be vastly improved and could produce a scalable approach in making multifunctional protein therapeutics. An alternative approach could be to develop a heterobifunctional PEG reagent with a one-pot-reaction, whereby one linker end could be conjugated to at a higher pH than the other linker end. This would remove the need for a 2-step conjugation approach and 2-CIEC steps, making multifunctional proteins an easier and scalable approach.

As discussed previously, the PEG_{20} di(*bis*)sulfone **4** is a flexible linker as it can be used to react with both polyhistidine tags and disulfide bridges. Therefore, is a very flexible approach. An interesting conjugate to make and test the functionality of would be a His_8IFN-PEG-Fab conjugate. This approach would combine the higher activity of His_8IFN (IFN conjugated to at the polyhistidine tag) with the conjugation of Fab at the disulfide.

Additionally, the PEG MW-structure-activity relationship could be further investigated. As in chapter 3, different MWs were investigated to determine if the PEG MW affected the activity of the IFN-PEG-IFN dimers. It is reported in literature that PEG MW does affect the activity of the protein. However, when making the IFN-PEG-Fab heterodimers, only a 20 kDa PEG was used to determine if multifunctional proteins could be prepared using PEG_{20} di(*bis*)sulfone **4**. Therefore it would be interesting to determine how/if PEG MW affects the functionality of the proteins and if this affects the conversion/yields of the multifunctional proteins. For example PEG MWs 10 and 20 kDa could be tested and the activity of IFN compared to conjugates (PEG-IFN and IFN-PEG-IFN) made in Chapter 3 using disulfide conjugation.

Table 4–12. Summary of IFN-PEG_{20}-Fab heterodimers prepared using disulfide conjugation and relevant controls. - = not tested, ND=could not be determined.

PEGylated conjugate	Purification method	Yield (%)	Purity (%)	AV mean Specific activity (MIU/mg)	Percentage retained activity (%)	AP mean Specific activity (MIU/mg)	Percentage retained activity (%)	K_D (nm)
His_8IFN α-2a	IMAC, AIEC	72 mg	100	231.31+10.95	100	329.36 ± 87.98	100	-
PEG_{20}-IFN	CIEC	29		3.95 ± 1.69	1.7	5.13 ± 1.44	1.56	-
IFN-PEG_{20}-IFN	CIEC, SEC	0.85		2.12 ± 0.64	0.94	0.81 ± 0.09	0.25	-
Fab_{beva}	Protein A	39	100	-	-	-	-	6.23 ± 0.67
IFN-PEG_{20}-Fab_{beva}	2× CIEC	IFN: 21 Fab_{beva}: 12	89	7.60 ± 2.56	3.3	34.62 ± 6.30	10.5	13.9 ± 0.24
PEG_{20}-Fab_{beva}	CIEC	44	83	-	-	-	-	6.04 ± 1.49
Fab_{alb}	Protein A	42		-	-	-	-	7.72 ± 0.70
IFN-PEG_{20}-Fab_{alb}	2× CIEC	IFN: 44 Fab_{alb}: 20.5		ND	ND	ND	ND	1.49 ± 0.03
PEG_{20}-Fab_{alb}	SEC	28.8		-	-	-	-	22.2 ± 1.15

Chapter 5 Summary of results and general conclusion

5.1 Summary of Results

The aim of this thesis was to determine if the homobifunctional PEG reagent **4** could be used to make therapeutic homodimeric and heterodimeric protein-protein conjugates that were based on IFN. First, IFN-PEG-IFN homodimers were prepared using two different site-specific conjugation methods (His-tag and disulfide). The PEG di(*bis*)sulfone **4** selectively undergoes *bis*-alkylation by a sequence of addition-elimination reactions with either the two free thiols from a reduced disulfide (Figure 1-13) or two histidine residues (Figure 1-14) within the polyhistidine tag. Site-specific histidine conjugation takes advantage of the his-tags, which are often used in the purification of recombinant proteins, as it can increase expression yields and aid refolding (Cong et al., 2012). Disulfide conjugation utilises the interchain disulfide bond, without the need for engineering in cysteines (Balan et al., 2007). Often, uncoupled cysteines are engineered into proteins for conjugation, however this is technically challenging as aggregation and disulfide scrambling often occurs during the refolding or purification process (Doherty et al., 2005). Disulfides have been conjugated to using maleimide conjugation, however it has been shown that this reagent undergoes hydrolysis leading to dePEGylation. Critically, it has been shown that maleimide based conjugation undergo exchange reactions to acidic by products *in vivo* (Alley et al., 2008; Shen et al., 2012).

Preparation of the His_8IFN-PEG-His_8IFN dimer and the other IFN dimers are examples of a recombinant-chemical conjugation approach to the preparation of dimeric and multifunctional proteins. IFN α and PEGylated IFN α are clinically used to treat Hepatitis B and C (Ahad et al., 2009). The PEG-IFNs that have been developed have become first line treatment and the PEGylation approach combines the advantages of reduced immunogenicity, increased body resistance time and protection from proteolytic digestion (Veronese and Morpurgo, 1999). The hope is that a hybrid approach to multifunctional proteins will be able to combine the advantages of site-specific conjugation with recombinant protein technology.

IFN was expressed recombinantly with an 8-polyhistidine tag (§3.2.2), which allowed the same molecule to be used throughout this PhD project. Both the polyhistidine tag and the natural disulfides could be conjugated site-specifically with

the PEG di(*bis*)sulfone reagent **4**. Like any thiol alkylation, the conjugation reaction with the protein cysteines is much more favoured than at other sites on the protein, including a histidine tag. Thiol conjugation only occurs if the IFN is first partially reduced. Without prior reduction, His-tag conjugation results. If the disulfides in IFN are first reduced, then conjugation to the cysteine thiols occurs. Thus, site-specific his-tag and disulfide conjugation was conducted on the His_8IFN α-2a to create IFN homodimers. It was hypothesised that the IFN dimers derived from conjugation at the polyhistidine tag would have greater activity than PEG-IFN conjugates, due to i) the site-specific nature of conjugation, reducing conjugation near or at the binding sites and ii) the greater number of IFNs present within the molecule which are able to bind to IFNAR complex.

Assessment of the activities of the different IFN-PEG-IFN homodimers was performed by optimised *in vitro* antiviral and antiproliferative assays (6.2-6.3Appendix II and III). Interestingly, it was found that His_8IFN-PEG_{20}-His_8IFN retained 2.95% activity compared to 0.92% activity for IFN-PEG_{20}-IFN (Table 3–7). This was thought to be due to the conjugation site. Conjugation to the polyhistidine tag is thought to be further away from the binding surfaces of IFN and this provides a conjugate with greater activity compared to the conjugation at an IFN disulfide that may be nearer to the IFN binding surface. The highest retained activity for IFN has been claimed to be at His^{34} (37% bioactivity) and the lowest retained activity was found at Lys^{164} (6% bioactivity) at the C-terminus of IFN (Wang et al., 2002). These PEG positional isomers were the result of random lysine conjugation preparing PEG-INTRON®, and showed the importance of conjugation away from the binding sites of the protein to retain a higher activity. Consequently, conjugation to H^{34} has been shown to be unstable where the PEG-H^{34} bond undergoes hydrolysis in aqueous solution, resulting in the de-conjugation of the PEG from the protein (Pedder, 2003; Wang et al., 2000). This inherent instability of PEG-H^{34} bond contributes to the relatively short-half-life of PEG-INTRON® (Pedder, 2003).

Alterative strategies have been described to prepare protein homodimers. These include DNL using an AD-DDD coupling to prepare PEGylated IFN dimers (Chang et al., 2009b) and flexible *bis*-maleimide cross linkers to prepare carbonic anhydrase II (Mack et al., 2011). The DNL 20 kDa monoPEGylated IFN-IFN dimer was reported to have an antiviral activity of 10×10^{12} U/mmol. The activity was reported to be 5-fold greater than PEGASYS® (Chang et al., 2009b). The His_8IFN-PEG_{20}-

His_8IFN (5.78 ± 1.62 MIU/mg) was found to be 2-fold more potent than PEGASYS® (2.75 ± 0.37 MIU/mg), while IFN-PEG_{20}-IFN (2.12 ± 0.64 MIU/mg) was found to have comparable activity to PEGASYS®. The DNL approach is a complex method, with several disadvantages; i) each protein/PEG molecule must be expressed/prepared with either the DDD or AD domain for fusing together to make the monoPEGylated dimer, ii) the AD and DDD peptides are 'locked' together by the cysteine residues forming a disulfide bridge, however during mild redox conditions during DNL conjugation some disulfides may reduce causing some proteins to aggregate or denature along with the AD and DDD peptides (Rossi et al., 2012). Further, in some cases fusion partners may have incompatible manufacturing properties, resulting in protein aggregation or misfolding of one of the fusion proteins, whilst the other partner maybe unharmed. In principle the recombinant-chemical approach described in this thesis may be more practical to implement. Precursor proteins can be recombinantly prepared using the optimum expression system and then dimerised by site-specific conjugation using the PEG di(*bis*)sulfone **4**.

It is well documented in literature that increasing PEG size correlates with decreasing protein activity. For example, a study found a 12 kDa monoPEGylated IFN was found to retain ~25% activity compared to 1.2% retained activity for the 40 kDa monoPEGylated IFN with the antiviral assay using A549 cells (Grace et al., 2005). Increasing PEG MW was also found to correlate with decreasing activity for the disulfide-conjugated IFN-PEG-IFN homodimers, PEG-IFN and $(PEG)_2$-IFN conjugates. Prior to potency testing, all of the disulfide conjugated IFN products were subject to anti-IFN Western blot and were found to be pure. The specific activity achieved for IFN-PEG_{10}-IFN was 5.99 ± 2.08 MIU/mg, whereas IFN-PEG_{20}-IFN achieved a specific activity of 2.12 ± 0.64 MIU/mg. Therefore the IFN-PEG_{10}-IFN dimer was found to retain a 2-fold greater activity compared to corresponding IFN-PEG_{20}-IFN

As discussed, enough of the different IFN-PEG-IFN dimers were prepared to characterise them in terms of their purity, identity and biological potency (Chapter 3). The His_8IFN-PEG_{20}-His_8IFN dimer was prepared pure but at low yield (1.5%; Table 3–7) when compared to PEG_{20}-His_8IFN (17.6%) producing using PEG *bis*-sulfone **1**. Disulfide-bridging conjugation was then examined to determine if IFN-PEG-IFN homodimers could be more efficiently prepared. It was found that the yield

of the IFN-PEG_{20}-IFN (0.85%;Table 3–7) and IFN-PEG_{10}-IFN (1.1%;Table 3–7) remained low, suggesting that the conjugation reactivity was not limiting the yield of the homodimers. Investigations into the PEG di(*bis*)sulfone **4** reagent revealed two possible factors affecting conversion and yield of the homodimers to be related to reagent purity and possible hydrolysis. Synthesis route 2, developed by G.Tekle, was used for the preparation of the PEG_{20} di($_{bis}$)sulfone **4** for preparing the IFN-PEG-Fab heterodimers. However, for the preparation of multifunctional protein-protein conjugates in larger quantities, more work needs to be done to optimise the synthesis route, purification and characterisation of PEG di(*bis*)sulfone **4**, to prepare the purest reagent to achieve better conversion and yield of protein-protein conjugates.

IFN-PEG_{20}-Fab_{beva} (IFN yield=21%; Fab_{beva}=12%) and IFN-PEG_{20}-Fab_{alb} (IFN yield=44%; Fab_{alb}=20.5%) were successfully prepared. Disulfide conjugation was used to conjugate both His_8IFN and Fab_{beva} to PEG_{20} di(*bis*)sulfone **4**. The rationale to examine the preparation of IFN-PEG_{20}-Fab_{beva} was based on the fact that bevacizumab plus interferon α is an approved treatment for metastatic renal cell carcinoma (RCC) (Rini et al., 2008). IFN-PEG_{20}-Fab_{alb} was prepared as a possible longer lasting form of IFN. The PEGylated Fabs, PEG_{20}-Fab_{beva} and PEG_{20}-Fab_{alb} were prepared as controls using PEG_{20} *bis*-sulfone **1**. PEG_{20}-Fab_{beva} were prepared with a final yield of 44% and were prepared in good purity (83%) (Table 4–12). However, it was found that PEG_{20}-Fab_{alb} was difficult to make, as an impurity assumed to be heavy or light chain was conjugating to PEG (PEG-heavy chain). The PEG-heavy chain was found to have a similar binding affinity to PEG_{20}-Fab_{alb} during CIEC, therefore SEC purification was used to purity the PEG_{20}-Fab_{alb}. A final yield of 28.8% was achieved of PEG_{20}-Fab_{alb} (Table 4–12). Site-specific disulfide conjugation has never been conducted on a polyclonal antibody or antibody fragment before. However it was found more difficult to prepare the PEG-Fab_{alb}, where the yield was lower than for PEG-Fab_{beva}, where Fab_{beva} was prepare from monoclonal bevacizumab IgG.

To determine if IFN, Fab_{alb} and Fab_{beva} had retained activity within the IFN-PEG_{20}-Fab_{alb} and IFN-PEG_{20}-Fab_{beva} heterodimers, *in vitro* assays were conducted. When conducting the antiviral and antiproliferative assays on IFN-PEG_{20}-Fab_{alb} conjugate, a 10-fold difference in IFN activity and a stunted sigmoid curve were observed. It was thought that Fab_{alb} was binding to components of the media. In spite of this complication, it does appear that the IFN component of IFN-PEG_{20}-Fab_{alb}

conjugate was active. However, an accurate specific activity for the IFN-PEG_{20}-Fab_{alb} could not be determined. If the assay was optimised with serum free media, a specific activity for the IFN-PEG_{20}-Fab_{alb} might be determined.

Bioactivity data was determined for IFN-PEG_{20}-Fab_{beva}, where in the antiviral assay a specific activity of 7.60 ± 2.56 MIU/mg, while in the antiproliferative assay a specific activity of 34.72 ± 6.30 MIU/mg was achieved (Table 4–12). This shows that IFN within the novel IFN-PEG_{20}-Fab_{beva} heterodimer had also retained its activity. Often when producing multifunctional proteins, the activity of the proteins is greatly reduced. For example, Albuinterferon, a HSA-IFN α fusion, retained 1% of IFN α (Subramanian et al., 2007). Often, reduced activity is due to the steric interference of the two proteins, in this case albumin and IFN. It was hoped by using the PEG as a spacer to link the two proteins, that both proteins would retain their activities. The order of activity determined by the antiviral and antiproliferative assays was; IFN (100% retained activity), IFN-PEG_{20}-Fab_{beva} (3.3% retained activity), PEG_{20}-IFN (1.7%) and IFN-PEG_{20}-IFN (10.5% retained activity, Table 4–12). Surprisingly, the IFN-PEG_{20}-Fab_{beva} heterodimer was found to have retained greater activity than PEG_{20}-IFN. This could possibly be due to the conformation of the heterodimer. It would be interesting to prepare an IFN-PEG_{20}-Fab_{beva} heterodimer, where the IFN has been conjugated to the PEG di(*bis*)sulfone **4** using his-tag conjugation.

It was also necessary to determine if Fab_{beva} and Fab_{alb} within the IFN-PEG_{20}-Fab_{beva} and IFN-PEG_{20}-Fab_{alb} heterodimers had retained binding. SPR was used to determine the binding of Fab_{beva} and Fab_{alb} within the IFN-PEG_{20}-Fab_{beva} and IFN-PEG_{20}-Fab_{alb}. It was observed that the association rate of IFN-PEG_{20}-Fab_{beva} was similar to Fab_{beva} (2.51 ± 0.32 $\times 10^4$ s^{-1}) and PEG_{20}-Fab_{beva} (2.38 ± 0.30 $\times 10^4$ s^{-1}), suggesting conjugation to the interchain disulfide does not impede binding to VEGF. A similar association rate of IFN-PEG_{20}-Fab_{alb} to Fab_{alb} (3.13 ± 0.31$\times 10^4$ s^{-1}) and PEG_{20}-Fab_{alb} (1.66 ± 0.47 $\times 10^4$ s^{-1}) was observed. Interestingly, when calculating the retained k_a IFN-PEG_{20}-Fab_{beva} and IFN-PEG_{20}-Fab_{alb}, in comparison to Fab_{beva} and Fab_{alb} respectively, both heterodimers retained ~54% association rates. The slower association rates achieved for the conjugated Fabs compared to the unconjugated Fabs could be due to steric shielding from the PEG, and the PEG+IFN for the heterodimers, explaining the similar retained association rates for the IFN-PEG-Fab heterodimers. The slowing of the association rates has also been described, with

varying PEG MW, where it is reported that the slower association rates could also be due to the PEGylated molecules blocking the association of other PEGylated molecules to bind to the ligands, especially at higher immobilised ligand densities (Khalili et al., 2012).

The dissociation rate gives an indication as to the propensity of an analyte to remain bound to the ligand. The dissociation rates of PEG_{20}-Fab_{beva} and PEG_{20}-Fab_{alb} were found to remain similar to that of Fab_{beva} ($1.55 \pm 0.10 \times 10^{-4}$ s^{-1}) and Fab_{alb} ($2.41 \pm 0.22 \times 10^{-4}$ s^{-1}, Table 4–8) respectively. The dissociation rates for IFN-PEG_{20}-Fab_{beva} ($1.79 \pm 0.30 \times 10^{-4}$ s^{-1}) and IFN-PEG_{20}-Fab_{alb} ($2.51 \pm 0.04 \times 10^{-4}$ s^{-1}) were found to increase slightly compared to Fab_{beva} and Fab_{alb} (Table 4–8). The faster dissociation rates observed for the heterodimers, could possibly be due to the monovalent binding of the Fab to the antigen, but also possibly the conjugation of the PEG may aid the diffusion from the bulk to the sensor surface. The dissociation of bevacizumab and $F(ab')_{2\text{-beva}}$ were found to be similar, with Fab_{beva} being quicker at dissociation, suggesting monovalent binding is quicker (Khalili et al., 2012). This data suggests that the novel IFN-PEG_{20}-Fab_{beva} and IFN-PEG_{20}-Fab_{alb} heterodimers have retained the activity of both the conjugated proteins. These are successful examples of how the PEG_{20} di(*bis*)sulfone **4** can be used in conjunction with disulfide-conjugation to prepare multifunctional proteins.

5.2 General discussion and conclusions

To further develop the concept of using PEG di(*bis*)sulfone **4** to prepare multifunctional proteins, it is important to investigate three areas: i) purity/quality of the starting reagents, ii) synthesis procedure to prepare PEG di(*bis*)sulfone **4**, iii) experimental procedure to prepare multifunctional proteins at larger scale with better conversions/yields. The main limitation with using the PEG di(*bis*)sulfone **4** reagent is the scalability of the current experimental approach. When producing the IFN dimers, it became apparent that the purity of the PEG di(*bis*)sulfone **4** affects the conversion and final yield of the end multifunctional protein. The purity of the PEG di(*bis*)sulfone **4** was found to be affected by the purity of the starting reagents used to prepare the PEG di(*bis*)sulfone **4** and the synthesis process used to prepare the PEG di(*bis*)sulfone **4**. For producing the heterodimers, an alternative synthesis route (2) was used to prepare PEG di(*bis*)sulfone **4**. The alternative synthesis route prepared higher conversion and yields of dimer compared to synthesis route 1 due to the purer

PEG di(*bis*)sulfone **4**. Therefore, to prepare higher yields of multifunctional proteins it is important to use the purest starting reagents to prepare the purest homobifunctional reagent **4**. Further, it is important to optimise the experimental process in preparing the multifunctional proteins, as the process must have as few steps as possible to minimise loss and to make the process scalable. For example, a one step synthesis could be investigated, such as conjugating one protein to one linker end at a lower pH, then increasing the pH to activate the other linker end for conjugating a second protein. As the main limitation with the current synthesis route for producing the IFN-PEG-Fab heterodimers, is that the unconjugated PEG di(*bis*)sulfone **4** reagent must be removed to ensure conjugation is conducted at the unconjugated linker end (X-PEG-Fab) to prepare the IFN-PEG-Fab heterodimer.

Further, it would be interesting to investigate maing a His_8IFN-PEG_{20}-Fab, conjugate. The functional activity of the His_8IFN-PEG_{20}-Fab would be interesting, as in chapter 3 it was found that the His_8IFN-PEG_{20}-His_8IFN dimer had greater activity than IFN-PEG_{20}-IFN. This is thought to be due to the conjugation site. The polyhistidine tag is thought to be further away from the protein-binding site than the thiols from the disulfides. Therefore it would of interest to investigate if, for example, His_8IFN-PEG_{20}-Fab_{beva} has greater activity than IFN-PEG_{20}-Fab_{beva}.

In chapter 3, different PEG MWs were investigated when making the IFN-PEG-IFN dimers, however this was not investigated when producing the IFN-PEG-Fab heterodimers. Therefore it would be interesting to investigate the PEG MW-structure-activity relationship with the heterodimers and if this affects the functional activity and conversion of the heterodimers. For example PEG MWs 10 and 20 kDa could be tested and the activity of IFN compared to conjugates (PEG-IFN and IFN-PEG-IFN) made in Chapter 3 using disulfide conjugation.

To develop the IFN-PEG_{10}-IFN, IFN-PEG_{20}-Fab_{beva} and IFN-PEG-Fab_{alb} conjugates, PK studies would need to be conducted to prove the conjugates are better than current treatments and ultimately have PK properties' better than current treatments. However, to do this the enough of the conjugates would need to be produced from one-batch. From the current experimental procedures this may be a problem, especially in case of IFN-PEG_{10}-IFN. Therefore, as stated previously, the purity of PEG di(*bis*)sulfone **4** would need to be improved to result in better conversions and yields of the conjugates. Further, the experimental procedures to make the conjugates would need to be improved for their scalability e.g. in the case

of IFN-PEG_{10}-IFN a SEC purification step would need to be replaced with CIEC for increased scalability.

The main achievements of this thesis, is that the IFN-PEG-IFN and IFN-PEG-Fab conjugates were prepared utilising two site-specific conjugation approaches and that the conjugates made were found to retain activity. The IFN-PEG-IFN conjugates were made using both his-tag and disulfide conjugation, where it was found that His_8IFN-PEG_{20}-His_8IFN retained 2.95% activity compared to 0.92% activity for IFN-PEG_{20}-IFN. This shows the flexibility of the homobifunctional reagent **4**, as two conjugation approaches can be used. It would be interesting to investigate the activity of His_8IFN conjugated to PEG di(*bis*)sulfone **4** by his-tag conjugation and conjugate Fab to the other end by disulfide conjugation to prepare His_8IFN-PEG_{20}-Fab_{beva}, as would this conjugate have greater activity than IFN-PEG_{20}-Fab_{beva}, further this demonstrates the possibilities available using the homobifunctional reagent **4**. As, the homobifunctional reagent utilises his-tags, which are often cleaved off after expression, as they often have no use. With the IFN-PEG-Fab heterodimers, it showed that PEG di(*bis*)sulfone **4** is able to conjugate two different proteins, allowing both proteins to retain activity, this had not been shown before with both antibodies and helical barrel proteins. To conclude, the work described in this thesis demonstrates encouraging results regarding utilising PEG di(*bis*)sulfone **4** to prepare protein-protein conjugates.

Chapter 6 Appendix

6.1 Appendix I: Calculations

Quantification of His_8IFN α-2a

ProtPram software was used to calculate the extinction coefficient for reduced and oxidised His_8-IFN α-2a, as can be seen below:

Extinction coefficients are in units of M^{-1} cm^{-1}, at 280 nm measured in water.

Ext. coefficient 18700
Abs 0.1% (=1 g/ l) 0.914, assuming all pairs of Cys residues form cystines

Ext. coefficient 18450
Abs 0.1% (=1 g/ l) 0.901, assuming all Cys residues are reduced

Calculating the protein concentration using UV (A=280 nm)

Beer-Lamberts Law calculation was used to calculate the concentration of the protein:

$$absorbance = extinction\ coefficient\ (\varepsilon)\ \times concentration \times length\ of\ pathway$$

To calculate the estimated protein concentration from UV at absorbance 280 nm, the following calculation was used:

$$Protein\ concentration = \frac{UV\ absorbance\ value\ (280\ nm)}{extinction\ coefficient\ (\varepsilon) \times length}$$

MicroBCA assay for Protein concentration determination

To calculate the protein concentration:

a) The average is calculated from each of the BCA standards and IFN α-2a samples

b) The average of the MicoBCA standard blank is subtracted from the MicroBCA standards and IFN α-2a samples.

c) The standard deviation is calculated for each MicroBCA standard and IFN α-2a sample.

d) 2nd order linear least squares regression model was used to calculate the protein concentration:

$$y = m_2x^2 + m_1X + b$$

This model was used as an alternative to 1st order least squares regression (y=mx+b), where absorbance vs protein concentration should form a liner curve. This is due to the some of the BCA calibration curve points not being within the linear part of the curve (200 µg/mL), furthermore some of the points between (20-0 µg/mL) may not completely fit within the linear of line of the curve due to pipetting errors etc. Thus to compensate the 2nd order linear least squares regression model is used to best fit the data of the MicroBCA assay.

Antiviral assay calculations

To calculate from the sample concentration to the starting concentration of the dilution plate the following calculation was used:

$$V_1 = C_2 \times V_2 \div C_1$$

To calculate from the sample ED_{50} (pg/ mL) to sample specific activity (IU/ mg), the following calculations were used:

a) $dilution\ factor\ of\ NIBSC\ IFN \propto -2a = \frac{NIBSC\ stock\ concentration\ (IU/\ mL)}{NIBSC\ ED_{50}(\ IU/\ mL)}$

b) $dilution\ factor\ for\ sample = \frac{sample\ stock\ concentration(\ pg/\ mL)}{sample\ ED_{50}(pg/\ mL)}$

c) potency of sample compared to NIBSC $= \frac{\text{sample dilution factor (b)}}{\text{NIBSC dilution factor (a)}}$

d) $sample\ activity\ (IU/\ mL) =$

$sample\ potency\ (c) \times NIBSC\ activity\ (63{,}000\ IU/\ mL)$

e) $sample\ specific\ activity\ (IU/\ \mu g) = \frac{(d)sample\ activity\ (IU/\ mL)}{sample\ stock\ concentration(\mu g/\ mL)}$

f) $sample\ specific\ activity\ (IU/\ mg) = sample\ specific\ activity\ (IU/\ \mu g)(e) \times 1000$

g) $sample\ specific\ activity\ (10^6\ IU/\ mg) = \frac{sample\ specific\ activity\ (IU/\ mg)(f)}{10^6}$

Table 6–1. Raw antiviral potency data achieved for disulfide PEGylated IFN compounds

Value	His_8IFN α-2a	PEGASYS®	PEG_5-IFN	$(PEG_5)_2$-IFN	PEG_{10}-IFN	$(PEG_{10})_2$-IFN	IFN-PEG_{10}-IFN	PEG_{20}-IFN	$(PEG_{20})_2$-IFN	IFN-PEG_{20}-IFN
Specific activity (×10^6 IU/ mg)	223.44 243.82 226.68	2.37 2.46 2.47	59.28 44.5	0.87 0.83 0.82	3.5 3.26 4.06 6.43 7.06	0.1 0.17 0.09	3.74 6.4 7.84	5.23 4.72 5.55	0.52 0.54 0.6	1.96 3.03 1.53 1.94
Mean specific activity (×10^6 IU/ mg)	231.31	2.43	51.89	0.84	4.86	0.12	5.99	3.95	0.55	2.12
ST.DEV of specific activity (×10^6 IU/ mg)	10.95	0.06	10.45	0.03	1.766	0.04	2.08	1.69	0.04	0.64
Percentage (%) retained activity	100	-	22.4	0.36	2.1	0.05	2.59	1.7	0.24	0.92
n number	3	3	2	3	5	3	3	5	3	4

6.2 Appendix II: Optimisation of the antiproliferative assay for the determination of the *in vitro* activity of IFN α and β

Interferons α and β have been shown not only to elicit antiviral activity, but also antiproliferative effects. The antiproliferative activity of IFNs was first described by Paucker in 1962 and colleagues who demonstrated that a 24 h exposure of L-cells to either UV-irradiated Newcastle disease virus or to IFN led to a temporary decline in cell growth. Interferons exert antiproliferative effects though cell cycle arrest particularly of the G0 and G1 phases (Sangfelt et al., 1997; Tiefenbrun et al., 1996). A variety of cell types including Daudi, ME15, H9 and U-266 cell lines have shown to be sensitive to the antiproliferative activity of IFNs and their conjugates (Borden et al., 1982; Foser et al., 2003; Sangfelt et al., 1997). However, human Burkitts lymphoma or Daudi cell line, shown in Figure 6-1, is the most widely utilised cell lines (Meager et al., 2001) and this is due it being highly sensitive to type I IFNs bit insensitive to type II and type III IFNs (Meager et al., 2001).

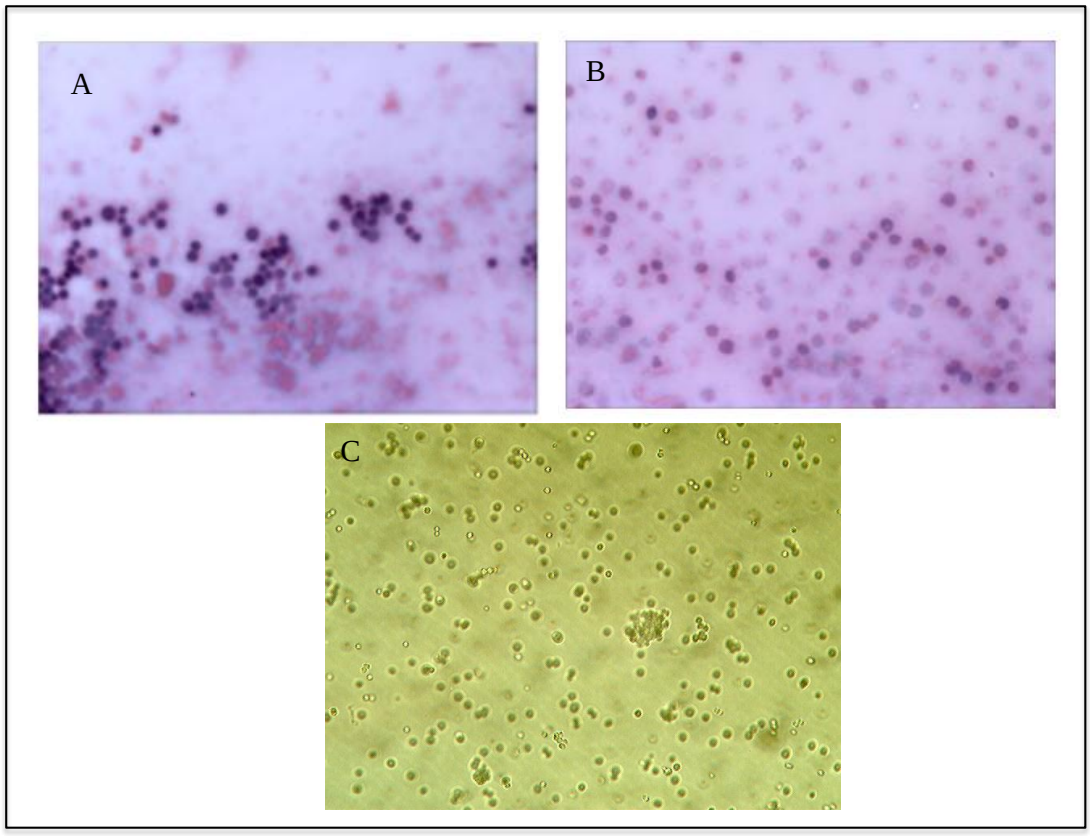

Figure 6-1. Microscopy images of Daudi cells, A-B) following haematoxylin and eosin (H&E) staining and C) growing in RPMI medium.

Growth characteristics of Daudi cells at different cell densities

Firstly to better understand the growth characteristics of the Daudi cells, a general growth curve was undertaken. A growth curve was conducted to determine if the Daudi cells were within the exponential phase after 72 h incubation required in the antiproliferative assay. The Daudi cell number was counted every 24 h and recorded over a five-day period (method 2.2.11.6). The Daudi cell growth curve in Figure 6-2, shows the initial lag phase (Figure 6-2, 1) which is the time it takes for the cells to recover from subculture and start to spread, which for Daudi cells is ~12 h. The Daudi cell number increases exponentially, this is the log phase (Figure 6-2, 2). The doubling time of the Daudi cells is ~24 h, thus if the cells were plated at 100,000 cells/well, the cells would be still be within the log phase of the growth curve after a 72 h incubation period. Thus, the assay is assessing the inhibition of the Daudi cells multiplication by IFN α-2a. The growth curve shows the cell number plateauing between days 3 and 4 (Figure 6-2, 3), this is where the culture becomes too confluent and the growth rate slows down or stops.

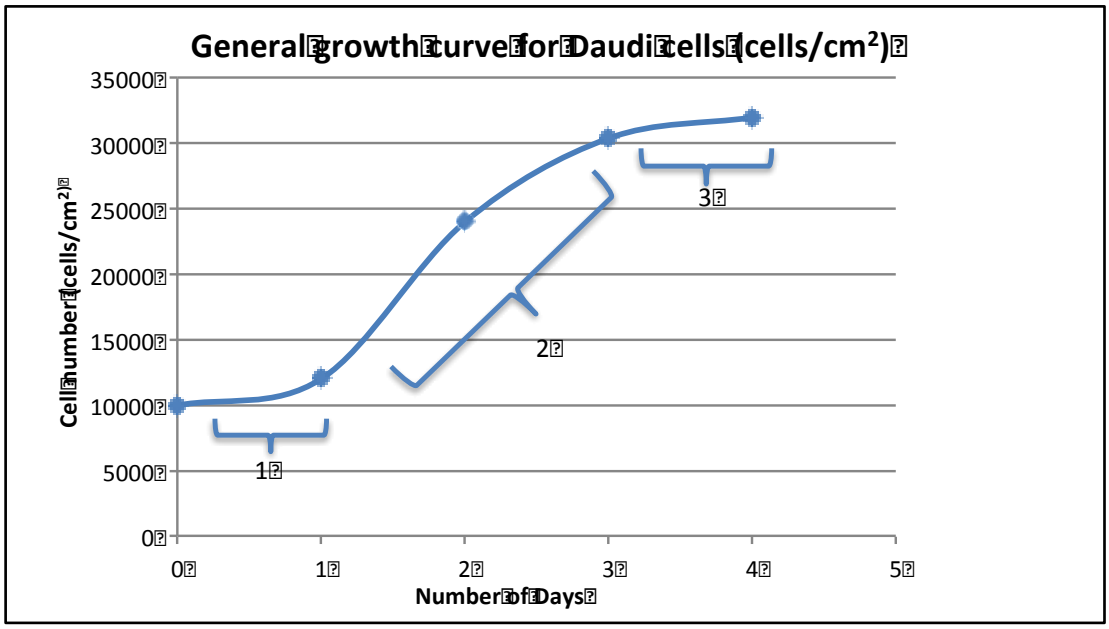

Figure 6-2. General growth curve for Daudi cells (cells/ cm^2)

The antiproliferative assay is built on the understanding that the cell growth in inhibited by the presence of IFN, thus it is necessary to determine a cell number, which over the incubation period (72 h), is within the exponential growth phase. Thus, confirming the inhibition of growth when in the presence of IFN rather than the cell death being due to alternative factors. In order to examine the response of the different seeding densities to MTT, different cell densities were seeded and the MTT

response was measured every day for 4 days in the absence of any IFN, method 2.2.11.6.

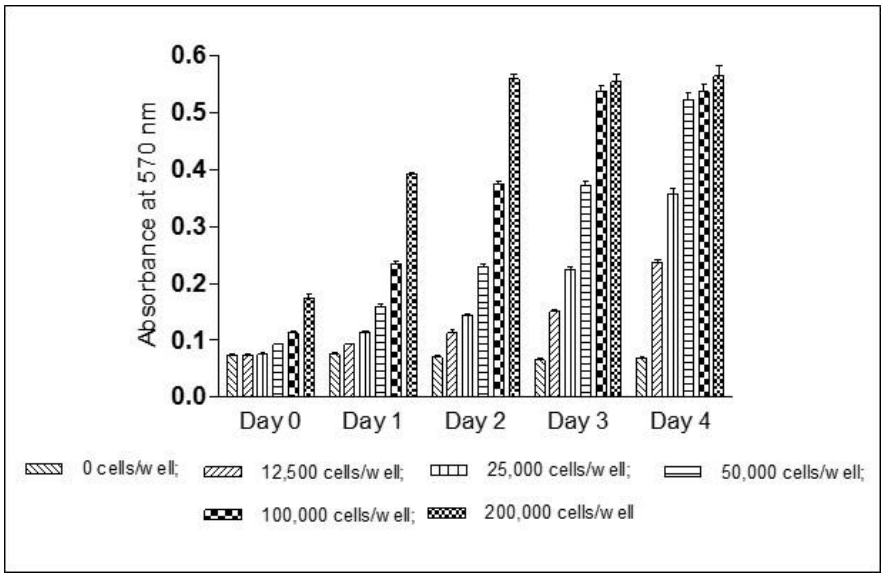

Figure 6-3. Daudi cell density optimisation for the antiproliferative assay

It can be observed in Figure 6-3 that all the all the cell densities showed an increase in cell number. At 200,000 cells/well, a steady growth rate peaked after 2 days and plateaued thereafter, which could be the result of exhaustion of media. The lowest cell densities tested (12,500 and 25,000 cell/ well) over the 4 days did not increase in number sufficiently, thus were unsuitable cell densities. The optimum seeding densities were 50,000-100,000 cells/ well due to them showing sufficient growth over 4 days as they provide a greater endpoint range to measure.

Optimisation of cell density

In order to achieve a sufficient decrease in cell viability, different cell numbers were tested in order to ensure the assay is assessing the inhibition of Daudi cell growth due to the presence of IFN. For this experiment (method 2.2.11.7) the Daudi cells were seeded at the densities of 4×10^5, 2×10^5, 1×10^5, 5×10^4, 2.5×10^4, 1.25×10^4 cells per well of a 96 well U-bottom plate along with 2-fold serial dilutions of the standards. For IFN-α, the two different standards used were PEGASYS® and NIBSC IFN α-2a. For IFN β, the two standards used were Betaferon® (IFN β-1b) and NIBSC IFN-β1b. The plates were incubated for 72 h (3 days) at 37 °C, cell viability was assessed by the addition of MTT. Following a 3 h incubation with MTT, the media was aspirated and the blue formazan crystals dissolved in sterile DMSO by agitation for 30 min. The absorbance at 570 nm was then measured using

a plate reader. In all experiments the appropriate controls (media alone and cell suspension) were included.

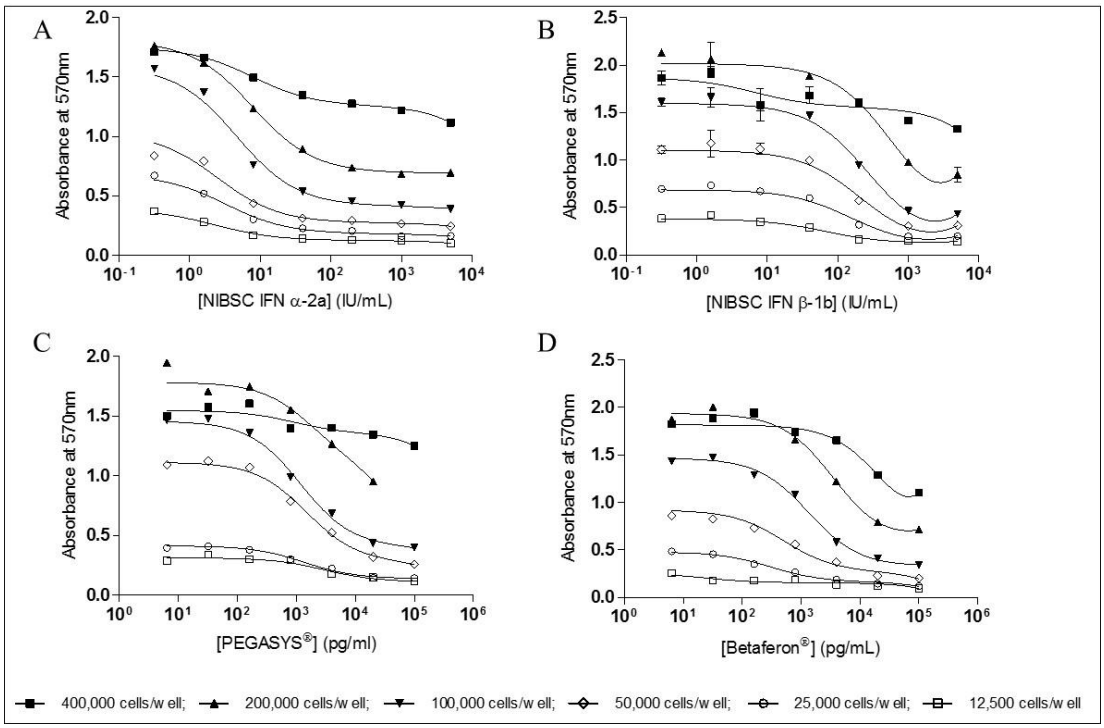

Figure 6-4. Effect of Daudi cell density on the antiproliferative effects of (A) NIBSC IFN α-2a, (B) PEGASYS®, (C) NIBSC IFN β-1b, (D) Betaferon®. Optimum seeding density was found to be 100,000 cell/ well.

Figure 6-4 that there is a dose dependent decrease in cell density from the dose response curves. At low seeding densities, only a very small change in absorbance was seen upon the additions of different concentrations of IFN α and –β. Whereas for the highest cell densities, large decreases in absorbance can be seen, this is likely a result of increased rate of nutrient depletion and build-up of toxic by-products caused by the increased amount of cells. It was deduced from this experiment that the optimum seeding density was 100,000 cells/well since this gave the greatest difference in absorbance from ~1.5 to 0.5 at 570 nm.

Optimisation of sample concentration

From Figure 6-5 it was observed that optimisation of sample concentration was required. Therefore, following method Effect of sample incubation time on cell viability Daudi cells were seeded at ~1×10^5 cells per well, the concentration of IFN-α or β was varied. A lower starting concentration of NIBSC IFN-α was used since in the previous experiment the curve did not plateau also a higher concentration NIBSC IFN-β since the cell viability did not reach the lowest cell viability. The results of

this experiment can be seen in Figure 6-5 where it can be observed that the cell viability does not decrease below 40%. Therefore, next different incubation times (72, 96 and 120 h) were then examined to see if the cell viability would decrease below 40%. Intriguingly, a much higher starting concentration of IFN β sample was required to prepare the same effects as IFN α suggesting that overall IFN α has greater antiproliferative effects than IFN β.

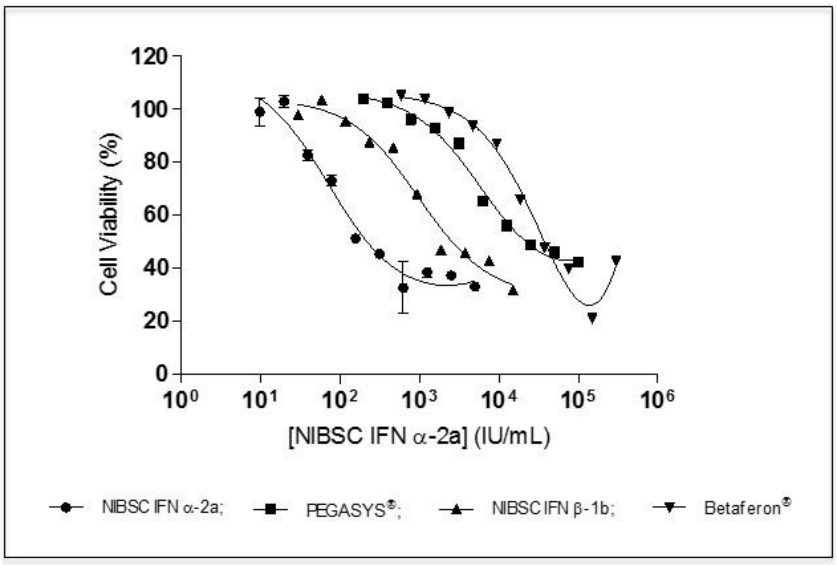

Figure 6-5. Optimisation of the concentration of NIBSC IFNα , PEGASYS®, NIBSC IFN β-1b and Betaferon® on the proliferation of Daudi cells.

Effect of sample incubation time on cell viability

To determine if the cell viability would decrease below 40% with the increased sample incubation time, the same sample concentrations were used and the plates were incubated for (72,96 and 120 h), method 2.2.11.8. As shown in Figure X, longer incubation times of 92 or 120 h did result in a reduction of cell viability to about 20% at the highest sample concentration. However, these increased incubation times were found to have decreased r-squared values. The r-squared value gives an indication of how well the line fits the data points on the graph. This variability may be from evaporation of media from the edges of the plate, which can be overcome by excluding the edges of the plate in future assays. Based on the data achieved, the incubation time of 72 h was decided on.

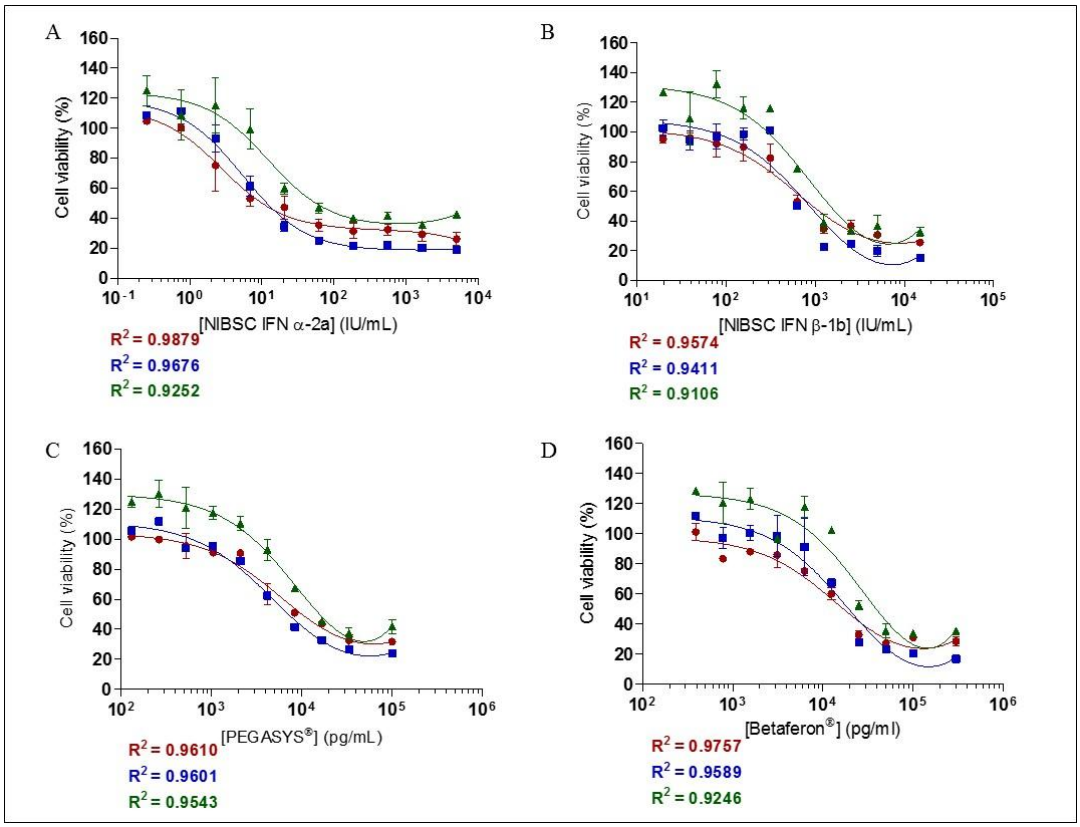

Figure 6-6. Effect of sample incubation time on the antiproliferative activity of (A) NIBSC IFN α-2a, (B) PEGASYS®, (C) NIBSC IFN β-1b and (D) Betaferon® on the proliferation of Daudi cells. The different incubation times were 72 h (blue line), 96 h (green line) and 120 h (red line).

6.3 Appendix III: Optimisation of the antiviral assay for IFN potency testing

50 % Tissue Culture Infective dose ($TCID_{50}$) assay for EMCV using A549 cells

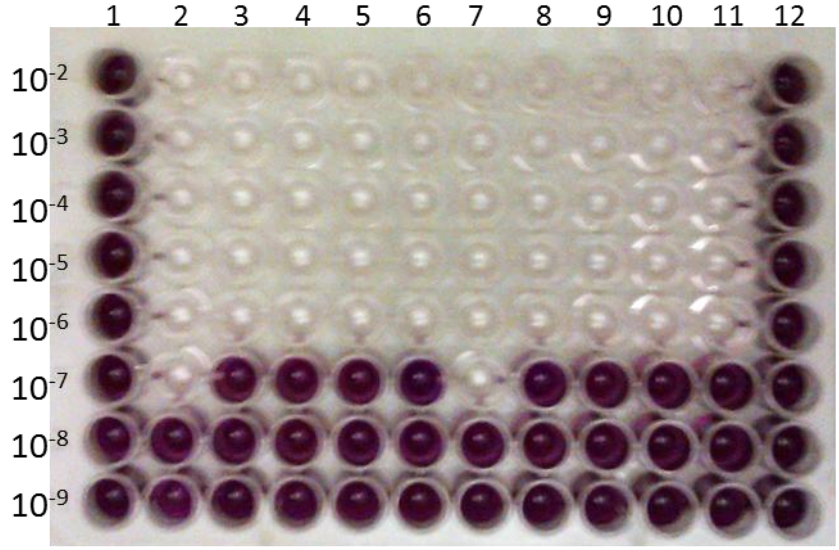

Figure 6-7. Results of the MTT assay to keep record of the $TCID_{50}$ for EMCV virus. Viable cells are coloured purple and virus infected cells are where no colour is visible. Columns 1 and 12 are negative controls.

To determine the EMCV virus stock strength a $TCID_{50}$ assay was used (§2.2.10.6). The $TCID_{50}$ can be defined as the dilution of the virus required to prepare a pathological change in 50% of the inoculated wells. A549 cells were infected with EMCV virus stock diluted to achieve concentrations of 10^{-2} to 10^{-9} and the CPE monitored from 72 to 96 h. The plates were harvested with MTT after 120 h, where MTT shows the effect of virus the wells are clear while wells containing viable cells are shown by a purple colour (Figure 6-7). Using MTT provided an easy, non-subjective assessment of viable cells rather than visual inspection, which is prone to error. To obtain the most accurate $TCID_{50}$ value, columns 2 to 11 were used for EMCV infection for each of the virus dilutions as opposed to using less replicates which would increase the variability and reduce the accuracy of the results. The plate shows 80% viability (CPE) at concentration of 10^{-7}. The $TCID_{50}$ was calculated using Reed and Muench's mathematical technique, for this assay it was found to be 1.63×10^{8} PFU/mL.

Bibliography

Ahad, M., Alim, M., and Ekram, A.S. (2009). Interferon to PEG-Interferon: A Review. TAJ J. Teach. Assoc. *17*, 2–5.

Akerström, B., Nielsen, E., and Björck, L. (1987). Definition of IgG- and albumin-binding regions of streptococcal protein G. J. Biol. Chem. *262*, 13388–13391.

Alley, S.C., Benjamin, D.R., Jeffrey, S.C., Okeley, N.M., Meyer, D.L., Sanderson, R.J., and Senter, P.D. (2008). Contribution of linker stability to the activities of anticancer immunoconjugates. Bioconjug. Chem. *19*, 759–765.

Alley, S.C., Okeley, N.M., and Senter, P.D. (2010). Antibody-drug conjugates: targeted drug delivery for cancer. Curr. Opin. Chem. Biol. *14*, 529–537.

Andersen, J.T., Cameron, J., Plumridge, A., Evans, L., Sleep, D., and Sandlie, I. (2013). Single-chain variable fragment albumin fusions bind the neonatal Fc receptor (FcRn) in a species-dependent manner: implications for in vivo half-life evaluation of albumin fusion therapeutics. J. Biol. Chem. *288*, 24277–24285.

Andrew, S.M., and Titus, J.A. (2001). Fragmentation of immunoglobulin G. Curr. Protoc. Cell Biol. *Chapter 16*.

Anguille, S., Lion, E., Willemen, Y., Van Tendeloo, V.F.I., Berneman, Z.N., and Smits, E.L.J.M. (2011). Interferon-α in acute myeloid leukemia: an old drug revisited. Leuk. Off. J. Leuk. Soc. Am. Leuk. Res. Fund, U.K *25*, 739–748.

Arai, R., Ueda, H., Kitayama, a, Kamiya, N., and Nagamune, T. (2001). Design of the linkers which effectively separate domains of a bifunctional fusion protein. Protein Eng. *14*, 529–532.

Arruebo, M., Valladares, M., and González-Fernández, Á. (2009). Antibody-Conjugated Nanoparticles for Biomedical Applications. J. Nanomater. *2009*, 1–24.

Baeuerle, P. a, and Reinhardt, C. (2009). Bispecific T-cell engaging antibodies for cancer therapy. Cancer Res. *69*, 4941–4944.

Bailon, P., and Won, C. (2009). PEG-modified biopharmaceuticals. Expert Opin. Drug Deliv. *6*, 1–16.

Bailon, P., Palleroni, A., Schaffer, C. a, Spence, C.L., Fung, W.J., Porter, J.E., Ehrlich, G.K., Pan, W., Xu, Z.X., Modi, M.W., et al. (2001). Rational design of a potent, long-lasting form of interferon: a 40 kDa branched polyethylene glycol-conjugated interferon alpha-2a for the treatment of hepatitis C. Bioconjug. Chem. *12*, 195–202.

Baker, M.P., and Jones, T.D. (2007). Identification and removal of immunogenicity in therapeutic proteins. Curr. Opin. Drug Discov. Devel. *10*, 219–227.

Balan, S., Choi, J.-W., Godwin, A., Teo, I., Laborde, C.M., Heidelberger, S., Zloh, M., Shaunak, S., and Brocchini, S. (2007). Site-specific PEGylation of protein disulfide bonds using a three-carbon bridge. Bioconjug. Chem. *18*, 61–76.

Bause, E., and Lehle, L. (1979). Enzymatic N-glycosylation and O-glycosylation of synthetic peptide acceptors by dolichol-linked sugar derivatives in yeast. Eur. J. Biochem. *101*, 531–540.

Beck, A., and Reichert, J.M. (2011). Therapeutic Fc-fusion proteins and peptides as successful alternatives to antibodies. MAbs *3*, 415–416.

Beckman, R. a, Weiner, L.M., and Davis, H.M. (2007). Antibody constructs in cancer therapy: protein engineering strategies to improve exposure in solid tumors. Cancer *109*, 170–179.

Bekisz, J., Baron, S., Balinsky, C., Morrow, A., and Zoon, K.C. (2010). Antiproliferative Properties of Type I and Type II Interferon. Pharmaceuticals (Basel). *3*, 994–1015.

Bell, S.J., Fam, C.M., Chlipala, E. a, Carlson, S.J., Lee, J.I., Rosendahl, M.S., Doherty, D.H., and Cox, G.N. (2008). Enhanced circulating half-life and antitumor activity of a site-specific pegylated interferon-alpha protein therapeutic. Bioconjug. Chem. *19*, 299–305.

Bendele, a, Seely, J., Richey, C., Sennello, G., and Shopp, G. (1998). Short communication: renal tubular vacuolation in animals treated with polyethylene-glycol-conjugated proteins. Toxicol. Sci. *42*, 152–157.

Bitonti, A.J., Dumont, J. a, Low, S.C., Peters, R.T., Kropp, K.E., Palombella, V.J., Stattel, J.M., Lu, Y., Tan, C. a, Song, J.J., et al. (2004). Pulmonary delivery of an erythropoietin Fc fusion protein in non-human primates through an immunoglobulin transport pathway. Proc. Natl. Acad. Sci. U. S. A. *101*, 9763–9768.

Borden, E.C., Hogan, T.F., and Voelkel, J.G. (1982). Comparative antiproliferative activity in vitro of natural interferons alpha and beta for diploid and transformed human cells. Cancer Res. *42*, 4948–4953.

Borden, E.C., Sen, G.C., Uze, G., Silverman, R.H., Ransohoff, R.M., Foster, G.R., and Stark, G.R. (2007). Interferons at age 50: past, current and future impact on biomedicine. Nat. Rev. Drug Discov. *6*, 975–990.

Brassard, D.L., Grace, M.J., and Bordens, R.W. (2002). Interferon-alpha as an immunotherapeutic protein. J. Leukoc. Biol. *71*, 565–581.

Brocchini, S., Balan, S., Godwin, A., Choi, J.-W., Zloh, M., and Shaunak, S. (2006). PEGylation of native disulfide bonds in proteins. Nat. Protoc. *1*, 2241–2252.

Brocchini, S., Godwin, A., Balan, S., Choi, J., Zloh, M., and Shaunak, S. (2008). Disulfide bridge based PEGylation of proteins. Adv. Drug Deliv. Rev. *60*, 3–12.

Vanden Broecke, C., and Pfeffer, L.M. (1988). Characterization of interferon-alpha binding sites on human cell lines. J. Interferon Res. *8*, 803–811.

Byrne, B., Donohoe, G.G., and O'Kennedy, R. (2007). Sialic acids: carbohydrate moieties that influence the biological and physical properties of biopharmaceutical proteins and living cells. Drug Discov. Today *12*, 319–326.

Carmeliet, P. (2005). VEGF as a Key Mediator of Angiogenesis in Cancer. Oncology *69(suppl 3*, 4–10.

Carnemolla, B. (2002). Enhancement of the antitumor properties of interleukin-2 by its targeted delivery to the tumor blood vessel extracellular matrix. Blood *99*, 1659–1665.

Carter, P.J. (2006). Potent antibody therapeutics by design. Nat. Rev. Immunol. *6*, 343–357.

Carter, P.J. (2011). Introduction to current and future protein therapeutics: a protein engineering perspective. Exp. Cell Res. *317*, 1261–1269.

Casi, G., and Neri, D. (2012). Antibody-drug conjugates: basic concepts, examples and future perspectives. J. Control. Release *161*, 422–428.

Chames, P., and Baty, D. (2009). Bispecific antibodies for cancer therapy: the light at the end of the tunnel? MAbs *1*, 539–547.

Chang, C. (2010). Dimeric alpha interferon PEGylated site specifically shows enhanced and prolonged efficacy in vivo.

Chang, C., Gupta, P., and Goldenberg, D.M.D. (2009a). Advances and challenges in developing cytokine fusion proteins as improved therapeutics. Expert Opin. Drug Discov. *4*, 181–194.

Chang, C.-H., Rossi, E.A., Cardillo, T.M., Nordstrom, D.L., McBride, W.J., and Goldenberg, D.M. (2009b). A new method to prepare monoPEGylated dimeric cytokines shown with human interferon-α2b. Bioconjug. Chem. *20*, 1899–1907.

Chapman, a P., Antoniw, P., Spitali, M., West, S., Stephens, S., and King, D.J. (1999). Therapeutic antibody fragments with prolonged in vivo half-lives. Nat. Biotechnol. *17*, 780–783.

Chaudhury, C., Mehnaz, S., Robinson, J.M., Hayton, W.L., Pearl, D.K., Roopenian, D.C., and Anderson, C.L. (2003). The Major Histocompatibility Complex-related Fc Receptor for IgG (FcRn) Binds Albumin and Prolongs Its Lifespan. J. Exp. Med. *197*, 315–322.

Chen, C., Constantinou, A., and Deonarain, M. (2011). Modulating antibody pharmacokinetics using hydrophilic polymers. Expert Opin. Drug Deliv. *8*, 1221–1236.

Chevallet, M., Luche, S., and Rabilloud, T. (2006). Silver staining of proteins in polyacrylamide gels. Nat. Protoc. *1*, 1852–1858.

Cines, D.B., Yasothan, U., and Kirkpatrick, P. (2008). Romiplostim. Nat. Rev. Drug Discov. *7*, 887–888.

Cleland, W.W. (1964). Dithiothreitol, a New Protective Reagent for SH Groups*. Biochemistry *3*, 480–482.

Cong, Y., Pawlisz, E., Bryant, P., Balan, S., Laurine, E., Tommasi, R., Singh, R., Dubey, S., Peciak, K., Bird, M., et al. (2012). Site-specific PEGylation at histidine tags. Bioconjug. Chem. *23*, 248–263.

Cooper, M. a (2002). Optical biosensors in drug discovery. Nat. Rev. Drug Discov. *1*, 515–528.

Coulter, a, and Harris, R. (1983). Simplified preparation of rabbit Fab fragments. J. Immunol. Methods *59*, 199–203.

Czajkowsky, D.M., Hu, J., Shao, Z., and Pleass, R.J. (2012). Fc-fusion proteins: new developments and future perspectives. EMBO Mol. Med. *4*, 1015–1028.

Davis, K. (2014). Amgen Recieves FDA Breakthrough Therapy Designation For Investigation BiTE Antibody Blinatumomab In Acute Lymphoblastic Leukemia.

Dennis, M.S., and Lazarus, R.A. (1994). Kunitz domain inhibitors of tissue factor-factor VIIa. I. Potent inhibitors selected from libraries by phage display. J. Biol. Chem. *269*, 22129–22136.

Doherty, D.H., Rosendahl, M.S., Smith, D.J., Hughes, J.M., Chlipala, E.A., and Cox, G.N. (2005). Site-specific PEGylation of engineered cysteine analogues of recombinant human granulocyte-macrophage colony-stimulating factor. Bioconjug. Chem. *16*, 1291–1298.

Duncan, R. (2003). The dawning era of polymer therapeutics. Nat. Rev. Drug Discov. *2*, 347–360.

Dytham, C. (2011). Choosing and using statistics: a biologist's guide (Wiley-Blackwell).

Ebersbach, H., Fiedler, E., Scheuermann, T., Fiedler, M., Stubbs, M.T., Reimann, C., Proetzel, G., Rudolph, R., and Fiedler, U. (2007). Affilin-novel binding molecules based on human gamma-B-crystallin, an all beta-sheet protein. J. Mol. Biol. *372*, 172–185.

Egrie, J.C., and Browne, J.K. (2002). Development and characterization of darbepoetin alfa. Oncology (Williston Park). *16*, 13–22.

Egrie, J.C., Dwyer, E., Browne, J.K., Hitz, A., and Lykos, M.A. (2003). Darbepoetin alfa has a longer circulating half-life and greater in vivo potency than recombinant human erythropoietin. In Experimental Hematology, (Elsevier Science Inc.,), pp. 290–299.

Eigentler, T.K., Weide, B., de Braud, F., Spitaleri, G., Romanini, A., Pflugfelder, A., González-Iglesias, R., Tasciotti, A., Giovannoni, L., Schwager, K., et al. (2011). A dose-escalation and signal-generating study of the immunocytokine L19-IL2 in combination with dacarbazine for the therapy of patients with metastatic melanoma. Clin. Cancer Res. *17*, 7732–7742.

Einstein, M.H., Baron, M., Levin, M.J., Chatterjee, A., Edwards, R.P., Zepp, F., Carletti, I., Dessy, F.J., Trofa, A.F., Schuind, A., et al. (2009). Comparison of the immunogenicity and safety of Cervarix and Gardasil human papillomavirus (HPV) cervical cancer vaccines in healthy women aged 18-45 years. Hum. Vaccin. *5*, 705–719.

Elliott, S., Lorenzini, T., Asher, S., Aoki, K., Brankow, D., Buck, L., Busse, L., Chang, D., Fuller, J., Grant, J., et al. (2003). Enhancement of therapeutic protein in vivo activities through glycoengineering. Nat. Biotechnol. *21*, 414–421.

Escudier, B., Pluzanska, A., Koralewski, P., Ravaud, A., Bracarda, S., Szczylik, C., Chevreau, C., Filipek, M., Melichar, B., Bajetta, E., et al. (2007). Bevacizumab plus interferon alfa-2a for treatment of metastatic renal cell carcinoma: a randomised, double-blind phase III trial. Lancet *370*, 2103–2111.

Escudier, B., Cosaert, J., and Jethwa, S. (2008). Targeted therapies in the management of renal cell carcinoma: role of bevacizumab. Biologics *2*, 517–530.

Evans, J.B., and Syed, B. a (2014). Next-generation antibodies. Nat. Rev. Drug Discov. 1–2.

Fahey, E.M., Chaudhuri, J.B., and Binding, P. (2000). Refolding of Low Molecular Weight Urokinase Plasminogen Activator by Dilution and Size Exclusion Chromatography—A Comparative Study. Sep. Sci. Technol. *35*, 1743–1760.

Farkas, H., and Varga, L. (2011). Ecallantide is a novel treatment for attacks of hereditary angioedema due to C1 inhibitor deficiency. Clin. Cosmet. Investig. Dermatol. *4*, 61–68.

Fee, C.J. (2007). Size comparison between proteins PEGylated with branched and linear poly(ethylene glycol) molecules. Biotechnol. Bioeng. *98*, 725–731.

Feldwisch, J., Tolmachev, V., Lendel, C., Herne, N., Sjöberg, A., Larsson, B., Rosik, D., Lindqvist, E., Fant, G., Höidén-Guthenberg, I., et al. (2010). Design of an optimized scaffold for affibody molecules. J. Mol. Biol. *398*, 232–247.

Fenselau, C. (1997). MALDI MS and strategies for protein analysis. Anal. Chem. *69*, 661A – 665A.

Ferrantini, M., Capone, I., and Belardelli, F. (2007). Interferon-alpha and cancer: mechanisms of action and new perspectives of clinical use. Biochimie *89*, 884–893.

Fish, E.N. (1992). Definition of receptor binding domains in interferon-alpha. J. Interferon Res. *12*, 257–266.

Folkman, J. (2007). Angiogenesis: an organizing principle for drug discovery? Nat Rev Drug Discov *6*, 273–286.

Forni, G., Giovarelli, M., and Santoni, a (1985). Lymphokine-activated tumor inhibition in vivo. I. The local administration of interleukin 2 triggers nonreactive lymphocytes from tumor-bearing mice to inhibit tumor growth. J. Immunol. *134*, 1305–1311.

Foser, S., Schacher, A., Weyer, K.A., Brugger, D., Dietel, E., Marti, S., and Schreitmüller, T. (2003). Isolation, structural characterization, and antiviral activity of positional isomers of monopegylated interferon α-2a (PEGASYS). Protein Expr. Purif. *30*, 78–87.

Foster, G.R. (2010). Pegylated interferons for the treatment of chronic hepatitis C: pharmacological and clinical differences between peginterferon-alpha-2a and peginterferon-alpha-2b. Drugs *70*, 147–165.

Fruijtier-Pölloth, C. (2005). Safety assessment on polyethylene glycols (PEGs) and their derivatives as used in cosmetic products. Toxicology *214*, 1–38.

Gebauer, M., and Skerra, A. (2009). Engineered protein scaffolds as next-generation antibody therapeutics. Curr. Opin. Chem. Biol. *13*, 245–255.

Gehlsen, K., Gong, R., Bramhill, D., Wiersma, D., Kirkpatrick, S., Wang, Y., Feng, Y., and Dimitrov, D.S. (2012). Pharmacokinetics of engineered human monomeric and dimeric CH2 domains. MAbs *4*, 466–474.

Getz, E.B., Xiao, M., Chakrabarty, T., Cooke, R., and Selvin, P.R. (1999). A comparison between the sulfhydryl reductants tris(2-carboxyethyl)phosphine and dithiothreitol for use in protein biochemistry. Anal. Biochem. *273*, 73–80.

Giard, D.J., and Fleischaker, R.J. (1984). A study showing a high degree of interlaboratory variation in the assay of human interferon. J. Biol. Stand. *12*, 265–269.

Gill, D.S., and Damle, N.K. (2006). Biopharmaceutical drug discovery using novel protein scaffolds. Curr. Opin. Biotechnol. *17*, 653–658.

Glennie, M.J., McBride, H.M., Worth, A.T., and Stevenson, G.T. (1987). Preparation and performance of bispecific F(ab' gamma)2 antibody containing thioether-linked Fab' gamma fragments. J. Immunol. *139*, 2367–2375.

Glue, P., Fang, J.W., Rouzier-Panis, R., Raffanel, C., Sabo, R., Gupta, S.K., Salfi, M., and Jacobs, S. (2000). Pegylated interferon-alpha2b: pharmacokinetics, pharmacodynamics, safety, and preliminary efficacy data. Hepatitis C Intervention Therapy Group. Clin. Pharmacol. Ther. *68*, 556–567.

Goding, J.W. (1996). Monoclonal antibodies: principles and practice (Academic Press).

Goodbourn, S. (2000). Interferons: cell signalling, immune modulation, antiviral response and virus countermeasures. J. Gen. … 2341–2364.

Grace, M., Youngster, S., Gitlin, G., Sydor, W., Xie, L., Westreich, L., Jacobs, S., Brassard, D., Bausch, J., and Bordens, R. (2001). Structural and biologic characterization of pegylated recombinant IFN-alpha2b. J. Interferon Cytokine Res. *21*, 1103–1115.

Grace, M.J., Lee, S., Bradshaw, S., Chapman, J., Spond, J., Cox, S., Delorenzo, M., Brassard, D., Wylie, D., Cannon-Carlson, S., et al. (2005). Site of pegylation and polyethylene glycol molecule size attenuate interferon-alpha antiviral and antiproliferative activities through the JAK/STAT signaling pathway. J. Biol. Chem. *280*, 6327–6336.

Hansen, R.E., and Winther, J.R. (2009). An introduction to methods for analyzing thiols and disulfides: Reactions, reagents, and practical considerations. Anal. Biochem. *394*, 147–158.

Harris, J.M., Martin, N.E., and Modi, M. (2001). Pegylation: a novel process for modifying pharmacokinetics. Clin. Pharmacokinet. *40*, 539–551.

Heinzel, F.P., Hujer, A.M., Ahmed, F.N., and Rerko, R.M. (1997). In vivo production and function of IL-12 p40 homodimers. J. Immunol. *158*, 4381–4388.

Helguera, G., Rodríguez, J. a, and Penichet, M.L. (2006). Cytokines fused to antibodies and their combinations as therapeutic agents against different peritoneal HER2/neu expressing tumors. Mol. Cancer Ther. *5*, 1029–1040.

Hermanson, G.T. (2008). Chapter 1 - Functional Targets. In Bioconjugate Techniques (Second Edition), G.T. Hermanson, ed. (New York: Academic Press), pp. 1–168.

Hjelm, H., Sjödahl, J., and Sjöquist, J. (1975). Immunologically active and structurally similar fragments of protein A from Staphylococcus aureus. Eur. J. Biochem. *57*, 395–403.

Holt, L.J., Herring, C., Jespers, L.S., Woolven, B.P., and Tomlinson, I.M. (2003). Domain antibodies: proteins for therapy. Trends Biotechnol. *21*, 484–490.

Holt, L.J., Basran, A., Jones, K., Chorlton, J., Jespers, L.S., Brewis, N.D., and Tomlinson, I.M. (2008). Anti-serum albumin domain antibodies for extending the half-lives of short lived drugs. Protein Eng. Des. Sel. *21*, 283–288.

Hopp, J., Hornig, N., Zettlitz, K.A., Schwarz, A., Fuss, N., Müller, D., and Kontermann, R.E. (2010). The effects of affinity and valency of an albumin-binding domain (ABD) on the half-life of a single-chain diabody-ABD fusion protein. Protein Eng. Des. Sel. PEDS *23*, 827–834.

Hu, S., Shively, L., Raubitschek, A., Sherman, M., Williams, L.E., Wong, J.Y., Shively, J.E., and Wu, A.M. (1996). Minibody: A novel engineered anti-carcinoembryonic antigen antibody fragment (single-chain Fv-CH3) which exhibits rapid, high-level targeting of xenografts. Cancer Res. *56*, 3055–3061.

Humphreys, D.P., Heywood, S.P., Henry, A., Ait-Lhadj, L., Antoniw, P., Palframan, R., Greenslade, K.J., Carrington, B., Reeks, D.G., Bowering, L.C., et al. (2007). Alternative antibody Fab' fragment PEGylation strategies: combination of strong reducing agents, disruption of the interchain disulphide bond and disulphide engineering. Protein Eng. Des. Sel. *20*, 227–234.

Isaacs, A., and Lindenmann, J. (1957). Virus Interference. I. The Interferon. Proc. R. Soc. B Biol. Sci. *147*, 258–267.

Ispolatov, I., Yuryev, A., Mazo, I., and Maslov, S. (2005). Binding properties and evolution of homodimers in protein-protein interaction networks. Nucleic Acids Res. *33*, 3629–3635.

Iyer, U., and Kadambi, V.J. (2011). Antibody drug conjugates - Trojan horses in the war on cancer. J. Pharmacol. Toxicol. Methods *64*, 207–212.

James E Seely, P.D., Scott D Buckel, P.., Green, P.D., and Richey, C.W. (2005). Making Site-specific PEGylation Work. BioPharm Int.

Jazayeri, J.A., and Carroll, G.J. (2008). Fc-based cytokines : prospects for engineering superior therapeutics. BioDrugs *22*, 11–26.

Jevsevar, S., Kunstelj, M., and Porekar, V.G. (2010). PEGylation of therapeutic proteins. Biotechnol. J. *5*, 113–128.

Johannsen, M., Spitaleri, G., Curigliano, G., Roigas, J., Weikert, S., Kempkensteffen, C., Roemer, A., Kloeters, C., Rogalla, P., Pecher, G., et al. (2010). The tumour-targeting human L19-IL2 immunocytokine: preclinical safety studies, phase I clinical trial in patients with solid tumours and expansion into patients with advanced renal cell carcinoma. Eur. J. Cancer *46*, 2926–2935.

Johnson, I.S. (1983). Human insulin from recombinant DNA technology. Science (80-.). *219*, 632–637.

Jones, M.C., and Patel, M. (2006). Insulin detemir: a long-acting insulin product. Am. J. Health. Syst. Pharm. *63*, 2466–2472.

Jorgensen, K.E., and Moller, J. V. (1979). Use of flexible polymers as probes of glomerular pore size. Am J Physiol Ren. Physiol *236*, F103–F111.

Khalili, H., Godwin, A., Choi, J., Lever, R., and Brocchini, S. (2012). Comparative binding of disulfide-bridged PEG-Fabs. Bioconjug. Chem. *23*, 2262–2277.

Khalili, H., Godwin, A., Choi, J.-W., Lever, R., Khaw, P.T., and Brocchini, S. (2013). Fab-PEG-Fab as a potential antibody mimetic. Bioconjug. Chem. *24*, 1870–1882.

Kinstler, O., Molineux, G., Treuheit, M., Ladd, D., and Gegg, C. (2002). Mono-N-terminal poly(ethylene glycol)-protein conjugates. Adv. Drug Deliv. Rev. *54*, 477–485.

Klaus, W., Gsell, B., Labhardt, a M., Wipf, B., and Senn, H. (1997). The three-dimensional high resolution structure of human interferon alpha-2a determined by heteronuclear NMR spectroscopy in solution. J. Mol. Biol. *274*, 661–675.

Kobsa, S., and Saltzman, W.M. (2008). Bioengineering approaches to controlled protein delivery. Pediatr. Res. *63*, 513–519.

Kontermann, R. (2011). Therapeutic proteins: strategies to modulate their plasma half-lives (John Wiley & Sons).

Kontermann, R. (2012). Dual targeting strategies with bispecific antibodies. MAbs *4*, 182–197.

Kontermann, R.E. (2005). Recombinant bispecific antibodies for cancer therapy. Acta Pharmacol. Sin. *26*, 1–9.

Kraulis, P.J., Jonasson, P., Nygren, P. a, Uhlén, M., Jendeberg, L., Nilsson, B., and Kördel, J. (1996). The serum albumin-binding domain of streptococcal protein G is a three-helical bundle: a heteronuclear NMR study. FEBS Lett. *378*, 190–194.

Kubota, T., Niwa, R., Satoh, M., Akinaga, S., Shitara, K., and Hanai, N. (2009). Engineered therapeutic antibodies with improved effector functions. Cancer Sci. *100*, 1566–1572.

Kurfürst, M.M. (1992). Detection and molecular weight determination of polyethylene glycol-modified hirudin by staining after sodium dodecyl sulfate-polyacrylamide gel electrophoresis. Anal. Biochem. *200*, 244–248.

Leader, B., Baca, Q.J., and Golan, D.E. (2008). Protein therapeutics: a summary and pharmacological classification. Nat Rev Drug Discov *7*, 21–39.

Leonard, J.P., Sherman, M.L., Fisher, G.L., Buchanan, L.J., Larsen, G., Atkins, M.B., Sosman, J. a, Dutcher, J.P., Vogelzang, N.J., and Ryan, J.L. (1997). Effects of single-dose interleukin-12 exposure on interleukin-12-associated toxicity and interferon-gamma production. Blood *90*, 2541–2548.

Libon, C., Corvaïa, N., Haeuw, J.F., Nguyen, T.N., Ståhl, S., Bonnefoy, J.Y., and Andreoni, C. (1999). The serum albumin-binding region of streptococcal protein G (BB) potentiates the immunogenicity of the G130-230 RSV-A protein. Vaccine *17*, 406–414.

Linke, R., Klein, A., and Seimetz, D. (2010). Catumaxomab: clinical development and future directions. MAbs *2*, 129–136.

Lipovsek, D. (2011). Adnectins: engineered target-binding protein therapeutics. Protein Eng. Des. Sel. *24*, 3–9.

List, T., and Neri, D. (2013). Immunocytokines: a review of molecules in clinical development for cancer therapy. Clin. Pharmacol. *5*, 29–45.

Lobstein, J., Emrich, C. a, Jeans, C., Faulkner, M., Riggs, P., and Berkmen, M. (2012). SHuffle, a novel Escherichia coli protein expression strain capable of correctly folding disulfide bonded proteins in its cytoplasm. Microb. Cell Fact. *11*, 56.

Lu, Y., Harding, S.E., Turner, A., Smith, B., Athwal, D.S., Grossmann, J.G., Davis, K.G., and Rowe, A.J. (2008). Effect of PEGylation on the solution conformation of antibody fragments. J. Pharm. Sci. *97*, 2062–2079.

Lunn, C.A., Davies, L., Dalgarno, D., Narula, S.K., Zavodny, P.J., and Lundell, D. (1992). An active covalently linked dimer of human interferon-gamma. Subunit orientation in the native protein. J. Biol. Chem. *267*, 17920–17924.

Luxon, B. a, Grace, M., Brassard, D., and Bordens, R. (2002a). Pegylated interferons for the treatment of chronic hepatitis C infection. Clin. Ther. *24*, 1363–1383.

Luxon, B. a, Grace, M., Brassard, D., and Bordens, R. (2002b). Pegylated interferons for the treatment of chronic hepatitis C infection. Clin. Ther. *24*, 1363–1383.

Mack, E.T., Snyder, P.W., Perez-Castillejos, R., and Whitesides, G.M. (2011). Using covalent dimers of human carbonic anhydrase II to model bivalency in immunoglobulins. J. Am. Chem. Soc. *133*, 11701–11715.

Mage, M. (1980). Preparation of Fab fragments from IgGs of different animal species. Methods Enzymol. *70*, 142–150.

Mahmood, T., and Yang, P.-C. (2012). Western blot: technique, theory, and trouble shooting. N. Am. J. Med. Sci. *4*, 429–434.

Malucchi, S., Sala, A., Gilli, F., Bottero, R., Di Sapio, A., Capobianco, M., and Bertolotto, A. (2004). Neutralizing antibodies reduce the efficacy of betaIFN during treatment of multiple sclerosis. Neurology *62*, 2031–2037.

Marianayagam, N.J., Sunde, M., and Matthews, J.M. (2004). The power of two: protein dimerization in biology. Trends Biochem. Sci. *29*, 618–625.

Markey, F. (1999). What is SPR anyway. BIA J. 14–17.

Marshall, S. a, Lazar, G. a, Chirino, A.J., and Desjarlais, J.R. (2003). Rational design and engineering of therapeutic proteins. Drug Discov. Today *8*, 212–221.

Martin, P. (2006). Beyond the next generation of therapeutic proteins. Protein Eng.

McDonagh, C.F., Huhalov, A., Harms, B.D., Adams, S., Paragas, V., Oyama, S., Zhang, B., Luus, L., Overland, R., Nguyen, S., et al. (2012). Antitumor activity of a novel bispecific antibody that targets

the ErbB2/ErbB3 oncogenic unit and inhibits heregulin-induced activation of ErbB3. Mol. Cancer Ther. *11*, 582–593.

Meager, A. (2002). Biological assays for interferons. J. Immunol. Methods *261*, 21–36.

Meager, A. (2006). Measurement of cytokines by bioassays: theory and application. Methods *38*, 237–252.

Meager, a, Gaines Das, R., Zoon, K., and Mire-Sluis, a (2001). Establishment of new and replacement World Health Organization International Biological Standards for human interferon alpha and omega. J. Immunol. Methods *257*, 17–33.

Meibohm, B. (2006). Pharmacokinetics and pharmacodynamics of biotech drugs: principles and case studies in drug development (John Wiley & Sons).

Metzner, H.J., Weimer, T., and Schulte, S. (2012). Half-Life Extension by Fusion to Recombinant Albumin. In Therapeutic Proteins, (Wiley-VCH Verlag GmbH & Co. KGaA), pp. 223–247.

Metzner, H.J., Pipe, S.W., Weimer, T., and Schulte, S. (2013). Extending the pharmacokinetic half-life of coagulation factors by fusion to recombinant albumin. Thromb. Haemost. *110*, 931–939.

Mintz, C.S., and Crea, R. (2013). Protein Scaffolds: the next generation of protein therapeutics? Bioprocess Int. *11*, 40–48.

Mire-Sluis, a R., Gaines Das, R., Zoon, K., Padilla, a, Thorpe, R., and Meager, a (1996). The biological properties, assay, and standardization of interferon-alpha: a need for a WHO collaborative study. J. Interferon Cytokine Res. *16*, 637–643.

Mitsui, Y., Senda, T., Shimazu, T., Matsuda, S., and Utsumi, J. (1993). Structural, functional and evolutionary implications of the three-dimensional crystal structure of murine interferon-beta. Pharmacol. Ther. *58*, 93–132.

Molineux, G. (2002). Pegylation: engineering improved pharmaceuticals for enhanced therapy. Cancer Treat. Rev. *28*, 13–16.

Monkarsh, S.P., Ma, Y., Aglione, A., Bailon, P., Ciolek, D., DeBarbieri, B., Graves, M.C., Hollfelder, K., Michel, H., Palleroni, A., et al. (1997). Positional isomers of monopegylated interferon alpha-2a: isolation, characterization, and biological activity. Anal. Biochem. *247*, 434–440.

Moore, S.J., and Cochran, J.R. (2012). Chapter nine - Engineering Knottins as Novel Binding Agents. In Protein Engineering for Therapeutics, Part B, K.D. Wittrup, and G.L. Verdine, eds. (Academic Press), pp. 223–251.

Mouratou, B., Schaeffer, F., Guilvout, I., Tello-Manigne, D., Pugsley, A.P., Alzari, P.M., and Pecorari, F. (2007). Remodeling a DNA-binding protein as a specific in vivo inhibitor of bacterial secretin PulD. Proc. Natl. Acad. Sci. U. S. A. *104*, 17983–17988.

Mullard, A. (2012). 2011 FDA drug approvals. Nat. Rev. Drug Discov. *11*, 91–94.

Myszka, D. (1997). Kinetic analysis of macromolecular interactions using plasmon resonance resonance biosensors. Curr. Opin. Biotechnol. 50–57.

Myszka, D.G. (2000). Improving biosensor analysis. J. Mol. Recognit. *12*, 279–284.

Nagabhushan, TL, Reichert P, W.M.. and M.N.. (2002). Type I interferon structures: Possible scaffolds for the interferon-alpha receptor complex. Can. J. … *1173*, 1166–1173.

Nanus, D.M., Pfeffer, L.M., Bander, N.H., Bahri, S., and Albino, A.P. (1990). Antiproliferative and antitumor effects of alpha-interferon in renal cell carcinomas: correlation with the expression of a kidney-associated differentiation glycoprotein. Cancer Res. *50*, 4190–4194.

Nuttall, S.D., and Walsh, R.B. (2008). Display scaffolds: protein engineering for novel therapeutics. Curr. Opin. Pharmacol. *8*, 609–615.

Okumura, M., Saiki, M., Yamaguchi, H., and Hidaka, Y. (2011). Acceleration of disulfide-coupled protein folding using glutathione derivatives. FEBS J. *278*, 1137–1144.

Osborn, B.L., Olsen, H.S., Nardelli, B., Murray, J.H., Zhou, J.X.H., Garcia, A., Moody, G., Zaritskaya, L.S., and Sung, C. (2002). Pharmacokinetic and pharmacodynamic studies of a human serum albumin-interferon-alpha fusion protein in cynomolgus monkeys. J. Pharmacol. Exp. Ther. *303*, 540–548.

Panowksi, S., Bhakta, S., Raab, H., Polakis, P., and Junutula, J.R. (2014). Site-specific antibody drug conjugates for cancer therapy. MAbs *6*, 34–45.

Pasche, N., and Neri, D. (2012). Immunocytokines: a novel class of potent armed antibodies. Drug Discov. Today *17*, 583–590.

Pasut, G., and Veronese, F.M. (2007). Polymer–drug conjugation, recent achievements and general strategies. Prog. Polym. Sci. *32*, 933–961.

Pasut, G., and Veronese, F.M. (2012). State of the art in PEGylation: the great versatility achieved after forty years of research. J. Control. Release *161*, 461–472.

Paulus, H. (1985). Preparation and biomedical applications of bispecific antibodies. Behring Inst. Mitt. 118–132.

Pedder, S.C.J. (2003). Pegylation of interferon alfa: structural and pharmacokinetic properties. Semin. Liver Dis. *23 Suppl 1*, 19–22.

Piedmonte, D.M., and Treuheit, M.J. (2008). Formulation of Neulasta (pegfilgrastim). Adv. Drug Deliv. Rev. *60*, 50–58.

Pisal, D.S., Kosloski, M.P., and Balu-Iyer, S. V (2010). Delivery of therapeutic proteins. J. Pharm. Sci. *99*, 2557–2575.

Pless, D., and Lennarz, W. (1977). Enzymatic conversion of proteins to glycoproteins. Proc. Natl. ….

Presta, L. (2003). Antibody engineering for therapeutics. Curr. Opin. Struct. Biol. *13*, 519–525.

Rader, R. (2012). FDA Biopharmaceutical Product Approvals and Trends in 2012. Bioprocess Int. *11*, 18–27.

Radhakrishnan, R., Walter, L.J., Hruza, a, Reichert, P., Trotta, P.P., Nagabhushan, T.L., and Walter, M.R. (1996). Zinc mediated dimer of human interferon-alpha 2b revealed by X-ray crystallography. Structure *4*, 1453–1463.

Ratner, M. (2014). Genentech's glyco-engineered antibody to succeed Rituxan. Nat. Biotechnol. *32*, 6–7.

Ravandi, F. (2011). Gemtuzumab ozogamicin: one size does not fit all--the case for personalized therapy. J. Clin. Oncol. *29*, 349–351.

Reeves, D., Cheveralls, K., and Kondev, J. (2011). Regulation of biochemical reaction rates by flexible tethers. Phys. Rev. E *84*, 021914.

Rich, R.L., and Myszka, D.G. (2000). Advances in surface plasmon resonance biosensor analysis. Curr. Opin. Biotechnol. *11*, 54–61.

Richter, A.W., and Åkerblom, E. (1983). Antibodies against Polyethylene Glycol Prepared in Animals by Immunization with Monomethoxy Polyethylene Glycol Modified Proteins. Int. Arch. Allergy Immunol. *70*, 124–131.

Richter, A.W., and Åkerblom, E. (1984). Polyethylene Glycol Reactive Antibodies in Man: Titer Distribution in Allergic Patients Treated with Monomethoxy Polyethylene Glycol Modified Allergens or Placebo, and in Healthy Blood Donors. Int. Arch. Allergy Immunol. *74*, 36–39.

Rini, B.I., Halabi, S., Rosenberg, J.E., Stadler, W.M., Vaena, D. a, Ou, S.-S., Archer, L., Atkins, J.N., Picus, J., Czaykowski, P., et al. (2008). Bevacizumab plus interferon alfa compared with interferon alfa monotherapy in patients with metastatic renal cell carcinoma: CALGB 90206. J. Clin. Oncol. *26*, 5422–5428.

Roberts, M.J., Bentley, M.D., and Harris, J.M. (2002). Chemistry for peptide and protein PEGylation. Adv. Drug Deliv. Rev. *54*, 459–476.

Rodewald, R. (1976). pH-dependent binding of immunoglobulins to intestinal cells of the neonatal rat. J. Cell Biol. *71*, 666–670.

Roopenian, D.C., and Akilesh, S. (2007). FcRn: the neonatal Fc receptor comes of age. Nat. Rev. Immunol. *7*, 715–725.

Rossi, E. a, Goldenberg, D.M., Cardillo, T.M., Stein, R., and Chang, C.-H. (2009). CD20-targeted tetrameric interferon-alpha, a novel and potent immunocytokine for the therapy of B-cell lymphomas. Blood *114*, 3864–3871.

Rossi, E. a, Rossi, D.L., Stein, R., Goldenberg, D.M., and Chang, C.-H. (2010). A bispecific antibody-IFNalpha2b immunocytokine targeting CD20 and HLA-DR is highly toxic to human lymphoma and multiple myeloma cells. Cancer Res. *70*, 7600–7609.

Rossi, E. a, Goldenberg, D.M., and Chang, C.-H. (2012). The dock-and-lock method combines recombinant engineering with site-specific covalent conjugation to generate multifunctional structures. Bioconjug. Chem. *23*, 309–323.

Rudnick, S.I., and Adams, G.P. (2009). Affinity and avidity in antibody-based tumor targeting. Cancer Biother. Radiopharm. *24*, 155–161.

Ryan, S.M., Mantovani, G., Wang, X., Haddleton, D.M., and Brayden, D.J. (2008). Advances in PEGylation of important biotech molecules: delivery aspects. Expert Opin. Drug Deliv. *5*, 371–383.

Sangfelt, O., Erickson, S., Castro, J., Heiden, T., Einhorn, S., and Grandér, D. (1997). Induction of apoptosis and inhibition of cell growth are independent responses to interferon-alpha in hematopoietic cell lines. Cell Growth Differ. *8*, 343–352.

Schlatter, D., Brack, S., Banner, D.W., Batey, S., Benz, J., Bertschinger, J., Huber, W., Joseph, C., Rufer, A., van der Klooster, A., et al. (2012). Generation, characterization and structural data of chymase binding proteins based on the human Fyn kinase SH3 domain. MAbs *4*, 497–508.

Schulte, S. (2009). Half-life extension through albumin fusion technologies. Thromb. Res. *124 Suppl*, S6–S8.

Schulte, S. (2013). Innovative coagulation factors: albumin fusion technology and recombinant single-chain factor {VIII}. Thromb. Res. *131, Suppl*, S2–S6.

Seely, J.E., and Richey, C.W. (2001). Use of ion-exchange chromatography and hydrophobic interaction chromatography in the preparation and recovery of polyethylene glycol-linked proteins. J. Chromatogr. A *908*, 235–241.

Seimetz, D. (2011). Novel monoclonal antibodies for cancer treatment: the trifunctional antibody catumaxomab (removab). J. Cancer *2*, 309–316.

Sekhon, B. (2010). Biopharmaceuticals : an overview. Thai J. Pharm. Sci. *34*, 1–19.

Senter, P.D. (2009). Potent antibody drug conjugates for cancer therapy. Curr. Opin. Chem. Biol. *13*, 235–244.

Shapiro, A.D., Ragni, M. V, Valentino, L. a, Key, N.S., Josephson, N.C., Powell, J.S., Cheng, G., Thompson, A.R., Goyal, J., Tubridy, K.L., et al. (2012). Recombinant factor IX-Fc fusion protein (rFIXFc) demonstrates safety and prolonged activity in a phase 1/2a study in hemophilia B patients. Blood *119*, 666–672.

Shaunak, S., Godwin, A., Choi, J.-W., Balan, S., Pedone, E., Vijayarangam, D., Heidelberger, S., Teo, I., Zloh, M., and Brocchini, S. (2006). Site-specific PEGylation of native disulfide bonds in therapeutic proteins. Nat. Chem. Biol. *2*, 312–313.

Shen, B.-Q., Xu, K., Liu, L., Raab, H., Bhakta, S., Kenrick, M., Parsons-Reponte, K.L., Tien, J., Yu, S.-F., Mai, E., et al. (2012). Conjugation site modulates the in vivo stability and therapeutic activity of antibody-drug conjugates. Nat Biotech *30*, 184–189.

Shewmake, T. a, Solis, F.J., Gillies, R.J., and Caplan, M.R. (2008). Effects of linker length and flexibility on multivalent targeting. Biomacromolecules *9*, 3057–3064.

Sievers, E.L., and Linenberger, M. (2001). Mylotarg: antibody-targeted chemotherapy comes of age. Curr. Opin. Oncol. KW - *13*.

Sievers, E.L., and Senter, P.D. (2013). Antibody-drug conjugates in cancer therapy. Annu. Rev. Med. *64*, 15–29.

Silverman, J., Liu, Q., Lu, Q., Bakker, A., To, W., Duguay, A., Alba, B.M., Smith, R., Rivas, A., Li, P., et al. (2005). Multivalent avimer proteins evolved by exon shuffling of a family of human receptor domains. Nat. Biotechnol. *23*, 1556–1561.

Sjölander, a, Nygren, P. a, Stahl, S., Berzins, K., Uhlen, M., Perlmann, P., and Andersson, R. (1997). The serum albumin-binding region of streptococcal protein G: a bacterial fusion partner with carrier-related properties. J. Immunol. Methods *201*, 115–123.

Smith, B.J., Popplewell, a, Athwal, D., Chapman, a P., Heywood, S., West, S.M., Carrington, B., Nesbitt, a, Lawson, a D., Antoniw, P., et al. (2001). Prolonged in vivo residence times of antibody fragments associated with albumin. Bioconjug. Chem. *12*, 750–756.

Solá, R.J., and Griebenow, K. (2010). Glycosylation of therapeutic proteins: an effective strategy to optimize efficacy. BioDrugs *24*, 9–21.

Spencer-Green, G. (2000). Etanercept (Enbrel): update on therapeutic use. Ann. Rheum. Dis. *59 Suppl 1*, i46–i49.

Stefan R. Schmidt (2013). Fusion Protein Technologies for Biopharmaceuticals. In Fusion Protein Technologies for Biopharmaceuticals: Applications and Challenges, S.R. Schmidt, ed. (Hoboken, NJ, USA: John Wiley & Sons, Inc.), pp. 3–24.

Stork, R., Müller, D., and Kontermann, R.E. (2007). A novel tri-functional antibody fusion protein with improved pharmacokinetic properties generated by fusing a bispecific single-chain diabody with an albumin-binding domain from streptococcal protein G. Protein Eng. Des. Sel. *20*, 569–576.

Subramanian, G.M., Fiscella, M., Lamousé-Smith, A., Zeuzem, S., and McHutchison, J.G. (2007). Albinterferon alpha-2b: a genetic fusion protein for the treatment of chronic hepatitis C. Nat. Biotechnol. *25*, 1411–1419.

Tamaskovic, R., Simon, M., Stefan, N., Schwill, M., and Plückthun, A. (2012). Chapter five - Designed Ankyrin Repeat Proteins (DARPins): From Research to Therapy. In Protein Engineering for Therapeutics, Part B, K.D. Wittrup, and G.L. Verdine, eds. (Academic Press), pp. 101–134.

Tayyab, S., Qamar, S., and Islam, M. (1991). Size exclusion chromatography and size exclusion HPLC of proteins. Biochem. Educ. *19*, 149–152.

Tessmar, J.K., and Göpferich, A.M. (2007). Matrices and scaffolds for protein delivery in tissue engineering. Adv. Drug Deliv. Rev. *59*, 274–291.

Thomas, H., Török, M., and Foster, G. (1999). Hepatitis C virus dynamics in vivo and the antiviral efficacy of interferon alfa therapy. Hepatology *29*, 1998–1999.

Thornton, J.M. (1981). Disulphide bridges in globular proteins. J. Mol. Biol. *151*, 261–287.

Tiefenbrun, N., Melamed, D., Levy, N., Resnitzky, D., Hoffman, I., Reed, S.I., and Kimchi, A. (1996). Alpha interferon suppresses the cyclin D3 and cdc25A genes, leading to a reversible G0-like arrest. Mol. Cell. Biol. *16*, 3934–3944.

Uzé, G., Di Marco, S., Mouchel-Vielh, E., Monneron, D., Bandu, M.T., Horisberger, M.A., Dorques, A., Lutfalla, G., and Mogensen, K.E. (1994). Domains of interaction between alpha interferon and its receptor components. J. Mol. Biol. *243*, 245–257.

Vazquez-Lombardi, R., Roome, B., and Christ, D. (2013). Molecular Engineering of Therapeutic Cytokines. Antibodies *2*, 426–451.

Veronese, F.M., and Morpurgo, M. (1999). Bioconjugation in pharmaceutical chemistry. Farmaco *54*, 497–516.

Veronese, F.M., and Pasut, G. (2005). PEGylation, successful approach to drug delivery. Drug Discov. Today *10*, 1451–1458.

Verwey, W.F. (1940). a Type-Specific Antigenic Protein Derived From the Staphylococcus. J. Exp. Med. *71*, 635–644.

Vicent, M.J., and Duncan, R. (2006). Polymer conjugates: nanosized medicines for treating cancer. Trends Biotechnol. *24*, 39–47.

Vincent, K.J., and Zurini, M. (2012). Current strategies in antibody engineering: Fc engineering and pH-dependent antigen binding, bispecific antibodies and antibody drug conjugates. Biotechnol. J. *7*, 1444–1450.

Waine, G.J., Tymms, M.J., Brandt, E.R., Cheetham, B.F., and Linnane, a W. (1992). Structure-function study of the region encompassing residues 26-40 of human interferon-alpha 4: identification of residues important for antiviral and antiproliferative activities. J. Interferon Res. *12*, 43–48.

Walker, A., Dunlevy, G., Rycroft, D., Topley, P., Holt, L.J., Herbert, T., Davies, M., Cook, F., Holmes, S., Jespers, L., et al. (2010). Anti-serum albumin domain antibodies in the development of highly potent, efficacious and long-acting interferon. Protein Eng. Des. Sel. *23*, 271–278.

Walsh, G. (2004). Second-generation biopharmaceuticals. Eur. J. Pharm. Biopharm. *58*, 185–196.

Walsh, G. (2010). Biopharmaceutical benchmarks 2010. Nat. Biotechnol. *28*, 917–924.

Walsh, G., and Jefferis, R. (2006). Post-translational modifications in the context of therapeutic proteins. Nat. Biotechnol. *24*, 1241–1252.

Wang, H.Z., Chang, C.H., Lin, C.P., and Tsai, M.C. (1996). Using MTT viability assay to test the cytotoxicity of antibiotics and steroid to cultured porcine corneal endothelial cells. J. Ocul. Pharmacol. Ther. *12*, 35–43.

Wang, W., Wang, E.Q., and Balthasar, J.P. (2008). Monoclonal antibody pharmacokinetics and pharmacodynamics. Clin. Pharmacol. Ther. *84*, 548–558.

Wang, Y.-S., Youngster, S., Grace, M., Bausch, J., Bordens, R., and Wyss, D.F. (2002). Structural and biological characterization of pegylated recombinant interferon alpha-2b and its therapeutic implications. Adv. Drug Deliv. Rev. *54*, 547–570.

Wang, Y.S., Youngster, S., Bausch, J., Zhang, R., McNemar, C., and Wyss, D.F. (2000). Identification of the major positional isomer of pegylated interferon alpha-2b. Biochemistry *39*, 10634–10640.

Webster, R., Didier, E., Harris, P., Siegel, N., Stadler, J., Tilbury, L., and Smith, D. (2007). PEGylated proteins: evaluation of their safety in the absence of definitive metabolism studies. Drug Metab. Dispos. *35*, 9–16.

De Weerd, N.A., Samarajiwa, S.A., and Hertzog, P.J. (2007). Type I interferon receptors: biochemistry and biological functions. J. Biol. Chem. *282*, 20053–20057.

Wu, A.M., and Senter, P.D. (2005). Arming antibodies: prospects and challenges for immunoconjugates. Nat. Biotechnol. *23*, 1137–1146.

Wu, W.-Z., Sun, H.-C., Shen, Y.-F., Chen, J., Wang, L., Tang, Z.-Y., Iliakis, G., and Liu, K.-D. (2005). Interferon alpha 2a down-regulates VEGF expression through PI3 kinase and MAP kinase signaling pathways. J. Cancer Res. Clin. Oncol. *131*, 169–178.

Wurch, T., Pierré, A., and Depil, S. (2012). Novel protein scaffolds as emerging therapeutic proteins: from discovery to clinical proof-of-concept. Trends Biotechnol. *30*, 575–582.

Xia, C.Q., Wang, J., and Shen, W.C. (2000). Hypoglycemic effect of insulin-transferrin conjugate in streptozotocin-induced diabetic rats. J. Pharmacol. Exp. Ther. *295*, 594–600.

Xie, D., Yao, C., Wang, L., Min, W., Xu, J., Xiao, J., Huang, M., Chen, B., Liu, B., Li, X., et al. (2010). An albumin-conjugated peptide exhibits potent anti-HIV activity and long in vivo half-life. Antimicrob. Agents Chemother. *54*, 191–196.

Yamaoka, T., Tabata, Y., and Ikada, Y. (1994). Distribution and Tissue Uptake of Poly(ethylene glycol) with Different Molecular Weights after Intravenous Administration to mice. J. Pharm. … *83*, 1–6.

Yang, J., Wang, X., Fuh, G., Yu, L., Wakshull, E., Khosraviani, M., Day, E.S., Demeule, B., Liu, J., Shire, S.J., et al. (2014). Comparison of Binding Characteristics and In Vitro Activities of Three Inhibitors of Vascular Endothelial Growth Factor A. Mol. Pharm.

Yeh, P., Landais, D., Lemaître, M., Maury, I., Crenne, J.Y., Becquart, J., Murry-Brelier, a, Boucher, F., Montay, G., and Fleer, R. (1992). Design of yeast-secreted albumin derivatives for human therapy: biological and antiviral properties of a serum albumin-CD4 genetic conjugate. Proc. Natl. Acad. Sci. U. S. A. *89*, 1904–1908.

Yokota, T., Milenic, D.E., Whitlow, M., and Schlom, J. (1992). Rapid tumor penetration of a single-chain Fv and comparison with other immunoglobulin forms. Cancer Res. *52*, 3402–3408.

Zhao, Y., Gutshall, L., Jiang, H., Baker, A., Beil, E., Obmolova, G., Carton, J., Taudte, S., and Amegadzie, B. (2009). Two routes for production and purification of Fab fragments in biopharmaceutical discovery research: Papain digestion of mAb and transient expression in mammalian cells. Protein Expr. Purif. *67*, 182–189.